24 0275432 0

FOREWORD

The work reported in this thesis was carried out both at Leeds University and at Imperial College, London (under the supervision of the late Prof. J.V. Watson). The bulk of the non-palaeomagnetic work, which formed a very important and integral part of the overall study, was performed at Imperial College. This work is referred to and discussed throughout the thesis, particularly in chapter 6 but also in parts of chapters 3, 5, 7 and 8. Selected raw data are given in appendices C and D. Conclusions based specifically on mineralogical and geochemical studies are given in sections 9.3 and 9.4

Imperial College &
Science Museum Libraries

London SW7 2AZ Issue Desk Tel. 020-7594 8810

LONG LOAN

To be returned by the last date stamped (normally one term), or after *three weeks* if the book is reserved by another reader. A fine may be charged if the book is returned late.

Palaeomagnetism of Old Red Sandstones and related rocks of the Orcadian Basin, including mineralogical studies of the remanence carriers

Martin A. Robinson

Submitted in fulfilment of the requirements of the

Diploma of the Imperial College (DIC)

Main department:

Dept. of Earth Sciences
The University
Leeds

Also at:

Dept. of Geology
Imperial College
London

February 1986

ABSTRACT

A wide range of rock types, including sediments, extrusive lavas and intrusive igneous rocks, have been analysed in an attempt to suggest a model for remanence acquisition in the Orcadian Basin.

Extrusive lavas and their baked contacts (of upper Middle ORS age) give a mean palaeomagnetic pole position of Lat. 10N, Long. 163E. This is proposed as a good estimate of the upper Middle ORS geomagnetic field with respect to northern Scotland. A similar pole to that of the lavas is found in many sediments, particularly those of Emsian or upper ORS age. The primary remanence is carried predominantly in hematite although a few sites which escaped early oxidation may show a primary magnetite component. Oxidation of detrital magnetite is considered to be the chief mechanism by which a primary hematitic remanence was acquired. Detrital grains often show marked martitisation textures indicative of oxidation; they give analyses strongly suggestive of hematite.

The primary remanence may be found in close association with a secondary Carboniferous-Permian component, often in the same specimen. Attempts have been made to characterise the nature of this secondary remanence using a variety of techniques, particularly electron microscopy and geochemical analysis. These would seem to suggest that much of the secondary remanence resulted from the diagenesis of ferroan carbonates; these may constitute a large part of the rock (e.g. the Midle ORS lacustrine laminites, which have been totally remagnetised) or may be present only as a minor cement (e.g. some of the Lower ORS and many other formations). Delayed martitisation probably also occurred, as evidenced by late diagenetic titanium oxides.

A model is proposed in which remagnetisation of sediments occurred during the Kiaman reversed polarity period as a result of a very deeply depressed water table level, resulting from extreme continentality and aridity. This enabled processes to occur to a very great depth which are normally associated with surface conditions. Such processes are those which require the free flow of water and/or high Eh, such as oxidation of magnetite and calcitisation and leaching of ferroan carbonate cements. By this means, a pervasive oxidative remagnetisation of a very great thickness of sediment could occur.

Such a model may be extended to many other Upper Palaeozoic sediments throughout Laurentia-Baltica which are currently being recognised as having suffered severe oxidative remagnetisation in the Kiaman. This has been tested by an analysis of Carboniferous sandstones on the Solway Firth which have been found to have acquired a post-tectonic remanence.

Any further studies of the Upper Palaeozoic, particularly sediments such as redbeds and carbonates, will need to follow a similar pattern of investigation in order to characterise their remanence sufficiently well to enable the apparent polar wander path for the period to have any validity. The use of the electron microscope in such studies is particularly recomended.

This thesis is dedicated to the memory of
Tarquin Teale

ACKNOWLEDGEMENTS

My thanks must go first and foremost to my two supervisors, Prof. J.C. Briden (Leeds University) and Prof. J.V. Watson (Imperial College). Their interest and enthusiasm for very different but closely inter-related aspects of Earth Sciences laid the foundations for a very varied and challenging research project.

Janet Watson's untimely death part way through the study was an enormous loss which will be felt very deeply by many people for a very long period of time. It was the loss not only of an outstanding and pioneering geologist but also of one of the most sincere, friendly and helpful people in the geological community.

I would like to thank Tim Astin, Dave Hatfield, Dave Ord, John Parnell and Doyle Watts, in addition to my supervisors, for invaluable advice and assistance in the field. Tim Astin is also thanked for organising a very useful and informative thematic conference on the Orcadian Basin.

The support and assistance of the 'Palaeomag Crew' (Martin Bates, Dave Hatfield, Buffy McClelland Brown, Bundan Mubroto, David Robertson and Mark Smethurst) is greatly appreciated, particularly the efforts of Mark Smethurst to bring computer graphics into the 21st century and of Dave Hatfield and Buffy McClelland Brown to keep equipment functional against all the odds.

On the technical side, the assistance of Mrs E. Bannerjee (ICP analysis), Dr. E. Condliffe, Mr. R. Giddens and Mr. P. Grant (electron microscopy), Mr. R. Boud (cartography), Dr. R. Clark (computing), Mr. F. Bouckley (ferrous iron determinations), Mr. A. Grey (sample preparation), Mr. F. Johnston (just about everything) and the technical and support staff of both Leeds University and Imperial College is gratefully acknowledged. The photography department of Leeds University made especial efforts in plate production.

In addition to names already mentionedd, discussion and help from many people including Mr. M. Enfield, Prof. E.H. Francis, Dr.M. Leeder, Dr.R. Raiswell and Prof.D. Shearman has been of invaluable assistance.

On a less formal note, the members of the departments of both Leeds and I.C. have a lot to answer for. I would particularly like to mention Jan Alexander, Mark Bennett, Sarah Drewery, Basem El-Haddadeh, Steve Flint, Alison Fraser, Rob Gawthorpe, Kathryn Loynes, Bob Maddock, Keith Myers, Clive Neal, Andy Sims, Ann Strudwick, Andy Thickpenny, Alastair Welbon (proof-reader and photocopier extraordinaire), John Wheeler and Jeremy Young, in addition to many other friends (both within these departments and in my 'other life'), from whom it would be unfair to select a small number of names.

Penultimately, I would like to offer my sincere gratitude to my family for their love and support, especially during the hard times.

The final months of this research were marred by the sudden death in Italy of Tarquin Teale, one of the closest friends one could wish to have. This thesis is dedicated to his memory.

SYMBOLS AND ABBREVIATIONS USED

a95	Circle of 95% confidence about a mean direction
A95	Semi-angle of the 95% cone of confidence about a VGP
AF	Alternating Field
APW	Apparent Polar Wander
ARM	Anhysteretic Remanent Magnetisation
B	Magnetic induction
Bc	Coercive force
Bs	Saturating field
Cong.	Conglomerate
CRM	Chemical Remanent Magnetisation
dp,dm	Oval of 95% confidence about a VGP
Dec.	Declination
DRM	Detrital Remanent Magnetisation
DW	Dykewidth Eh Redox potential
EM	Eday Marls
EPMA	Electron Probe Microanalysis
EV	Eday Volcanics
f	Frequency factor
GGF	Great Glen Fault
H	Magnetic field
ICP	Inductively-coupled plasma spectroscopy
IRM	Isothermal Remanent Magnetisation
J	Magnetisation
K	Conductivity
k	Diffusivity
k	Estimate of Fisher's precision parameter
LES	Lower Eday Sandstone
M	Magnetic dipole moment per unit volume
Ms	Saturation Magnetisation
Mr	Unsaturated IRM
Mrs	Saturation IRM
MCR	Multi-component Remanence
md	multidomain
MES	Middle Eday Sandstone
m.y.	Million years
N	Number (of observations etc)
Nsp,Nsi	Number of specimens/sites
NRM	Natural Remanent Magnetisation
ORS	Old Red Sandstone
PEF	Present Earth's Field (direction)
psd	pseudo-single domain
PTRM	Partial Thermoremanent Magnetisation
PWP	Polar Wander Path
Q	Koenigsberger Ratio
R	Resultant (of N unit vectors)
SCR	Single-Component Remanence
sd	single-domain
SEI	Secondary Electron Image
SEM	Scanning Electron Microscope

Tb	Blocking Temperature
Tc	Curie Temperature
Tco	Contact Temperature
TCRM	Thermo-Chemical Remanent Magnetisation
Th	Thermal
Ti	Intrusion temperature
TiMt	Titanomagnetite
TRM	Thermoremanent Magnetisation
UES	Upper Eday Sandstone
v	Volume (of a magnetic grain)
VGP	Virtual Geomagnetic Pole
VRM	Viscous Remanent Magnetisation
Z	Atomic Number
χ	Volume Susceptibility
χ_i	Initial Susceptibility
τ	Relaxation time

CONTENTS

Abstract i
Dedication ii
Acknowledgements iii
Symbols and abbreviations iv
Contents vi
Figures x
Tables xii
Plates xiii

CHAPTER 1 INTRODUCTION

1.1. Preface 1
1.2. Sampling strategy and objectives 4
1.3. Structure of thesis 5
1.4. Experimental techniques
1.4.1. Palaeomagnetic techniques 5
1.4.2. Other techniques 8
1.5. Palaeomagnetic units 8

CHAPTER 2 GEOLOGICAL AND PALAEOMAGNETIC BACKGROUND

2.1. The Orcadian Basin
2.1.1. The Orcadian Basin in context 10
2.1.2. Old Red Sandstone of the Orcadian Basin 10
2.1.3. Bulk analyses and source areas 20
2.1.4. Origin of the basin 20
2.1.5. Structure 22
2.1.6. Post-Devonian history of the basin 24
2.2. Major transcurrent faulting 26
2.3. The Old Red Continent 29
2.4. ORS palaeomagnetism of Laurentia-Baltica
2.4.1. Great Britain 30
2.4.2. Laurentia-Baltica 34
2.5. Post-ORS palaeomagnetism 35
2.6. The Kiaman remagnetisation hypothesis 36
2.7. The acquisition of a magnetic remanence
2.7.1. Introduction: NRM 37
2.7.2. TRM-PTRM-VRM 38
2.7.3. DRM-PDRM 41
2.7.4. CRM 42
2.7.5. IRM (natural) 43
2.7.6. Spurious magnetisations 43
2.8. Palaeomagnetism of carbonates 44
2.9. Palaeomagnetism of redbeds 47

CHAPTER 3 THE EDAY LAVAS AND EDAY FLAGS

3.1. Introduction 54
3.2. Geology
3.2.1. Contemporaneous volcanic rocks 54
3.2.2. The Eday Lavas 55
3.3. Sampling 59
3.4. Palaeomagnetism: Eday Lavas
3.4.1. Previous work 59
3.4.2. NRM 64
3.4.3. Thermal demagnetisation 67
3.4.4. AF demagnetisation 72
3.5. Palaeomagnetism: Eday Flags
3.5.1. Eday Flags distant from the Eday Lavas 72

3.5.2. Eday Flags beneath the Eday Lavas 74
3.6. Hysteresis of NRM
3.6.1. Eday Lavas 77
3.6.2. Eday Flags 81
3.7. Origin of the remanence
3.7.1. Eday Lavas 82
3.7.2. Eday Flags 84
3.7.3. Summary 86

CHAPTER 4 PALAEOMAGNETISM OF CLASTIC SEDIMENTS

4.1. Introduction 89
4.2. Sediments of southern Caithness and the Moray Firth
4.2.1. Lower ORS 90
4.2.2. Middle-Upper ORS 99
4.2.3. Discussion 100
4.3. The Lower and Lower Middle ORS of Caithness
4.3.1. Geology and sampling 100
4.3.2. Palaeomagnetism: previous studies 104
4.3.3. Palaeomagnetism 105
4.3.4. Age of the remanence 114
4.4. Eday Group: Geology and sampling
4.4.4. Sedimentology 117
4.4.2. Sampling 125
4.5. Eday Group: palaeomagnetism
4.5.1. Introduction 127
4.5.2. The A component 134
4.5.3. The B component 138
4.5.4. The C component 141
4.5.5. Other sites 144
4.5.6. IRM and magnetic mineralogy 146
4.5.7. Age of the magnetisation 149
4.6. The Upper ORS of Dunnet Head and Hoy
4.6.1. Geology and sampling 152
4.6.2. Palaeomagnetism 153
4.7. The Yesnaby Group, Orkney
4.7.1. Geology and sampling 155
4.7.2. Palaeomagnetism 157
4.8. Synthesis 157

CHAPTER 5 PALAEOMAGNETISM OF LACUSTRINE SEDIMENTS

5.1. Introduction 161
5.2. Geology and sampling 165
5.3. Palaeomagnetism
5.3.1. Previous studies 169
5.3.2. Laminated 'fishbed' horizons 170
5.3.3. Other lacustrine sediments 175
5.3.4. Hysteresis of NRM 178
5.4. Summary 182

CHAPTER 6 SEDIMENTS: MAGNETIC MINERALOGY AND REMANENCE ACQUISITION

6.1. Introduction 184
6.2. Bulk geochemistry 185
6.3. Iron-Titanium oxides
6.3.1. Introduction 191
6.3.2. Detrital oxides: morphology 192
6.3.3. Secondary oxides: morphology 196
6.3.4. Composition analysis 201
6.3.5. Discussion 207
6.4. Carbonates

6.4.1. Introduction 210
6.4.2. Lacustrine sediments 211
6.4.3. Clastic sediments 225
6.5. Sheet silicate diagenesis
6.5.1. Geochemistry 235
6.5.2. Biotite in the Orcadian Basin 236
6.6. Fine-particle hematite
6.6.1. Iron-rich overgrowths 241
6.6.2. Pigmentary reddening 246
6.7. Synthesis
6.7.1. Introduction 251
6.7.2. Acquisition of a syngenetic remanence 255
6.7.3. Acquisition of a secondary remanence 258
6.7.4. A model for Kiaman remagnetisation 260

CHAPTER 7 THE PERMIAN DYKE SWARM

7.1. Introduction 263
7.2. Geology and sampling
7.2.1. Tectonics 263
7.2.2. Geochemistry 264
7.2.3. Age 266
7.2.4. Sampling 267
7.3. Dyke material: palaeomagnetism
7.3.1. Previous work 267
7.3.2. NRM 270
7.3.3. Progressive demagnetisation 273
7.3.4. Origin of the NRM 277
7.4. Dyke margins: palaeomagnetism
7.4.1. Introduction 277
7.4.2. Lacustrine laminites 278
7.4.3. Upper ORS, Caithness 289
7.4.4. Eday Marls 290
7.5. Synthesis 303

CHAPTER 8 OTHER INTRUSIVE BODIES AND THEIR AUREOLES

8.1. Introduction 308
8.2. Duncansby Vent
8.2.1. Geology, sampling and age 308
8.2.2. Palaeomagnetism 314
8.3. John o'Groats Sandstone
8.3.1. Geology, age and sampling 322
8.3.2. Palaeomagnetism 324
8.3.3. Origin of the NRM 329
8.4. Other vents 334
8.5. Summary 336

CHAPTER 9 CONCLUSIONS

9.1. The syngenetic remanence in context
9.1.1. Intra-basin 339
9.1.2. Great Britain 343
9.2. Post-ORS directions in context
9.2.1. Remagnetised sediments 348
9.2.2. Intrusive igneous rocks 354
9.3. Relevance to the remagnetisation hypothesis
9.3.1. A model for Kiaman remagnetisation 356
9.3.2. Extension to Laurentia-Baltica 358
9.4. Summary 361

REFERENCES 363

APPENDICES

A	Experimental techniques	A1
B	Site details	A10
C	ICP whole-rock analyses	A13
D	EPMA analyses	
	D.1 Carbonates	A23
	D.2 Iron-titanium oxides	A27
	D.3 Miscellaneous	A32
E	Ferrous iron determination	A33
F	Carboniferous sediments of the Kirkbean Outlier	A34

FIGURES

2.1. Upper Palaeozoic basins of the British Isles 11
2.2. Stratigraphy of the Orcadian Basin 17
2.3. ORS of the Orcadian Basin 18
2.4. Carbonates: stable and unstable phases 46
2.5. The $FeO-Fe_2O_3-TiO_2$ ternary system 49
2.6. Eh-pH diagrams, iron oxides/carbonates 51

3.1. Eday Lavas and Eday Flags: site locations 61
3.2. Eday Lavas and Eday Flags: detailed site locations 62
3.3. Eday Lavas: NRM directions 65
3.4. Eday Lavas: Koenigsberger ratios 66
3.5. Eday Lavas (type I): orthogonal projections 68
3.6. Eday Lavas: demagnetisation curves 69
3.7. Eday Lavas (type I): site means 71
3.8. Eday Lavas (type II): orthogonal projections 73
3.9. Eday Flags (beneath lavas): orthogonal projections 76
3.10. Eday Flags (beneath lavas): site means 78
3.11. Eday Flags: demagnetisation curves 79
3.12. Eday Lavas and Eday Flags: Hysteresis of NRM 80
3.13. Eday Flags (beneath lavas): bulk geochemical variation 85
3.14. Eday Flags (beneath lavas): combined mean directions 87

4.1. Site locations, southern part of basin 91
4.2. Lower ORS (Foyers): orthogonal projections 93
4.3. Lower and lower Middle ORS: stratigraphy 96
4.4. Lower ORS (Braemore): orthogonal projections 98
4.5. Sarclet area: location map 101
4.6. Sarclet area: orthogonal projections (SCR) 106
4.7. Sarclet area: orthogonal projections (MCR) 107
4.8. Sarclet area: Progressive demagnetisation (stereonets) 109
4.9. Sarclet area: stable component directions 111
4.10. Sarclet area: contoured stable component distribution 112
4.11. Sarclet area: site mean directions 115
4.12a Eday Group: location maps 118
4.12b Eday Group: site locations, northern islands 119
4.12c Eday Group: site locations, eastern Mainland 120
4.12d Eday Group: site locations, southern islands 121
4.13. Eday Group: schematic lithological variation 124
4.14. Eday Group: contoured stable component distribution 128
4.15. Eday Group: orthogonal projections (A+C components) 131
4.16. Eday Group: inclination ranges of stable components 133
4.17. Eday Group: orthogonal projections (A component) 136
4.18. Eday Group: site mean directions 137
4.19. Eday Group: orthogonal projections (B component) 140
4.20. Eday Group: orthogonal projections (C component) 142
4.21. Eday Group: hysteresis of NRM 147
4.22. Eday Group: Mean directions (A,B and C groups) 151
4.23. Upper ORS and Yesnaby Group: orthogonal projections 154

5.1. Lacustrine sediments: site locations 162
5.2. Achanarras Limestone: Orthogonal projections 173
5.3. Achanarras Limestone: Site mean directionses 176
5.4. Latheron Group: Orthogonal projections 179
5.5. Latheron Group: Stable component directions 180
5.6. Lacustrine sediments: hysteresis of NRM 181

6.1. Eday Group: ICP analyses (Fe and Al) 189
6.2. Magnetic stability and total iron content 190
6.3. X-ray spectra for secondary iron minerals 202
6.4. EPMA analyses of iron-titanium oxides: total analysis 204
6.5. EPMA analyses of iron-titanium oxides: FeO and TiO_2 206
6.6. Evolution of continental red beds 209
6.7. Carbonate compositions: (i) lacustrine sediments 212
6.8. Calcitised dolomite: line traverse 220
6.9. Carbonate compositions: (ii) Sarclet Group dolomites 227
6.10. Fresh dolomite: line traverse 228
6.11. Carbonate compositions: (iii) Calcite in clastics 233
6.12. Carbonate compositions: (iv) Yesnaby Sst dolomites 233
6.13. Alteration of biotite: digimap 240
6.14. X-ray spectra, silicate overgrowths 245

7.1. Dyke swarms of Scotland 265
7.2. Dyke occurrences in the Orcadian Basin 268
7.3. Dyke material: Koenigsberger Ratio 271
7.4. NRM intensity variation across dyke ROD07 272
7.5. Dyke material: NRM directions 274
7.6. Dyke material: progressive demagnetisation 275
7.7. Dyke margins (laminites): NRM variation with distance 280
7.8. Hysteresis of NRM, site ROD05 282
7.9. Dyke margins: progressive demagnetisation 284
7.10. Dyke margins: intensity profiles 285
7.11. Dyke margins (site ROD02): bulk geochemistry 288
7.12. ROD74: NRM variation with distance 292
7.13. ROD74: progressive demagnetisation (orthogonal 293
7.14. ROD74: progressive demagnetisation (stereographic) 295
7.15. ROD74: thermal profile 296
7.16. ROD74: bulk geochemistry variation 301
7.17. ROD74: intensity profile 302
7.18. Dyke margins: site mean directions 304
7.19. APWP with dyke directions 305

8.1. Intrusive igneous bodies of the Orcadian Basin 309
8.2. Duncansby Ness: site locations 310
8.3. The John o'Groats Sandstone 311
8.4. Duncansby Vent (matrix): progressive demagnetisation 316
8.5. Duncansby Vent: high-temperature directions 317
8.6. Duncansby Vent (xenoliths): prog. demagnetisation 319
8.7. Duncansby Vent: site mean directions 321
8.8. EPMA analyses of TiMt, Duncansby Vent 321
8.9. John o'Groats Sst.: progressive demagnetisation 327
8.10. John o'Groats Sst.: specimen component directions 330
8.11. Mean directions, Duncansby Ness area 331
8.12. Contact zone of vent: bulk geochemistry 331

9.1 Site mean directions, syngenetic remanence 341
9.2 Formation mean directions, syngenetic remanence 342
9.3 APWP with syngenetic remanence poles 346
9.4 Mean directions, secondary remanence 351
9.5 APWP with secondary and igneous poles 353

A.1 Hysteresis loop for an ideal ferromagnetic material A5
F.1 Carboniferous of the Kirkbean Outlier A36
F.2 Carboniferous: progressive demagnetisation A37
F.3 Carboniferous: site mean directions A38

TABLES

1.1.	Sampling and treatment summary	6
2.1.	Mean ICP analyses	21
2.2.	Great Glen Fault: lateral displacements	28
3.1.	Eday Lavas and Eday Flags: site details	60
3.2.	Previous work, Orcadian Basin volcanics	63
3.3.	Eday Lavas (type I): site means	70
3.4.	Eday Lavas (type II): site means	70
3.5.	Eday Flags (beneath lavas): susceptibility and NRM	75
3.6.	Eday Flags (beneath lavas): site means	75
3.7.	Eday Lavas and Eday Flags: IRM characteristics	82
3.8.	Mean directions: effect of tectonic correction	83
3.9.	Eday Lavas and Eday Flags: combined statistics	88
4.1.	Moray Firth and Southern Caithness: site means	94
4.2.	Sarclet area: sampling details	103
4.3.	Sarclet area: site means	108
4.4.	Sarclet area: rock magnetism	114
4.5.	Eday Group: sampling details	126
4.6.	Eday Group: multi-component remanence directions	130
4.7.	Eday Group: site means, A component	135
4.8.	Eday Group: site means, B component	139
4.9.	Eday Group: site means, C component	144
4.10.	Eday Group: grain size-magnetic reliability	145
4.11.	Eday Group: rock magnetic characteristics	148
4.12.	Upper ORS and Yesnaby Group: specimen components	156
4.13.	Chapter 4: summary	159
5.1.	Lacustrine sediments: Site details	166
5.2.	Lacustrine sediments: selected ICP analyses	168
5.3.	Lacustrine palaeomagnetism: previous studies	171
5.4.	Achanarras Limestone: anomalous directions	174
5.5.	Achanarras Limestone: Site means	175
5.6.	Lacustrine sediments: Rock magnetism summary	182
6.1.	Eday Group: ICP characteristics	187
6.2.	Iron oxide occurrence and age of remanence	208
6.3.	Remanence acquisition and magnetomineralogy	256
7.1.	Dykes: K-Ar age determinations	266
7.2.	Dykes and dyke margins: site details	269
7.3.	Dyke material: stable end points	276
7.4.	Dyke margins: site mean directions	283
7.5.	ROD74: whole-rock Fe analyses	300
8.1.	Permian vents: site details	313
8.2.	Duncansby Vent: site mean directions	315
8.3.	Duncansby Vent: IRM characteristics	322
8.4.	John o'Groats Sst.: site details	324
8.5.	John o'Groats Sst.: recalculated means	325
8.6.	John o'Groats Sst.: site mean directions	328
8.7.	Minor vents: site mean directions	336
8.8.	John o'Groats Sst.: remanence and deformation	337
9.1.	Primary ORS mean directions: summary	340
9.2.	Secondary mean directions: summary	349
9.3.	Intrusive igneous rocks: summary	355
F.1	Kirkbean Outlier: site mean directions	A35

PLATES

2.1.	Orcadian Basin: field characteristics I	12-13
2.2.	Orcadian Basin: field characteristics II	14-15
3.1.	Eday Lavas and Eday Flags	57-58
5.1.	Lacustrine sediments: field characteristics	163-164
6.1.	Detrital iron-titanium oxides	193-194
6.2.	Secondary iron-titanium oxides I	197-198
6.3.	Secondary iron-titanium oxides II	199-200
6.4.	Primary carbonates	213-214
6.5.	Calcitisation of dolomite (i) Lacustrine sediments	221-222
6.6.	Calcitisation of dolomite (ii) Element distributions	223-224
6.7.	Calcitisation of dolomite (iii) Clastic sediments	230-231
6.8.	Alteration of sheet silicates	237-238
6.9.	Silicate grain coatings	242-243
6.10.	Miscellaneous features	253-254

CHAPTER 1

INTRODUCTION

1.1. PREFACE

Palaeomagnetism of the 'Old Red Continent' has long been controversial, ever since the pioneering studies of Creer (1957), on sediments from Pembrokeshire, and Stubbs (1958) on lavas from the Midland Valley of Scotland. Palaeopole positions from these investigations, of latitude 40°N and 10°S respectively, have separately been proposed as representing the Devonian geomagnetic field with respect to Great Britain (the DI and DII poles of Creer & Embleton, 1967).

Later progressive demagnetisation of the Pembrokeshire sandstones demonstrated that their remanence was multi-component, with both DI and, at higher blocking temperatures, DII components; this suggests that they have been remagnetised (Chamalaun & Creer, 1964). DII was proposed as the best approximation to a primary Devonian palaeopole.

Palaeomagnetic results from elsewhere in eastern Laurentia-Baltica, generally from group DI, led Creer (1968) to suggest that much of the continent had been subjected to severe oxidative remagnetisation in the Permo-Carboniferous (since the DI pole greatly resembled demonstrably primary poles from Permo-Carboniferous rocks).

The picture was further complicated by the possible presence of a third primary magnetisation axis, largely reported from the Orcadian Basin by workers from Bergen University (Waage & Storetvedt, 1973; Storetvedt et al 1978; Storetvedt & Carmichael 1979; Storetvedt & Torsvik, 1983).

Such poles have since been largely discredited (van der Voo & Scotese, 1981) as they do not appear to be based on valid data.

The remagnetisation hypothesis discussed above was slowly accepted for much of western Europe, particularly Great Britain, but North America (which also gave almost exclusively DI poles), was not suspected of having been remagnetised. This led to the necessity of large-scale strike-slip movements between North America and Europe to account for the palaeopole discrepancy between the two continents (after correcting for the opening of the Atlantic). Examples include van der Voo & Scotese (1981), who proposed 2000 km displacement along the Great Glen Fault, and Briden et al (1984) who put the fault further west, in the Atlantic.

This discrepancy may largely have been resolved by the recent recognition that many of the formations in North America which were originally believed to carry a primary remanence only may also have been pervasively remagnetised (e.g. Irving & Strong, 1984a). The remagnetisation would thus appear to have affected almost all of the Laurentia-Baltica continent.

The precise nature of the remagnetisation process has not been comprehensively investigated. It generally involves the creation or remagnetisation of hematite and so has long been recognised as an oxidative process (Creer, 1968), although other investigations invoked a deep-burial thermal remagnetisation (Chamalaun & Creer, 1964). The conclusions of many later studies (e.g. Turner & Archer, 1975; Tarling et al, 1976; Roy & Morris, 1983) is summarised by Irving & Strong (1984a) who suggest that the depressed water table

level resulting from the 'unprecedented continentality' of Pangaea enabled remagnetisation to occur, whether it resulted from dehydration of ferric oxy-hydroxides, oxidation of magnetite, oxidation of biotite or any combination of these and several other possible causes.

The affinity of a number of possible microplates, such as Spitsbergen, Acadia, Avalonia and Scotland north of the Great Glen Fault, are not yet resolved. This may largely be because it is not easy to demonstrate the presence of a remagnetisation event in a restricted selection of facies as would be found on a small land mass.

The Orcadian Basin (a large internal basin of essentially continental sediments with occasional lavas) belongs to the fourth of these possible microplates, being separated from the remainder of NW Europe by the Great Glen Fault. There are a number of published palaeomagnetic studies of the basin, including Waage & Storetvedt (1973), Turner & Archer (1975), Tarling et al (1976), Turner (1977), Storetvedt & Carmichael (1979) and Storetvedt et al (1978). Palaeopoles from these studies have variously been interpreted as representing a primary or secondary remanence; no conclusions have been reached as to what does, in fact, represent the primary Devonian field direction with respect to the Orcadian Basin. A number of continental reconstructions have been proposed, based on comparing these studies with data from elsewhere (North America, Norway and southern Britain). These include Storetvedt (1974a), Turner et al (1976) and van der Voo & Scotese (1981).

It is the aim of this work to investigte the palaeomagnetic and diagenetic characteristics of sediments and lavas of the basin, particularly with regard to

suggesting a viable model for secondary remanence acquisition. This model will then be tested for applicability to the Laurentia-Baltica continent as a whole, and also used to re-assess previous work on the Orcadian Basin.

Any primary palaeomagnetic poles revealed during the course of the study will, despite being essentially a 'by-product' of the main investigation, be of immense importance in determining the continental affinity of the area. This is particularly important as very few, if any, reliable primary Devonian poles have previously been found from Britain north of the Great Glen Fault.

1.2. SAMPLING STRATEGY AND OBJECTIVES

Early sampling of sediments of the Orcadian Basin was largely aimed at investigating the palaeomagnetic and geochemical effects of Permo-Carboniferous dykes and vents on the surrounding sediments. This was initiated by the possibility that hydrothermal activity, instigated by these bodies, may have been a possible mechanism of remagnetisation. Samples were thus collected from the aureoles of a number of intrusions as well as from the intrusions themselves. Subsequent laboratory work showed the intrusions and the remagnetisation to be contemporaneous but not directly linked.

Further sampling was aimed firstly at identifying those facies which were likely to carry a stable ancient remanence. As wide a facies variation as could be found was sampled, from coarse conglomerates through reddened and unreddened sandstones and mudstones to basic lavas and their baked contacts. This inevitably produced a number of sites which did not, in fact, carry a stable or interpretable

remanence.

Those facies which gave the most useful information were studied in greater detail. These include the basal Lower ORS of Caithness, the most carbonate-rich lacustrine laminites of the Middle ORS and Eday Group sediments and lavas of the upper Middle ORS. Sampling is summarised in table 1.1. Individual site details may be found in appendix A.

1.3. STRUCTURE OF THESIS

Following brief review of the Old Red Sandstone in chapter two, the palaeomagnetism of the Eday Lavas will be found in chapter 3. A possible primary pole for the basin is derived from these and used, together with other factors, in the interpretation of the palaeomagnetism of clastic and lacustrine sediments in chapters 4 and 5. This will be followed by a detailed investigation of the origin and diagenesis of iron oxides in these sediments in chapter 6. Chapters 7 and 8 form a somewhat discrete study of the palaeomagnetism of Permo-Carboniferous intrusive bodies in the basin.

Pole positions derived in chapters 3,4,5,7 and 8 will be synthesised in chapter 9 and, where applicable, used to modify and assist in the interpretation of Upper Palaeozoic polar wander for Laurentia-Baltica.

1.4. EXPERIMENTAL TECHNIQUES

1.4.1. Palaeomagnetic techniques

In the majority of cases, cylindrical samples were drilled in the field using a standard 2.5 cm diameter drill bit. Specimens were oriented individually using a

Table 1.1.
Sampling & treatment summary.

Age	Subdivision			Chapter/ section	N_{si}	N_{sp}	Treatment								
							Thermal		AF		AF+				
							Pr	Cl	Pr	Cl	Th		Chem	None	
U. ORS	S. Basin			4.2	4	45	10	8	-	-	-		2	25	
	Caithness			4.6	7	56	46	-	2	-	-		4	4	
	Orkney			4.6	1	14	6	-	-	-	-		-	8	
UPPER M. ORS	EDAY GROUP	Sediments	Upper Eday Sst.	4.4,4.5	8	114	40	8	2	-	-		2	62	
			Eday Marls	4.4,4.5	8	100	49	-	5	-	-		2	44	
			Middle Eday Sst.	4.4,4.5	11	135	70	-	7	-	-		3	55	
			Eday Flags	3	3	26	8	-	-	-	-		-	18	
			Lower Eday Sst	4.4,4.5	15	183	53	14	4	-	-		3	109	
		Volcanics	Lavas	3	9	100	61	-	6	-	-		-	33	
			Contact zone	3	4	45	33	-	7	-	-		-	5	
	John o'Groats Group			8.3	5	64	38	-	1	-	3		-	22	
LOWER M. ORS	Lacustrine sediments	Fishbeds		5	10	93	57	-	34	2	-		-	-	
		Other		5	10	98	19	-	31	4	3		-	41	
	Clastic sediments			4.2,4.3	2	27	14	-	-	-	-		1	12	
L. ORS	S. Basin			4.2	4	43	31	-	6	-	-		2	4	
	Sarclet			4.3	8	85	63	-	3	1	2		-	13	
	Orkney			4.7	5	35	17	-	2	-	-		-	16	
U.CARB-TRIAS	Duncansby	Matrix		8.2	2	23	9	2	2	8	2		-	-	
		Xenoliths		8.2	3	31	8	3	-	-	8		-	12	
	Vent	Contact zone		8.3	1	15	13	-	2	-	-		-	-	
	Other vents			8.4	3	21	6	-	11	-	4		-	-	
	Dykes	Dyke material		7	4	40	32	-	8	-	-		-	-	
		Contact zones		7	9	105	78	-	6	20	1		-	-	
CARB.	Criffel			App.F	9	95	9	67	2	-	-		3	14	
	Totals				145	1593	770	102	141	35					
							872		176		23		25	497	

N_{si} = No. of sites
N_{sp} = No. of specimens

Pr: Progressive demagnetisation.
Cl: Thermal/AF single-step cleaning.
Chem: Chemical demagnetisation.

combination, where possible, of sun and magnetic compass. Ideally 5 to 8 cores were drilled at any one site, although occasionally fewer (particularly in a very hard or awkward exposure) or more may have been collected. Individual specimens for analysis (1 to 4 per sample) were cut to 2.3 cm height.

Where field drilling was impossible or impracticable, individually orientated block samples were taken, later drilled in the laboratory. These sites may occasionally also include field-drilled cores.

The remanence of some of the material collected during the first field season, and also all strongly-magnetised specimens, were measured on a Digico spinner magnetometer; weaker samples were measured on a CCL cryogenic magnetometer. The vast majority of specimens were progressively demagnetised, using either thermal or AF demagnetisation. Susceptibility changes were carefully monitored during thermal demagnetisation (for details of these methods see appendix A).

A small number of specimens was treated by the chemical demagnetisation technique, although this was largely found to be unsuccessful due to the tendency of carbonate cements to dissolve in acid, resulting in rapid specimen disintegration. Specimens which did not disintegrate tended to be of very low porosity/permeability and hence were not amenable to the method anyway.

Those specimens subjected to progresive demagnetisation were routinely plotted on cartesian co-ordinates (As, 1960); the application of this method to multi-component investigations is discussed by Zijderfeld (1967) and Dunlop (1979). The horizontal projection of a vector position is

shown as a solid symbol, with separate treatment steps being joined by a solid line. The vertical projection is shown as open symbols and dotted lines. In addition, directional data were plotted stereographically using an equal angle projection; solid (open) symbols represent the lower (upper) hemisphere respectively. Blocking temperature/coercivity spectra were also routinely constructed. All of the above graphical techniques use standard computer programs.

Individual components, apparent as straight-line segments on orthogonal projections, were identified and quantified using the linefind program of Kent et al (1983), which takes into account intrinsic measurement error as defined by Briden & Arthur (1981).

Conventional Fisher statistics (Fisher, 1953) were applied to component directions so derived, both at the site and higher levels as appropriate.

Routine rock magnetic methods used were susceptibility measurement and determination of hysteresis of NRM, both described in appendix A.

1.4.2. Other techniques

A variety of techniques were used during investigation of remanence acquisition; experimental details are given in appendix A. These include electron microscopy (both backscattered and secondary electron modes in addition to EPMA analysis), conventional microscopy, bulk analysis using the Inductively-Coupled Plasma spectroscopy (ICP) method, x-ray diffraction and 'wet chemical' ferrous iron determination.

1.5 PALAEOMAGNETIC UNITS

Both CGS and SI units are widely used in the

palaeomagnetic literature. Relationships between the two are described by Payne (1981) and Shive (1986).

In this thesis, SI units are used as far as possible, e.g. magnetic dipole moment per unit volume (M) in A/m and magnetic induction B in Tesla.

CHAPTER 2

GEOLOGICAL AND PALAEOMAGNETIC BACKGROUND

2.1. THE ORCADIAN BASIN

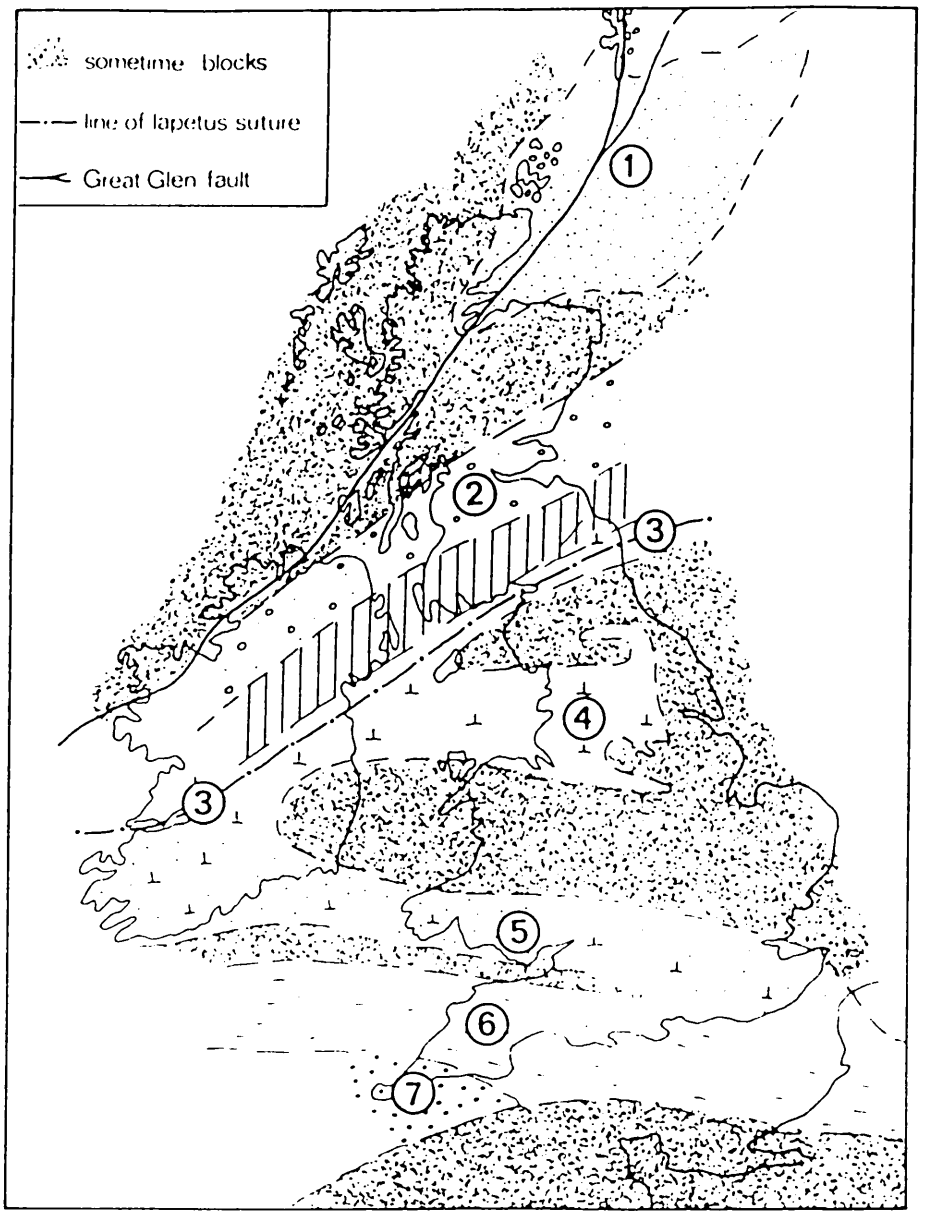
2.1.1. The Orcadian Basin in context

The Orcadian Basin is the northernmost of five or more major Old Red Sandstone (ORS) basins within the British Isles (fig. 2.1). These show a northerly progression from largely Hercynian control (e.g. South British and Rheno-Hercynian basins) to Caledonian control (e.g. Midland Valley and Orcadian Basins; Leeder, 1982). Relict Caledonian controls include the location of the Iapetus Suture and the positions of the Newer Granites (Thirlwall, 1981; Watson, 1984) whereas the Hercynian Orogeny played a somewhat different role (e.g. lithospheric stretching and back-arc spreading; Dewey, 1983).

Sedimentation was generally of continental facies, regardless of whether a basin was 'internal' (e.g. Orcadian Basin) or 'external' (e.g. Southern Britain; Anderton et al, 1979). Fluvial sedimentation in the Scottish basins was dominated by local drainage into enclosed basins within a stable block, whereas the southern basins were characterised by broad coastal alluvial plains.

2.1.2. Old Red Sandstone of the Orcadian Basin

The depositional history of the Orcadian Basin can be broadly subdivided into four main episodes. These comprise (i) the Lower ORS (immature fluvial sediments) (ii) the lower Middle ORS (lacustrine laminites) (iii) The upper



The major Upper Palaeozoic basinal areas of the British Isles, together with the location of (sometime) blocks, the Iapetus suture and Great Glen fault system. 1 - Orcadian (M-U O,R,S) basin; 2 - Midland Valley basin (M Silurian-U Carboniferous); 3 - Northumberland-Solway-Dublin-Limerick basins along line of the Iapetus suture; 4 - S Pennine basin and smaller basins; 5 - S Wales-S Ireland basin; 6 - Rheno-Hercynian zone of SW England-Belgium-Germany; 7 - S Cornish flysch trough (Gramscatho).

Fig. 2.1. The Orcadian Basin in relation to other major Upper Palaeozoic basins of the British Isles (after Leeder, 1982).

PLATE 2.1

ORCADIAN BASIN: FIELD CHARACTERISTICS (I)

(a) Middle Eday Sandstone (sites ROD16 and 17): interbedded sheet sands and overbank sandy mudstones. Water bottles 80cm high.

(b) Neptunian dyke (carbonate) intruding granitic basement. Yesnaby, Orkney (see also plate 2.2c). Lens cap 5cm.

(c) Conformable contact between lacustrine horizon and unreddened sandstone, near the boundary between the Rousay Flags and the Lower Eday Sandstone. Hammer 35cm.

(d) Yesnaby Sandstone, Mainland Orkney (sites ROD14-15). Contact with granitic basement.

(e) Upper ORS, Dunnet Head (sites RCD10 and 47). Reddened zone within an otherwise buff-drab sequence. Lens cap 5cm.

(f) Liesegang rings in the Upper ORS, site RCD13. Diameter of drilled cores 2.54cm.

(g,h) Post-depositional reddening in the Eday Marls, Eday (sites ROD53 and 54). Note general horizontal boundary between red and green sediment which is not directly related to bedding orientation. Hammer 35cm.

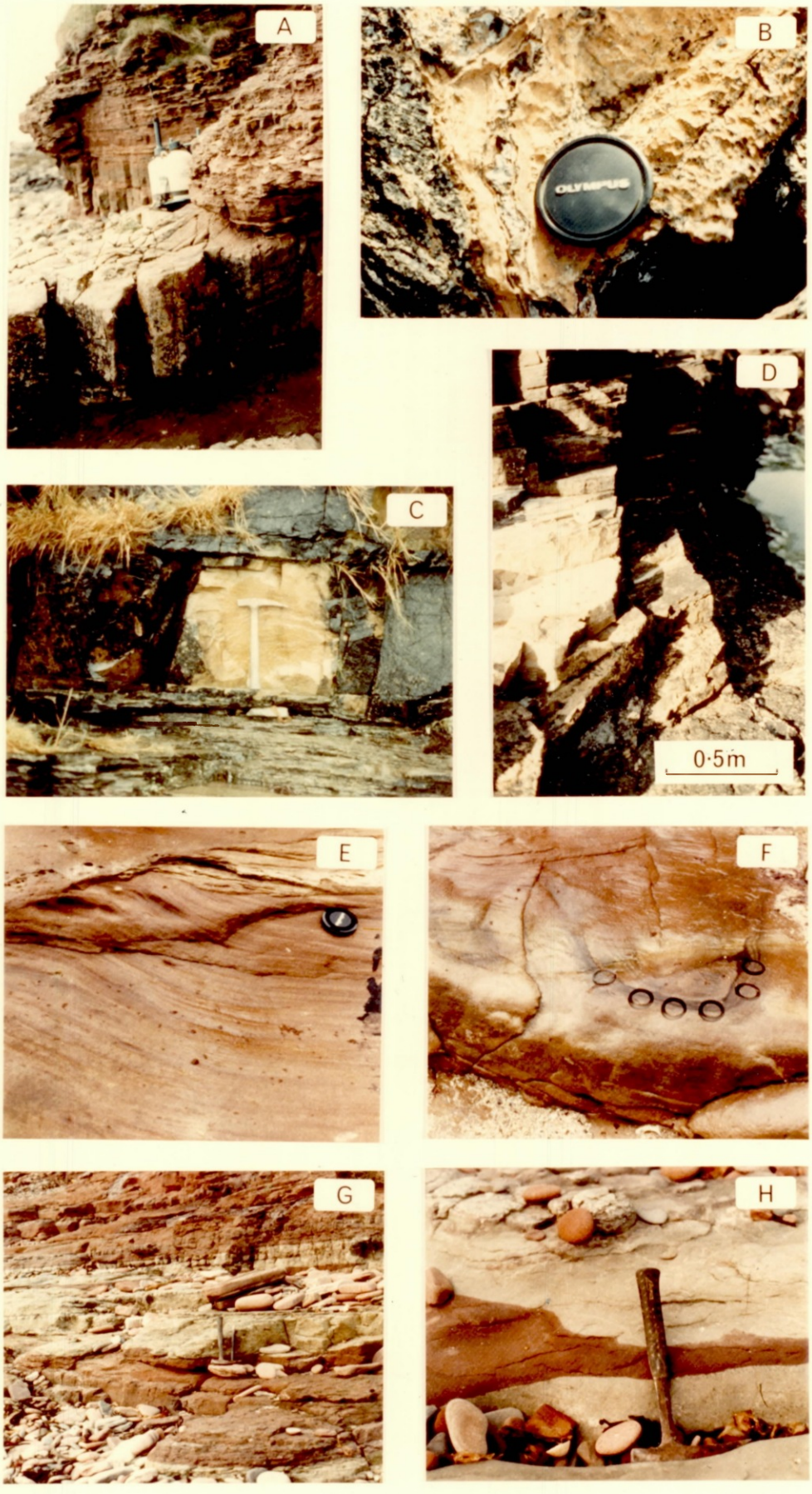


PLATE 2·1

PLATE 2.2
ORCADIAN BASIN: FIELD CHARACTERISTICS (II)

(a) RCD54; Upper ORS, Dornoch. Reddened mudstone rip-up clasts within fine-grained sandstone.

(b) ROD53-54; Middle Eday Sandstone, Eday. Boundary between reddened and unreddened (green) sandy mudstone.

(c) Section through neptunian dyke, intruding downwards into granitic basement. Yesnaby, Orkney.

(d) Pyritic pseudomorphs of evaporite (gypsum) needles. Basal ORS, Lothbeg, Sutherlandshire.

(e) ROD29; Niandt Limestone, Skaill. Bitumenous hydrocarbon accumulation. Lens cap 5cm.

(f) RCD03; Permo-Triassic vent, Duncansby Ness. Fine-grained matrix material with xenoliths of sandstone and mudstone. Engine width 50cm.

(g) RCD06; Monchiquite dyke intruded into Thurso Flags. Castletown, Caithness. Hammer 35cm.

(h) ROD03-06; Camptonite dyke intruded into Upper Stromness Flags. Note well-developed jointing, both in dyke and contact zone. Hammer 35cm.

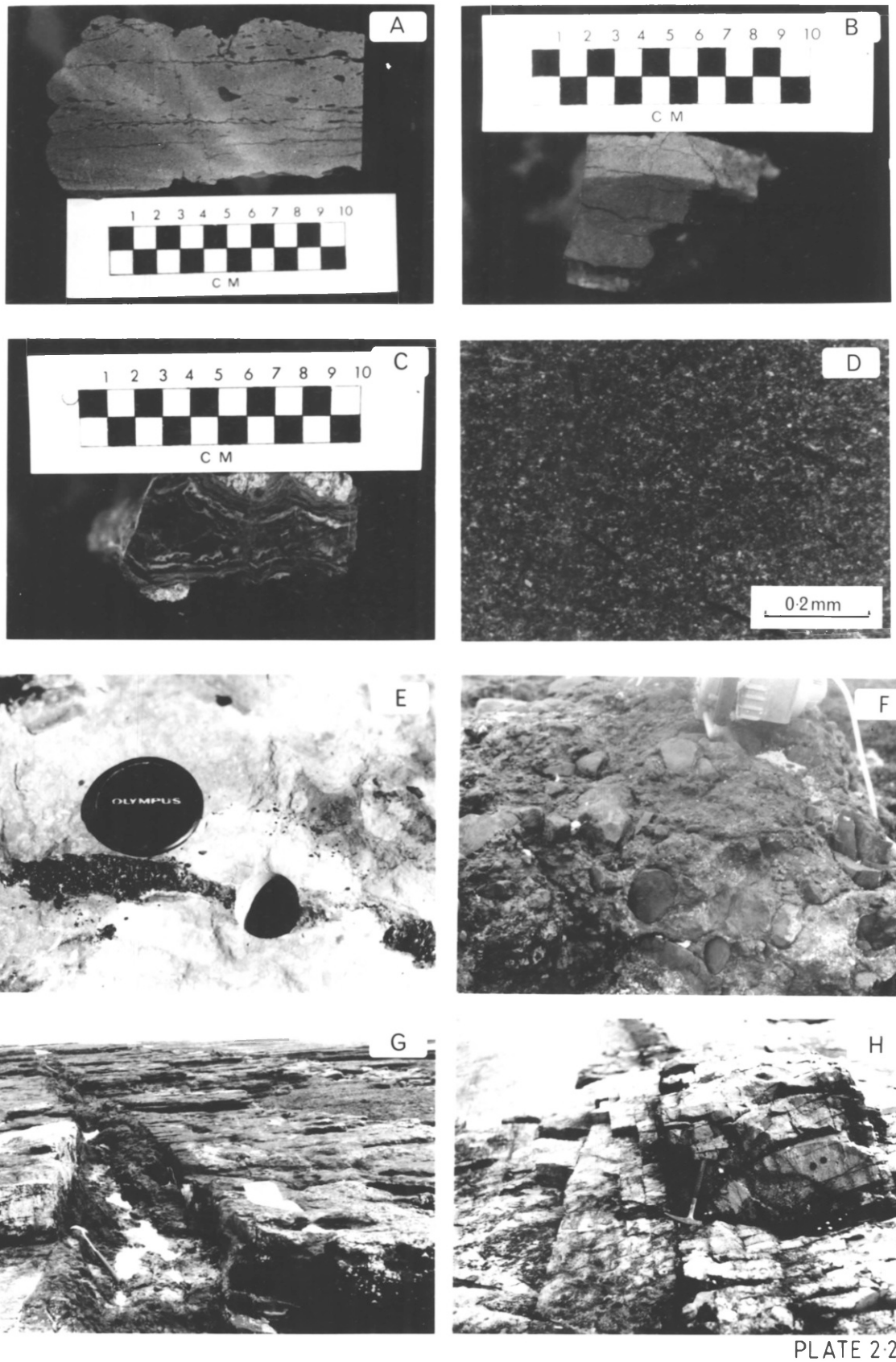

A
1 2 3 4 5 6 7 8 9 10
C M
B
1 2 3 4 5 6 7 8 9 10
C M
C
1 2 3 4 5 6 7 8 9 10
C M
D
0·2mm
E
OLYMPUS
F
G
H

PLATE 2·2

Middle ORS and (iv) the Upper ORS. The latter two subdivisions, separated by a major unconformity, mark a return to predominantly fluvial processes.

Stratigraphy of the basin is summarised in fig. 2.2; local details will be considered, where relevant, in later chapters. The main areas of Lower, Middle and Upper ORS sedimentation are shown in fig. 2.3. These will be discussed individually below.

(i) Lower ORS (sections 4.2.1; 4.3; 4.7). The basal Lower ORS consists of a breccia-conglomerate (e.g. Sarclet Conglomerate of Caithness and the Bochruben Formation of Loch Ness) or a coarse arkose (e.g. the Ousdale Arkose of southern Caithness). These are overlain by fine-grained purplish sands, silts and muds (e.g. Ousdale Mudstone, upper members of the Sarclet Group and the Foyers formation of Loch Ness). Lower ORS sediments are largely absent from northern Caithness and Orkney, with the Middle ORS being deposited directly onto the Caledonian basement; the exception is in the Yesnaby area of Orkney, where locally-derived talus-scree deposits blanket exposed basement outcrop (plate 2.1b,d). The sediments were deposited in a series of intermontane basins along the eastern margin of the Caledonian mountain chain, in alluvial fans, local river systems and small ephemeral lakes.

(ii) lower Middle ORS (chapter 5). The Middle ORS sometimes conformably overlies the Lower ORS (as in the Sarclet area) or it may follow a limited period of erosion and mild deformation. It consists of a basal conglomerate overlain by barren red flaggy sandstones, passing upwards into a great

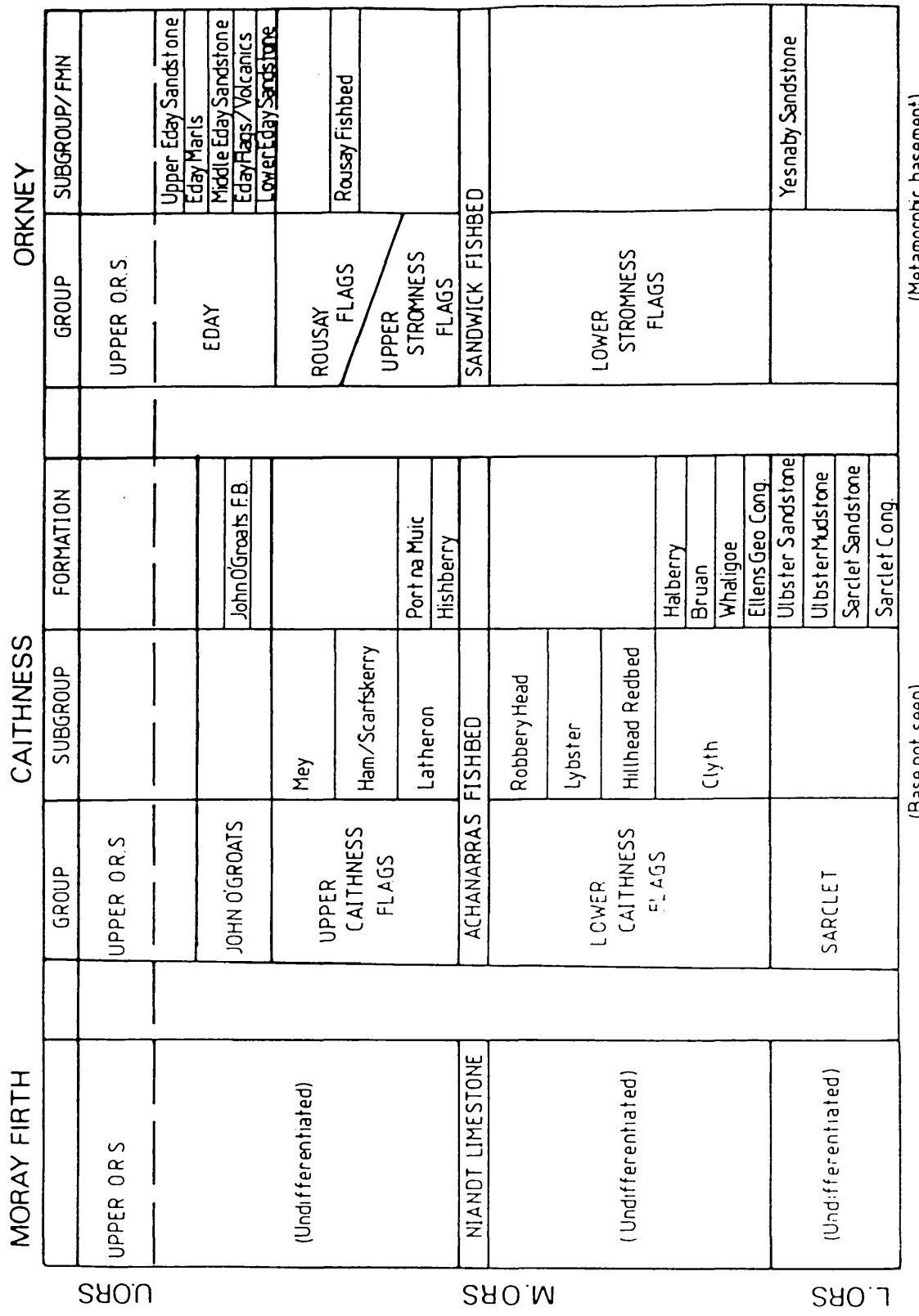


Fig. 2.2. Simplified stratigraphy of the Orcadian Basin. Largely based on Donovan et al (1974) and regional memoirs.

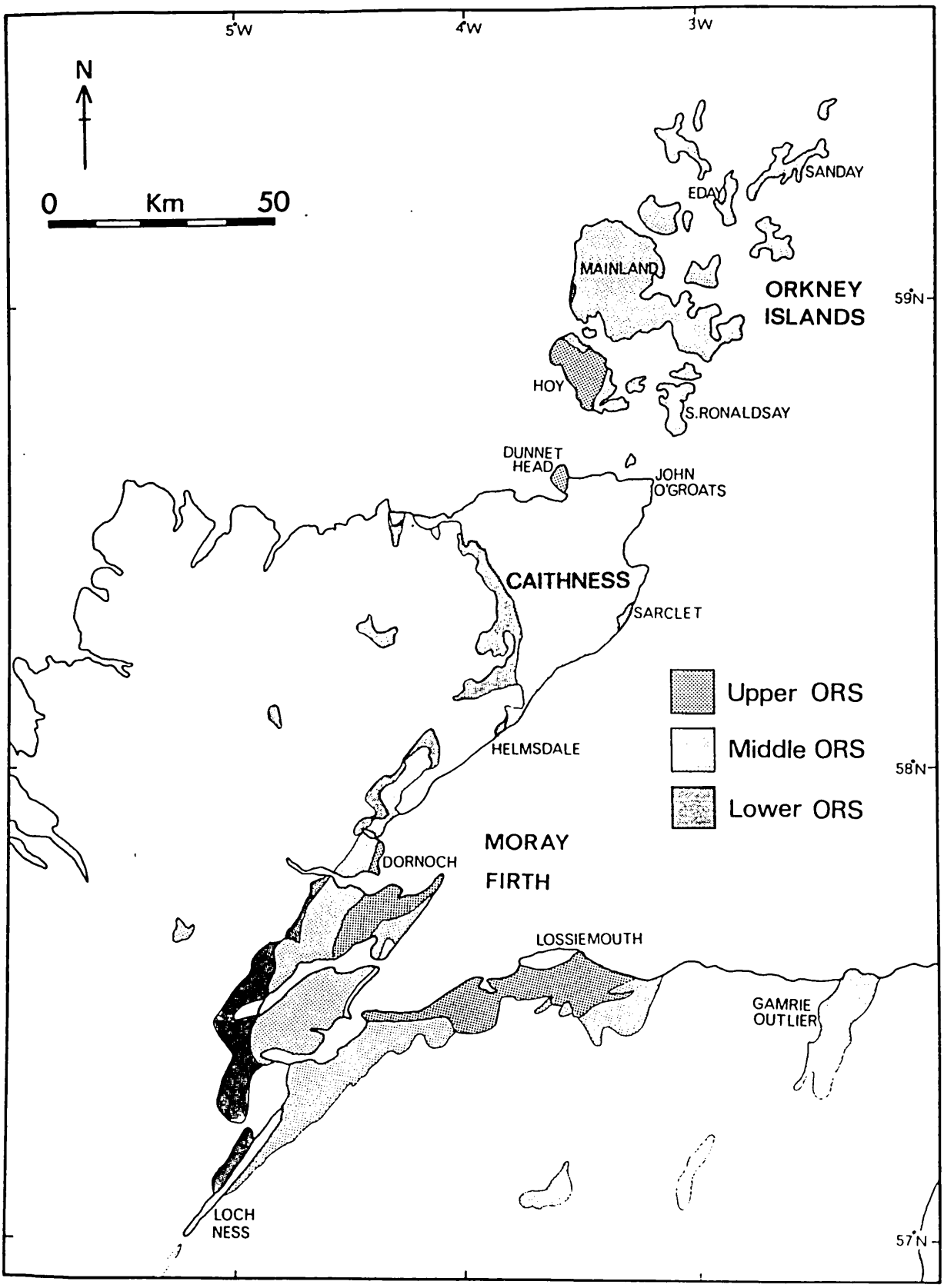


Fig. 2.3. Principal areas of Lower, Middle and Upper ORS in the Orcadian Basin (excluding Shetland). Based on IGS 1:625000 northern sheet. Note that some of the sediment south of Lossiemouth may be of Middle rather than Upper ORS age

thickness of uniform grey carbonate-rich flags (the Caithness Flags, Stromness Flags and equivalents; see chapter 5). These display a pronounced large-scale cyclicity, representing fluctuations in lake water level and the repeated silting-up of a large shallow lake. Occasional fluvial incursions occur (e.g. the Hillhead Redbed). Individual formations may be traced over great distances, suggesting that local faulting was of only limited significance.

(iii) upper Middle ORS (sections 4.4; 4.5; 8.3). The upper Middle ORS of Caithness and Orkney (the John o'Groats and Eday Groups) marks a pronounced change in depositional environment (plate 2.1c). Composed largely of fluvial sands and muds (plate 2.1a,g,h; 2.2b), they were deposited by rivers crossing the plain of the largely filled-in lake. Syn-sedimentary faulting played an important role, as evidenced by the lava flows within the Eday Flags (chapter 3). Short-lived lakes still sometimes formed as occasional lacustrine horizons (such as the John o'Groats Fishbed) may be found. The prevailing tectonic environment appears to have been somewhat similar to that of the Lower ORS; for example, the Eday Group appears to have been deposited in small sub-basins within a NE-SW trending graben (Ridgway, 1974) following a line of crustal weakness marked by later igneous activity (Watson, 1985).

(iv) Upper ORS (section 4.6). The Upper ORS (medium grained fluviatile sandstones, occasionally conglomeratic in the south; plate 2.1e, 2.2a) occurs chiefly in three isolated outcrops, whose stratigraphic relationship with underlying

sediments is usually obscure but presumably unconformable (House, 1977; McAlpine, 1978). Extensive lavas occur below the yellow (occasionally reddened) sandstone of Hoy.

2.1.3. Bulk analyses and source areas

Whole-rock ICP bulk analyses of many of the sediments studied have been made (method described in appendix A; results in appendix C). Aspects of these results will be referred to elsewhere in the text; taken as a whole they may provide an insight into sediment source areas.

Mean analyses for four main groupings of clastic sediment and for lacustrine laminites are given in table 2.1. These may be compared with global mean analyses for sandstones (Pettijohn, 1963). Most major elements are within a range of half to twice the global mean, with the exception of Na and K which are particularly depleted and enriched respectively. This is probably due to the relative geochemical instability of albite relative to orthoclase but may also provide some information regarding source areas.

Of the minor and trace elements, enrichments of V, Cr, Mo, Co and Ni and depletion in Cu may suggest a preponderance of basic rocks in the source areas, largely to the south and west. High Sr is probably associated with carbonates and La with organic matter.

2.1.4. Origin of the basin

The early evolution of the basin can thus be seen to adhere well to the model of McKenzie (1978); an early rifting phase with local sub-basins is followed by the progressive onlapping of the Middle ORS (the flexural

Table 2.1
Mean ICP analyses

	Caithness Lower ORS (n=10)	John o'Groats Sandstone (n=5)	Caithness M&U ORS (n=8)	Eday Group (n=40)	Lacustrine Laminites (n=12)
Na	0.4	0.2	0.1	0.2	0.3
K	3.4	1.9	2.1	2.4	2.3
Mg	1.1	1.0	0.6	1.3	2.8
Ca	1.2	1.3	2.4	0.6	4.4
Al	1.2	0.7	0.8	0.9	1.1
Ti	1.2	0.5	0.7	0.6	0.9
Fe	1.0	0.5	0.7	0.6	0.6
Li	0.7	1.1	1.3	1.7	2.4
Rb	1.4	0.9	1.2	1.0	1.2
Sr	3.5	2.9	4.3	3.1	13
Ba	2.5	1.7	2.2	2.2	2.1
La	28	16	19	18	23
V	3.5	1.3	2.3	2.4	5.3
Cr	4.2	1.1	2.1	1.6	4.2
Mo	10.0	26	21	5.5	25
Mn	1.6	0.8	2.4	0.6	1.4
Co	70	80	48	33	31
Ni	22	5.5	8.0	8.5	29
Cu	0.5	0.4	0.4	1.1	1.9
Ag	3.1	2.2	5.3	1.2	2.6
Zn	1.7	0.7	1.2	1.4	4.1
Cd	3.3	8.5	6.5	2.2	2.0
Pb	2.2	1.3	1.7	1.8	5.1
P	1.6	0.7	0.8	0.8	1.4

Analyses expressed as a proportion of a global average for sandstones (Pettijohn, 1963).

phase). However, there was a later period of reversion to active rifting towards the end of the Middle ORS and into the Upper ORS, particularly in Caithness and Orkney. This has been related to crustal updoming above a mantle 'hotspot' (as described by Bott, 1981), which could also be responsible for the upper Middle ORS igneous activity of Shetland and Orkney (Astin, 1982).

Such a straightforward analysis of the evolution of the basin may not be valid. An alternative model involves the reactivation of earlier faults related to Caledonian thrusting (Brewer & Smythe, 1984). Normal faulting along reactivated thrust planes could have allowed the accumulation of Devonian and younger sediments in the numerous half-graben structures seen in seismic sections.

2.1.5. Structure

Early discussion of the structure of the basin (Crampton & Carruthers 1914; Wilson et al 1935) regarded it as very simple, although detailed discussion is not given. Later work (Donovan et al 1974; Mykura 1976; Enfield, pers. comm.) shows that it is much more complex and that deformation was possibly of greater duration than previously recognised. Part of the reason for this is that many faults are low-angle thrusts, confined to certain horizons (e.g. sandstone bands within conglomerates or fish-bearing bedding planes within lacustrine laminites) which are not always easy to recognise in the field.

The main tectonic features throughout the basin are block faulting, low-angle thrust faulting, gentle open folding, strong joint development (especially within

lacustrine sediments) and occasional small-scale angular folding within some lithologies. The most important features (such as the Sarclet Anticline and Eday Syncline) are shown in figs. 4.5 and 4.12.

Analysis of the directional distribution of joints, fold axes, fault trends and dyke orientations (Donovan et al, 1974) suggests that most of these are the result of approximately E-W compression. This may be resolved into a dominant compression from the ESE and a local compression component from the SW.

In contrast to this, extensional tectonics appear to have operated throughout much of the depositional history of the area (although much of this may be due to wrench fault movements; Watson 1984). Some of the major faults were active during sedimentation, such as the North Scapa Fault, across which large sediment thickness variations can be seen (Mykura 1976, p9).

Such faults have often been reactivated during the later compressive phase of deformation which was responsible for most of the thrusting. A post-compressional phase of deformation resulted in normal faulting which may cut earlier thrusts (Enfield, Pers. Comm.).

The original memoirs (Crampton & Carruthers 1914; Wilson et al 1935) suggest a pre-Upper ORS age for deformation of the Middle ORS; a substantial thickness of sediment appears to have been removed during this interval. Other distinct deformation episodes seem to have occurred locally at the base of the Middle ORS and also possibly post-ORS.

The large-scale, open folding of the Middle ORS is, however, generally accepted as an early feature (Wilson et al 1935; Watson 1984), possibly related to late Caledonian movements which ceased entirely before the Upper ORS (Sutton, 1963 p257; Watson & Plant 1979).

Although material from a number of categories of structural feature has been sampled in the present study (e.g. syn-sedimentary folds, small-scale angular folds and large, open folds) it is only material from the last category which has given any reliable palaeomagnetic information. Most sites show only a low angle of dip (typically 10-20°) apart from a few sites in the Eday Syncline. In most cases the plunge of individual folds is not determinable, although it is generally low or non-existent. This is not of great significance palaeomagnetically; plunges as great as 40-50° do not materially affect palaeomagnetic declination if bed dip is less than 30-40° (MacDonald, 1980).

Possibly the most important and fundamental tectonic feature of the area is the Great Glen Fault, which has apparently undergone large-scale strike-slip (transcurrent) motion. This will be discussed in section 2.2.

2.1.6. Post-Devonian history of the basin

(a) Sedimentation.

Since the Devonian, N.E. Scotland has acted as a stable massif (Watson, 1985) with only limited erosion or deposition. The principal post-ORS features of the area will be outlined below.

Upper ORS and Carboniferous sediments are preserved to the north and west of the Orkney Islands, possibly in a large half-graben system (Bott & Watts, 1970) of which the Hoy and Dunnet Head outcrops of Upper ORS are the most easterly development. Elsewhere, post-ORS sediments are of only limited onshore outcrop in the Highlands. Thin Permo-Triassic sandstones along the coast south of the Great Glen Fault represent thicker deposits offshore in the Moray Firth (Sunderland, 1972), as proven by boreholes. These are overlain by Jurassic sands and shales, preserved onshore in a small faulted graben south of Helmsdale (Pickering, 1984).

In summary, there is no evidence for there ever having been substantial accumulations of post-ORS sediments on the main massif. It appears to have acted as a stable block, separating the rift systems of the North Sea and the Hebrides. There appears to be no increase in organic maturity with depth (Hillier & Marshall 1985) confirming that burial of the sediments has never been great.

(b) Magmatism. Onshore intrusive igneous activity in the Orcadian Basin is restricted to one period. During the Permo-Carboniferous, extensive dyke swarms formed over much of Northern Britain, together with associated vents. Orientation of the Orcadian swarm (the most northerly of nine) was controlled by deep dislocations in the upper crust or mantle (Rock, 1983; Baxter & Mitchell 1984). There is no direct geological evidence for the dykes having acted as feeders to the surface (Watson, 1985). Detailed geology and palaeomagnetism of dykes and vents are discussed in chapters 7 and 8 respectively (see plates 2.2f,g,h).

(c) Hydrocarbons. Much of the Lower and Middle ORS, particularly the lacustrine sediments, have a high organic carbon content (Plate 2.2e). Some of this has not migrated, but some undoubtedly has. Parnell (1981, 1985b) suggests that migrated hydrocarbon distribution is largely related to major fracture systems, and that migration could have occurred at any time between the Upper ORS and the Permian, possibly having been delayed until facilitated by secondary porosity generation and faulting in the Permian. Marshall et al (1985) suggest that the peak of hydrocarbon generation occurred fairly soon after deposition, at the time when maximum burial occurred.

(d) Sulphide mineralisation. As with hydrocarbons, much of the sulphide mineralisation in the basin is of syngenetic origin. Remobilisation occurred during the movement of pore fluids during sediment compaction (Muir & Ridgway, 1975) which presumably occurred at an early stage. Further local transfer took place in the vicinity of Permo-Carboniferous dykes (chapter 7).

(e) Diagenesis. Sediments in the Orcadian Basin have undergone numerous diagenetic reactions, of which a number are of immense importance palaeomagnetically. This will be considered in detail in chapter 6.

2.2. MAJOR TRANSCURRENT FAULTING

A number of major transcurrent faults transect Northern Britain; they have a dominant NE-SW trend. Of these, the Great Glen Fault (GGF) is perhaps the most important, although several of the others show lateral displacements of 5 to 10 km (Smith, 1977, fig.1). The GGF is marked by a

deeply-eroded linear valley which exposes a broad crush zone (with occasional mylonites) several hundred metres wide (Eyles & MacGregor 1952). Recognised as a major fault for a long time (for historical references see Smith 1977), numerous attempts have been made to quantify fault displacement, particularly in a lateral sense. No general concensus has yet been reached. One of the aims of the present study is to investigate the validity of these arguments, especially those based on palaeomagnetic correlation across the fault.

A representative selection of estimates of fault displacement are given in table 2.2. These are based largely on comparing one (or several) feature(s) on either side of the fault (such as location of igneous bodies, basement characteristics, palaeomagnetic pole position etc.) and resolving any discrepancy by transcurrent movement along the fault. As pointed out by Anon (1974) and Mykura (1975), most results have been used 'with equal facility to demonstrate dextral or sinistral movement of varying magnitudes'. Geological estimates suggest a maximum displacement of 160 km, although if net displacement was greater than about 200 km it would not be quantifiable as this is the total exposure length of the fault.

Serious objections can be raised to many of the published palaeomagnetic estimates of fault displacement, as these are either below the resolution of the method (e.g. Storetvedt 1974a) or based on unreliable data or invalid palaeomagnetic correlation (e.g. Van der Voo & Scotese 1981). This is summarised by Esang & Piper (1984b) who

Table 2.1

Great Glen Fault: estimates of lateral displacement.

Reference	Displacement km sense	Timing	Criteria used	Objections
Kennedy 1946	105 SIN	U.ORS-L.Carb.	Equivalence of Foyers & Strontian granites	Unequivalence of granites (Ahmad 1967; Munro 1973) Lack of extensive mylonites (Shand 1951)
Shand 1951	Small		Lack of mylonites	Lack of mylonites disproved (Eyles & MacGregor 1952)
Holgate 1969	134 SIN 30 DEX	L.-M. ORS Tertiary	Dist. of sediments Dist. of dykes	Bacon & Chesher 1975
Garson & Plant 1972	120 DEX 32 DEX	L.ORS U.Cret.	Basement characteristics	Speight & Mitchell 1979
Winchester 1973	160 SIN	Post L.ORS	Dist. of metamorphic zones	
Storetvedt 1974a,b;1975 Winchester 1974 Storetvedt 1977	>200 SIN 500 SIN	Late or post Devonian	Palaeomagnetism	Turner et al 1976; Mykura 1976; Donovan et al 1976; This study etc.
Bacon & Chesher 1975	Small	Mesozoic-Tert. only	Lack of faulting in younger rocks	Flinn 1975
Speight & Mitchell 1979	8 DEX	Post Permo-Carboniferous	Offset of dyke swarm	
Van der Voo & Scotese 1981,82	2000 SIN	Carboniferous	Palaeomagnetism	Invalidity of palaeomagnetic correlation etc. (Donovan & Meyerhoff 1982; Parnell 1982; Smith & Watson 1983; This study etc.)
Smith & Watson 1983	100-200 SIN	Pre-U.ORS	Correlation of basement & ORS sediments	
Esang & Piper 1984b	Indeterminate	Post-Caledonian	Palaeomagnetism of Caledonian Intrusives	

Abbreviations: SIN = Sinistral, DEX = Dextral, Dist. = Distribution, Cret. = Cretaceous, Tert. = Tertiary

Table 2.2. Great Glen Fault: Estimates of lateral displacement.

suggest that any realistic palaeomagnetic quantification of fault displacement is impossible due to intrinsic uncertainties in the method.

It has been suggested (e.g. Morris, 1976; Briden et al, 1984) that a major transcurrent fault system may be necessary to account for the dissimilarity of British and North American Palaeozoic polar wander paths; the GGF has often been selected for this role. However, it would now appear that such comparisons are invalid (Irving & Strong 1984a) due to the widespread Kiaman remagnetisation of North America currently being recognised (section 2.4.2); hence such major fault displacements may no longer be necessary. This will be discussed in greater depth in chapter 9.

2.3. THE OLD RED CONTINENT

The supercontinent of Pangaea was formed during the Carboniferous by the joining of three pre-existing continents, Gondwanaland (Antarctica, Australia, Africa and South America), Siberia and Laurentia-Baltica. The latter (the 'Old Red Continent') originally consisted of two smaller continents (or possibly more : Soper & Hutton, 1984; Barber, 1985.) on either side of the Iapetus suture, which closed during the Caledonian orogeny (Wilson, 1966; Phillips et al, 1976; Briden et al, 1984). Fragments of the resultant orogenic zone are now preserved on either side of the Atlantic (the Caledonides of Britain and Scandinavia and the Appalachians of North America).

Laurentia consisted of much of N. America, Northern Scotland, Greenland and parts of Spitsbergen. It collided with Baltica (Scandinavia, Western USSR and Britain south of

the Iapetus suture) during the Caledonian orogeny (Barker & Gayer, 1985) after which they acted as a single continent until the opening of the North Atlantic (Le Pichon et al, 1977).

The final major plate movement during the formation of Pangaea was the collision of Laurentia-Baltica with Gondwanaland during the Carboniferous, with related obduction of oceanic lithosphere (e.g. the Lizard complex). The resulting Hercynian Orogeny caused severe deformation south of the Hercynian Front (Anderton et al, 1979, chapter 12); this passes through southern Ireland, South Wales and Somerset and into Holland, Belgium and West Germany. It is covered by later sediments in much of S.E. England. The Pangaean 'supercontinent' was now at its maximum extent prior to breakup in the late Triassic.

The existence and approximate form of the larger continents referred to above is now generally accepted. Controversy exists, however, regarding (i) relative movements of the continents, particularly the North American craton and Western Europe and (ii) the affinities of several postulated microcontinents such as Spitsbergen, Acadia and Avalonia (including western and eastern Newfoundland respectively) and also Scotland north of the Great Glen Fault. This will be discussed briefly below and in more detail in chapter 9.

2.4. ORS PALAEOMAGNETISM OF LAURENTIA-BALTICA: A REVIEW

2.4.1. Great Britain

Despite the study of a number of discrete areas of ORS rocks within the British Isles, there are still no universally accepted primary pole positions, particularly

for the Middle and Upper ORS. The main reasons for this are uncertainties regarding palaeomagnetic correlation across possible large-scale strike-slip faults and the pervasive Permo-Carboniferous remagnetisation which has particularly affected sediments.

The palaeomagnetic poles most widely accepted as representing the Devonian geomagnetic field with respect to the British Isles are those obtained from lavas, particularly from the Midland Valley (Stubbs, 1958; Embleton, 1968; McMurry, 1970; Sallomy & Piper, 1973; Latham & Briden, 1975 and Torsvik, 1985b). These are all of Upper Silurian - Lower Devonian age. They give both normal and reversed directions, directed upwards to the NE or downwards to the SW. Their validity has been questioned by Storetvedt & Halvorsen (1967) and Storetvedt (1968a, 1970a,b and elsewhere) who suggested that laboratory treatment, particularly in the earlier studies, was inadequate. These objections do not appear to be valid.

Less extensive lavas of Middle or Upper ORS age occur in the Orcadian Basin. The earliest study (Storetvedt & Petersen, 1972) of the Eday Lavas uses unsatisfactory statistical treatment (see chapter 3). Further work by Morris et al (1973) gave a poorly-defined mean direction of more southerly declination but of similar inclination to the Midland Valley lavas. This has been confirmed by Robinson (1985 and this study). The laterally equivalent Esha Ness Ignimbrite of Shetland gives a more shallow, southerly, mean direction (Storetvedt & Torsvik, 1985); this may represent only a 'spot reading' which has not averaged the effects of

secular variation.

Recent re-investigation of the Hoy Lavas (Upper ORS) by Storervedt & Meland (1985) gave a direction of normal polarity but in good agreement with the upper Middle ORS lavas investigated by Robinson (1985 and this study). This is not, however, regarded by the original authors as representing a valid direction.

Large intrusive igneous bodies of Upper Silurian-Lower Devonian age (such as the Newer Granites) have been investigated by Briden (1970), Turnell (1982, 1985), Turnell & Briden (1983), Torsvik et al (1983) and Torsvik (1984, 1985a). While precise correlation with sediments and lavas is impossible, these studies tend to confirm the Lower Devonian pole position discussed above (see chapter 9).

Palaeomagnetic characteristics of British ORS sediments are much more controversial than those of igneous rocks. This has been apparent since the earliest investigations, due to the large palaeomagnetic differences between the NRM of ORS sediments of South Wales (Creer, 1957) and the Midland Valley lavas (Stubbs, 1958). This was resolved by progressive demagnetisation which revealed the presence of a low-T_B remagnetisation in the sediments. At higher temperatures, a component resembling that found by Stubbs (op. cit.) was found (Chamalaun, 1964; Chamalaun & Creer, 1964). These studies showed that the remagnetisation occurred while the sediments were partly folded, since inter-site precision was greatest after partial tilt correction. The authors suggest that the low-T_B remanence is a PTRM acquired during burial (although there is no

geological evidence for this). It is unlikely that remagnetisation of the Pembrokeshire ORS was directly related to deformation, as flat-lying sediments nearby are similarly remagnetised (Creer, 1957); hence the remagnetisation could equally well be a CRM acquired during a deformation hiatus. Such results are confirmed by McClelland Brown (1983) although the more complicated relationship between deformation and remanence acquisition suggested by the study does not appear to be justified due to the small sample size.

Later studies of other ORS sediments have generally shown that magnetic components fall into one or more of three main groupings. Sediments may occasionally show a remanence direction of comparably steep inclination to lavas of the Midland Valley but of variable, generally southerly, declination. This has been found at Jedburgh (Upper ORS; Nairn, 1960), the Gamrie Outlier (Lower ORS; Turner & Archer, 1975) and the Sarclet Sandstone (Storhaug & Storetvedt, 1985). Elsewhere, a southerly direction of low (positive) inclination has been proposed as representing the Devonian pole relative to Scotland (e.g. Waage & Storetvedt, 1973; Storetvedt & Carmichael, 1979; Storetvedt & Torsvik, 1983; all from the Orcadian Basin). Such directions are not rigorously derived. These and similar directions from a supposedly Devonian igneous body (the Duncansby Ness vent, reliably dated to Permo-Triassic; chapter 8) have been comprehensively discredited by Van der Voo & Scotese (1981) as well as being superceded by the present study.

The third category of palaeomagnetic direction is

grouped around a southerly, upwards mean. This has been found to be widespread in the Orcadian Basin (e.g. Tarling et al, 1976; Turner, 1977; Robinson, 1985). It may often be found in close association with directions from the first group (e.g. Turner & Archer, 1975 and this study). These directions have been proposed as representing a largely diagenetic remagnetisation, acquired in the late Carboniferous to early Triassic (the Kiaman reversed polarity period).

2.4.2. Laurentia-Baltica

The same basic controversy as discussed above for Great Britain also applies throughout much of Laurentia-Baltica, although this has been widely recognised only recently. The main reason for this may be the relative absence of rocks comparable to the Midland Vally lavas; most published studies are of sediments (which are now suspected of having been pervasively remagnetised).

The basic problem is illustrated by some formations which were originally considered to carry a primary remanence, but have been shown at a later date to have been remagnetised. An example from North America is the Catskill Formation (Upper Devonian), originally studied by Kent & Opdyke (1978) and van der Voo et al (1979) but shown by Miller & Kent (1985) to have been remagnetised, acquiring much of its remanence during folding. Similarly, the Onondaga Limestone of New York State has recently been shown to have been totally remagnetised in the Permian (Scotese et al, 1982; Kent, in press) despite the fact that it was originally suspected that it might carry a primary remanence

only (Graham, 1954; Kent, 1979). There do not appear to be any primary Devonian poles derived from N. America which can be shown conclusively not to have been at least partially remagnetised.

The Devonian of the remainder of Laurentia-Baltica has received much less attention than that of Great Britain and North America. The status of published results from Norway (Storetvedt & Gjellestad, 1966; Storetvedt et al, 1968; Lie et al, 1969) is highly uncertain, as shown by Smethurst (in prep). Remagnetisations may be very widespread. The same may apply to Spitsbergen (Storetvedt, 1972; Lovlie et al, 1984; Torsvik et al, 1985; Jelenska, 1985). It would also appear that much of the Devonian of France has been remagnetised (e.g. Edel & Coulon, 1984; Courtillot et al, 1985; Perroud et al, in press), as may much of Western USSR, although apparently primary directions have been able to survive here (Creer, 1968; McElhinny & Cowley, 1977, 1979).

2.5. POST-ORS PALAEOMAGNETISM

The post-Carboniferous polar wander path for Western Europe and North America is, on the whole, fairly well-defined and generally accepted (an exception being the Jurassic for which few results are available). Summaries may be found in McElhinny (1973); polar wander paths based on this and other publications will be used in chapter 9.

The Carboniferous, however, is not as straightforward, both in terms of global tectonics (particularly transcurrent fault movements in the N. Atlantic) and also regarding palaeopole positions relative to cratonic regions.

This second point is illustrated by the hypothesis of

rapid polar transitions during the Carboniferous (e.g. Turner & Tarling, 1975), suggested as an explanation for an apparent 20° inclination difference in rocks of comparable ages. An alternative explanation is that many early Carboniferous rocks have been affected by later (Kiaman) remagnetisation in a similar fashion to ORS sediments discussed above (Roy & Morris, 1983). This has been found in, for example, the Pendleside Limestone (Addison et al, 1985), the Mauch Chunk Formation of the Appalachians (Kent & Opdyke, 1985) and sandstones near Criffel (appendix F). Widespread Kiaman remagnetisation would also account for apparent strike-slip movements proposed on the basis of palaeomagnetic inclination differences (e.g. Kent & Opdyke, 1979 and Kent, 1982, since refuted by Irving & Strong, 1984a,b and 1985). British palaeomagnetic results are reviewed by Turner & Tarling (1975) and magnetostratigraphy by Palmer et al (1985).

2.6. THE KIAMAN REMAGNETISATION HYPOTHESIS

The possibility that Kiaman remagnetisation of Lower Palaeozoic (or even older) rocks may be a continent-wide phenomenon was first suggested by Chamalaun (1964) based on his work with Creer. Despite a general lack of acceptance at the time (e.g. van Hilten, 1965), it has gradually been recognised in more widespread, and lithologically variable, rocks, as discussed above.

Although explanations of the cause of the remagnetisation may vary greatly in detail, they generally suggest that it was oxidative in nature (with occasional

exceptions, such as possible thermoviscous remagnetisation of magnetite; Kent, in press). Creer (1968) suggested that it was a direct result of the continental configuration and position in the Permo-Carboniferous, and used this to explain why other continents (e.g. Siberia) were not similarly remagnetised.

Van der Voo & McCabe (1985), referring specifically to eastern USA, suggest that partial or complete Kiaman remagnetisations are the rule, rather than the exception. It appears from the above discussion that this may be a valid observation for the whole of the Laurentia-Baltica continent.

It is also interesting to note that Kiaman remagnetisations may be found in pre-Devonian rocks as varied as the Peerless Formation (Dubois et al, 1985; Cambrian), the Trenton Limestone (McCabe et al, 1984; Ordovician), the Builth Volcanics (Briden & Mullan, 1984; Ordovician), the St Georges Group limestones of Newfoundland (Deutsch & Prasad,1985; Ordovician) and the Red Mountain Formation (Perroud & van der Voo, 1984; Silurian) and many other studies (see chapter 9). It has, however, generally not been found in Pre-Cambrian rocks (Irving & Strong, 1985). This is presumably due to the fact that the majority of Pre-Cambrian rocks are crystalline basement of low porosity and permeability and hence not susceptible to diagenetic remagnetisation.

2.7. ACQUISITION OF A MAGNETIC REMANENCE

2.7.1. Introduction: NRM

The Natural Remanent Magnetisation (NRM) of a specimen

is the (vector) summation of all of its remanence components which were acquired by natural processes (as distinct from, for example, laboratory-induced remanence). The constituent component(s) may be acquired via one or several mechanisms, either during formation of the rock (cooling, deposition etc.) or at any stage in its history. Such mechanisms will be discussed briefly below; reference should be made to standard texts (e.g. Irving, 1964; Stacey & Bannerjee, 1974).

2.7.2. TRM-PTRM-VRM

Most established theories of thermoremanent magnetisation (TRM) are based on single-domain (s.d.) grains, when grain size is, by definition, equal to magnetic domain size. For such grains, Neel (1949) has shown that the relaxation time τ of a grain of volume V, saturation magnetisation J_S and intrinsic coercivity H_C is:

$$\tau = \left(\frac{1}{f}\right) \exp\left(\frac{V\ J_S H_C}{2\ k\ T}\right) \qquad \text{.....(1)}$$

where k = Boltzmann's constant
T = Absolute temperature
f = Frequency factor (approx. constant).

Hence for any s.d. grain

$$\ln(\tau) \propto V/T \qquad \text{.....(2)}$$

A grain of any given size will have a specific temperature, the Blocking Temperature (T_B) above which it will behave superparamagnetically and below which a remanence acquired during cooling in a unit applied field

will become 'blocked' for a specified time period (usually greater than the duration of the experiment).

$$\text{i.e.} \quad \frac{V J_S H_C}{2 k T} = \ln(f\tau) = C \quad \text{.....(3)}$$

where C is the blocking constant

Individual blocking temperatures for an assemblage of grains of identical composition in a unit field will thus be dependent only on grain size, being higher for larger grain sizes. This leads to the 'law of additivity of partial thermoremanent magnetisations (PTRM)', whereby the TRM at room temperature will always be equal to the summation of magnetisations acquired at higher temperatures.

The Curie Temperature (T_C) for a particular composition is defined as the temperature above which a ferro- or ferrimagnetic substance will behave paramagnetically.

A TRM may be acquired by any rock cooling from the highest T_B of any of the magnetic grains within the rock. Cooling from lower temperatures (as in cooling after contact matamorphism) will produce a PTRM.

It should be noted that T_B is highly dependent on time; from (3) it can be seen that heating a rock to temperature T_1 for time τ_1 will be equivalent to heating it to a temperature T_2 for time τ_2, i.e.

$$T_1 \ln(f\tau_1) = T_2 \ln(f\tau_2) \quad \text{.....(4)}$$

This is the basic explanation for acquisition of a Viscous Remanent Magnetisation (VRM); for example, a rock

kept at ambient surface temperatures for a long period of time in a steady field will become remagnetised with maximum T_B much higher than the ambient temperature. Such components, aligned with the Present Earth's Field (PEF) direction, may be found in the vast majority of rocks (the only exceptions being those which do not have mineral grains of sufficiently low T_B range).

This also shows that apparent (un)blocking temperatures revealed during progressive thermal demagnetisation will not be equivalent to actual temperatures reached during, for example, cooling. Conversion from one to the other would necessitate knowledge of the length of time for which the material in question was at elevated temperatures (Dodson & McClelland Brown, 1980; McClelland Brown, 1981).

The theories outlined above apply only to s.d. grains. Larger grains may be characterised by pseudo-single domain (p.s.d.) or multi-domain (m.d.) behaviour (Dunlop, 1983). Transitions between these occur at the following grain sizes (Dunlop, 1972b; Day, 1977):

	s.d.-p.s.d.	p.s.d.-m.d.
Hematite	0.15cm	-
Magnetite	0.05-0.1μ	-
Titanomagnetite	0.1-20μ	15-40μ

The theory of m.d. behaviour (Neel, 1950; Merrill, 1981) is not well understood, and the effects of differences with s.d. behaviour (which is more amenable to theoretical modelling) are not well known. It is suggested that such

problems are not of great importance in the present study (which largely concerns rocks which have been highly oxidised) although it would be in a palaeomagnetic study of, for example, contact metamorphism of magnetite-bearing rocks.

It should be noted in passing that large titanomagnetite grains are not necessarily multidomain, as they may be subdivided into numerous sub-regions by exsolution lamellae (Price, 1980); these may then fall within the s.d. or p.s.d. size range of magnetite, particularly if the inevitable sub-grain shape irregularity is taken into account.

2.7.3. DRM-PDRM

The only mechanism by which sediments may acquire a net remanence during deposition is by alignment of detrital magnetic particles with the ambient field during deposition (a Detrital Remanent Magnetisation or DRM; Verosub, 1977) or very shortly after deposition (Post-Depositional Remanent Magnetisation or PDRM; Payne & Verosub, 1982). The theory is discussed by Collinson (1965a), who suggests that grain alignment may be a very rapid process, not needing more than a few centimetres water depth.

A DRM will be most easily assumed by small (to reduce hydrostatic forces), strongly-magnetised, grains: these will often tend to be magnetite. A DRM may, however, occur in detrital hematite (Steiner, 1983; Tauxe & Kent, 1984).

Natural shape irregularities present in many grains will result in them becoming rotated out of magnetic alignment so that their long axes tend to become parallel or

sub-parallel to the depositional surface. This may cause the net remanence of a sediment to become of artificially shallower inclination than the ambient field. Such effects have been produced in the laboratory (King, 1955) but have not been conclusively shown to occur naturally.

2.7.4. CRM

The acquisition of a Chemical Remanent Magnetisation (CRM) involves the alteration of pre-existing minerals or the introduction of new magnetic material from outside. The theory of CRM is similar to that of TRM but with grain size, rather than temperature, as the variable. The relationship between blocking temperature τ and volume V is given in (2) above; with T constant,

$$\ln(\tau) \propto V \qquad \text{.....(4)}$$

There is thus a critical volume V_c through which a grain must grow to become blocked; beyond this, continued growth results in increased relaxation time (until m.d. behaviour occurs).

Mechanisms by which a CRM may be acquired are many and varied. They fall into one of two classes: (i) In situ alteration of a pre-existing magnetic mineral, e.g. oxidation of detrital magnetite or (ii) production of a magnetic mineral from a previously non-magnetic source (e.g. dedolomitisation of ferroan dolomite or serpentinisation of olivine). Mechanisms of CRM formation in redbeds and carbonates (the principal rock types studied here) will be

discussed in sections 2.8 and 2.9. CRM in other sediments or igneous rocks is beyond the scope of this study.

It should be noted in passing that a CRM aligned with the PEF is a frequent phenomenon, caused by recent oxidative weathering. If this produces hematite (rather than iron oxy-hydroxides) it may have very high T_B and may hence be the most thermally stable component present. This is contrary to the outdated belief that the most stable remanence is the oldest, and it devalues the concept of single-step 'cleaning' of NRM. Examples of both high- and low-T_B recent components are illustrated in chapter 4.

2.7.5. IRM (natural)

An Isothermal Remanent Magnetisation or IRM (Graham, 1961) is acquired at constant temperature by a material subjected to an applied direct field (generally strong). It will characteristically have low coercivity and high T_B (and hence may be readily distinguishable from TRM or CRM on the basis of response to thermal and AF demagnetisation). Lightning strikes, in which a strong field is imposed for a short time, will tend to produce an IRM, found particularly in material from exposed outcrop (hilltops, cliff edges etc.).

2.7.6. Spurious Magnetisations

A spurious or meaningless remanence, acquired during collection or treatment, may sometimes be difficult to detect. They may arise from (i) remagnetisation during

drilling; (ii) misorientation during collection or treatment or (iii) presence of an applied field during thermal or AF demagnetisation. Other additional causes may be suggested. Most may be reduced or eliminated by careful equipment design and operation.

2.8. PALAEOMAGNETISM OF CARBONATES

No pure carbonate minerals are able to carry a stable ancient remanence, as all are diamagnetic or paramagnetic at room temperature. Carbonate rocks, however, may often be of great palaeomagnetic interest, due either to a non-carbonate detrital remanence or to diagenetic alteration of iron-bearing carbonate minerals.

Many instances of carbonates carrying a primary or very early diagenetic remanence are documented; it is usually a DRM in magnetite (e.g. Perry, 1979; Hornafius, 1984). This is not an intrinsic property of carbonates as a comparable remanence could be acquired by other sediments under similar conditions. It will be susceptible to diagenetic alteration under similar circumstances to redbed sediments discussed below.

Iron-bearing carbonate minerals include siderite, $FeCO_3$, the calcite-siderite system $(Ca,Fe)CO_3$ and the ferroan dolomite-ankerite system $Ca(Fe,Mg,Mn)(CO_3)_2$. Diagenetic alteration of these often results in the formation of iron oxides or oxyhydroxides; under suitable conditions these may acquire a palaeomagnetic remanence.

Principal among such processes are straightforward dissolution, particularly of ferroan calcite, and the dedolomitisation of ferroan dolomite-ankerite. In the latter

process, iron and magnesium carbonates are replaced by calcium carbonate. Large amounts of iron are incompatible with the calcite crystal lattice due to ionic radius contrast; iron will thus tend to be released into the system during calcitisation. As it is less soluble than the magnesium ion it will often tend to stay in close proximity to its original location.

Dedolomitisation textures are widespread in the Orcadian Basin, particularly in the carbonate-rich lacustrine horizons. Detailed mineralogy and geochemistry of the dedolomitisation process will be discussed in chapter 6 in conjunction with palaeomagnetic evidence that it occurred during the Kiaman reversed polarity interval.

Dedolomitisation has recently been established as a viable method of delayed remanence acquisition in carbonates (Elmore et al, 1985). Carbonate rocks have often been reported as showing remagnetisation (Turner et al, 1979; McCabe et al, 1983; Addison et al, 1985; Courtillot et al, 1985; Deutsch & Prasad, 1985; Elmore & Loucks, 1985; Salmon et al, 1985; Kent, in press). Within North America, van der Voo & McCabe (1985) suggest that carbonates are more susceptible than other lithologies to remagnetisation. It is interesting to speculate whether much of this is due to diagenesis of iron-bearing carbonates.

The dedolomitisation process is greatly enhanced by a high concentration of calcium ions (fig. 2.4), low Pco_2 and low temperature (Garrels & Christ, 1965; Evamy, 1967; Back et al 1983). It has usually been interpreted as a recent phenomenon (e.g. Al-Hashimi & Hemingway, 1973) and hence not

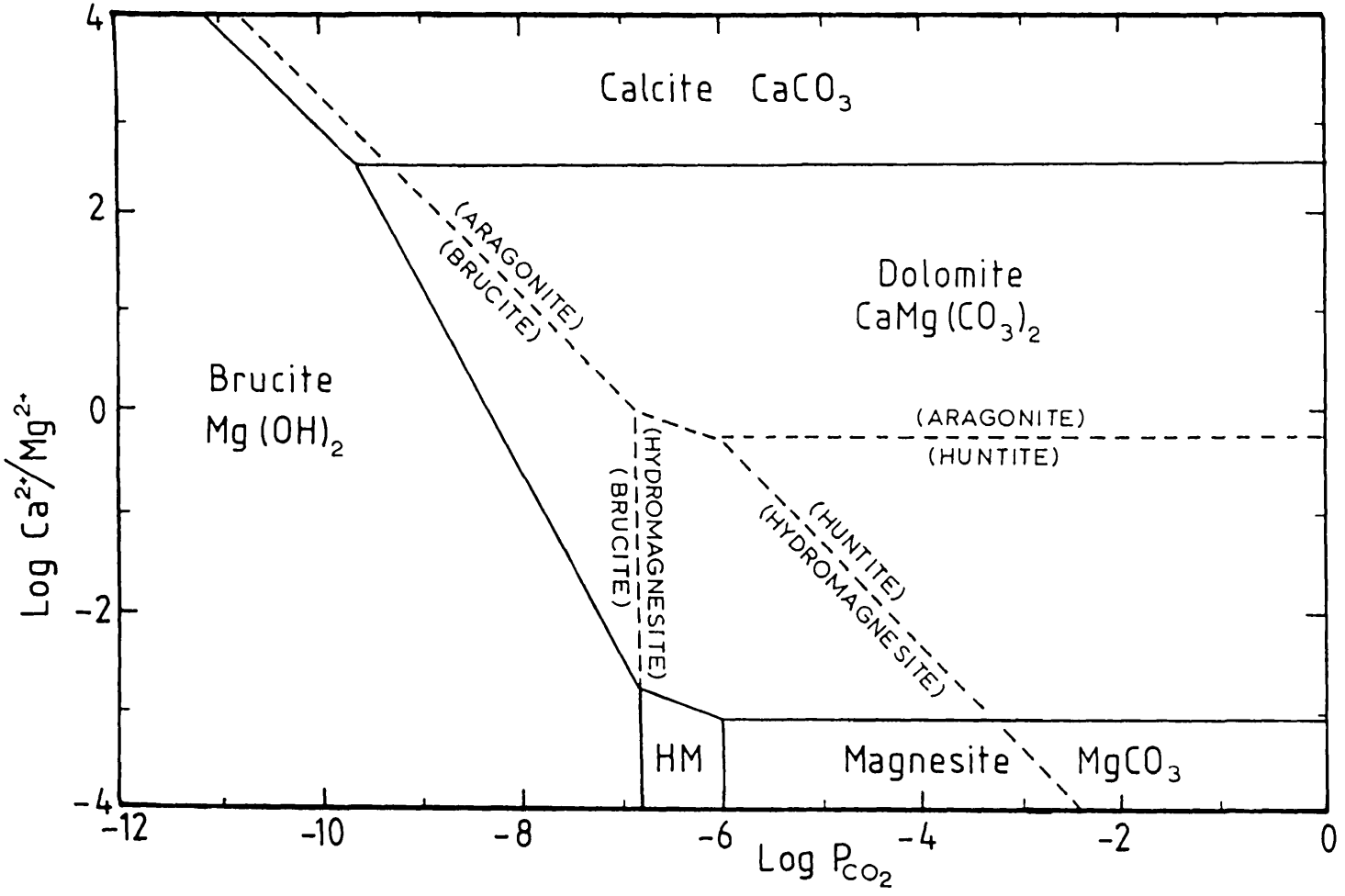


Fig. 2.4. Relationships of calcium and magnesium carbonates at 25° C and 1 atm. pressure, as a function of Pco_2 and Ca/Mg ionic ratio. Stable phases in bold/solid, unstable light/dashed. HM = hydromagnesite. (After Garrels & Christ, 1965, fig. 10.18).

a viable mechanism for the production of an ancient yet secondary remanence. This need not necessarily be the case; it is suggested in chapter 6 that suitable conditions existed during the Permian and early Triassic for the reaction to occur.

2.9. PALAEOMAGNETISM OF REDBEDS

As outlined above, the chief mechanisms by which a sediment may acquire a stable magnetic remanence are by alignment of detrital magnetic grains with the ambient field (DRM-PDRM) or by later diagenetic alteration or production of magnetic phases (CRM). The relative contributions of these two processes may vary widely from one sediment to another, although CRM acquisition is generally considered to be by far the more important process.

Some of the various mechanisms of remanence acquisition in redbeds will be discussed briefly below. General reference should be made to van Houten (1968, 1973) and Turner (1979, 1980).

(i) Detrital iron-titanium grains.

Detrital iron oxide grains are without doubt a major constituent of most redbeds. They may often be shown to be responsible for carrying much or all of the magnetic remanence in a sediment.

The majority of such grains are specularite (α-Fe_2O_3). Many authors have suggested that they carry a DRM (e.g. Roy & Park 1972; Collinson, 1974; Tauxe & Kent, 1984), the grains having been oxidised prior to or during transportation (Steiner, 1983). This need not necessarily be the case.

These grains can often be shown on textural evidence to have been diagenetically oxidised (van Houten, 1968; Reynolds, 1982). They may originally have carried a DRM but this has since been replaced by a hematitic CRM.

Diagenetic oxidation of magnetite need not be total, as demonstrated by a recent study of the Torridonian Sandstone (Robinson & McClelland Brown, in prep.). Although most sites show a single ancient remanence carried in hematite, some show a more complex remanence with a low-T_B component of opposite polarity to a higher-T_B one. That the lower-T_B one is carried in magnetite is suggested by its maximum T_B (575-585^{o}C); the presence of magnetite is confirmed by Parry (1957) on the basis of rock magnetic properties. Oxidation of detrital magnetite must thus have occurred a significant time (at least one field reversal) after deposition.

A typical martitisation texture is exsolution lamellae (of hematite, ilmenite or rutile) within an oxide grain; examples are illustrated in chapter 6. The martitisation process is described by Readman & O'Reilly (1972) and O'Reilly (1984). Observable magnetic characteristics are decreases in NRM intensity and susceptibility and a rise in Curie Temperature. Partial oxidation may result in cation-deficient (titano)maghemites (Gallagher et al, 1968; Readman & O'Reilly, 1972). This will usually be evident during thermal demagnetisation as a decrease in susceptibility at 350-400^{o}C due to the inversion of maghemite to hematite.

Oxidation without exsolution or removal of TiO_2 will proceed along lines of equal Ti-Fe ratio, as illustrated in fig. 2.5.

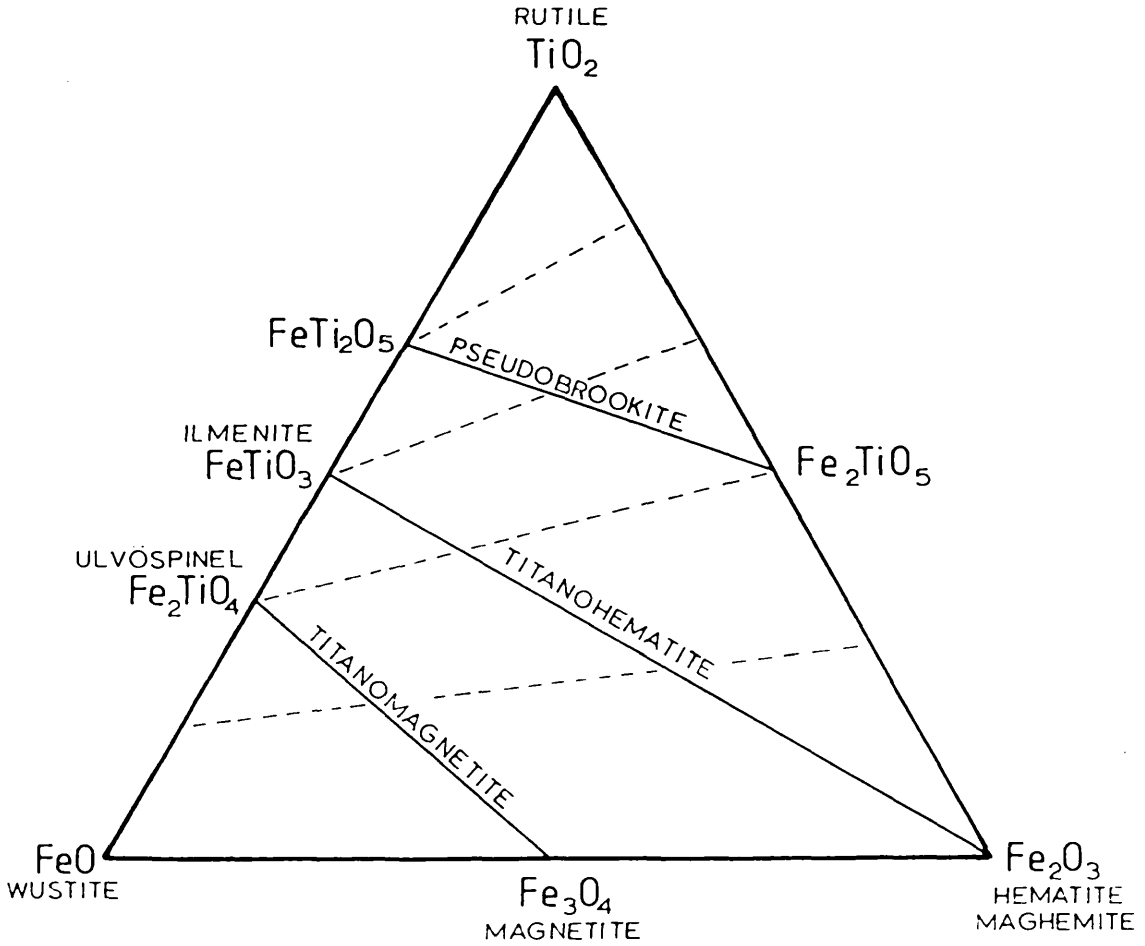


Fig. 2.5. The FeO-Fe_2O_3-TiO_2 ternary system. Dashed lines are of equal Fe-Ti ratio (modified after Turner, 1980, fig. 6.1).

(ii) Diagenesis of iron oxyhydroxides.

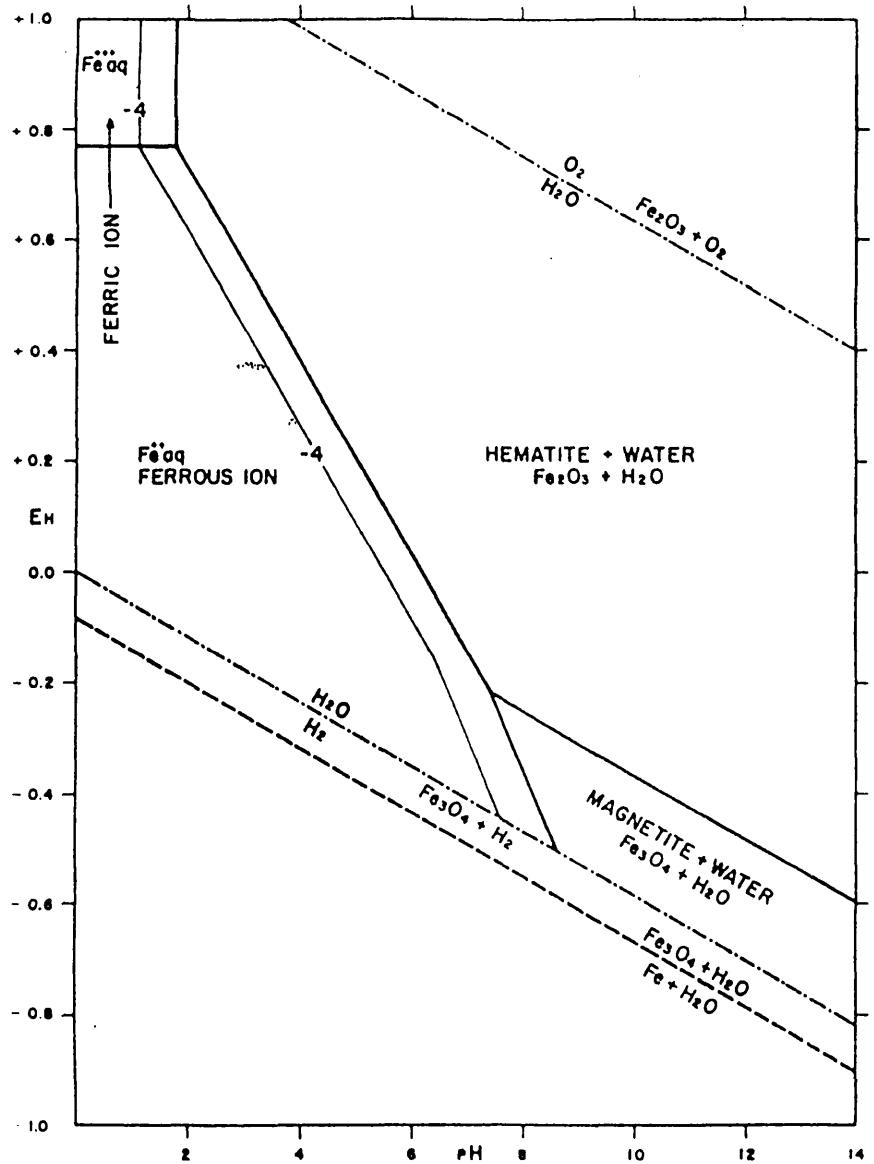
There are a wide variety of naturally-occurring oxyhydroxides of iron, of which the most important are goethite, lepidocrocite, amorphous FeO.OH and limonite ($FeO.OH.nH_2O$); Brown, (1961). They are a frequent component of the detrital clay fraction in recent, and hence by inference ancient, redbeds. They may also form diagenetically during the breakdown of ferromagnesian minerals.

The 'ageing' of iron oxyhydroxides to hematite has long been considered as an integral part of redbed formation (e.g. van Houten, 1968, 1973). Limonitic goethite, for example, has been shown by Berner (1969) to be thermodynamically unstable relative to hematite and water under most geological conditions. Eh-pH stability fields for iron oxides, oxyhydroxides and carbonates are illustrated in fig. 2.6. These show that the hot, dry conditions once considered necessary for dehydration, and which led to the widespread use of redbeds as a palaeoclimatic indicator, are not a prerequisite for the reaction.

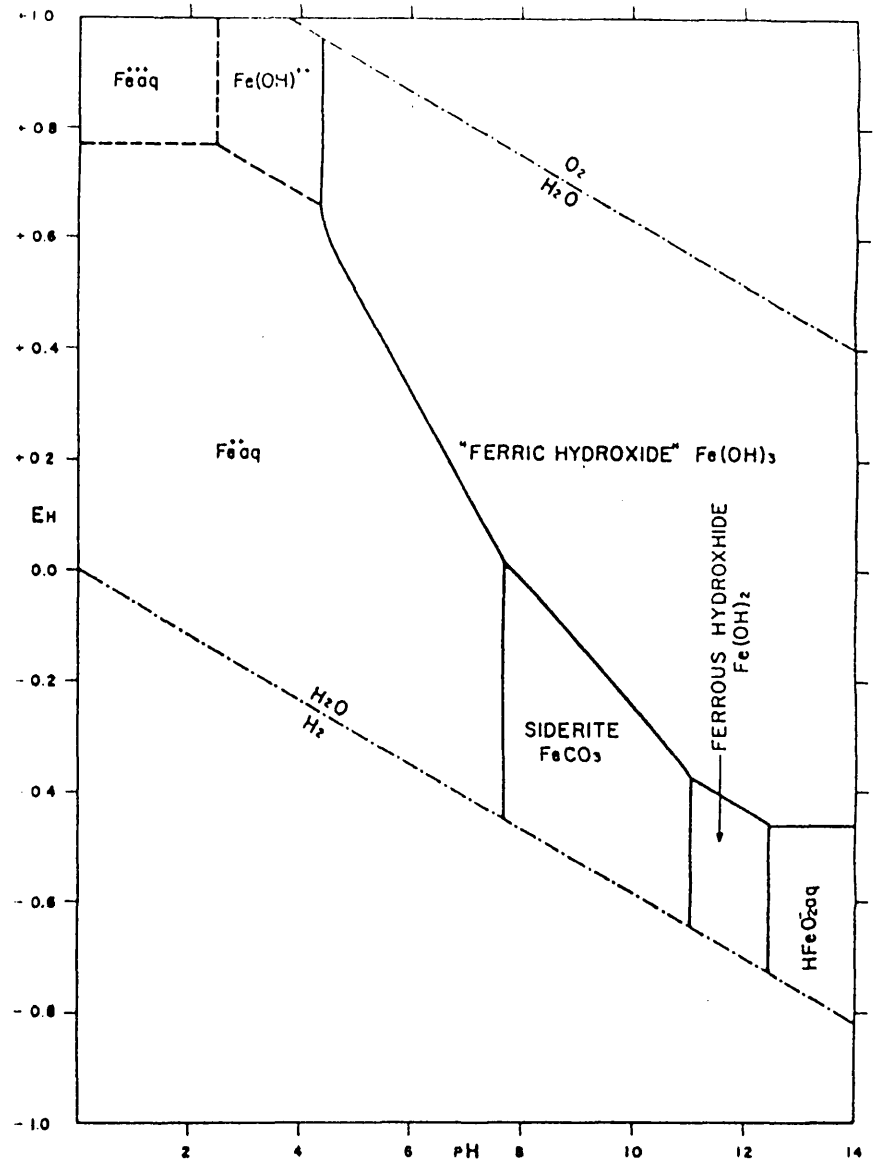
Whether the hematite so formed carries a stable remanence is a separate question, dependent largely on the grain size of the resulting oxide. Even though hematite has a very low 'critical diameter' (probably less than 1μ, below which it is superparamagnetic), clay-fraction hematite may easily be of finer grain size than this (see section 6.6).

The relative role of pigment in the NRM of redbeds has been extensively discussed. Early assumptions that it played a dominant role have been largely disproved by, for example, Collinson, (1974), Turner & Archer, (1975) and Turner & Ixer,

Fig. 2-6. Eh-pH diagrams for iron oxide-carbonate species under various conditions. After Garrels & Christ (1965) figs. 7-6 and 7-14.



A Composite diagram showing stability fields of hematite and magnetite in water. Fields of ions are designated where total activity of dissolved species are $> 10^{-6}$. Fields of ions are labeled with dominant species. Contour of log [dissolved species] = −4 is included to show slope of activity change. Plot at 25 °C and 1 atmosphere total pressure.



B Diagram showing the relations among the metastable iron hydroxides and siderite at 25 °C and 1 atmosphere total pressure. Boundary between solids and ions at total activity of dissolved species = 10^{-6}. Total dissolved carbonate species = 10^{-2}. Dashed lines are boundaries between fields dominated by the labeled ion.

(1977), who showed that specularite carried the bulk of the stable remanence. Pigment magnetisation was of relatively low T_B range. Exceptions may be found, in cases where, for instance, the growth of hematite has been of long duration allowing the formation of larger grains.

(iii) Silicate alteration and pseudomorphism.

Many detrital silicate/ferromagnesian minerals are chemically unstable in some or all of the transport-deposition-diagenesis system. Replacement, alteration or dissolution often occur.

If iron oxides or oxyhydroxides are produced then the reaction will be of significance palaeomagnetically. A good example illustrating the possible complexity of such processes is the breakdown of detrital mica, particularly biotite (the trioctohedral micas being more unstable in oxidising conditions than dioctohedral ones). This is discussed by Turner (1980).

Potassium is generally lost, often accompanied by vermiculisation. Other changes may involve replacement of hydroxyl ions by oxygen and the loss of octohedral iron, which can often be seen forming flakes of iron oxide within cleavage planes of the mica. An oxyhydroxide intermediary may be involved (Farmer et al, 1971) which will be susceptible to similar alteration processes to those described above. Under suitable conditions, a magnetic remanence can be acquired.

The exsolution process could occur at any stage of the history of the biotite, either before or during weathering, transport, deposition or diagenesis. Iron-rich haloes

surrounding partially-oxidised biotite (e.g. Walker et al, 1978) are conclusive proof that *in situ* oxidation has occurred. Pre-depositional oxidation could account for the lack of such haloes elsewhere (e.g. Turner & Archer, 1977; Wilson & Duthie, 1981). Perhaps the most sensitive method for assessing the relative ages of deposition and biotite oxidation is palaeomagnetism; this will be discussed further in section 6.5.

The alteration of other ferromagnesian minerals such as hornblende and pyroxene (e.g. Walker et al, 1967), will generally occur rapidly during diagenesis. The resulting dissolved ions may act as an important source of iron, which may later acquire a CRM.

(iv) Cement diagenesis.

Many redbeds are cemented by carbonates. If these are iron-bearing, they may acquire a diagenetic remanence in a similar way to carbonate sediments described in section 2.7. Examples will be discussed in chapter 6.

CHAPTER 3

THE EDAY LAVAS AND EDAY FLAGS

3.1 INTRODUCTION

Within the sediments of the Orcadian Basin, whose palaeomagnetic characteristics are the chief topic of study in this work, are a number of interbedded contemporaneous volcanic horizons of limited geographical extent, chiefly of upper Middle ORS age. The main object of studying these lavas palaeomagnetically is to try to obtain an irrefutable primary Middle ORS palaeopole for Scotland north of the Great Glen Fault with which to compare poles derived from sediments, as discussed in more detail in the previous chapter.

Due largely to their relative accessibility, the only lavas to have been investigated in this study are the Eday Lavas, which have been sampled throughout their geographical range. In addition, data from a number of sites in the Eday Flags immediately above and below are reported since their stable remanence appears to be contemporaneous with that of the lavas and possibly dependent upon them.

3.2 GEOLOGY

3.2.1. Contemporaneous volcanic rocks of the Orcadian Basin

Volcanic rocks of Middle ORS age are widely distributed in Shetland (Mykura, 1976), with a wide range of lithology including basic and acid tuffs and agglomerates, rhyolites, andesites, basalts and ignimbrites. They are much less common in Orkney (Wilson et al, 1935), being restricted to the basal Upper ORS of Hoy , (dated to 376 $\pm$ 8 Ma; Halliday et al, 1977), and within the Eday Flags

of the southern Orkney Islands (Kellock, 1969), both of which are alkaline in nature and bear a strong resemblance to the Carboniferous teschenites and basanites of the Midland Valley (MacGregor & MacGregor, 1948).

The onset of volcanism appears to be associated with a severe change in depositional environment. For example, the Eday Lavas occur at the same time as the rapid change from the prolonged low energy, slow deposition of the fine-grained Rousay Flags to immature clastic sandstones of the lower Eday Group (plate 2.1c); this possibly results from syn-sedimentary fault movement. The Hoy volcanics follow a period of folding and faulting at the end of the Middle ORS.

Astin (1982) has argued that the distribution of Middle ORS volcanism in the Orcadian Basin defines a thermal high, aligned approximately N-S and centered on the large plutons of West Shetland. The extent of surface volcanicity decreases to the north and south of this centre, with the Eday Lavas representing the southern limit.

3.2.2. The Eday Lavas

The presence of extrusive volcanic rocks in the Orkney Islands has been recognised for a long time (e.g. Flett, 1898). This work recognises the folded lavas of Deerness and equates them with similar rocks in Shapinsay and Black Holm of Copinsay. It also suggests that some of the outcrop represents near-surface volcanic feeders, as confirmed by later studies.

Geochemistry of the lavas is discussed by Kellock (1969), in which they are described as highly altered olivine dolerites and teschenites. Olivine is usually serpentinised or replaced by carbonate; plagioclase

microphenocrysts are usually replaced by mica. The groundmass is largely sericitised feldspar with clinopyroxene and a mesostasis of chlorite, analcime, natrolite and anorthoclase. Fresh iron oxides are highly titaniferous, with local alteration to leucoxene and rutile; no lamellar textures have been noted (plate 3.1c-e,g,h).

The main outcrops of the Eday Lavas are on Deerness (Eastern Mainland), Black Holm of Copinsay and Shapinsay (fig. 3.1; plate 3.1a,b). On Deerness, they occur as a narrow faulted belt around the Deerness syncline. At Point of Ayre (fig. 3.2a), the lavas reach a thickness of 7m and consist of at least two flows, one of which is highly amygdaloidal (Wilson et al, 1935). Grain size decreases towards towards the top and bottom of the flow. At the other end of the syncline (Muckle Castle, fig. 3.2b) the outcrop is an isolated stack capped by sediment. Although considered to be a flow by Wilson et al (1935) this appears to be an intrusive body (Flett, 1898; Kellock, 1969). Above it there are several layers of tuff with lapilli. The outcrop at Black Holm of Copinsay (fig. 3.2c) is very similar; it shows severe alteration of the underlying sediment. Inland exposures in the Deerness area are highly decomposed and hardly recognisable; they have not been sampled in this study.

There are possibly two distinct flows present on Shapinsay, separated by minor faulting (fig. 3.2d). There is no doubt that they are extrusive, with the upper surfaces showing the vesicular, blocky texture typical of sub-aerial flows. In addition, overlying sediments are unbaked and have a clear depositional relationship with the uneven upper surface of the lava.

PLATE 3.1
EDAY LAVAS AND EDAY FLAGS

(a) Contact between Eday Lavas (above) and laminated Eday Flags (below); sites ROD68-73, Shapinsay. Water bottle in left-hand corner 0.8m.

(b) Isolated outcrop of Eday Lavas with baked contact in Eday Flags below. Site ROD19, Deerness.

(c-d) Skeletal magnetite in Eday Lavas (type I sites). Site ROD38, Deerness. (BEI; Jeol 733).

(e) Enlargement of a single branch of a skeletal magnetite. Details as above.

(f) Eday Flags (site ROD19): baked contact beneath Eday Lavas. Detrital quartz (Q) and orthoclase (K); groundmass (G) of clays (high Mg, Al, Fe), being replaced by calcite (C). Carbonate cementation possibly contemporaneous with lava emplacement (see text). (BEI; Jeol 733).

(g-h) Skeletal magnetite in Eday Lavas (type I). Site ROD38, Deerness. (BEI; Jeol JXA-50A).

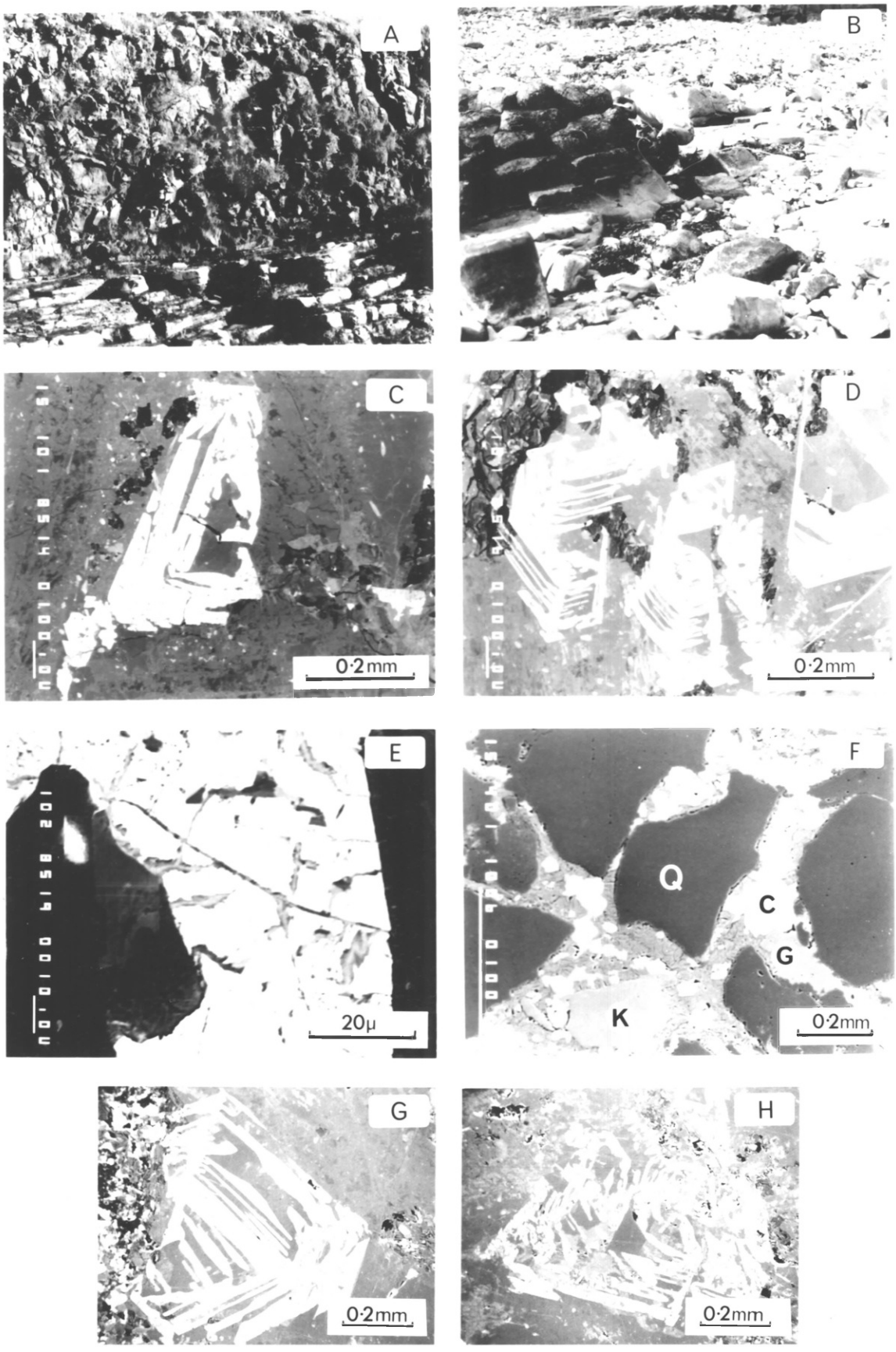


PLATE 3·1

Despite disagreements over the exact nature (i.e. intrusive or extrusive) of some of the outcrops of the Eday Lavas, all authors agree that they are essentially coeval and contemporaneous with deposition of the Eday Flags in the upper Middle ORS.

3.3 SAMPLING

The total geographical extent of the Eday Lavas and sampling localities within it are shown in fig. 3.1, and details of some relevant outcrops in fig. 3.2. Sampling is, of necessity, restricted to coastal exposures due to the very limited outcrop inland and the extremely weathered nature of the lavas at the surface (Kellock, 1969). Of the sixteen sites discussed in this chapter, three are from the Eday Flags from above the lavas or well separated from them, and hence with palaeomagnetic characteristics presumably independent of them. Nine are from the lavas themselves and four are from the Eday Flags immediately below; these show varying degrees of baking or alteration close to the contact. Characteristics of each individual site are given in table 3.1.

3.4 PALAEOMAGNETISM: EDAY LAVAS

3.4.1. Previous work

There are several previously published palaeomagnetic studies of the lavas of Orkney. Storetvedt & Petersen (1972), in a study of both the Eday and Hoy lavas, derived a result based on 7 samples selected from the 60 analysed which showed an apparent high-temperature stable end-point (table 3.2). Those specimens which reach a consistent

Table 3.1
Eday Lavas and Eday Flags: Site details

Site no.	Formation	Location	Dist. from lava (m)	N_{sa}	N_{sp}	Treatment None	Th	AF	Tectonic Correction
ROD19	Contact	Deerness	0-1.20	13	20	1	14	5	10°/090
ROD20	Lavas		-	11	14	-	10	4	
ROD32	Flags	Kirkwall	-	5	7	5	2	-	20°/230
ROD34	Lavas		-	5	10	-	10	-	
ROD35	Lavas		-	5	8	5	3	-	26°/334
ROD36	Flags	Deerness	-	7	7	5	2	-	
ROD37	Flags		-	6	12	8	4	-	17°/290
ROD38	Lavas		-	7	10	-	9	1	10°/090
ROD68	Lavas		-	6	6	-	6	-	
ROD69	Contact		0-0.20	4	8	4	4	-	
ROD70	Contact	Shapinsay	0.20-0.27	5	7	-	6	1	14°/200
ROD71	Contact		0.27-0.50	5	10	-	9	1	
ROD72	Lavas		-	5	9	5	4	-	
ROD73	Lavas		-	5	10	-	10	-	
ROD77	Lavas	Copinsay	-	12	23	16	7	-	8°/200
ROD78	Lavas		-	6	10	7	2	1	
Totals				107	171	54	102	13	

N_{sa} = No. of samples
N_{sp} = No. of specimens
Th = Thermal treatment

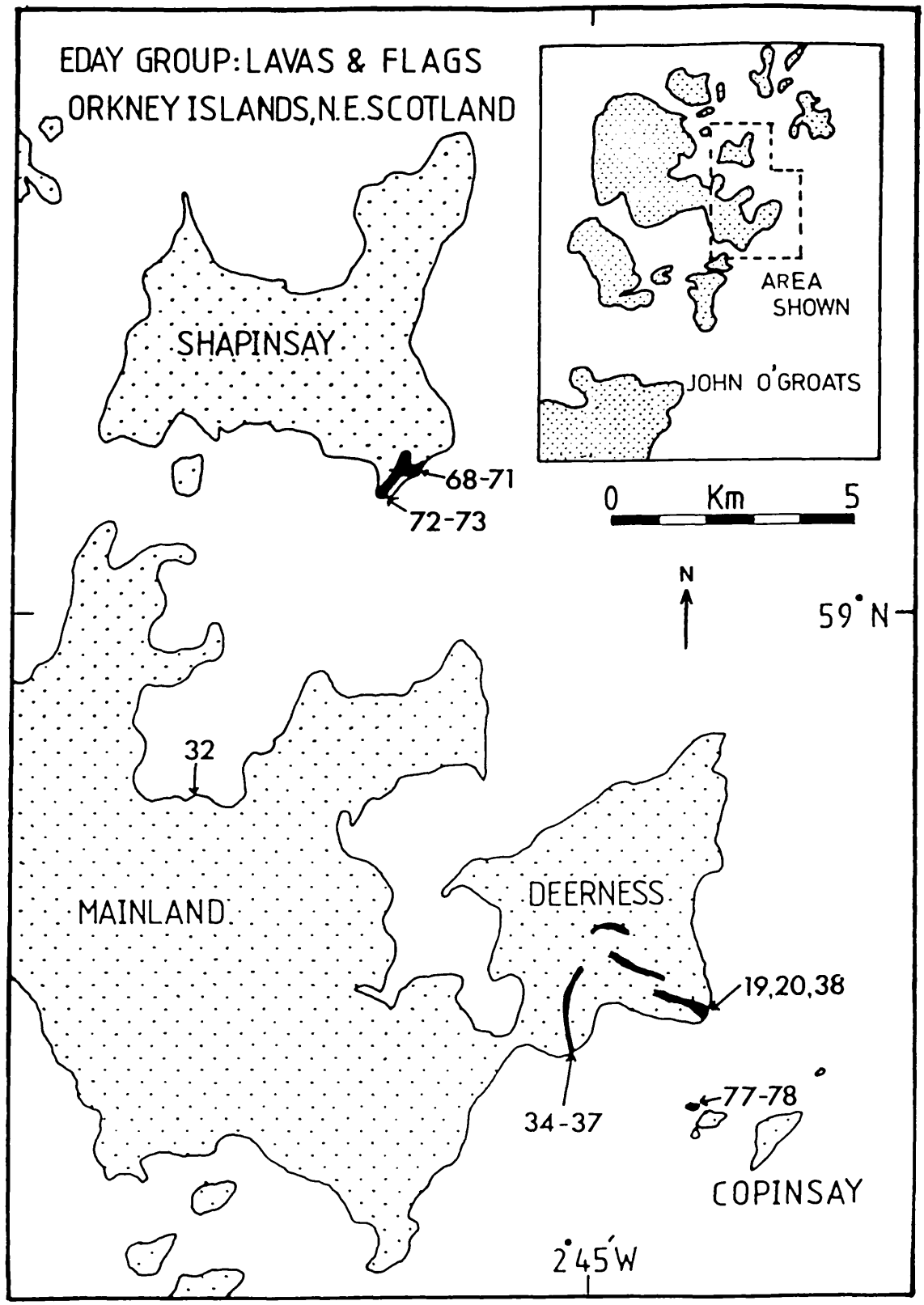


Fig. 3.1. Eday Lavas and Eday Flags: Site locations. Approximate outcrop of lavas shown in solid black.

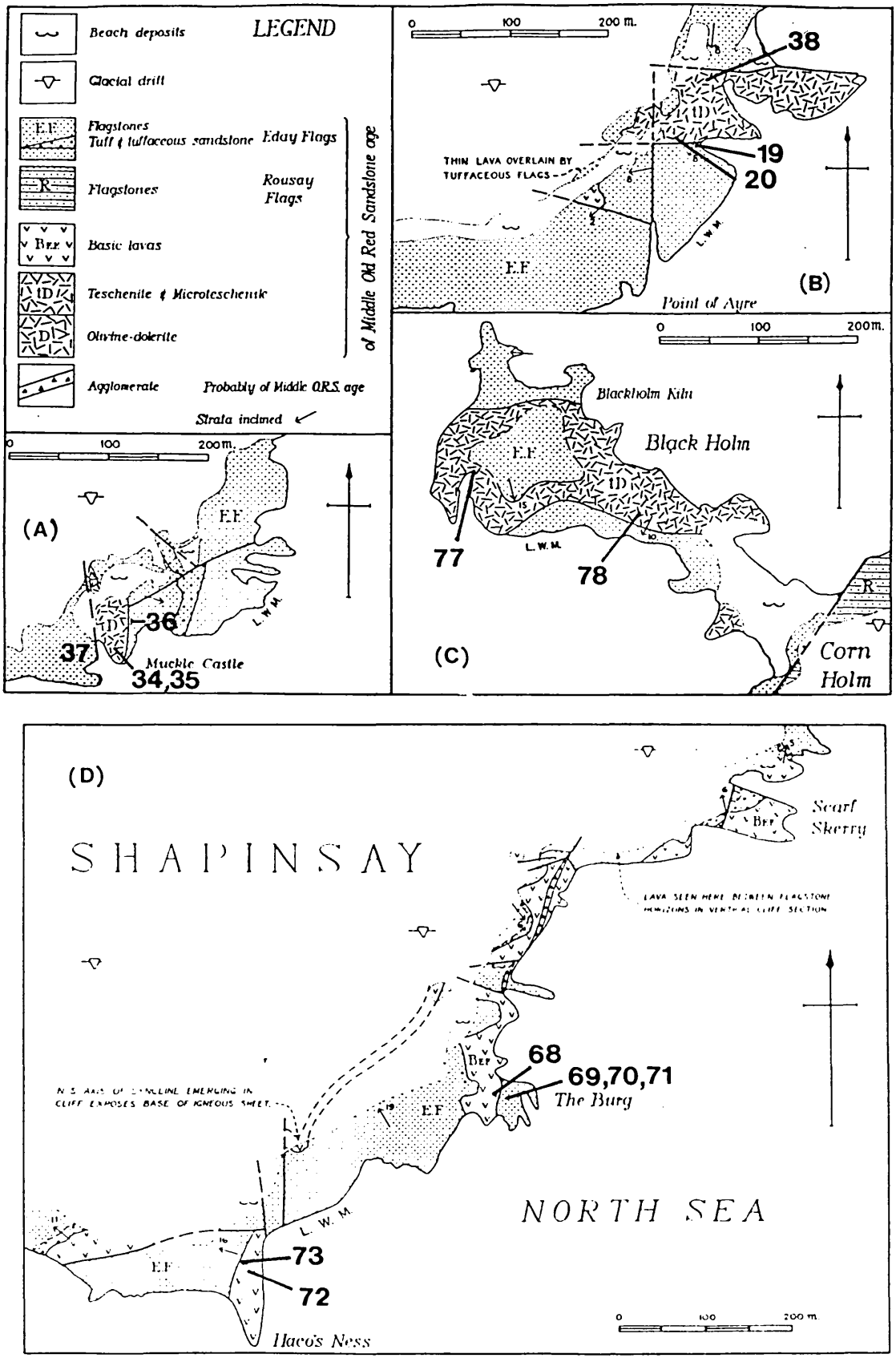


Fig. 3.2. Eday Lavas and Eday Flags: Site locations (large-scale local details). Base maps after Kellock (1969).

direction up to a temperature around 550 - 580 °C are usually rejected. The implications of this work are discussed in greater detail in section 3.7.

Table 3.2
Previous work, Orcadian Basin volcanic rocks.

Location	Dec	Inc	N	k	a_{95}	Pole position		Ref.
Orkney (Hoy, Eday)	205.0	8.4	7^1	45	9.1	24 °N	149 °E	1
Orkney (Eday) *	273	67	9^1	17		42 °S	17 °E	2
Orkney & Shetland	216	46	7^2	18		2 °S	147 °E	2
Orkney (Eday)	191.3	40.8	6^2	20	15.2	7 °N	164 °E	(3)
Shetland	220.4	3.1	55^1	53	2.6	21 °N	135 °E	4
Orkney (Hoy)	023	-28	22^1?	66	3.8	14 °N	154 °E	5

1 : Unit weight to specimens
2 : Unit weight to sites
* : Included in result below

References (and method of treatment)
1 Storetvedt & Petersen (1972) Thermal (Selected samples)
2 Morris et al (1973) AF cleaning
3 Robinson (1985) Thermal (superceded by this study)
4 Storetvedt & Torsvik (1985) Thermal
5 Storetvedt & Meland (1985) Thermal + AF

The Orkney lavas have also been studied by Morris et al (1973); one site (9 specimens) from the Point of Ayre gave a westerly, downwards direction based on single-step AF or thermal cleaning. Three of the four sites in the Hoy volcanics gave a more southerly, downwards direction (table 3.2). A more recent study (Storetvedt & Meland, 1985) records a direction of normal polarity in good directional agreement with the reversed direction from the Eday Lavas (this study). This was found both in lavas and their baked contacts. (The direction is not accepted by the original authors who prefer a southerly, low-inclination direction found only in the lavas).

The Esha Ness ignimbrite of Shetland is considered to be approximately coeval with the Eday Lavas, despite being calc-alkaline rather than alkaline, it has been investigated by Storetvedt & Torsvik (1985), who found a high-stability hematitic remanence which defines a clear

southwesterly, horizontal, direction (table 3.2). This does not appear to be open to the objections raised in chapter 2 to similar directions found elsewhere in the Orcadian Basin by the same authors (e.g. Storetvedt et al, 1978; Storetvedt & Carmichael, 1979; Storetvedt & Torsvik, 1983) although it can only represent a single spot reading of the ambient field at the time of formation and hence is open to inaccuracy. The result is discussed further in chapter 9.

Some of the results described in this chapter are summarised in Robinson (1985), although this paper was written at a somewhat earlier stage of analysis and is superseded by the present study.

3.4.2. NRM

NRM directions are generally steeply downwards (fig. 3.3) with a slight bias to the south and west. Scatter is very large, reflecting the presence of large, magnetically soft, viscous components. NRM intensities vary considerably, between the extremes of 33 and 1315 mA/m (emu cm^{-3}). Initial volume susceptibilities, which range between 0.3 and 11.7 $x10^{-4}$ mA/m, are shown plotted against NRM intensities in fig. 3.4. The ratio between these (the Koenigsberger Ratio, Q), varies widely. Higher values, which may have a general relationship with higher magnetic stability (Stacey 1967) are found throughout the distribution range of NRM intensity, even in specimens showing a recent magnetisation only (type II sites, as discussed below), so Q does not appear to be a reliable indicator of palaeomagnetic stability in this instance.

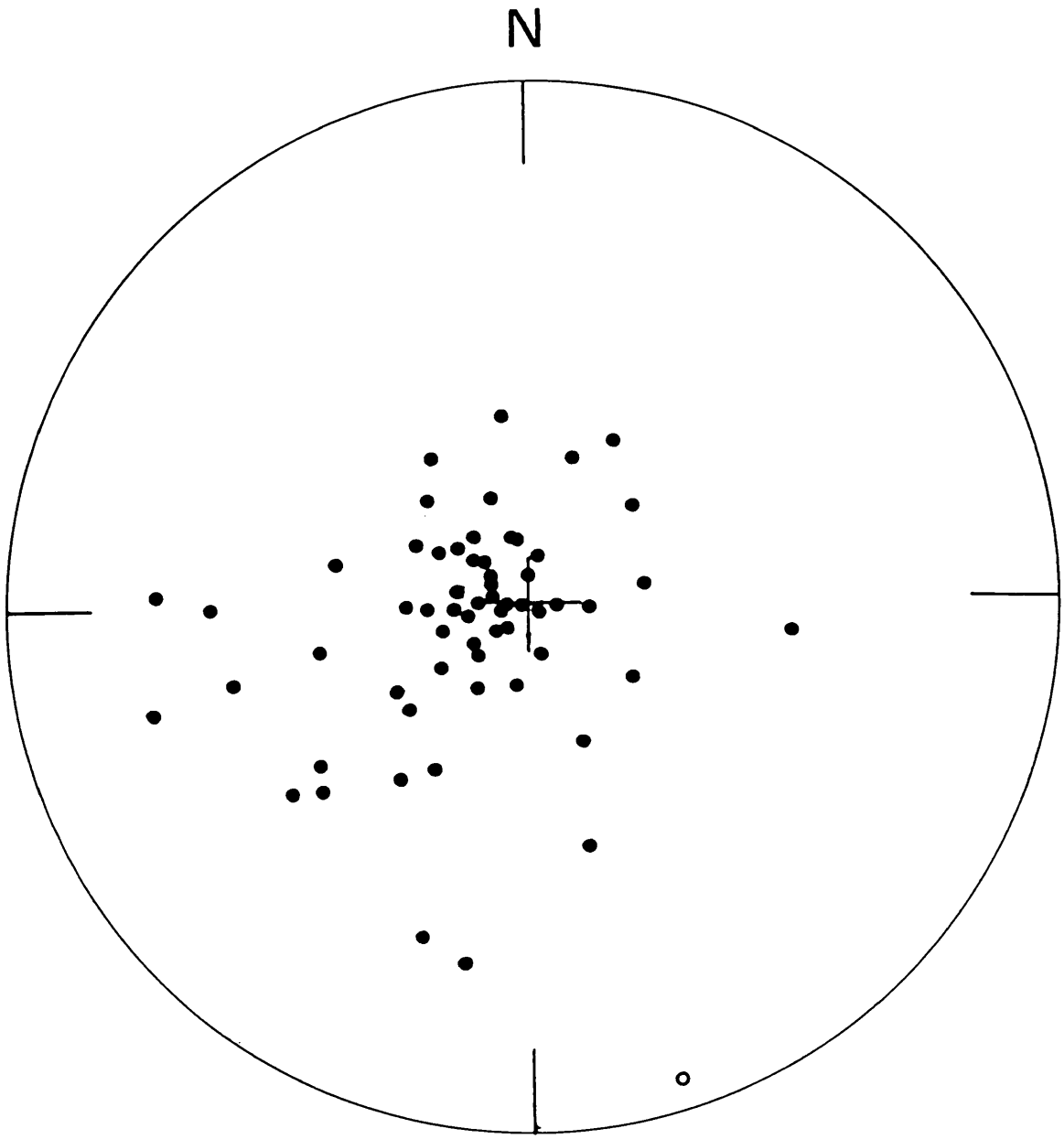
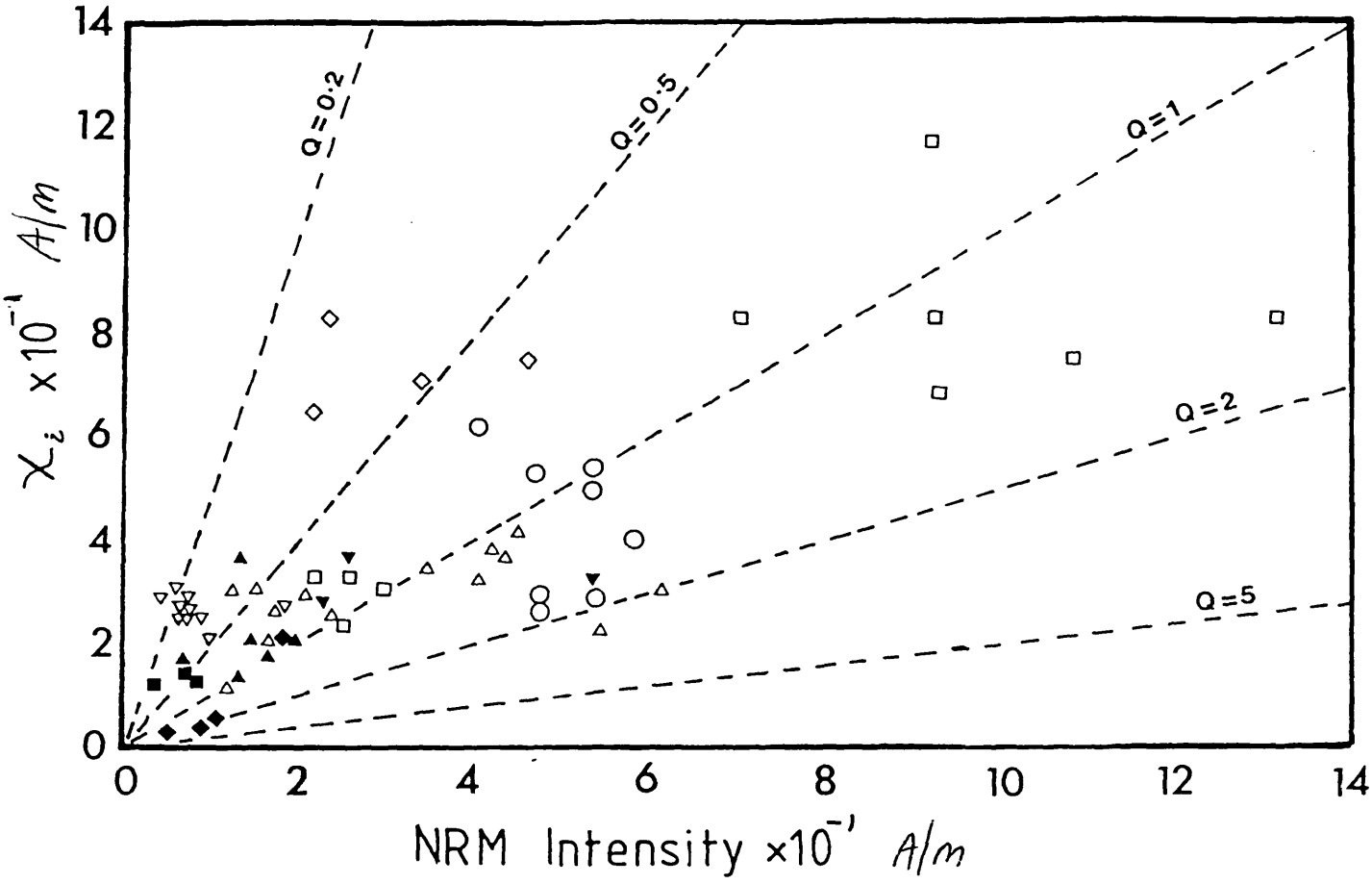


Fig. 3.3. Eday Lavas: NRM directions.



Type I sites

- ROD20
- ROD34
- ROD38
- ROD68
- ROD73

Type II sites

- ROD35
- ROD72
- ROD77
- ROD78

Fig. 3.4. Eday Lavas: Koenigsberger Ratio (Q) of type I and type II sites (see section 3.4.2.).

3.4.3. Thermal Demagnetisation

Of the 115 samples analysed the majority, 102, were subjected to progressive thermal demagnetisation, including representatives from each of the 9 sites (table 3.1). Demagnetisation results in one of two types of behaviour:

(a) Type I lavas

Type I lavas usually give a low-T_B component close to the Present Earths Field (PEF) direction followed by a component directed downwards to the south at higher temperatures. Typical examples, illustrated as orthogonal and stereographic projections, are shown in fig. 3.5. The 'soft' component has a maximum T_B of between 110 and 415°C, with a mean of 227°C. As it is predominantly aligned with the PEF, it presumably represents a recently-acquired VRM. Some of the most viscous specimens such as ROD3802b (fig. 3.5a) show a multi-component VRM, a higher stability one between 210 and 415 °C aligned with the PEF and also one of very low-T_B which survives up to 128-210 °C, probably acquired during storage after collection. Above 415°C a well-defined component directed downwards and to the south, is revealed. Demagnetisation was continued above 580 °C to determine whether any significant hematitic components are present, as suggested by Storetvedt & Petersen (1972); this was found not to be the case. Directional behaviour becomes erratic at temperatures above 550-580 °C; specimens left in zero field within the magnetometer for long periods of time before measurement do not give reproducible results.

Typical demagnetisation curves are shown in fig. 3.6a&b for two specimens with very different NRM intensities and degrees of magnetic viscosity. Demagnetisation is complete by the Curie point of magnetite.

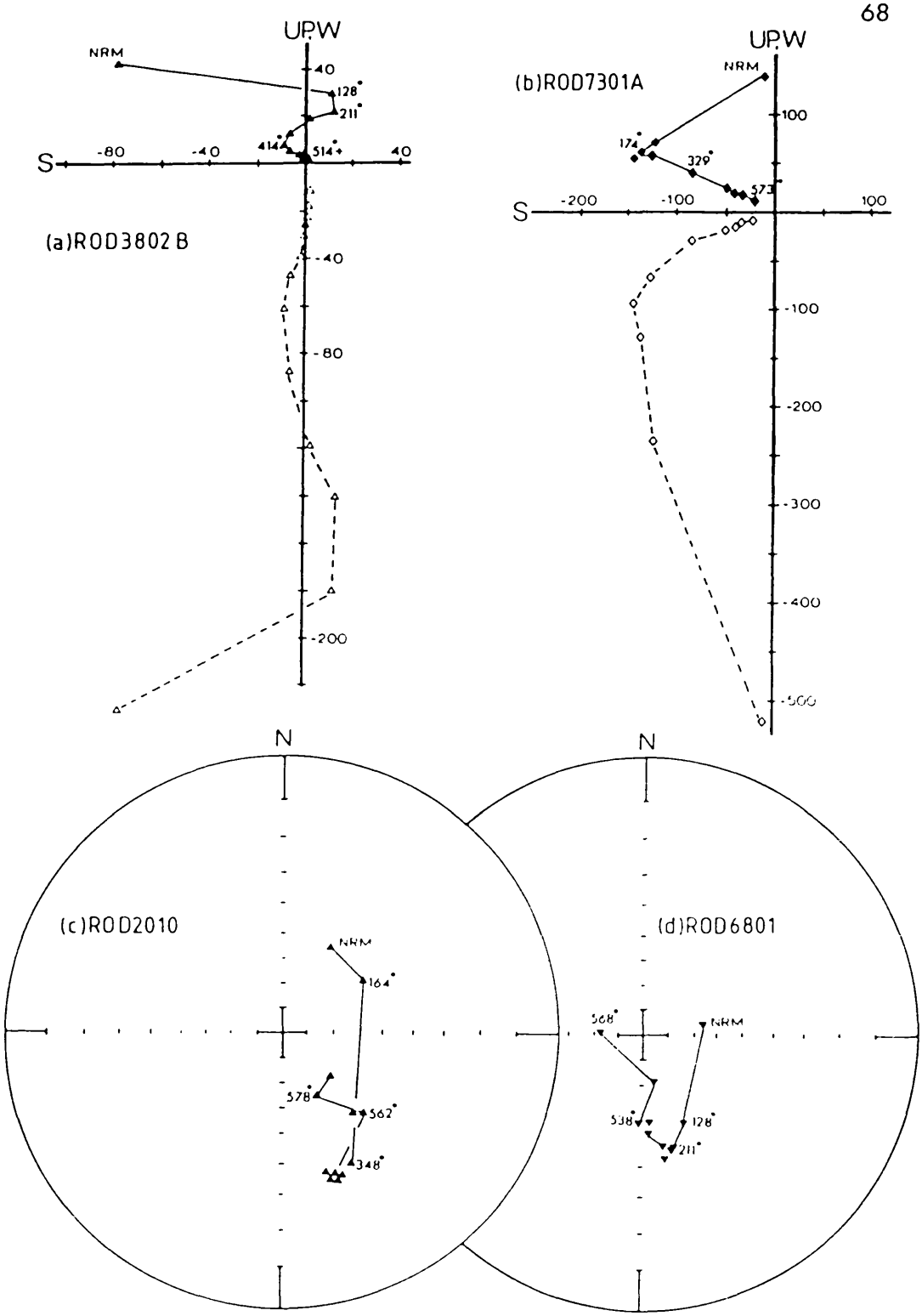


Fig. 3.5. Eday Lavas (type I sites): demagnetisation characteristics (orthogonal and stereographic projections, as described in section 1.4.1.). Demagnetisation temperatures in °C; axes of orthogonal projections in mA/m.

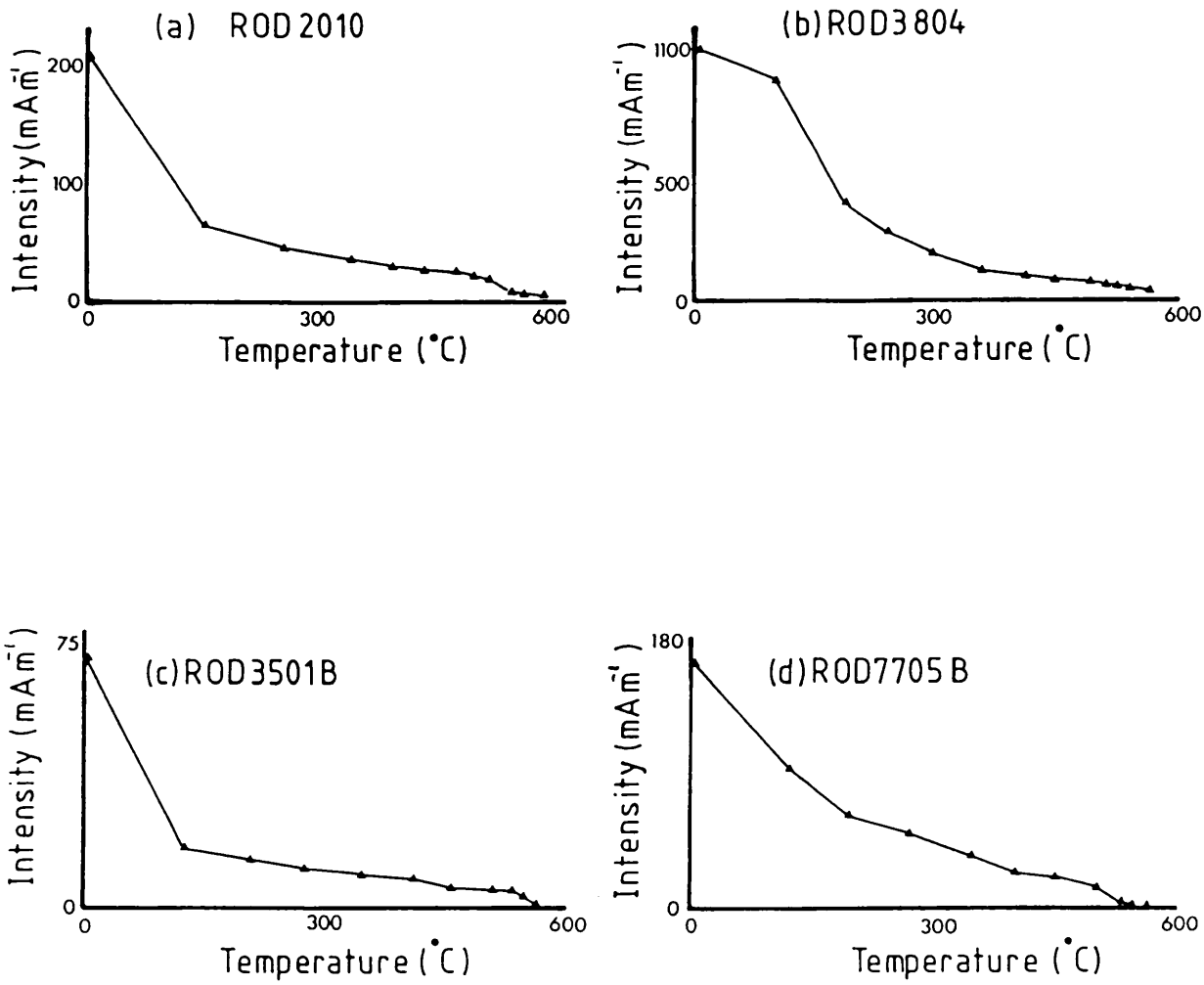


Fig. 3.6. Eday Lavas: Intensity decrease during thermal demagnetisation. (a) and (b): Type I sites. (c) and (d): Type II sites.

Site-level statistics for the intermediate T_B range components are given in table 3.3, and presented stereographically in fig. 3.7. It will be seen that there is a wide range in the precision parameter, with ROD20 in particular having a very low value. This represents innaccuracy due to a directional distribution somewhat strung to the west. Further reference to this direction will be made below.

Table 3.3
Eday Lavas: Type I sites

	Treatment					Mean				
Site no.	N_{SA}	N_{SP}	Th	AF	Rejected	Dec	Inc	N	k	a_{95}
ROD20	11	14	10	4	2 (+4AF)	190.8	34.2	8	6	24.8
ROD38	7	9	9	1	2 (+1AF)	188.1	35.4	7	20	13.7
ROD68	6	6	6	-	2	201.9	38.3	4	12	27.8
ROD73	5	10	10	-	3	203.5	23.0	7	21	13.3
Mean	29	40	35	5	9 (+5AF)	195.6	32.2	26[1]	11	8.9
						196.2	32.9	4[2]	75	10.7

N_{SA} = No. of samples
N_{SP} = No. of specimens
1 = Unit weighting to specimens
2 = Unit weighting to sites
Rejected samples: Low intensity/PEF (6)
Suspected misorientations (3)

Table 3.4
Eday Lavas: Type II sites

			Treatment			Mean				
Site no.	N_{SA}	N_{SP}	Th	AF	None	Dec	Inc	N	k	a_{95}
ROD34	5	10	10	-	-	210.5	69.7	8	4	31.5
ROD35	5	8	3	-	5	281.3	55.7	3	7	50.3
ROD72	5	9	4	-	5	156.6	84.0	4	14	7.8
ROD77	12	23	7	1	15	195.2	86.2	7	20	13.8
ROD78	6	10	3	-	7	005.8	88.5	3	14	34.0
Mean	33	60	27	1	32	226.5	80.6	25[1]	8	11.2
						243.9	80.5	5[2]	21	17.0

N_{SA}= No. of samples
N_{SP}= No. of specimens
1 = Unit weighting to specimens
2 = Unit weighting to sites

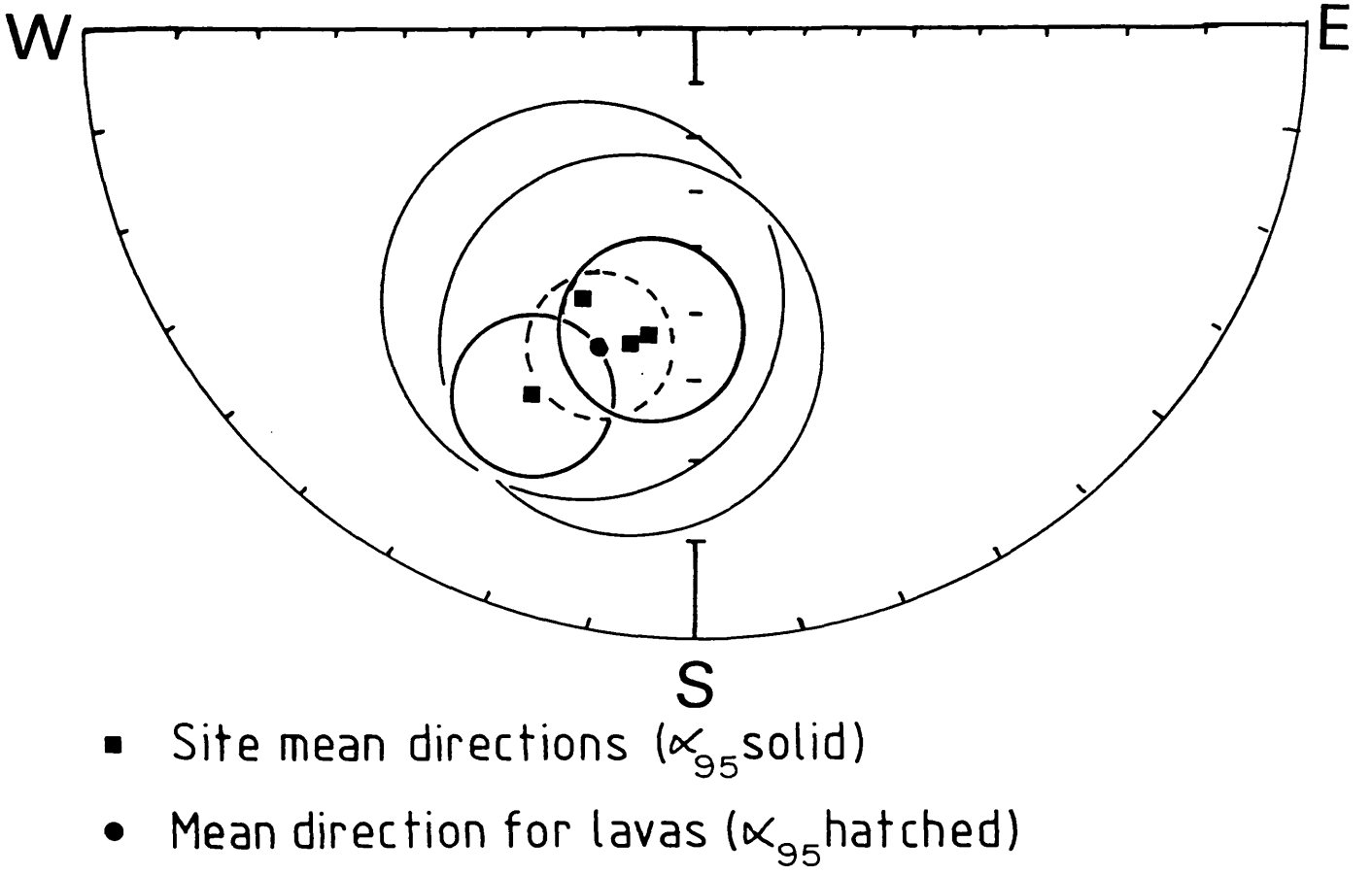


Fig. 3.7. Eday Lavas (type I sites): Site mean directions. Solid 95% circles of confidence for sites (unit weighting to specimen directions), hatched circle for formation mean direction (unit weighting to sites). Statistics given in table 3.3.

(b) Type II lavas.

The characteristic of the second group (type II; sites ROD34, 35, 72, 77 and 78) is that their remanence is essentially single-component (or there may be a very low-stability VRM). Representative specimens only were analysed from these five sites, typical examples being illustrated in fig. 3.8. Mean directions at site level are given in table 3.4. Three of them, sites ROD72, 77 and 78, give a steeply downwards direction approximating to the PEF. The other two, ROD34 and 35, give a westerly, downwards direction similar to that found by Morris et al (1973), this also being the direction towards which the stable component distribution of site ROD20 is elongated.

3.4.4. AF demagnetisation

Six samples treated by progressive AF demagnetisation (table 3.1) show that this is a very ineffective method of separating NRM components; specimens show little deviation from a PEF direction at low fields and erratic directional behaviour at higher fields (above about 30 mT). Such specimens are not included in site statistics and are not considered further.

3.5 PALAEOMAGNETISM: EDAY FLAGS

3.5.1. Eday Flags distant from the lavas

Three of the sites from the Eday Flags are sufficiently far from the lavas (geographically and/or stratigraphically) for them to be effectively independent of them palaeomagnetically (fig. 3.1; table 3.1). ROD32, from near Kirkwall Airport, is a well bedded, very fine grained laminated quartz-rich muddy sandstone with alternating carbonaceous and siliceous layers. Sedimentary features

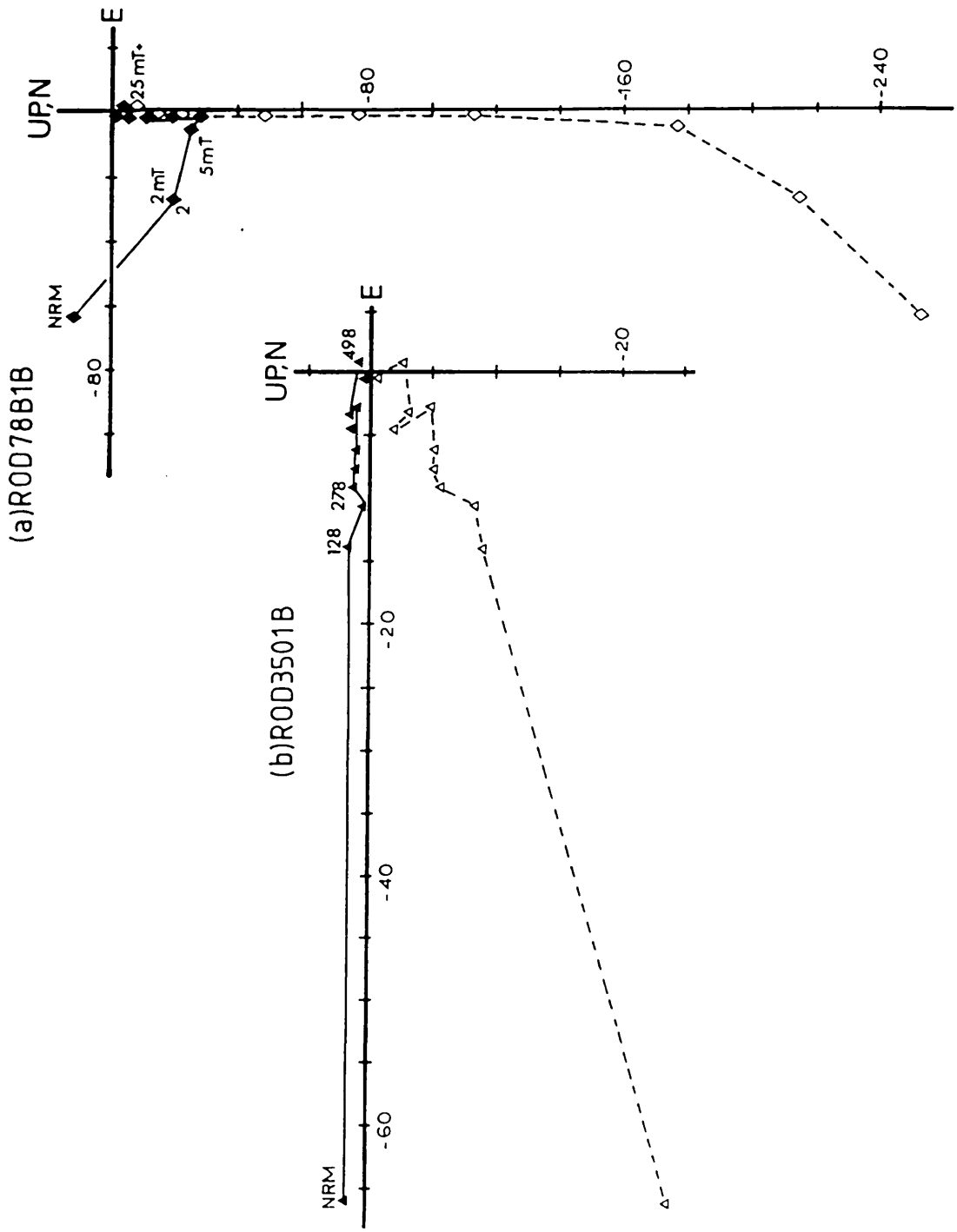


Fig. 3.8. Eday Lavas (type II sites): Demagnetisation characteristics (orthogonal projections, as described in section 1.4.1.). Demagnetisation temperatures in °C or demagnetising fields in mT. Axes in mA/m.

observed nearby indicating periodic emergence (such as raindrop imprints and desiccation polygons) testify to the extremely shallow water during deposition. ROD36 and 37, in a laminated carbonate-rich flagstone, are from 2m above and 10m beneath the lavas of sites ROD34-35 respectively.

Two or three samples from each site were subjected to progressive thermal demagnetisation. The main points of palaeomagnetic interest are that NRM intensity is very low (average 0.40 mA/m) while susceptibility is relatively high (average 6.1×10^{-6} mA/m). Demagnetisation results in little directional change from a steeply downwards PEF direction and is completed by 300-350°C, with no indication of a stable ancient remanence. Susceptibility does not change significantly during heating.

3.5.2. Eday Flags adjacent to the lavas

At two localities (fig.3.1), samples from the Eday Flags immediately below the lavas, at distances of 0.01 to 1.20 m from the base, show palaeomagnetic characteristics contrasting with those discussed in section 3.5.1. Site ROD19 consists of 11 samples at various distances below the lavas of site 20 (fig. 3.2a; plate 3.1b) while on Shapinsay (fig. 3.2d; plate 3.1a), three sites (ROD69,70 and 71) are 0.12-0.20m, 0.20-0.27m and 0.27-0.50 m respectively beneath site ROD68.

As might be expected, these all show a very much lower NRM intensity (0.50-12.61 mA/m) and initial susceptibility (4.5 to 15.4 $\times 10^{-6}$ emu cm^{-3}) than the overlying lavas. It appears that both of these parameters tend to change with distance (table 3.5). Initial susceptibility decreases by about 50% beyond 0.1m to slightly above the background for

the Eday Flags (see section 3.5.1.). NRM intensity, however, decreases by the same amount beyond 0.1m but to a level well above the background value.

Table 3.5
Eday Flags (Contact zone beneath lavas)
Susceptibility and intensity variation with distance

Distance beneath base of lava (m)	Initial Susceptibility X ($\times 10^{-6}$ mA/m)	N	NRM Intensity I (mA/m)	N
0.01-0.10	13.4	6	4.73	8
0.10-0.20	8.2	6	2.85	10
0.20-1.20	7.5	23	2.75	28
Distant sediments (section 3.5.1)	6.1	8	0.40	15

(N = No. in mean)

Table 3.6
Eday Flags (Contact zone): Site statistics

Site no.	Treatment N_{SA}	N_{SP}	Th	AF	None	Rejected	Mean Dec	Inc	N	k	a_{95}
ROD19	13	19	14	5	-	3 (+5AF)	174.8	41.8	11	21	10.1
ROD69	4	8	4	-	4	4	-	-	-	-	-
ROD70	5	7	6	1	-	1 (+1AF)	204.8	50.8	5	10	25.2
ROD71	5	10	9	1	-	3 (+1AF)	195.8	32.1	6	21	15.1
Mean	27	44	33	7	4	11 (+7AF)	186.9	41.8	22^1	14	8.7
							191.4	42.2	3^2	31	22.6

N_{SA}= No. of samples
N_{SP}= No. of specimens
1 = Unit weighting to specimens
2 = Unit weighting to sites

Rejections: Weak PEF direction only (9)
Suspected misorientation (2)

Directional behaviour is very similar to that shown by type I lavas (section 3.4.2), with removal of a low-T_B VRM followed by a component directed downwards to the south. Typical examples are shown in fig. 3.9. Of the four sites, three (ROD19,70 and 71) give a well-defined southerly component, generally of higher precision than adjacent sites from the lavas, with no tendency to show a directional streaking to the west as found in one of the lava sites.

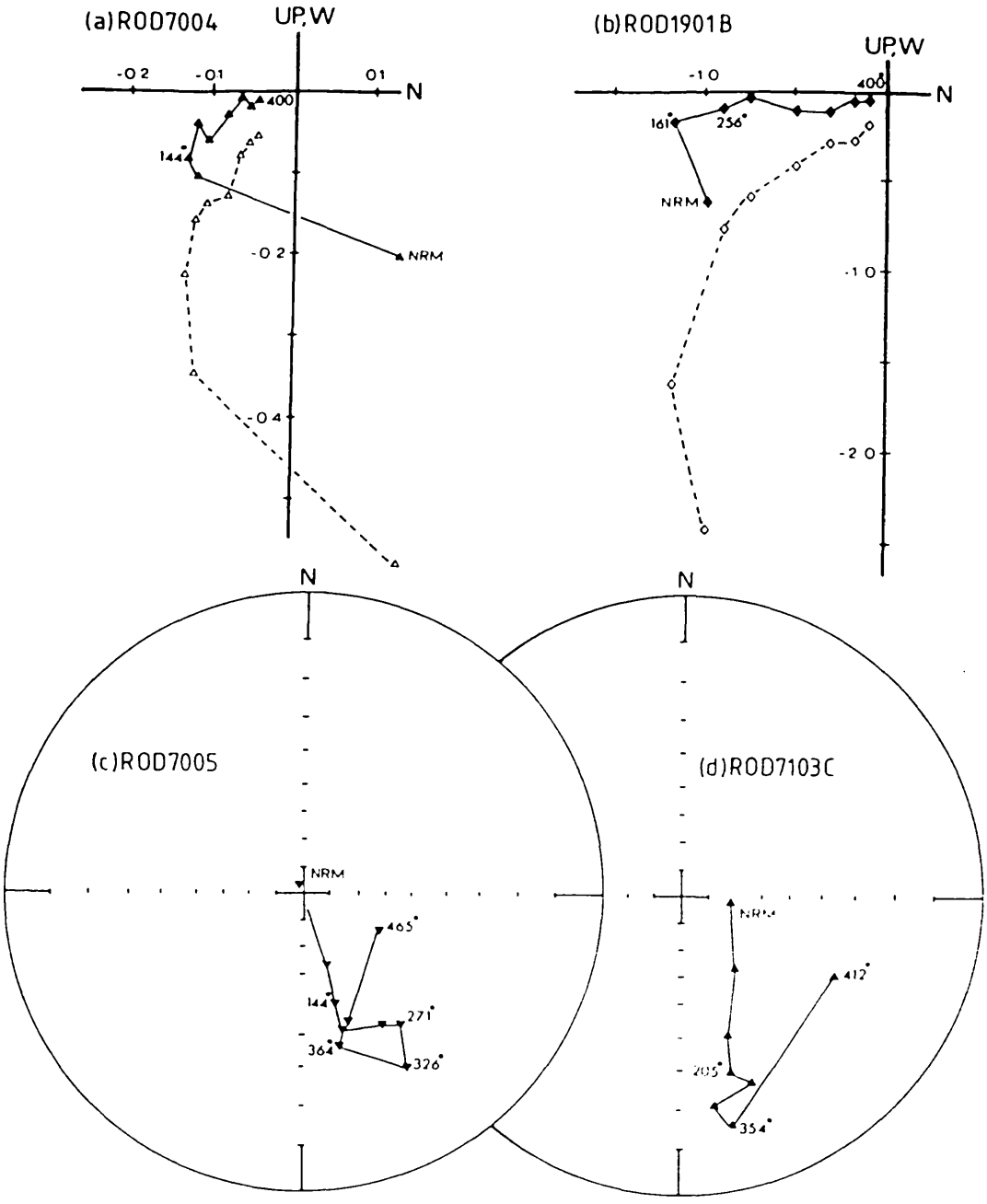


Fig. 3.9. Eday Flags (baked contact beneath Eday Lavas): Demagnetisation characteristics (orthogonal and stereographic projections, as described in section 1.4.1.). Demagnetisation temperatures in °C; axes of orthogonal projections in mA/m.

Site-level statistics are given in table 3.6 and shown stereographically in fig.3.10. The fourth site, ROD69, shows a PEF component only and is not included in the statistics.

Demagnetisation curves show that remanence in the Eday Flags from beneath the lavas typically has a maximum T_B of 500-580 °C (fig. 3.11a-d). In many specimens intensity increase at high temperatures (e.g. fig. 3.11a) combined with a randomising of magnetic orientation suggests that thermochemical alteration of the magnetic mineralogy is occurring. Any possible remanence above these temperatures is thus obscured.

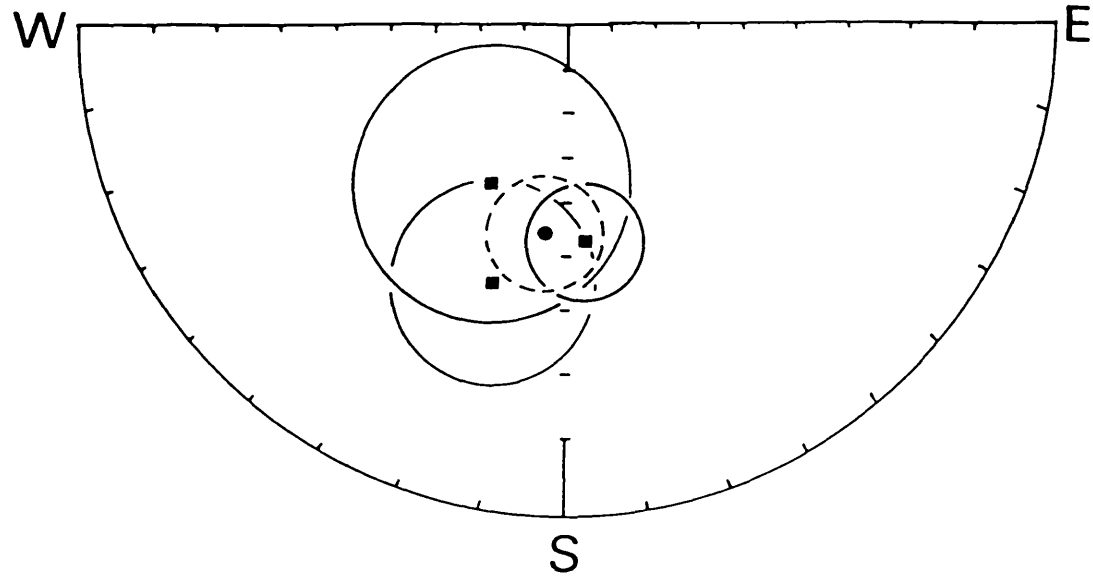
Progressive AF demagnetisation of seven samples produces similar behaviour to that shown by the lavas (section 3.4.4.) with no separation of NRM components, so AF results are not considered further.

3.6 HYSTERESIS OF IRM

3.6.1. Eday Lavas

The two categories of lava sites show markedly contrasting IRM characteristics (see appendix A). Although both show typical features of a magnetite-dominated remanence, the type I sites (which generally show a suspected primary TRM) saturate in fields of over 200 mT whereas type II sites saturate in 100-150 mT (fig. 3.12a). Saturation magnetisations are at least an order of magnitude greater in type I sites (table 3.7), which also have higher coercivities than type II (B_c = 45-90 mT and <30 mT respectively).

This demonstrates a possible reason for the contrast in remanence characteristics: type II sites can be seen to be dominated by grains of low coercivity, which will have a tendency to acquire a VRM in the ambient field. These sites



- Site mean directions (α_{95} solid)
- Mean direction for baked contact (α_{95} hatched)

Fig. 3.10. Eday Flags (baked contact beneath Eday Lavas): Site mean directions. Solid circles of 95% confidence for site means; hatched circle for formation mean (both unit weighting to specimens). Statistics given in table 3.6.

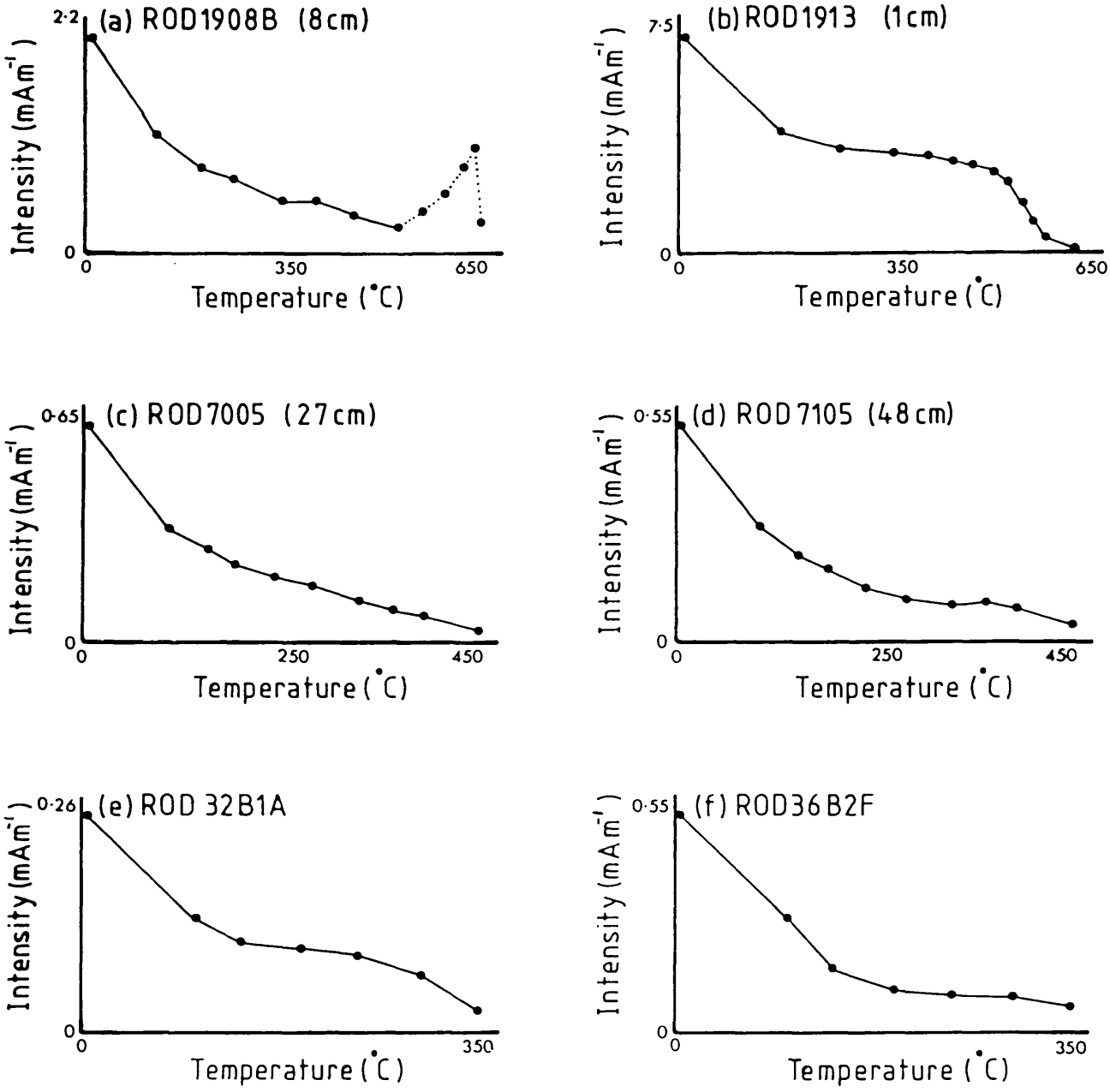


Fig. 3.11. Eday Flags: Intensity decrease during thermal demagnetisation. (a to d): Baked contact beneath Eday Lavas (e,f): Sediments distant from lavas.

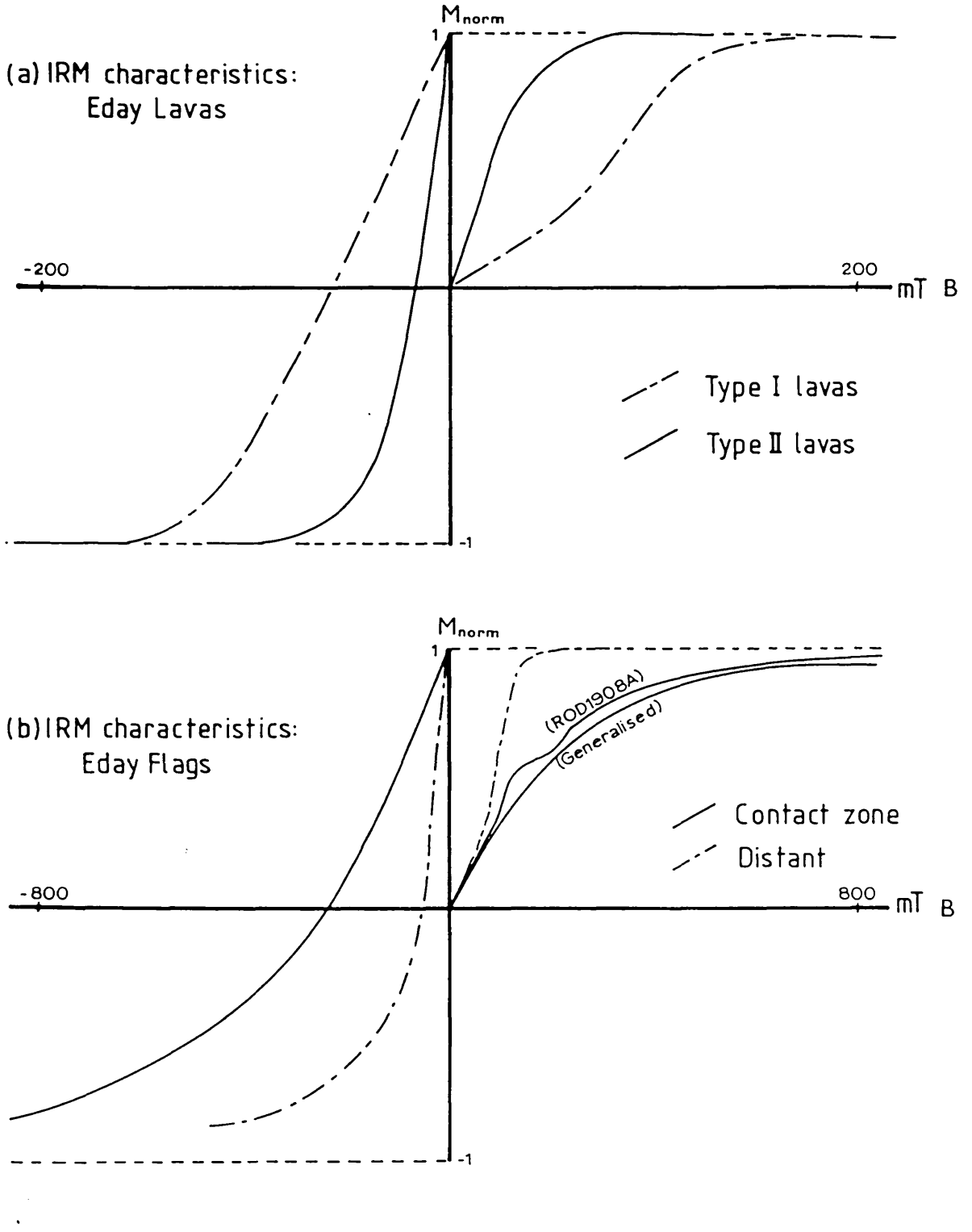


Fig. 3.12. Hysteresis of NRM. (a) Eday Lavas: Contrast between type I and type II sites. (b) Eday Flags: Contrast between baked contact beneath Eday Lavas and distant sediments (see table 3.7.).

do not have grains of higher stability which, in type I sites, are presumably responsible for the observed primary remanence. This is most likely to be a grain size effect, possibly related to cooling rate.

3.6.2 Eday Flags

Five specimens from the contact zone beneath the Eday Lavas (site ROD19) do not show significant variation in IRM characteristics with distance from the lava, although the only fresh specimens available were collected from 8cm, 80cm and 120cm beneath the lava (table 3.7). Saturation is usually achieved by 1200 mT, although two specimens do not saturate in the maximum field available of 1250 mT; this shows that hematite is present in all samples, although it is not necessarily contributing to the remanence. A point of inflexion is clearly seen for specimen ROD1908A, suggesting that magnetite and hematite may both be present (fig. 3.12b).

Of more importance, perhaps, than the lack of significant within-site variation is the contrast with sites in the Eday Flags distant from the lava (table 3.7, fig. 3.12b). These have a saturation magnetisations an order of magnitude lower than those in the contact zone, and they saturate in very low fields. This contrast suggests that thermo-chemical alteration in the contact zone may have occured. The exact nature of this is somewhat unclear, and it cannot be modelled due to uncertainties regarding the chemical environment at the time; it appears to involve the production of small quantities of high-coercivity magnetite and also hematite, although the latter may be the product of recent oxidation.

Table 3.7
Eday Lavas and Flags: IRM characteristics

	Specimen	M_S (mA/m)	B_C (mT)	B_S (mT)
Type I lava	ROD2004B	217000	61	225
	ROD3807A	766000	55	236
Type II lava	ROD3505B	11200	<34	102
	ROD7705C	43000	<47	140
8cm	ROD1908A	4090	220	1200
8cm	ROD1909	4940+	240	1250+
Contact 80cm	ROD1902A	3810	95	1185
Zone 80cm	ROD1903B	4570+	105	1250+
120cm	ROD1905A	6890	150	1170
Eday Flags	ROD32B2G	263	<47	180
	ROD36B2A	230	50	365

3.7. ORIGIN OF THE REMANENCE

3.7.1. Eday Lavas

Although the Eday Lavas are generally reported as being badly decomposed (section 3.2.), there is often a wide range of degree of weathering, and it proved possible to find relatively unweathered parts of outcrops where sampling could be concentrated. Opaque oxides are generally fairly fresh. Typical examples are illustrated in plate 3.1c-e,g,h; these show the characteristic cruciform shape of magnetite grains which have undergone rapid chilling, as illustrated in Haggerty (1976) fig. Hg-25i. They show a simple set of orthogonal cross-arms corresponding to the crystallographic axes. Crystallisation occurred along the entire length of each of the primary cross-arms along directions parallel to the (111) spinel planes. Such examples show beyond doubt that the primary magnetic mineralogy has survived intact. Similar crystal morphologies have also been found by Wilkinson (1957) who found skeletal titanomagnetites only in the upper and lower parts of thick

sills, indicating their relationship to rapid cooling.

This conclusion is in contrast with that of Storetvedt & Petersen (1972) who suggested that the original remanence has been replaced by a subsequent low-temperature CRM acquired over a long time interval. It is also contrary to the suggestion of Van der Voo & McCabe (1985) that hematite-bearing volcanic rocks are the best candidates for preserving an early characteristic magnetisation which is capable of escaping severe Kiaman remagnetisation, as also suggested by Storetvedt (1970) for the Devonian lavas of Scotland as a whole.

Unfortunately, as with most of the southern Orkney Islands, between-site variation in tectonic dip is insufficient to ascertain incontrovertibly the relative ages of remanence acquisition and deformation in type I sites by the use of the fold test of, for example, McFadden & Jones (1981). The effects of tectonic correction on site means, both for the lavas and their contact zone in the Eday Flags, are shown in table 3.8.

Table 3.8
Tectonic correction, lavas and their contact zone

	In Situ					Dip Corrected				
	Dec	Inc	N	k	a_{95}	Dec	Inc	N	k	a_{95}
Lava (type I)	192.9	37.6	4	59	12.0	196.2	32.9	4	75	10.7
Contact zone	183.6	44.2	3	38	20.4	191.4	42.2	3	31	8.7
Combined	189.2	40.5	7	47	8.9	194.3	36.9	7	46	9.0

IRM characteristics of type II sites (which show a single-component remanence directed steeply downwards or aligned with the PEF) show them to be dominated by grains of very low coercivity which are highly susceptible to VRM acquisition. There is little magnetic material of higher stability, unlike type I sites where it presumably carries

the primary TRM.

3.7.2. Eday Flags

The three sites from the Eday Flags which are spatially separated from the lavas (section 3.5.1.) show that the formation carries no intrinsic stable ancient remanence; a weak PEF component has a maximum T_B of 300-350°C. In contrast, sites from beneath the lava show a stable remanence of an approximately similar orientation to that in the overlying lavas. Such components have demagnetisation characteristics contrasting with those of distant sites, with magnetic stability up to the Curie point of magnetite (fig. 3.12).

Geochemical analysis for site ROD19 shows that there is a narrow zone, perhaps 0.1m thick, within which there is possible enrichment of total Fe (fig.3.13a). Such a pattern is not clearly seen in sites ROD69-70-71 (fig.3.13b) so it may represent natural variations in bulk analysis. 'Wet chemical' analysis for FeO, however, shows the iron to be progressively less reduced (or more oxidised?) with distance (fig.3.13c). This suggests that the lava may have caused a net thermochemical reduction of iron in the contact zone with associated acquisition of a magnetitic remanence. This is confirmed by IRM experiments (table 3.7), which demonstrate the presence of high-coercivity magnetite; this is not present in distant flagstone sites.

The only other consistent changes in bulk geochemistry with distance are in Ca, Mg and Mn (fig.3.13d). This suggests either that remobilisation of the original mineralogy has occurred or that induration of the Flags due to baking has affected the nature of later secondary

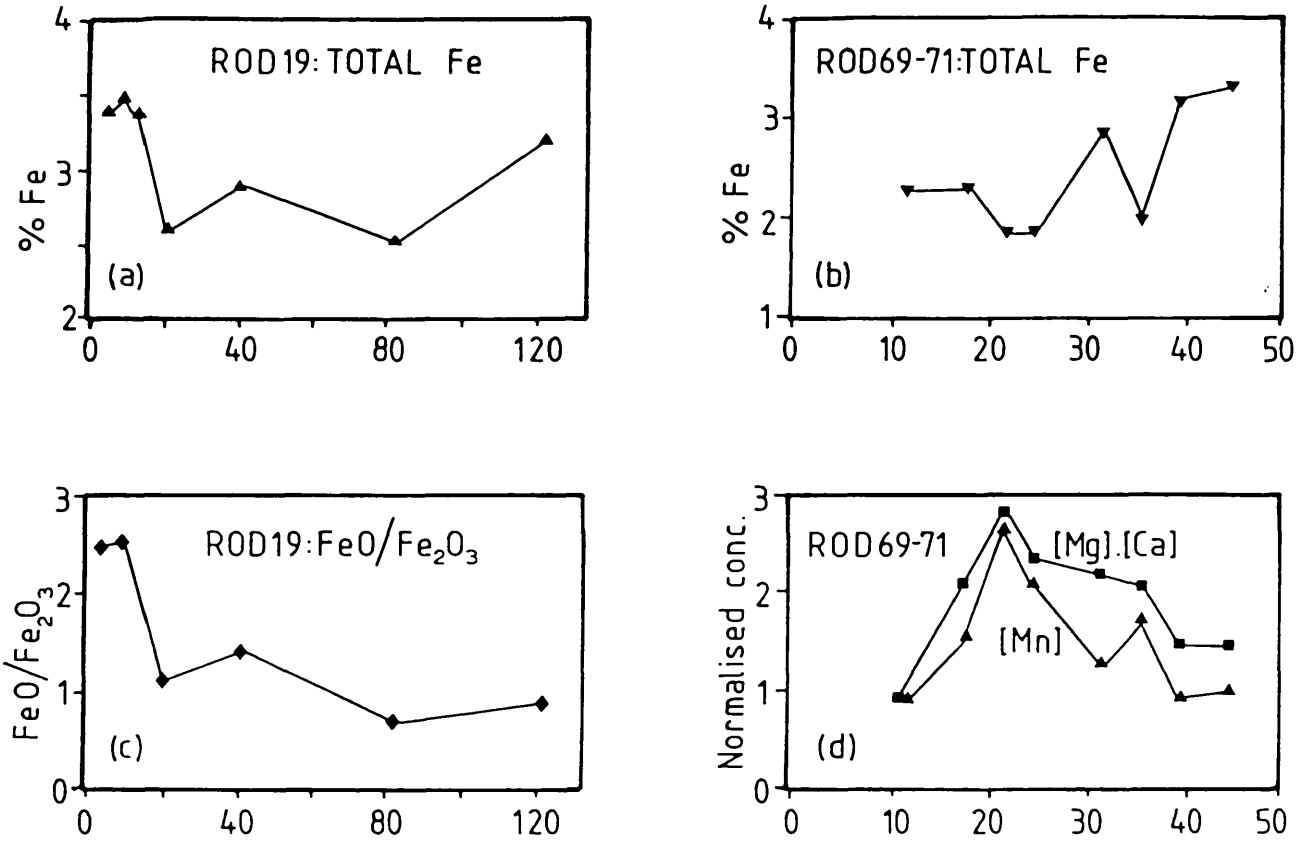


Fig. 3.13. Eday Flags (baked contact): Bulk geochemical variation with distance beneath Eday Lavas (described in section 3.7.2.). Full analyses (ICP spectroscopy) given in appendix C.1b. Note that in fig. 3.13d, carbonates are represented by the product MgxCa.

carbonate cementation. Thin section observation (plate 3.1) of the Eday Flags gives little additional information about their magnetic mineralogy; opaque oxide grains are very sparse.

In summary, it would appear that remanence in the Eday Flags beneath the lavas is directly related to their emplacement, although the exact nature of processes within the sediment, beyond being a net reduction of Fe, is not clear. Palaeomagnetic consistency between the two lithologies, discussed below, is additional strong evidence that the remanence is primary.

3.7.3. Summary

The mean directions for the Eday Lavas and their contact zone in the Eday Flags, derived in table 3.9, are illustrated in fig.3.14. The directions are statistically identical, suggesting that they are contemporaneous (contact test type D; McElhinny, 1973). Additional geochemical evidence seems to suggest that the remanence in the contact zone is a TRM/TCRM directly related to lava emplacement (i.e. contact test type B; McElhinny, op. cit.). The only geologically feasible method by which the two very different lithologies could have acquired an identical remanence at a later date is by a deep-burial induced PTRM, for which there is no evidence elsewhere in the Orcadian Basin.

Based on the evidence discussed above, therefore, it is suggested that it is valid to consider a mean primary direction for the Eday Lavas and their baked contact together (table 3.9) which corresponds to a dip-corrected palaeopole position of 10°N, 163°E. This will be discussed in relation to other postulated primary ORS palaeopoles from

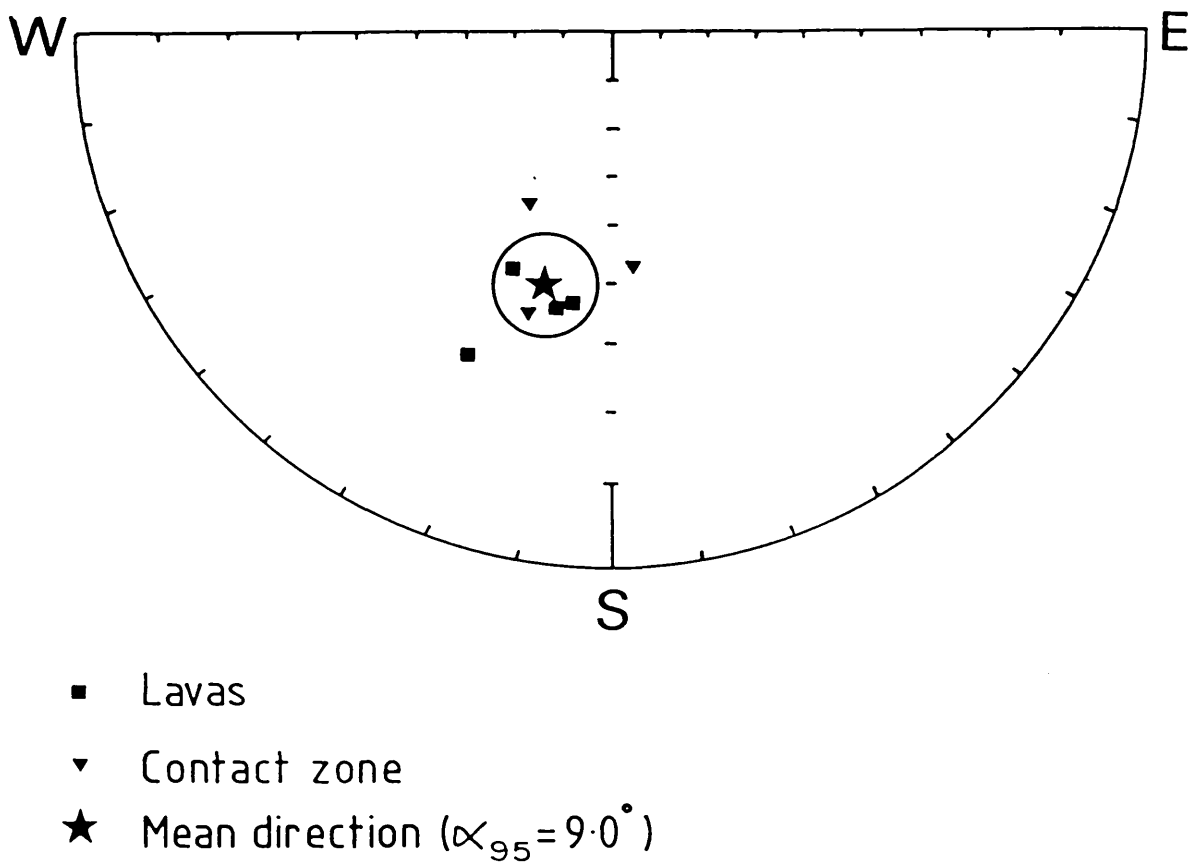


Fig. 3.14. Eday Flags and Eday Lavas: Combined mean directions. 95% circles of confidence for overall mean direction (unit weighting to site) shown solid. Statistical details given in table 3.9.

Table 3.9
Eday Lavas and Eday Flags: Combined statistics (dip corrected)

	Mean Dec	Mean Inc	N	k	a_{95}	Palaeopole
Lavas (type I)	195.6	32.2	26[1]	11	8.9	12.8°N 161.8°E
	196.2	32.9	4[2]	75	10.7	12.3°N 161.2°E
Contact zone	186.9	41.8	22[1]	14	8.7	7.1°N 170.6°E
	191.4	42.2	3[2]	31	22.6	6.4°N 166.8°E
Combined	191.8	36.7	48[1]	12	6.3	10.3°N 165.7°E
	194.3	36.9	7[2]	46	9.0	9.9°N 163.4°E

1 = Unit weighting to specimens
2 = Unit weighting to sites

Scotland and elsewhere in chapter 9, and will also be used as a reference upper Middle ORS direction during discussion of the palaeomagnetic properties of sediments within the Orcadian Basin.

It should be noted that this chapter supersedes an earlier report of the work (Robinson, 1985). In particular, IRM characteristics have shown that site ROD34, which originally gave a somewhat anomalous direction, belongs to type II rather than type I. Additional data are also now included. The revised mean direction is of somewhat lower inclination than suggested in the earlier work, and is of slightly greater precision.

CHAPTER 4

PALAEOMAGNETISM: CLASTIC SEDIMENTS

4.1 Introduction

Clastic sediments in the northern Orcadian Basin form a relatively minor part of the stratigraphy of the area, which is dominated by carbonate-rich lacustrine rocks, as discussed in chapter 5. The chief occurrences are (i) the south and west of the basin, including both sides of the Moray Firth (ii) much of the Lower and basal Middle ORS, including the Foyers-Loch Ness area, a strip to the north of Berriedale flanking the lacustrine sediments to the west, the Sarclet area and the Yesnaby Sandstone of Orkney (iii) occasional clastic formations within the Middle ORS, such as the Hillhead Redbed (iv) the upper Middle ORS (the Eday and John o'Groats Groups, of which the latter is discussed in chapter 8) and (v) the Upper ORS of Hoy and Dunnet Head. Total surface exposure north of Helmsdale is perhaps one third of that of the lacustrine sediments.

These five main occurrences of clastic sediments have all been sampled in the present study, but with highly variable intensity. Sampling strategy was dictated by several factors including palaeomagnetic reliability, extent of earlier study, degree of exposure and accessibility.

As a result of a combination of all of these factors, over half of the collected sites are from Eday Group sediments of Orkney. These comprise 43 out of a total of 73 sites, in addition to a further three sites in the Eday Flags discussed in chapter 3. The 9 sites from the Sarclet Sandstone and related rocks demonstrate their palaeomagnetic importance, as reflected in several earlier studies. The

areas around the Moray Firth, Loch Ness and Berriedale have only been very sparsely sampled; they appear to justify a separate study in themselves. Other sediments discussed in this chapter (the Upper ORS of Dunnet Head and Hoy and the Yesnaby Sandstone of Mainland Orkney) are either of very restricted outcrop, inaccessible or unsuitable for palaeomagnetic study.

In this chapter, the geological and palaeomagnetic characteristics of each of the above mentioned groups of sites will be considered individually, followed by a general synthesis. An analysis of possible remanence carriers and their modes of origin, considered within the context of the overall diagenetic history of the basin, will be given in chapter 6, and discussion of the results in a wider context in chapter 9.

4.2 Sediments of southern Caithness and the Moray Firth

4.2.1. Lower ORS

(a) Foyers

Clastic ORS sediments occur in a narrow strip along the eastern edge of the Great Glen (fig. 4.1). There is a wide variety of sedimentary lithology, including granite and schist breccias, conglomerates, arkosic grits, shales and sandstones. They have been interpreted as fault-bounded alluvial fan deposits derived from the SE (Mould, 1946; Stephenson, 1972, 1977; Mykura, 1982), lying unconformably on a Caledonian-Moinian basement. A palaeogeographic reconstruction by Stephenson (1977) shows highlands of granitic material to the east flanked by talus slopes which shallow off into more flat-lying areas with ephemeral lakes. The sediments are shattered in places and are cut by many

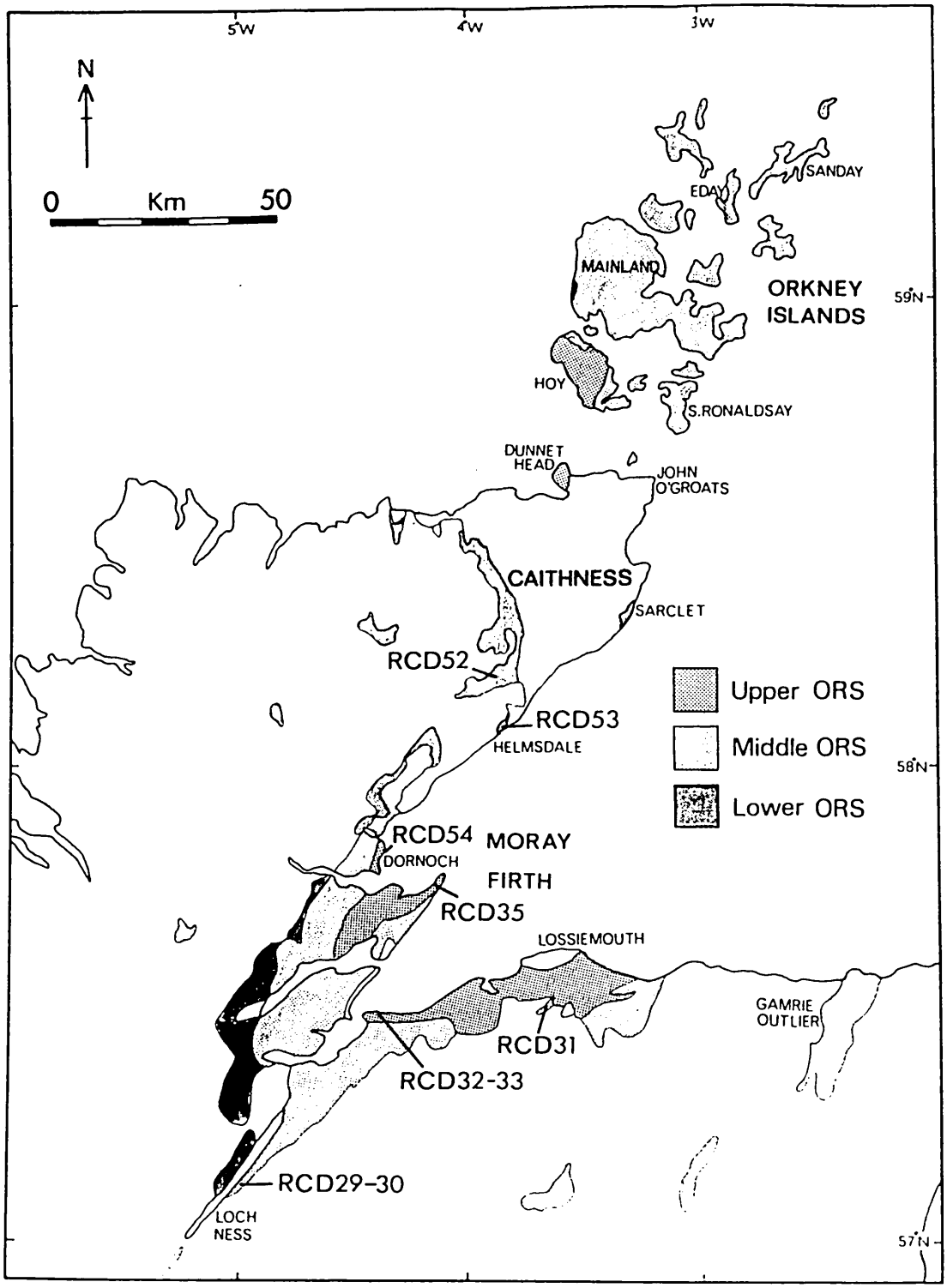


Fig. 4.1. Site locations in the ORS of the southern part of the Orcadian Basin.

minor faults, although movement during and after sedimentation appears to be predominantly vertical (Stephenson, op. cit.). Bedding orientation in the sampled outcrops can be clearly seen due to graded bedding sequences.

The only palaeomagnetic study of sediments of the area (Kneen, 1973) gives site mean directions for five or six 'acceptable' (i.e. $a_{95} < 20^{\circ}$) sites, although statistics for the Foyers Granite and the unconformably overlying ORS sediments are not separated. Recalculation by Morris (1976) and Van der Voo & Scotese (1981) for sediments alone gives a southerly, flat-lying mean direction. However, it is not stated whether the original results are corrected for local tectonic dip (which is considerable, and highly variable, throughout the area). The recalculated result also does not include site F69 which, although stated to be in the granite appears from fig.1 of the original publication to be in the ORS.

The nearby Foyers Granite has been more extensively investigated (Kneen, 1973; Torsvik, 1984) but it considerably predates the sediments so a direct comparison between the two is not valid (c.f. Kneen 1973). Results from the granite will thus be considered in chapter 9 only.

The two sites in the present study are from a fine-grained grey sandstone near the Foyers power station (RCD29) and a coarser-grained feldspathic grit (RCD30) from between the Foyers and Glen Liath faults (Mykura 1982, fig.3). *In situ* remanence of both sites is dominated by a northerly component I, generally of shallow, upward inclination (fig. 4.2, table 4.1). This has a maximum T_B of 590-695°C showing it to be carried by hematite. In addition there is often a

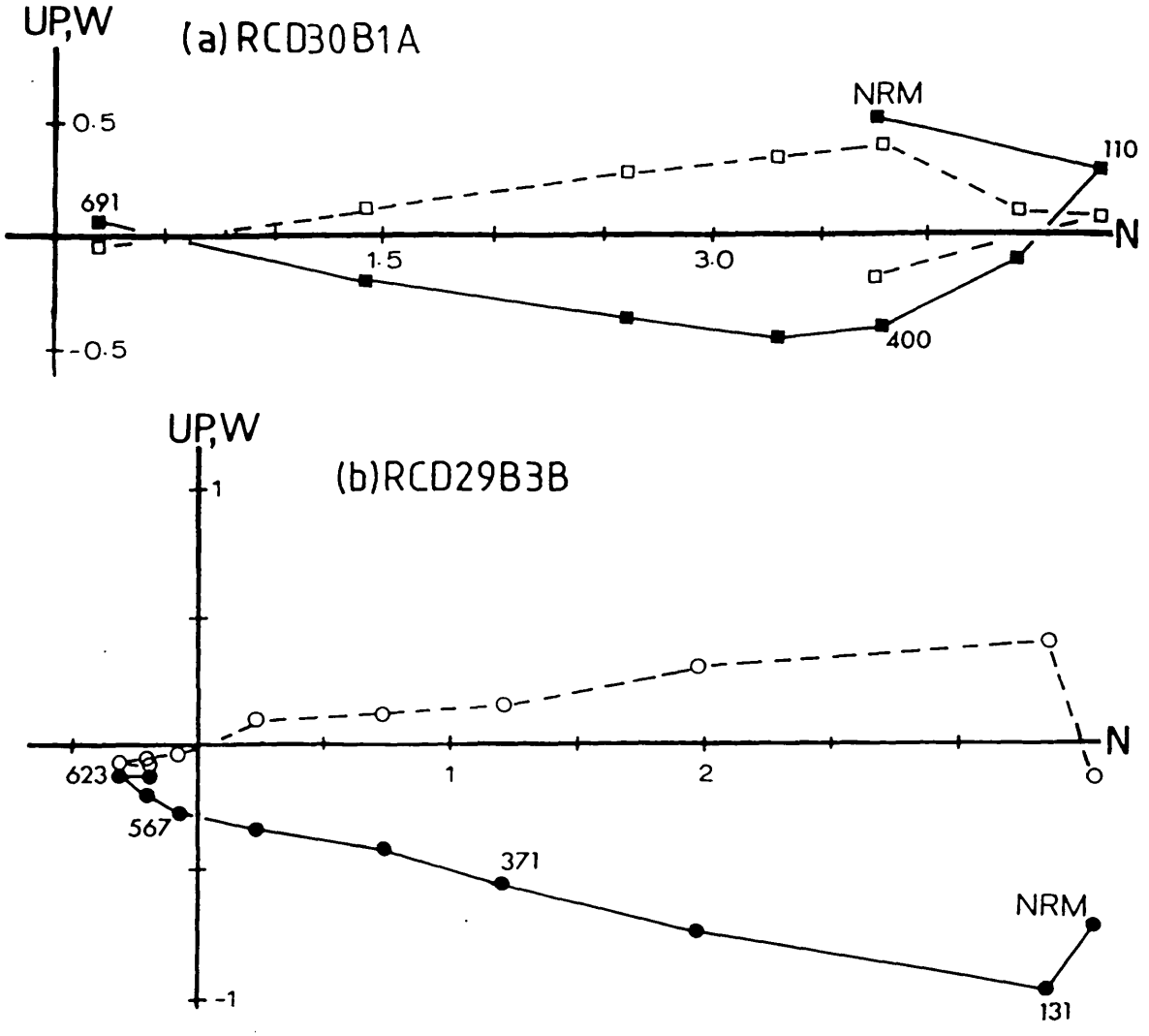


Fig. 4.2. Lower ORS, Foyers: Progressive thermal demagnetisation, illustrated as orthogonal projections (section 1.4.1). Demagnetisation temperatures in °C; axes in mA/m.

low-temperature VRM, and an unresolved high-T component (possibly a CRM of recent origin) is suggested by the fact that the demagnetisation trajectory of the dominant component, illustrated on an orthogonal projection, rarely passes through the origin. Dip correction of I produces a more steeply upward mean direction (table 4.1).

This dip-corrected direction is not in good agreement with the recalculated direction for Lower ORS sediments reported by Morris (1976) based on work by Kneen (1973) which suggests that the remanence is of very low inclination, rather than the 20-25° suggested here. It should also be noted that the results are of opposite polarity.

Table 4.1

MORAY FIRTH-SOUTHERN CAITHNESS: SITE MEAN DIRECTIONS

Site no. (RCD)	In Situ Dec	In Situ Inc	Dip Corrected Dec	Dip Corrected Inc	N	k	a_{95}	T_B max (°C)
			Low Blocking Temperature Components					
52	189.6	-0.6a	194.9	-14.6	5	37.1	12.7	632-665
			High Blocking Temperature Components					
29	003.1	-5.0	354.6	-25.6	12	15.5	11.4	600-694
30	343.6	6.2	341.6	-21.5	9	12.1	15.4	660-685
52	034.1	18.5	045.7	12.7	5	54.0	10.5	685-690
53	014.1	18.0	015.5	-10.8	8	26.8	10.9	450-665
54	359.1	-21.5	353.3	-15.7	7	24.6	12.4	600-665
Mean directions	004.0	2.2	-	-	41[1]	9.1	7.8	
	-	-	002.2	-16.3b	41[1]	8.0	8.4	
	006.5	3.5	-	-	5[2]	10.6	24.6	
	-	-	006.1	-13.3c	5[2]	8.2	28.5	

(1) Unit weighting to specimens
(2) Unit weighting to sites

Palaeopole positions:
(a) Long. 165.0E, Lat. 31.6N (dp=6.4, dm=12.7)[1]
(b) Long. 173.5E, Lat. 23.8N (dp=4.5, dm=8.7)[2]
(c) Long. 169.2E, Lat. 25.2N (dp=14.8, dm=29.1)[2]

(b) Berriedale - Braemore

Two sites have been analysed from the strip of Lower ORS to the west of the Middle ORS lacustrine sediments of Caithness (fig. 4.1). The Ousdale mudstone (site RCD52) has been dated to Lower Emsian, based on its spore and macroflora assemblage (Collins & Donovan, 1977) which suggests that it is an approximate equivalent of the Ulbster/Riera Geo Mudstone of Sarclet (fig.4.3; see section 4.2.3). The Braemore Mudstone (RCD53) is very similar to the Ousdale Mudstone and is without doubt an exact equivalent (Crampton & Carruthers, 1914, p26-27). Both sites are in a fine-grained micaceous purple-red mudstone. Unfortunately most outcrop is highly inaccessible, forming (with interbedded sandstones and conglomerates) much of the high ground of the Morven-Scaraben area. The two sampled outcrops are in a recent road cutting and stream section respectively.

These or similar sediments have been the subject of a number of earlier studies (Waage & Storetvedt 1973, sites 2-12; Tarling et al 1976, sites 35-39; Eustance 1981 site CF9 and Storetvedt & Torsvik 1983). None of these are sufficiently rigorous in experimental technique and/or treatment of results to give a reliable indication of the palaeomagnetic history of the area.

The earliest study (Waage & Storetvedt 1973) based on two sites (10 samples) from the Ousdale area and 9 sites (42 samples) from Berriedale gives a bi-polar mean direction (based on six selected samples only) which is directed upwards to the NNE, although this direction has no validity as it is based on postulated stable end-points only. The authors suggest that the complex results are due to the

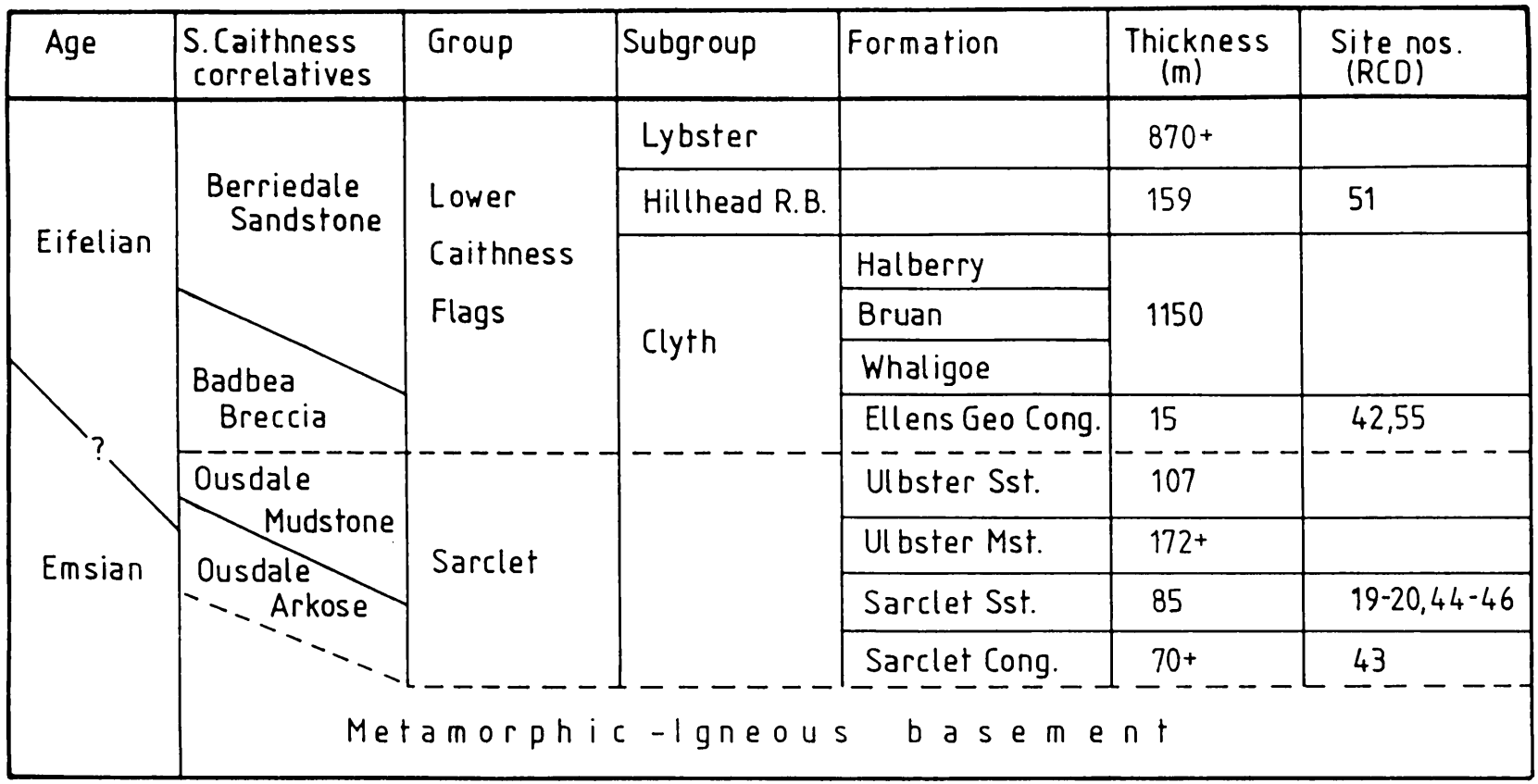


Fig. 4.3. The Lower and lower Middle ORS of Caithness: stratigraphical representation. (after Donovan et al, 1974 and Collins & Donovan, 1977). Not drawn to scale.

presence of up to four components, some of which are of opposing polarity. More recent revision and extension of this study (Storetvedt & Torsvik, 1983) gives no improvement in statistical rigour but confirms the multi-component nature of the remanence. A single site in the Ousdale Mudstone (Eustance, 1981) gives a westerly direction after thermal cleaning. Similar treatment by Tarling et al (1976) gives 'significant' (i.e. $a_{95} < 15^{\circ}$) results for three sites out of seven, which bear little relation to each other. In summary, therefore, there is no reliable published work on these sediments.

Progressive thermal demagnetisation of samples from site RCD52 (fig. 4.4; table 4.1) shows the remanence to be composed of two ancient components (after removal of a recent VRM). The lower-T_B component I is of very low inclination to the south; correction for tectonic dip produces a mean direction of shallow, upwards inclination. At higher temperatures, a component H directed downwards to the north is removed, which, upon dip correction, becomes more shallow. Both seem to be held in hematite (table 4.1) with a maximum T_B of 632-665°C and 685-690°C respectively. There is no indication of a magnetitic contribution to the remanence. Unfortunately the sediments are not suitable for chemical demagnetisation; disintegration occurs very shortly after immersion in acid, as with many sediments of the basin (presumably due to rapid carbonate cement dissolution).

Site RCD53, in contrast to the above, shows a northerly component of intermediate T_B (after removal of a low-stability VRM) which is of shallow to moderately steeply downward inclination (fig. 4.4). After dip correction, this becomes of upward inclination (table 4.1). At higher

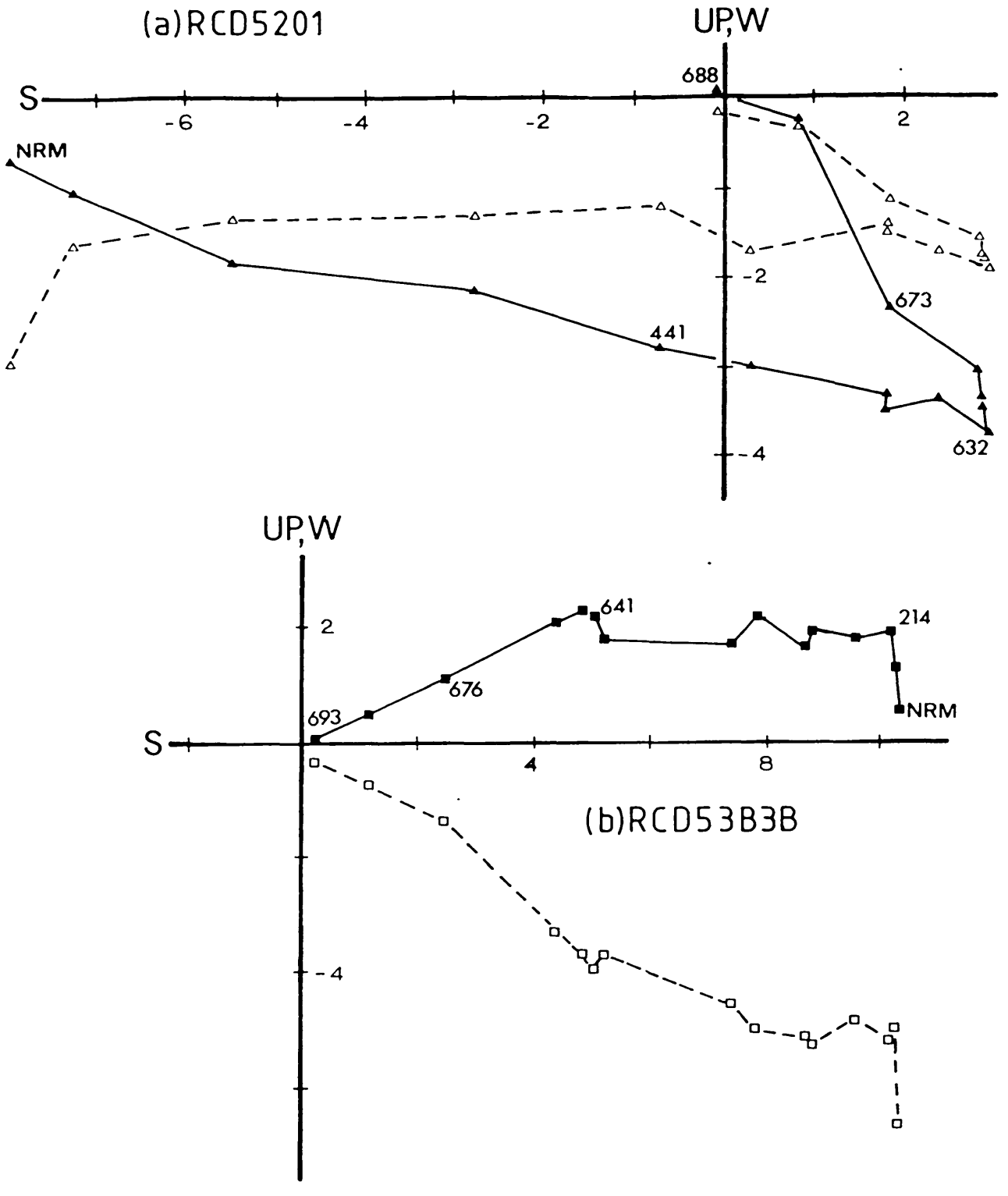


Fig. 4.4. Lower ORS, Berriedale-Braemore. Progressive thermal demagnetisation, illustrated as orthogonal projections (section 1.4.1). Demagnetisation temperatures in °C; axes in mA/m.

temperatures, a northerly component directed steeply downwards is generally removed: this may correspond to a CRM acquired during recent weathering. Again both components appear to be carried by hematite, with T_B ranges of 200-250°C to 450-665°C and 580-665°C to 685-693°C respectively.

4.2.2. Middle-Upper ORS.

A total of five sites from the Middle-Upper ORS (three from south of the GGF, and two from the north) have been examined (fig. 4.1). Of these only one (RCD54; Upper ORS) shows a well-defined ancient remanence, so background discussion will be kept to a minimum. The only previous investigation of the area (Tarling et al 1976) gives a result for one site (two specimens) only.

All sediments south and east of the GGF (i.e. the Middle ORS conglomerate south of Lossiemouth, a fine-grained red sandstone near Nairn and the Upper ORS of Portmahomack: fig. 4.1) have a remanence dominated by PEF components, or of completely random orientation. They have presumably been the target of recent severe oxidative weathering; the results are not considered further.

Site RCD54, in a cross-bedded red micaceous sandstone of Upper ORS age from north of the Dornoch Firth (plate 2.2a), has a stable hematitic remanence directed upwards to the north (fig. 4.4; table 4.1) with a maximum T_B of 600-670°C. Due to the high degree of directional stability, the majority of specimens were treated by single-step thermal cleaning with no adverse effects on precision of the resultant mean direction.

4.2.3. Discussion.

Five of the nine sites from the Moray Firth area have interpretable palaeomagnetic mean directions, including four from the Lower ORS and one from the Upper ORS. The remaining four sites have been severely affected by recent oxidation which has obscured or replaced any earlier remanence.

All five reliable sites have a northerly component of shallow inclination which, after correction for tectonic dip, gives a mean direction directed upwards to the north, as shown in table 4.1. This is carried purely in hematite. There is no reason to suppose that this does not represent a syn-depositional remanence (as discussed in chapters 6 and 9).

One site, from western Caithness, has an additional lower-T_B component; this is of very low upward inclination to the south and is also of high-T_B (fig. 4.4; table 4.1). Inclination steepens after dip correction; it thus probably represents a secondary magnetisation. Origin of the NRM (both northerly and southerly components) is discussed in chapter 6 and related to the Palaeozoic polar wander path in chapter 9.

4.3 The Lower and lower Middle ORS of Caithness

4.3.1. Geology and sampling.

The Sarclet Group (Donovan et al, 1974; fig. 4.5) forms an isolated outcrop of Lower ORS (the Barren or Basement Group of Crampton & Carruthers, 1914). The base is not seen but is probably very near to the surface as the lowest member of the Group is a coarse basal conglomerate (the Sarclet Conglomerate). The top of the sequence has a

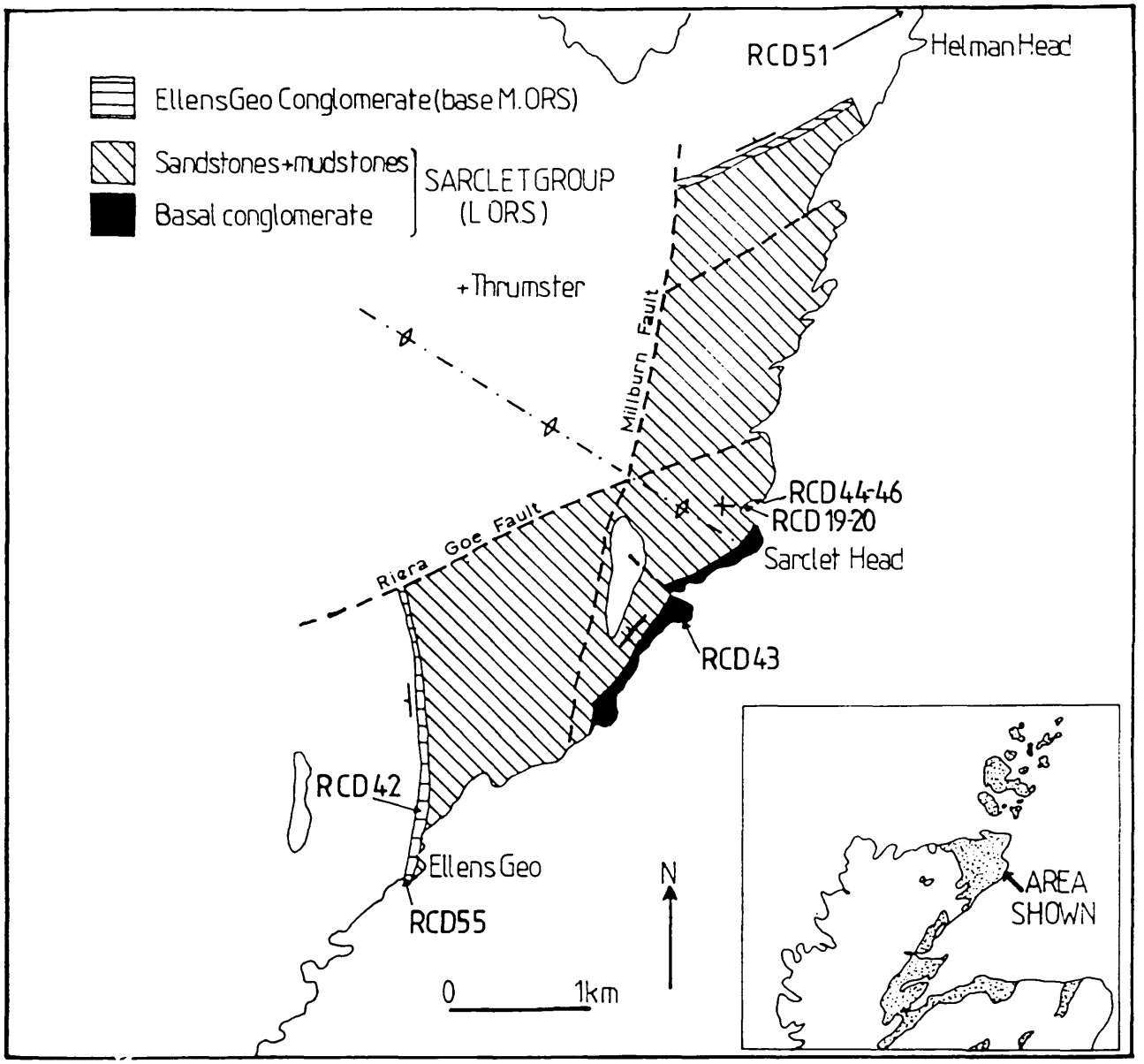


Fig. 4.5. Lower and basal Middle ORS of the Sarclet area: simplified structure and site locations.

severely carbonised but identifiable spore assemblage (Collins & Donovan, 1977) which suggests an upper Emsian age; this is somewhat younger than the Ousdale Mudstone discussed in section 4.2.1., although lower, possibly laterally equivalent, members of the Group are totally barren. Similar sediments elsewhere in NE Scotland (also referred to the Basement Group) are geographically separated and may have formed as distinct sub-basins, dominated by fluvial processes, which were later blanketed by the lacustrine sediments discussed in chapter 5.

The major structure of the area is the Sarclet Anticline or Sarclet Dome (fig. 4.5) in the core of which the oldest sediments are found. Numerous cross-cutting faults, sometimes with large vertical displacements, and a complex thrusting pattern, dissect the area into a complicated arrangement of fault blocks. Faulting is intimately associated with folding and has been interpredted as the result of long-term E-W compression which has continued since ORS deposition (Donovan et al, 1974). Recent work (Enfield, in progress) has demonstrated the importance of low-angle faulting in the area; some faults may have been rejuvenated at a late stage in their history.

Sampling and treatment details are shown in table 4.2. The lowest exposed formation, the Sarclet Conglomerate (site RCD43; fig 4.3) consists of a polymict assemblage of large and small sub-rounded blocks of granite, quartzite, schist and basalt, together with autochthonous sandstone fragments, in a red arkosic matrix (from which the sampled material comes). It had been hoped to sample some of the larger clasts, in particular sandstones, in order to perform a conglomerate test (Graham, 1949). This was found to be

impossible, due to restricted outcrop, extreme hardness, awkward exposure and strong tendency to fracture. The rock as a whole is very well indurated.

Table 4.2.
Lower/lower Middle ORS sediments:
Sampling details.

Site	Formation	Th	Treatment AF	Th+AF	Chem	IRM
RCD19		8		1		
RCD10		15		1	1	1
RCD44	Sarclet	6	1			
RCD45	Sandstone	7	2			
RCD46		9			1	
Sarclet Sst. total		45	3	1	2	1
RCD42	Sarclet Cong.	8	1	1	1	1
RCD43	Ellens Geo Cong.	11	1		1	1
RCD51	Hillhead Redbed	10			1	
RCD55	Ellens Geo Cong.	6	1			1
Total		80	6	3	5	4

The conglomerate is rapidly succeeded by the Sarclet Sandstone (sites RCD19-20; RCD44-46), a fairly uniform, well-cemented red arkose with occasional grit bands, which fines upwards into the Ulbster Mudstones and Sandstones (not sampled). The Ellens Geo Conglomerate (sites RCD42,55) marks a period of rejuvenation at the base of the Middle ORS (although it is included in this section due to its great similarity with underlying sediments). Source areas were somewhat different to those of the Sarclet Conglomerate below, as granitic clasts are absent; otherwise they are of a similar nature.

Also included in this section is the Hillhead Redbed (site RCD51) which marks a temporary return to fluvial sedimentation within the drab lacustrine sediments which quickly succeed the Ellens Geo Conglomerate (fig. 4.3). This is a red sandstone with high organic carbon content, bearing a general similarity to the Berriedale Sandstone with which

it is correlated (section 4.2.1.).

4.3.2. Palaeomagnetism: Previous Studies.

The Sarclet Sandstone has been the subject of several previous palaeomagnetic studies, which demonstrate the complexity of the remanence but have not satisfactorily resolved it. Waage & Storetvedt (1973) and the updated study Storetvedt & Torsvik (1983) show, on the basis of two sites (13 and 14), that remanence characteristics are essentially the result of extreme stability spectrum overlap between components of opposing polarity. Statistical details are not given, but it appears that the southerly component(s) is generally of shallow to moderately steeply upward inclination, as is the northerly component(s): i.e. they are not exactly anti-parallel (see Storetvedt & Torsvik, 1983, fig. 3b). The demagnetisation trajectory is generally along a great circle between these two directions. Tarling et al, 1976, (sites 29-31) and Eustance, 1981, (site CF5), using thermal cleaning at 250-300°C, isolated the southerly, upwards component only. Turner (1977) presents no statistical information but suggests that the remanence is dipolar and of high scatter, using this information to propose an essentially Devonian age for the magnetisation, a conclusion not apparently supported by definite evidence.

Storhaug & Storetvedt (1985) present a more rigorous analysis than most earlier studies. Component directions of both normal and reversed polarity are divided (non-statistically) into two subgroups. One is of moderately steep inclination (mean of 33°); this is proposed as a syngenetic remanence. A component of lower inclination (mean of 6°) may represent a later remagnetisation.

4.3.3. Palaeomagnetism.

Palaeomagnetic characteristics of the Sarclet Group and related rocks confirm the general findings of previous workers (see above), namely that most ancient components lie in a north-south plane. The distribution of these components (which may be of northerly or southerly declination and of variable inclination) is inhomogeneous within the sediments studied, some having a single ancient component, others being more complex. Resolution into discrete components is greatly hindered in some specimens by very high magnetic viscosity after high-temperature thermal demagnetisation, often rendering the high-T_B remanence difficult or impossible to quantify.

The four sites showing only one resolvable ancient component are RCD19, 45, 46 and 55 (table 4.3) although the latter three also tend to show an unresolved high-T_B remanence. A low-stability magnetisation, often aligned with the PEF direction, is also usually present; this has maximum T_B of around 300°C. Typical examples of demagnetisation behaviour during thermal demagnetisation are illustrated in fig. 4.6.

Characteristics of the remaining sites are perhaps best illustrated by reference to a few of the clearest examples (fig.4.7). Specimens RCD20B1K, RCD43BIF and RCD4405, for example, show a low-T_B viscous component followed at higher temperatures by a component of northerly declination and shallow, upward inclination. Above about 500-600°C, the declination changes to southerly and the inclination steepens but is still upward.

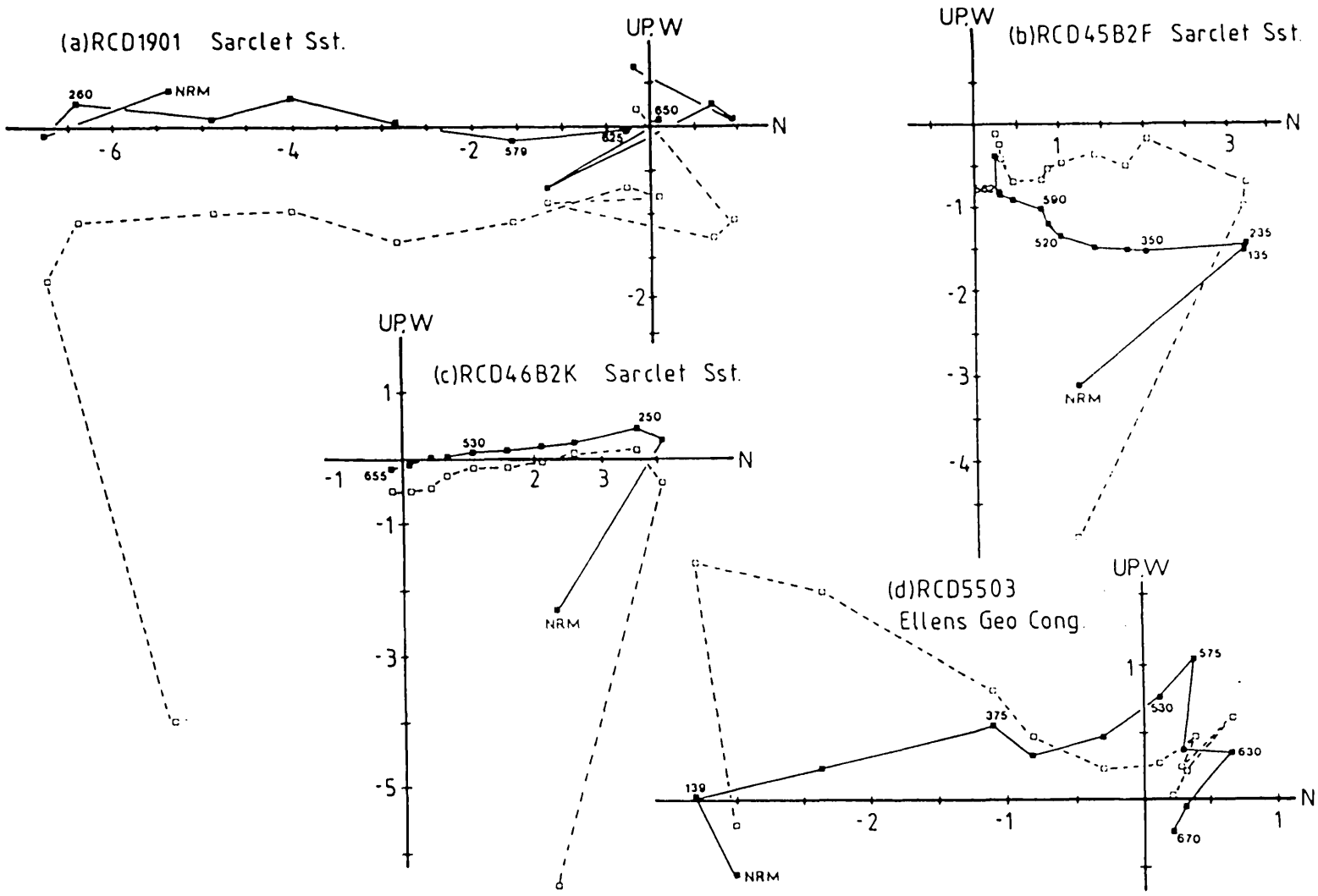


Fig. 4.6. Lower and basal Middle ORS of the Sarclet area: progressive thermal demagnetisation of samples from sites showing a single resolvable component. Illustrated as orthogonal projections (section 1.4.1). Demagnetisation temperatures in °C; axes in mA/m.

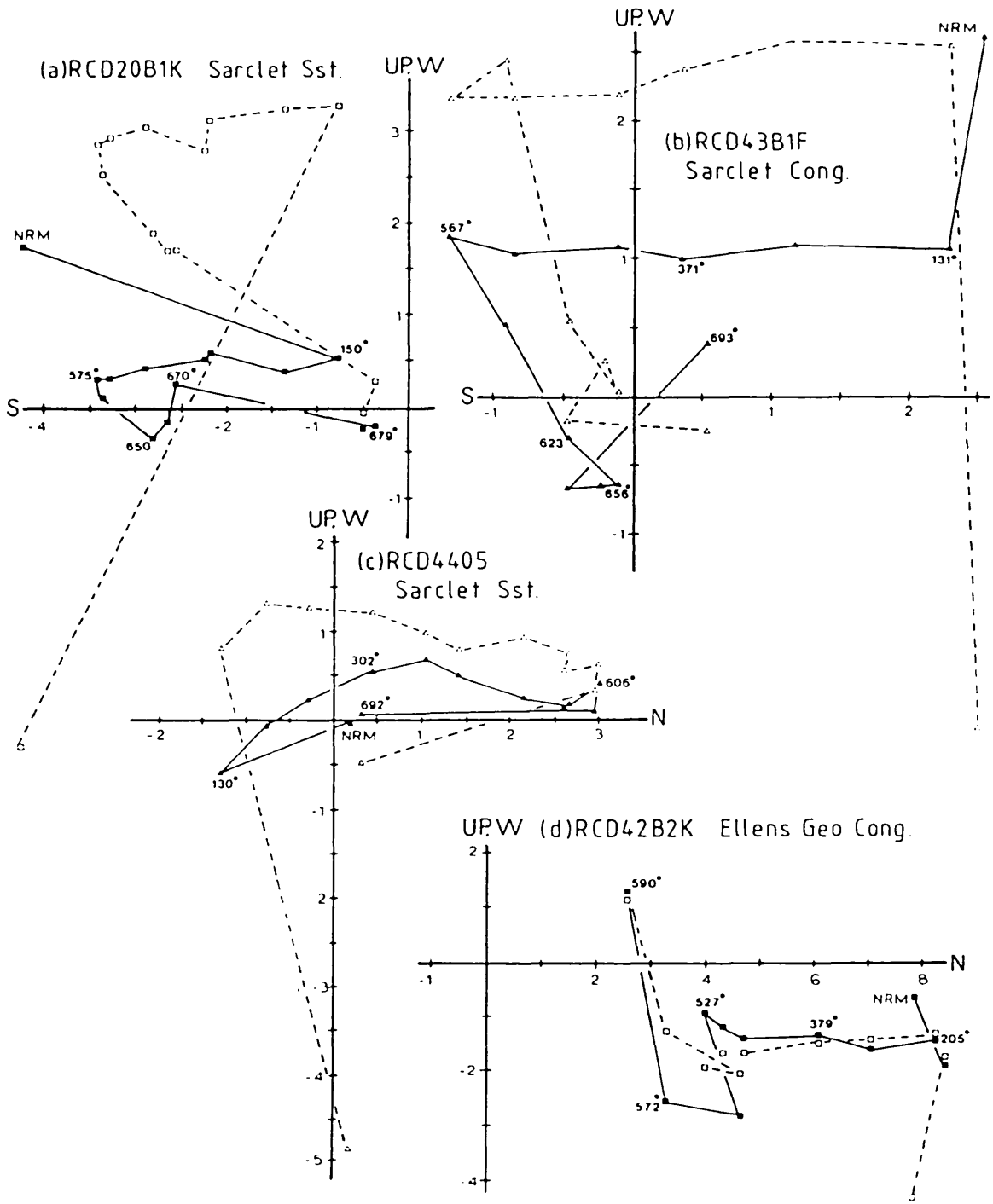


Fig. 4.7. Lower and basal Middle ORS of the Sarclet area: progressive thermal demagnetisation of samples from sites showing a multi-component remanence, illustrated as stereographic projections. Demagnetisation temperatures in °C; axes in mA/m.

Table 4.3
Lower-lower Middle ORS, Caithness:
Site mean directions.

Site	In Situ Dec.	In Situ Inc.	Dip Corrected Dec.	Dip Corrected Inc.	N	k	a_{95}
			Northerly Components				
RCD20	013.1	-13.1	(013.1	-13.1)	13	21.7	9.1
RCD42	353.2	-10.9	357.9	-16.9	6	57.2	8.9
RCD43	351.8	-8.2	353.7	-23.9	10	46.9	7.1
RCD44	003.9	-12.4	(003.9	-12.4)	3	52.7	17.2
RCD45	029.8	-8.9	(029.8	-8.9)	7	28.1	11.5
RCD46	013.5	-8.6	(013.5	-8.6)	6	15.7	17.4
Mean directions	007.6	-10.7	-	-	45	17.3	5.3
	-	-	009.0	-15.0a	45	17.7	5.2
	007.5	-10.6	-	-	6	32.4	11.9
	-	-	008.8	-14.1	6	34.5	11.6
			Southerly Components				
RCD19	178.2	1.8	(178.2	1.8)	9	42.7	8.0
RCD20	177.7	-26.1	(177.7	-26.1)	4	9.7	31.1
RCD42	215.2	-7.9	211.3	-15.9	2	-	-
RCD43	210.4	-20.5	206.2	-11.5	1	-	-
RCD44	190.8	-3.4	190.8	-3.4	4	46.5	13.1
RCD51	185.1	-23.6	181.8	-22.0	10	11.1	15.2
RCD55	178.4	-4.1	177.0	0.0	5	22.6	16.4
Mean directions	184.5	-11.1b	-	-	35^1	11.9	7.3
	-	-	**182.9**	**-7.9**	35^1	**13.9**	**6.7**
	182.1	-11.1	-	-	5^2	27.0	13.1
	-	-	183.3	-8.4	5^2	41.3	12.0

Palaeopoles: (a) Long. 167.2°E, Lat. 24.1°N (dp=6.0°, dm=11.8°)
(b) Long. 167.1°E, Lat. 34.9°N (dp=6.6°, dm=13.2°)

(1): Unit weighting to specimens
(2): Unit weighting to sites (N>4)

An example more typical of the majority of specimens is RCD42B2K, in which the lower-T_B component is easily identifiable, but randomised directional behaviour occurs at higher temperatures, presumably due to thermochemical alteration during demagnetisation. There are, however, no significant net changes in bulk IRM characteristics between thermally treated and untreated specimens. The behaviour described above is thus probably due to very small amounts of highly viscous material which do not have a detectable effect on bulk properties.

Stereographic projections (fig. 4.8) clearly show the

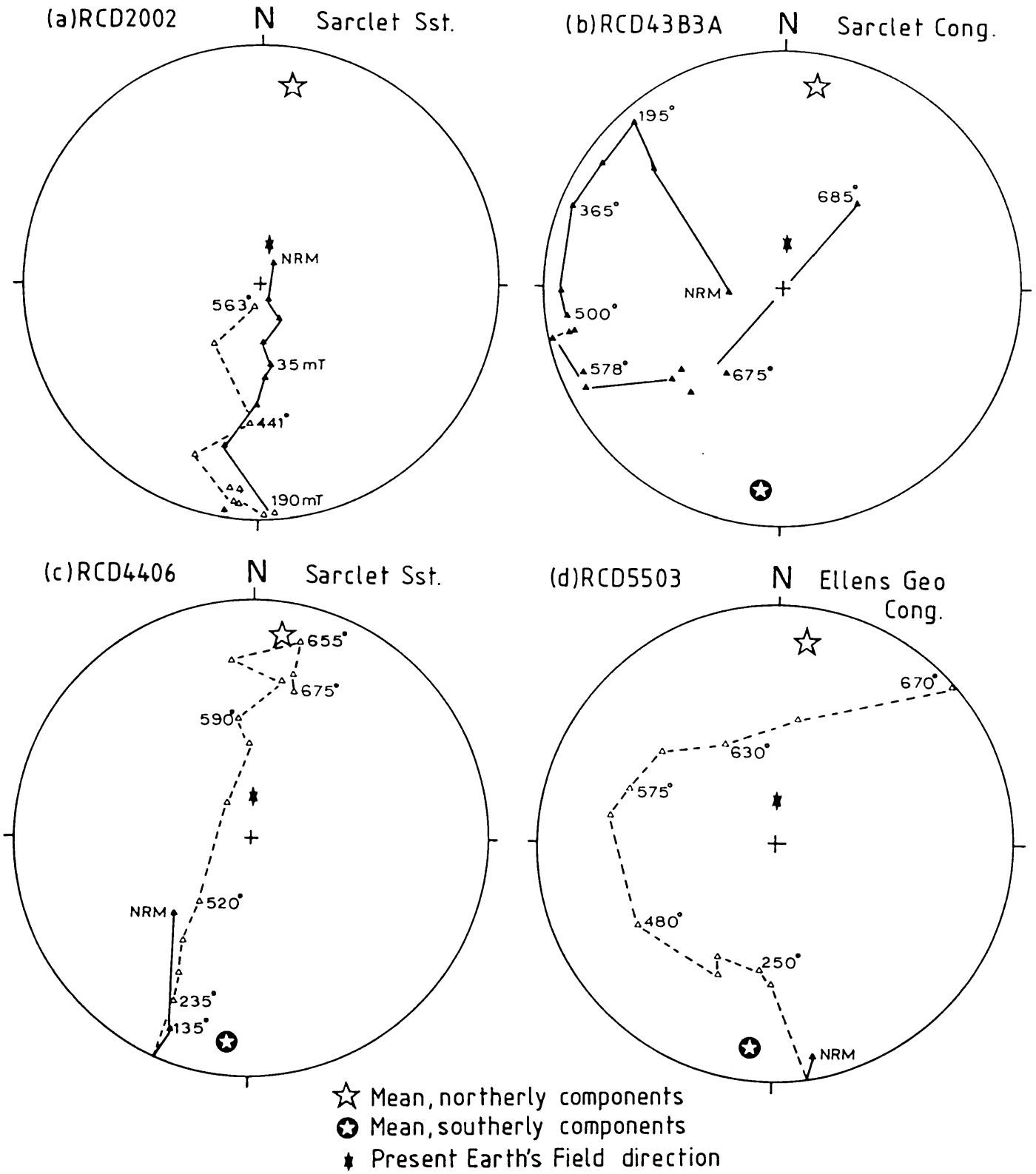


Fig. 4.8. Lower and basal Middle ORS of the Sarclet area. Multi-component remanences, illustrated as stereographic projections. Demagnetisation temperatures in °C.

nature of the remanence. The demagnetisation trajectory is usually confined to a N-S plane; this may have any inclination between 0 and 90°. There may be a stable direction at high and/or low temperature, but more typically only a portion of the full great circle is seen; this suggests severe T_B overlap between the two (or more) components present.

A few specimens were AF demagnetised (table 4.2); this was generally an ineffective method of multi-component separation. It was sometimes able, however, to selectively demagnetise recently-acquired PEF components, as illustrated in fig. 4.8a, in which AF demagnetisation was followed by thermal. The PEF component can be seen to survive a demagnetising field of up to 190 mT.

Chemical demagnetisation was found to be totally ineffective, as with most other sediments studied.

All resolvable component directions are illustrated stereographically in fig. 4.9, in which directions included in formation means are distinguished from those considered as spurious. Many of these spurious directions presumably result from severe T_B overlap of two or more stable components, including the PEF direction.

It would appear that most components fall into two main groupings, one of northerly declination, one of southerly. The former is almost certainly a single population, as shown by fig. 4.10 which illustrates a contoured distribution of all components of negative inclination (using the STATIS program: Woodcock, 1977). There is an approximately Fisherian distribution around the calculated mean northerly direction. Southerly components show a peak around an almost horizontal inclination.

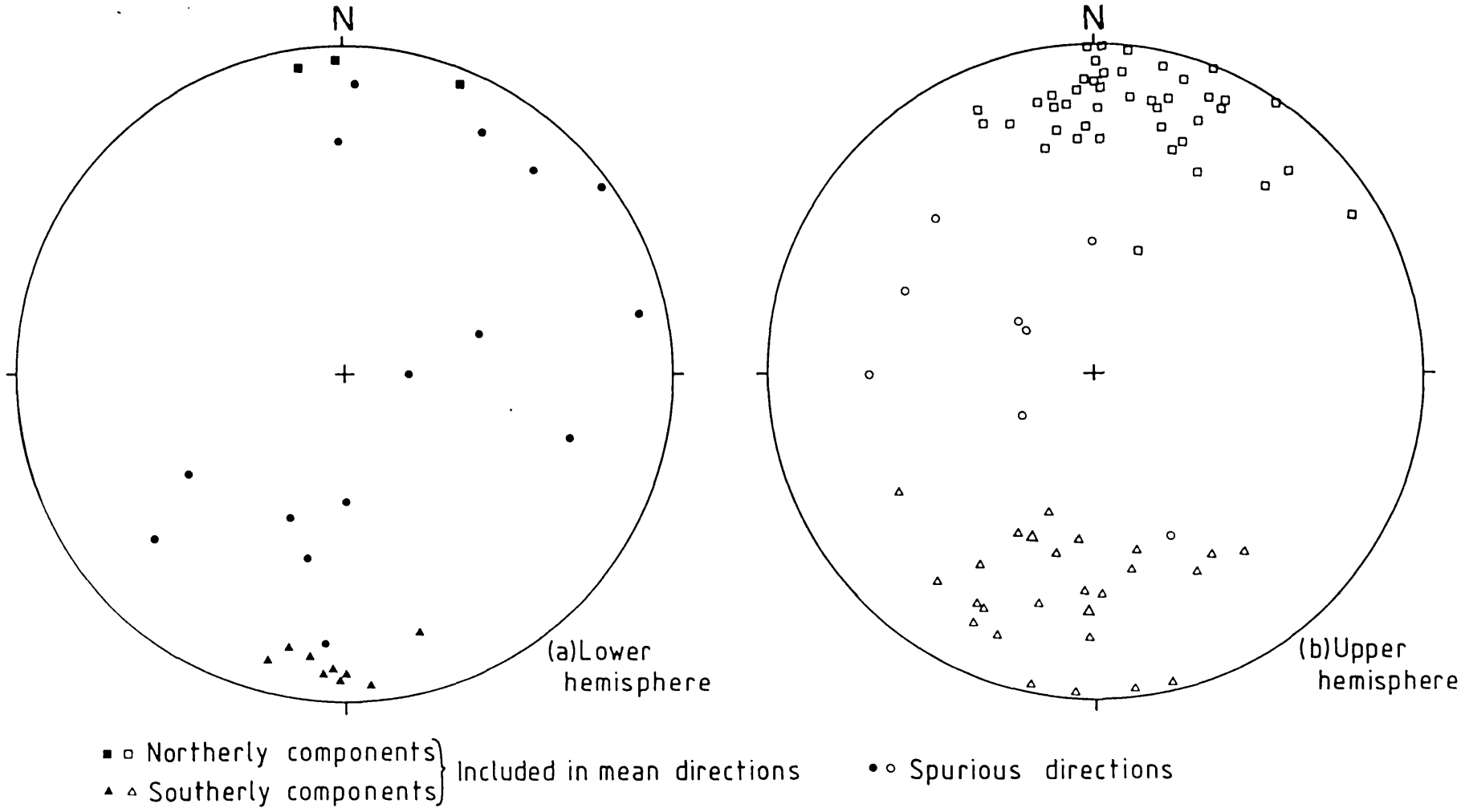


Fig. 4.9. Lower and lower Middle ORS of the Sarclet area: all valid stable components, illustrated as stereographic projections.

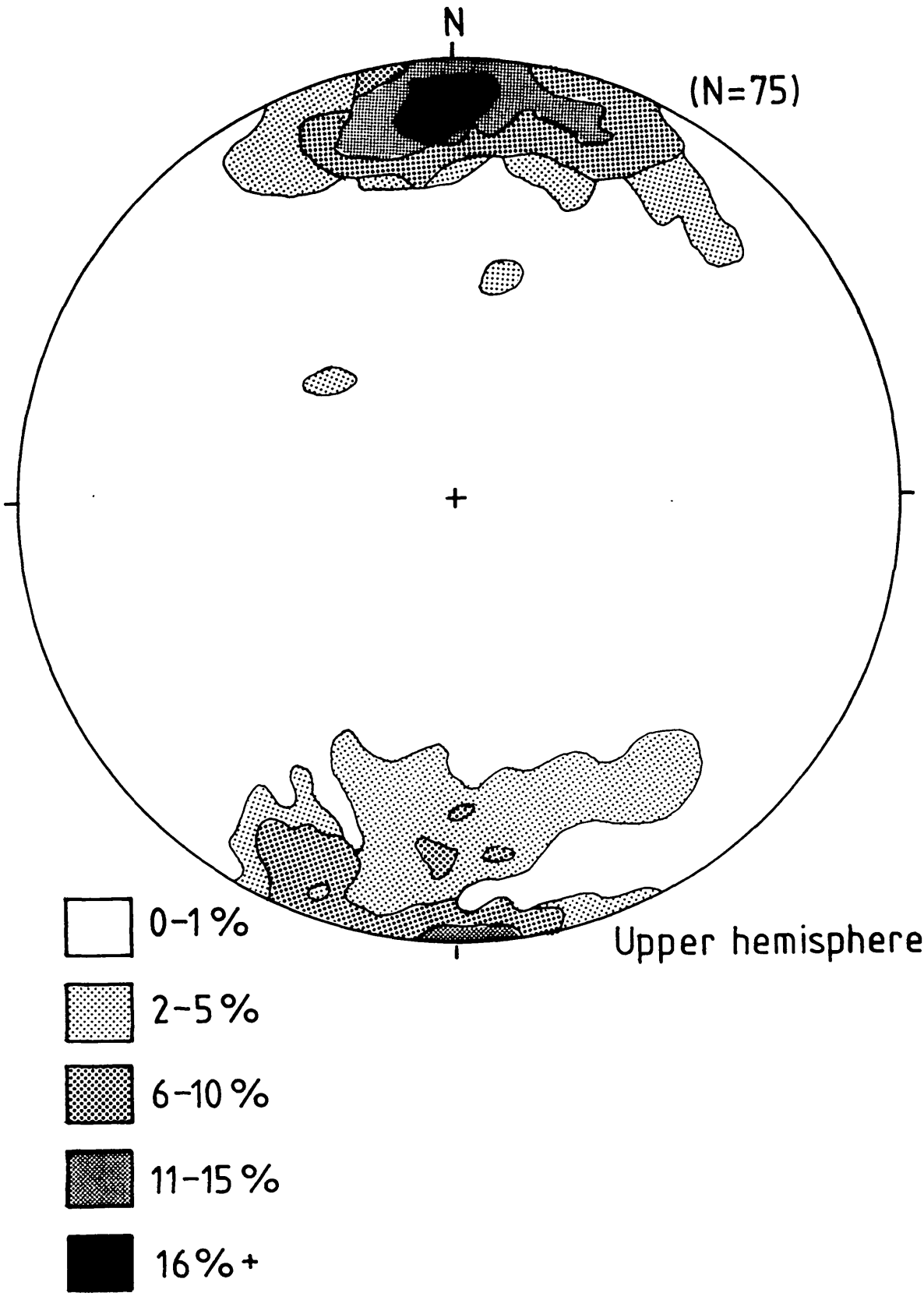


Fig. 4.10. Lower and basal Middle ORS of the Sarclet area: all components (upper hemisphere only), contoured using the STATIS program (Woodcock, 1977). Uses the distribution illustrated in fig. 4.9. Shows a pronounced peak of northerly declination and a more dispersed area of southerly declination.

Unfortunately the number of components of positive inclination is insufficient to produce a corresponding contoured distribution. The majority are of southerly declination with a low inclination (0-10°) but a few (5-7) have a more steeply downward inclination. It is not clear whether these form a distinct population representing an ancient remanence or if they result from a large degree of T_B-overlap with another component, possibly a PEF direction resulting from recent weathering. Due largely to the fact that there are never more than one or two such components from this sub-group in any one site they cannot be distinguished from a random remanence; they are not considered in greater detail or treated statistically. Further work, however, may confirm that they are part of a meaningful and significant population.

Site mean directions for both northerly, upward and southerly, low-inclination components are given in table 4.3. Only four of the nine sites have a tectonic dip and this is generally low, so there is no statistical difference between *in situ* and dip corrected mean directions.

Details of maximum blocking temperatures and IRM characteristics are given in table 4.4. It would appear that the dominant remanence carrier is hematite as maximum T_B is often above 600°C and magnetic saturation does not occur below 1T. However, the northerly component in several sites (RCD20, 42 and 43) has a maximum T_B resembling the T_C of magnetite and there is often a slight point of inflexion during IRM determination corresponding to an applied field of about 200 mT. Magnetite may thus be present, although in some cases, possibly all, all components appear to be carried by hematite, often with much T_B overlap.

Table 4.4
Sarclet Group: Rock Magnetic Properties.

Site	Max. T_a (N-)	Max. T_B (S-)	B_S	M_r (mA/m)	B_c (mT)
RCD19	-	590-660	-	-	-
RCD20	530-600	560-625	-	9000	220
RCD42	520-560	460-520	-	8600	230
RCD43	560-595	(558)	-	8100	210
RCD44	560-692	589-662	-	-	-
RCD45	560-692	-	-	-	-
RCD46	558-655	-	-	-	-
RCD51	-	570-640	-	-	-
RCD55	-	530-565	-	3400	280

4.3.4. Age of the remanence.

Site mean directions, both *in situ* and dip corrected, for the northerly and southerly components are illustrated in fig. 4.11, together with overall mean directions and associated error circles. It is apparent that the two directions are both in the same hemisphere, i.e. they are not exactly antiparallel. That they represent discrete populations can be demonstrated using the test of McFadden & Lowes (1981). It is shown below that each of the directions is statistically distinct from the opposite polarity of the other with greater than 95% confidence.

Comparison of the two groups of direction suggests that the southerly component probably represents a secondary remanence; it also has a similar palaeopole position to other sediments elsewhere in the basin which can be shown to have been remagnetised. The pole falls on a significantly post-Devonian portion of the NW European polar wander path discussed in chapter 9. These results should be compared with those of Storhaug & Storetvedt (1985); this also suggests an essentially similar history of remanence acquisition.

The northerly remanence probably predates the

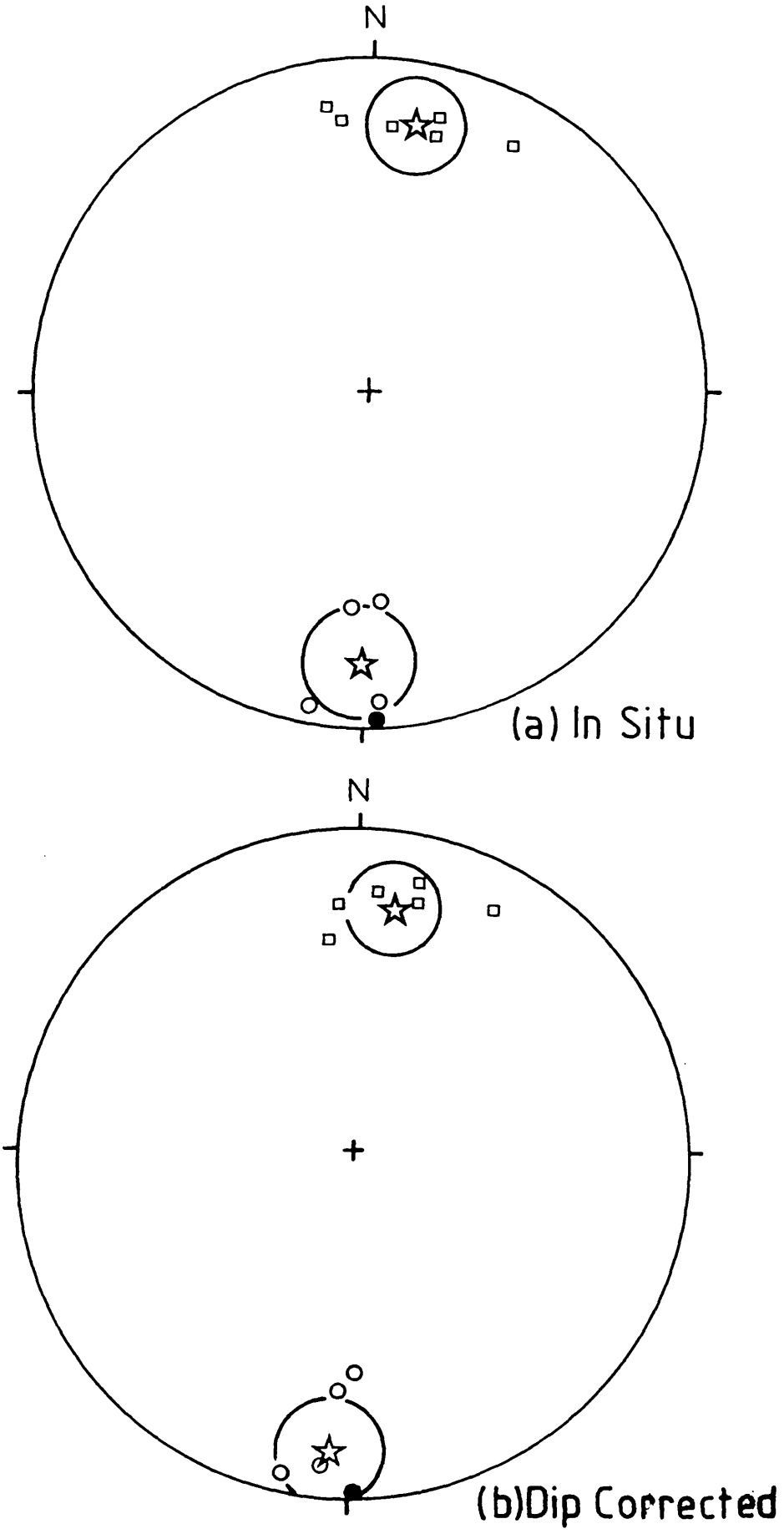


Fig. 4.11. Lower and lower Middle ORS of the Sarclet area: site mean directions, both in situ and dip corrected. Statistics given in table 4.3.

Discrimination of northerly and southerly components:

Southerly components: $N_1=5$ $k_1=33.7$ $R_1=4.88128$

Northerly components: $N_2=6$ $k_2=32.4$ $R_2=5.84584$

Combined: $N=11$ $R=10.58335$

$r = k_2/k_1 = 0.961$

Using the test of McFadden & Lowes (1977);

$$\frac{r\left[(R_1+R_2)^2 - R^2\right]}{2\left[(N_1-R_1) + r(N_2-R_2)\right](R_1 + rR_2)} > \left(\frac{1}{p}\right)^{1/N-2} - 1$$

LHS=0.525, RHS=0.395: i.e. the groups are statistically distinct with 95% confidence.

If LHS=RHS, then $\left(\frac{1}{p}\right)^{1/N-2} - 1 = 0.525$, i.e. $p=0.022$.

The test is thus significant at the 98% significance level.

---

southerly; it may thus represent an original magnetisation or possibly an earlier remagnetisation. Comparison of the corresponding palaeopole with other postulated primary palaeopoles for the Lower ORS (such as the Midland Valley lavas) shows that it is not in very good agreement, particularly with respect to magnetic declination. This difference may be accounted for, at least partially, by the younger age of the Sarclet sequence (upper Emsian) compared with the Midland Valley lavas (Ludlovian-Geddinian). This

will be discussed further in chapter 9.

4.4 The Eday Group: Geology and Sampling.

4.4.1. Sedimentology.

Sediments of the Eday Group (Mykura, 1976; Wilson et al, 1935) constitute the majority of the clastic sediments of the Orkney Islands, along with the Upper ORS (restricted to Hoy) and the Yesnaby Sandstone (Lower ORS) of Western Orkney. Outcrop area is limited to the southern and eastern parts of the islands (fig. 4.12). Sedimentation, largely restricted to a NE-SW trending basin, was predominantly fluvial. The basin has been interpreted as a fault-bounded graben, with sediment transport predominantly to the NE, although some areas show E-W palaeocurrents suggesting clastic input from the western flanks of the graben (Ridgway, 1974). It is interesting to note that the orientation of the graben is parallel to the major lineation marked by Permo-Carboniferous igneous activity (fig. 8.1) which probably marks a period of fault rejuvenation.

The origin of the graben may be related to updoming above an upwelling 'hotspot' (Bott, 1981) which also produced the intrusive and extrusive upper Middle ORS igneous activity centered on west Shetland (Astin, 1982; see section 3.2.1).

The total thickness of around 1000m can be subdivided into three coarse clastic units (the Lower, Middle and Upper Eday Sandstones) and two finer grained units (the Eday Flags and Eday Marls; fig. 2.2) although these subdivisions are highly diachronous (fig. 4.13). The lower units have been correlated with the John o'Groats Sandstone of Caithness (chapter 8) on the basis of the faunal assemblage of the Eday Flags (Wilson et al, 1935).

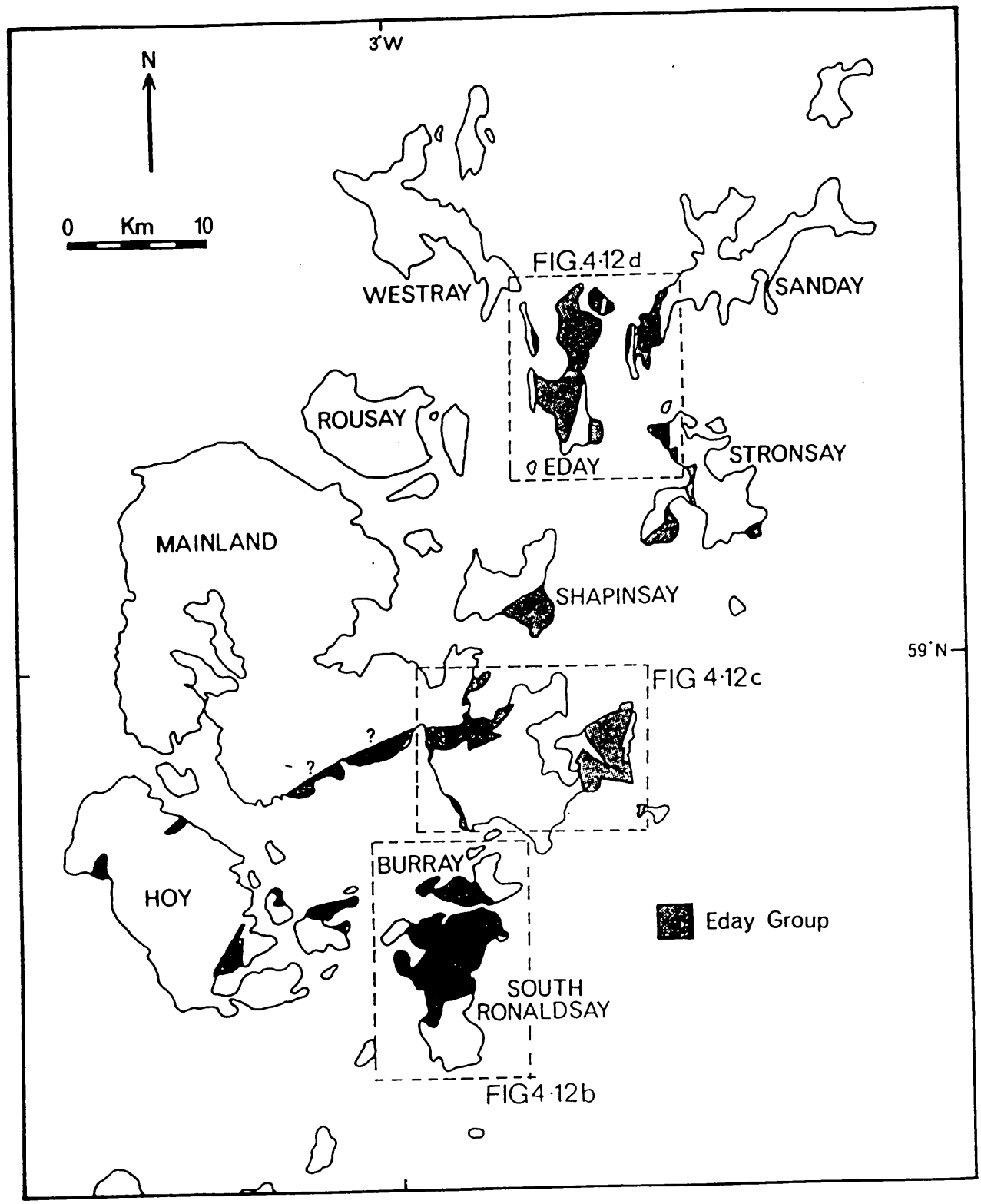


Fig. 4.12a. Eday Group: location maps.

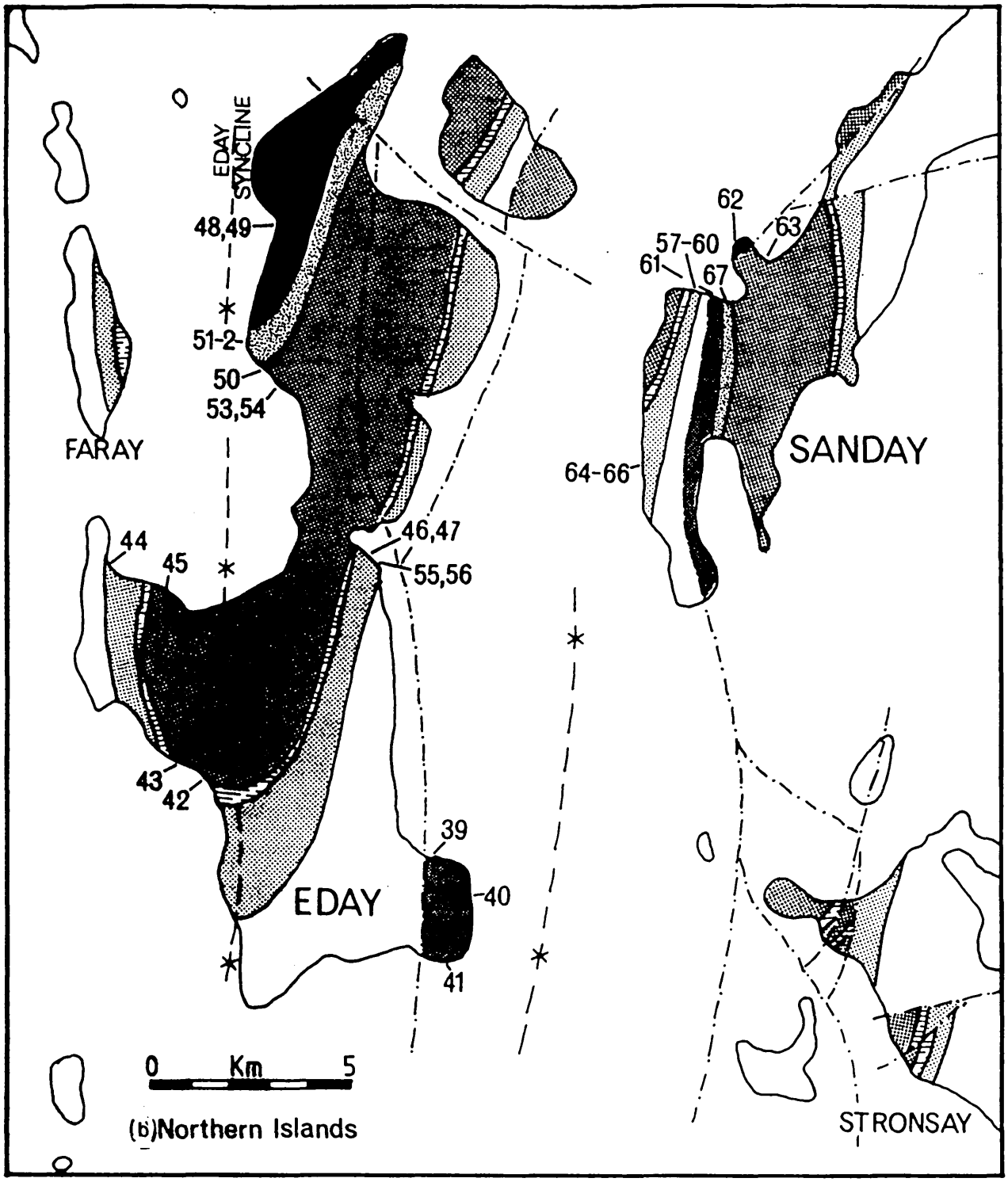


FIG.4.12b. Eday Group: site locations, northern islands of Eday and Sanday.

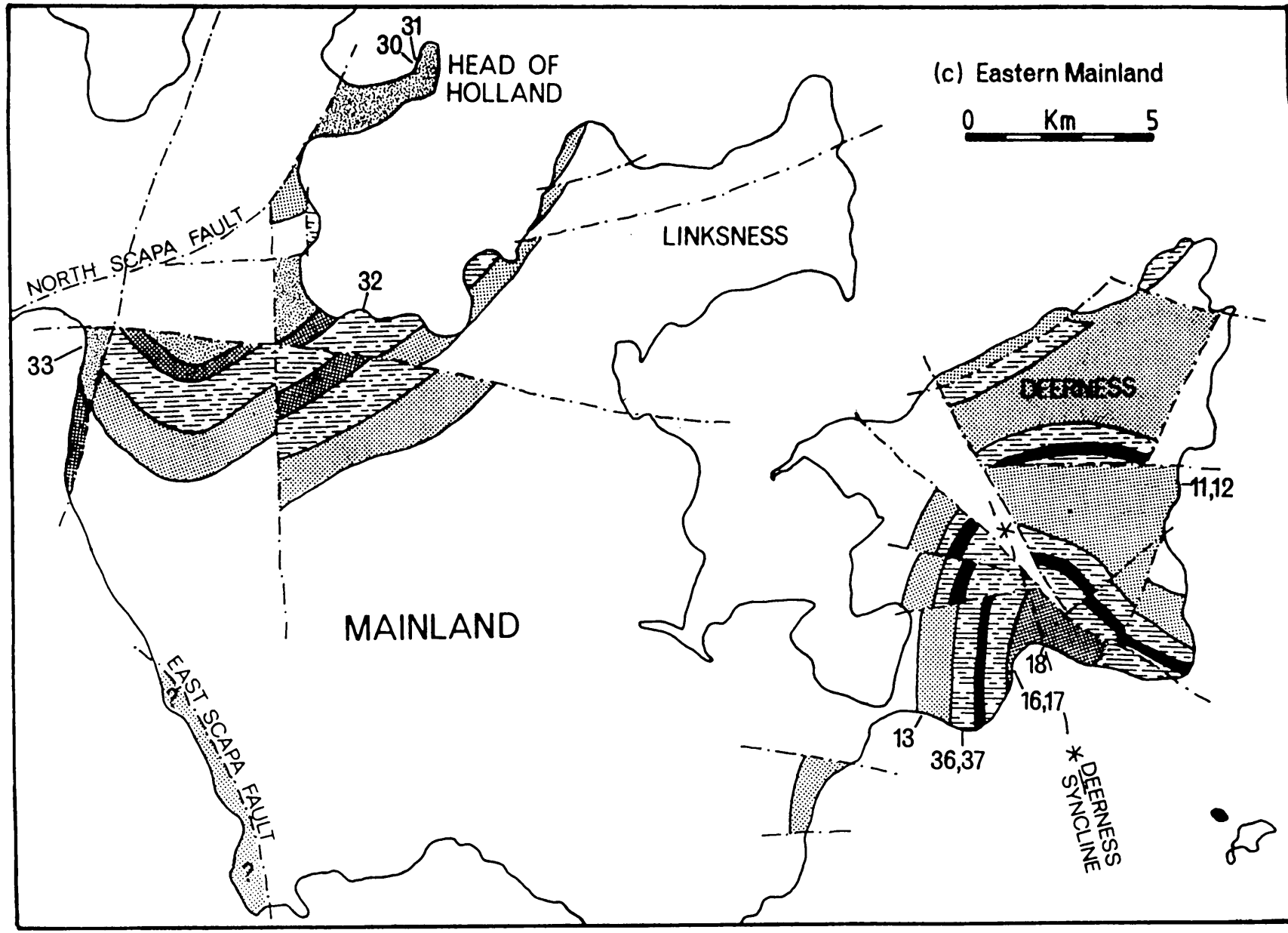


Fig. 4.12c. Eday Group: site locations, eastern Mainland Orkney. For key see fig. 4.12b.

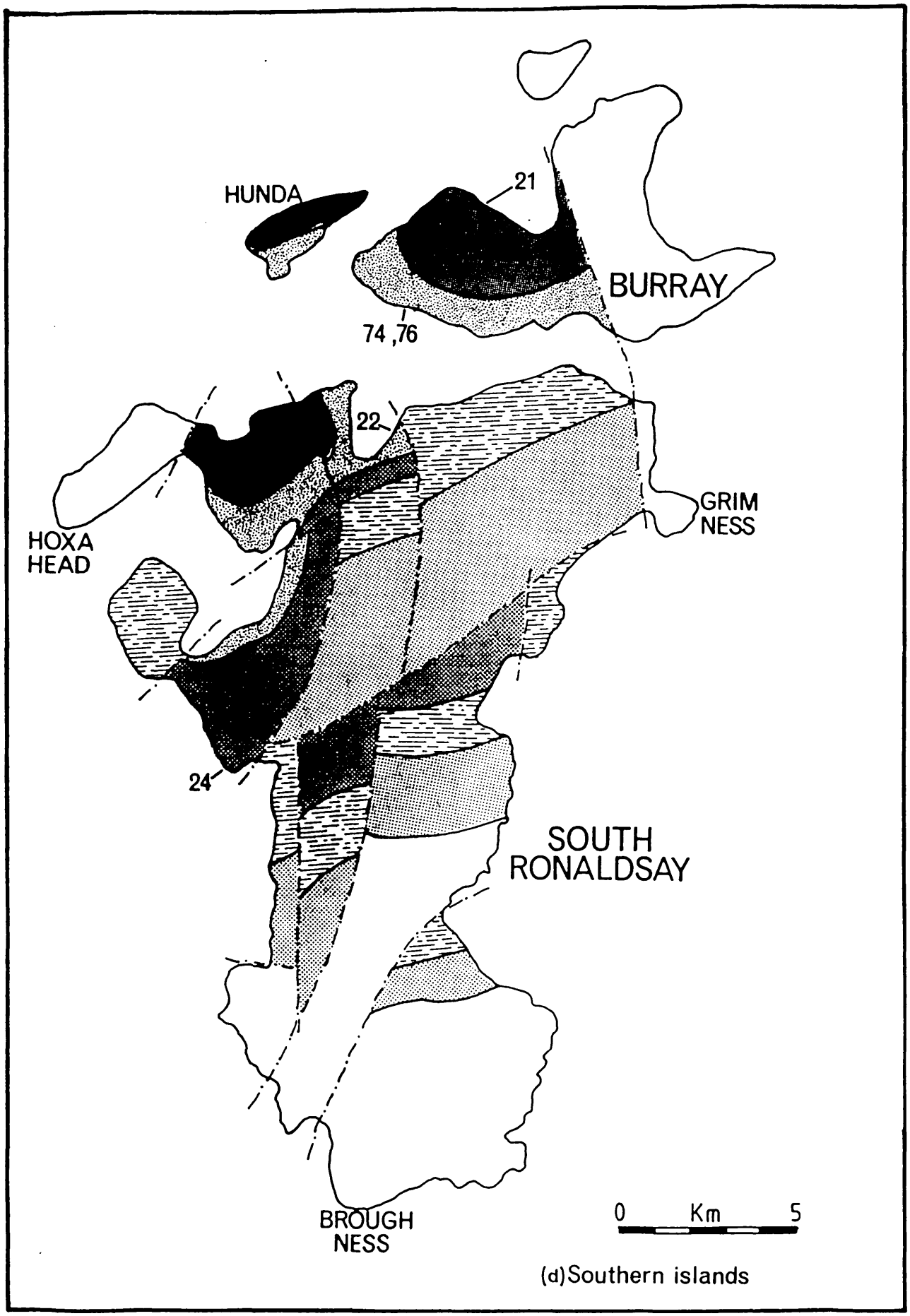


Fig. 4.12d. Eday Group: site locations, southern islands of Burray and South Ronaldsay. For key see fig. 4.12b.

Stratigraphy, detrital petrology and sedimentology of the Eday Group are discussed in detail in Ridgway (1974) and also in the regional memoirs (Mykura, 1976; Wilson et al, 1935). From these and field observations relevant details will be given for each of the five units in turn.

(i) Lower Eday Sandstone. This is probably the most variable unit of the five, both laterally and vertically. It is the subject of a very intensive palaeogeographic study by Astin (1985), to which reference should be made.

Outcrop in the Northern Isles (Eday and Sanday) can be subdivided into two. The lower part, (facies A of Ridgway, 1974), is a purple to red sandstone with lenses of coarse polymict conglomerate, interpreted as lag deposits (Mykura, 1976). Transition from the underlying Rousay Flags (plate 2.1c) is gradual, with interbedded lacustrine and aeolian facies (the Passage Beds of Wilson et al, 1935). The upper beds are typically yellow, pink or white medium-grained sandstones (facies B), generally devoid of pebbles and showing large-scale cross-bedding. Colour banding is common. Facies C, a more uniform, well-indurated yellow sandstone, is restricted to the southern islands of Mainland, Stronsay and South Ronaldsay. Liesegang rings are common (as in the Bay of Skaill and Taracliff Bay, Deerness). Occasional bands of fine calcareous shales and silts, sometimes with fish remains, are found at the southern limits of the formation.

(ii) Eday Flags. These are discussed in chapter 3, together with the extrusive volcanic rocks occurring within them. Transition, both from the Lower Eday Sandstone below and into the Middle Eday Sandstone above, is highly diachronous, resulting in large apparent thickness variations from north to south. The sediments are the product of restricted high-

sinuosity channels and floodplain lakes, and are predominantly drab or grey-brown in colour. Reddening is not apparent.

(iii) Middle Eday Sandstone. This is the dominant unit in the northern islands, where it forms up to 400m thickness; this thins to only 90m in South Ronaldsay (fig. 4.13). Grain size increases both to the north and south from Deerness; the extreme development of this is the very coarse polymict conglomerate of Hegglie Ber, Sanday, which includes lava clasts presumably derived from the Eday Lavas below. Colouration is a fairly uniform red or purple, occasionally yellow in the south. Most sediments are of fluvial origin, with interbedded sheet sands and finer-grained overbank deposits of sandy mudstone (plate 2.1a). Resemblance to the overlying Eday Marls increases towards the top of the group, the two sometimes being indistinguishable.

(iv) Eday Marls. The Eday Marls are typically bright red or green, particularly when fine-grained. Rhythmic fining-upwards cycles are the result of meandering streams with overbank deposits. Thickness decreases progressively to the north, although this may be due in part to the similarity with upper horizons of the Middle Eday Sandstone. Average grain size decreases towards the middle of the formation.

(v) Upper Eday Sandstone. Northern outcrops can be subdivided into a lower red/yellow sandstone, occasionally pebbly (resembling the Middle Eday Sandstone); this fines upwards into a red or purple marly sandstone. Outcrop in the southern islands is a less well-indurated sandstone/marl of more variable colouration (red, pink, yellow, green).

Coarser-grained deposits of the Eday Group have been

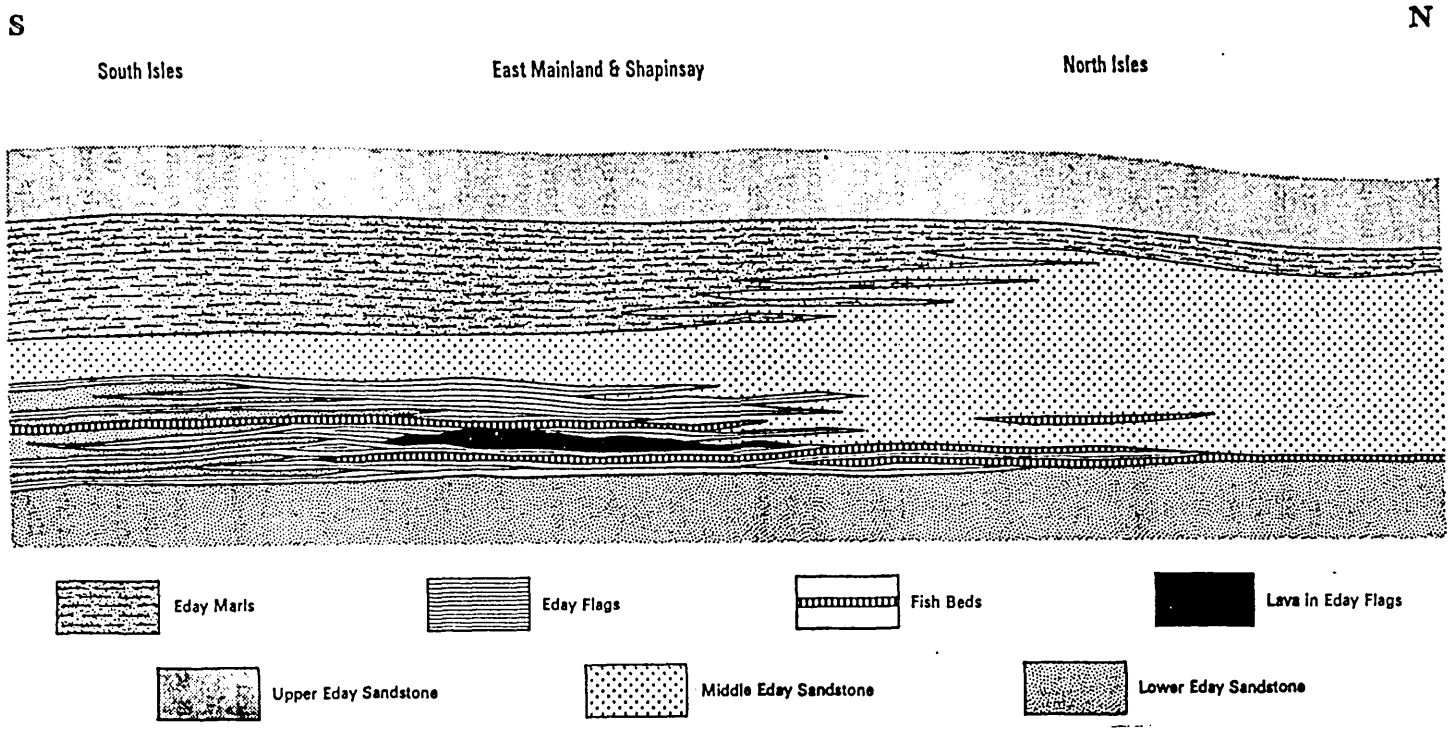


Fig. 4.13. Schematic representation of lithological variation within the Eday Group. After Mykura (1976), fig. 20. Length of section about 60km.

WATTS LIBRARY

interpreted as predominantly of fluvial origin; finer-grained members as overbank or floodplain deposits. Larger-scale variations, such as the period of reversion to lake-dominated processes in the Eday Flags, are the result of relative changes in lake water level, which may either be due to climatic change or related to local fault movements.

Petrological and diagenetic characteristics of the sediments referred to in this chapter will be discussed in chapter 6, particularly where relevant to possible models for the origin of the remanence.

4.4.2. Sampling

Within the constraints of accessibility and degree of exposure, an attempt has been made to sample a broad range of facies within the group, over much of its geographic range. Sampling and treatment details are summarised in table 4.5.

As will become apparent in the remainder of this chapter, a number of sites have been collected from outcrop which would not appear to be an obvious first choice from the point of view of an investigation of stable ancient remanence. Such sites serve as a useful comparison with those sites found to be palaeomagnetically reliable. This applies particularly to a number of sites in lightly-coloured (white-fawn-buff) sandstones which may often be weakly magnetised (such as much of the Lower Eday Sandstone).

Paucity of fresh inland exposure dictates that the majority of sites are from inter-tidal or supra-tidal coastal outcrop. Such sites tend to be vulnerable to recent oxidative weathering, which in many cases has obscured or replaced any earlier remanence. These effects are enhanced

TABLE 4.5
EDAY GROUP: CLASTIC SEDIMENTS

(a) Sampling details

	LES	MES	EM	UES
Eday	5	6	2	5
Sanday	7	1	1	2
Central Mainland			3	
Deerness	3	3		
Burray			2	1
S. Ronaldsay		1	1	

(b) Treatment details

	Sampling		Treatment		
	No. of sites	No. of samples	None	Thermal	AF
UES	8	114	64	48	2
EM	9	111	47	59	5
MES	11	135	58	70	7
LES	15	183	112	67	4
Total	43	543	281	244	18

by groundwater percolation, as this is often acidic (and hence highly corrosive) after passage through the extensive peat deposits which cover much of the islands.

4.5. Eday Group: Palaeomagnetism.

4.5.1. Introduction.

Palaeomagnetic characteristics of the 43 sites in clastic sediments from the Eday Group are extremely varied, reflecting large contrasts in such factors as lithology, porosity, permeability, grain size, cementation, original conditions of deposition, geographic and stratigraphic position and type of exposure. The large number of sites studied means that each one cannot be discussed individually. The approach used, therefore, will be to discuss typical examples of each of the major classes of magnetic behaviour and to present most information in tabulated form.

The majority of specimens have been treated by progressive demagnetisation (predominantly thermal, with some AF and chemical) although a few specimens from sites showing stable single-component magnetisations have been treated by a single-step cleaning technique.

All stable components have been plotted stereographically and contoured using the STATIS program (Woodcock, 1977) as illustrated in fig. 4.14. This shows that there are four main groupings of palaeomagnetic orientation, of which two are distinct and two have a degree of overlap. These are:

(i) A Components. These are of southerly declination, shallow to moderately steeply downward inclination. This group has a degree of overlap with (iii).

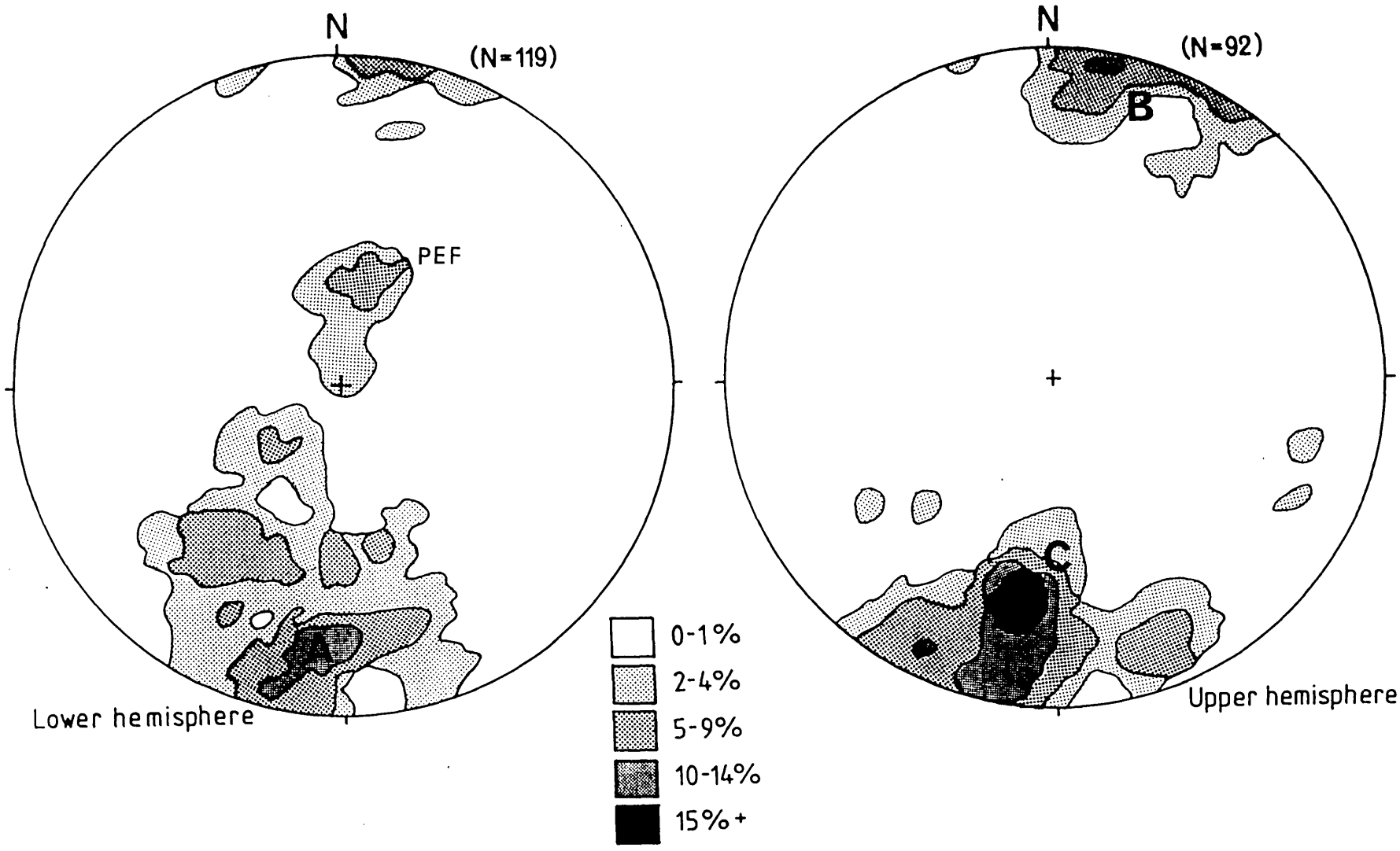


Fig. 4.14. Eday Group: all stable components plotted on stereographic projections and contoured using the STATIS program of Woodcock (1977). See discussion in section 4.5.1., para.3. Main component groups shown as A, B, C and PEF.

(ii) B Components. Northerly declination, shallow, generally upward, inclination.

(iii) C Components. Southerly declination, shallow to moderately steeply upward inclination. This group has a pronounced peak around an inclination of about -20°.

(iv) Northerly declination, steeply downward inclination.

Of these four groups, the first three are considered to represent ancient components; they will be referred to as A, B and C components respectively. The fourth group bears a strong resemblance to the PEF and thus presumably represents a recent remagnetisation.

Components which lie outside the four groups referred to above are rejected as anomalous, resulting from stability spectrum overlap of more than one stable component, a recently-acquired IRM, laboratory-induced remanence or possibly occasional misorientation during field collection. They will not be considered in any more detail.

The only apparent ambiguity is in distinguishing groups A and C, both of southerly declination but with an inclination spread of between $+70^{\circ}$ and -60° It is crucial to determine whether this spread is due to the presence of discrete component groups or, alternatively, to severe but variable degrees of T_B/coercivity overlap between a component directed upwards to the south and the PEF.

Fortunately, a few specimens show a multicomponent remanence (fig. 4.15), with components directed both upwards and downwards to the south. These directions are given in table 4.6, from which it may be seen that they are readily divisible into two groups, one group having a low to steeply downward inclination and the other being generally

Table 4.6

Eday Group: Multi-component remanence directions.

Specimen	'A' component I.S. Dec	Inc	'A' component D.C. Dec	Inc	'C' component I.S. Dec	Inc	'C' component D.C. Dec	Inc	N	R	k	a_{95}
1701 MES	209.3	44.5	190.7	52.2	208.9	-5.2	208.9	4.9				
2201 EM	183.5	64.1	199.6	71.6	149.7	-13.8	149.7	-3.8				
2205 EM	217.6	72.2	250.1	73.3	190.3	-7.5	189.8	0.1				
2206 EM	221.2	73.7	256.2	73.9	211.9	-4.3	211.6	0.4				
3103B EM	185.0	55.0	172.6	30.4	192.5	-0.7	196.3	-20.9				
3104A EM	212.0	17.3	207.5	2.9	193.9	-22.4	207.4	-40.4				
3104C EM	226.6	30.5	213.6	20.7	193.1	-4.1	198.1	-23.8				
3105B EM	160.0	50.0	156.9	22.2	181.6	-29.9	197.3	-51.8				
3106C EM	180.0	50.0	170.6	24.5	185.0	-2.0	189.0	-24.5				
3907C UES	170.4	5.7	144.3	38.5	157.7	-12.4	154.3	18.2				
4801A UES	223.3	44.4	241.2	40.0	221.7	-48.6	200.1	-45.3				
4802B UES	160.3	34.6	171.2	50.9	190.6	-31.8	182.2	-20.6				
	194.1	48.0	-		-		-		12	10.805	9.2	15.1
	-		186.8	45.8	-		-		12	10.325	6.6	18.3
	-		-		189.2	-15.9	-		12	11.032	11.3	13.5
	-		-		-		190.0	-18.2	12	10.644	8.1	16.2

Formations: UES = Upper Eday Sst EM = Eday Marls
MES = Middle Eday Sst LES = Lower Eday Sst

Test for distinct groupings (McFadden & Lowes, 1981) (In Situ)

$$\frac{r\left[(R_1+R_2)^2 - R^2\right]}{2\left[(N_1-R_1)+r(N_2-R_2)\right]\left[R_1+rR_2\right]} > \left(\frac{1}{p}\right)^{1/N-2} - 1$$

where $r=k_2/k_1=1.233$ $R_1=10.80522$ $N_1=12$
$p=0.05$ $R_2=11.03184$ $N_2=12$
$R=18.50821$ $N=24$ $(=\sum N_i)$

L.H.S.=1.41 i.e. the two groups are statistically distinct.
R.H.S.=0.15

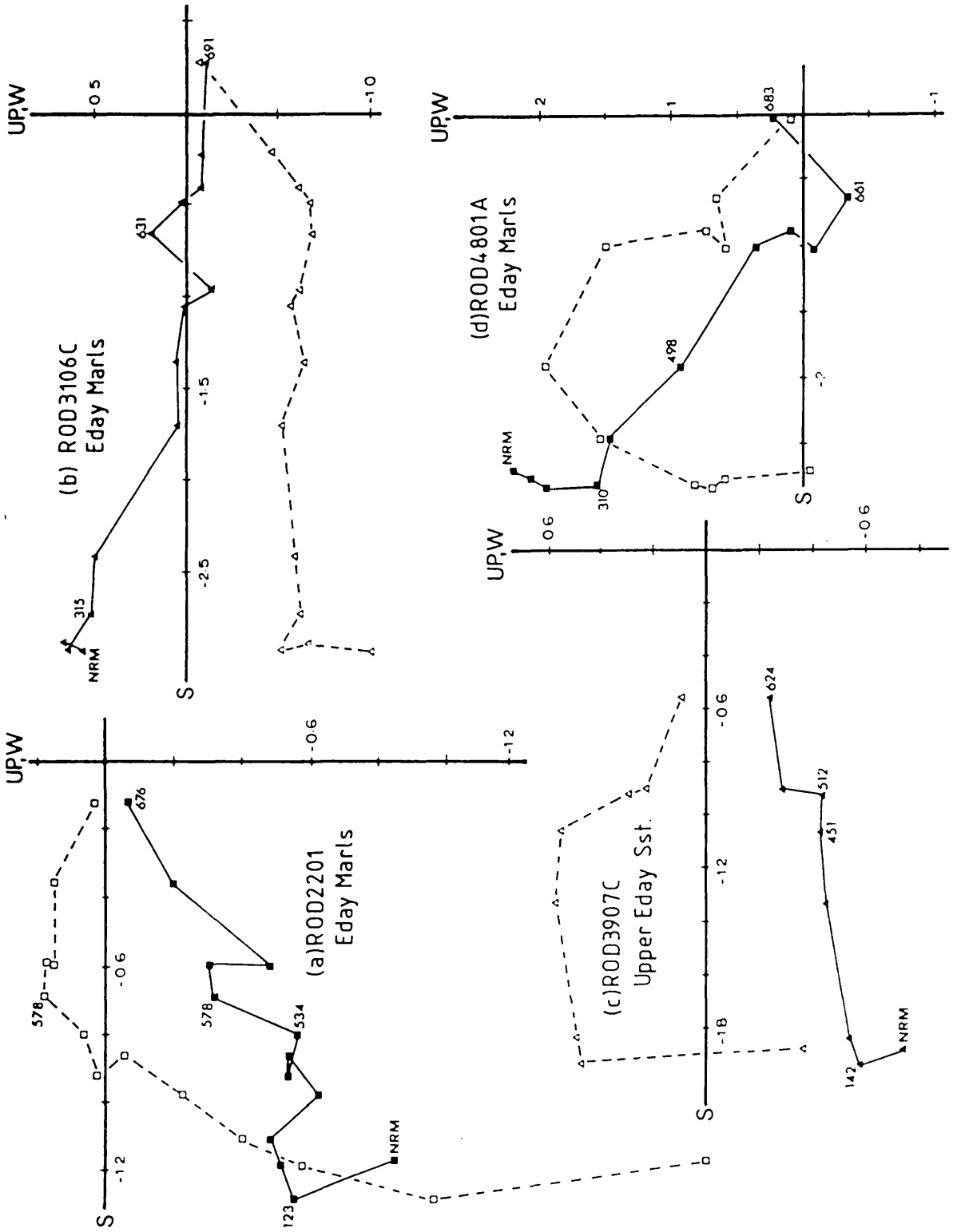


Fig. 4.15. Eday Group: Specimens showing a possible multi-component remanence (A and C components). Orthogonal projections (section 1.4.1); demagnetisation temperatures in °C, axes in mA/m.

of upward inclination. It should be noted, however, that neither group is exclusively of higher or lower T_B range than the other. The two groups are statistically distinct (using the test of McFadden & Lowes, (1981).

It would thus appear that it is valid to consider components of southerly declination to be divisible into two distinct groups on the basis of magnetic inclination variation. However, the assignation of a particular component direction to one group or the other is not always straightforward, as suggested by the inclination range overlap between groups A and C shown in fig. 4.16. For specimens with inclinations in the range approximately between $+20^{\circ}$ and -20°, other factors must therefore be taken into account.

Such factors include (i) the effects of tectonic dip correction, since it is suggested below that the A magnetisation is pre-tectonic while the C magnetisation is largely post-tectonic (ii) mineralogy of the phases responsible for carrying the remanence as revealed by IRM analysis, T_B spectra and mineralogical investigations: see chapter 6 and (iii) comparison with other specimens from the same site or other sites of similar lithology nearby. However, a degree of ambiguity is inevitable for some specimens, particularly in sites for which tectonic dip correction causes movement from a palaeomagnetic orientation resembling one group (or the PEF) to one resembling another group. Specimens or sites for which such ambiguities exist will be specifically identified and discussed.

Characteristics of each of the three groups of ancient component will now be discussed individually, followed by a general discussion of the nature and age of the remanence.

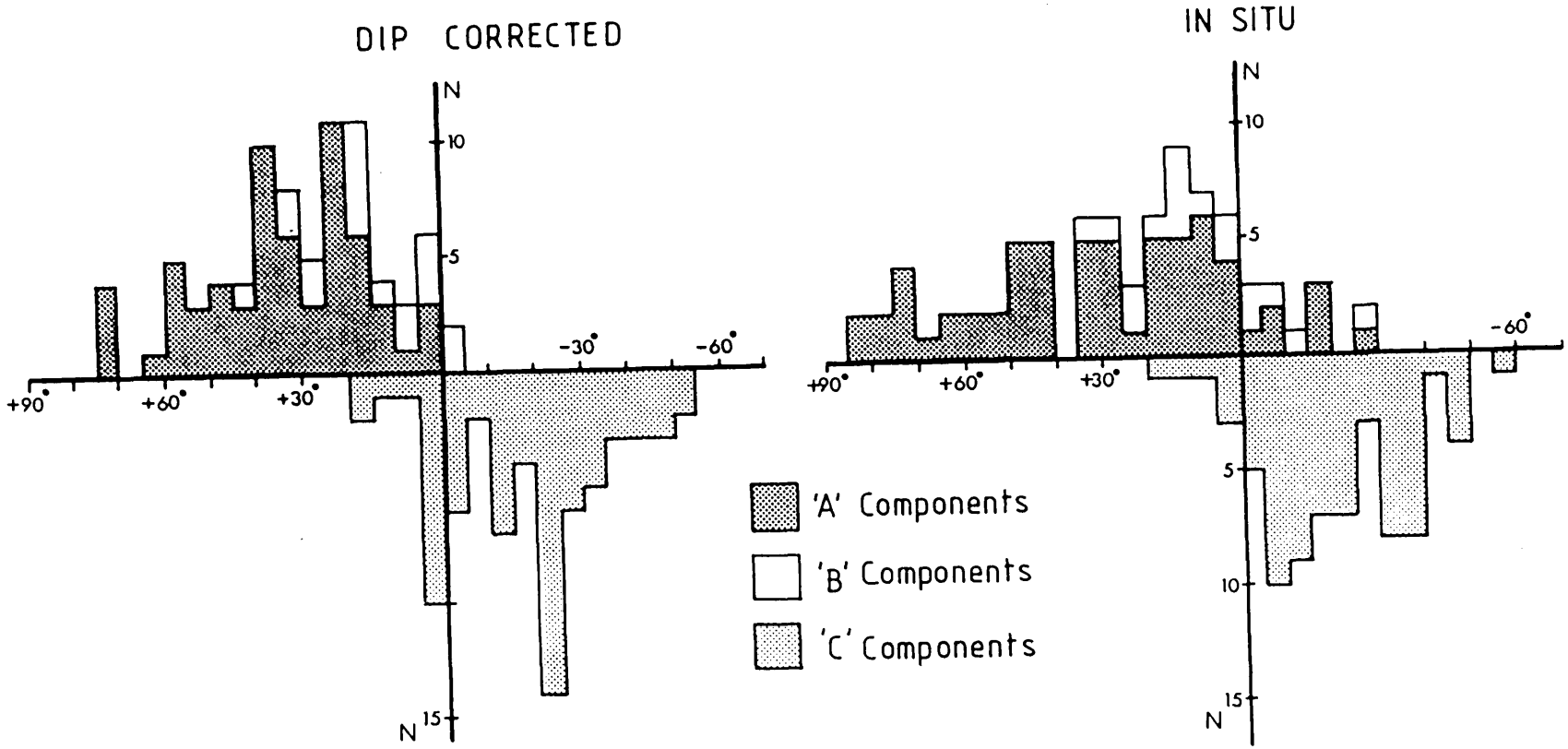


Fig. 4.16. Eday Group: Inclination ranges of stable components. A and B (suspected syngenetic remanence) separated from C (suspected late remagnetisation). Possible causes of the overlap discussed in section 4.5.1.

4.5.2. The A component.

Sites showing an A component (directed downwards and to the south) occur in all four of the clastic units discussed in this section, although there is often an additional B or C component present in the same specimen or the same site.

A number of sites show only an A component (together with a recent, low-T_B remanence). Typical examples are illustrated in fig. 4.17; site mean directions are given in table 4.7 and illustrated in fig. 4.18.

Up to 10 of the 16 sites showing possible A components also show a C component; some of these sites show both occurring in the same specimen, as discussed above and illustrated in fig. 4.15. They may be of discrete T_B range (e.g. site ROD22; fig. 4.15a) or there may be a significant degree of overlap (e.g. ROD4801A; fig. 4.15d). The only other identifiable components present are a low-stability VRM, presumably of recent origin, and an unresolved high-T_B remanence (e.g. ROD3106C; fig. 4.15b); this is often of northerly declination and downward inclination and may represent a CRM of recent origin.

Apart from the two sites (ROD17 and ROD46) for which the A component is present in one specimen only (and hence is statistically indistinguishable from a random magnetisation, particularly where this is found elsewhere in the site) there are three sites for which a degree of uncertainty regarding component group designation exists. Two of these (ROD22 and ROD59) show a steeply downward *in situ* remanence, which bears as much of a resemblance to the PEF as to the mean A direction. Dip correction of the mean direction for ROD59, however, gives a result which is

Table 4.7
EDAY GROUP: A COMPONENT SITE STATISTICS

Site no. (ROD)	In Situ Dec	In Situ Inc	Dip Corrected Dec	Dip Corrected Inc	N	k	a_{95}
16 MES	181.3	27.2	171.8	27.7	3	-	-
17 MES	209.3	44.5	190.7	52.2	1	-	-
18 MES	193.3	45.6	200.6	39.5	2	-	-
22 EM	188.5	67.5	210.4	74.1	5	30.1	14.1
31 EM	191.3	40.9	181.6	18.2	6	10.6	21.6
39 UES	180.4	-10.9	168.6	36.6	8	11.5	17.1
40 UES	203.6	12.6	218.8	41.0	5	12.0	23.0
44 LES	187.0	37.3	166.9	33.2	5	16.6	19.3
46 LES	192.9	45.0	173.7	29.3	1	-	-
48 UES	193.9	39.6	211.6	45.6	8	9.1	19.4
49 UES	171.8	08.3	175.6	22.8	2	-	-
50 MES	177.5	14.5	184.4	25.2	4	27.3	17.9
51 EM	170.8	30.4	177.4	37.6	4	15.5	24.1
53 MES	183.6	10.7	186.6	18.7	5	80.1	8.6
59 LES	153.7	81.8	209.7	35.2	8	68.6	6.7
67 EM	200.0	38.0	212.0	23.9	7	19.1	14.2
Mean directions	187.0	34.3	-	-	74[1]	6.4	7.0
	-	-	191.7	36.2a	74[1]	9.4	5.7
	187.2	33.8	-	-	16[2]	10.9	11.7
	-	-	188.4	36.1	16[2]	16.8	9.3
	186.8	33.2	-	-	11[3]	8.8	16.3
	-	-	191.8	36.5b	11[3]	14.1	12.6

(1) Unit weighting to specimens
(2) Unit weighting to sites
(3) Unit weighting to sites (for which N>3)

Formations: LES = Lower Eday Sst EM = Eday Marls
MES = Middle Eday Sst UES = Upper Eday Sst

Palaeopoles (a) Long. = 166.1°E Lat. = 10.0°N (dp=3.8° dm=6.6°)
(b) Long. = 165.8°E Lat. = 10.1°N (cp=8.6° dm=14.7°)

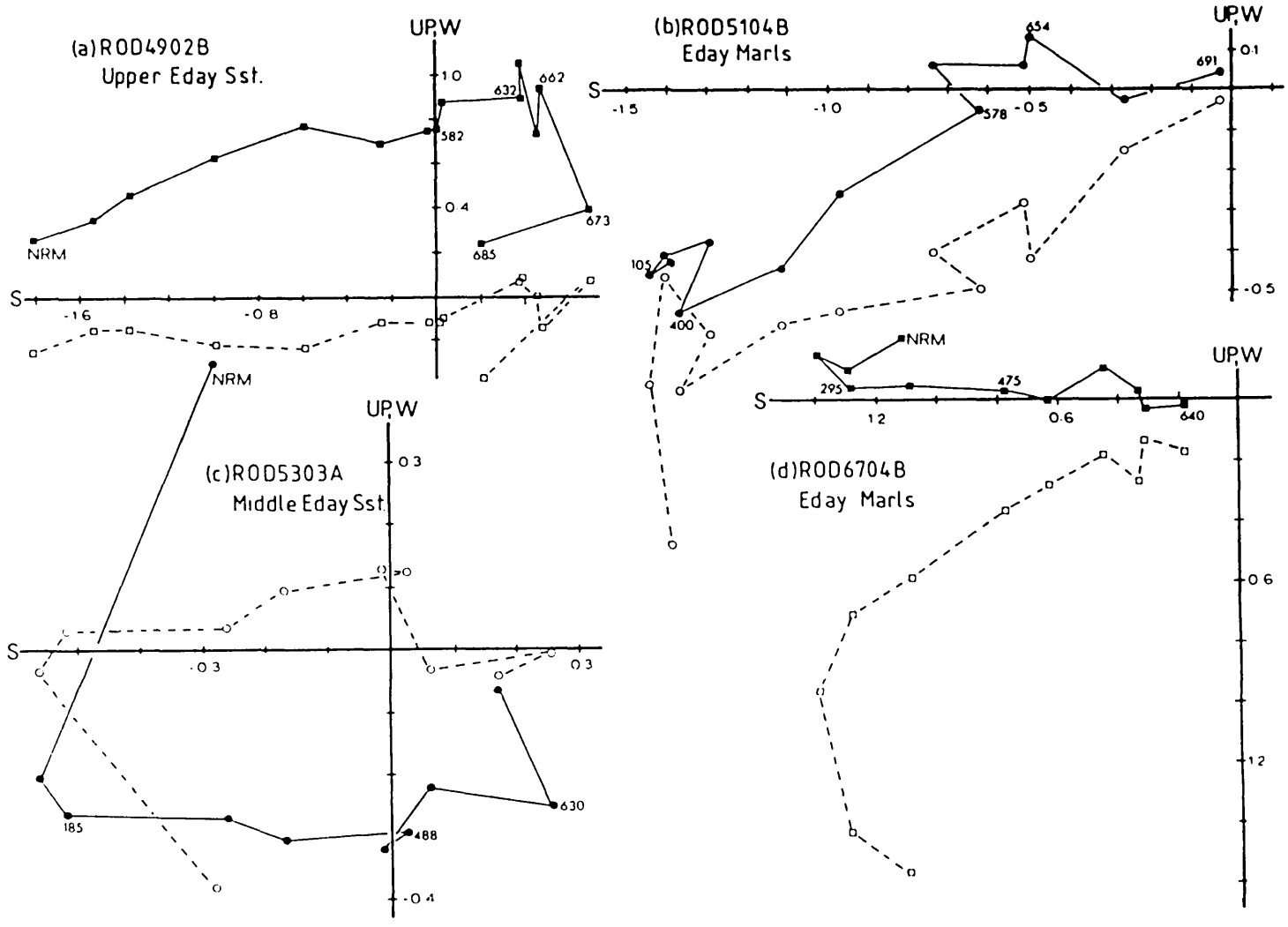


Fig. 4.17. Eday Group: A components (+VRM and unresolved high stability remanence). Orthogonal projections: demagnetisation temperatures in °C, axes in mA/m.

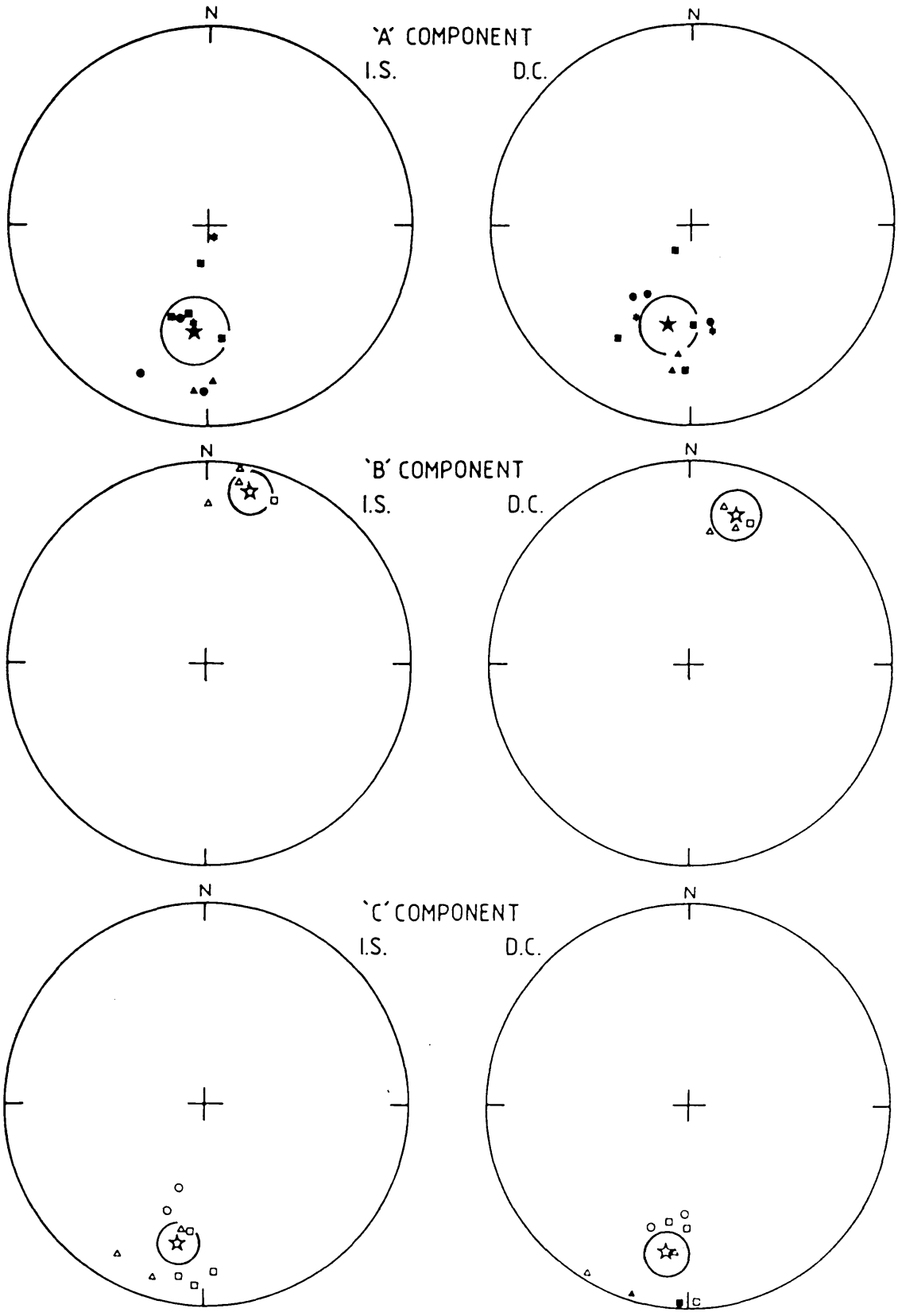


Fig. 4.18. Eday Group: Site mean directions (A, B and C components).

statistically indistinguishable from the A direction. This is not the case for site ROD22, for which a degree of uncertainty must hence remain. ROD39 gives an *in situ* mean which is very similar to the C direction discussed below but dip correction moves the mean towards the A group. Assignation to group A rather than group C is thus a somewhat subjective decision, although one specimen (ROD3907C; fig. 4.15c, table 4.6) shows two components, of which the higher-T_B one bears a greater resemblance (*in situ*) to the C group than the same component, corrected for tectonic dip, does to the A group. The reverse is true for the lower-T_B component. Similarity of the T_B range of the remainder of the site to the lower-T_B component of ROD3907C (which, it would appear from the above evidence, is more likely to be group A than C) suggests that the predominant remanence of the site belongs to group A.

The mean direction for group A (table 4.7) shows considerable improvement in the precision parameter, k, after correction of individual components for tectonic dip although this is insufficient to pass the fold test of McElhinny (1964) at the site level, either when considering all sites or only those for which four or more directions have been averaged. This suggests, but does not prove, that the remanence was acquired prior to the main deformation episode.

4.5.3. The B component.

In a small number of sites (table 4.8) a component of north-easterly declination and low, generally negative, inclination (the B component) is removed; it is particularly apparent in sites ROD54 and 74. In addition to these, two

other sites show a possible B component in two or three specimens.

Table 4.8
EDAY GROUP: B COMPONENT SITE STATISTICS

Site no. (ROD)		In Situ Dec	In Situ Inc	Dip Corrected Dec	Dip Corrected Inc	N	k	a_{95}
33	EM	010.6	0.6	024.5	-25.3	2	-	-
50	MES	001.7	-14.4	008.6	-23.7	3	27.3	17.9
54	MES	009.2	-6.6	011.9	-13.6	4	49.6	13.2
74	EM	023.8	-8.4	024.1	-16.2	7	12.5	17.8
Mean directions		014.4	-8.1	-	-	16[1]	11.6	11.3
		-	-	018.1	-18.0a	16[1]	12.2	11.0
		011.4	-7.3	-	-	4[2]	54.9	12.5
		-	-	017.2	-19.8	4[2]	70.3	11.0

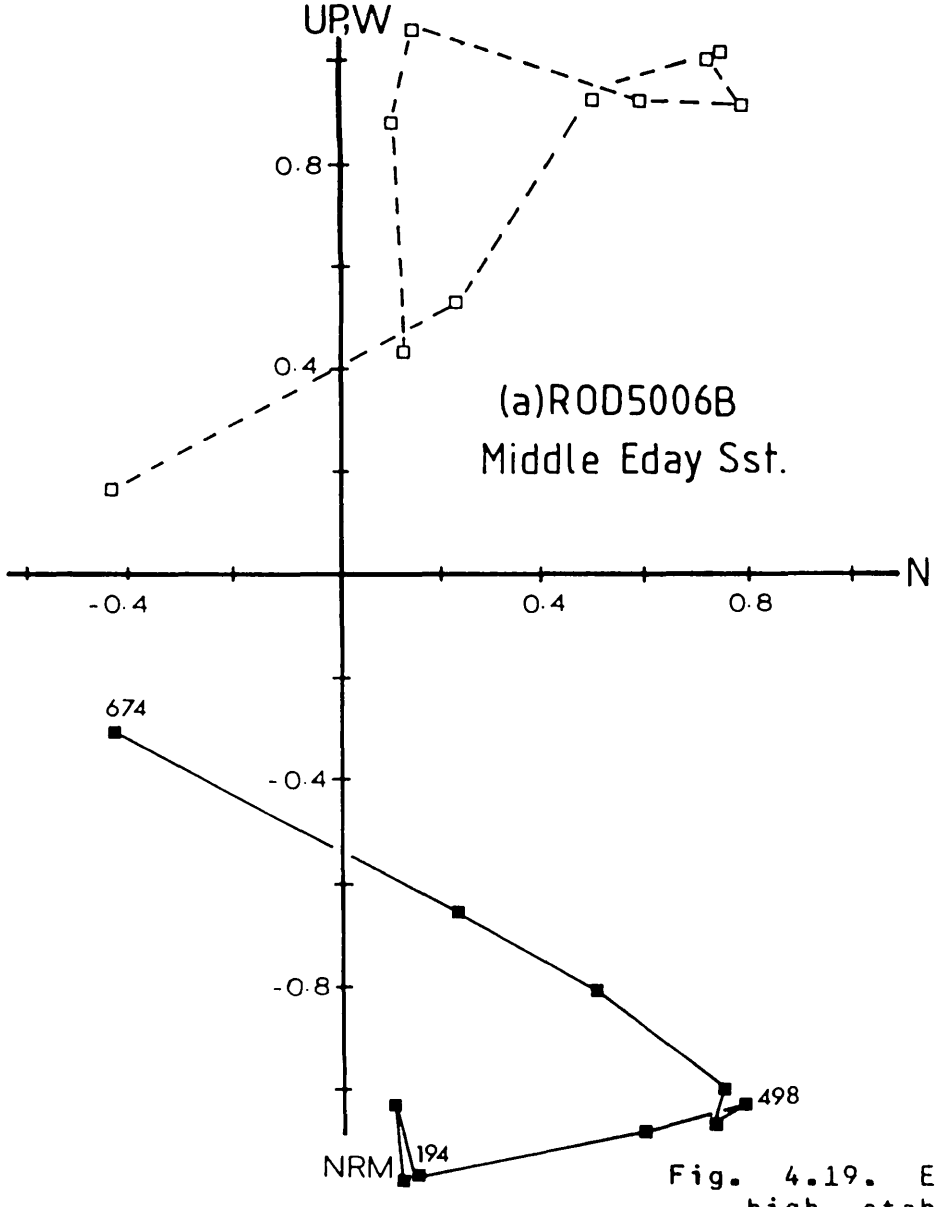
Palaeopole: (a) Long. 157.9°E, Lat. 20.6°N (dp=5.9°, dm=11.4°)

(EM: Eday Marls MES: Middle Eday Sandstone)

(1) Unit weighting to specimens
(2) Unit weighting to sites

Site ROD74, collected at various distances from a Permo-Carboniferous dyke intruded into the Eday Marls (in the baked contact zone) is discussed in detail in section 7.4.4., with particular regard to the TRM/TCRM overprint due to the dyke. At high temperatures a north-easterly, upwards component is removed (fig. 7.13). This steepens somewhat after dip correction (table 4.8).

Site ROD54 is in a green sandy mudstone from the Middle Eday Sandstone (plate 2.1g,h 2.2b). It shows a two-component remanence: a component directed steeply downwards to the north (?PEF) is removed at low temperatures, followed by a northerly, upwards component (fig. 4.19). This has a maximum T_B of 510-575°C or peak demagnetising field of 25-30 mT. NRM intensity is very low (average 0.64.mA m^{-1}). This site should be compared with ROD53, in a reddened lithology intimately associated with the green mudstone, which shows



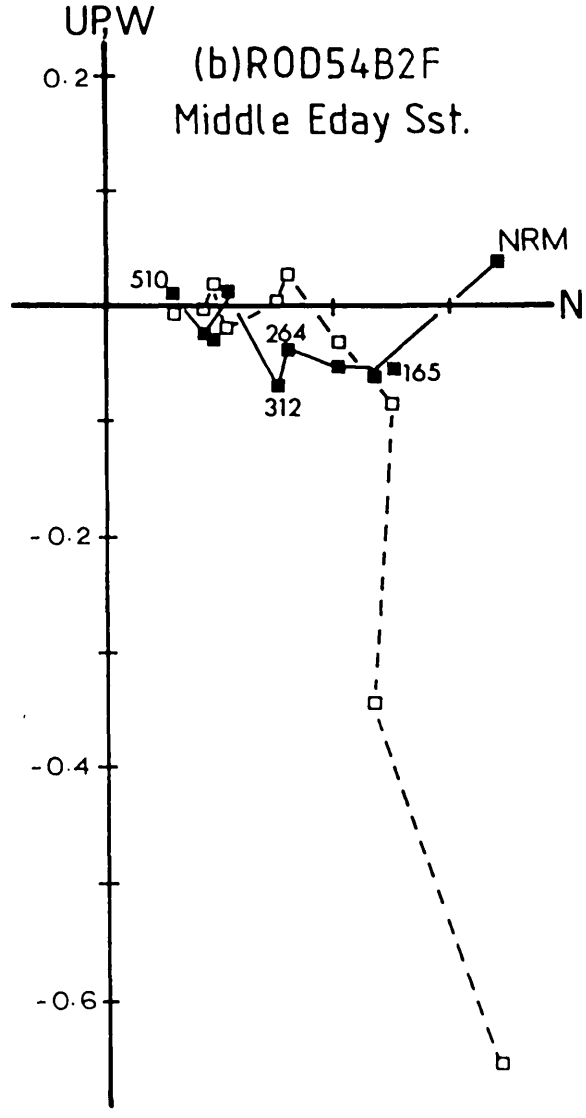


Fig. 4.19. Eday Group: B components (+VRM and unresolved high stability remanence). Orthogonal projections (section 1.4.1): demagnetisation temperatures in °C, axes in mA/m.

only high-T_B components with a southerly declination, or resembling the PEF (see section 4.5.4.).

Two other sites show a clear B magnetisation in two or more specimens. In ROD33, the bulk of the remanence in the site is a steeply downwards PEF direction; this has apparently replaced any earlier remanence which has survived at high temperatures in one or two specimens only. Three specimens from ROD50 show a possible B component at high temperatures, in addition to both A and C components elsewhere in the site. Three sites show a possible B component in one specimen only, which is not sufficient to give such directions any great significance.

Site mean directions for the B component are given in table 4.8 and illustrated in fig.4.18. Precision is insufficient, either at the site or sample level, to give a conclusive fold test result (McElhinny, 1964).

4.5.4. The C component.

C components, of southerly declination and shallow positive to moderately steeply negative inclination (fig. 4.16) form a distinct group from the A magnetisation, as discussed above. Unlike the A magnetisation, it occurs only in the upper members of the Eday Group (Middle Eday Sandstone, Eday Marls and Upper Eday Sandstone). In three sites, it forms the only stable ancient remanence (fig. 4.20) where it may be very well-defined; elsewhere, there is an additional stable component, usually of group A (the difference in inclination being used to discriminate between the two), as illustrated in fig. 4.15. In two cases, component B is also possibly present. PEF components, both of low-T_B (VRM?) and sometimes high-T_B (CRM?) are often evident (e.g. ROD2106, fig. 4.20a, which has a component

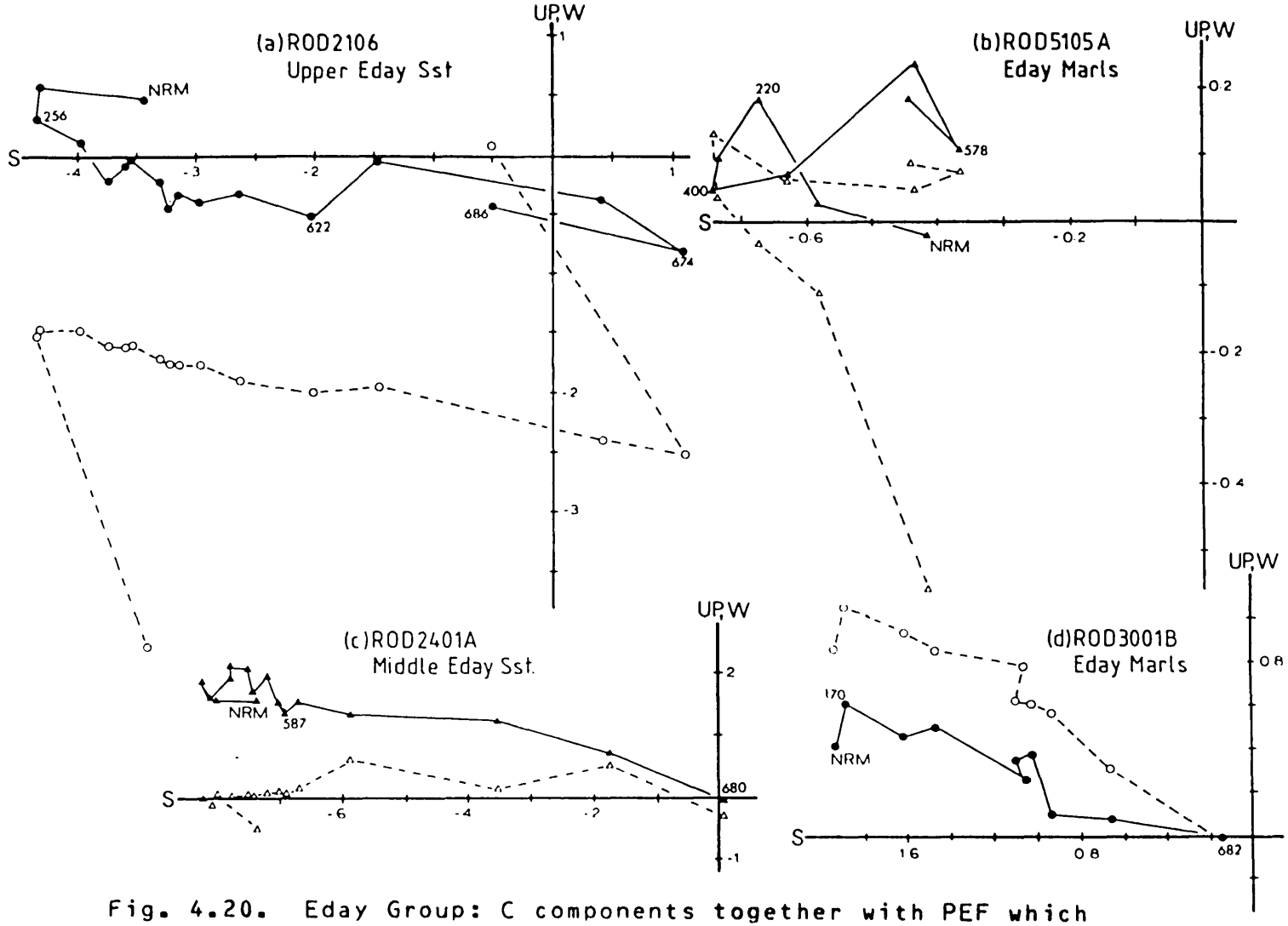


Fig. 4.20. Eday Group: C components together with PEF which is sometimes of both low and high T_B. Orthogonal projections; demagnetisation temperatures in °C, axes in mA/m.

resembling the PEF direction at both high and low T_B, presumably resulting from the acquisition of a recent CRM and VRM respectively.

Individual components from specimens showing a multi-component remanence inevitably do not always have discrete stability ranges, although this may sometimes be the case (e.g. site ROD22, fig. 4.15a). This is particularly evident in cases where all components appear to be of high T_B (as discussed below). Such effects may be the cause of some of the apparent inclination overlap between groups A and C, although it is not considered to be a significant problem in more than a few specimens.

Site mean directions for component C are given in table 4.9 and illustrated stereographically in fig.4.18. As with the A component, some sites show a clear remanence in only one or two specimens. It is well-defined in 9 of the 14 sites suspected of carrying the C component.

There is no indication in relative values of the precision parameter k as to whether remanence acquisition was pre- or post-tectonic. Such a conclusion would not be surprising if the remanence does not represent a single reading of the geomagnetic field, as could be the case if it was acquired over a long time period. If this was so then the effects of net apparent polar wander could mask the effects of tectonic correction which, in most cases, is not great.

Table 4.9
EDAY GROUP: C COMPONENT SITE STATISTICS.

Site no. (ROD)		In Situ Dec	In Situ Inc	Dip Corrected Dec	Dip Corrected Inc	N	k	a_{95}
16	MES	176.7	-24.2	184.4	-22.4	3	-	-
17	MES	209.0	-9.7	210.2	-1.8	5	104.4	7.5
21	UES	197.9	-31.3	197.3	-25.0	4	13.0	26.5
22	EM	177.1	-10.0	176.6	-1.0	4	7.9	34.9
24	MES	189.1	-25.3	185.2	-18.4	13	36.3	7.0
24A	MES	196.2	-6.2	195.7	2.2	5	42.5	11.9
30	EM	186.6	-25.0	180.2	-28.0	10	47.1	7.1
31	EM	188.4	-10.9	198.8	-31.9	8	35.1	9.5
39	UES	157.7	-12.4	154.3	18.2	1	-	-
48	UES	204.2	-41.2	190.0	-33.3	2	-	-
49	UES	196.4	-42.5	183.0	-32.2	6	12.3	19.8
50	MES	198.6	-18.5	192.5	-12.9	2	-	-
51	EM	181.8	-5.6	181.3	0.2	4	10.3	30.1
53	MES	188.8	-27.3	183.7	-18.4	2	-	-
Mean directions		190.3	-21.1a	-	-	69[1]	14.3	4.7
		-	-	188.0	-18.4b	69[1]	12.5	5.0
		188.8	-21.2	-	-	14[2]	22.0	8.7
		-	-	186.5	-15.1	14[2]	16.5	10.1
		190.1	-18.2c	-	-	9[3]	22.7	11.0
		-	-	189.0	-14.9d	9[3]	21.1	11.5

Palaeopoles: (a) Long. 163.7°E, Lat. 41.1°N (dp=2.6°, dm=4.9°)
(b) Long. 166.8°E, Lat. 39.9°N (dp=2.7°, dm=5.2°)
(c) Long. 164.0°E, Lat. 39.7°N (dp=6.0°, dm=11.5°)
(d) Long. 165.7°E, Lat. 38.1°N (dp=6.0°, dm=11.8°)

(1) Unit weighting to specimens
(2) Unit weighting to sites
(3) Unit weighting to sites (N>3)

MES: Middle Eday Sst; EM: Eday Marls; UES: Upper Eday Sst.

4.5.5. Other sites

In the preceding discussion, palaeomagnetic results from only 24 of the 44 sites collected (and analysed) from the Eday Group have been examined. The remaining 20 sites are considered, for one reason or another, not to give a reliable ancient remanence. Some sites, such as those with a very low NRM intensity, have been rejected after the demagnetisation of only one or two specimens. Others, particularly those showing a stable but apparently randomly-orientated remanence, have been investigated in more detail.

There are several independent characteristics which can be identified in such sites distinguishing them from those showing a stable ancient remanence, which together may explain the origin of the remanence in most of the sites in question.

(i) NRM intensity. Of the 7 sites showing NRM intensity less than 1 mA m^{-1}, six do not carry a stable remanence. Such sites are found particularly in the three sites in facies A (Ridgway, 1974) and unreddened sites in facies C of the Lower Eday Sandstone, and also in the Middle Eday Sandstone. The one exception is site ROD54 in unreddened, fine grained Middle Eday Sandstone, which preserves a low-intensity, low-T_B B component.

(ii) Grain size. All sites collected have been approximately categorised (using a somewhat subjective visual examination only) into four detrital grain size groupings. Table 4.10 shows that the rejected sites are exclusively of coarser grain size. This may be due to one or both of (i) the relative ease of leaching and/or recent oxidative weathering of coarser-grained (i.e. higher porosity-permeability) sandstones compared to finer sands and muds or (ii) the higher percentage of iron oxide minerals intrinsically associated with fine-grained rocks (Turner, 1980, fig. 6.30).

Table 4.10
EDAY GROUP: GRAIN SIZE-MAGNETIC RELIABILITY.

Grain size	Coarse	Medium	Fine	Very Fine
All Sites	9	24	7	4
Rejected Sites	4	16	0	0
% of all sites	45%	67%	0	0

(iii) Koenigsberger Ratio. The mean Koenigsberger Ratio

(Q), determined for each site, shows an overall range of between 1 and several hundred. In all, 10 sites have Q >30; of these, 7 carry a remanence dominated by steeply downward (?PEF) components or components of apparently random orientation. Anomalously high Q is a reliable indicator of IRM acquisition (e.g. McElhinny, 1973); this may provide an explanation of remanence acquisition in these sites. This category includes site ROD55, from the reddened basal Lower Eday Sandstone of Eday, immediately above the transition from the Rousay Flags, and also three sites in a sharp ruck fold in the Lower Eday Sandstone on the south-east coast of Eday; both of these outcrops appear from field observation to be homogeneously reddened over a large area and might otherwise have been expected to carry a stable ancient remanence.

4.5.6. IRM and magnetic mineralogy.

IRM experiments on representative specimens from the Eday Group (table 4.11; fig. 4.21) confirm that, in the majority of cases, hematite is the principal magnetic mineral (but not always necessarily contributing to the remanence). B_c is, in all cases but one, greater than 150 mT and occasionally as high as 380 mT. The one exception is ROD54, a green sandy mudstone from the Middle Eday Sandstone, which is 90% saturated by 200 mT suggesting that magnetite is the main magnetic mineral present. (This site has a B magnetisation only).

Curie Points revealed during progressive thermal demagnetisation suggest that magnetite may possibly be present in some sites, particularly in finer-grained sediments from the southern islands, which show a southerly, downward (A) magnetisation, such as ROD22,39 and 40. There

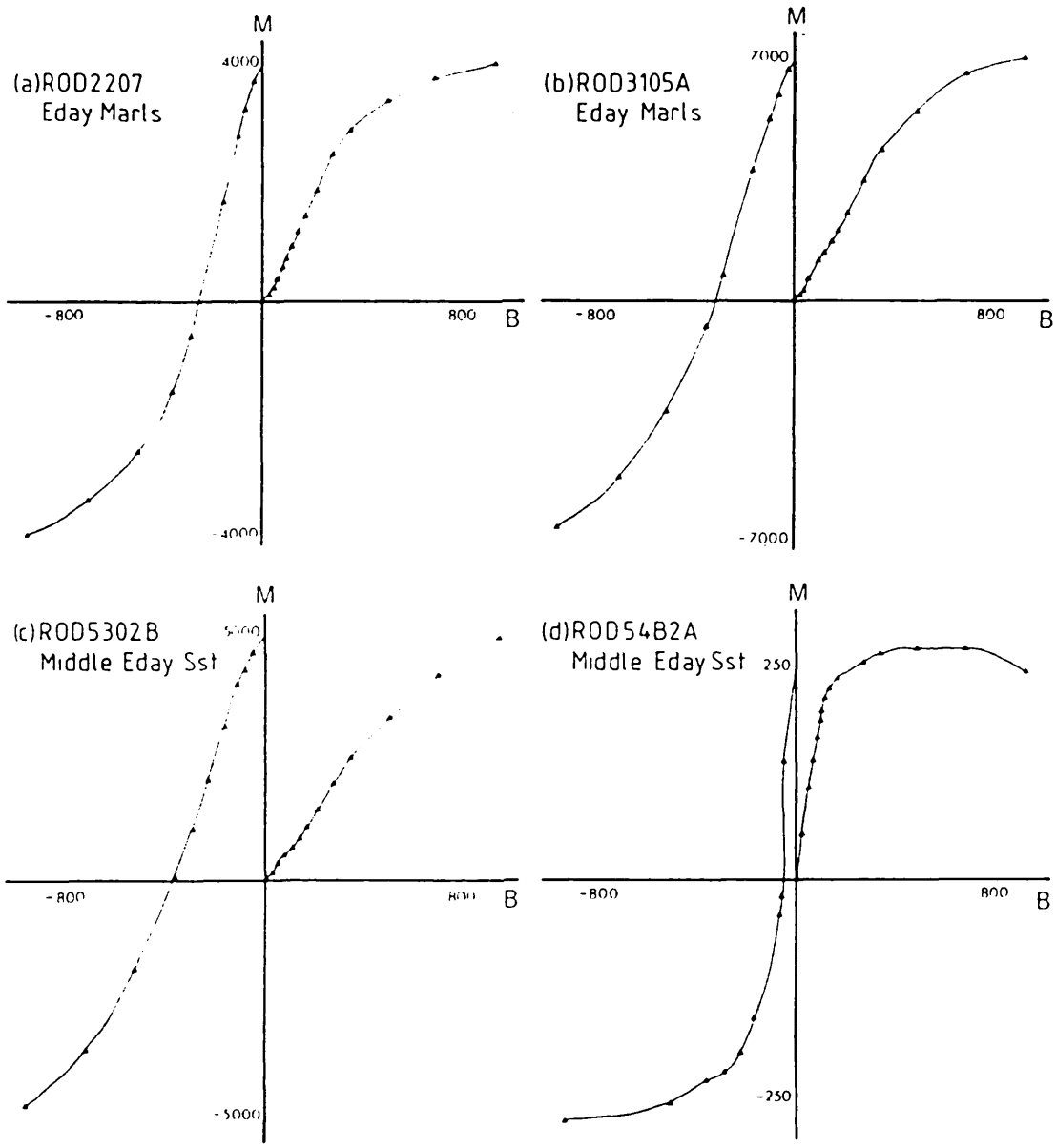


Fig. 4.21. Eday Group: hysteresis of IRM (representative examples). M in mA/m, B in mT. Numerical details in table 4.11.

Table 4.11
EDAY GROUP: ROCK MAGNETIC CHARACTERISTICS

Site no. (ROD)	Components	T_B max	Components	T_B max	Components	T_B max.	M_r (mA m^{-1})	B_s (mT)	B_c (mT)
16	A	596			C	650	(800)	800	170
17	A	668			C	681	6800		320
18	A	670					5400		250
22	A	587			C	676	4000		250
31	A	684			C	676	7100		320
39	A	590			(C)	625+	2200		180
40	A	570					3200		180
51	A	676			C	595	2300		270
53	A	585+			C	655	4900		380
54			B	475			(266)	400	40

M_r = Magnetic moment at B=1000 mT, except () = M_{rs}

is little indication in IRM curves, however, that magnetite is present apart from possible points of inflection at around 150-200 mT in a few specimens. There are two possible explanations of this:

(i) Magnetite is not present, the low-T_B remanence being carried in low-coercivity hematite with maximum T_B coincidentally resembling the T_c of magnetite.

(ii) Magnetite is present but only in very small quantities; indications of its presence in IRM curves are masked by substantial quantities of low-coercivity hematite. The amount of magnetite present would have to be very small compared to that of hematite; Dunlop (1972a) has estimated that magnetite need be present in a concentration of only 0.5 to 1% of that of hematite for each to contribute equally to the saturation remanence. However, site ROD54 shows that a stable ancient magnetitic remanence can have a low B_s (table 4.11) when compared with those sites containing large amounts of hematite. It is thus suggested that much of the hematite in the Eday Group (in, for example, oxidised biotite) may not in fact carry a net remanence even though

it may contribute overwhelmingly to M and thus could effectively swamp any small quantities of magnetite which may be present. This will be discussed further in chapter 6.

Analysis of Curie Temperatures, combined with IRM analysis for certain ambiguous sites (table 4.11), suggests the following conclusions:

(i) The A magnetisation is carried predominantly in hematite, with the exception of five sites (ROD16,22,39,40 and 50) in which it may be carried, at least partly, in magnetite. Sites in which it is carried exclusively in hematite have generally high maximum T_B (660-690°C).

(ii) The B magnetisation appears to be carried exclusively in hematite (although it is well-defined in only three sites) with the exception of ROD54 in which it is carried only in magnetite. Hematitic components are again of high maximum T_B (672-685°C).

(iii) The C magnetisation is exclusively hematitic. Maximum T_B generally appears to be somewhat lower than for groups A and B, generally in the range 580 to 680°C but with most being around 650°C.

4.5.7. Age of the magnetisation.

As discussed earlier in this volume, there are no previously-published reliable palaeomagnetic data for the ORS of Scotland north of the Great Glen Fault. The palaeomagnetic pole from the Eday Lavas and their baked contact in the Eday Flags has, however, been established in chapter 3 (and Robinson, 1985) as a reliable record of the palaeopole relative to N.E. Scotland in the upper Middle ORS. It is intended to use this as a reference direction with which to compare the three ancient components (A, B and C) derived above for Eday Group sediments.

(i) The A and B components.

Mean directions for these two component groups (derived and illustrated above) are compared with the mean direction for the Eday Lavas and their baked contact in fig. 4.22. It can be seen that they are indistinguishable (when considering the B magnetisation to be of opposite polarity to the lavas; this is denoted B'). Similarity of the two groups is confirmed using the test of McFadden & Lowes (1981), which shows that A and B' are indistinguishable with greater than 99% confidence.

It is thus suggested that both A and B (B') components represent an early remanence, acquired during or shortly after sedimentation, and that the mean directions provide a further approximation to the upper Middle ORS palaeopole relative to N.E. Scotland. Such a conclusion is also broadly compatible with other palaeopoles for the Devonian (predominantly Lower ORS) from elsewhere in N.W. Europe, as discussed in chapter 9.

(ii) The C component.

Comparison of the mean direction for the C component with that of the Eday Lavas (fig. 4.22) shows that they are statistically distinct. As will be discussed in more detail in chapter 9, the corresponding palaeopole falls on the Permo-Carboniferous portion of the APW curve for N.W. Europe. The exclusively reversed nature of the remanence over a large area suggests that it dates from the Kiaman Magnetic Interval. A large degree of between-site scatter, which masks the effects of tilt correction, suggests that the population of site mean directions could encompass a significant length of time (and hence APW), as might be expected between the beginning and end of the Kiaman which

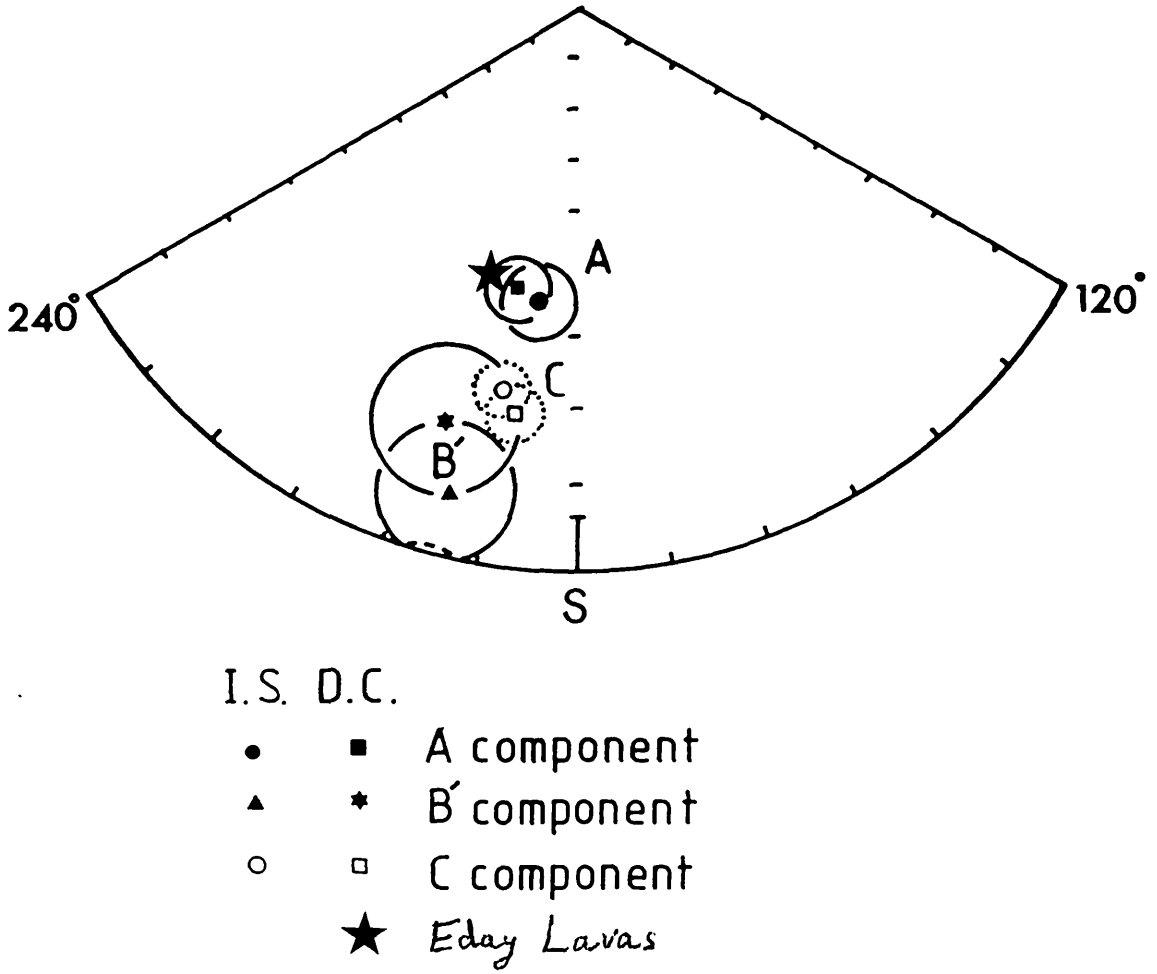


Fig. 4.22. Eday Group: Mean directions of A, B and C group components (B group represented as reversed polarity equivalent, B'.) 95% circles of confidence shown for each direction.

covers a period of perhaps 40 to 60 Ma.

4.6. The Upper ORS of Dunnet Head and Hoy.

4.6.1. Geology and sampling.

In addition to outcrop around the Moray Firth (discussed in section 4.2.2.), Upper ORS sediments occur as isolated outcrops on Dunnet Head (northern Caithness) and also on Hoy, southern Orkney. They are not recognised elsewhere north of the Dornoch Firth.

The Upper ORS of Dunnet Head (Crampton & Carruthers, 1914), dated by means of Holoptychius scales found within green clay horizons (McAlpine, 1978), consists almost entirely of yellow, red or buff sandstones with occasional clay horizons. It has been interpreted as a fluvial deposit, frequently trough cross-bedded, with palaeocurrents predominantly from the SE. Pebbles from various formations, such as the Durness Limestone and Moine, have been identified (House et al, 1977; McAlpine, 1978).

Sampled material is from a representative suite of the lithologies found in the area, including an inhomogeneously reddened sandstone horizon (RCD10,11 and 47; plate 2.1e), a finely laminated pink-grey sandstone (RCD9), a homogeneously reddened sandstone (RCD12) and two sites in drab sandstones showing pronounced liesegang ring structures (RCD13-14; plate 2.1f). In addition, three sites from the margin of a Permo-Carboniferous dyke (RCD15,16 and 17) are discussed in section 7.4.3.

The Upper ORS of Hoy (Wilson et al, 1935; Mykura, 1976; McAlpine, 1978) was apparently deposited over now-deformed Middle ORS lacustrine sediments (although the relative age of deformation is open to question; see chapter 2). It

consists of over 1000m of massive, current-bedded red and yellow sandstones with thin marly partings. At the base of the sandstones are found the Hoy Lavas referred to in chapter 3. A total of four oriented blocks have been collected, grouped together as a single site (ROD28) despite the large area covered. Sampling was severely restricted due to extreme wind conditions.

4.6.2. Palaeomagnetism.

Previous work, restricted to Dunnet Head, suggests that the Upper ORS is of very limited use as a palaeomagnetic recorder. 18 sites collected by Tarling et al (1976) show no consistency and are magnetically unstable. Collinson (1980), finding similar results to Tarling et al (op. cit.), suggests that the NRM, (shown to reside largely in pigment rather than specularite), was acquired in the Permo-Triassic during a period of disturbed ambient field, such as might be found during a polarity transition. Material discussed in both studies is a reddish-brown, medium-grained sandstone, similar to that of site RCD12 in the present study.

Of the 8 sites analysed here, only two show a well-defined ancient remanence. Of the remainder, two are weakly magnetised (RCD9 and 11, both with NRM intensities below 0.6 mA m^{-1}). Site ROD28 on Hoy shows stable but randomly-orientated components of relatively high intensity but low susceptibility, as might be anticipated for a hilltop exposure vulnerable to IRM acquisition. Three sites (RCD12, 13 and 14) show palaeomagnetic characteristics similar to those reported by Tarling et al (1976) and Collinson (1980) for similar lithologies, namely a remanence generally of southerly declination but of variable, inconsistent

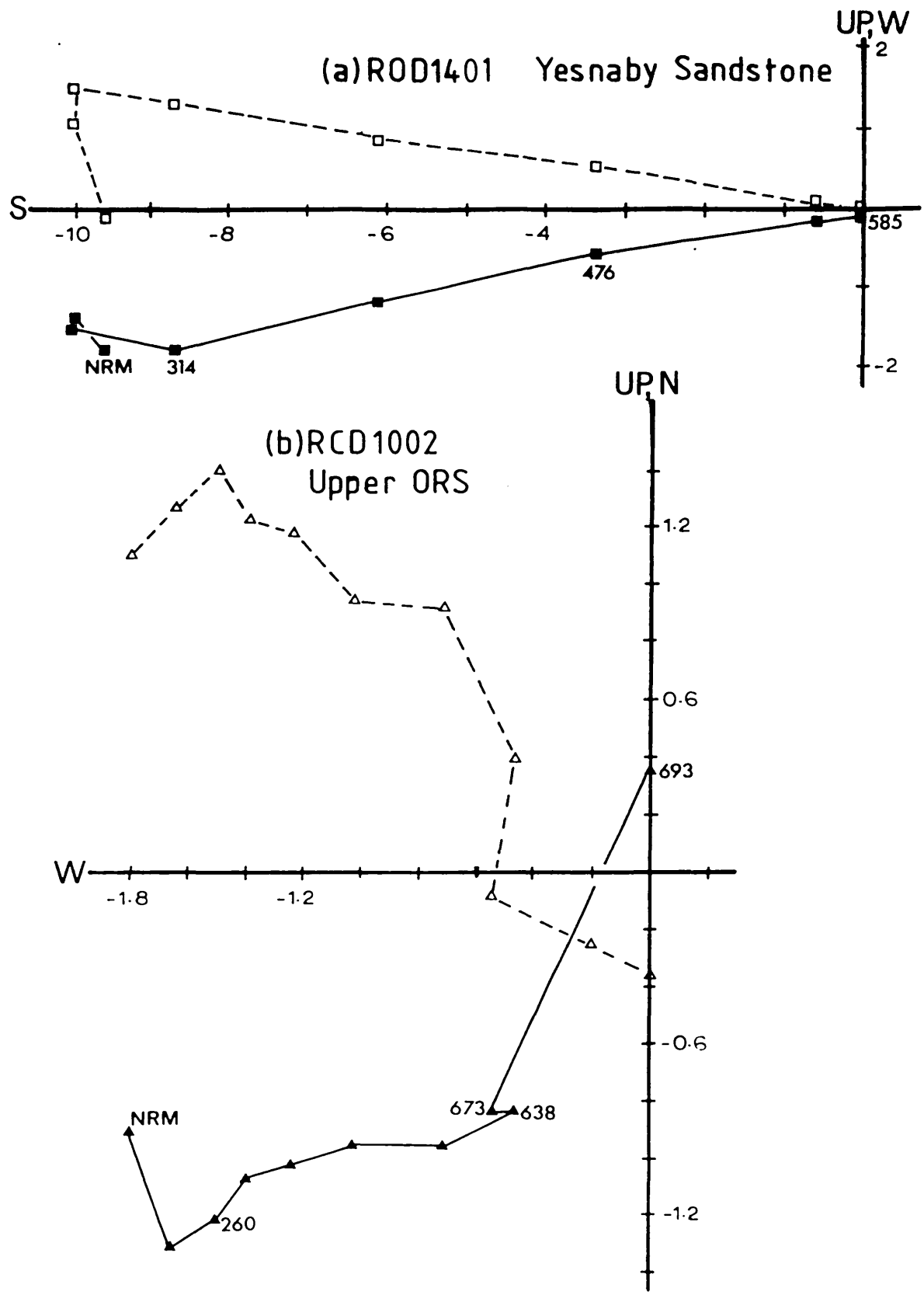


Fig. 4.23. Upper ORS (Dunnet Head) and Lower ORS (Yesnaby). Thermal demagnetisation, presented as orthogonal projections (section 1.4.1). Demagnetisation temperatures in °C, axes in mA/m.

inclination. Well-defined components are rarely apparent in these sites, presumably as the result of the interaction of more than one stable magnetisation.

Sites RCD10 and 47, however, generally show a stable remanence with a T_B range between 155-280 and 535-666 °C (fig. 4.23). These two sites are from a reddened horizon within a largely buff sandstone (site RCD11) which, as mentioned above, is of very low NRM intensity and reveals no stable ancient components during progressive demagnetisation. It would thus appear that the reddening may be responsible for carrying the remanence of RCD10 and 47. Mean directions (table 4.12) from these two sites correspond to palaeopoles of apparent Permo-Carboniferous age. Causes of delayed reddening such as this will be discussed in chapter 6.

4.7 The Yesnaby Group, Orkney.

4.7.1. Geology and sampling.

In the SW of Mainland, Orkney, small outcrops of basement material (granite, schist, biotite gneiss; Wilson et al, 1935) form an eroded pre-ORS land surface, which possibly extends beneath the ORS under much of western Orkney (McQuillin, 1968). Over this, the Yesnaby Sandstone Group (including the Harra Ebb and Yesnaby Sandstone Formations) forms an apron-like deposit (plate 2.1b,d; 2.2c). It is composed of up to 100m of interbedded fluviolacustrine sandstones, siltstones, conglomerates and breccias, with palaeocurrents in the lower members being radial to exposed basement highs. A detailed investigation (Michie & Cooper, 1979) was carried out due to the presence of anomalously high uranium concentrations associated with phosphates found in the finer-grained members; these form a substantial sub-economic

Table 4.12
Upper ORS and Yesnaby Group:
Palaeomagnetic components (In Situ).

Site	Specimen	Dec	Inc	T_B range (°C)	Mean direction Dec	Inc	N	k	a
				Upper ORS					
RCD10	01	222.2	-37.3	260-540					
	02	254.5	-29.5	260-595					
	04	210.0	-8.4	NRM-576					
	05	214.3	-42.6	155-590					
	06	206.4	-34.9	190-585					
	07	199.9	-47.2	190-666					
					218.2	-34.7	6	14.9	17.9
RCD47	01A	213.1	-15.8	280-660					
	02	185.3	-8.3	190-535					
	03	178.6	-5.6	190-585					
	04	185.0	-0.4	315-585					
					190.0	-7.7	4	26.0	18.4
RCD10+47					205.4	-24.4a	10	9.6	16.4
				Yesnaby Sandstone					
ROD14	01	171.5	-8.4	115-585					
	02	178.5	-3.2	NRM-100mT					
	03	183.6	3.7	120-508					
	04	179.3	-6.8	20-70mT					
	05	174.1	-1.9	NRM-557					
					177.4	-3.3b	5	148.0	6.3

Palaeopoles: (a) Long. 143.6E, Lat. 40.5N (dp=9.4, dm=17.6)
(b) Long. 179.8E, Lat. 32.6N (dp=3.2 dm= 6.3)

reserve. The age of the sediments is generally accepted as Lower ORS, as there appears to be an angular unconformity with the overlying Lower Stromness Flags. This is disputed by Fannin, 1970, who suggests that the transition is rapid and conformable, both laterally and vertically. Supporting evidence for a Lower ORS age comes from borehole data (Michie & Cooper, 1979) showing thick purple silts which bear a strong resemblance to the Lower ORS in the south of the basin.

Samples have been analysed from the Harra Ebb Formation, immediately above the basement (ROD14 and 15) at Garthna Geo, an inland exposure of the Yesnaby Sandstone to the east of Garthna Geo (ROD79) and the bitumen-rich Yesnaby Sandstone opposite Stromness (ROD80, 81).

4.7.2. Palaeomagnetism.

Four of the five sites analysed do not carry a stable ancient remanence; of these, two are magnetised in the PEF direction only, one carries stable but totally random components and one is unmagnetised. Such findings are somewhat unexpected, since material selected for sampling in most cases is a dark, bitumen-rich fine-grained sandstone/silt. Any primary iron oxides might thus be expected to have escaped severe post-depositional alteration (although bituminous pore infillings in black members of the Yesnaby Sandstone are considered to be secondary; Fannin, 1970).

The one site showing a stable remanence (ROD14 in the Harra Ebb Formation) gives a mean In Situ direction of Dec.= 177.4°, Inc.= -3.3° (table 4.12) with a maximum T_B of 450-585°C (fig. 4.23). Correction of this for apparent dip gives a direction of Dec.= 177.3°, Inc.= 14.6° but this is not necessarily a valid correction as the dip appears to be that of a syn-sedimentary slope. Such a conclusion is supported by Wilson et al (1935) who suggests that the 'slope of the land surface...was...rather greater than 1 in 4'. The direction is therefore considered to represent a secondary remanence (chapter 9), not affected by later tectonic activity. This conclusion is supported by evidence for remagnetisation of the formation as discussed in chapter 6. Unfortunately no fresh material is available for IRM analysis, so the magnetic mineralogy is somewhat uncertain.

4.8 Synthesis.

Clastic sediments of the Orcadian Basin have been shown to have a wide range of palaeomagnetic characteristics. Of

the 78 sites studied, 32 carry a total or partial primary remanence; these range in age from Lower ORS through to Upper ORS.

The most well-defined primary direction is perhaps that from the upper Middle ORS, largely from the Eday Group. Rocks carrying a primary remanence include extrusive lavas and their baked contacts (chapter 3) as well as a wide range of sediment type, including fine-grained marls, sandstones and conglomerates.

An ancient but secondary remanence has been found to occur widely, sometimes in close association with a primary remanence, sometimes totally obscuring or replacing it. Only sediments show a remagnetisation of this nature and it is without exception hematitic.

It should be noted that the results reported here update and supercede those of Robinson (1985).

Discussion in the next chapter of a very different type of sediment, the lacustrine laminites of the Middle ORS, will be followed by a general investigation of magneto-mineralogical and diagenetic characteristics, particularly in sediments. The aim of this will be to attempt to define as precisely as possible the conditions under which some sediments became susceptible to remagnetisation and to discover why others have been able to retain a primary remanence.

The main conclusions of this chapter will, for ease of reference, be tabulated below. Discussion of the relationship of palaeomagnetic poles from this study with previously-determined poles from elsewhere may be found in chapter 9.

Table 4.13
Chapter 4: Summary.

Formation/Group	Primary remanence		Secondary remanence	
Upper ORS, Dunnet			*	Hem
Upper ORS, S. Basin	*	Hem		
Upper Eday Sst.	*	Hem	*	Hem
Eday Marls	*	Hem (Mt?)	*	Hem
Middle Eday Sst.	*	Hem, Mt	*	Hem
Lower Eday Sst.	*	Hem		
L.ORS, Foyers	*	Hem		
L.ORS, S. Basin	*	Hem	*	Hem
L.ORS, Orkney			*	?
L.ORS, Sarclet	*	Hem (Mt??)	*	Hem

Magnetic mineralogy: Hem = Hematitic
Mt = Magnetitic

CHAPTER 5

LACUSTRINE SEDIMENTS

5.1 Introduction

The ORS succession of the Orcadian Basin (chapter 2) is dominated by lacustrine sediments of the Middle ORS (Anderton et al, 1979). These form a stratigraphic thickness of up to 5 km (Donovan et al, 1974), which accumulated over a very short period of time. The majority of the sediments are varved flagstones, although some relatively minor clastic horizons occur. Included within the flagstones are several carbonate-rich laminated fish-bearing horizons, including the world-famous Niandt-Achanarras-Sandwick-Melby fishbed, which extends from south of the Moray Firth to Shetland in the north (fig. 5·1).

The sediments have been the subject of several palaeontological, palaeoenvironmental and stratigraphical studies, largely due to their unique fauna (plate 5.1b), which provide the only basis for accurate stratigraphic correlation within the basin (since there is only a very limited fossil record within the Lower and Upper ORS.

Lacustrine sediments of the basin have been investigated palaeomagnetically several times (Turner, 1977; Turner et al, 1978; Eustance, 1981). It was originally expected that they might yield a primary Devonian palaeopole carried in detrital magnetite, since the generally high organic content of the laminites shows that they have not undergone severe post-depositional oxidation. However, few, if any, such results have been found to date; any stable remanence appears to be of post-Devonian age. The aim of the present study, therefore, is to extend the sampling range of

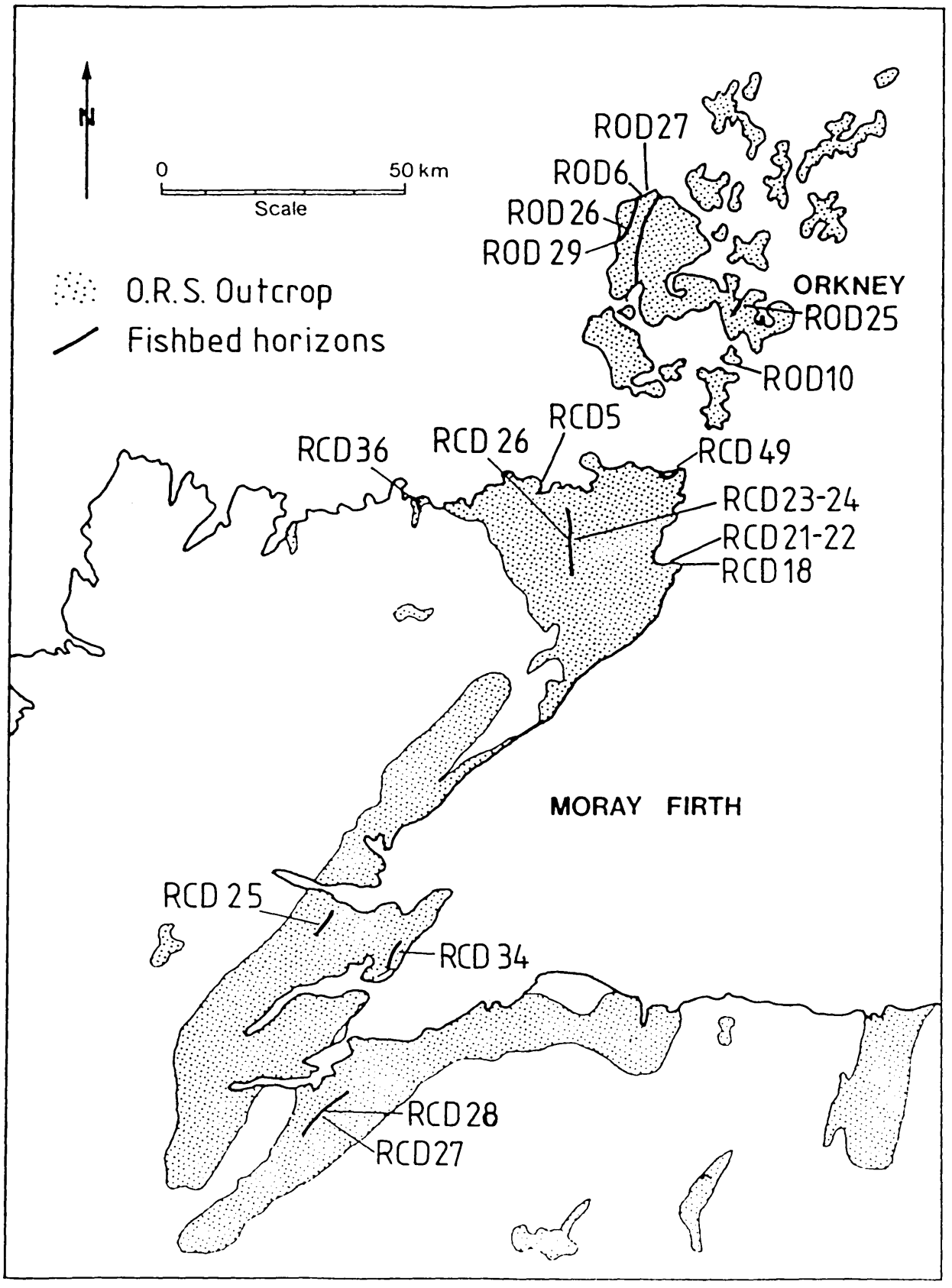


Fig. 5.1. Lacustrine sediments: Site locations.

PLATE 5.1

LACUSTRINE SEDIMENTS: FIELD CHARACTERISTICS

(a) Early diagenetic carbonate nodule in fishbed horizon, site RCD34. Shows the degree of post-concretion sediment compaction. (Pen 15cm).

(b) Typical fish preserved within the lacustrine sediments of the Orcadian Basin. (after Mykura, 1976, plate XIII).

(c) Laminated lacustrine sediments, Achanarras Quarry (site RCD26), showing extreme fissility. (Hammer 35cm).

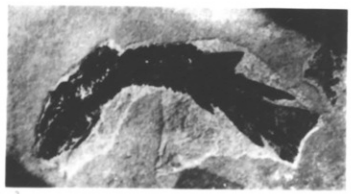
(d) Syn-sedimentary deformation in the Rousay Flags. Gearsan, Deerness (HY079594). Lenscap 5cm.

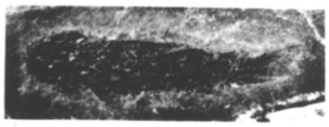
(e) Laminated sediments above the Achanarras Fishbed, Achanarras Quarry, site RCD26. The fishbed (s.s.) is in the flooded quarry below.

(f) Shrinkage cracks in the Upper Caithnes Flags, suggesting sub-aerial exposure. Site RCD7, Dunnet Bay, Caithness. Hammer 35cm.

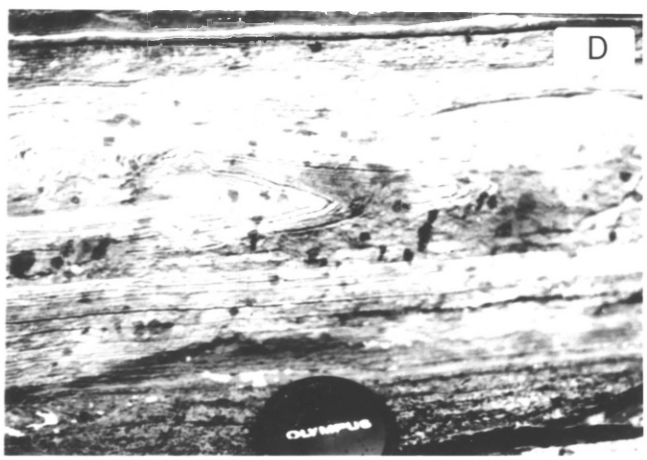












E



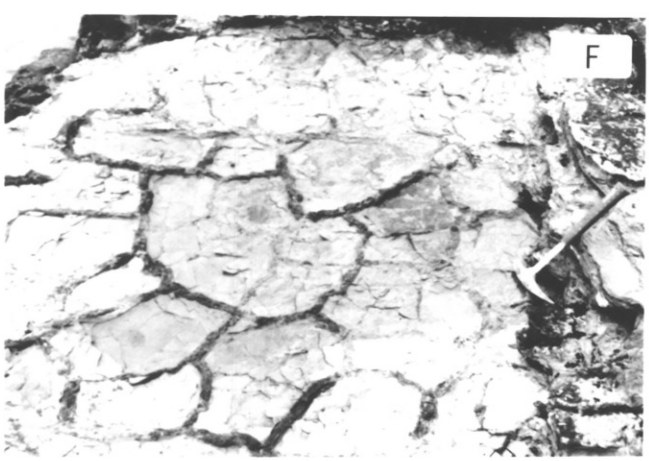


PLATE 5·1

WATTS LIBRARY

the Niandt limestone itself, to investigate the surrounding laminites and to attempt to clarify the nature and cause of the previously-recognised remagnetisation.

5.2 Geology and sampling

The stratigraphic range covered in this chapter extends from just above the base of the Middle ORS (using the stratigraphy recommended by Donovan et al, 1974) to the base of the upper Middle ORS sediments of the John o'Groats sandstone (chapter 8) and the Eday Group (chapter 4) but excluding Middle ORS clastic horizons from the Moray Firth area and southern Caithness (discussed in chapter 4). Also included is the John o'Groats fishbed, of very similar lithology to the main fishbed horizons. The Eday Flags, also of broadly comparable facies, are discussed chiefly in chapter 3 rather than in this chapter as they do not carry an intrinsic stable remanence. Site details are given in table 5.1.

The geology of the lacustrine sediments of the basin is discussed by Rayner (1963), Fannin,(1970), Donovan et al (1974), Donovan (1975,1980), Trewin (1976), Armstrong (1977) and Allen (1981). In addition, there are local descriptions (e.g. Crampton & Carruthers, 1914; Mykura, 1976) and many earlier studies predominantly concerned with the fish fauna (see Rayner (1963) for such references; detailed discussion is beyond the scope of the present study). Hydrocarbon source-rock potential has also been of interest (Parnell 1981, 1985a,b; Marshall et al, 1985).

The major features of the Middle ORS (using data from all references mentioned above) suggest intricate interplay between a large non-marine lake and its neighbouring clastic

Table 5.1
Lacustrine sediments: site details

Site no.	Group/Formation	Location	N_{sa}	N_{sp}	Treatment None	Th	AF
		Laminated Fishbeds					
RCD25		Blackpark	6	9	-	6	3
RCD26		Achanarras	5	9	-	7	2
RCD27		Inverness	3	3	-	1	2
RCD28	Achanarras FB	Inverness	5	5	-	3	2
RCD34		Hilton	6	7	-	6	1
RCD36		Baligill	7	9	-	6	3
ROD26		Cruaday	9	17	-	11	6
ROD29		Skaill	7	15	-	6	9
RCD49	John o'Groats FB	Duncansby	6	10	-	5	5
ROD25	Rousay FB	Kirkwall	7	10	-	6	4
Total			61	94	-	57	37
		Other laminites					
RCD05	Mey beds (U.C.F.)	Thurso	2	6	-	1	5
RCD07	Thurso Flags	Thurso	6	7	-	6	1
RCD18	Robbery Head (L.C.F.)	Staxigoe	6	11	7	2	2
RCD21	Field (U.C.F.)	Ackergill	5	12	3	2	7
RCD22		Ackergill	6	9	5	2	2
RCD23	Staxigoe (U.C.F.)	Spital	6	6	-	1	2
RCD24		Spital	5	8	-	1	7
ROD06	U. Stromness Flags	Brough	5	9	6	1	2
ROD10	Rousay Flags	Burray	9	17	14	1	2
ROD27	U. Stromness Flags	Whitaloo	11	14	12	2	-
Total			61	99	47	19	33

source areas. Deeper-water varved sediments, found predominantly in the more central (i.e. north-eastern) parts of the basin, represent seasonal fluctuations with algal blooms during warm, dry periods and clastic input during the cooler, wetter season. Clastic sedimentation was largely via minor density currents, reaching far out into the basin, often producing very thin laminae (0.1-1.0 mm). Palaeocurrents indicate source areas to the west and south. Water depth during deposition was never great, as subaerial desiccation features are frequent, even in the more distal parts of the basin (plate 5.1f). A maximum water depth of about 50m has been suggested (Fannin, 1970).

On a large scale, it can be seen that fluvial fining-upwards cycles become increasingly prevalent towards the top

of the succession (Anderton et al, 1979). This suggests a major fluvio-lacustrine regression with time, culminating with deposition of the predominantly coarse clastic John o'Groats and Eday Groups, although occasional regressions to lake-dominated processes resulted in, for example, the John o'Groats fishbed.

Lithologically, the lacustrine sediments are somewhat variable, depending mainly on position within the ancient lake. For example, marginal limestones (Donovan, 1975; Parnell, 1983a) are devoid of the organic matter which is characteristic of deeper-water facies (Parnell, 1983b, 1985b). Typical features of the sediments are illustrated in plate 5.1.

The lacustrine fishbeds are composed largely of two main groups of minerals, one consisting of detrital silicates and the other a carbonate matrix. Bulk geochemical analyses (summarised in table 5.2; full analyses in appendix C1d) show that the relative contributions of these, as characterised by Si and Ca-Mg respectively, are somewhat variable. Silicates constitute a greater percentage of the total in sites near the lake margin (such as the marginal limestone of RCD36 and in the Inverness area) when compared with sites from north of the Cromarty Firth and in the Orkney Islands. There is also a tendency for total alkalis (representing feldspars) to decrease as total silicates decrease, suggesting increasing mineralogical maturity of the detrital contribution with distance from the clastic source area.

Calcium and magnesium (largely as carbonates) are present in highly variable proportions, reflecting the dominant carbonate mineralogy of any particular site. Sites

Table 5.2

Fishbed sites: ICP bulk analyses (selected elements).

	RCD25	RCD26	RCD27	RCD28	RCD34	RCD36	RCD49	ROD25	ROD26	ROD29
Ca	26.0	5.6	4.3	4.5	15.1	7.1	6.9	5.3	12.6	11.6
Mg	1.01	1.99	1.42	1.92	1.69	0.63	3.1	2.7	2.5	2.2
Fe d4	1.11	2.7	3.3	1.18	1.91	1.85	2.6	3.7	2.1	2.3
Na (%)	0.03	2.3	0.93	1.03	0.94	1.34	0.49	1.62	1.72	1.82
K	1.07	2.0	4.8	2.1	1.55	3.1	2.8	3.2	1.3	1.53
Al	2.5	5.6	7.0	3.8	4.1	5.2	5.8	6.5	4.2	4.8
Ti	0.15	0.35	0.42	0.15	0.20	0.34	0.31	0.39	0.28	0.32
Sr	450	370	400	300	510	182	240	340	1130	1120
Mn	900	710	470	420	760	980	730	380	560	520
Ba (ppm)	190	430	590	430	360	470	570	590	440	480
P	300	540	650	340	400	510	510	580	1510	520
H.M.	125	169	417	101	150	203	240	591	175	177
Total (%)	32.1	20.8	22.9	14.9	25.7	19.8	22.2	23.6	25.1	24.9
Balance (%)	68.2	79.4	77.8	85.3	74.5	80.4	78.0	76.6	75.3	75.4

H.M.: Heavy metals (Co, Ni, Cu, Ag, Zn, Pb etc).
Balance: Largely Si and anions.

Figures given to the limit of accuracy of the method; full analyses given in appendix C.

RCD25, RCD34, ROD26 and ROD29, the four sites with highest total calcium, also have the highest strontium, which is often a minor constituent of calcite (Veizer, 1983). Heavy metals (e.g. Zn, Pb) are present at well above the global averages for carbonates (Pettijohn, 1963); this probably represents a syngenetic mineralisation (Muir & Ridgway, 1975). Minor and trace elements show little systematic variation. Analyses reported by Muir et al (1956) for two sites in the fishbed horizon (SL163 and SL 167) show a somewhat higher ratio of Ca to Mg (3:1 and 5:1, compared with an average of about 2.5:1 in the present study).

There is generally a high level of Th-U in the sediments. They appear from qualitative microprobe analyses to reside in fish scales deposited with the sediment (in association with La and Ce), presumably as a diagenetic replacement. Rare earth elements frequently replace Ca in apatite (Deer, Howie & Zussman, 1966). Nearby Jurassic sediments, sourced largely from the Middle ORS (Pickering, 1984) have inherited this radiometric signature (Myers, Pers. Comm.).

Laminated fishbed horizons have been sampled over much of their geographical range (fig. 5.1; table 5.1) including two sites south of the Great Glen Fault and three on Orkney. In addition, a number of sites in the laminated flagstones which form the bulk of the ORS of N.E. Scotland are examined, most sites being from above the main fishbed.

5.3 Palaeomagnetism

5.3.1. Previous studies

The lacustrine sediments of the Orcadian Basin have been the

subject of several published studies (table 5.3). Turner (1977) found no stable ancient remanence in the Lower Caithness Flags but a remanence directed steeply upwards to the south (?Mesozoic) was found in the Achanarras Limestone, and a southerly component of shallower inclination in the Latheron Group, immediately above the limestone. Turner et al (1978) used IRM and ARM methods as well as thin-section examination in an investigation of remanence acquisition in these sediments. They concluded that the dominant magnetic carrier in the Latheron Group is magnetite of very fine grain size. The Mesozoic NRM of the Achanarras Limestone was found to be carried in hematite and/or magnetite, with a wide range of coercivities. Occasional chrome-spinels were found, within which hematite exsolution may have occured. Eustance (1981) found a similar pattern in the fishbed horizon at Achanarras and Blackpark (table 5.3) although magnetic inclinations were lower than reported by Turner (1977).

5.3.2. Palaeomagnetism: Laminated fishbed horizons

A total of 8 sites from the main Achanarras fishbed have been analysed, over much of its outcrop range (fig. 5.1). This has been shown to represent more or less a single horizon (Trewin, 1976). In addition, results are reported for one site in the John o'Groats fishbed and one in the Rousay fishbed near Kirkwall. NRM intensity is very low (generally in the range 0.1 to 1.5 mA/m, with a maximum of 6.5 mA/m in one or two specimens).

One of the basic problems in multicomponent analysis of Orcadian Basin sediments, particularly those of low NRM intensity, is that the three major axes of magnetisation

Table 5.3
Palaeomagnetism: Previous studies

Formation & location	Site no. (published)	Site no. (this study)	Direction[1] Dec	Inc	N[2]	k	a_{95}	Ref.
Fishbed (Achanarras Quarry)	?	RCD26	170	-50	33[3]	?	?	A
	CF2		171	-2[4]	15	9	27	B
Fishbed (Blackpark)	CF9		177	-18	6	99	7	
	CF10	RCD25	163	-22	3	146	10	B
	CF11		179	-26	6	17	17	
L.C.F.	?	RCD18	No stable remanence					A
	CF4		No stable remanence					B
U.C.F. (South Head)	CF3	-	191	7[4]	12	3	63	B
U.C.F. (Whaligoe)	CF6	-	197	26[4]	15	5	39	B
U.C.F. (Spital)	?	RCD23-24	Southerly, low-inc.					A
	CF1		191	-1[4]	11	3	73	B

1: In Situ directions
2: Unit weighting to specimens
3: Statistical details not given (N estimated from diagram)
4: No great reliance placed on these directions; note very large error circles
L.C.F. = Lower Caithness Flags
U.C.F. = Upper Caithness Flags
? = not quoted in reference

References: A Turner (1977)
B Eustance (1981)

(Devonian, Permo-Carboniferous and recent) are all approximately coplanar. This problem is compounded by the fact that components acquired at these times will frequently have different origins (e.g. DRM, CRM and VRM) and thus may have severely overlapping stability spectra. Resolution of a magnetisation consisting of two or more of these components will thus require a substantial number of demagnetisation steps. This is the problem found by earlier studies on the lacustrine rocks of the basin, particularly Turner (1977) who used a single-step cleaning technique; a component distribution was highly strung along a north-south

plane gives no clear indication as to whether two or three constituent components are involved. Previously-published mean directions for flagstone sites (Eustance 1981, table 5.3) have very low precision, presumably reflecting varying degrees of effectiveness of separation of NRM components.

Progressive demagnetisation techniques used during the present study have been able to reduce this problem somewhat by using the stipulation that a single component should be defined by at least three, ideally more, demagnetisation steps. Even so, a degree of ambiguity still remains in some specimens, particularly those treated by AF demagnetisation, as discused below.

Of the ten sites analysed, three (RCD28, south of the Great Glen Fault, RCD36, from the marginal limestone of Baligill and RCD49 from the John o'Groats fishbed) give a remanence dominated by PEF and/or random components; they are not considered further. The remaining seven display a wide range of intra-site precision, largely reflecting the relative ease of component separation. Most specimens show a low-stability component, presumably a VRM, which is demagnetised by 100-200 °C or 2-20 mT. Such components may sometimes dominate the remanence of an individual specimen, particularly in site RCD26.

Components of higher stability, with a southerly declination and usually low inclination (+5 to -25°) are often also present. Typical examples illustrated by both thermal and AF demagnetisation, are illustrated in fig. 5.2a,b and 5.2c respectively. Maximum peak demagnetising fields are typically 30-75 mT or maximum temperatures of 350-450 °C, above which directional instability and substantial susceptibility increases occur.

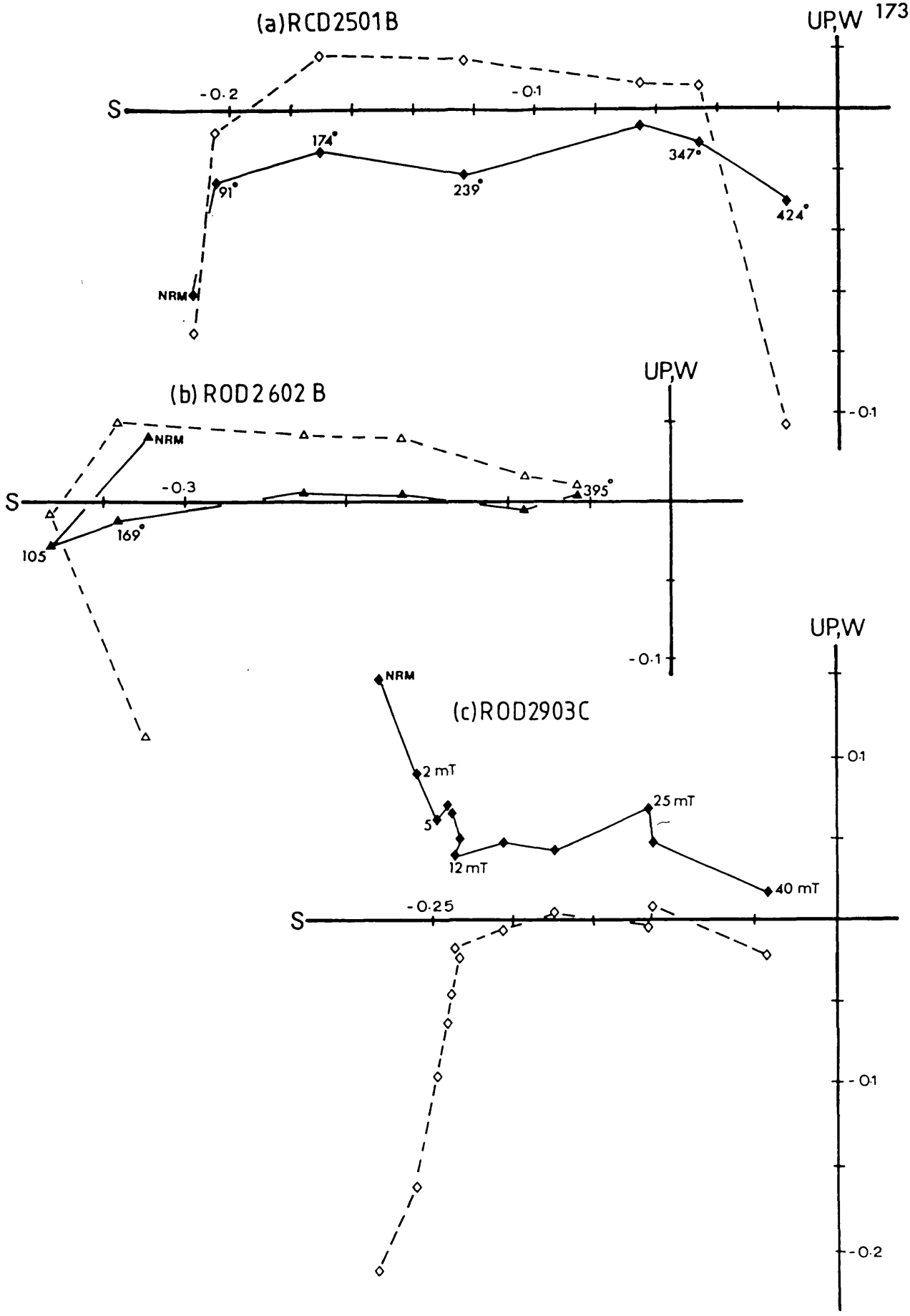


Fig. 5.2. Achanarras Limestone: Demagnetisation characteristics (orthogonal projections, as described in section 1.4.1.). Demagnetisation temperatures in °C or demagnetising field in mT. Axes in mA/m.

However, one or two specimens from each of four sites (RCD26, RCD34, ROD25 and ROD26) show a contrasting remanence directed downwards to the south, with inclinations of +20° to +40° (table 5.4). This could represent a distinct population, which could then be interpreted as representing an early (?DRM/PDRM) remanence as it is in approximate concordance with a Middle ORS direction for the area (chapter 3). Alternatively, these could be composite 'pseudo-components' resulting from a high degree of T_B/coercivity spectrum overlap between the PEF and the dominant low-inclination remanence. Of these six samples, four were treated by AF demagnetisation, which appears to be a less effective method of multi-component NRM separation than thermal analysis in most of the sediments studied elaewhere in the basin. On balance, therefore, the latter possibility is considered to be the most likely, especially as such specimens may occur in the same samples as ones showing a component clearly directed upwards to the south.

Table 5.4
Achanarras Limestone: Anomalous directions.

Site	Specimen	Direction Dec	Inc	N	k	a	Treatment
RCD26	02B	192.8	21.3				Thermal
RCD34	02	207.7	31.9				Thermal
	06A	213.1	32.8				AF
ROD25	05A	181.3	38.6				AF
ROD26	04B	172.2	20.6				AF
	05B	179.5	15.9				AF
Mean		190.6	27.6	6	23	9.7	

Site statistics are given in table 5.5; excluded from these statistics are a total of 16 specimens. These show either an unresolved magnetisation with no clearly-defined components (accounting for 10 specimens) or a PEF direction only. Also excluded are the six anomalous directions given

in table 5.4 which probably represent a discrete population. Site mean directions are shown in fig. 5.3. There is very little difference in precision between in situ and dip corrected mean directions, since two sites have no tectonic dip and the remainder are only very gently inclined.

Comparison of these directions with a general APW path for N.W.Europe, and also with other results derived from the basin (chapter 9), suggests that the dominant remanence is post-Devonian, and is probably Permo-Carboniferous in age. The exclusively reversed (southerly) declination suggests that it may have been acquired during the Kiaman reversed polarity period, as may be the case elsewhere in much of the basin.

Table 5.5
Achanarras Limestone
Site mean directions (in situ)

	With anomalous directions					Without anomalous directions				
Site	Dec	Inc	N	k	a_{95}	Dec	Inc	N	k	a_{95}
RCD25	170.5	-16.1	9	17	12.7	(170.5	-16.1	9	17	12.7)
RCD26	177.0	0.6	4	12	27.1	171.9	-6.4	3	18	29.6
RCD27	203.4	-7.1	3	12	37.4	(203.4	-7.1	3	12	37.4)
RCD34	184.4	3.6	6	5	33.8	172.3	-12.1	4	8	35.5
ROD25	185.6	-10.0	5	5	36.4	186.8	-21.7	4	9	32.1
ROD26	182.3	-5.6	14	28	7.7	183.4	-9.5	12	44	6.6
ROD29	179.5	-7.9	13	23	8.9	(179.5	-7.9	13	23	8.9)
Mean	180.9	-7.1	54	12	5.7	179.8	-11.2	48	17	5.2
	183.3	-6.1	7	45	9.1	181.1	-11.7	7	41	9.6

1: Unit weighting to specimens
2: Unit weighting to sites

5.3.3. Other lacustrine sediments

The remaining sites in lacustrine sediments (table 5.1) may, with the exception of those immediately above the Achanarras Limestone (sites RCD23-24), be discussed very briefly. Few, if any, show a consistent stable ancient

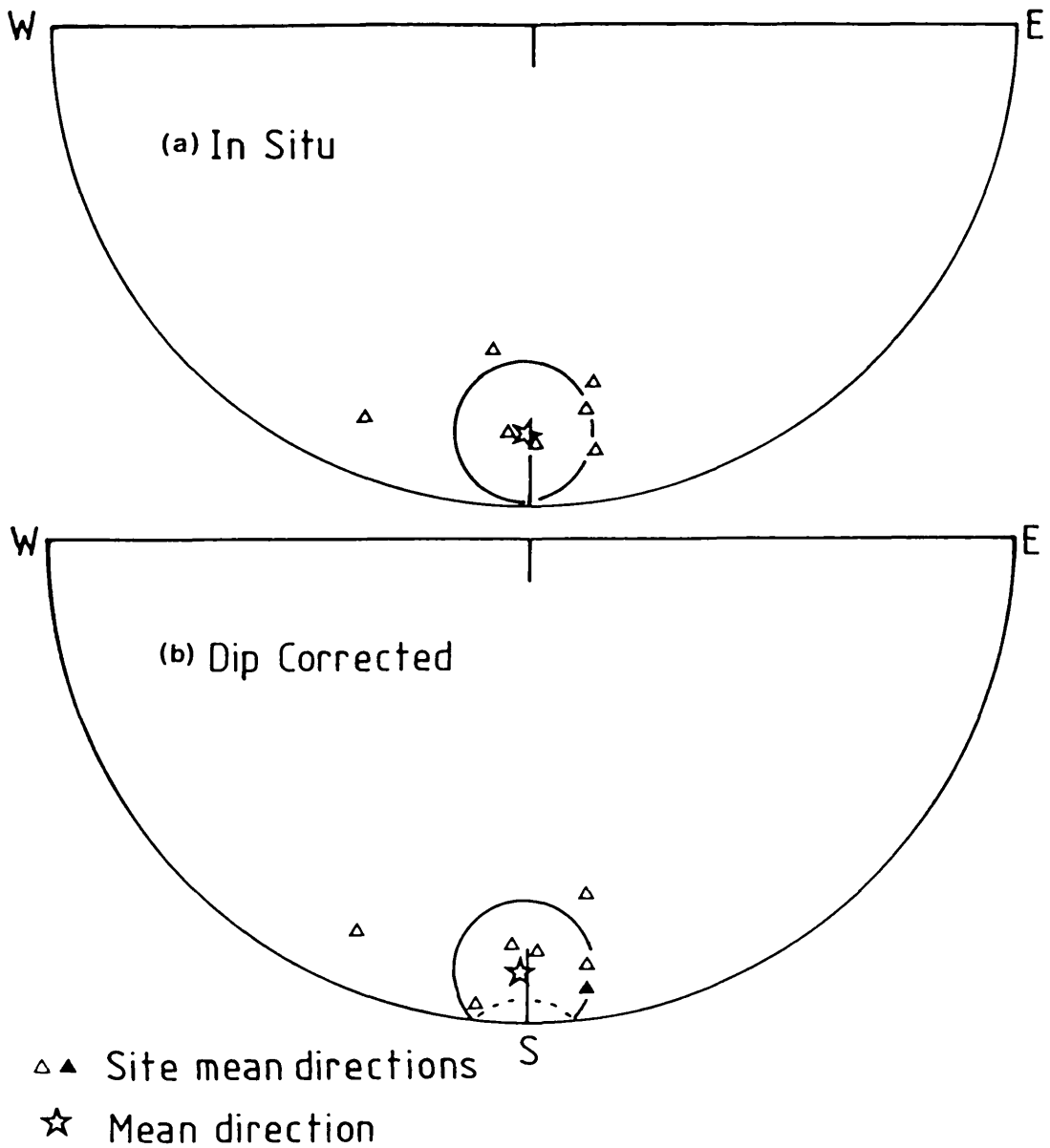


Fig. 5.3. Achanarras Limestone: Site mean directions, *in situ* and dip corrected. 95% circle of confidence for overall mean direction (unit weighting to sites) shown. Statistics given in table 5.5.

remanence, and only representative specimens have been analysed. NRM intensity is very low (typically 0.2 to 0.5 mA/m) and demagnetisation is generally complete at very low temperatures (250-300°C) or applied fields (15-30 mT). Increases in susceptibility at higher temperatures (above 400°C) may be indicative of thermal dehydration of iron oxy-hydroxides or of oxidation of pyrite (Eustance, 1981). These findings are in accordance with those of Turner (1977) and include the Eday Flags (discussed in chapter 3) and the Caithness, Stromness and Rousay Flags of Caithness and Orkney; they will not be considered in any more detail. Their main value is in comparison with sites in similar lithologies which have undergone contact metamorphism (chapter 7).

The two sites in the highly laminated flags of Spital Quarry, immediately above the Achanarras Fishbed, are worthy of somewhat more detailed consideration. Similar material has previously been investigated by Turner (1977), Turner et al (1978) and Eustance (1981), as summarised in table 5.3. after cleaning at 30 mT, directional distribution is reported by Turner (1977) to be highly strung between the PEF and a shallow, southerly direction. This is interpreted as an early diagenetic magnetisation held in magnetite, acquired over more than one polarity interval, but reinterpreted by Turner et al (1978) as a relict Devonian magnetisation with a stronger Mesozoic overprint of normal polarity. Eustance (1981) reports a southerly mean direction of low inclination for this and other similar locations (table 5.3) but these are of very low precision and must be treated with some caution.

Individual components are generally fairly poorly

defined, largely due to the generally low NRM intensity (typically less than 1.0 mA/m). Demagnetisation characteristics are somewhat similar to those shown by the main fishbed horizon (section 5.3.2), with a high-intensity, low-stability VRM and also a more stable component of higher T_B (fig. 5.4). (The high magnetic viscosity is demonstrated by leaving specimens for several months between repeat NRM measurements; they may show intensity changes of 50-80 %). The stable component is of more variable inclination than that in the fishbed, however, with a range between +70° to the north and -30° to the south (fig. 5.5). This is a similar distribution to that shown by Turner (1977) for AF cleaned specimens from the same outcrops. There is no evidence for a valid southerly, downwards component carried by authigenic magnetite, as suggested by Turner (op. cit.). The distribution appears more likely to be the result of variable degrees of T_B /coercivity overlap between a viscous PEF component and a late Palaeozoic/early Mesozoic overprint.

The small number of specimens from these two sites showing a clear high-stability component makes derivation of site mean directions impracticable; the main point is that there is, without doubt, a late Palaeozoic - early Mesozoic overprint in these sediments.

5.3.4. Hysteresis of NRM

Fig. 5.6 shows typical saturation IRM hysteresis curves for representative lacustrine sediments, including both true fishbeds and other laminites. Results are summarised in table 5.6. M_S is low (700 to 7000 mA/m) and saturation was sometimes not achieved below 350 mT. This indicates that hematite must be present, at least in some samples, since

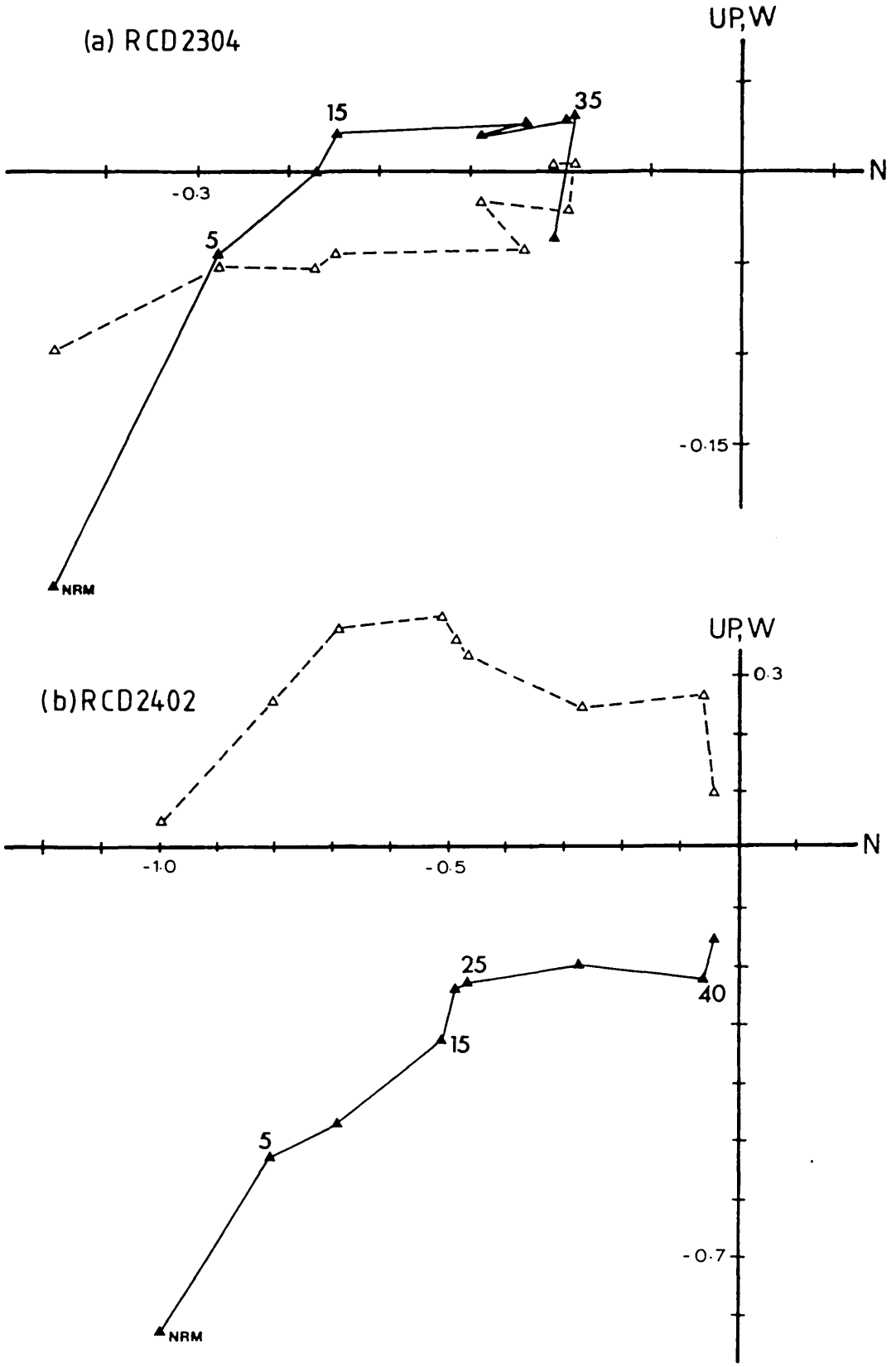


Fig. 5.4. Latheron Group (Staxigoe Formation): Demagnetisation characteristics (orthogonal projections, as described in section 1.4.1.). Demagnetising field in mT; axes in mA/m.

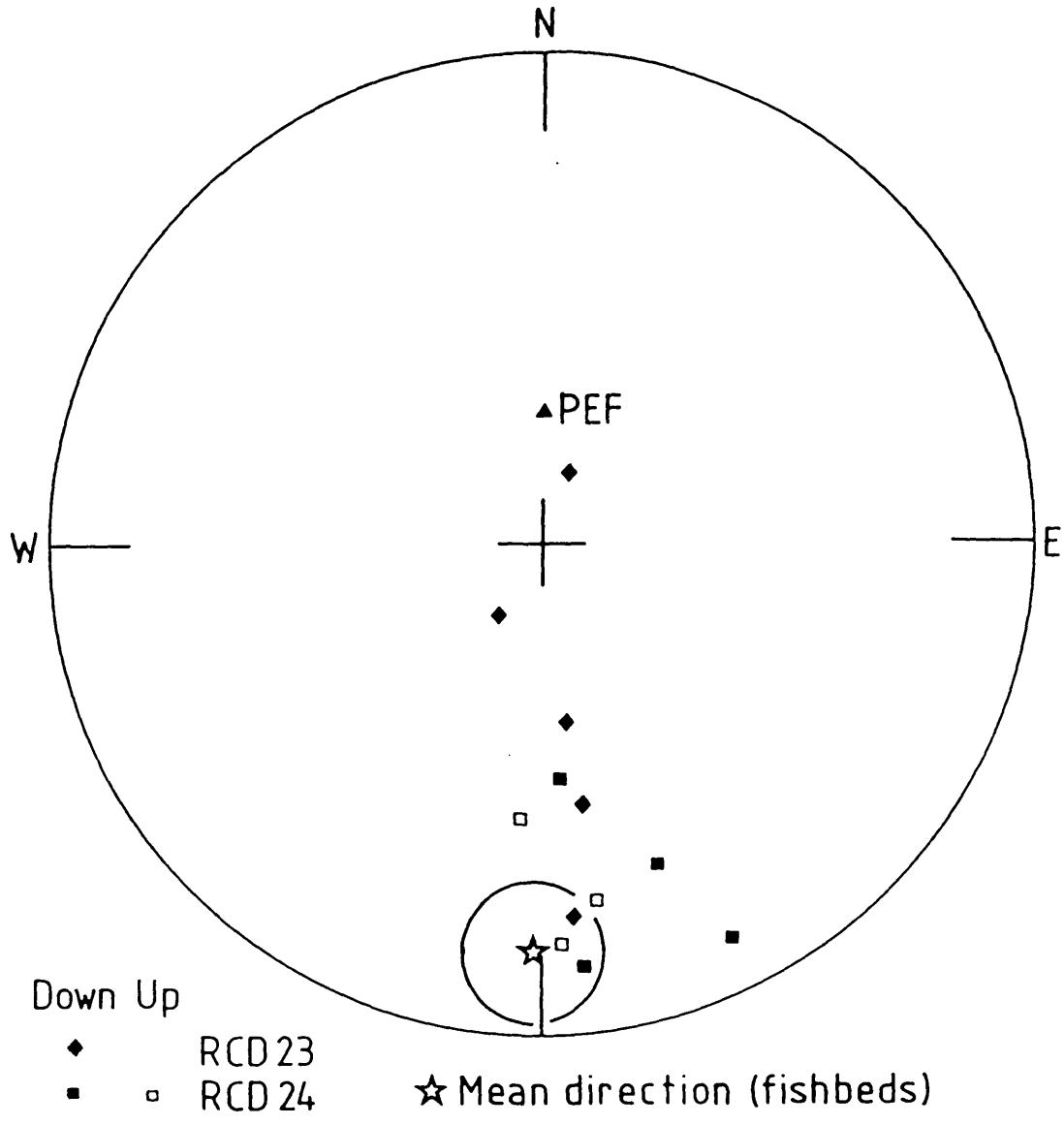


Fig. 5.5. Latheron Group (Staxigoe Formation): Stable component directions. Mean direction from Achanarras Limestone shown for comparison.

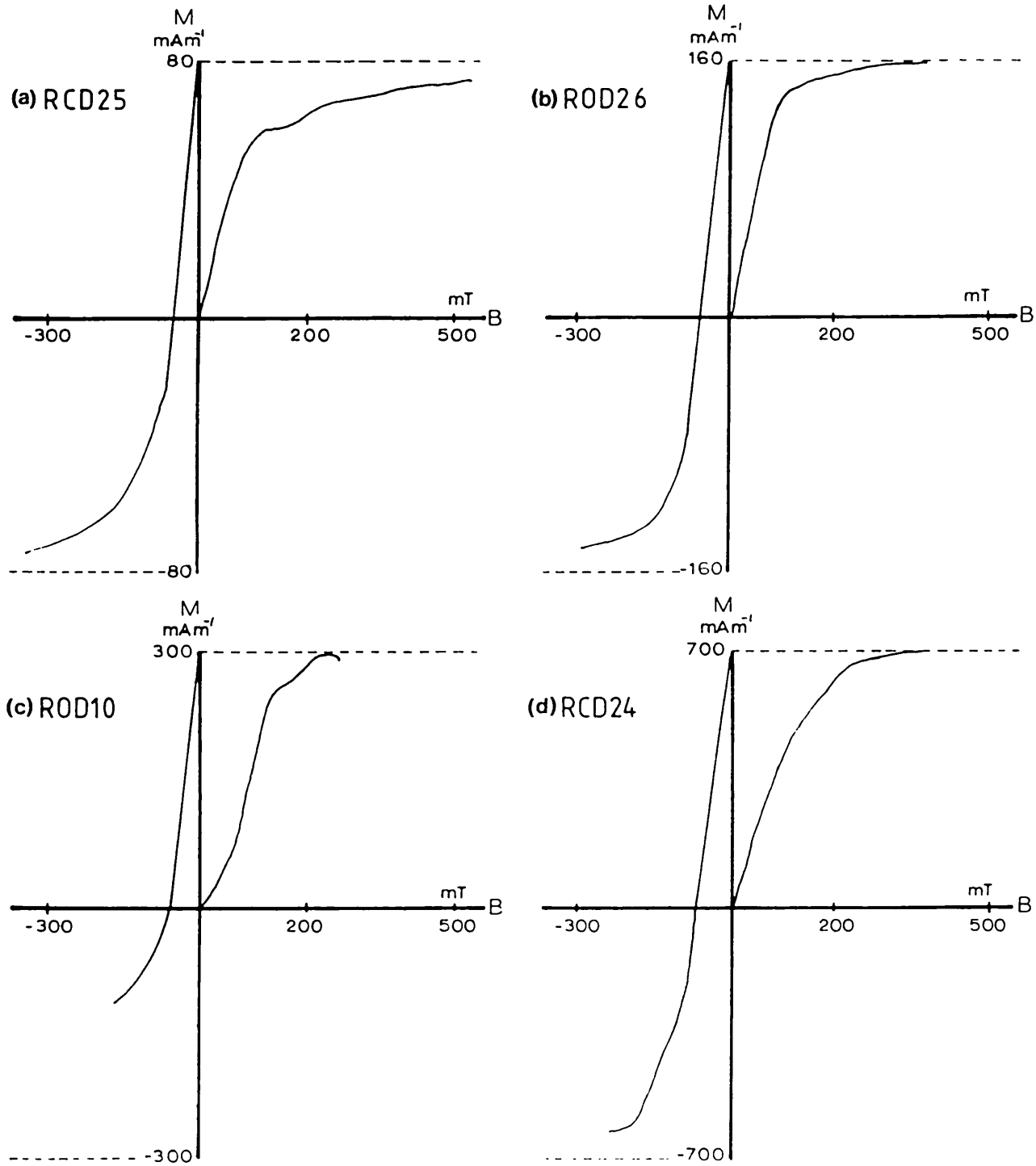


Fig. 5.6. Lacustrine sediments: Hysteresis of NRM. (a) and (b): Achanarras Limestone (c) Rousay Flags (d) Latheron Group (Staxigoe Formation).

magnetite and maghemite saturate in fields of 100-150 mT, even when single-domain (Dunlop, 1972a).

Table 5.6
Lacustrine Sediments: Rock magnetic characteristics.

Site	Fmn.	T_{max} (°C)	B_c (mT)	B_s (mT)	M_s (mA/m)	Reliability	Magnetic Mineralogy
RCD24	1	-	50-90	>300	700	1	H ± M
RCD25	2	400-500	<66	>350	80	3	H ± M
RCD26	2	400-450	<47	>120	350	1,2	M and/or H
RCD27	2	300-370	40-47	365	198	3	H ± M
RCD28	2	-	-	-	-	0	
RCD34	2	300-400	<66	>350	80	2	H ± M
RCD36	2	-	-	-	-	0	
RCD49	3	<300	40-47	120	116	0	?
ROD10	4	-	<47	>120	300	0	
ROD25	5	400-500	<47	>160	360	2	M and/or H
ROD26	2	400-500	47-61	365	156	3	H ± M
ROD29	2	350-400	<110	>200	180	3	H ± M

Formations: 1 Staxigoe
2 Achanarras Fishbed
3 John o'Groats Fishbed
4 Rousay Flags
5 Rousay Fishbed

Magnetic Mineralogy: M: Magnetite H: Hematite

Reliability: 0 = No ancient remanence
1 = Ancient remanence present but not resolvable
2 = Ancient remanence quantifiable but inaccurate
3 = Ancient remanence well-defined

5.4 Summary

The lacustrine sediments of the Orcadian Basin have been shown to carry little or no primary remanence components. This is somewhat surprising, as detrital iron oxides are widespread in many of the coarser clastic sediments nearby; much of this was probably originally deposited as magnetite (chapter 6). Any magnetite which was deposited in the lacustrne environment might be expected to have escaped severe oxidation due to the high organic content of the rocks. Even if the hydrodynamic properties of detrital magnetite prevented it reaching the deeper-water facies under discussion, other processes such as aeolian deposition or authigenic production at the sediment-water

interface (Creer et al, 1972) might be expected to have operated.

Stable remanence is carried predominantly in hematite, which is entirely of secondary origin. The origin of the remanence will be discussed together with that of the clastic sediments (chapter 4) in the next chapter.

CHAPTER 6

SEDIMENTS: MAGNETIC MINERALOGY AND REMANENCE ACQUISITION

6.1 Introduction.

The palaeomagnetic characteristics of a wide range of sediment types, from predominantly chemical carbonate sediments to coarse clastic rocks, have been analysed in the previous two chapters. It has been shown that there has been a partial remagnetisation affecting many of the sediments (but not contemporaneous lavas); this has often replaced or obscured any possible primary remanence. A suspected primary remanence may often occur in close association with this, sometimes within the same specimen.

It is proposed to examine the paragenesis of three major categories of sediment in more detail than the remainder. These categories are (i) the Eday Group of Orkney (sections 4.4 and 4.5), (ii) the Sarclet Group and related rocks of Caithness (section 4.3) and (iii) the Niandt Limestone (chapter 5) which has been sampled throughout much of the geographical extent of the basin. The first two show intimately associated primary and secondary components while the third has been totally remagnetised. Characteristics of the remaining sites (the Upper ORS and the rest of the Lower ORS) will be considered alongside the above but in lesser detail.

Palaeomagnetic work suggests that most stable ancient remanence is carried by hematite (table 4.13). This applies without exception to the remagnetisation and also to most primary components with the exception of a small number of sites in the Eday Group and possibly in the Sarclet Group.

Observations and deductions from a number of separate

viewpoints will be discussed in this chapter. These will then be integrated to assist in the construction of a model for remanence acquisition in the Orcadian Basin.

6.2. Bulk Geochemistry.

The bulk chemical composition of a sandstone is a complex function of source rock characteristics, primary weathering processes, transport history and diagenesis. It can give much valuable information about the nature of the rock, ideally enabling the effects of some or all of the above-mentioned variables to be modelled.

Whole-rock ICP analyses for a number of sites in sediments of the basin are tabulated in appendix C1. These include 15 analyses for the Sarclet Group (appendix C1e), 40 for the Eday Group (appendix C1f) and 13 for other Middle and Upper ORS sediments (appendic C1g). Analyses for laminated sediments (appendix C1d) are described in chapter 5. It is suggested that these analyses provide a moderately good indication of the true mean rock composition, as most are based on offcuts from a number of discrete specimens, selected to avoid surface weathering features. Exceptions are a small number of analyses of thermally-treated specimens for which fresh material was not available.

The bulk of the data, despite being of interest in several respects, is not of direct relevance to the theme of this study. Salient points, particularly for the Eday Group (for which sufficient data is available to make more detailed interpretation), will be discussed below and referred to elsewhere in this chapter. The implications of regional mean analyses with regard to source rock characteristics are discussed in chapter 2.

(i) Total Analysis. The ICP method analyses all major and

most minor elements with the exceptions of silicon, carbon and anions; hence the total analysis provides an indication of the total non-silicate content of the rock. Mature sandstones with a low ferromagnesian/feldspar content will thus give a lower total analysis than mineralogically immature sediments, and coarser-grained sediments a lower total than fine-grained (Pettijohn, 1963). Mean total analyses for the Eday Group have been categorised according both to grain size (as given in appendix B) and to individual formation. This shows the relative mineralogical immaturity of finer-grained sediments compared with coarser (table 6.1a). It also suggests that the upper and lower sandstone formations are generally more mature than the Eday Marls and Middle Eday Sandstone. This is in accord with field and thin-section observation that the latter two formations bear a greater facies resemblance to each other than either does to the Lower or Upper Eday Sandstone.

(ii) Total Iron. Total iron content is over three times greater in fine-grained sediments (table 6.1b) than in medium or coarse sandstones, reaching a maximum of over 4% in very fine-grained horizons in the Eday Marls. This is consistent with the frequently-observed relationship between the two parameters (e.g. Walker & Honea 1969).

This relationship does not in itself show that iron constitutes a greater proportion of the non-silica analysis; it could simply be a dilution effect caused by increasing SiO_2 in coarse sandstones. However, table 6.1c, in which iron content is expressed as a percentage of the total analysis, shows that iron generally constitutes an increasingly greater proportion as grain size decreases.

The reason for the apparent iron enrichment in fine-

Table 6.1.

ICP Characteristics.

(a) Total Analysis (%)

	VF	F	M	C	Mean
UES	-	-	9.68	6.95	8.90
EM	20.45	11.83	8.00	-	12.04
MES	22.60	16.33	9.20	9.20	14.33
LES	-	13.80	9.50	8.10	9.51
Mean	21.70	14.04	9.18	8.22	

(b) Total Iron (%)

	VF	F	M	C	Mean
UES	-	-	1.09	1.43	1.19
EM	3.90	4.30	0.87	-	1.83
MES	2.83	2.30	1.16	0.60	1.81
LES	-	1.17	1.03	1.01	1.04
Mean	3.26	2.03	0.99	0.96	

(c) Total Iron/Total Analysis (%)

	VF	F	M	C	Mean
UES	-	-	11.3	14.8	12.3
EM	19.1	36.3	10.9	-	21.2
MES	12.5	14.1	12.6	6.5	11.4
LES	-	22.8	11.2	10.8	11.3
Mean	15.3	16.1	11.7	9.1	

(d) Na-K Ratio

	VF	F	M	C	Mean
UES	_	_	0.61	0.38	0.55
EM	0.37	0.66	0.51	-	0.53
MES	0.41	0.33	0.43	0.41	0.39
LES	-	0.33	0.47	0.50	0.42
Mean	0.39	0.48	0.48	0.43	

Formation

UES Upper Eday Sandstone
EM Eday Marls
MES Middle Eday Sandstone
LES Lower Eday Sandstone

Grain size

C Coarse
M Medium
F Fine
VF Very Fine

grained sediments has been discussed extensively (see Turner, 1980). It is suggested by Carroll (1958) that a significant amount of iron may be transported in close association with the sediment clay fraction, possibly as a thin surface film around clay particles. This would be an enhanced effect in environments of high Eh in which ferromagnesian minerals in the coarser fraction would tend to be unstable.

Association of some of the iron with clays is suggested by fig.6.1; there is a linear relationship in fine-grained sediments between Fe and Al, both of which are generally high. (Al is used as a first approximation to the amount of clay minerals). In coarse sediments, total Al has a restricted range of 3-4% which thus presumably represents detrital silicates (feldspars etc.), little clay being observable in thin section.

Analyses for Fe^{2+}/Fe^{3+} (appendix A) were made for only a very small number of samples. Results are summarised in appendix E; only a few are from sediments unaffected by later igneous intrusions (RCD10 and 11 and ROD54G&P). Reference will be made to these below.

It is interesting to relate total iron content to palaeomagnetic properties, illustrated for the Eday and Sarclet Groups in fig.6.2. This shows two main features: (i) High iron content is always associated with a stable ancient remanence, and (ii) Rocks carrying no stable ancient remanence are always of low iron content, although the reverse is not true. This is presumably a direct function of grain size; finer grained sediments generally have a high iron content, as shown above, and are also less vulnerable to weathering processes which may be responsible for the

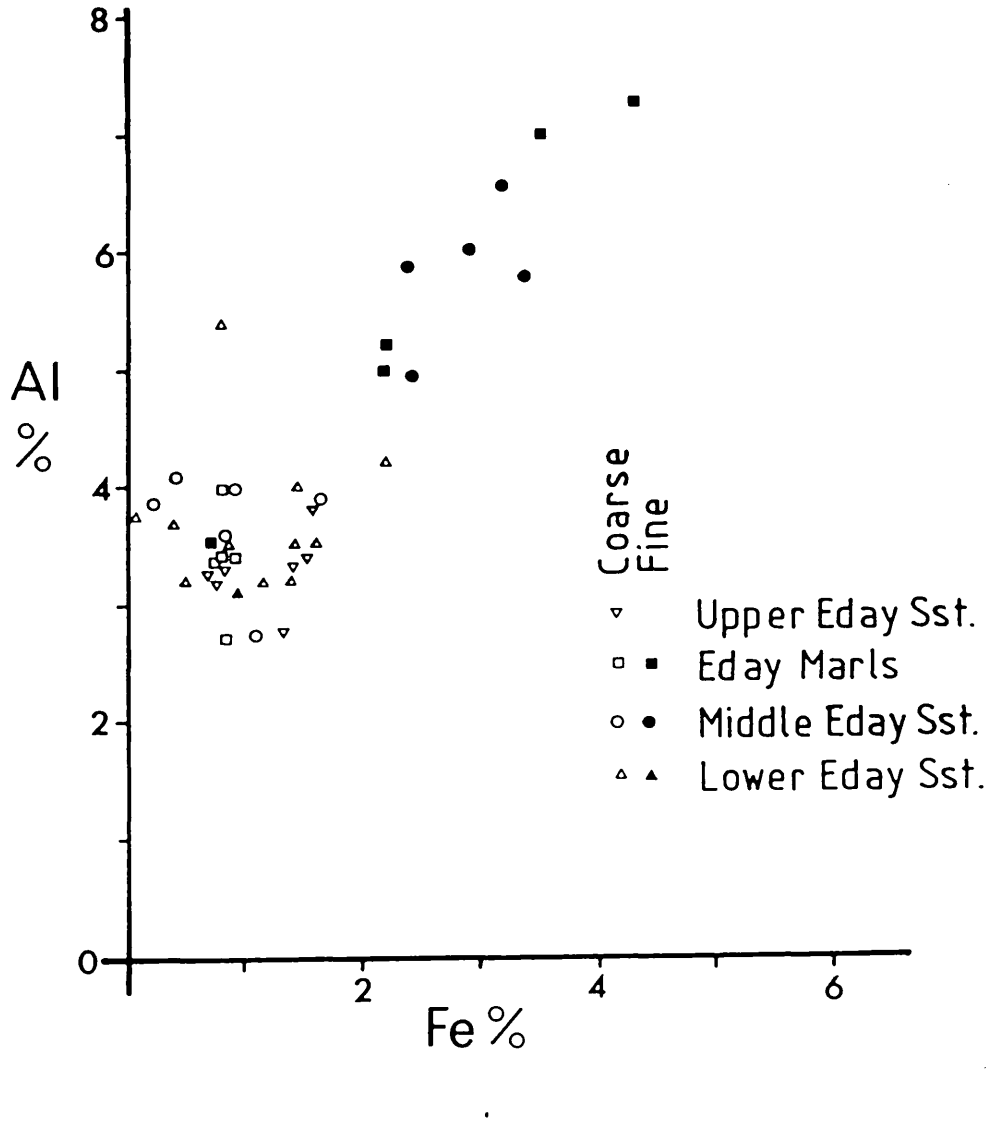


Fig. 6.1. ICP analyses, Eday Group. Relationship between Al and total Fe according to grain size. 'Coarse' corresponds to grain sizes M and C, 'Fine' to F and VF, as listed in appendix B.

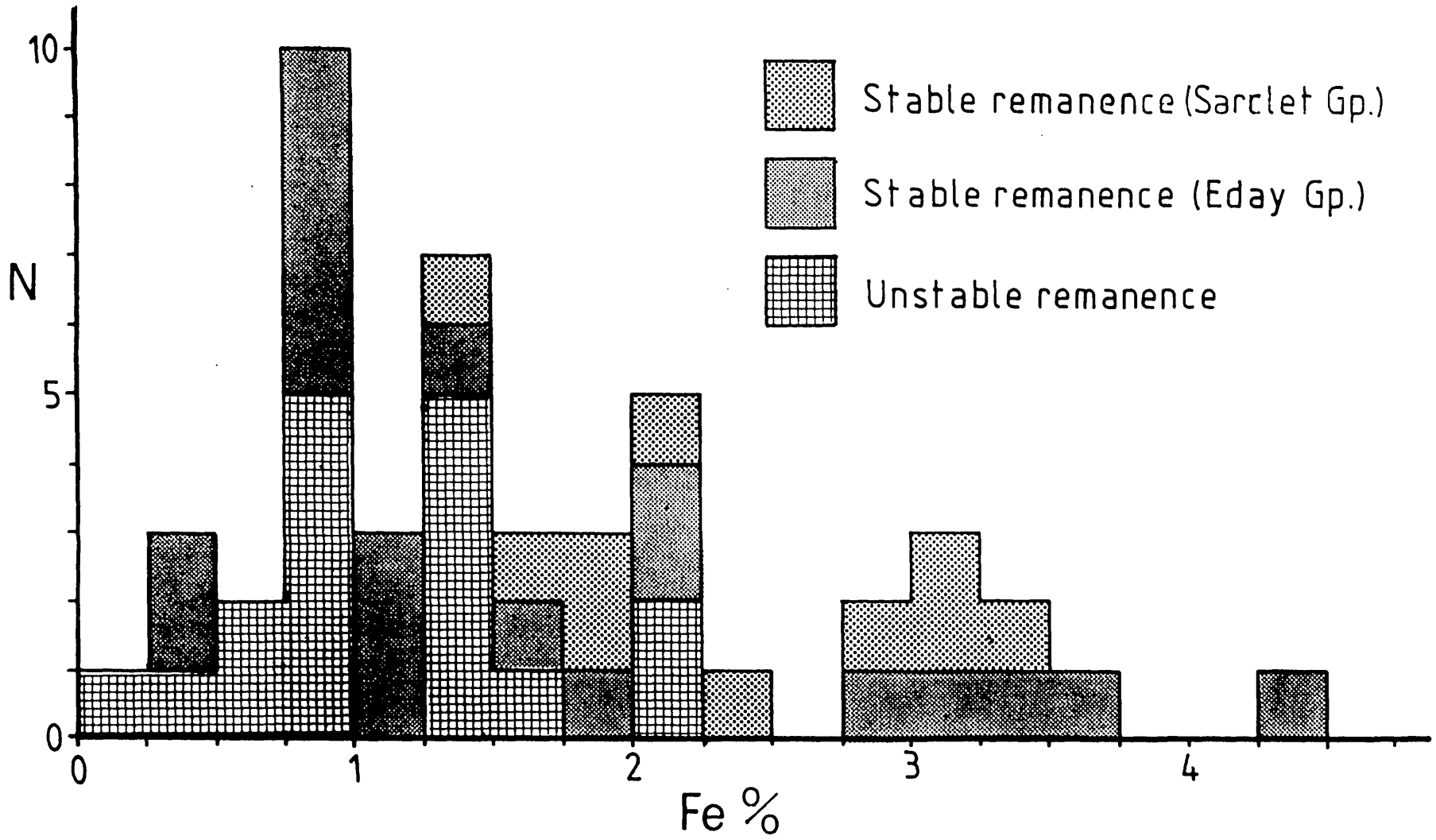


Fig. 6.2. Stable and 'unstable' (i.e. not geologically meaningful) remanence according to total Fe content; Eday and Sarclet Groups.

alteration or destruction of much of the magnetic mineralogy.

(iii) Other elements. Other criteria may be used as an approximate indicator of mineralogical maturity, such as the Na/K ratio, since albitic feldspars will tend to decompose more rapidly than orthoclase (Bramlette, 1941). Mean values of this ratio for Eday Group sediments (table 6.1d) show an increase from 0.38-0.40 in the Lower and Middle Eday Sandstones to 0.53-0.55 in the Eday Marls and Upper Eday Sandstone. Calcium and magnesium, largely associated with carbonate cements, will be discussed below. Regional implications of mean values (appendix C2) are discussed in chapter 2.

6.3. Iron-Titanium Oxides.

6.3.1. Introduction.

Iron-titanium oxides are a ubiquitous constituent of nearly all redbed successions. They are easily detectable qualitatively but more detailed information (mineralogy, diagenetic history etc.) is often obscure to a greater or lesser degree and infrequently investigated.

In Orcadian Basin sediments it is possible to subdivide iron-titanium oxides into two distinct groups, according to whether they originally formed part of the detrital fraction of the sediment or if they appear to be secondary in origin. The distinction is usually straightforward, based largely on morphological characteristics. Detrital grains, particularly in more mature sediments, will tend to be rounded or sub-rounded while secondary oxides may often be subhedral or even perfectly euhedral. They may often grow freely in open pore spaces.

Secondary oxides will tend to acquire a palaeomagnetic

remanence during their growth through the appropriate critical blocking diameter (chapter 2). The time at which this occurred may be quantifiable palaeomagnetically if it is a sufficient time after deposition and/or tectonic activity.

Detrital oxides may acquire a remanence during or very shortly after deposition (a DRM; see chapter 2). If the grain is (at this or any later stage in its history) metastable with respect to another phase or phases then it may undergo diagenetic alteration. As with secondary oxides, this may result in remanence acquisition or remagnetisation. Processes which may occur in sediments are usually oxidative, and will often result in, for example, the oxidation of magnetite to maghemite or hematite.

Iron oxides from the Orcadian Basin, both detrital and secondary, have been investigated in the present study, largely using electron microscopy. Attempts have been made to characterise the compositions of various categories of iron oxide using EPMA spot analyses; results and problems encountered will be discussed in the following sections.

6.3.2. Detrital Oxides: Morphology.

Grains which would appear to be of detrital origin are ubiquitous in nearly all of the clastic sediments studied. Recognisable largely from grain outline, a variety of textures and morphologies are illustrated in plate 6.1.

In addition to anhedral grain shape (e.g. plate 6.1h), additional evidence of detrital origin for such grains is provided by plate 6.1f, in which a detrital sheet silicate is deformed around an iron oxide grain, presumably during sediment compaction. Oxides may also occasionally form part

PLATE 6.1
DETRITAL IRON-TITANIUM OXIDES

(a) RCD10; Upper ORS, Dunnet Head. Deeply-pitted titaniferous iron oxide grain. (BEI, Jeol 733).

(b) RCD46; Sarclet Sandstone, Sarclet Haven, Caithness. Strongly martitised iron oxide grain but still with significant Ti content (analysis 150, appendix D2i). (BEI, Jeol 733).

(c) RCD54; Upper ORS, Dornoch. Detrital grain with pure TiO_2 (T) and titaniferous iron oxide (F). (BEI, Jeol 733).

(d) Detail from (c), showing exsolution lamellae within the iron oxide portion of the grain. Higher Ti in the darker lamellae (analyses 181,183) than in the lighter (analysis 182, appendix D2iii). (BEI, Jeol 733).

(e) ROD17; Middle Eday Sandstone, Deerness. Strongly martitised iron oxide grain with low Ti content (analysis 094, appendix D2ii). (SEI, Jeol 733).

(f) ROD22; Eday Marls, S. Ronaldsay. Iron-titanium oxide grain (F); detrital origin suggested by the sheet silicate (S), deformed around the grain, possibly during early sediment compaction. (BEI, Jeol 733).

(g) ROD18; Middle Eday Sandstone, Deerness. Iron-titanium oxide grain (F) with negligible Ti (analysis 193, appendix D2ii). (BEI, Jeol JXA-50A).

(h) ROD18, Middle Eday Sandstone, Deerness. Rounded detrital iron-titanium oxide (analysis 192, appendix D2ii). Surrounding material is largely silica. (BEI, Jeol JXA-50A).

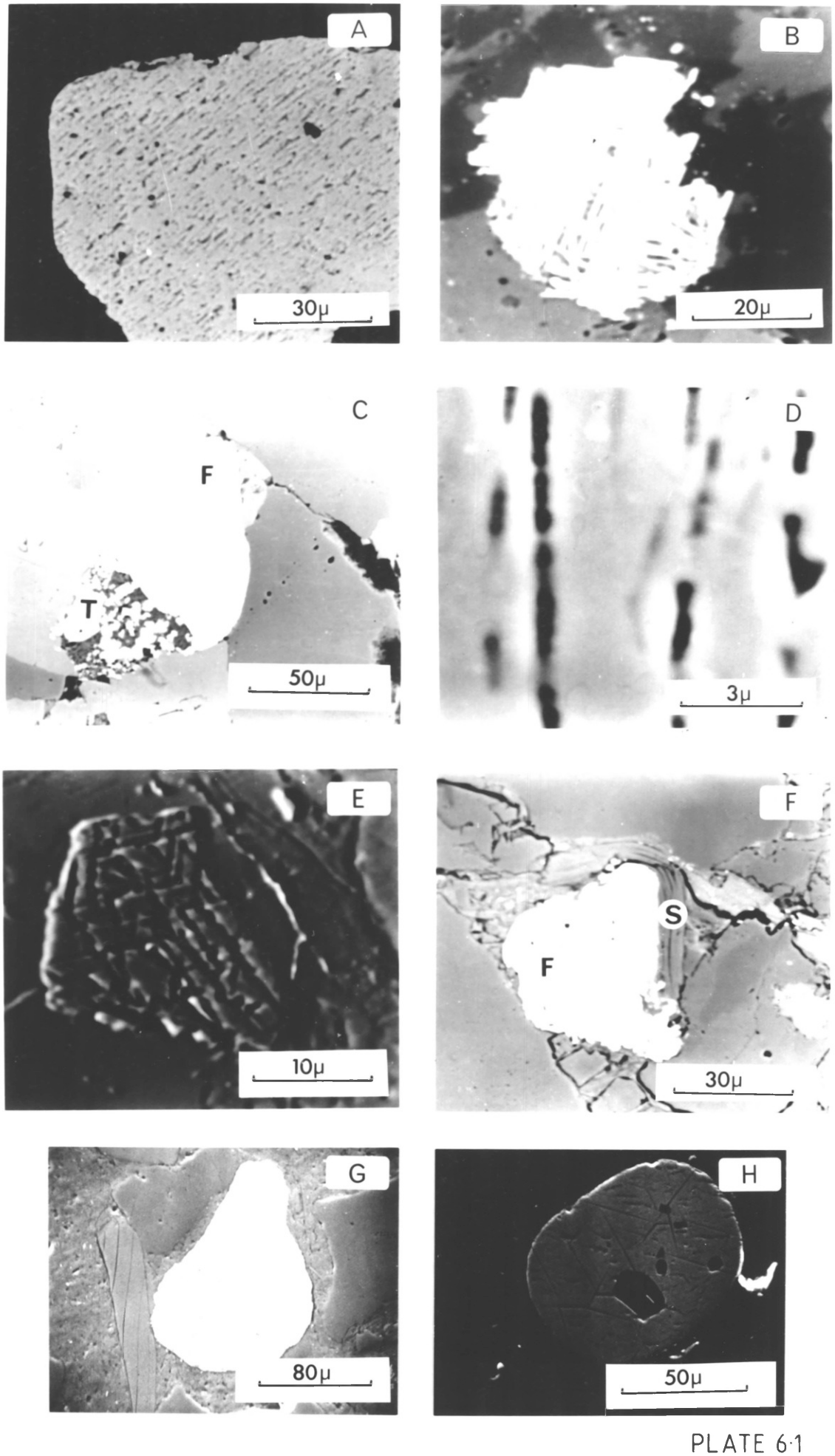


PLATE 6·1

of a larger rock fragment, as in plate 6.1c.

Some grains do not give such clear indications of their detrital origin. Plate 6.1b, for example, shows a grain which is of irregular, angular outline but which has been severely martitised. One set of exsolution lamellae has been selectively removed by dissolution, producing the observed shape. Additional irregularities may have been caused by later syntaxial overgrowths. Based largely on the fact that the grain is an alteration product of a precursor magnetite (which is very unlikely to have formed diagenetically), it is probably a detrital grain.

The texture of many detrital oxides gives conclusive evidence of martitisation having occurred, as described by van Houten (1968), Turner (1980) and Reynolds (1982). Typical examples, showing a range of degree of martitisation, are shown in plate 6.1. Exsolution may be of very fine scale, as shown in plate 6.1d, or may be very coarse (plate 6.1e). Individual lamellae may be much less than 1μ in width and show a variation in Ti content (e.g. analyses 181-183, appendix D2iii). Analyses at this scale will tend to be very imprecise as the beam diameter is significantly greater than the width of a single lamella.

Some grains (e.g. plate 6.1g) would appear to be almost totally fresh while others (e.g. plate 6.1a,b,e) have undergone later dissolution of the exsolved ilmenite/rutile. It would appear from palaeomagnetic characteristics (chapter 4) and also EPMA analyses (see below) that magnetite is not present in these samples in significant amounts. The grains are thus presumably all hematitic.

Whether the apparently fresher grains have undergone pervasive but extremely fine-scale oxidation from a

magnetite precursor or were deposited as hematite is not apparent. Detrital hematite is described by Steiner (1983) and Tauxe & Kent (1984) but is very difficult to distinguish from secondary hematite unless a well-developed cleavage is present.

6.3.3. Secondary Oxides: Morphology.

Plates 6.2 and 6.3 illustrate the very wide range of types of secondary iron-titanium oxide/oxyhydroxide present in clastic sediments of the Orcadian Basin. Most are either of highly irregular (but angular) shape or are perfectly euhedral, both of which preclude transport in the high-energy depositional system indicated by other detrital grains.

Euhedral hexagonal hematite crystals (plate 6.2a,f) show a range of grain size, from 1-2μ to over 40μ. They may occur either within a sediment now of low porosity-permeability (e.g. plate 6.2a) or may grow into open pore space (plate 6.2f).

A close association with authigenic clays is suggested by plate 6.2d, in which anhedral iron oxides occur within kaolinite (s.l.) in a large open pore space. The origin of other irregular grains, such as those shown in plate 6.2b,c and e, is less clear; they may result from pseudomorphing of precursor ferromagnesian minerals.

Other forms of pore-filling iron oxides, sometimes with traces of other elements typical of clays (Al, Mg) are shown in plate 6.3. Plate 6.3a-c show the two discrete morphologies of secondary iron oxides present in the Middle Eday Sandstone and elsewhere; there is an early phase of subhedral (type I) crystals, 1 to 10μ in diameter, and a

PLATE 6.2
SECONDARY IRON-TITANIUM OXIDES (I)

(a) RCD20; Sarclet Sandstone, Sarclet Haven. Euhedral iron oxide with 3% Ti (analysis 154, appendix D2i). (BEI, Jeol 733).

(b) RCD20; Sarclet Sandstone, Sarclet Haven. Irregular (secondary) iron-titanium oxide (F) with quartz (Q) and orthoclase (K). Oxide shows 7.5% Ti (analysis 155, appendix D2i). (BEI, Jeol 733).

(c) RCD51; Hillhead Redbed, Wick. Sheet of low-Ti iron oxide (F) (analyses 118,119; appendix D2i), occupying a minor cleavage plane. Surrounding detrital grains of quartz (Q) and orthoclase (K). (BEI, Jeol 733).

(d) ROD30; Eday Marls, Kirkwall. Low-Ti iron oxides (analyses 233,234; appendix D2iii) closely associated with kaolinite (K) and apparently growing into porosity (O). (BEI, Jeol 733).

(e) ROD30; Eday Marls, Kirkwall. Low-Ti iron oxide of highly irregular shape (not analysed quantitatively). (BEI, Jeol JXA-50A).

(f) RCD42; Ellens Geo Conglomerate, Ulbster. Hexagonal hematite crystals growing in pore space. Slight Ti detected qualitatively. (BEI, Jeol JXA-50A).

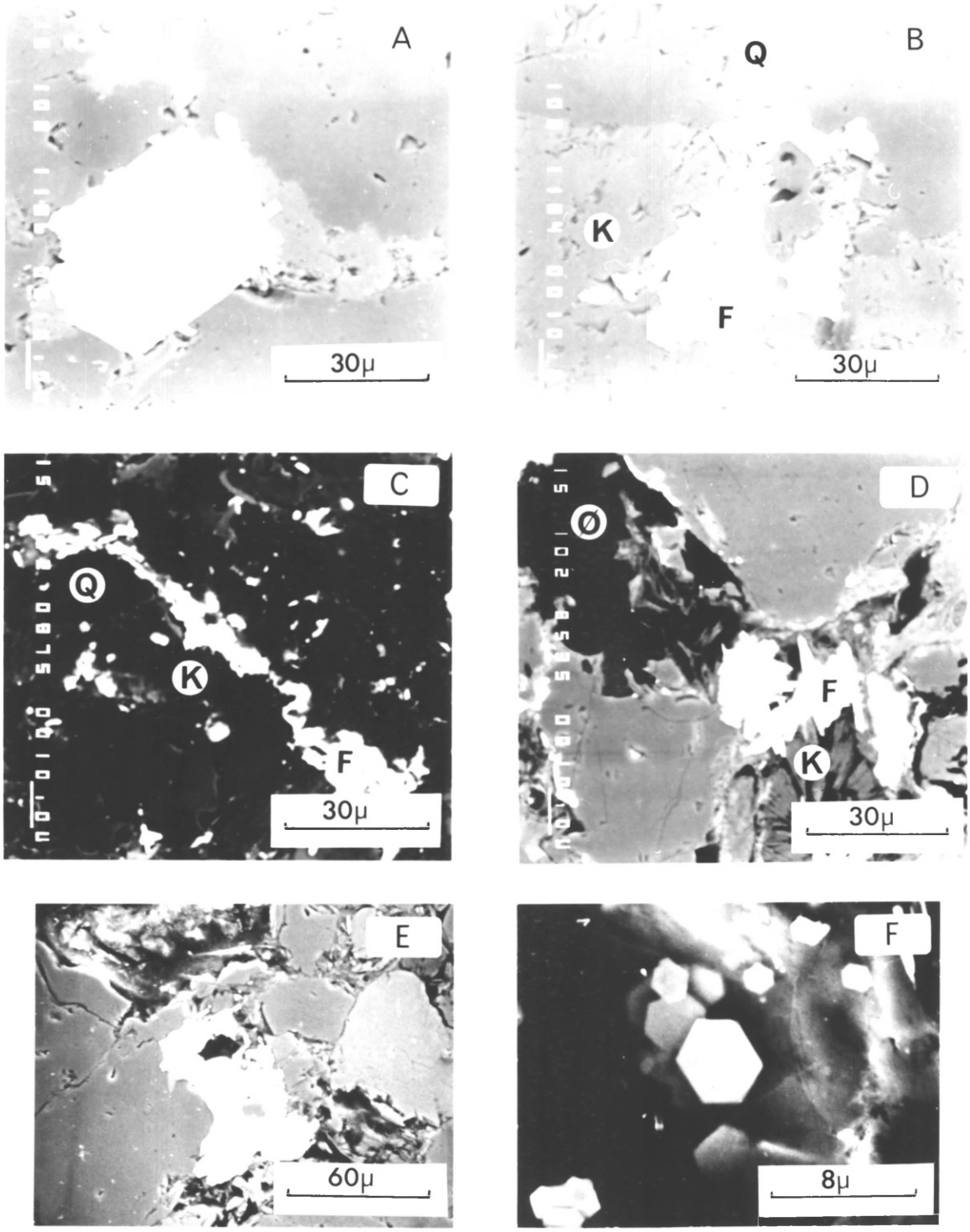


PLATE 6·2

PLATE 6.3
SECONDARY IRON-TITANIUM OXIDES (II)

(a) ROD24; Middle Eday Sandstone, S. Ronaldsay. Pore-lining secondary iron oxide growths. (BEI, Jeol 733).

(b) ROD24; Middle Eday Sandstone, S. Ronaldsay. Detail of fibrous iron oxides, growing into open pore space.

(c) ROD24; Middle Eday Sandstone, S. Ronaldsay. Enlargement of (a) showing two-phase growth of iron oxides, with inner subhedral crystals (A) and an outer zone of needle-like growths (B) within open pore space. X-ray spectra for both types of growth shown in fig. 6.3. (BEI, Jeol 733).

(d) ROD22; Eday Marls, S. Ronaldsay. Iron-titanium oxide grain (F) with later overgrowths of iron oxide. (BEI, Jeol 733).

(e) ROD22; Eday Marls, S. Ronaldsay. Authigenic iron-titanium oxide laths (analysis 210, appendix D2iii) growing into pore space. (BEI, Jeol 733).

(f) RCD42; Ellens Geo Conglomerate, Ulbster. Split-screen image showing partial iron oxide pseudomorphing of an original detrital grain. Right-hand side is an Fe x-ray map of the left-hand side field of view. Isolated patch of high Fe is a detrital iron oxide grain. (SEI, Jeol 733).

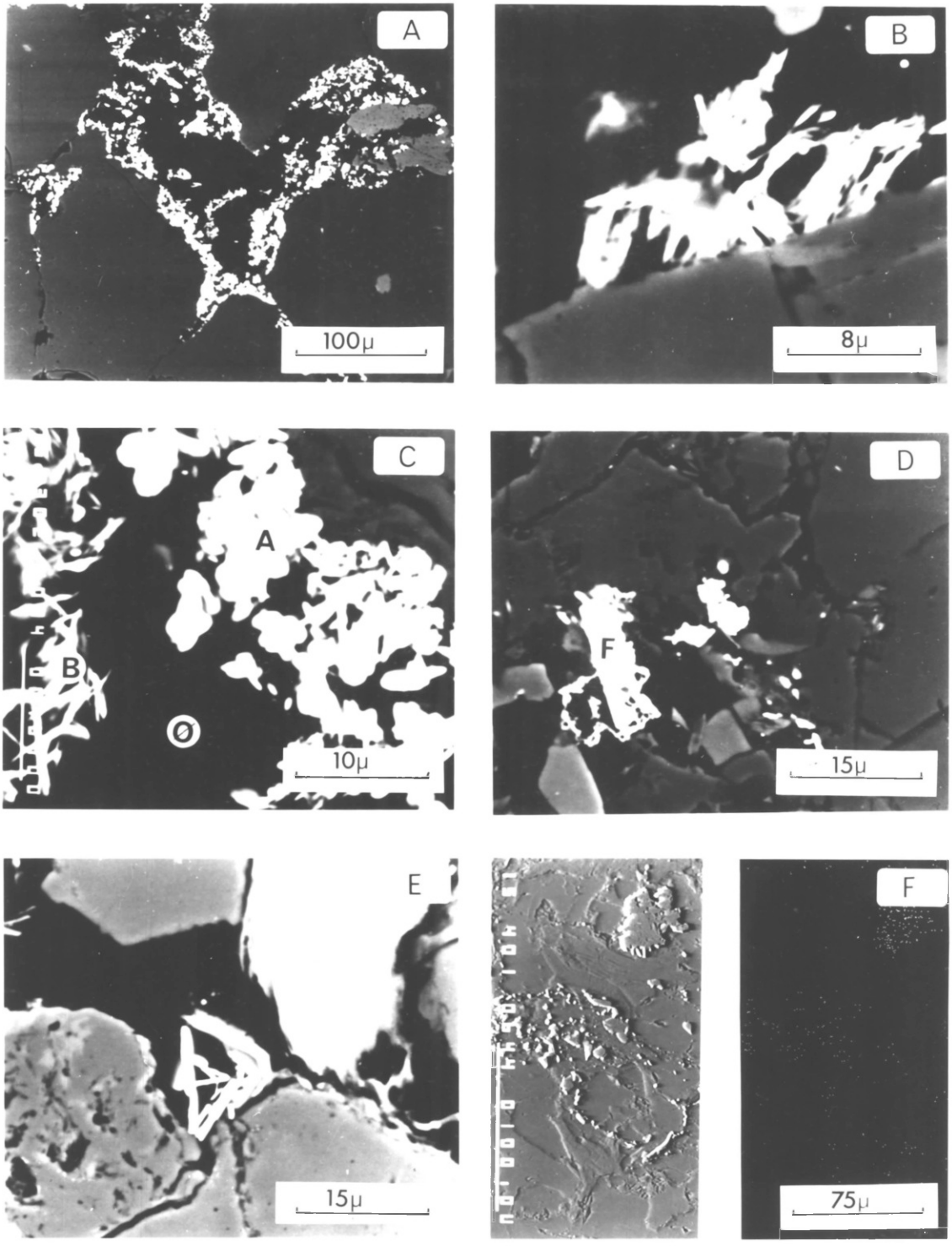


PLATE 6·3

later phase of needle-like growths (type II). Type II crystals may be seen to postdate subhedral (?authigenic) iron oxide grains in the Eday Marls (plate 6.3d). A very similar occurrence is described and illustrated by Welton (1984, p219). The rounded discs are described as hematite and the radiating, rod-shaped crystals as goethite. Of particular interest is that both occur together within a partially calcitised dolomite rhomb, from which calcite has been artificially etched away.

A rare occurrence of secondary iron oxides is shown in plate 6.3f, in which iron oxides appear to have partially pseudomorphed a detrital grain. This will be discussed further below.

6.3.4. Iron-Titanium Oxides: Composition Analysis.

(i) Qualitative analysis.

Not all occurrences of iron oxides are amenable to EPMA analysis. This is largely a function of the ability of the material being analysed to return a coherent beam to the detector. Many materials which do not present a uniformly-polished surface exactly perpendicular to the beam (e.g. clays) will thus give a low count-rate; accurate quantitative analysis will then be impossible. Additionally, the presence of volatiles (particularly water) will result in non-reproducible analyses.

A qualitative indication of the composition of such materials may better be provided by an x-ray spectrum. These are shown for type I and type II oxides for the Middle Eday Sandstone of site ROD24 (fig. 6.3). Iron is the dominant element present, together with Al and Si; Ti is found only in type II oxides, and then only in small amounts. Similar results are found for other similar secondary oxides not

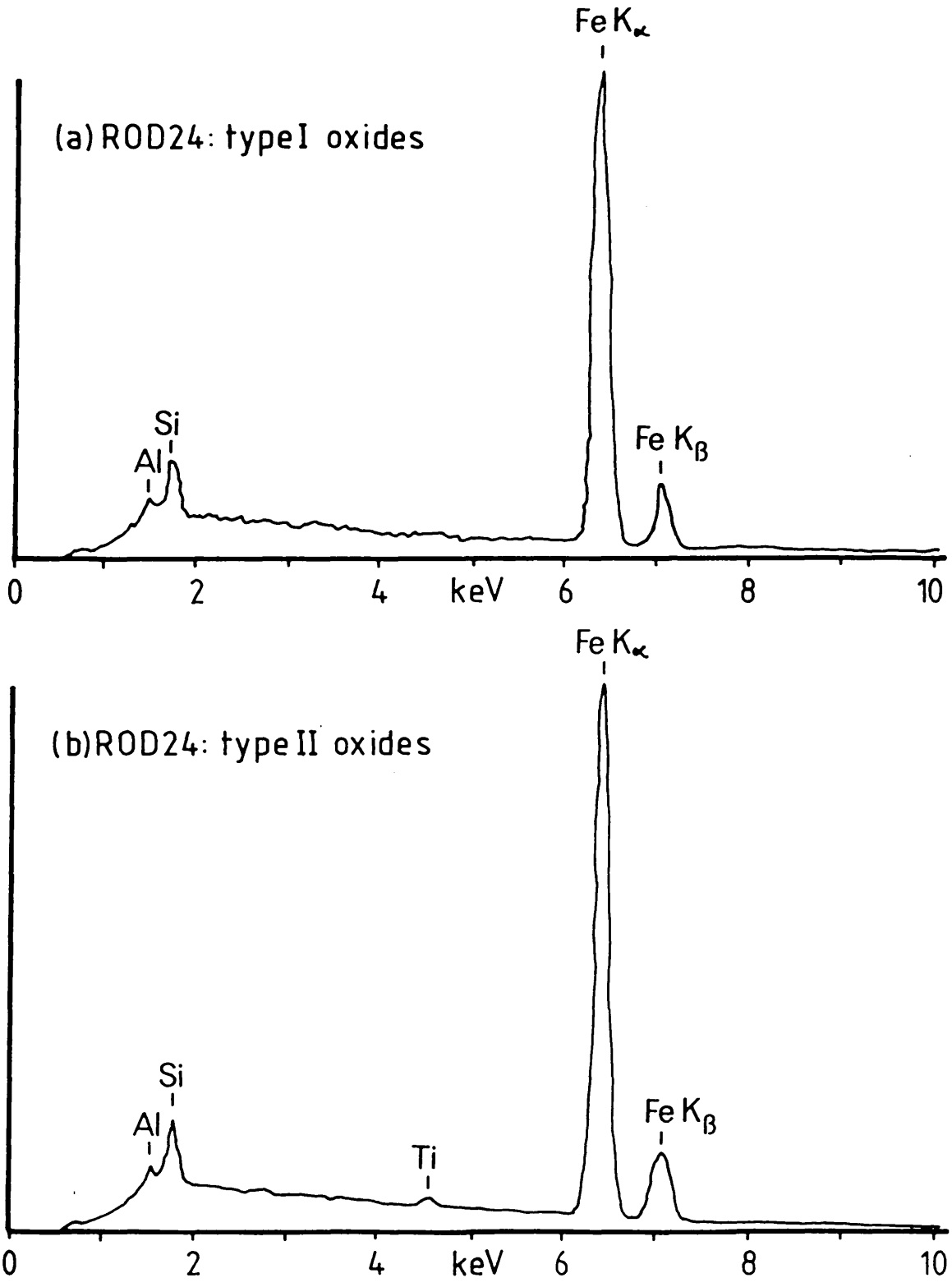


Fig. 6.3. X-Ray spectra for secondary iron oxides or oxyhydroxides, site ROD24 (see section 6.3.4.i). All peaks are K_α unless otherwise stated.

analysed quantitatively.

(ii) Quantitative Analysis.

94 EPMA analyses of iron-titanium oxides are given in appendix D2. These are categorised according to formation, site and detrital/secondary origin.

In principle, it should be possible to use EPMA analyses to determine exactly the relative abundances of FeO and Fe_2O_3. Iron is traditionally expressed as FeO; any Fe_2O_3 present will thus have the effect of reducing the total analysis figure (due to unanalysed oxygen being present). If it can be assumed that this is the only factor causing a low total, the relative amounts of FeO and Fe_2O_3 will be directly related to the amount by which the analysis is less than 100%.

ZAF-corrected total analyses for all iron-titanium oxides are shown in fig. 6.4, subdivided according to the origin of the oxide. The range of theoretical total analyses for hematite (i.e. 100% Fe_2O_3) to magnetite (50% Fe_2O_3) is shown. It can be seen that the majority of analyses appear, on this criterion alone, to be between magnetite and hematite in composition. None have less Fe_2O_3 than would be expected for magnetite although 17 of the 94 analyses have lower totals than would be expected for pure hematite. Obviously additional causes for low analysis totals must be found.

A small number of individual analyses were recalculated using an on-line program (developed by Dr E. Condliffe) which performs an iterative recalculation taking stoichiometry into account and thus making an allowance for other elements being present. These eight analyses are given in appendix D2v.

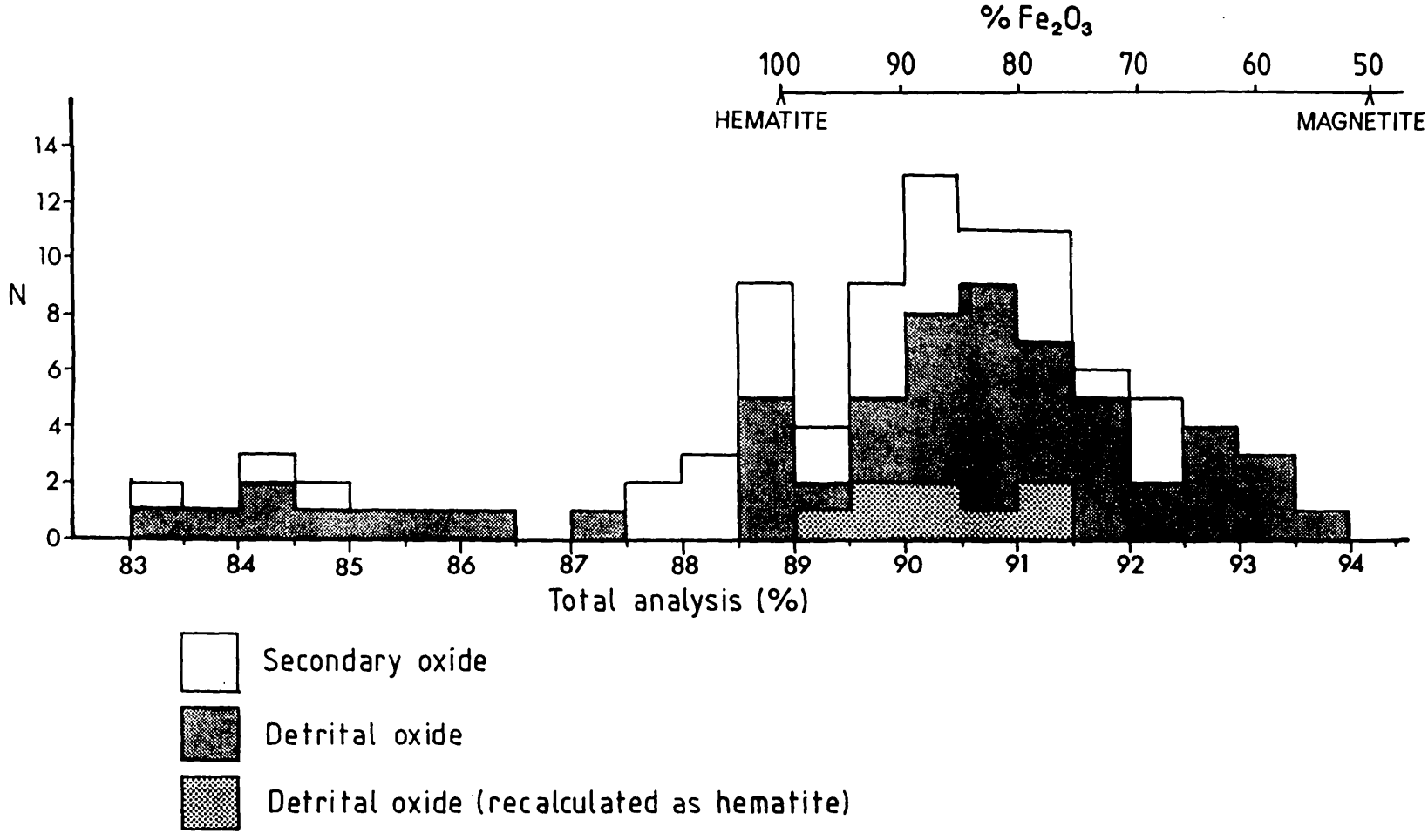


Fig. 6.4. Iron-titanium oxides: total ZAF-corrected EPMA analyses according to origin of the oxide. Theoretical total analyses for hematite, magnetite and intermediate compositions shown. Recalculated analyses are definitely of hematite.

Raw (ZAF-corrected) analyses, with iron calculated as FeO, are iteratively recalculated, maintaining a charge balance between divalent and trivalent cations in the crystal structure, for both a three-oxygen and four-oxygen formula unit and allowing both FeO and Fe_2O_3 to be present. Whichever gives a total analysis nearer to 100% will be indicative of the true formula unit ratios of the two oxidation states. One of the chief advantages of this method is that cation deficiencies, frequently found in iron oxides (Deer et al, 1962; Lindsley, 1976), will not greatly affect the result.

It would appear that all eight analyses are of moderately pure hematite, despite estimates of Fe_2O_3 contents as low as 75% using the more simplistic recalculation discussed above (fig. 6.4). This would thus suggest that definite inferences regarding chemical composition should not be made from the raw data alone. There is, however, no doubt that many of the analysed grains are hematitic; there is also no basis for suggesting that any of the analyses made are conclusively of magnetite.

It is interesting to investigate the abundances of other elements in the oxide minerals under discussion (predominantly titanium). Fig. 6.5 shows the ratio of TiO_2 to FeO, for all analyses showing greater than 3% TiO_2, divided according to origin of the oxide. It is striking that none of the secondary oxides has greater than 5-8% TiO_2, and most have less. Such analyses are consistent with a hematitic composition; Deer et al (1962) suggest that hematite may contain up to 10% TiO_2 before exsolution of ilmenite will occur (although they report work which indicates a lower figure of 5%).

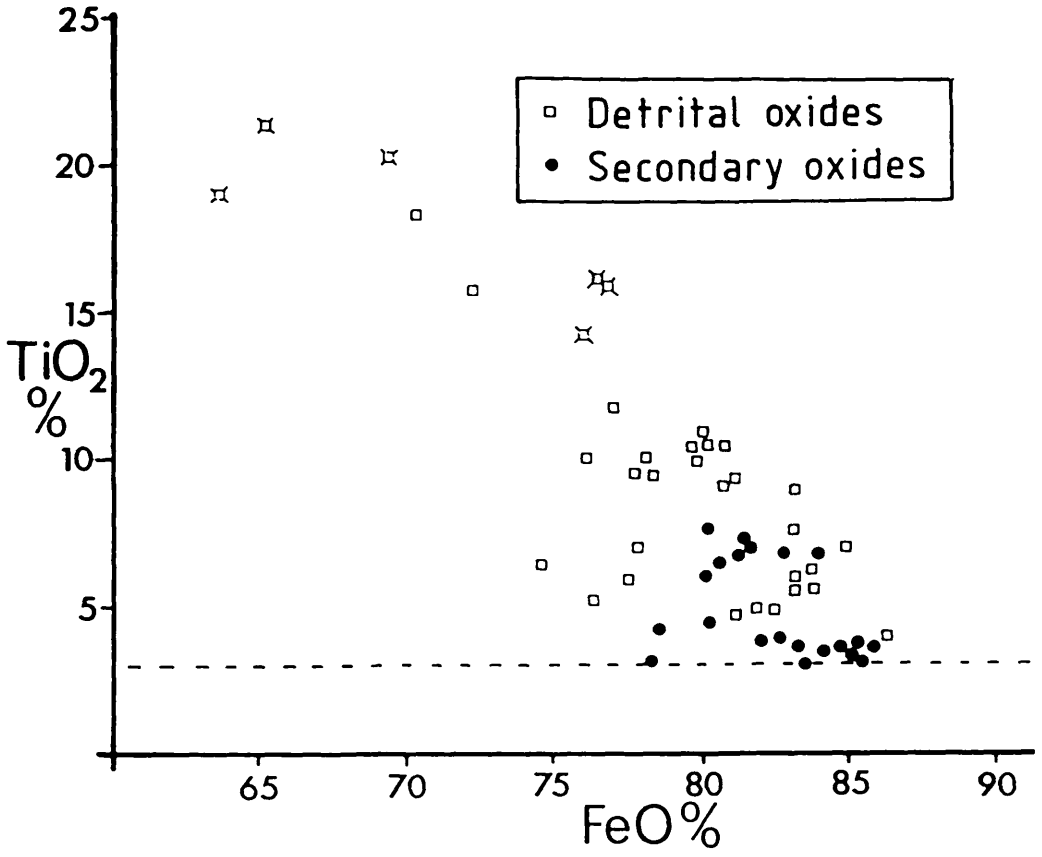


Fig. 6.5. Iron-titanium oxides: ZAF-corrected EPMA analyses according to origin of the oxide. Only analyses with TiO_2 > 3% shown; many analyses from both categories of oxide have less than this.

The TiO_2 content of detrital oxides, on the other hand, may reach 20-25% even though magnetic analysis suggests that titanomagnetite is not present. The majority of those analyses with high Ti are from ilmenitic exsolution lamellae in martitised grains. Only two (with TiO_2=15.8% and 18.3%) are from apparently fresh grains; higher magnification may reveal that they too have been oxidised.

6.3.5. Discussion.

Recalculated EPMA analyses discussed above provide conclusive evidence that hematite is present in many sites, both as detrital grains, now largely martitised, and also as secondary growths. There is no conclusive evidence for the presence of magnetite.

It would appear that most, if not all, of the hematite could be of post-depositional origin, although pre- or syn-depositional oxidation cannot be ruled out. It has formed either from the oxidation of and/or exsolution within a detrital magnetite grain or from growth of a new (hematitic) crystal. There is no textural evidence to constrain the timing of martitisation. It can be seen from fig. 2.9 that magnetite is metastable under most diagenetic conditions in a clastic sediment. This is enhanced in conditions of high Eh and pH, irrespective of dissolved carbonate concentration.

Martite may be found both in sites which carry an early (syngenetic) remanence and also in those which have been remagnetised (table 6.2). Detrital oxides have been noted in every site carrying an early remanence. Secondary oxides, however, are generally found only in sites which have been remagnetised. The only exception is site RCD29 in the Lower

ORS of Foyers which has not been investigated in detail but has an apparently complex diagenetic history despite carrying only a single, well-defined ancient remanence.

Table 6.2. Iron Oxide occurrence and age of remanence.

Site	Formation	Oxide occurrence		Remanence	
		Detrital	Secondary	Primary	Secondary
RCD01	John o'Groats	+	+	-	+
RCD10	Upper ORS	+	.	-	+
RCD19	Sarclet Sst.	.	+	-	+
RCD20	Sarclet Sst.	+	+	+	+
RCD29	Lower ORS	+	+	+	-
RCD38	John o'Groats	+	+	-	+
RCD41	John o'Groats	+	.	+	-
RCD42	Ellens Geo Cong.	+	+	+	+
RCD43	Sarclet Sst.	+	+	+	+
RCD46	Sarclet Sst.	+	+	+	?
RCD50	John o'Groats	-	-	-	-
RCD51	Hillhead RB	.	+	-	+
RCD54	Upper ORS	+	.	+	-
RCD55	Ellens Geo Cong.	.	+	-	+
ROD16	Middle Eday Sst.	+	.	+	+
ROD17	Middle Eday Sst.	+	+	+	+
ROD18	Middle Eday Sst.	+	.	+	-
ROD22	Eday Marls	+	+	+	+
ROD24	Middle Eday Sst.	-	+	-	+
ROD30	Eday Marls	+	+	-	+
ROD39	Upper Eday Sst.	+	+	+	+
ROD40	Upper Eday Sst.	+	.	+	-
ROD48	Upper Eday Sst.	+	.	+	+
ROD67	Eday Marls	+	.	+	-

+ Definitely present
- Definitely absent
. Not seen

The close associations of an early remanence with detrital (now martitised) oxides and of late remagnetisation with secondary oxides and/or martite gives an important insight into a possible model for remanence acquisition. Early oxidation of detrital magnetite could produce a very early hematitic remanence (i.e. a type A redbed of Turner, 1980; see fig. 6.6). Long-delayed martitisation and/or the generation of secondary hematite could result in remagnetisation. Those sites which show both an early remanence and a Kiaman remagnetisation (chapter 4) would

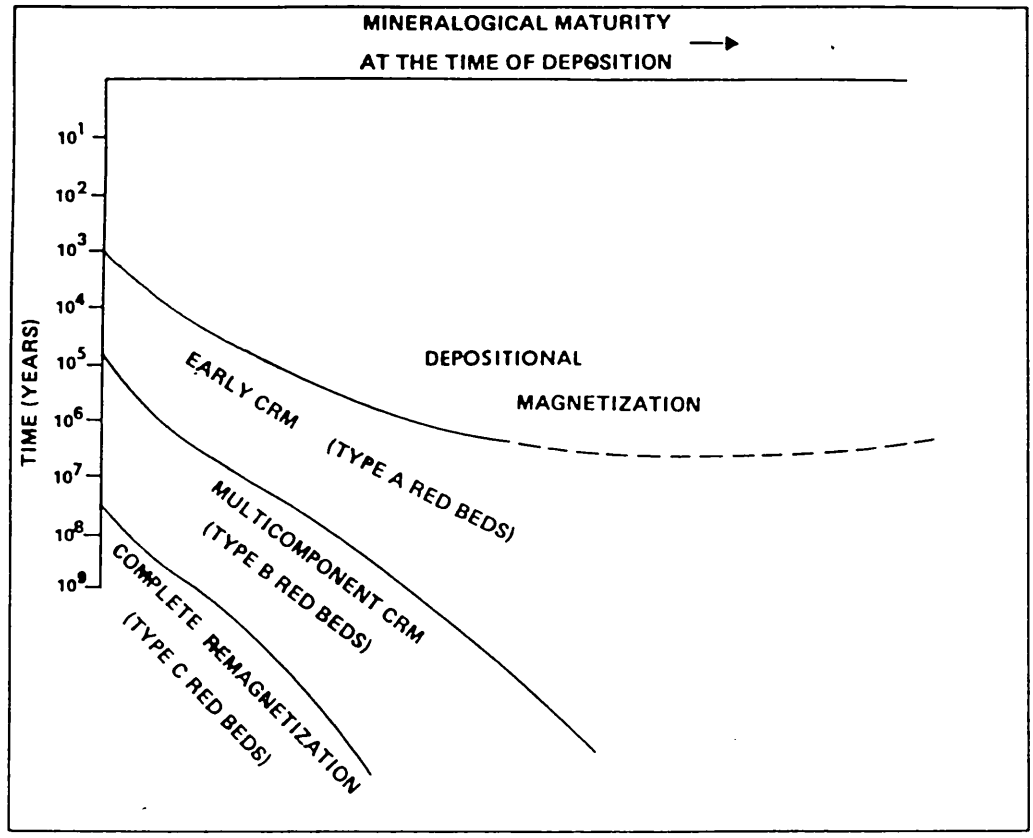


Fig. 6.6. Evolution of continental redbeds (after Turner, 1980, fig. 8.34).

fall into the type B redbed grouping (e.g. many sites in the Sarclet area and in the Eday Group), whereas completely remagnetised sediments (e.g. the Hillhead Redbed and some of the Eday Group) are type C redbeds.

To which category (A,B or C) a sediment belongs will be a complex function of many parameters, including original mineralogy, degree of cementation, porosity-permeability history and stratigraphic position. The relevance of such points to remanence acquisition will be discussed later in this chapter.

6.4. Carbonates.

6.4.1. Introduction.

Carbonates, particularly calcite and dolomite-ferroan dolomite-ankerite, occur widely in the Orcadian Basin. Within clastic sediments, calcite and dolomite cements are frequently seen, although these have often been greatly affected by late dissolution and secondary porosity generation. Such effects are particularly pronounced in the Eday Group, where many sites show little or no carbonate (as evidenced by low Ca,Mg ICP analyses: appendix C1f). Finer-grained sediments (e.g. the Sarclet Group and Yesnaby Sandstone) may retain a considerable amount of carbonate.

Of very different character are the laminated lacustrine sediments such as the Niandt Limestone which are dominated by calcium-magnesium-iron carbonates. Some of the carbonates may be a primary precipitate but some are undoubtedly diagenetic (Rayner, 1963).

The possible relevance of carbonates to palaeomagnetic studies is discussed in section 2.8. Since it would appear that many of the carbonates in the Orcadian Basin have undergone diagenetic reactions relevant to the acquisition

of a palaeomagnetic remanence, they will be considered in some detail below.

6.4.2. Lacustrine sediments.

As described in chapter 5, the Niandt Limestone is composed mainly of a mature detrital component (largely quartz), organic matter and carbonates. The latter occur in several distinct forms, all of which may be seen in plate 6.4a.

(i) Primary/early diagenetic precipitate.

Anhedral dolomite crystals, 5 to 30μ in diameter, may often form a dense interlocking mosaic surrounding detrital grains. They may be of variable iron content but are generally ferroan to some degree. This is considered by Rayner (1963) to be a primary precipitate; alternatively it could be a very early diagenetic replacement, forming seasonally during periods of high pH. (High pH appears to promote early dolomitisation; Chilingar & Bissell, 1967). A Recent analogue is described by Alderman & Skinner (1957) in a very shallow lake in South Australia. Apparently synchronous calcite deposition is described by Rayner (1963) but not seen in this study.

(ii) Rhombic dolomite.

Large, isolated euhedral dolomite rhombs occur throughout the fishbed (plate 6.4a); these may be over 100μ in length. Zonation is characteristic, with an inner zone, invariably of low iron content, and an outer zone of ferroan dolomite which may be of ankeritic composition. Fig. 6.7b shows EPMA analyses of such rhombs (full analyses given in appendix D1i). There is a clear distinction between the inner and outer zones on the basis of (Fe+Mn) content. Both

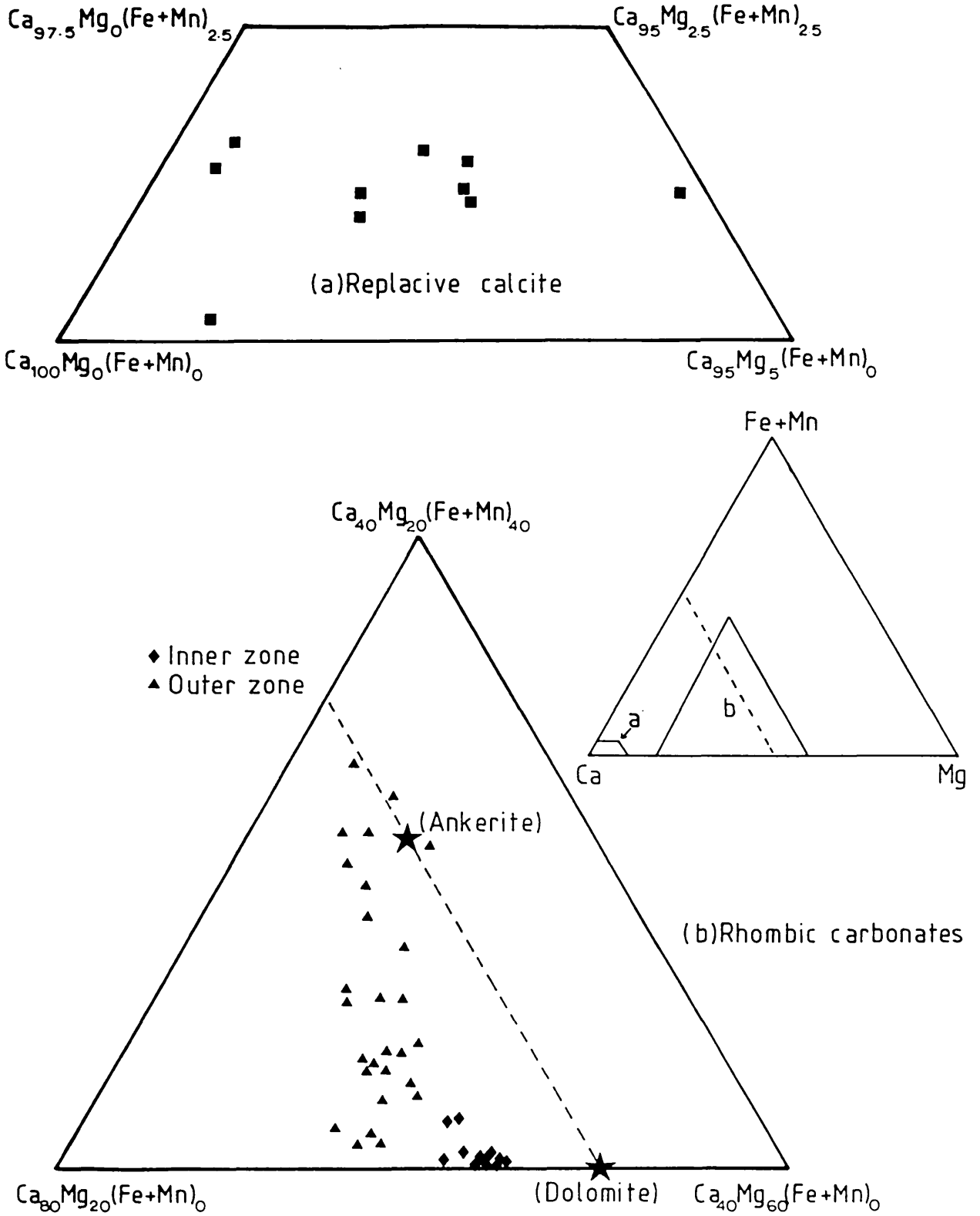


Fig. 6.7. EPMA analyses of carbonates (i) Lacustrine sediments. Ideal compositions of dolomite and ankerite shown; dashed line is Ca/Mg=1.

PLATE 6.4
PRIMARY-EARLY DIAGENETIC CARBONATES

(a) ROD26; Niandt Limestone, Cruaday Quarry. Zoned dolomite (D) and ferroan dolomite (F) rhomb. Surrounding material largely quartz (Q) and calcite (C). (BEI, Jeol 733).

(b) ROD14; Yesnaby Sandstone, Yesnaby. Multiple concentric zonation of a ferroan dolomite rhomb. Z-contrast due largely to variations in Mg-Fe ratio, as illustrated by analyses 099-102 (analysis points indicated by arrows, with 099 on the left and 102 on the right). Note inner core of highly ferroan dolomite (analysis 103). (BEI, Jeol 733).

(c) Carbonate vein intruding granitic basement; Yesnaby, Mainland Orkney (HY152217). Lower part composed of alternating dolomite and ferroan dolomite overgrowths (D) followed by barite (B: very high-Z). Dolomite cut by a later calcite vein (C) prior to deposition of ferroan dolomite (F) of more uniform composition. Precise cause of the zonation is uncertain. (BEI, Jeol 733).

(d) Enlargement of dolomite-ferroan dolomite alternations shown in (c). Analyses 097 (dolomite,D) and 098 (ferroan dolomite,F; appendix D1i). (BEI, Jeol 733).

(e) ROD17; Middle Eday Sandstone, Deerness. Subtly zoned ferroan dolomite crystal D. Analyses 040 (lighter zone) and 041 (darker zone; appendix D1i). (BEI, Jeol 733).

(f) ROD67; Eday Marls, Sanday. Calcite (C) cement in quartz (Q) and feldspar (K) sandstone. Analyses 281-283 (appendix D1ii). (BEI, Jeol 733).

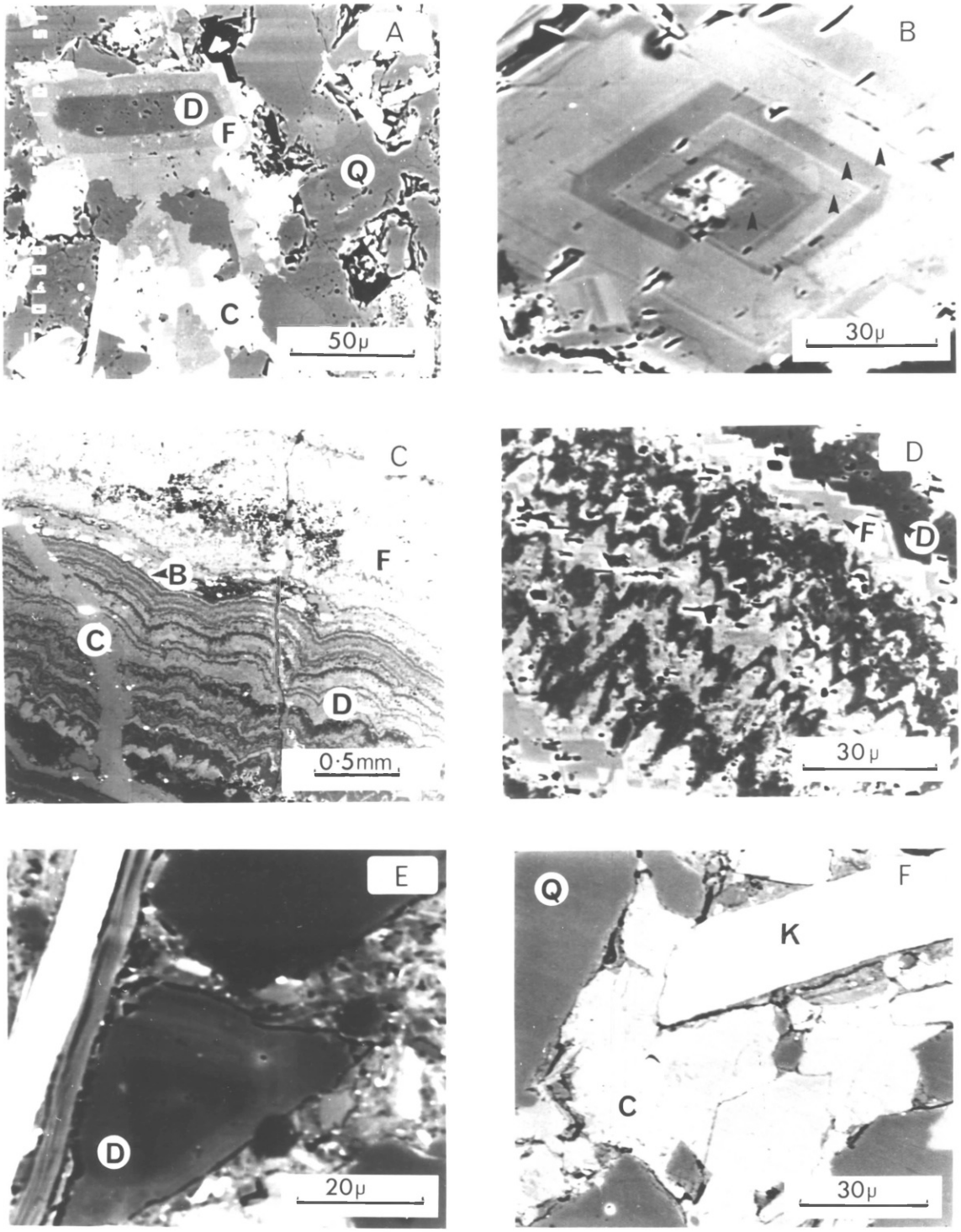


PLATE 6·4

are generally of high molar% $CaCO_3$, which may often reach 60-65%. Molar% $CaCO_3$ increases slightly with decreasing (Fe+Mn) content.

Similar compositional variations have been observed by Gawthorpe (1985 and in press) in the Carboniferous of the Bowland Basin, and may be characteristic of 'saddle' or 'baroque' dolomites (Radke & Mathis, 1980). The excess of calcium in such situations was explained by Lipmann (1973, p48) and Reeder (1983) as being due to irregular stratification of magnesitic/ankeritic and calcitic layers, producing an excess of the latter. Katz (1971), however, suggests that early diagenetic calcian dolomites may be related simply to a high Ca^{2+}/Mg^{2+} ratio in the dolomitising fluids.

$CaCO_3$ content is generally fairly uniform, any major variations being in the relative proportions of $FeCO_3$, $MgCO_3$ and $MnCO_3$. The latter is present only in small quantities (up to 1.2%, but generally less) and does not show a clear relationship with $FeCO_3$.

These rhombs are clearly diagenetic. There is little textural evidence to suggest a relative age for their formation. Near-surface authigenic dolomite rhombs are widely reported (e.g. Muller et al, 1972; Irwin et al, 1977; Friedman & Muruta, 1979; Irwin, 1980 and Pye, 1985), often associated with the sulphate reduction zone. Such dolomite is unlikely to be ferroan as any Fe^{2+} from decomposing detrital ferromagnesian minerals would combine rapidly with free H_2S to form pyrite (Berner, 1984). Strong evidence of a sulphate reduction zone is the presence of much dispersed diagenetic pyrite throughout the sediment. Pyrite is seen in higher concentrations than is typical for freshwater lakes,

for which Berner (1984) records a maximum of 0.5% sulphur. This compares with up to 2% in 'normal' marine sediments (Berner & Raiswell, 1983).

In addition, organic carbon may have been indirectly important for the formation of early diagenetic dolomite; Baker & Brown (1985) suggest that low inorganic carbon contents tend to preclude dolomite formation in continental margin sediments.

Below the zone of sulphate reduction, however, sulphide ions will no longer be available to combine with ferrous iron which may then be incorporated into carbonates, producing the outer zone of ferroan dolomite-ankerite.

Isotopic analysis would assist greatly in confirming the diagenetic environments suggested above (Land, 1980). Samples submitted for analysis have not yet been processed.

(iii) Late replacive calcite.

(a) The calcitisation process.

The calcitisation of dolomite (an equivalent term to the widely-used 'dedolomitisation'; Smit & Swett, 1968) has been described by many authors. Replacement textures would appear to fall into one of two categories, centrifugal or centripetal.

'Centrifugal' replacement, in which dolomite is wholly or partially replaced by finer-grained calcite (often from the core outwards) is described by Shearman et al (1961), Schmidt (1965), Evamy (1967), Folkman (1968), Harwood (1981), Frank (1981) and Elmore et al (1985). 'Centripetal' dedolomite, i.e. the replacement of dolomite by coarser-grained calcite, is described by Shearman et al (1961), Katz (1971) and Zenger (1973). Here, the calcite may form a syntaxial overgrowth with the relict crystal or it may

totally replace a large volume of dolomite.

The geochemistry, necessary conditions and relative timing of the process are somewhat controversial, highly variable and generally difficult to prove. Experimental work by De Groot (1967), together with carbonate phase diagrams (Garrells & Christ, 1965; see fig. 2.6) suggest that conditions of low Pco_2, low temperature, high Ca^{2+}/Mg^{2+} ratio and efficient fluid transfer, are important controlling factors in the reaction. This, combined with the undoubtedly recent nature of some calcitisation, has led many workers to regard it as a Recent, and hence geologically unimportant, process. It has sometimes been related to ancient weathering surfaces (now unconformities), for example by Schmidt (1965), Folkman (1968) and Larsen & Chilingar (1979).

A study by Back et al (1985) of the relationship of recent dedolomitisation to groundwater flow suggests that it is occurring widely at the present day, and to considerable depth. They consider that dissolved evaporites in slow-moving groundwater are the driving mechanism of the process. This example may provide an analogue to some ancient occurrences.

In addition to dedolomitisation beneath ancient weathering surfaces (see above) and of Recent age (e.g. Evamy, 1967; Al-Hashimi & Hemingway, 1973), some occurrences have been ascribed to syn-depositional replacement (Katz, 1971; Zenger, 1973; Wood & Armstrong, 1975). These studies suggest that syntaxial borders around a dolomitic centre formed synchronously with crystal growth, during periods of pore-water dilution which produced a high Ca^{2+}/Mg^{2+} ratio. All the other physical pre-requisites of the process

described above would be met in such an environment.

The basic (idealised) reaction is

$$CaMg(CO_3)_2 + Ca^{2+} = 2CaCO_3 + Mg^{2+}$$

An association with pyrite has frequently been noted (Evamy, 1963; Folkman, 1968; Zenger, 1973). Pyrite oxidation may greatly enhance the process (Larsen & Chilingar, 1979), as:

$$FeS_2 + \tfrac{7}{2}O_2 + H_2O = Fe^{2+} + 2SO_4^{2-} + 2H^+$$

and

$$Fe^{2+} + \tfrac{1}{4}O_2 + \tfrac{5}{2}H_2O = Fe(OH)_3 + 2H^+$$

The resultant acidification of pore waters will promote the reaction

$$CaMg(CO_3)_2 + 2H^+ = CaCO_3 + Mg^{2+} + CO_2 + H_2O$$

Iron intrinsic to ferroan dolomite has been omitted from the above equations for the sake of simplicity. During calcitisation, any iron present in the original dolomite will tend to be released. The reasons for this are somewhat uncertain but are probably due to Fe being associated with the Mg layer of dolomite. Relative ionic radii may also be significant.

It is not known whether the iron is released directly as hematite or whether there is an intermediate stage of hydrated oxide. This could then dehydrate to hematite (Langmuir, 1971).

This is the reaction of significance to palaeomagnetism; the hematite will have a tendency to acquire a remanence corresponding to the time of calcitisation. Such a process has recently been dated

palaeomagnetically (Elmore et al, 1985).

(b) Calcitisation of lacustrine sediments.

Calcite in the fishbed occurs in one of two forms. In plate 6.4a, it can be seen as an irregular patch, intimately associated with early diagenetic anhedral dolomite and apparently replacing it. Such occurrences are possibly those considered by Rayner (1963) to have formed synchronously with the dolomite.

Elsewhere, calcite may be seen replacing parts of the larger dolomite rhombs referred to above. Typical examples of this are shown in plate 6.5. It would appear to be a late replacement, as it often cuts across earlier zone boundaries within the dolomite.

Fig. 6.8 shows molar % carbonate variations across a typical partially calcitised rhomb. It shows the replacement to be a straightforward substitution of Ca for Mg and Fe; Mn would appear to have retained an earlier zonation related to the dolomite-ferroan dolomite boundary and not to have been expelled during calcitisation. The reason for this is obscure but may be related to the fact that it is present in significantly smaller amounts than iron.

Replacive calcite is generally fairly pure (fig. 6.7a), with $MgCO_3$ up to 3.5%, $FeCO_3$ up to 1.1% and $MnCO_3$ up to 0.7%. These elements are presumably inherited from the replaced dolomite.

A clearer indication of the nature of the replacement is shown by plate 6.6, in which the relative concentrations of the three major elements involved are individually mapped using the electron microscope. Calcitisation has progressed around the boundary between ferroan and non-ferroan dolomites, and has replaced both, particularly the latter.

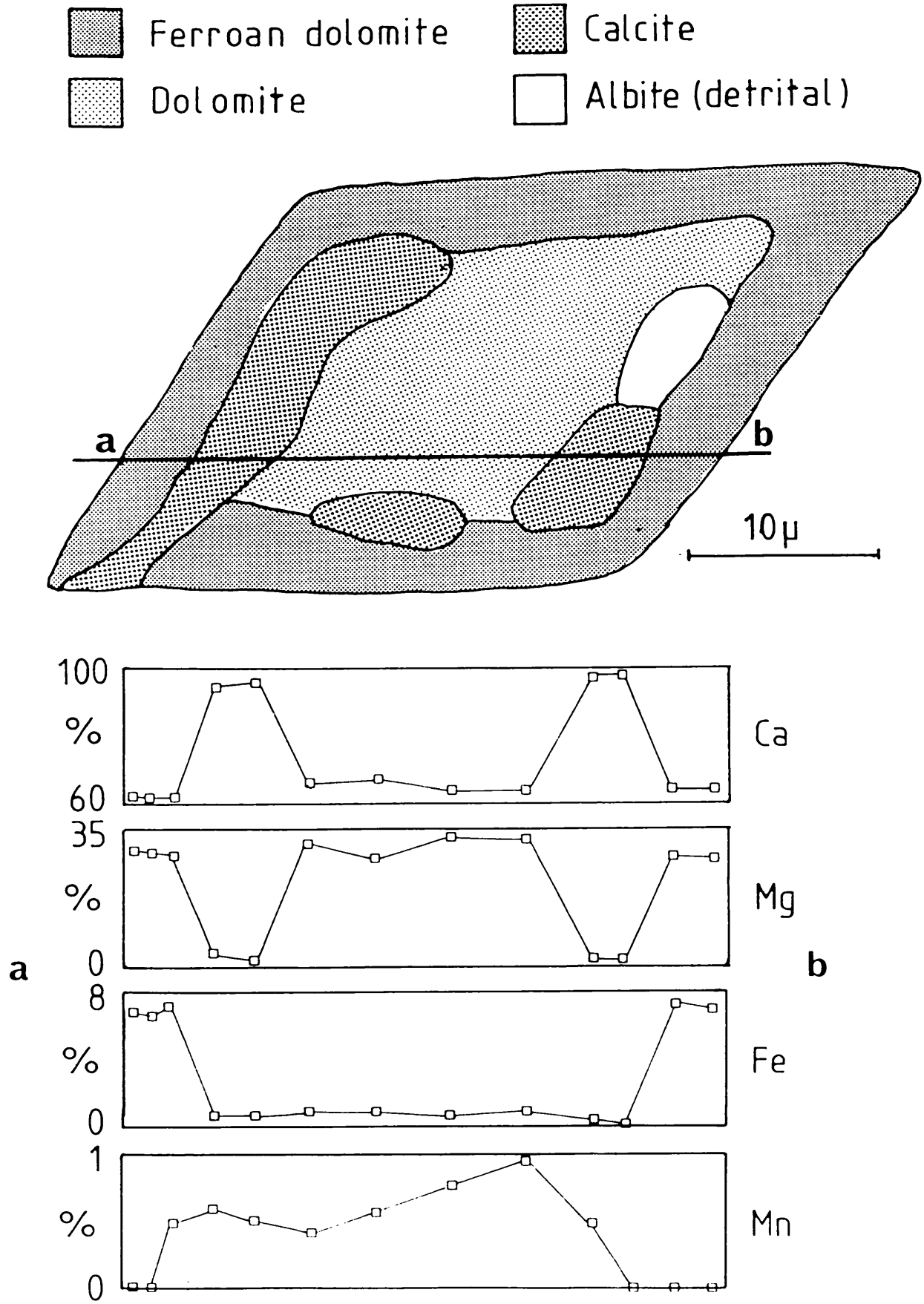


Fig. 6.8. Calcitised dolomite rhomb, site ROD26. Analysis points along traverse line a-b.

PLATE 6.5
CALCITISATION OF DOLOMITE: LACUSTRINE SEDIMENTS (I)

(a-b) ROD26; Niandt Limestone, Cruaday Quarry, Mainland Orkney. Early diagenetic dolomite (D) and ferroan dolomite (FD) with later calcite (C) replacement, particularly of the inner dolomitic zone. (BEI, Jeol 733).

(c) ROD29; Niandt Limestone, Skaill, Mainland Orkney. As above but possibly with a third early zone intermediate between dolomite (D) and ferroan dolomite (FD). (BEI, Jeol 733).

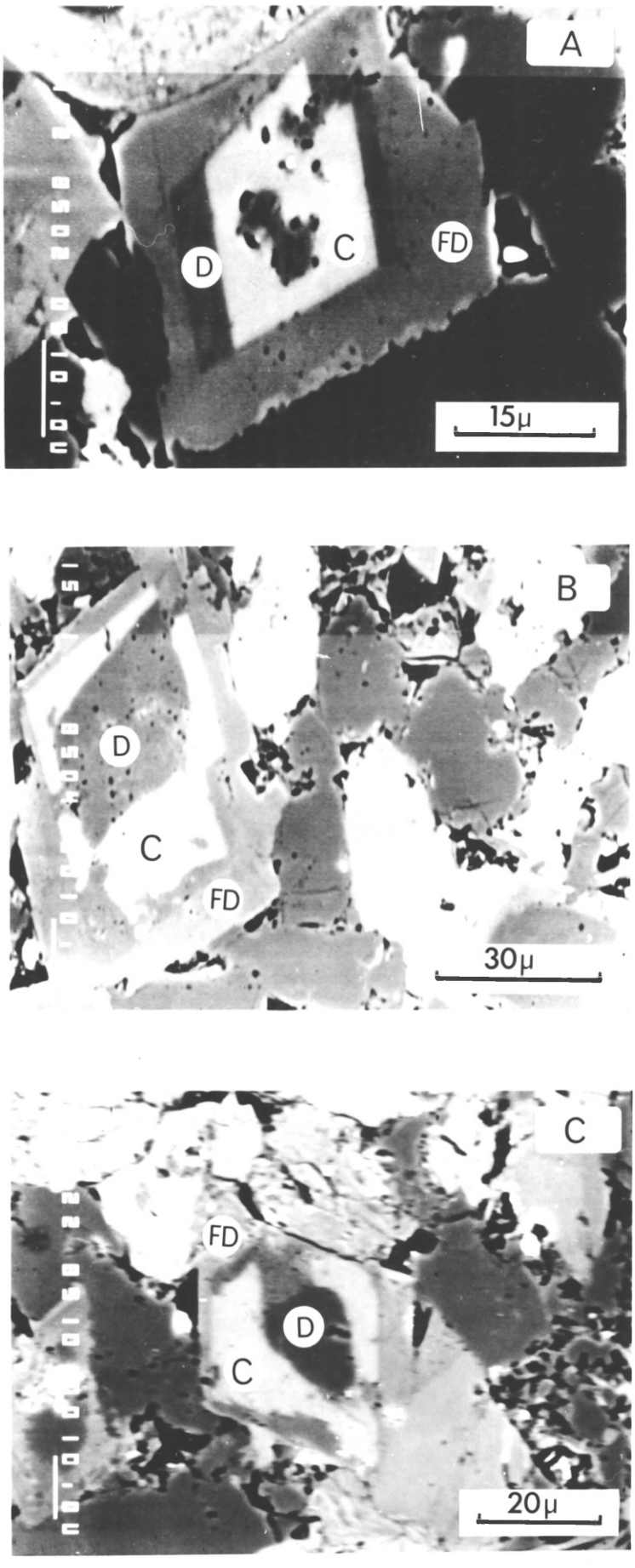


PLATE 6·5

WATTS LIBRARY

PLATE 6.6
CALCITISATION OF DOLOMITE: LACUSTRINE SEDIMENTS (II)

Element 'digimaps' produced on the SEM. Element concentration corresponding to a particular colour is variable between each map.

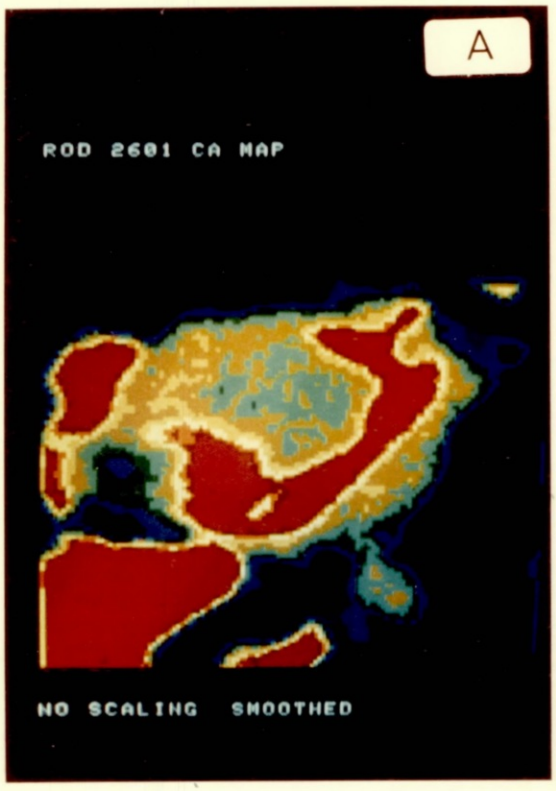
(a) Calcium. Peak values (red) correspond to calcite, lighter tones to dolomite and ferroan dolomite.

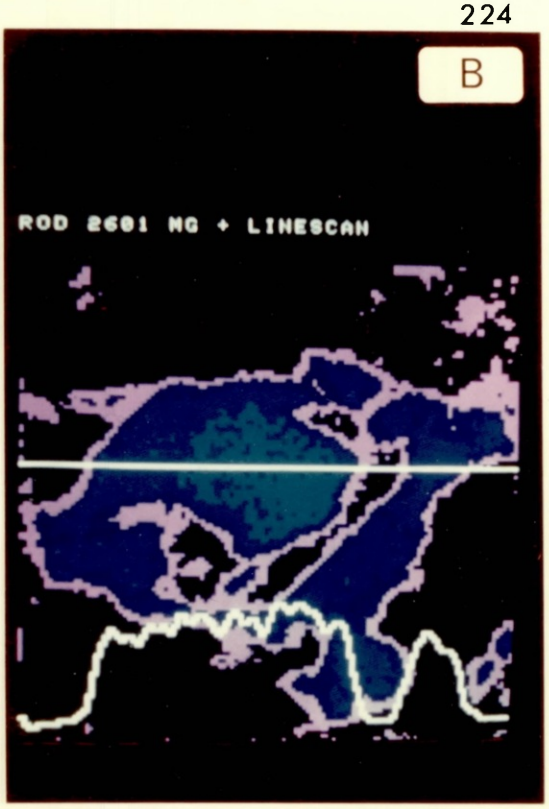
(b) Magnesium. Peak values correspond to dolomite (light blue centre) or ferroan dolomite (dark blue rim). Line scan across centre of crystal marked by a white line: vertical scale arbitrary.

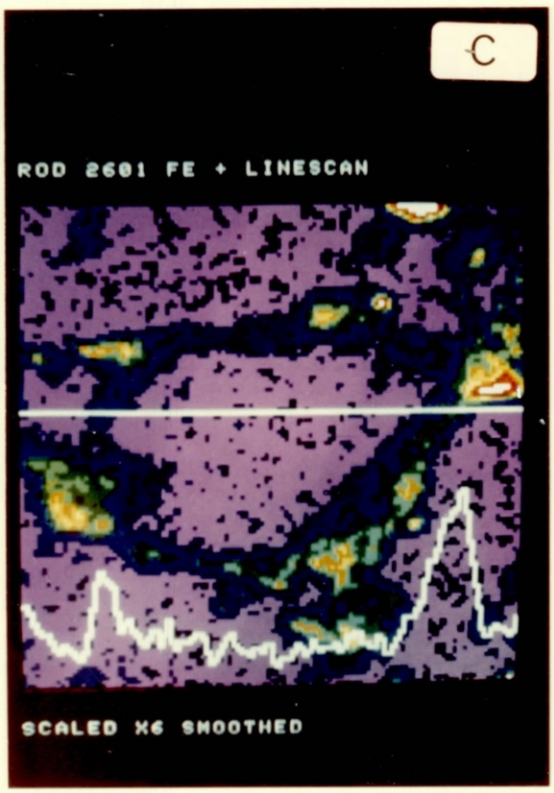
(c) Iron. Linescan across centre of crystal marked by a white line: vertical scale arbitrary.

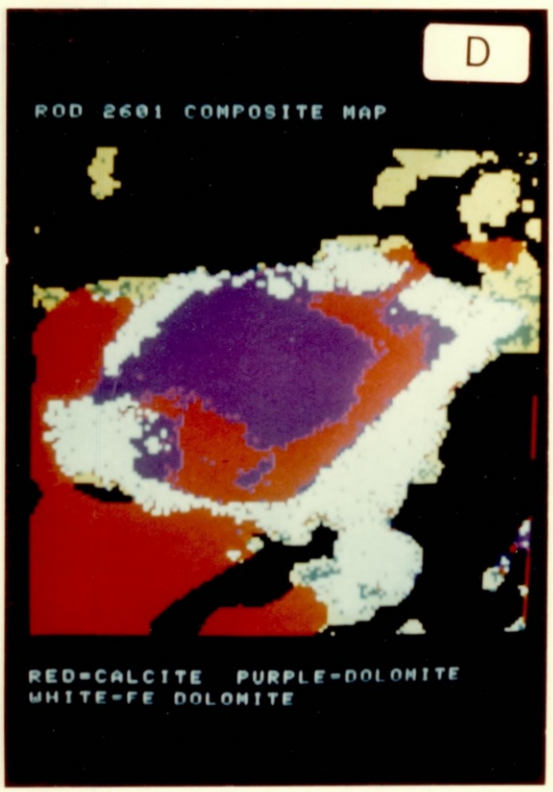
(d) Composite map

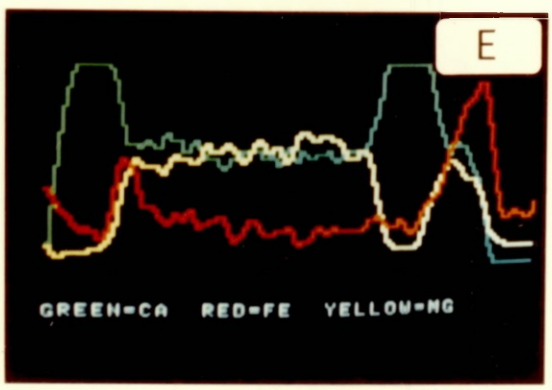
(e) Composite linescan for Ca, Mg and Fe. Scan position shown by white line on (b) and (c).


A
ROD 2601 CA MAP
NO SCALING SMOOTHED


B
ROD 2601 MG + LINESCAN


C
ROD 2601 FE + LINESCAN
SCALED X6 SMOOTHED


D
ROD 2601 COMPOSITE MAP
RED=CALCITE PURPLE=DOLOMITE
WHITE=FE DOLOMITE


E
GREEN=CA RED=FE YELLOW=MG

20μ

PLATE 6·6

That the calcite was not formed syngenetically between the two phases of dolomite precipitation (as discussed by Katz, 1971; Zenger, 1973; Wood & Armstrong, 1975) is indicated by the fact that it has replaced both dolomite and ferroan dolomite zones.

A possible microfracture in the outer ferroan zone (plate 6.6a) appears to have been calcitised. This could have allowed the penetration of calcitising fluids to the remainder of the crystal.

It is shown above that calcitisation and resultant release of iron has occurred at some stage since the termination of dolomitisation. Textural evidence does not permit closer constraining of the exact time of this process.

Palaeomagnetic characteristics of the fishbed (chapter 5) show that it acquired a hematitic remanence during the Kiaman reversed polarity period, i.e. Late Carboniferous to Late Permian. Calcitisation is a valid mechanism by which to generate secondary iron oxides; extensive examination of the sediments has not suggested any other possible mechanism for delayed remanence acquisition. It is thus proposed that calcitisation of dolomite was a principal agent responsible for the remagnetisation. This will be discussed further below.

6.4.3. Clastic sediments.

As mentioned previously, carbonates are widespread within clastic sediments of the Orcadian Basin. However, discussion will be largely confined to those sediments in which the diagenesis of carbonates has played an important role in remanence acquisition, namely the Sarclet Group and

the Lower ORS of Orkney; the John o'Groats Group and Carboniferous sandstones of Criffel are discussed in chapter 8 and appendix F respectively.

(a) Sarclet Group.

Early Diagenetic dolomite: As in the lacustrine sediments described above, isolated euhedral rhombs of dolomite are widespread in the Sarclet Group, and they are of comparable dimensions (10-80μ). Compositionally they are somewhat dissimilar. Fig. 6.9 shows that nearly all are of calcic ankerite composition, with only two non-ferroan dolomite analyses and one of intermediate composition.

Individual rhombs show a fine-scale zonation, as illustrated in fig. 6.10. This example has a small core of non-ferroan dolomite, represented by one analysis, and an outer zone which displays a progressive 20-30% increase in $FeCO_3$ and $MnCO_3$ towards the perimeter of the rhomb. This example is atypical, most being composed only of ferroan dolomite, with an average composition of $Ca_{1.08}\ Mg_{0.54}\ Fe_{0.35}\ Mn_{0.03}\ (CO_3)_2$.

The origin of diagenetic dolomite in lacustrine sediments is discussed above. In contrast to this model, it is suggested that the depositional environment of the Sarclet Group was not appropriate for the precipitation of early diagenetic anhedral dolomite. A very shallow, possibly ephemeral, sulphate reduction zone could have produced the small non-ferroan euhedral rhomb cores described above. This is consistent with the limited amounts of pyrite present. Lack of significant organic carbon and/or sulphate enabled the sediment to pass rapidly with burial to below the sulphate reduction zone; ferroan dolomite could now form.

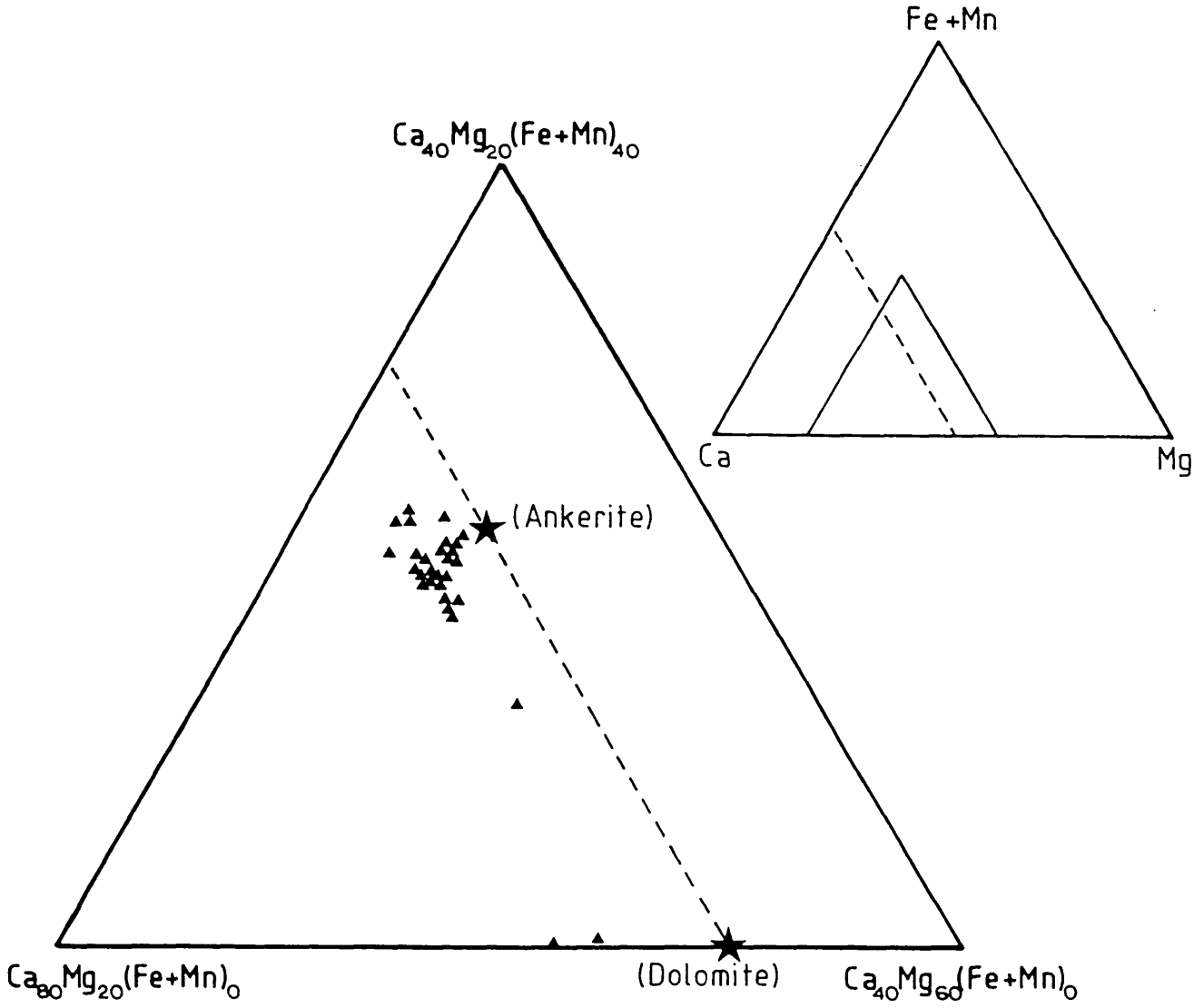


Fig. 6.9. EPMA analyses of carbonates (ii) Dolomites from the Sarclet Group. Ideal compositions of dolomite and ankerite shown; dashed line is Ca/Mg=1.

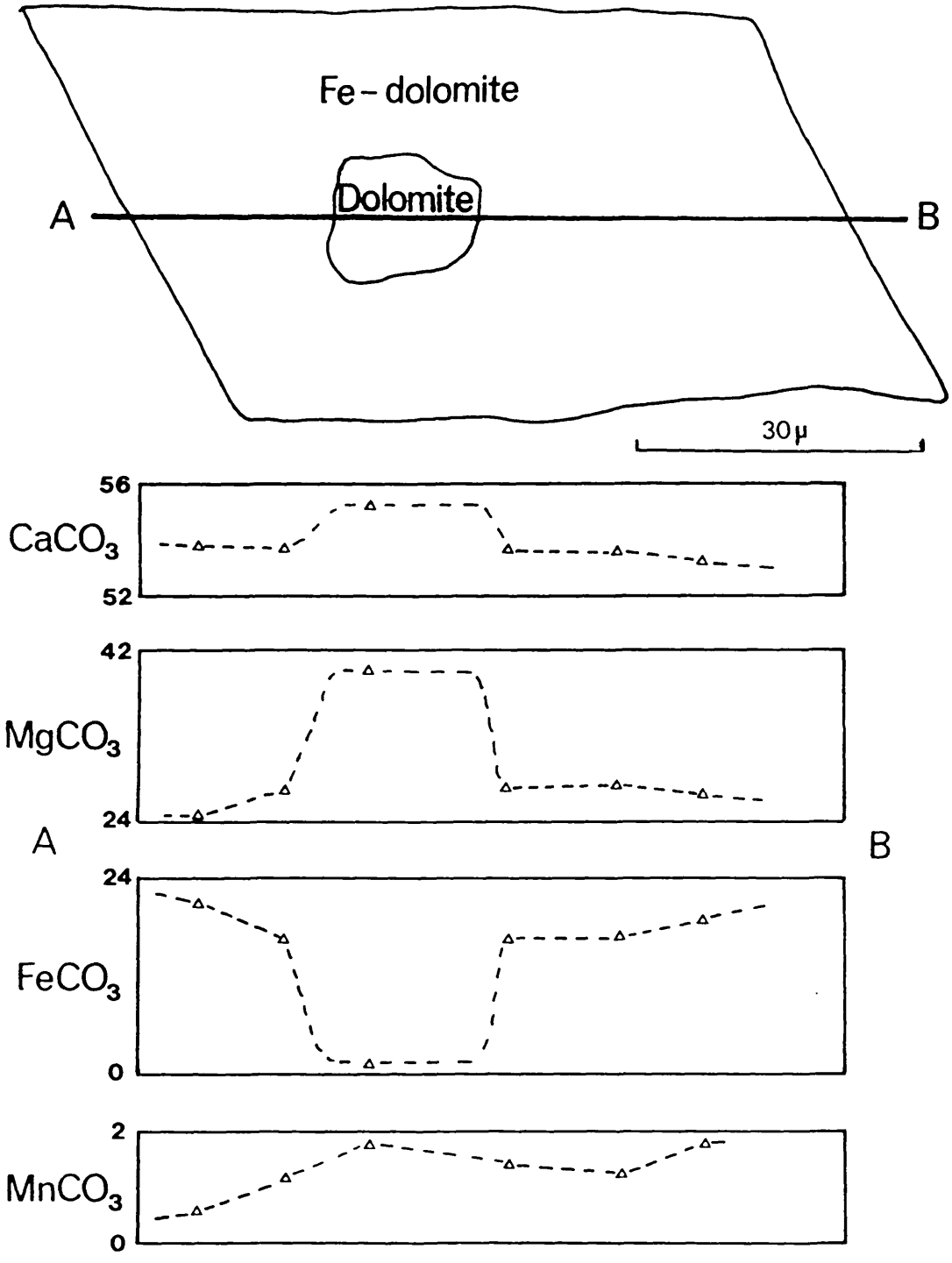


Fig. 6.10. Unaltered dolomite rhomb, Sarclet Sandstone (site RCD19). Analysis points along traverse line A-B

The boundary between non-ferroan and ferroan dolomites is fairly sharp, suggesting a rapid environmental transition (and/or very slow crystal growth). The cause of the fine-scale zonation within the dolomite is not obvious, but could be related to variations in the flux of iron and manganese from decomposing detrital minerals.

Replacive calcite: The Sarclet Group has undergone extensive diagenetic and textural alteration, due largely to its relatively immature detrital mineralogy. It would appear that much carbonate material has been removed (resulting in secondary porosity generation). Some of the less porous horizons have, however, retained an indication of diagenetic carbonate textures. Plate 6.7a shows a rhombic outline of iron oxides (x-ray map plate 6.7b) which is of similar size to the early diagenetic rhombs described above. Within this outline, patches of calcite (plate 6.7c) occupy interstitial spaces between silicate grains (plate 6.7d). This is interpreted as representing an early diagenetic euhedral ferroan dolomite rhomb which grew to envelop detrital quartz and feldspar, and which was later calcitised. The iron released during this process has accumulated on the exterior surface of the original rhomb.

This would appear to the author to be conclusive evidence of the close link between dolomite diagenesis and iron oxide formation (and hence palaeomagnetic remanence acquisition). Presumably such textures would not be preserved in a more open system; iron oxides could accumulate in a form not demonstrating the close genetic link shown here. Some of the secondary growths discussed earlier (plates 6.2,6.3) may represent iron oxide generated by the above mechanism.

PLATE 6.7
CALCITISATION OF DOLOMITE: CLASTIC SEDIMENTS

(a) RCD42; Ellens Geo Conglomerate, Ulbster. Rhombic outline of iron oxide (F), possibly describing a relict dolomite crystal outline, now entirely replaced by calcite (C). The original rhomb would appear to have grown around and between detrital quartz grains (Q). (BEI, Jeol 733).

(b) Fe x-ray map of (a), showing the rhombic form of the iron oxides.

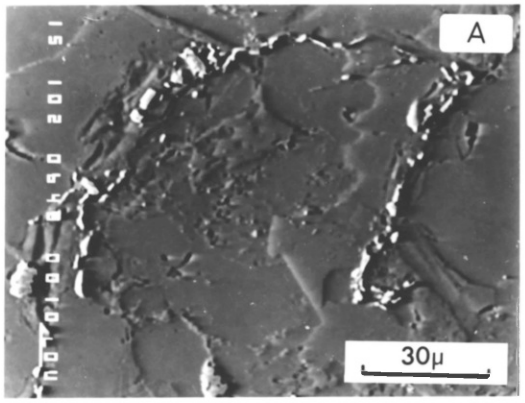
(c) Ca x-ray map of (a), showing patches of (?secondary) calcite within the rhomb.

(d) Si x-ray map of (a), showing detrital silicate grains.

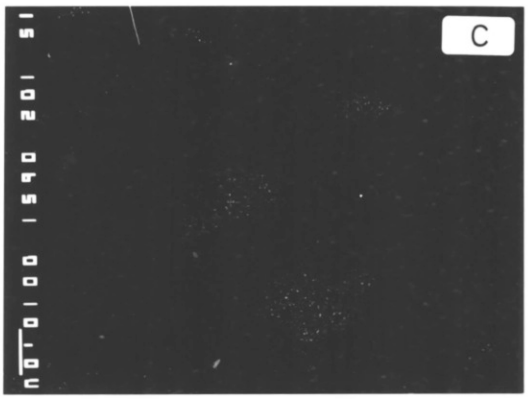
(e) ROD14; Yesnaby Sandstone, Yesnaby. Irregular zones of ferroan dolomite (D) and calcite (C). the latter possibly being a late replacive feature. (BEI, Jeol 733).

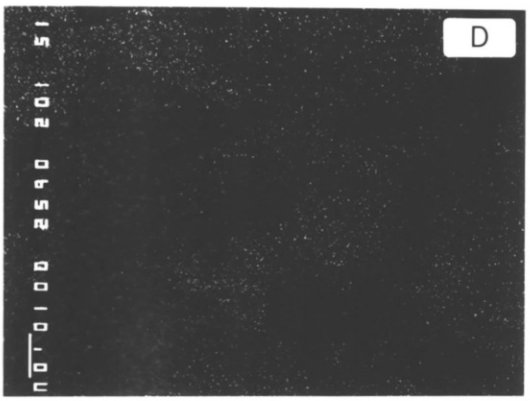
(f) ROD14; Yesnaby Sandstone, Yesnaby. Patchy calcitisation of ferroan dolomite (D) by calcite (C). Original rhombic crystal shape outlined by pyrite (P). (BEI, Jeol 733).

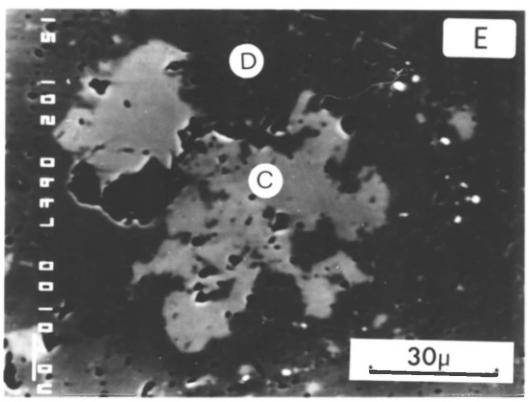
(g) Basal ORS, Sutherlandshire. Replacement of hematite-stained dolomite (D) by calcite (C). Photograph supplied by Dr. J. Parnell; (Transmitted light).

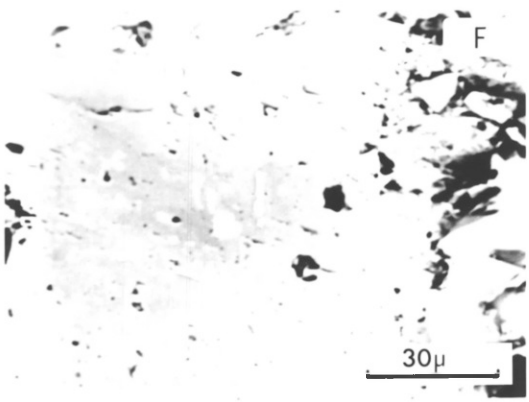












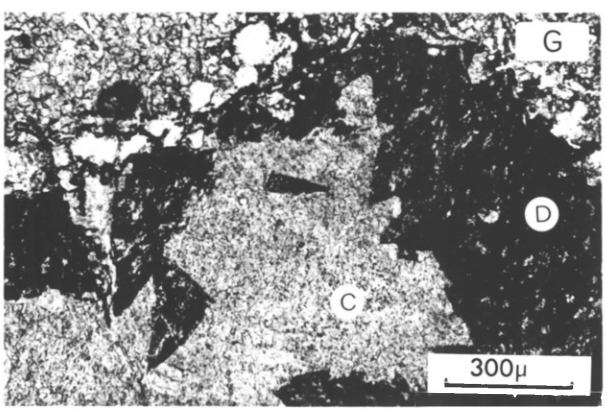


PLATE 6·7

Late diagenetic calcite in the Sarclet Group (fig. 6.11) is generally of very low Mg content but may contain up to 1.7% Fe and 1.2% Mn. Calcite is almost invariably associated with secondary oxides (although this could purely be a function of available porosity space).

Palaeomagnetism of the Sarclet Group (section 4.3) shows that it carries both a primary remanence and also a Kiaman hematitic remagnetisation. Calcitisation of ferroan dolomite during this period would provide a suitable means by which to effect such a remagnetisation.

(b) The Yesnaby Sandstone.

The carbonate content of the Yesnaby Sandstone (illustrated in plate 2.1d) is very high. This is illustrated by ICP analysis ROD14 (appendix C1e) which shows 28% $CaCO_3$, 7% $MgCO_3$ and 2.5% $FeCO_3$ (assuming iron to be present as carbonate). These figures suggest that there are approximately similar proportions of calcite and dolomite.

Dolomite was often of variable, rhythmic composition (plate 6.4b); some rhombs have nucleated around a core of highly ferroan dolomite. Compositional variation is largely in the relative proportions of Fe and Mg. Again the dolomites are over-calcic (fig. 6.12) and are possibly of two distinct compositional groups.

Dolomitisation may have occurred during the emplacement of neptunian dykes (plate 2.1b, 2.2c) which cut down from the Middle ORS, through the Lower ORS (Parnell, pers, comm.) and into the granitic basement. These show a very fine-scale alternation of dolomite and ferroan dolomite (plate 6.4c,d) and may show ?syngenetic barite mineralisation. They are of unusual composition for such bodies, which generally tend to

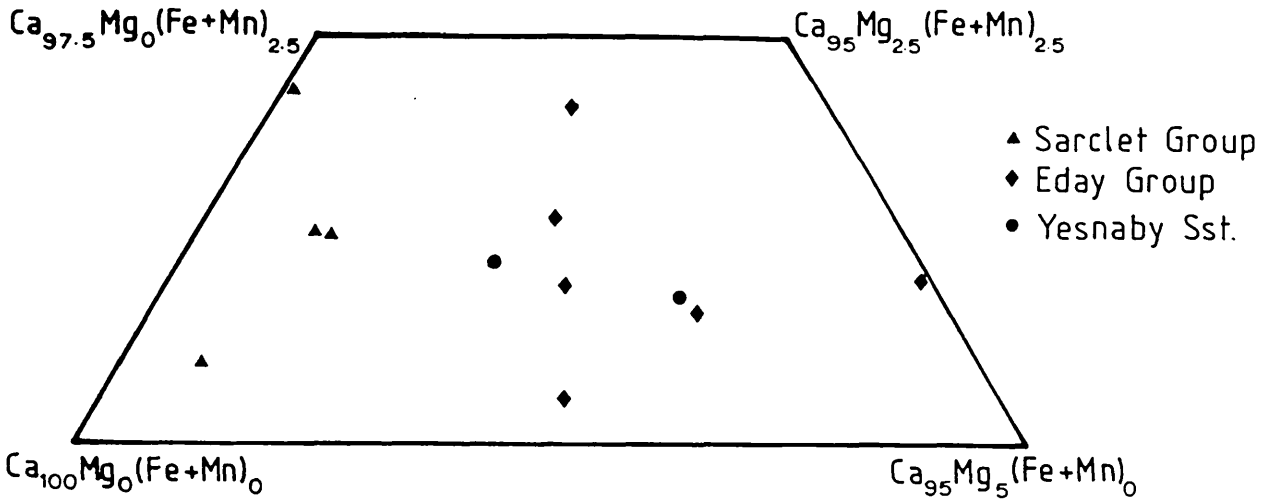


Fig. 6.11. EPMA analyses of carbonates (iii) Calcite in clastic sediments.

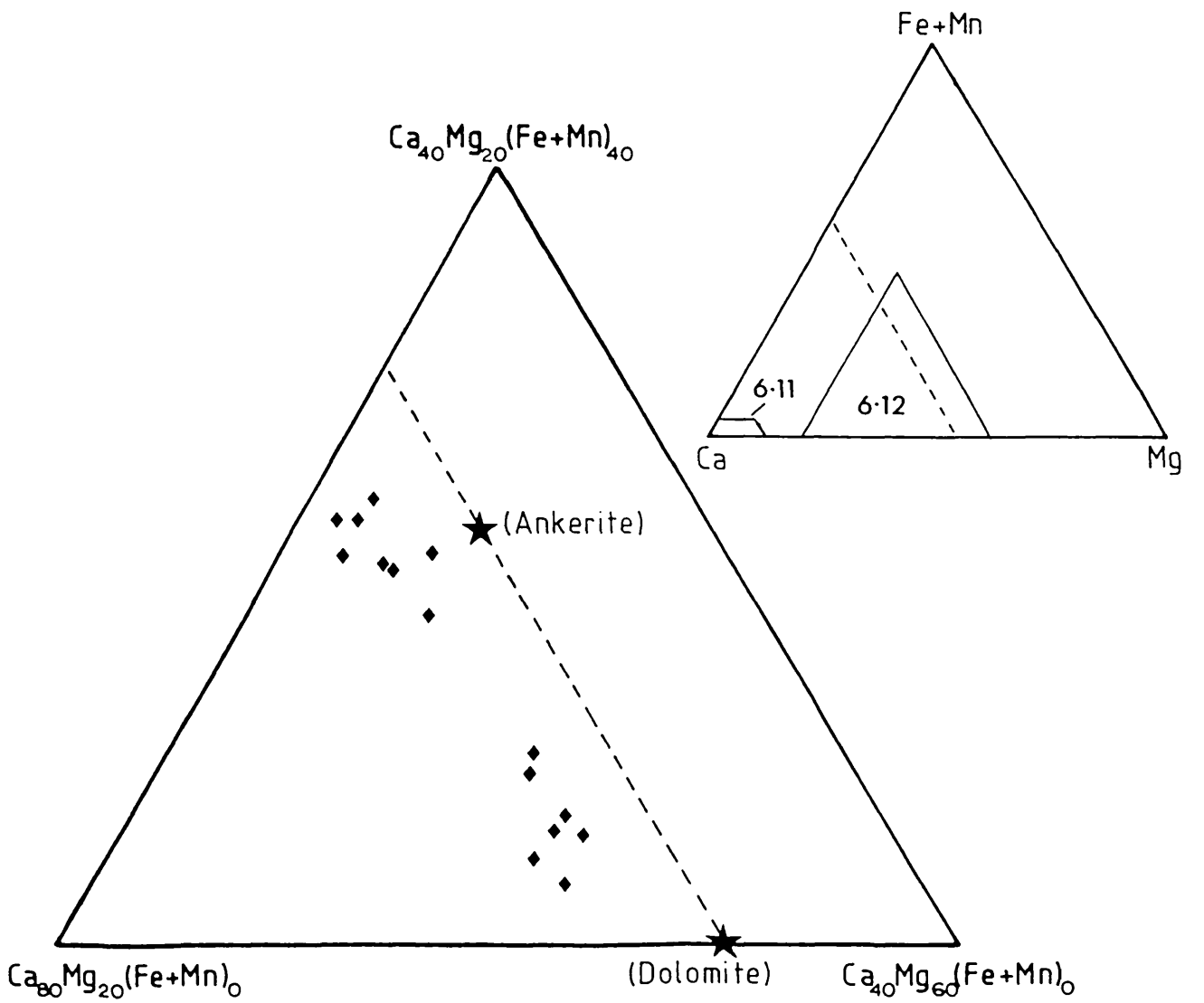


Fig. 6.12. EPMA analyses of carbonates (iv) Dolomites from the Yesnaby Sandstone. Ideal compositions of dolomite and ankerite shown; dashed line is Ca/Mg=1.

be calcitic (Rigby, 1984). ICP analysis ROD14H (appendix C1e) shows them to be composed of 38% $CaCO_3$, 15% $MgCO_3$ and 14% $FeCO_3$. Textural features are reminiscent of stromatolitic growth, although this might be expected to have high base-metal concentrations which are not seen.

Dolomite in the Yesnaby Sandstone has been calcitised, both on a large scale (plate 6.7e) and also as small dispersed patches (plate 6.7f). The latter is often seen in association with pyritic rhombs. The origin of these is unclear; an alternative to their being related to calcitisation is formation during periods of syngenetic sulphate reduction, outlining a dolomite rhomb at a particular stage during its growth.

It does not, therefore, constrain the timing of calcitisation which could have occurred at any late stage in the diagenetic history of the sediment. As with the lacustrine sediments and the Sarclet Group already discussed, calcitisation during the Kiaman reversed polarity interval would have been capable of producing the observed remagnetisation (section 4.7).

(c) Other sediments.

Carbonates in other clastic sediments such as the Eday Group (dolomite: plate 6.4e, calcite: plate 6.4f; calcite compositions shown in fig. 6.11) are often seen but but their precise role in the acquisition of a palaeomagnetic remanence is somewhat obscure. Clear calcitisation textures have not been seen in the Eday Group or in the Upper ORS.

Even if extensive calcitisation has occurred, it might perhaps not be expected to be apparent due to the generally higher porosity and permeability of these sediments compared

with those discussed above. Later selective leaching of carbonates (producing the widespread secondary porosity now seen) would remove any clear evidence of the process apart from any secondary iron oxides (which are widespread in the basin). It is interesting to note that the morphology of some of the secondary iron oxides is identical to that shown by Frank (1981) and Welton (1984) as occurring within a partially calcitised dolomite rhomb.

That the process has occurred elsewhere in Northern Scotland is shown by plate 6.7g; this is of basal ORS from Lothbeg, Sutherlandshire (material supplied by J. Parnell) and shows replacement of dolomite (hematite stained) by calcite. This formation has not been sampled palaeomagnetically.

The John o'Groats Group (chapter 8) also shows calcitisation, possibly associated with remanence acquisition in the late Permian or Triassic. This has been linked to extensive fluid movements around the Duncansby Ness vent, and would not appear to have a direct link with other sediments discussed in this chapter.

6.5. Sheet silicate diagenesis.

6.5.1. Geochemistry.

The alteration of biotite is a very complex process which may occur under a wide range of conditions. Decomposition at elevated temperatures in a parent igneous body will cause biotite of annite composition to break down to sanidine + magnetite or hematite, according to temperature, fO_2, fH_2O and Fe/Mg ratio (Wones & Eugster, 1965; Eugster & Wones, 1962). Such effects have been observed in the Jersey Granites (Duff, 1978), producing a characteristic 'schiller' texture. An important point about

this is that it does not involve the loss of potassium.

Once a biotite is in the sedimentary system, very different physicochemical conditions obtain. The simplest type of alteration is vermiculisation, in which K is replaced by hydrated cations (Ca, Mg) from an external solution. It is usually more complex; iron in high-Fe biotites is almost invariably ejected from octohedral sites in order to maintain a charge balance (Farmer et al, 1971). It would appear that such changes in the state of octohedral iron cannot occur unless K is lost (Rice & Williams, 1969; Wilson & Duthie, 1981).

6.5.2. Biotite in the Orcadian Basin.

Studies of the role of biotite in the ORS of Scotland (Higham, 1976; Turner & Archer, 1977; Wilson & Duthie, 1981) have shown it to be oxidised to a variable degree. The former study suggests that migration out of the mica to form an iron-rich halo has occurred; this would be conclusive proof of intrastratal alteration. Turner & Archer (1977) and Wilson & Duthie (1981), on the other hand, suggest that little or no iron has been lost and hence the micas have not contributed significantly to the reddening of the sediment.

Turner & Archer (1977) discuss the environment in which oxidation occurred, and conclude that hematisation may have taken place prior to the final accumulation in the sediment, possibly during several stages of sedimentary reworking. This conclusion is based on the lack of correlation between the degree of biotite oxidation (which was found to be highly variable even on a small scale) and other oxidative diagenetic characteristics.

A number of sheet silicates from the Orcadian Basin are illustrated in plate 6.8. The wide range in both degree and

PLATE 6.8
SHEET SILICATES

(a) ROD22; Eday Marls, S. Ronaldsay. Sheet silicates of uncertain composition, showing complete lack of diagenetic alteration. (BEI, Jeol 733).

(b) ROD22; Eday Marls, S. Ronaldsay. Highly oxidised biotite. Intra-cleavage iron oxides: analysis 208 (appendix D3ii). (BEI, Jeol 733)

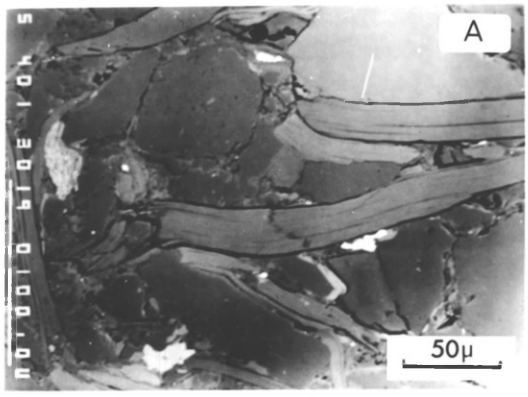
(c) RCD41; John o'Groats Sandstone, Duncansby Ness. Biotite flake showing incipient oxidation along a few cleavage planes. (BEI, Jeol 733).

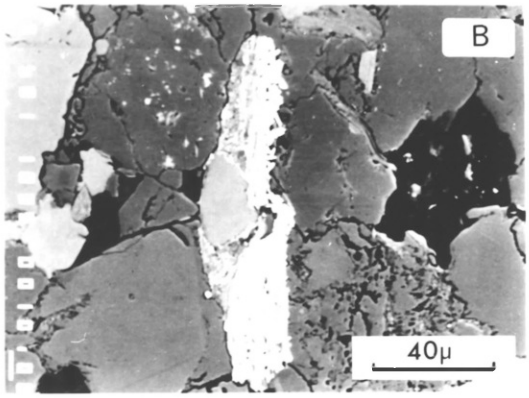
(d) RCD41; John o'Groats Sandstone, Duncansby Ness. Biotite flake almost entirely pseudomprphed by iron oxide of very low Ti content. (BEI, Jeol 733).

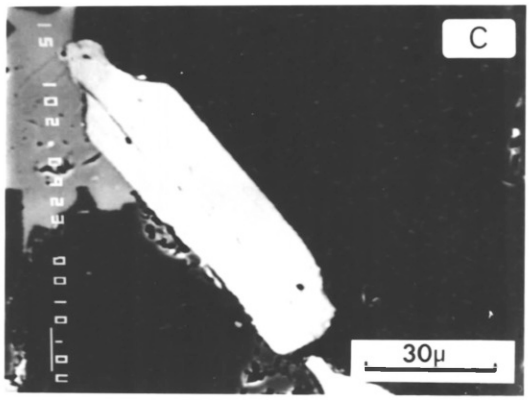
(e) RCD54; Upper ORS, Dornoch. Large biotite flake showing partial oxidation. (BEI, Jeol 733).

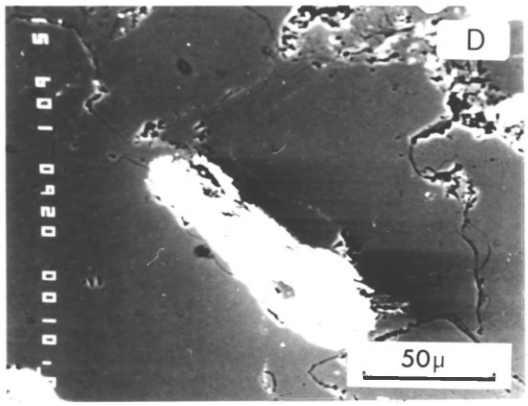
(f) RCD54; Upper ORS, Dornoch. Enlargement of (e), showing the sub-micron size of individual particles of iron oxide. (BEI, Jeol 733).

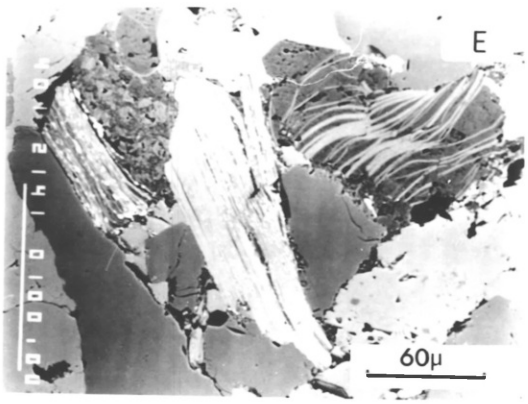
(g) ROD18; Middle Eday Sandstone, Deerness, Mainland Orkney. Oxidised biotite, showing the grain analysed by 'digimap' (fig. 6.13). (BEI, Jeol JXA-50A).

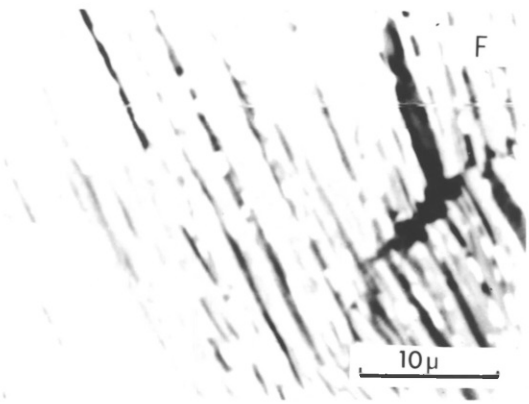












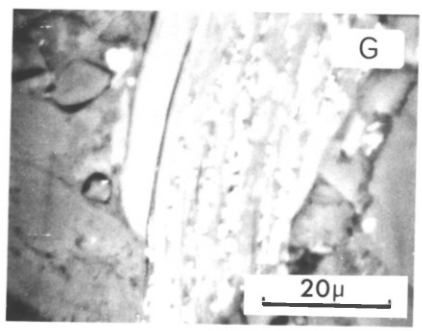


PLATE 6·8

style of oxidation is demonstrated by, for example, plates 6.8c&d which are of discrete biotites in very close proximity (1-2mm) to each other. Biotites which are almost unoxidised may be seen adjacent to those almost entirely pseudomorphed by iron oxides.

A very different texture is shown in plates 6.8e&f; this may be indicative of high-temperature alteration (as described in section 6.5.1) rather than oxidation within the sedimentary system.

A small number of biotite analyses (042, 059 and 090: appendix D3ii) shows them to have between 15-25% FeO, although some may have less (analysis 043, with 1.5% FeO). The iron-rich varieties correspond to an annite-siderophyllite composition (Deer, Howie & Zussman, 1966). Two analyses of iron oxides within cleavage planes (appendix D3ii) show them to be composed almost entirely of Fe and Ti (with interference from Mg, Al and Si due to the very small size of the grains).

The detailed geochemistry of biotite oxidation is illustrated by fig. 6.13, which corresponds to plate 6.8g. Regions of high Fe concentration, towards the centre and right of the flake, correspond precisely to regions of low K (confirming the conclusions of Rice & Williams, 1969 and Wilson & Duthie, 1981). This is indicative of oxidative vermiculisation rather than the high-temperature decomposition referred to earlier. Fig. 6.13d shows a manipulation of the raw data, in which areas of very high K, corresponding to orthoclase, are artificially annulled prior to re-plotting the data with a lower peak K value. This illustrates variation within the biotite-vermiculite flake more clearly.

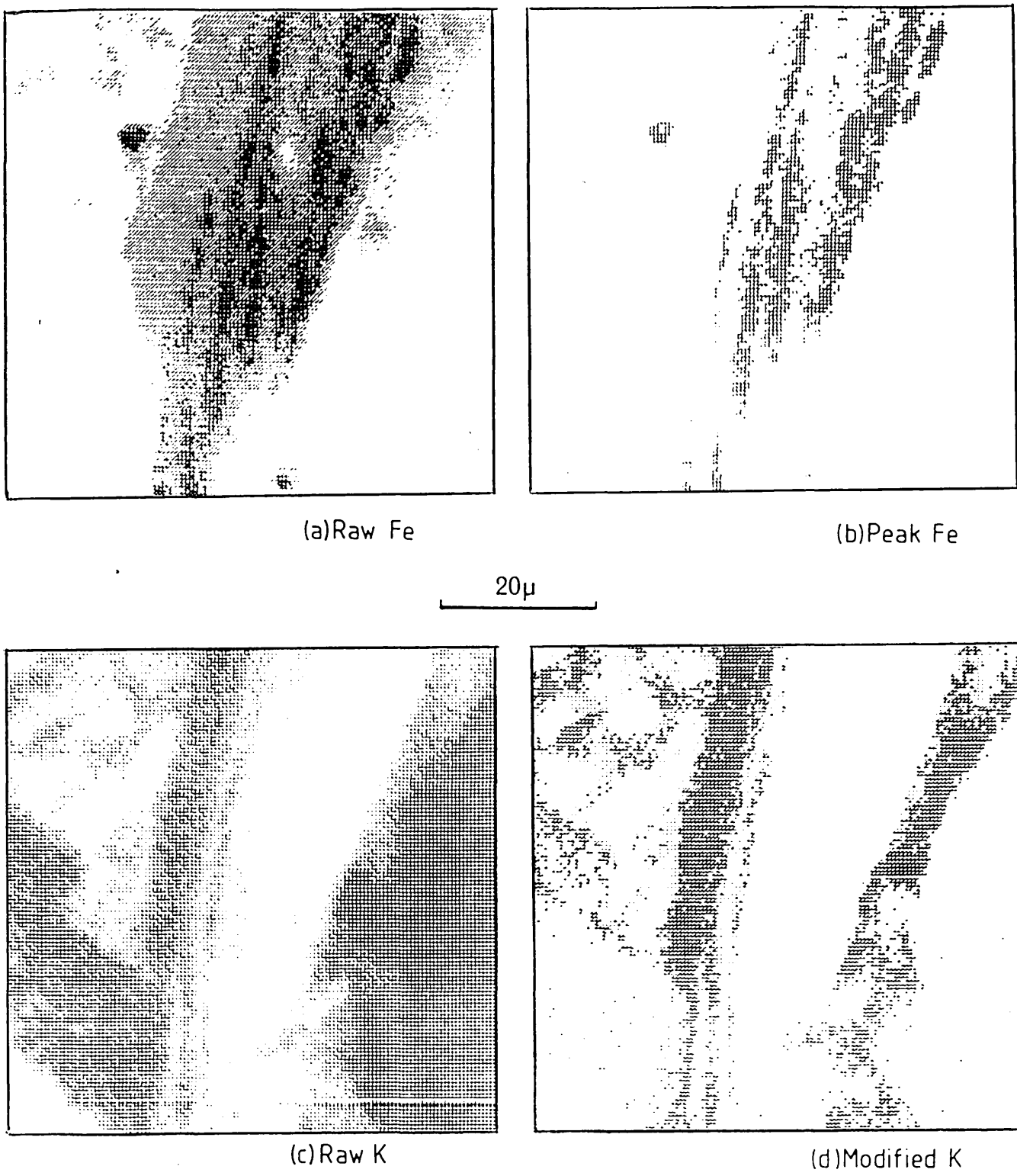


Fig. 6.13. Alteration of biotite: element distribution maps of Fe and K. Note coincidence of high Fe with low K.

The following points regarding biotite oxidation may be made.

(i) Most oxidation occurred within the sedimentary system.

(ii) Biotites with a wide range of degree of oxidation may be found in very close proximity.

(iii) Oxidised and unoxidised biotites may both be found in sediments carrying a syn-depositional remanence only.

(iv) Oxidised biotites may be found in sites which do not carry a net stable remanence.

(v) Oxidised biotites may be found in sites with very low NRM intensity (but often with a susceptibility comparable with other sediments).

Taking all the above evidence into consideration, it would appear that biotite underwent much or all of its oxidation prior to or during sedimentation. If any intrastratal oxidation occurred, it would not appear to contribute significantly to the stable NRM.

Other sheet silicates (muscovite, chlorite etc.) are widespread and common throughout the basin, but are unlikely to be of great significance to the palaeomagnetic record and hence will not be considered further.

6.6. Fine-particle hematite.

6.6.1. Iron-rich grain coatings

Post-depositional iron-rich grain coatings are a common feature of clastic sediments in the Orcadian Basin. They generally coat the exterior surfaces of detrital silicate grains, particularly quartz. A representative selection are illustrated in plate 6.9.

These are unsuitable for precise EPMA analysis, due to small grain size, the difficulty of achieving a finely-polished surface and the possible presence of

PLATE 6.9
GRAIN COATINGS

(a) RCD01; John o'Groats Sandstone, Duncansby Ness. Detrital quartz grains (Q) with iron-rich coatings (F). See spectrum S.5 (fig. 6.14a). (BEI, Jeol 733).

(b) RCD37; John o'Groats Sandstone, Duncansby Ness. Clay overgrowths (O) on detrital quartz (Q). (BEI, Jeol 733).

(c) RCD38; John o'Groats Sandstone, Duncansby Ness. Overgrowths (O) on quartz (Q) show show only Fe and Mg (BEI, Jeol 733).

(d) RCD38; John o'Groats Sandstone, Duncansby Ness. Diagenetic feldspar (K) laths on detrital quartz (Q_1) with later silica overgrowths (Q_2). The boundary of the original grain is not seen due to lack of Z-contrast. (BEI, Jeol 733).

(e) RCD42; Ellens Geo Conglomerate, Ulbster. Iron-rich grain coating (spectrum S.20; fig. 6.14c) around a detrital quartz grain (Q_1). Later silica overgrowths (Q_2) have destroyed the original porosity. Diagenetic replacement by calcite (C) occuring. (BEI, Jeol 733).

(f) RCD54; Upper ORS, Dornoch. Iron-rich grain coating (F), (spectrum S.12), between grains of feldspar (K) and quartz (Q). (Spectrum S.12, fig. 6.14b). (BEI, Jeol 733).

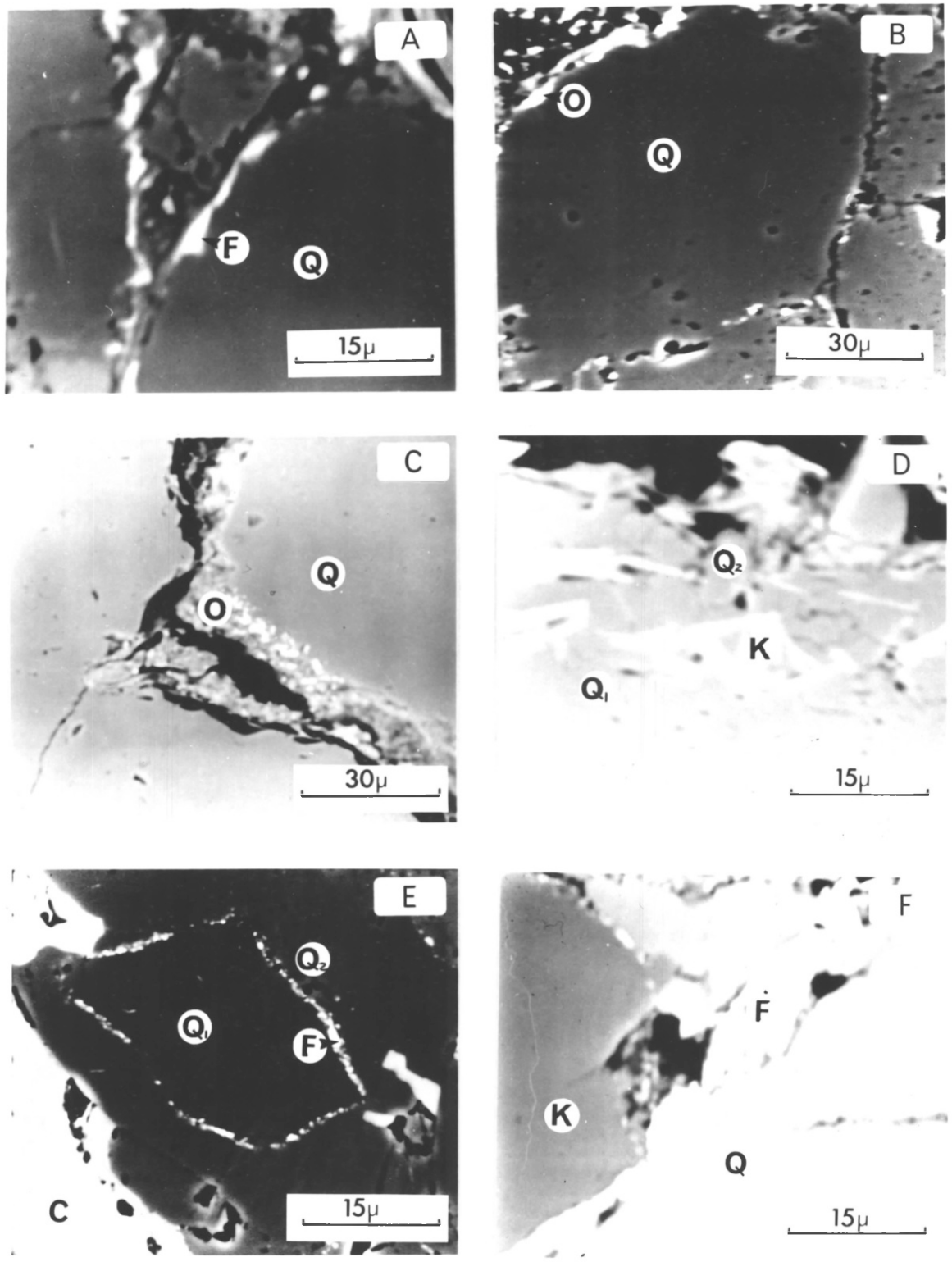


PLATE 6·9

volatiles. An indication of composition may be gained from x-ray spectra (fig. 6.14). These will often be contaminated by the host grain (e.g. a falsely high Si peak for quartz overgrowths). These spectra show iron to be the dominant element in the overgrowths, and that it is usually associated with minor amounts of Ti and Al. The latter would be expected, perhaps in a much greater proportion, if the coats were purely a detrital clay deposit. That it is only present in small amounts suggests that an alternative origin should be found.

Intrastratal alteration and decomposition of detrital ferromagnesian minerals is often cited as a method of generating grain coatings and reddening in sediments (e.g. Walker et al, 1967, and as suggested for the Upper ORS of NE Scotland by McAlpine, 1978). Within most of the sediments studied, however, there is little indication of relict ferromagnesian minerals, although there are occasional exceptions such as that shown in plate 6.3f. Additional evidence against extensive intrastratal alteration is the relatively fresh state of many biotite flakes, which would not be expected to preferentially survive severe oxidation.

Wilson (1971) suggests that most iron in grain coatings was derived indirectly from the sediment source areas, forming via recrystallisation from a precursor oxyhydroxide. The iron would presumably have been transported as colloidal $Fe(OH)_3$, as discussed above. A somewhat different interpretation, but involving the same principle, was suggested by Foster (1972) for the John o'Groats Sandstone. He suggested that the original (?colloidal) iron was incorporated into ferroan carbonates; these have later been selectively leached, leaving behind residual iron oxides.

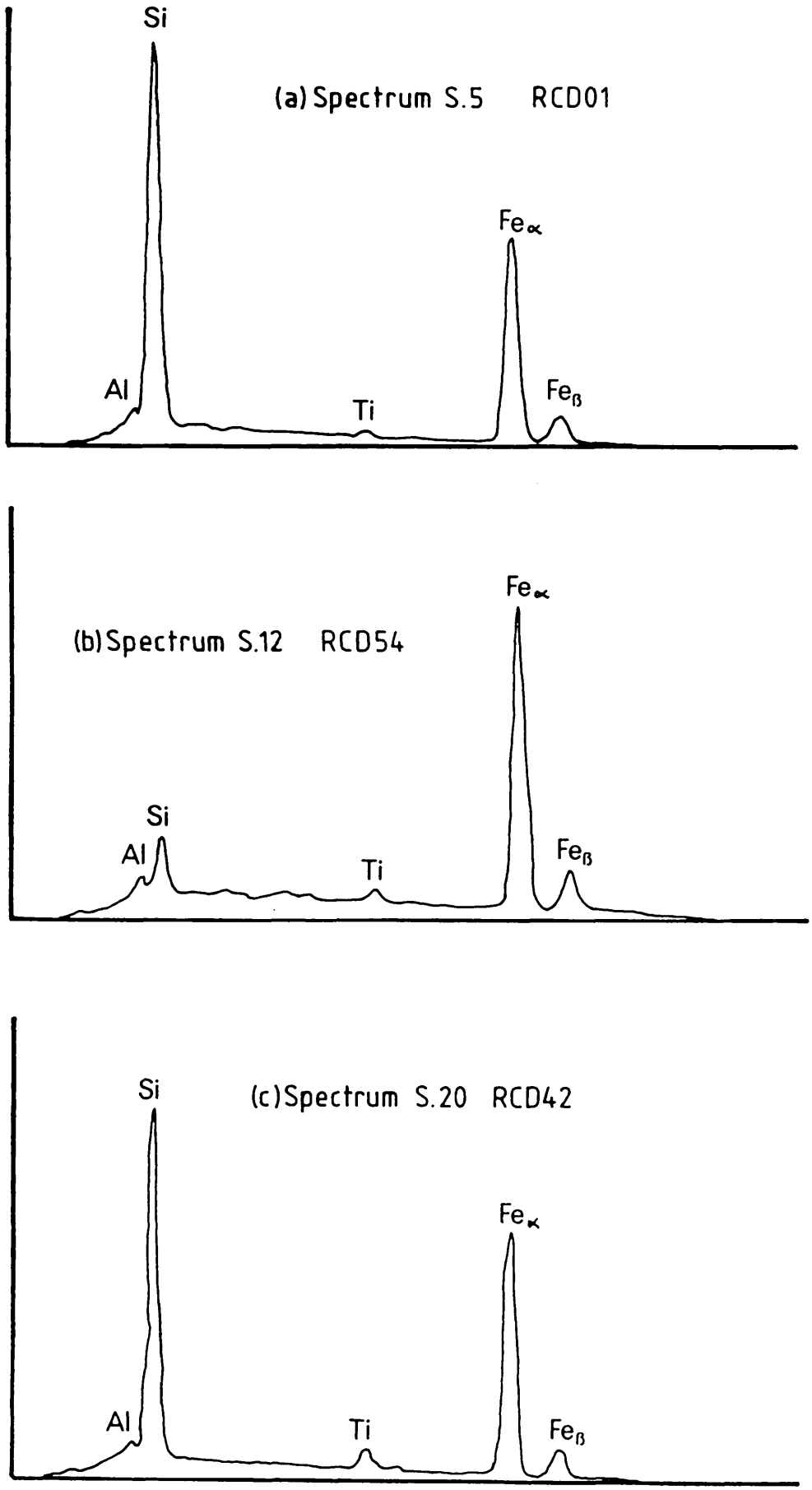


Fig. 6.14. Silicate grain overgrowths: x-ray spectra. All peaks K_{α} unless otherwise stated.

This would be enhanced if there was an intermediate stage of calcitisation of ferroan dolomite, where appropriate, as calcite is more readily soluble.

The relevance of such grain coatings to the palaeomagnetic record is not clear. In some cases (such as the John o'Groats Sandstone) they would appear to be the main remanence carrier. Elsewhere, similar lines of evidence to those listed for biotite oxidation (section 6.5.2) apply, suggesting that coatings do not contribute substantially to stable magnetic remanence. Chemical demagnetisation would easily test this; unfortunately most sediments studied are not amenable to the method.

6.6.2. Pigmentary reddening: a sedimentological model.

(a) Early reddening.

The grain coatings described above will tend to impart a red colouration to the sediment. 'Pigmentary' (i.e. fine-particle) hematite (the main cause of reddening: Collinson, 1974) is not, however, confined to such coatings.

Sedimentary reddening has often been ascribed to diagenesis of the clay fraction, particularly the dehydration of iron oxyhydroxides such as goethite. The principle of this is described by Hedley (1968) and Berner (1969). The latter study showed that goethite is unstable with respect to hematite + water under most geological conditions, even when below the water table. The potential for 'ageing' of goethite to produce hematite is thus very great.

Several workers in north-east Scotland (Wilson, 1971; Ridgway, 1974; Higham, 1976) have suggested that early

oxides (Wilson) or oxyhydroxides (Ridgway, Higham) pre-dated much of the hematite now seen in the matrix of many sandstones. Despite the observation that goethite is unstable even in aqueous conditions, the rate of the dehydration will depend greatly on the surrounding pH and Eh. This will, in turn, be a function of the original sedimentary conditions, organic carbon content and diagenetic history. It is thus possible that the diagenetic history of iron-rich clays will closely parallel that of detrital magnetite, as both will become unstable under similar conditions.

Unfortunately (from this point of view) most of the sediments sampled in this study are homogeneously reddened. These will provide little information about the original sedimentary geochemical environment and hence about processes which have operated to produce the characteristics seen today.

An area which may be crucial in this respect is in the Middle Eday Sandstone of Eday (sites ROD53 and 54). The former is a green sandy mudstone which occurs in close association with a reddened equivalent (as illustrated in plates 2.1g,h and 2.2b). Reddening is obviously post-depositional as it is discordant to bedding.

There is no significant bulk geochemical contrast between the two facies. ICP whole-rock analyses (appendix C1fii) of which ROD53 and 54G represent green horizons and ROD54P reddened, do not show noteworthy contrast. Neither is there a significant difference in the bulk oxidation state of the iron (appendix E). This implies firstly that reddening does not involve large-scale mass transfer and secondly that it involves only a very small proportion of

the total iron content, insufficient to materially affect the bulk oxidation state.

Palaeomagnetism of the two sites (section 4.5) shows that the green member carries an apparently primary ('B') component of normal polarity and of very low NRM intensity. The reddened member, in contrast, carries a hematitic remanence of opposite polarity but essentially similar age ('C' components). This shows that:

(i) Detrital magnetite carries a stable (primary) remanence in unreddened sediments and

(ii) Magnetite is not found in contemporaneously reddened sediments, which carry a (presumably later) hematitic remanence, here of opposite polarity.

Two inferences may be drawn from this:

(i) Reddening is associated with a hematitic remanence and

(ii) Acquisition of a hematitic remanence involves the simultaneous destruction or replacement of a magnetitic one.

Hence either pigmentary hematite formed during reddening and/or post-depositionally oxidised magnetite (oxidation presumably intimately associated with reddening) carry the stable hematitic remanence.

A 70% NRM intensity increase in the reddened horizon compared with the green would tend to suggest the former conclusion (although this is not necessarily the case if magnetite in the green sediment carries an unsaturated DRM). Further work is needed to assess the relative contributions of the two processes.

It is suggested by Higham (1976) and others that most sediments in the basin originally received detrital colloidal $Fe(OH)_3$; this has survived only in unreddened sediments. In oxidised sediment it has largely been

converted to hematite by a dehydration mechanism (Hedley, 1968; Berner, 1969).

Control of the timing of this reaction would be provided by the original depositional environment, particularly the presence or otherwise of organic carbon. Despite the scarcity of this in fluvial sediments now exposed, it is considered by Higham (1976) once to have been ubiquitous. While it was preserved (e.g. in fine-grained overbank muds) mildly reducing conditions would prevail. Subaerial exposure during sedimentation would allow it to oxidise and hence would enable both the dehydration of iron oxyhydroxides and the oxidation of magnetite to occur, with the resultant acquisition of a syngenetic hematite remanence.

Oxidative conditions in the case discussed above would not appear to have prevailed immediately after deposition, as the magnetitic and hematitic components are of opposite polarity. Morphology of the reddened zones is more suggestive of fluid flow within the sediment (although detailed mapping is needed to confirm this). Oxidation thus presumably occurred during the passage of fluids through the sediment at some later stage; these could possibly be related to early sediment dewatering. In other sediments, features have been noted which would suggest more rapid oxidation, often affecting a whole area (as in homogeneously reddened sediments which carry only a primary remanence).

(b) Late reddening.

It is not possible to demonstrate a direct link between any possible late reddening and the undoubtedly delayed remanence acquisition seen in many sediments. It has not been demonstrated that fine-particle hematite in the basin

is capable of carrying a stable remanence. Studies of hematite produced artificially by goethite dehydration (Chevallier, 1951; Dunlop, 1971; Dubey & Dunlop, 1971) show that it is generally superparamagnetic. This is in contrast to other forms of synthetic hematite (from magnetite oxidation or thermal decomposition of ferrous sulphate) which may carry a stable remanence (summarised in Dunlop, 1971). Studies of natural sediments tend to confirm that pigmentary hematite plays a relatively minor role in the total NRM (Collinson, 1965b, 1974).

It is tentatively suggested that despite the lack of evidence for pigmantary reddening being directly associated with remanence, its development is closely linked to the diagenetic history of detrital magnetite. Physico-chemical conditions which enhance the dehydration of oxyhydroxides will closely parallel those for magnetite oxidation.

Palaeomagnetic evidence (chapter 4) suggests that oxidation of clastic sediments was often delayed until the Kiaman. Reddening may often have accompanied this, neither process operating noticeably until the very deep penetration of oxidative agents relatively late in the history of the area (as discussed below). The extent and pervasiveness of this will be a complex function of porosity and permeability, and may vary on a very small scale (as shown by Turner & Archer, 1975).

Suitable conditions for both processes are again operative at present, during surface weathering. It should not, therefore, be surprising that many sediments, even those which appear to be homogeneously reddened, carry a recent CRM only. Of sediments which have escaped syn-depositional and Kiaman oxidation, it is only those of

sufficiently low permeability or mature mineralogy which have been able to escape recent oxidation.

An alternative cause of reddening is suggested by Foster (1972), namely the production of iron oxides from ferroan carbonate cements. These would tend to be of larger grain size than oxides produced by dehydration, and hence may be able to carry a stable remanence.

Such a model could be applicable to many of the coarser-grained sediments which carry a secondary hematitic remanence (such as the Upper ORS of Dunnet Head and some of the coarser members of the Eday Group). In these sediments, post-depositional reddening is probably associated with a Kiaman oxidative remagnetisation.

The Upper ORS, for example, is characterised by ferroan carbonate cements (Foster, 1972: McAlpine, 1978). Leaching of these in a restricted zone of fluid migration could produce the reddening pattern seen today (plate 2.1e) leaving little or no trace of the original carbonate. Such a model would be particularly applicable to coarse sediments which would have received little detrital clay and would also have been more susceptible to carbonate cementation.

6.7. Synthesis

6.7.1. Introduction

Palaeomagnetic investigation has shown that both 'primary' (i.e. detrital or early diagenetic) and 'secondary' magnetisations may be found in sediments of the Orcadian Basin. These may often be closely associated, within a single site or even a single specimen.

In this chapter, a review of possible remanence carriers and their history has been made. These include detrital and secondary iron-titanium oxides, ferroan

carbonate diagenesis, sheet silicate diagenesis and fine-grained hematite (both as grain coatings and as part of the interstitial clay mineralogy).

As mentioned previously, there are many mechanisms by which a secondary remanence may be acquired. Deep burial, effecting a viscous PTRM, has been invoked before to explain 'remagnetisation' (op. cit.) of, for example, the Duncansby Ness vent and the John o'Groats Sandstone (Storetvedt et al, 1978; Storetvedt & Carmichael, 1979). There would appear to be overwhelming geological evidence against there ever having been sufficient depth of burial to remagnetise hematite of high T_B (e.g. Watson, 1985). This is confirmed by pyrolysis data (Marshall et al, 1985) which shows that burial, even of the basal formations, has never exceeded 5-6 km (in the late Devonian) and was less than 2 km for the Upper ORS and John o'Groats Groups.

Intensive study of the dyke swarm (chapter 7) and other igneous bodies (chapter 8) has shown that they did not cause a regional remagnetisation; TCRM overprints in dyke aureoles is restricted to within a few dykewidths.

Liesegang ring structures (plate 2.1f, 6.10d) were originally suggested as evidence for regional hydrothermal fluid circulation, possibly related to the dyke swarm. They do not, however, carry a stable remanence and would appear to involve chiefly the remobilisation of Mn (compare analyses 13L and 13N; appendix C1g).

The remaining option is a diagenetic remagnetisation, as discussed in detail in this chapter.

Of the possible mechanisms discussed above, a stable ancient remanence is considered to have one (or more) of the following origins:

PLATE 6.10
MISCELLANEOUS

(a) ROD16; Middle Eday Sandstone, Deerness. Calcite (C) replacing quartz (Q). (BEI, Jeol 733).

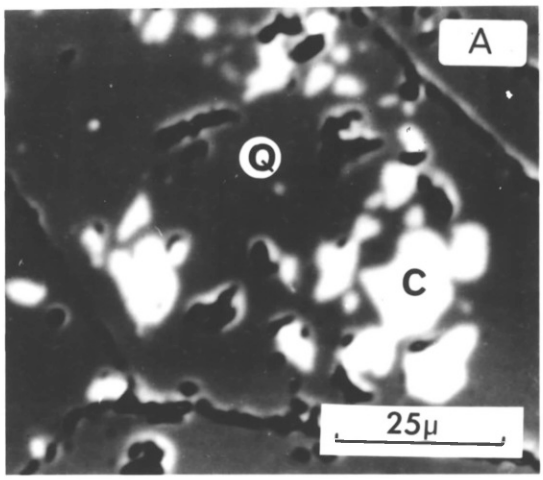
(b) ROD24; Middle Eday Sandstone, S. Ronaldsay. Euhedral authigenic anatase/rutile growing in porosity space in sandstone. Intergrown with diagenetic silica. (BEI, Jeol 733).

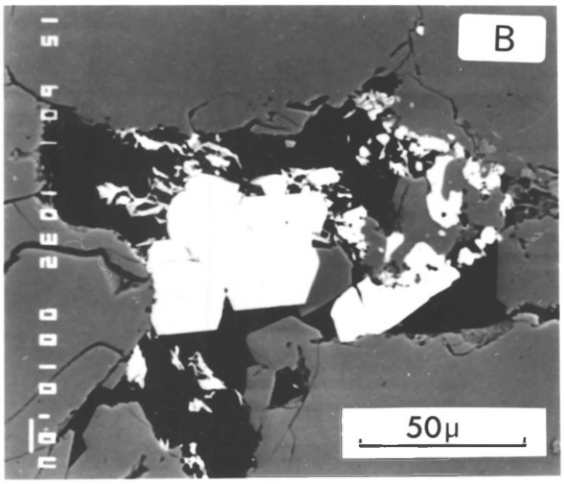
(c) ROD30; Eday Marls, Kirkwall. Coxcomb kaolinite (?dickite) overgrowing iron- and titanium-rich coating (F) on quartz grain (Q). (BEI, Jeol 733).

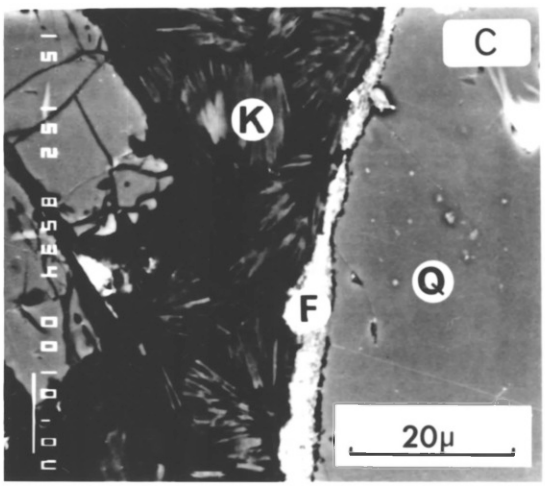
(d) ROD11; Lower Eday Sandstone, Deerness. Pore space (Ø) in sandstone showing liesegang rings. Lining of the pore is of characteristic clay composition. (BEI, Jeol 733).

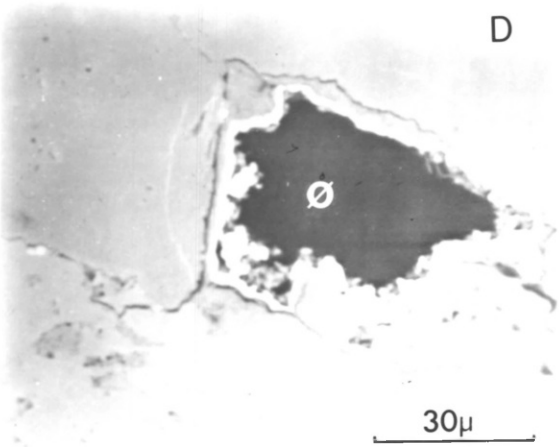
(e) ROD22; Eday Marls, S. Ronaldsay. Small-scale porosity-permeability variation. (BEI, Jeol 733).

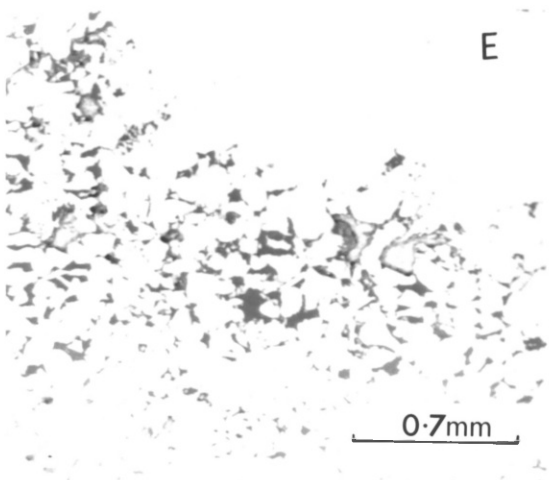
(f) RCD50; John o'Groats Sandstone, Duncansby Ness. Mature sandstone composed almost entirely of quartz (Q) and Orthoclase (K) grains with some porosity (Ø). Main diagenetic feature is silica overgrowths. (BEI, Jeol 733).











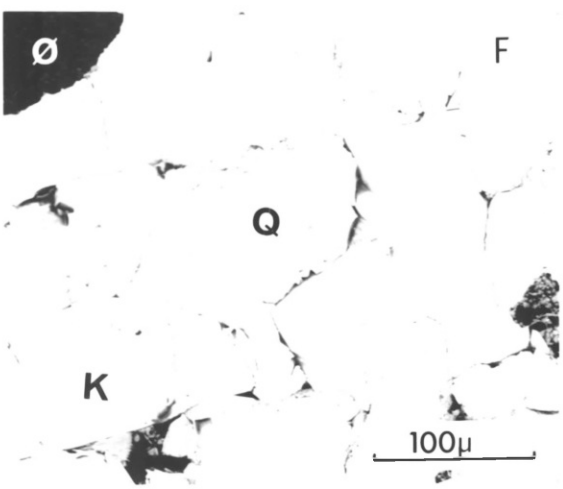


PLATE 6·10

(a) 'Primary' remanence:

(i) DRM in magnetite

(ii) Early oxidation of detrital magnetite

(iii) Early dehydration of iron oxyhydroxides

(b) 'Secondary' remanence:

(i) Calcitisation of iron-bearing dolomite

(ii) Late oxidation of detrital magnetite

(iii) Late dehydration of iron oxyhydroxides

Other possible candidates (DRM in hematite, hematitic grain coatings and diagenesis of sheet silicates) are not believed to be of great significance regionally, as discussed above. Remanence acquisition processes according to sediment grouping are summarised in table 6.3.

6.7.2. Acquisition of a syngenetic remanence

It is very difficult to separate the relative contributions of coarse- and fine-grained hematite in, for example, the Eday Group. This is largely due to problems associated with chemical demagnetisation. Tauxe et al (1978), finding a similar problem in the Siwaliks, performed rock magnetic experiments on mineral separates from very similar sediments to those described here. This showed that specularite (either detrital or formed by very early diagenetic oxidation) carried a remanence acquired during or shortly after deposition. Red pigment carried a later remanence, often of opposite polarity and contrasting stability.

Most or all of the iron-titanium oxides analysed in this study would appear to be hematite. This includes both

TABLE 6.3

REMANENCE ACQUISITION

Group	REMANENCE Primary	Secondary	Detrital magnetite	Early hematite	Calcitisation	Late hematite
Upper ORS		++			?	?
John o'Groats	+	++			++	
Eday	++	++	+	++	++?	++
Lacustrine		++			++	
S. Basin	++	+		++		?
Yesnaby Sst.		++			++	
Sarclet	++	++		++	++	?

detrital (rounded) and secondary occurrences. Most or all of the detrital grains have been oxidised and may show fine-scale exsolution lamellae. These may have originally been deposited as magnetite.

It is proposed that early oxidation of detrital magnetite was responsible for much of the early hematite remanence acquisition. Similar conclusions have been reached elsewhere by, for example, Turner, 1974; Walker & Larson, 1976; Turner & Ixer, 1977; Purucker et al, 1980; Walker et al, 1981 and Larson et al, 1982.

Evidence from the Eday Group suggests that magnetite was deposited in the original sediment. This has been able to survive (retaining a stable remanence, presumably a DRM) only in very fine-grained sediments, where it has been able to escape oxidation at a later date. Elsewhere, magnetite was probably oxidised rapidly prior to deep burial (as discussed by Reynolds, 1982). Oxidation was apparently intimately associated with post-depositional reddening (as also described by Friend, 1966) although the relative contributions of the two processes are uncertain in this case.

The rate or efficiency of magnetite oxidation would have been intimately related to depositional environment and would have been closely dependent on organic carbon contents. Astin (1982) has suggested that reddening of the Trona Scord Formation of Shetland was related to water table level during deposition; streams with variable discharge rates would be more prone to a low water table than lake margin sediments. Such a model probably explains the acquisition of most primary NRM directions (Foyers Sandstone; Sarclet Group northerly components; most

sediments around the Moray Firth; site RCD41 in the John o'Groats Sandstone and most A and B components in the Eday Group).

The only sediments suitable for accurate magnetostratigraphy are those which have retained a magnetite DRM as it is impossible to precisely date the timing of hematite generation. In the Orcadian Basin, such sites are restricted to one in the Eday Marls and possibly one in the Middle Eday Sandstone.

6.7.3. Acquisition of a secondary remanence

Many sediments carry only a secondary remanence (of Upper Palaeozoic or early Mesozoic age). Others may show both primary and secondary components in close association. Secondary components are exclusively hematitic.

Textural evidence regarding the timing of secondary remanence acquisition is rarely forthcoming; a martitised magnetite grain will have a similar appearance whenever it was oxidised. Delayed oxidation of magnetite would, however, be a possible mechanism for remagnetisation, particularly if syngenetic oxidation was precluded by a high water table or high organic carbon content. Indirect evidence of the late oxidation of magnetite may occasionally be seen, as in plate 6.10b which shows an authigenic titanium oxide grain (?anatase) occupying a secondary porosity space. Authigenic titanium oxides have been connected with martitisation as they will tend to form from excess Ti in the original magnetite (Ixer et al, 1979; Morad & Aldahan, 1982).

Secondary iron oxides (section 6.3) are characteristic of sites showing a remagnetisation. That these may often occupy secondary porosity space (plate 6.3) is testament to

their late origin. It is suggested that much of the iron originated in ferroan carbonate cements (which in turn probably acquired much of their iron from interstitial breakdown of detrital grains). These cements have since been extensively leached, leaving only remnant patches. An intermediate calcitisation stage may not be essential for the generation of iron oxides from carbonates, as ferroan calcite will also tend to release iron during leaching.

Alternative or additional sources of iron could also be suggested; sufficient evidence does not remain in the sediment for conclusions to be drawn. This could include the dissolution of feldspars (which may sometimes contain significant amounts of iron).

Conclusive evidence of the role of calcitisation in secondary hematite production is shown by the Sarclet Group; it is suggested that remagnetisation of the Sarclet Group is largely due to this process. The relatively fine grain size (compared with much of the Eday Group) may explain why textural evidence of calcitisation has survived here. An important point about such a process of remagnetisation is that it will tend to produce iron oxides of differing morphology to those produced by early martitisation; this would explain how both primary and secondary hematitic components with contrasting stability ranges may be found, even in the same specimen (e.g. Sarclet and Eday Groups).

Small-scale variations in the extent and efficiency of the remagnetisation process would tend to depend greatly on porosity and permeability variation. Plate 6.10e shows a field of view from site ROD22, which carries both a syngenetic remanence (?DRM) and also a Kiaman remagnetisation. Fine-scale porosity variation, on the sub-

millimetre scale, would allow great contrasts in stable magnetic mineralogy over a small distance, as found by Turner & Archer (1975) in the nearby Gamrie Outlier.

In some sediments (lacustrine laminites and the Yesnaby Sandstone, both of which have been completely remagnetised), the only evidence of diagenetic reactions involving secondary hematite generation is the calcitisation of dolomite. This is thus proposed as the principal mechanism of remagnetisation in such sediments.

There are sites which carry no stable remanence atall; an example is illustrated in plate 6.10f. The site has a very mature mineralogy (quartz and feldspar) and no carbonate cements or iron oxides- and hence no mechanism by which to effect a remagnetisation.

6.7.4. A model for Kiaman remagnetisation

The remagnetisation process outlined above is essentially oxidative. Reactions have apparently occurred at a relatively late stage in the history of the basin which are usually considered to be near-surface processes requiring high Eh. Previous investigations of sediments showing a Kiaman remagnetisation (see section 2.6 and chapter 9) have nearly all suggested a similar conclusion.

This was summarised by Creer (1968), who related the pervasive Kiaman remagnetisation of Lower Palaeozoic rocks from Laurasia to the continental configuration and position at the time. A large landmass was situated at low latitudes for a prolonged period during the Permian; the environment was 'favourable for the formation of red beds on a scale never since repeated'.

The essential point is that being a large landmass near the equator it would be extremely arid. This would enable the water table to sink to an extremely low level, perhaps to depths never since repeated, even in modern desert environments. Buried sediments would then be subjected to conditions resembling those of the surface, i.e. in the phreatic zone with free oxygen available.

As discussed in chapter 2, these are the ideal conditions for oxidative diagenesis, both of iron oxides and of carbonates. This would explain why processes normally believed to occur only at the present land surface could have occurred to a great depth.

Moving groundwater within the phreatic zone would also tend to enhance the calcitisation process, particularly if evaporites (plate 2.2d) were carried in solution.

Observations of post-depositional oxidative diagenesis ('reddening') in the British Isles were first made many years ago. Bailey (1926)suggested that the red colouration of the Carboniferous of Arran was not original but was '...connected in some way with the New Red Sandstone...' It may be significant that the sandstones in question are described as carbonate-rich. Trotter (1939, 1953, 1954) found reddening '...associated with dolomite..' in Carboniferous sediments of the Carlisle Basin and Lancashire. Observations such as '...the ferrous carbonates...have been wholly converted into ferric oxide...' suggest that regional calcitisation of dolomite has occurred. He suggests that this was associated with deep oxidative penetration in a semi-arid climate during the Carboniferous-Permian interval. A maximum penetration of 1700 feet (520m) is proposed.

Anderson & Dunham (1953) found a much shallower zone of reddening in the coal measures of Durham. Mykura (1960) suggested that reddening of originally grey Upper Carboniferous sediments and the replacement of coal by limestone in Ayrshire were related to oxidation beneath the late Carboniferous to early Permian land surface; a somewhat greater depth of 1950 feet (600m) is suggested.

In addition to the above observations, the Carboniferous of Criffel would also appear to have been remagnetised (appendix F), again possibly associated with calcitisation.

It is suggested that the fact that geological observations of late reddening have been commented on in the Carboniferous but not the Devonian is largely a function of original expectation: the Devonian is generally assumed to have acquired a syngenetic reddening. Since both the Devonian and the Carboniferous have been susceptible to the same processes and it would appear that much of the Devonian underwent delayed oxidative remagnetisation this may also apply to reddening.

In conclusion, this study would seem to suggest that the ORS of the Orcadian Basin underwent severe oxidative diagenesis , particularly of ferroan carbonates, during the late Carboniferous to late Permian (the Kiaman reversed polarity period), and acquired much of its palaeomagnetic remanence at this time.

CHAPTER 7

THE PERMIAN DYKE SWARM

7.1 Introduction

Late Palaeozoic intrusive igneous activity is widespread in N. Scotland, with a number of localised Permo-Carboniferous dyke swarms such as those in the Outer Isles, Inner Hebrides, and southern Scottish Highlands, as well as in the northern Orcadian Basin. In addition, there are several possibly related volcanic plugs in Caithness and Orkney, the most well-known of these being Duncansby Ness (see chapter 8).

Age determinations on dykes from the Orcadian Basin (section 7.2.3) suggest that they were emplaced at a similar time to the postulated Kiaman (Upper Carboniferous-Permian) chemical remagnetisation in surrounding sediments (chapter 9 etc). Hence much of the earlier emphasis of the present research was aimed at investigating the palaeomagnetic and geochemical effects of dyke emplacement on surrounding sediments and determining the extent to which it was a significant remagnetising agent, either on a local scale or as part of a large-scale heat influx which could also have caused regional hydrothermal fluid circulation with related chemical remagnetisation.

7.2 Geology and sampling

7.2.1 Tectonics

The Orcadian dyke swarm is the northernmost onshore expression of Permo-Carboniferous igneous activity in Northern Scotland. A total of some 250 dykes have been recognised, out of more than 3000 throughout the Highlands

and Islands, which are grouped into 8 major swarms (Rock, 1983); these are separated by areas of very low dyke incidence (fig.7.1). The swarms are concentrated on the margins of tectonic basins and coincide in azimuthal orientation with the faults controlling such basins (Baxter & Mitchell,1984; Watson,1985). This orientation changes progressively from NW-SE in the south of Scotland to NE-SW in Orkney. In particular, the Orcadian swarm appears to coincide in orientation with the Great Glen Fault and its extension the Walls Boundary Fault (Baxter & Mitchell,1984). Even though Permo-Carboniferous sediments corresponding to these basins are no longer found on land, they have been recognised offshore, to the west of Orkney (Kent,1975).

Total crustal dilation associated with the dykes is extremely low, as none is more than a few metres in thickness. Even within the densest swarms of Northern Scotland, crustal dilation does not exceed 4% over 0.5-2.0 km (Rock,1983; Speight & Mitchell,1979).

7.2.2 Geochemistry

In general, the dykes are alkaline lamprophyres, predominantly camptonites and monchiquites, which have a mineralogy dominated by olivine, hornblende and augite with subsidiary biotite, feldspar (predominantly plagioclase), iron oxides and a glassy groundmass. The dykes sampled belong to both of these subgroups (4 are camptonites and 3 monchiquites). In addition, there are a few dykes of extremely felsic composition. All variants are considered to have a common origin, the range of compositions reflecting varying degrees of high-level fractionation. The widespread occurrence of dense ultrabasic mantle xenoliths within dykes suggests that the magma did not reside in the upper crust

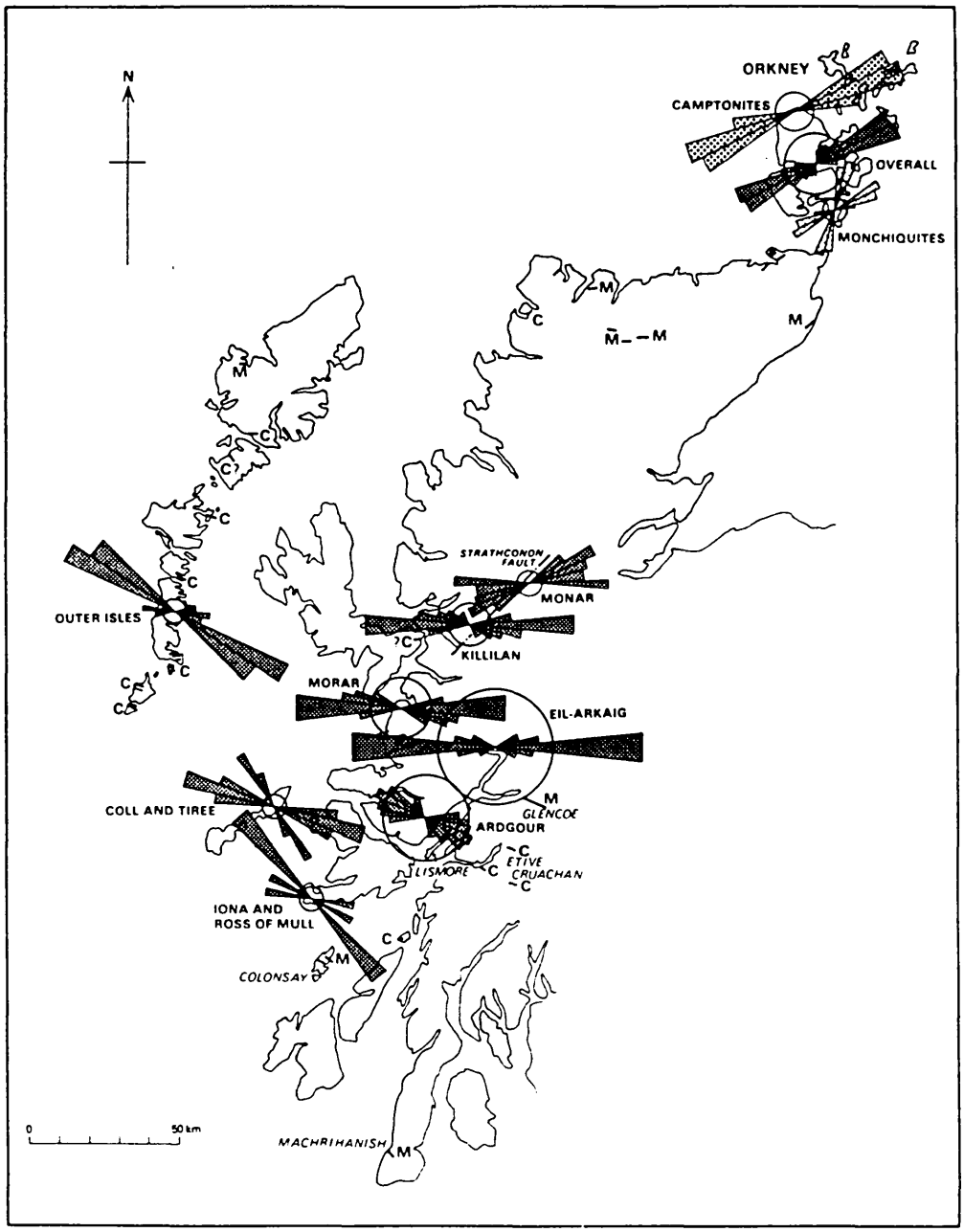


Fig. 7.1. Permo-Carboniferous dyke swarms of Scotland (after Rock, 1983).

for any significant length of time prior to intrusion (Rock, 1983). This has important implications in consideration of net regional heat flow changes due to magmatism during this period.

7.2.3. Age

The age of the Orcadian dyke swarm was for a long time in considerable doubt, with early authors considering it to be either Tertiary (e.g. Flett,1900) or late Carboniferous-Permian (eg Richey, 1939). The recent publication of reliable isotopic dates (Brown,1975; Baxter & Mitchell,1984; table 7.1) suggests a Mid-Upper Permian age, in agreement with earlier estimates based on petrographic similarity with well-dated Permo-Carboniferous rocks further south in Scotland (Francis,1968). These dates are somewhat later than those for other monchiquitic dyke swarms of Northern Scotland which appear to cover a time-span of about 90 m.y. (see table 7.1), although Mykura (1976) reports data by N.J.Snelling which give a Lower Permian age for some of the Orkney dykes, more in agreement with dates from the remainder of Scotland.

Table 7.1
Scottish Permo-Carboniferous dykes:
Potassium-Argon age determinations

Location	Age (Ma)	Reference
Loch Eil, Loch Arkaig	326±8	Baxter & Mitchell (1984)
Loch Monar	323±9	Baxter & Mitchell (1984)
Ardgour (Mull)	291±5	Speight & Mitchell (1979)
Orcadian Basin	288±9*	Snelling (in Mykura, 1976)
Colonsay	281±8	De Souza (1979)
Mull	275±7*	Beckinsale & Obradovitch (1973)
Orcadian Basin (Thurso)	252±10	Baxter & Mitchell (1984)
Orcadian Basin (Orkney)	240±12*	Browne(1975)
Orcadian Basin (Hoy)	235	Halliday et al (1977)

* : Pre-1977 dates corrected as per Steiger & Jaeger (1977)

7.2.4.Sampling

A total of seven distinct dykes and/or dyke margins have been investigated, including three monchiquites and four camptonites (fig.7.2, table 7.2). The camptonites are all from Orkney, as is one of the monchiquites. This reflects the spatial distribution of the two dyke types, camptonites being more abundant further north. Five of the dykes are intruded into fine-grained lacustrine sediments and two into clastic rocks. Of the 12 sites, 4 are from dyke material, wherever this was found in the field to be fresh enough to sample, and the remainder from contact zones in the surrounding sediments, where a site may represent a number of specimens collected in a linear traverse at various distances from a dyke margin. These will be considered separately, followed by a synthesis of results.

7.3. Dyke material-Palaeomagnetism

7.3.1. Previous work

To date, the only one of the Permo-Carboniferous dyke swarms to have been thoroughly investigated palaeomagnetically is that in Argyllshire (Esang & Piper, 1984a) from which fifteen sites define a mid-Carboniferous palaeopole at 355 E, 35 S, in excellent agreement with an isotopic age for the swarm of 320±4 Ma (Baxter & Mitchell, 1984). Eight sites from five Permian dykes and/or dyke margins intruding the Strontian Granite (McClelland Brown 1980) give a well-defined mean direction of Dec. 183°, Inc -41° (k=69, a=7°) A single dyke cutting the Peterhead granite of Aberdeenshire (Torsvik, 1985a) gives a broadly comparable direction of Dec 192°, Inc -19°, the remanance being carried predominantly in magnetite; sampling in the contact zone in the granite was not successful. The

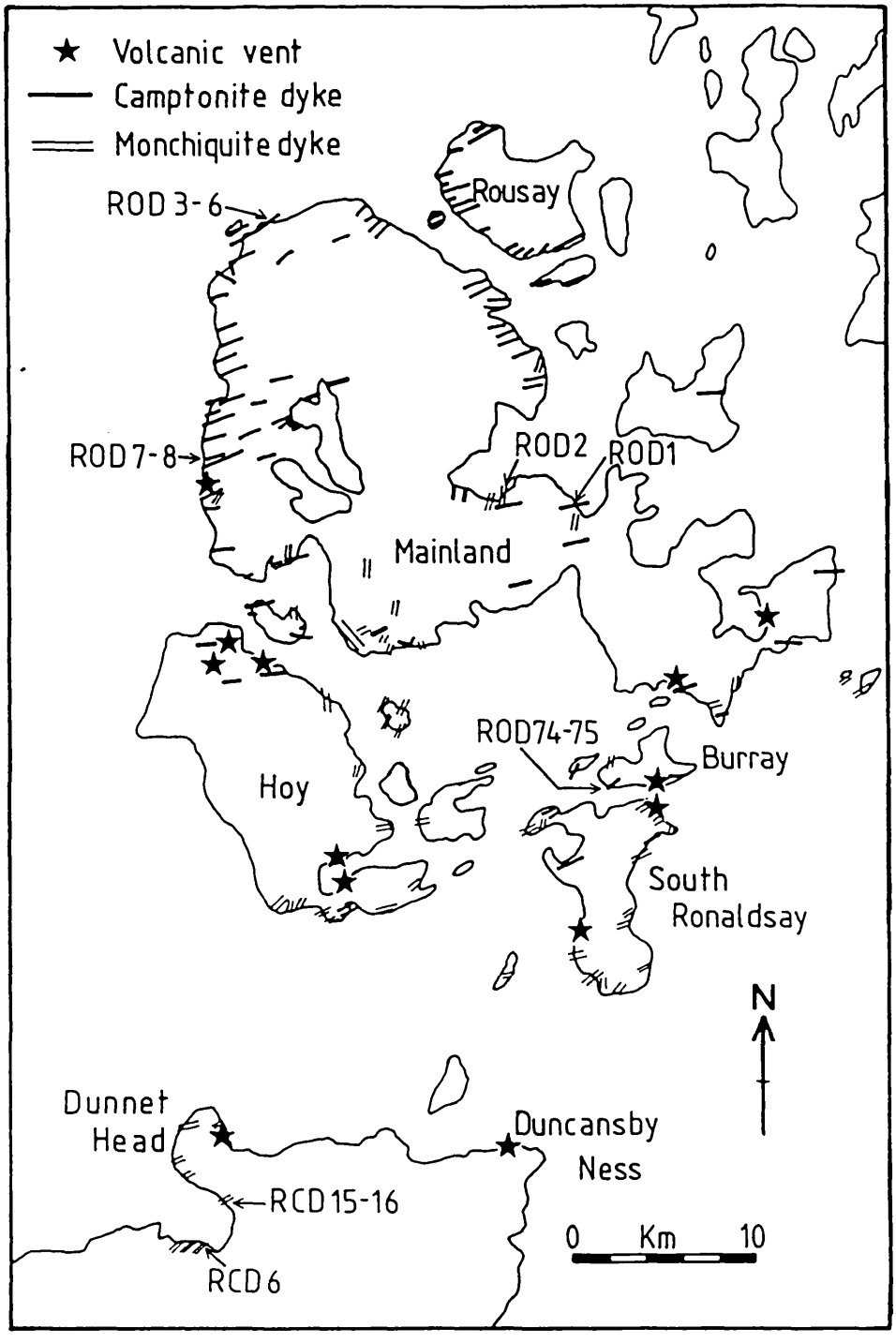


Fig. 7.2. Dyke occurrences in the Orcadian Basin, with site locations.

Table 7.2
Dykes and dyke margins: Site details

Site no. Dyke	Site no. Margin	Dyke type	Host rock	Dyke Width	Margin Limit	N_{sa}	N_{sp}	Treatment Th	Treatment AF	Treatment AF+Th
-	RCD6	M	Thurso Flags	0.65m	1.09m	14	14	12	2	-
-	RCD15	M	Upper ORS		(10cm)	5	7	6	-	1
-	RCD16				(1.3m)	5	9	9	-	-
ROD1	-	C	Rousay Flags	0.85m	-	6	6	6	-	-
-	ROD2	M	Rousay Flags	1.50m	0.80m	12	21	16	5	-
ROD3	-				-	6	10	9	1	-
-	ROD4	C	U. Stromness	1.00m	0.66m	5	7	7	-	-
-	ROD5		Flags		0.84m	8	13	-	13	-
ROD7	-	C	L. Stromness	2.75m	-	9	16	11	5	-
	ROD8		Flags		2.90m	9	13	9	4	-
-	ROD74	C	Eday Marls	0.58m	0.96m	8	11	9	-	2
ROD75	-				-	5	8	6	2	-
Total						92	123	100	32	3

N_{sa} = No. of samples
N_{sp} = No. of specimens
C = Camptonite
M = Monchiquite

Orcadian swarm (the subject of the present study) has not previously been studied palaeomagnetically.

7.3.2 NRM

As might be anticipated for basic dykes, NRM intensities are very much higher than any found in surrounding sediments. Apart from two cores (ROD0304 and ROD0701), NRM intensity varies between 1115 and 3140 mA/m with a mean of 1985 mA/m and initial susceptibility, measured for several samples per site, between 750 and 3750 mA/m. The ratio of the two, Q, varies between 0.4 and 1.6, suggesting fairly good palaeomagnetic stability (Irving, 1964; Stacey, 1967). However, this ratio is only a very approximate guide to reliability, especially when some or all of the magnetic phases are of secondary origin, as may be the case here. The presence of low-coercivity magnetite may also artificially increase the value of Q (Collinson, 1982, section 10.2). Lower NRM intensities tend to be found towards the outer (chilled) margins, as exemplified by site ROD7 (fig 7.4) which shows a systematic increase in intensity towards the centre of the dyke. The lowest intensity of all is found in a core from the outer margin of this dyke, possibly reflecting the inclusion and partial absorption of a sedimentary clast during emplacement. The overall pattern of intensity variation is presumably due to the partial dependence of grain size and/or domain state of the magnetic carrier on cooling rate, although no detailed microscopic observations have been made to confirm this. Such an intensity distribution could be a useful discriminator between single- and multi-phase intrusions, as several dykes have been reported which have internal cooled margins (Rock, 1983); this does not appear

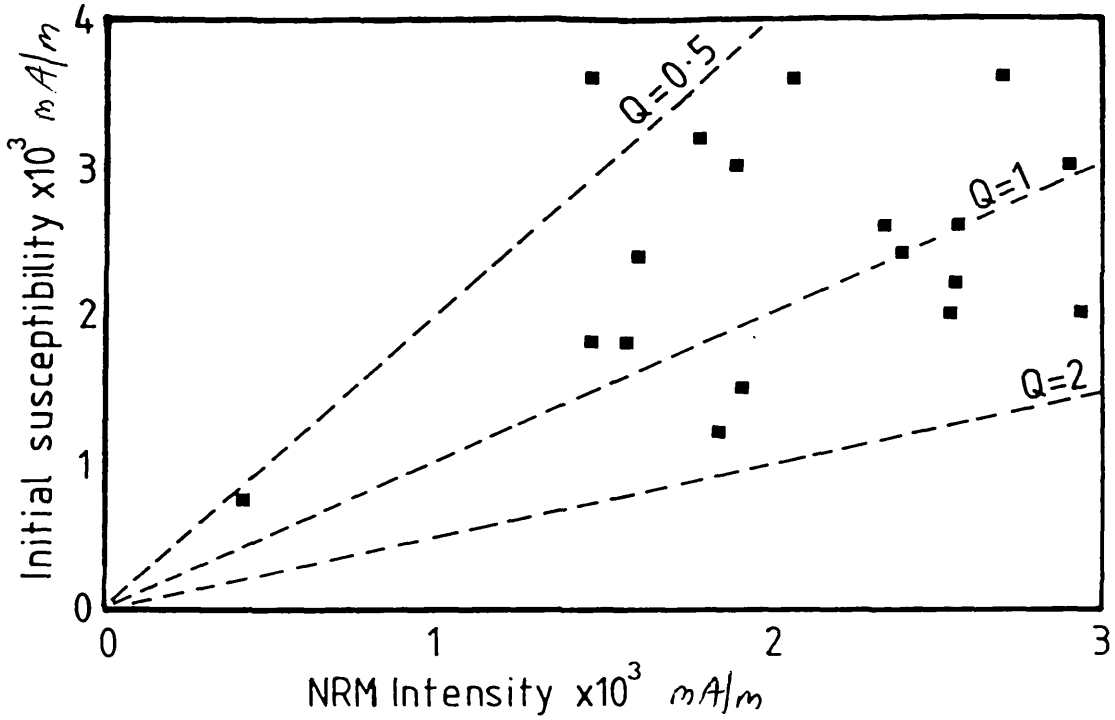


Fig. 7.3. Dyke material: Koenigsberger Ratios.

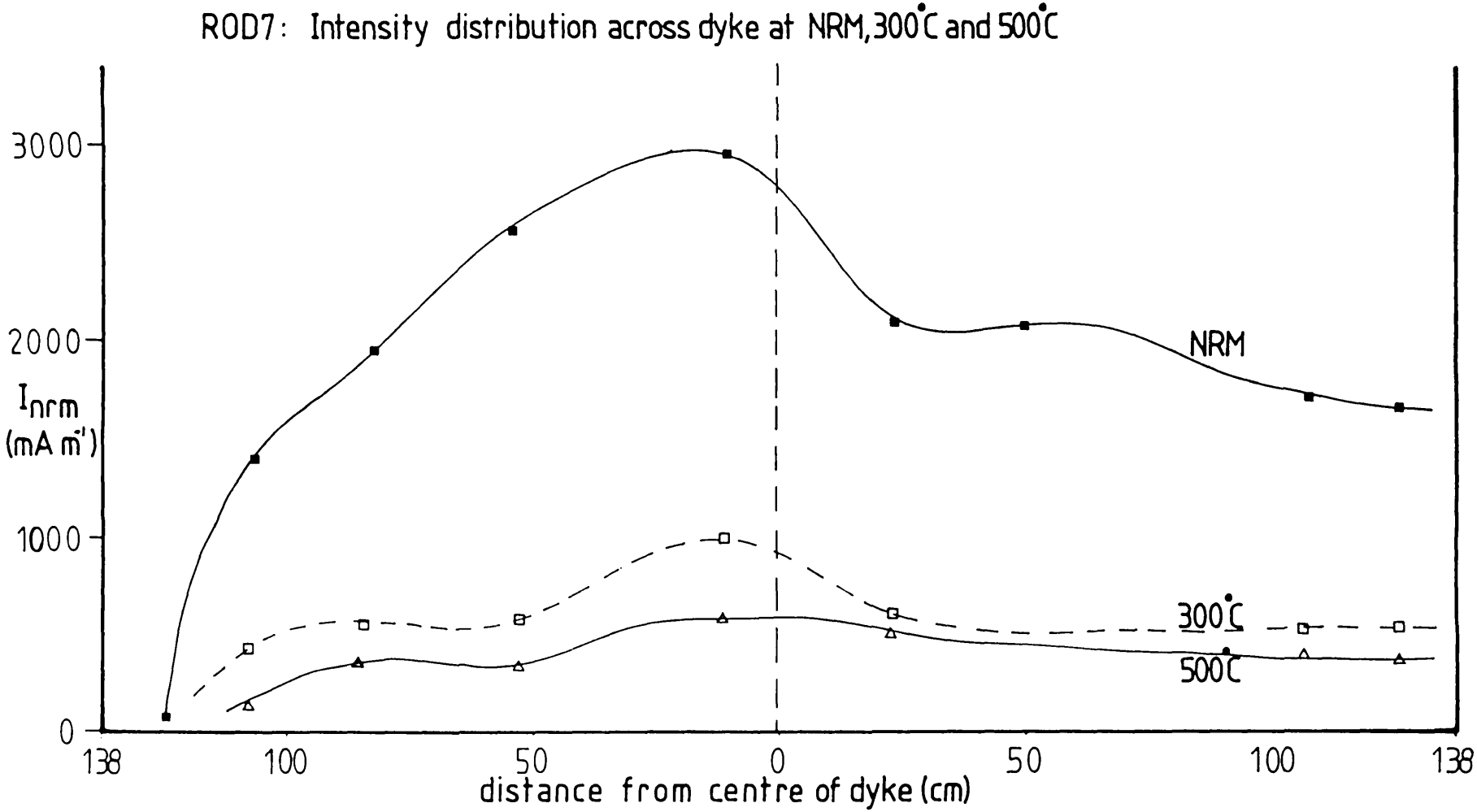


Fig. 7.4. Magnetic intensity variation across dyke ROD07 (showing it to be a single-phase intrusion).

to be the case here.

NRM directions are all steeply downwards, with inclinations frequently greater than 60 (fig 7.5). There is a general clustering around the PEF direction, particularly for sites ROD1 and ROD75. The majority of the remainder have a distribution elongated to the S or SE of the PEF, suggesting that they represent a composite of this with a southerly component.

7.3.3. Progressive demagnetisation

All samples were subjected to progressive demagnetisation, both thermal and AF, in an attempt to separate the NRM components. Both methods give a very rapid decrease in measured intensity, often with decreases to 10-30% of the NRM value after one demagnetisation step (100-150 C or 2-5mT) and frequently with a similar decrease after the second step (fig.7.6b,c). There is generally a southward movement of magnetic orientation during treatment, with inclination changes of 5-15 per step, presumably representing the removal of a viscous PEF component. Typical examples, represented as stereographic projections, are given in fig.7.6a. Many, such as specimen ROD0301B, obviously do not reach a stable end-point; others (e.g.ROD0105), would appear to do so, which could lead to the suggestion that this represents a meaningful direction. Such directions are given in table 7.3; the mean would appear to correspond approximately to a Devonian palaeopole, as discussed in chapters 2 and 9. This apparent incongruity with isotopic dating (section 7.2.3) is resolved by comparison of these results with those derived from baked dyke margins (section 7.4) which can be shown beyond doubt to represent a magnetisation acquired during dyke

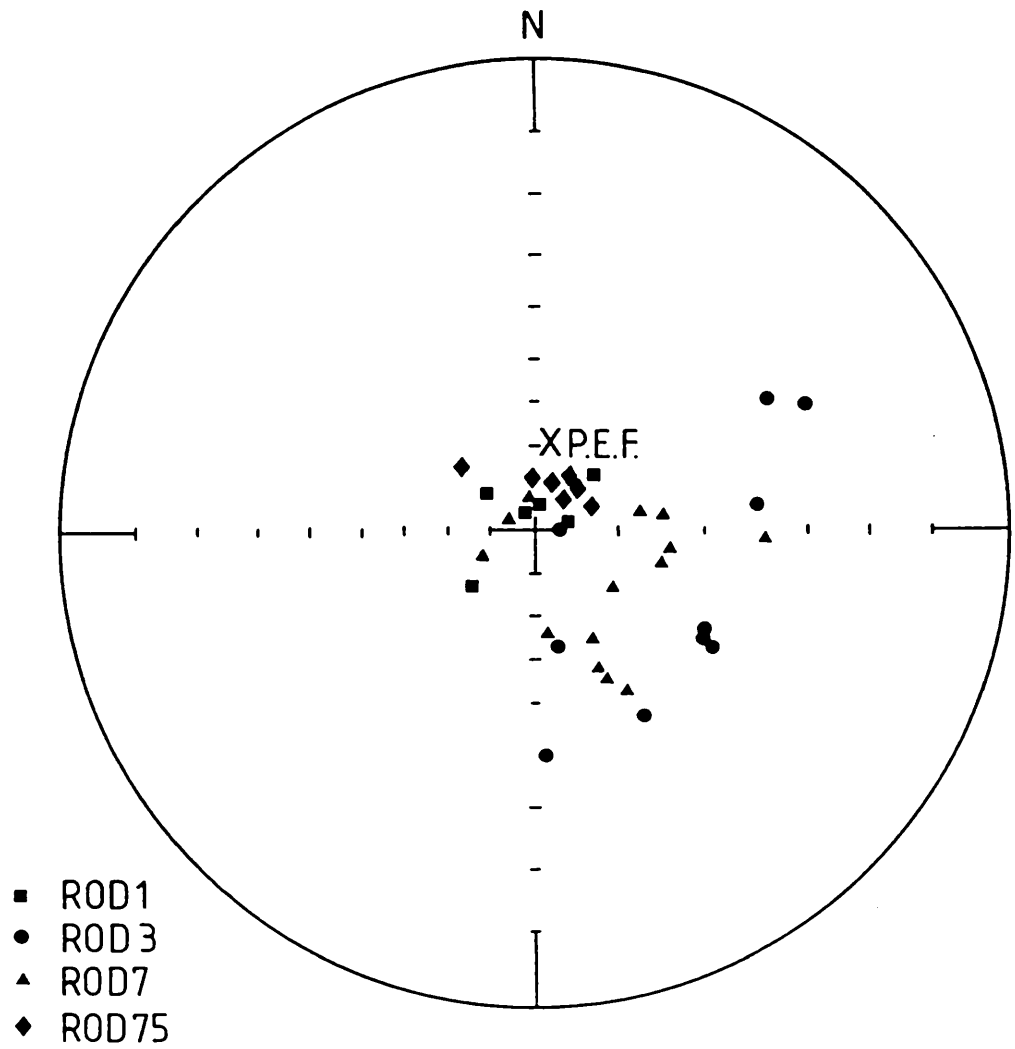


Fig. 7.5. Dyke material: NRM directions.

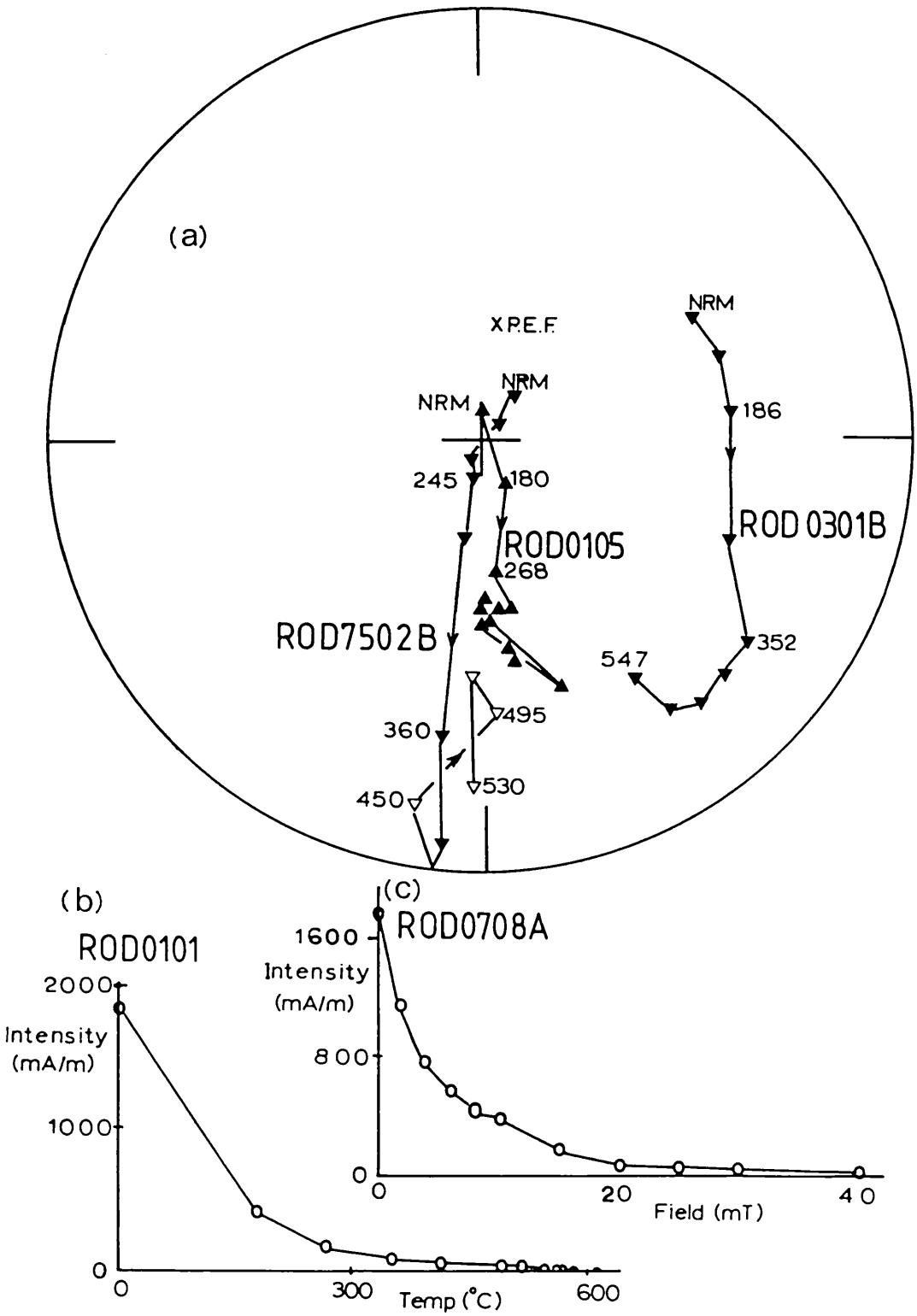


Fig. 7.6. Dyke material: Progressive demagnetisation (stereographic projections and typical stability spectra) for both AF and thermal demagnetisation. Demagnetisation temperatures in °C; applied fields in mT.

emplacement, and which have a characteristic Permo-Carboniferous direction. Hence the dyke material does not actually achieve a meaningful stable end-point direction; ancient and recent components must therefore have similar blocking temperature/coercivity ranges, with both being removed simultaneously during demagnetisation.

Table 7.3
Dyke material: stable end-points

Site	Specimen	Dec.	Inc
ROD01	01	185	60
	02	183	10
	03	200	65
	04	160	60
	05	175	46
ROD03	02	154	12
	03A	280	60
	03B	152	23
	04	165	23
	05A	150	18
	06A	140	70
	06B	172	20
ROD07	02A	150	30
	02B	142	30
	03A	168	17
	07A	170	30
	09	172	00

Mean direction: Dec 166°, Inc 36° (N=17, k=8, a=13.6°)

It would, in principle, be possible to use the converging circles of remagnetisation method (Halls, 1976,1978) to estimate the two directions. However, remanence in all specimens is the vector sum of the same two components (PEF and dyke direction) so great circles of demagnetisation for each sample will tend to be very similar, resulting in indeterminacy in estimating intersections. Since NRM directions associated with dykes are very well defined by studies of their margins it is not considered useful to attempt to use this method. The only dyke of the four to give an end-point in approximate agreement with its margin direction is ROD75, (e.g. specimen

ROD7502B, fig.7.6a) although it is poorly defined.

7.3.4. Origin of the NRM

The high NRM intensity and the fact that no stable remanence survives above 550-580 °C indicates that magnetite and/or maghemite are the dominant magnetic minerals in the dyke material, as found by Esang & Piper (1984a) in the dykes of Argyllshire. Decreases in susceptibility of up to 50-80% during thermal demagnetisation suggests that partial alteration of maghemite to hematite is taking place, hematite having much lower specific susceptibility.

It appears probable that the bulk of the PEF component is carried in maghemite formed by recent low-temperature oxidation of magnetite, and the primary direction, towards which most specimens converge during demagnetisation, is carried by titanomagnetite of high blocking temperature. This would explain the blocking temperature/coercivity spectrum overlap of the two components which appears to be greater than would be expected for a purely viscous overprint in magnetite.

7.4. Dyke margins-Palaeomagnetism

7.4.1. Introduction

A total of 8 sites have been analysed from the contact zones and aureoles of 6 separate dykes intruded into a variety of rock types (table 7.2; fig. 7.2). Each of these sites consists of a number of cores collected in an approximately linear traverse perpendicular to dyke margins, at distances of up to between 0.5 and 1.7 dykewidths (DW), i.e. 66 to 290 cm, from the dyke. The exception to this is the dyke intruded into the Upper ORS of Dunnet Head, where samples from three discrete sites were

collected, all samples from a particular site being from a fixed distance from the dyke margin.

Of the 92 samples analysed (from 63 cores) the majority, (65), were thermally demagnetised, 26 AF demagnetised and 1 by a combination of both methods. Palaeomagnetic behaviour is very different between the three lithologies sampled (lacustrine laminites, fine-grained red marls and medium-grained sandstone) so they will be considered individually.

7.4.2. Lacustrine Laminites

7.4.2.1. Palaeomagnetism

Samples from five sites in the aureoles of four separate dykes intruded into lacustrine laminites of the Middle ORS have been analysed (table 7.2; fig.7.2), as well as from a number of sites in the same or similar horizons but greater than 5-10 DW distant from the contact. The latter were discussed in more detail in chapter 5; in summary, none have a stable ancient remanence, with NRM being predominantly aligned with the PEF and of low intensity, typically 0.2-0.8 mA/m. It should not be expected, therefore, that specimens from contact zones in lacustrine laminites should possess a remanence pre-dating dyke emplacement. This is in contrast with the site in the Eday Marls (section 7.4.4.) with which these results should be compared.

Specimens collected from near to dyke margins usually show very limited low-T_B viscous components, resulting in directional distribution of NRM being very similar to that of stable components. More distal samples, however, have a greater contribution from PEF components, giving NRM directions distributed along a great circle between the dyke

direction and the PEF.

The distribution of NRM intensity, however, is more revealing about the origin of the remanence. There is a significant contrast between the two groups sampled in the Orkneys. Site ROD2, from the Rousay Flags, shows a 97% decrease in NRM intensity between 5 and 80 cm (about 0.5 DW) with a peak of over 200 mA/m. The lowest intensity, at 80 cm, is still about ten times that of typical Rousay Flags (chapter 5). In strong contrast to this, the three sites in the Stromness Flags have a maximum intensity of 4.2 mA/m (apart from one specimen immediately adjacent to the dyke which is somewhat higher), decreasing to 1.6-2.9 mA/m at 0.5 DW distant and 0.7-1.4 mA/m (broadly comparable with background) at the sampling limit of 0.7-1.0 DW. This suggests that in all cases there has been addition to, alteration of, or net magnetic realignment of the magnetic mineralogy, but to a different degree in the two Groups studied.

Considering the three sites from the Stromness Flags first, NRM characteristics appear to define two distinct zones (fig. 7.7a). A narrow zone of between 0.1 and 0.2 DW has somewhat higher NRM intensity than the remainder which then show only a very gradual decrease with distance. All three sites appear to behave very similarly, with comparable intensities at any particular distance. However, if NRM intensity is plotted using true linear distance, rather than distance as a function of dyke width, as the independent variable (fig. 7.7b) this is no longer the case; there is now no overlap in intensity spectra between the sites. This strongly suggests that the efficiency of the magnetic overprinting process at any particular distance from the

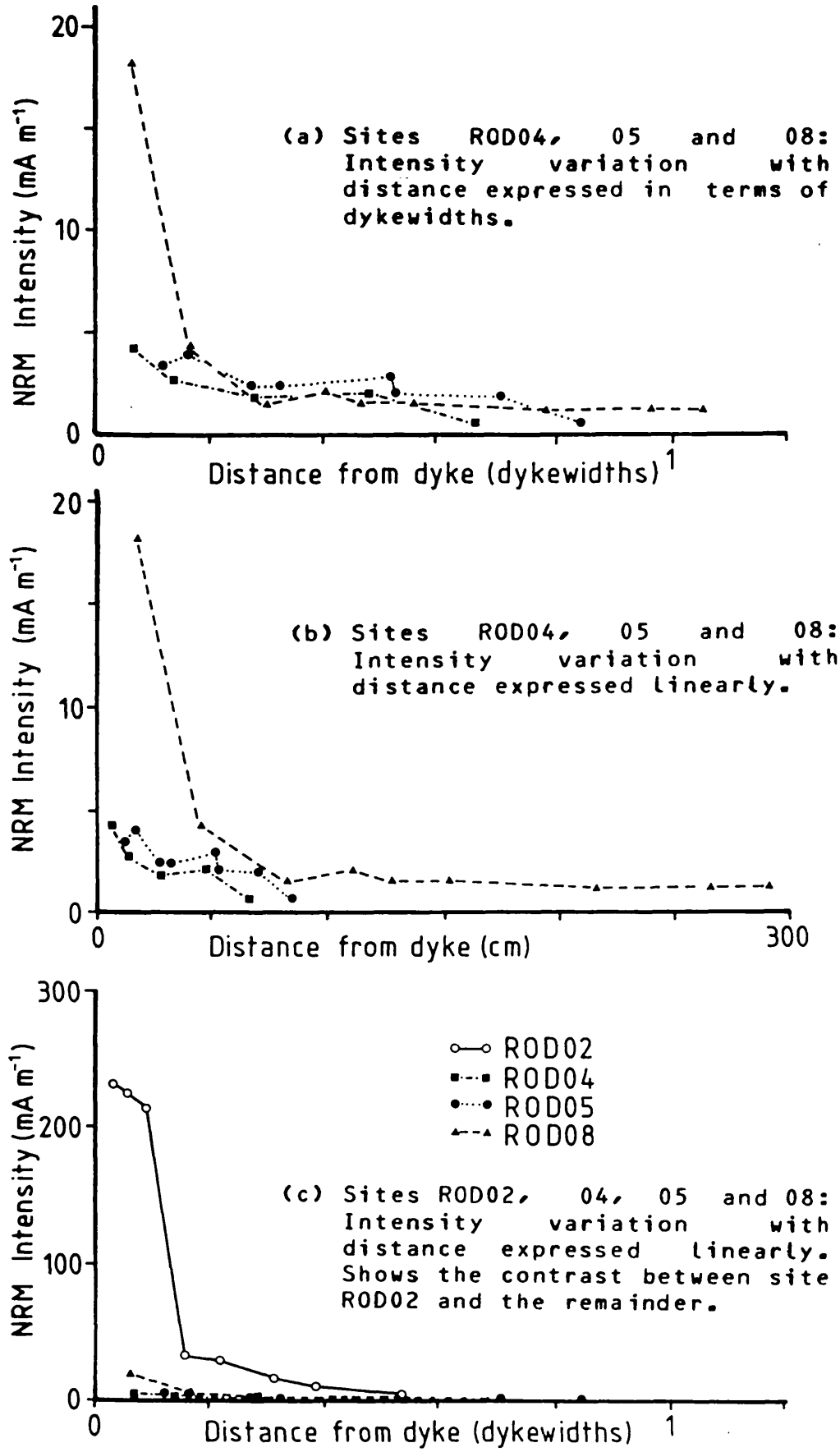


Fig. 7.7. Dyke margins: NRM Intensity variation with distance for sites ROD02,04,05 and 08.

dyke is directly related to the dyke thickness (i.e. temperature).

The fact that this is predominantly a CRM is illustrated by the IRM characteristics of four specimens (site ROD5) at various distances from dyke ROD3 (fig. 7.8). This shows that there is a progressive increase in M. towards the dyke. Points of inflection in fields of 100-130 mT suggest that both magnetite and hematite are present. Much of the contrast between the four samples occurs in the range 50-150 mT, consistent with net changes in the amount of magnetite present, as discussed below.

The site in the Rousay Flags (ROD2) shows a more pronounced inner zone of high NRM (fig. 7.7c) which is much higher than the sites already considered. NRM intensity drops rapidly beyond 0.15 DW but remains significantly higher than that in both the Stromness Flags and 'background' Rousay Flags throughout the sampling range of 0.53 DW. IRM analysis of the two available specimens (5 cm and 80 cm from the dyke) show 95-98 % saturation in fields of 150-200 mT. There is a great contrast in M_S (21000 and 980 mA/m respectively) indicative of the decreasing effectiveness of CRM acquisition with distance from the dyke (i.e. temperature).

The site in the Upper Caithness Flags, RCD6, shows less coherent behaviour than those from Orkney. No dyke-induced remanence is observed beyond 0.66 DW. NRM intensity decreases from 2.7-6.2 mA/m in the three most proximal cores to 0.4 mA/m, comparable with background, at 0.66 DW. Sampling frequency is insufficient to constrain intensity profiles to the same degree as those already discussed, so the site will not be considered in as much detail.

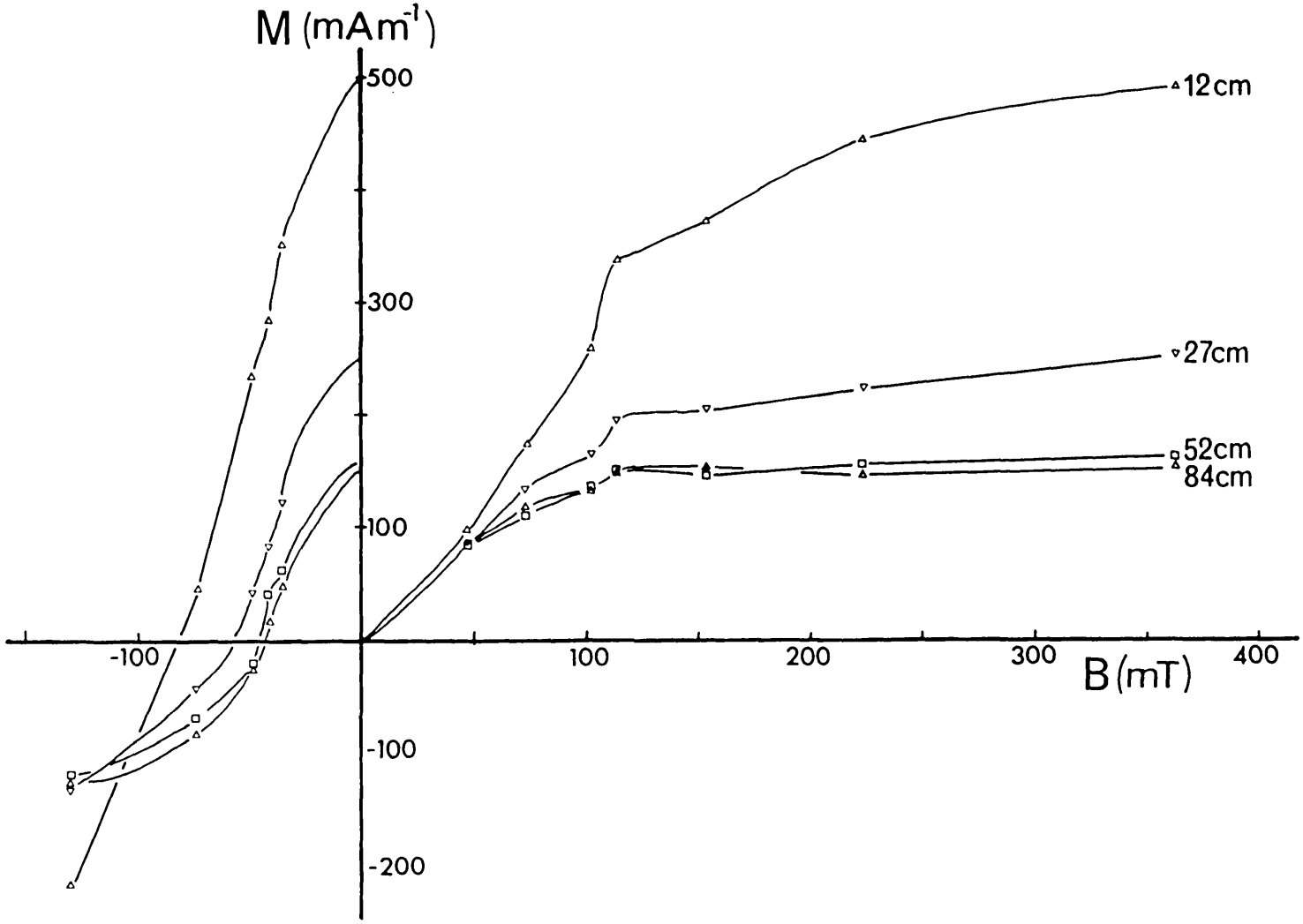


Fig. 7.8. Hysteresis of IRM, site ROD05: variation with distance from the dyke margin (expressed in cm). There appears to be little variation beyond 50cm, suggesting that this is the limit of chemical alteration.

Progressive demagnetisation, both thermal and AF, shows the NRM to be composed of two components, a low stability one easily removed at low temperatures (100-150°C) or fields (2-10 mT), usually aligned with the PEF, and a well-defined high-stability component with maximum T_B of 580 °C, often lower, or coercivities of 100-120 mT. No stable remanence ever survives above 580 °C. Typical examples are presented in fig.7.9. Due to the high degree of directional stability, it was considered appropriate to subject a number of specimens to single-step AF cleaning; this did not adversely affect the precision of the mean direction.

Stable component directions show a remarkable degree of intra-site precision, with 95% circles of confidence as low as 1.6. Site level statistics are given in table 7.4 and the results discussed in detail in section 7.5.

Table 7.4
Dyke margins: Site mean directions

Site	Dec	Inc	N	k	a_{95}	
RCD6	168.8	-8.2	4	98	9.3	
RCD15	178.1	-23.2	7	275	3.6	
RCD16	174.1	0.5	9	17	12.9	
ROD2	186.2	-46.0	21	374	1.6	
ROD4	174.1	-0.3	7	73	7.1	
ROD5	178.6	-4.6	13	71	5.0	
ROD8	168.4	-25.8	13	133	3.6	
ROD74	168.1	-23.4	9	26	10.3	
Mean (with	175.8	-21.4	83	15	4.1	
RCD16)	174.2	-16.3	8	23	11.9	
Mean (without	176.0	-24.1	74	17	4.1	
RCD16)	174.2	-18.7	7	23	12.8	(*)

Palaeopole (*) Lat. 40 N, Long. 184.6 E.

As with discussion of NRM, it is interesting to investigate the distribution of intensity at various temperatures with distance from the dyke. This is presented for a number of dyke traverses (fig. 7.10) in the form of a contoured intensity-distance-temperature distribution.

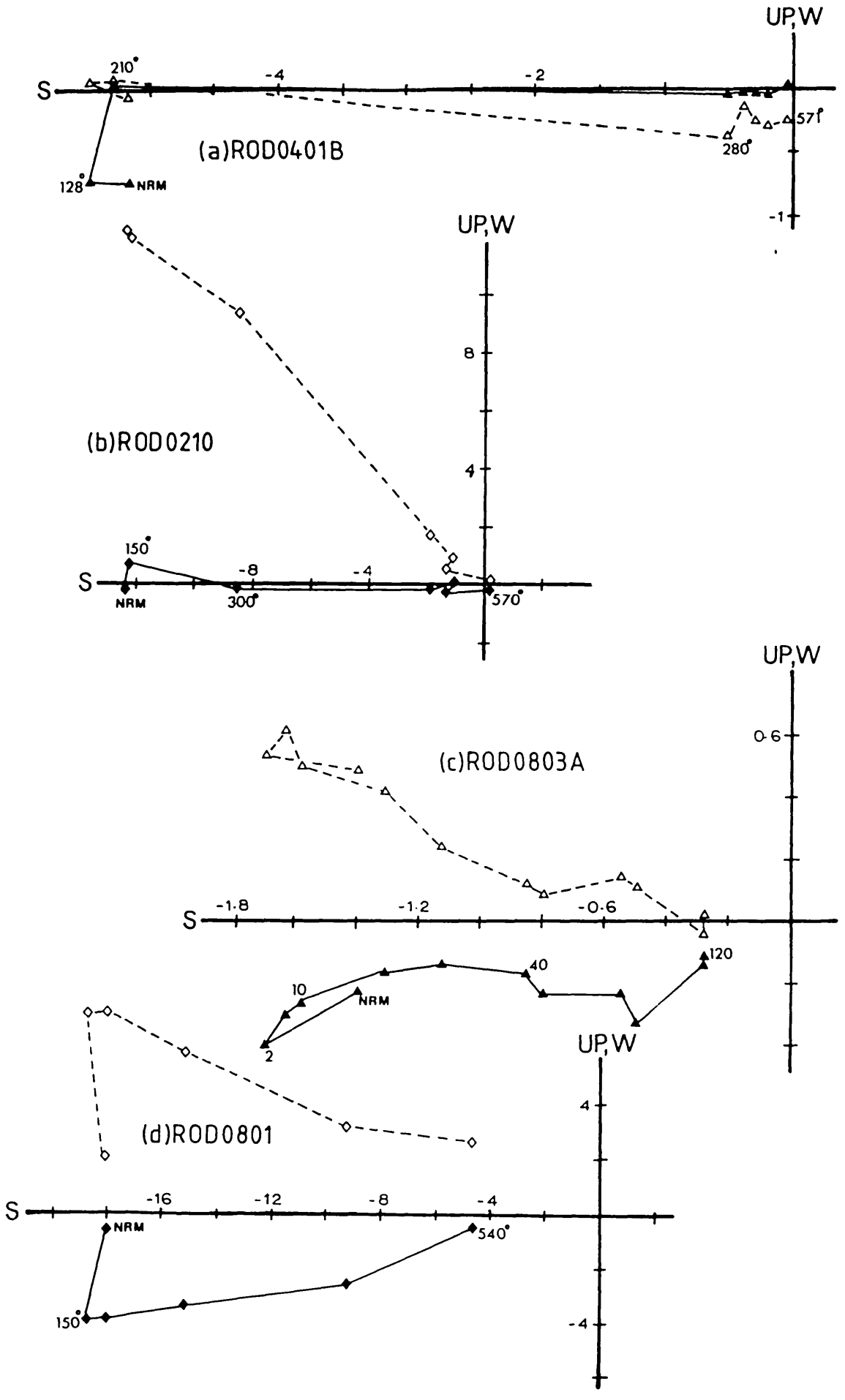


Fig. 7.9. Dyke margins: progressive demagnetisation (orthogonal projections). Demagnetisation temperatures in °C or applied fields in mT; axes in mA/m.

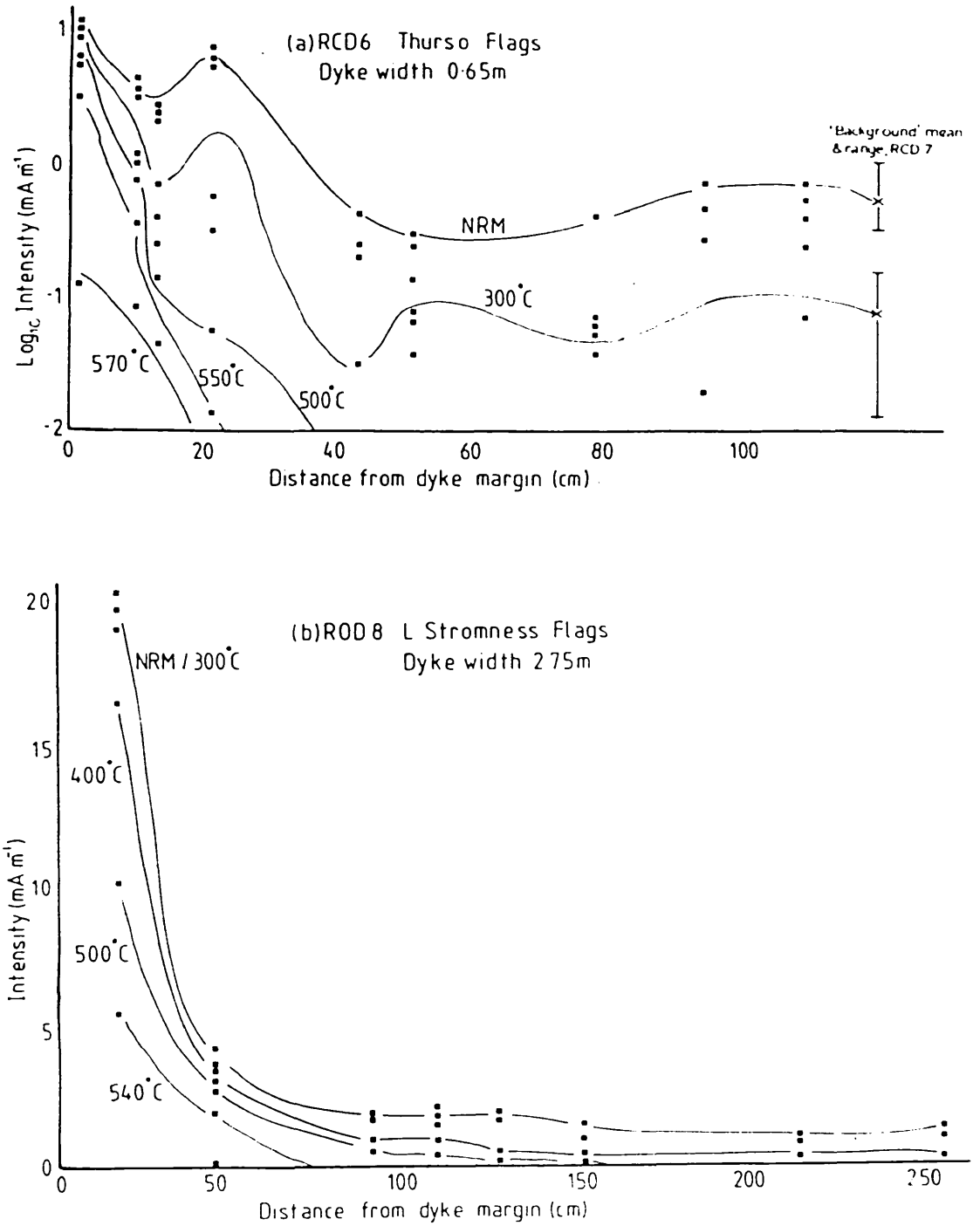
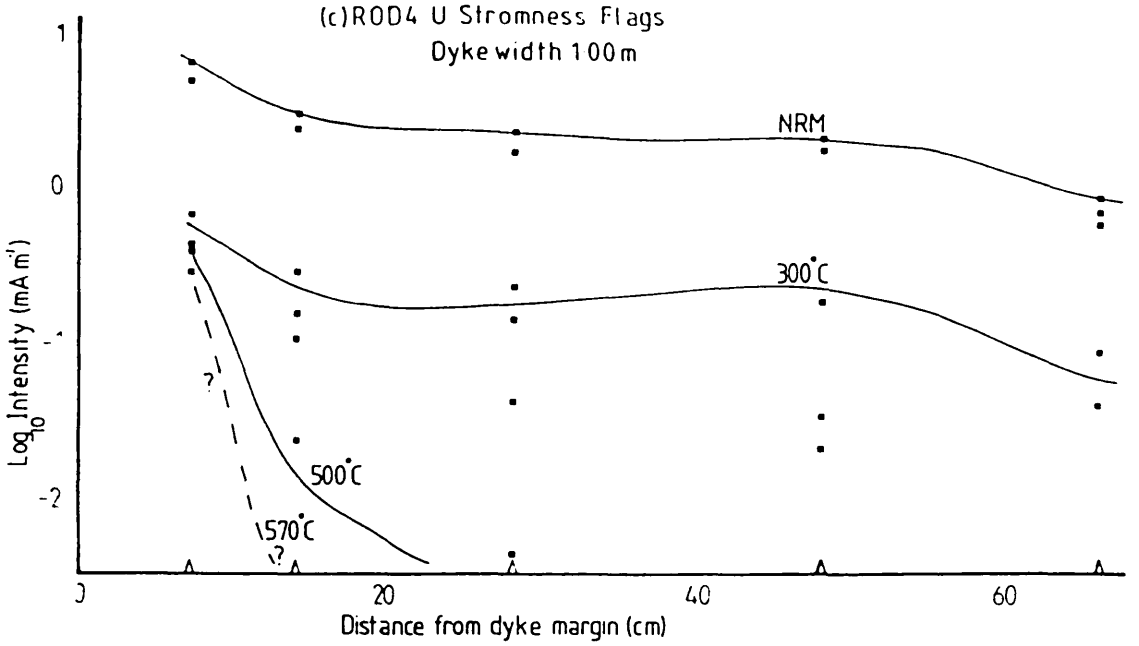


Fig. 7.10. Dyke margins: Intensity variation at various demagnetisation temperatures as a function of distance. Each symbol represents remaining intensity at any particular temperature; these have been contoured for selected temperatures. Margins in which no chemical alteration has occurred should show no variation with distance. Regional background shown for site RCD06.



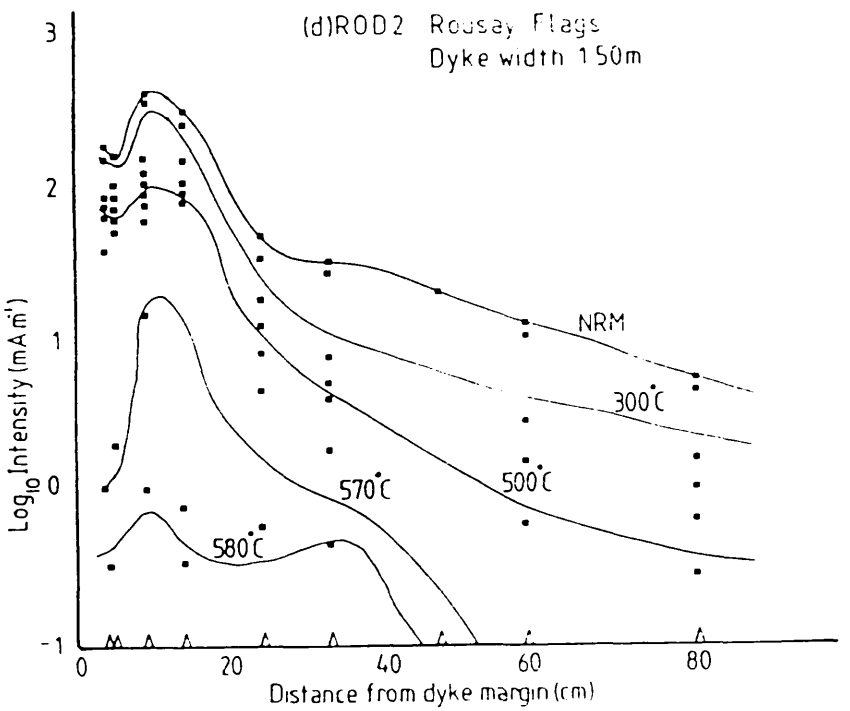


Fig. 7.10. (continued).

Beyond the narrow zone of 0.1-0.15 DW referred to above, all show a consistent decrease in intensity with distance at all temperatures, down to the background level at low temperatures (NRM to 400-500°C) or noise level (500-580°C), here taken to be around 0.1 mA/m. The intersection of these contours with the x-axis at the noise level gives the approximate distribution of maximum T_B with distance. The limit of the 500 °C contour defines the extent of the overprint for RCD6 but for ROD4 it extends well beyond this. The limit of the 500°C contour is not reached for ROD2, consistent with the somewhat different nature of its remanence.

7.4.2.2. Geochemical Studies

One of the principal aims of the study of dykes and their aureoles in the Orcadian Basin is to establish the extent and nature of any remagnetisation in surrounding sediments. To this end, representative samples from ROD2 were analysed by ICP for major and minor elements (appendix C1a). For iron, this shows that there is a narrow zone of apparent enrichment (fig. 7.11a) immediately adjacent to the dyke. Beyond this there is no systematic behaviour, any variations presumably being inherited characteristics of the rock. It would appear, therefore, that there has been no large-scale redistribution of iron outside the immediate contact zone. Unfortunately it was found to be impossible to determine whether there is any net change in the oxidation state of the iron present using the wet chemistry method of FeO determination (chapter 1), as the large content of inorganic carbon renders such analyses invalid (Hillerbrand et al, 1953).

Analyses were made for a complete range of elements for

WATTS LIBRARY

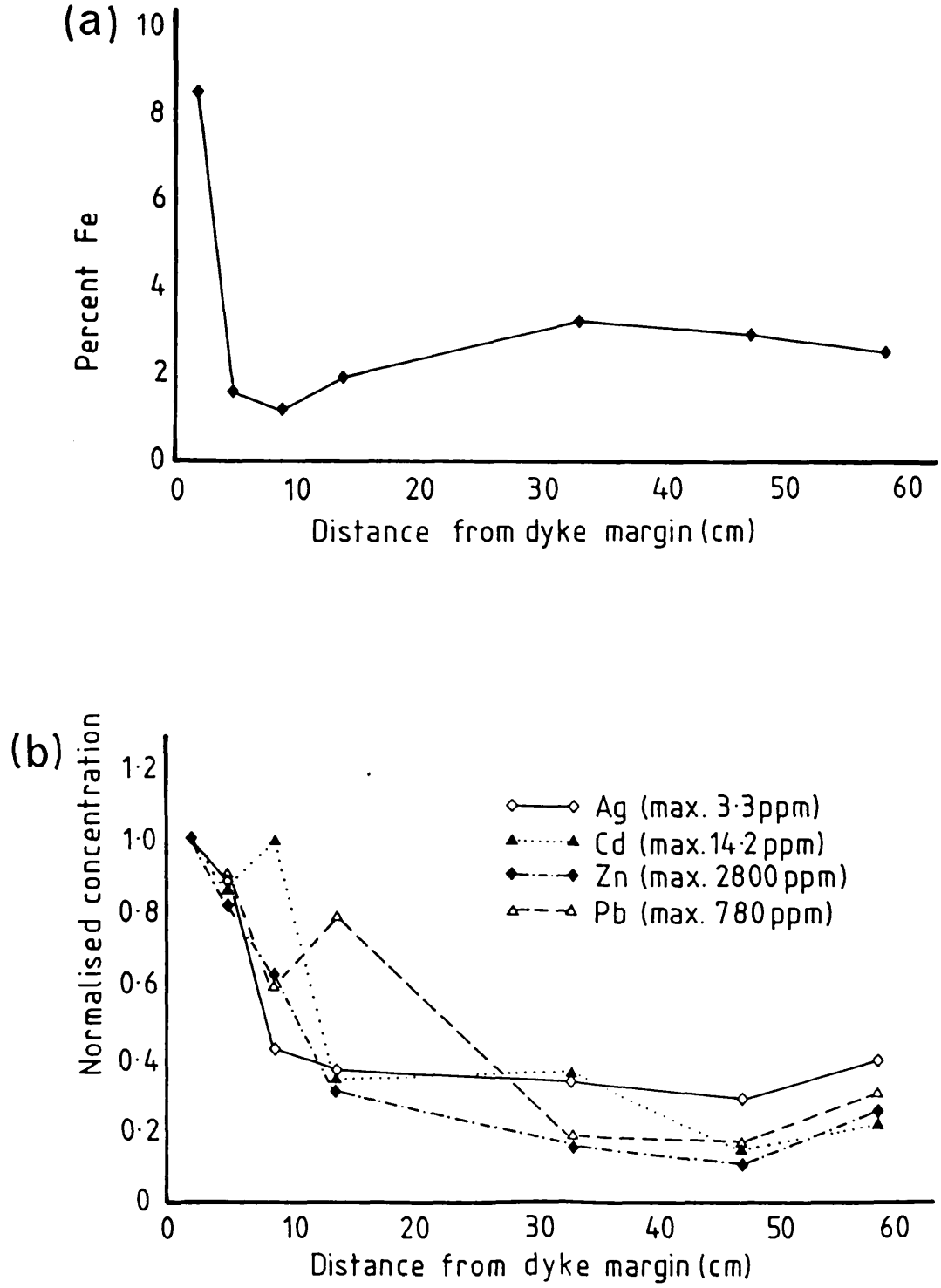


Fig. 7.11. Dyke margins (site ROD02). Bulk geochemical variation with distance from the dyke: (a) Total Fe (b) Selected heavy metals. Concentrations of heavy metals normalised to the analysis closest to the dyke; peak concentrations (in ppm) given.

ROD2, but the only other ones to show any systematic behaviour were the base metals (fig. 7.11b) which all show progressive enrichment towards (or depletion away from) the dyke margin. Syngenetic base-metal mineralisation is well-known in the Devonian lacustrine rocks of Orkney (Muir & Ridgway, 1975). It would thus appear that redistribution of pre-existing mineralisation has occurred during dyke emplacement, possibly in a localised small-scale hydrothermal cooling system (since no mineralisation is known to be directly related to the dykes).

Looking at base-metal distribution in more detail (fig. 7.10b), there is a suggestion of an increase in relative concentrations at the sampling limit (58 cm) with values here perhaps tending towards the regional background, which may often be very high (e.g. Pb 2000 ppm, Zn 1000 ppm; Muir & Ridgway, 1975). This suggests that possibly the intermediate zone (33-47 cm) has been scavenged for base metals with redistribution towards the dyke. Such a remobilisation may well also have included iron.

7.4.3. Upper ORS, Caithness

Three sites from the margin of a monchiquite dyke intruded into the Upper ORS of Dunnet Head, Caithness, show somewhat different characteristics from the lacustrine sediments discussed above. The three sites, RCD15,16 and 17, are spaced at 5-10 cm, 1.3 m and 10.0 m respectively from the dyke margin.

RCD15, closest to the dyke, shows essentially single-component behaviour with a maximum T_B of 580-585 °C or demagnetising field of 100-120 mT, corresponding to p.s.d. magnetite. The site mean is defined to a high degree of precision (table 7.4). Remanence at site RCD16 (1.3 m) is

somewhat less well-defined, both during demagnetisation and also at site level (table 7.4). In contrast to site 15 the remanence is of high T_B, up to 680 °C, showing it to be hematitic. There is no indication in T_B spectra to suggest that magnetite contributes to the remanence. The reason for the low precision of the site may be indicated by site RCD17, 10 m distant and well beyond the effects of the dyke, which has a stable remanence of comparable intensity to site 16 but of apparently random orientation. Vestiges of such a remanence in site 16 may be sufficient to cause high dispersion. The mean direction for the site, which is at variance with that of site 15, is thus not given any great significance.

The contrast of dyke aureoles in the Upper ORS with those in lacustrine horizons is considered to be directly related to their original magnetic mineralogy, in particular the absence of organic carbon in the sandstones. The Upper ORS, being a mature, coarse-grained sandstone, has allowed fluid permeation immediately adjacent to the dyke; further away, remagnetisation is predominantly a TRM since the primary mineralogy is thermally stable.

7.4.4. Eday Marls

7.4.4.1. Palaeomagnetism

Due to the scarcity of dykes intruded into sediments of the Eday Group (the majority being found in the Middle ORS lacustrine horizons, presumably a function of their ease of fracture) only one such margin site has been collected, from the Eday Marls of Burray (fig. 7.2). Site ROD75, from the dyke itself, has already been discussed (section 7.3). Site 74 consists of eight cores at distances of 4 to 96 cm (0.07-1.66 DW) from the contact. It provides a great

contrast to those sites already discussed in this chapter in that firstly there is a pre-existing stable NRM direction in the country rock and secondly that there does not seem to be any significant chemical overprint, the dyke-induced NRM being a pure TRM/PTRM.

The presence of two components is suggested by the directional distribution of NRM (fig. 7.12). Samples from close to the dyke are grouped around a southerly, upwards direction corresponding to the dyke direction (component I). NRM directions found in specimens further away from the dyke margin are distributed along a great circle joining I and a NE, upward direction (approximating to component H). The proportion of I to H decreases with distance. It is suggested that H represents a primary direction. (A low-T_B component L is also present in most specimens, approximating to the PEF, and causing a shift of the great circle referred to above towards the PEF direction).

Progressive demagnetisation reveals that the relative proportions of the two stable components I and H vary with distance from the dyke. Specimen 7401, 4 cm/0.06 DW from the margin, is composed entirely of I (fig. 7.13a,7.14a). 7403 (11 cm/0.19 DW) has a suggestion of a high-temperature component above 662 ^{o}C (fig. 7.13b,7.14b) which becomes more obvious in 7405 (29 cm/0.5 DW; fig. 7.13c,7.14c) until at 45 cm/0.78 DW (7406, fig 7.13d,7.14d) it has T_B as low as 535-600 ^{o}C. Unfortunately, there is some overlap of T_B between I and H so their exact limits cannot be precisely determined.

Two specimens were subjected to AF demagnetisation, both of which have thermally-treated sister cores for comparison. 7404B shows a decrease of 50% in intensity up to

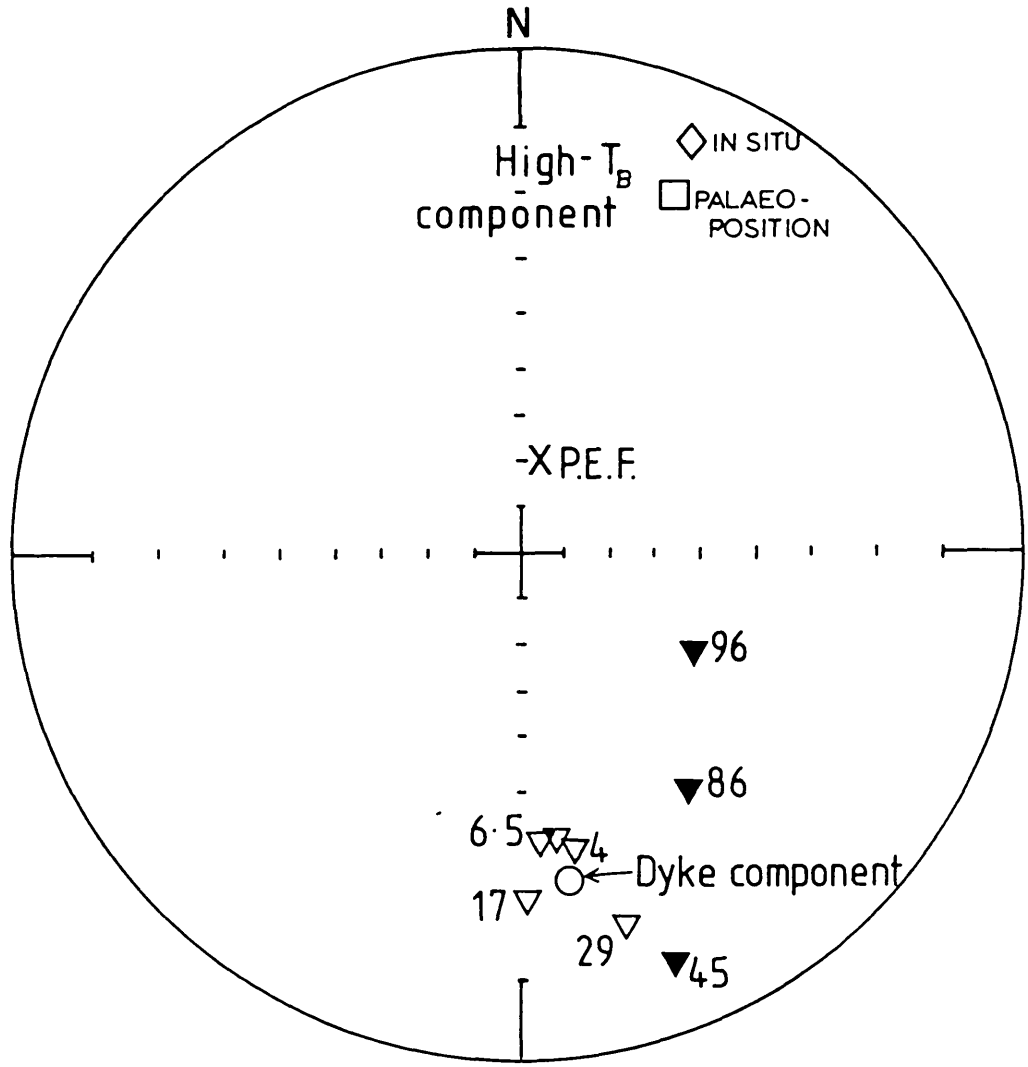


Fig. 7.12. ROD74: Variation of NRM direction with distance from the dyke (site ROD75). Distances expressed in cm. Mean directions for both low-T_B ('dyke component') and high-T components shown.

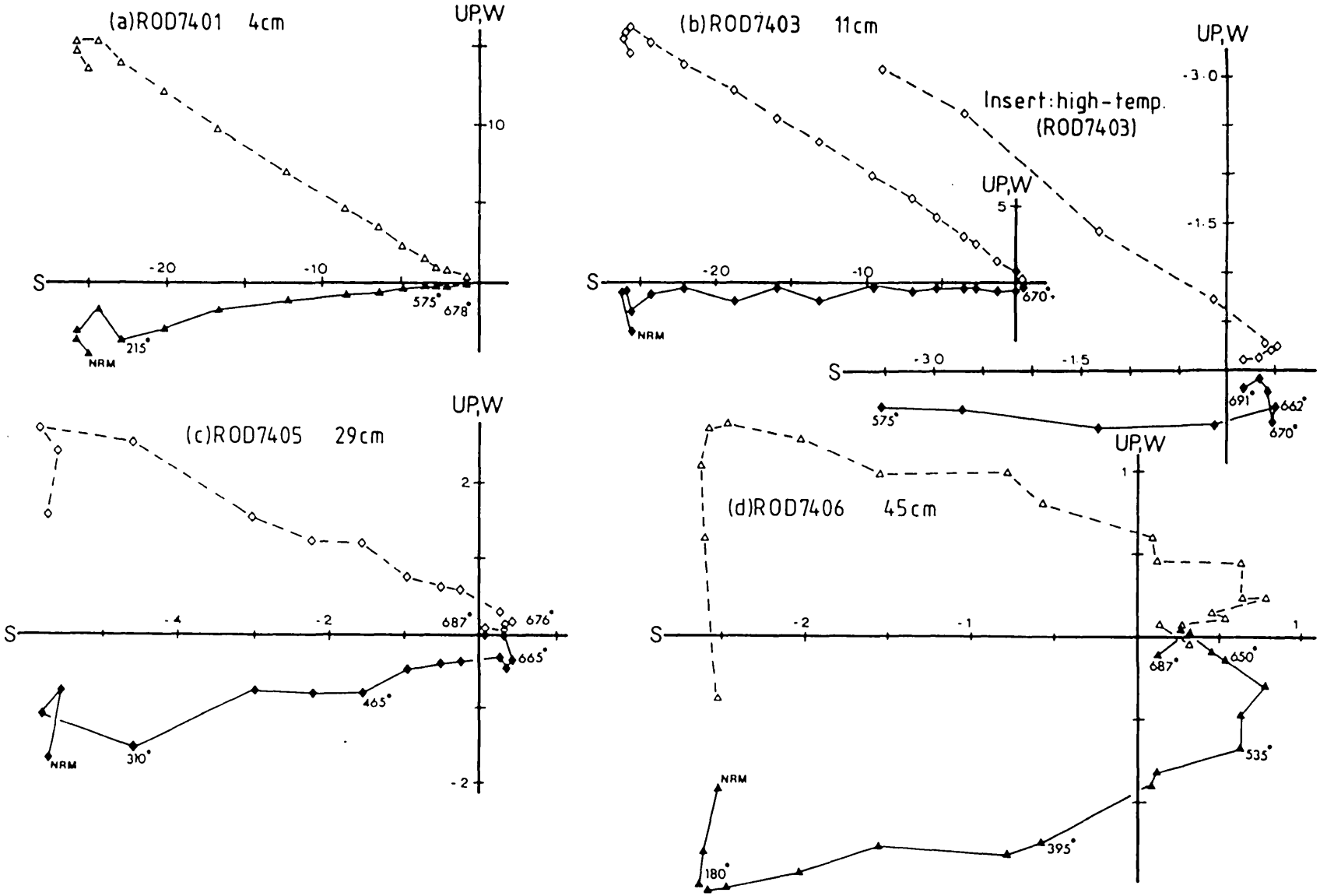


Fig. 7.13. ROD74: Thermal demagnetisation (orthogonal projections). Demagnetisation temperatures in °C; axes in mA/m.

190 mT but no significant movement in net vector orientation. This indicates that the remanence is purely hematitic, with no contribution from magnetite, and that the minimum coercivity of component H is above 190 mT. Thermal demagnetisation after AF treatment produces no directional change below 605 °C, after which vector movement is to the north, towards the postulated primary direction (fig. 7.14f).

Using estimates from orthogonal and stereographic projections of the maximum temperature reached during heating, an approximate temperature profile away from the dyke can be constructed (fig. 7.15). Such a profile can be used to estimate laboratory equivalents of the actual temperatures reached during contact metamorphism (McClelland Brown, 1981), although it must firstly be established that there is no CRM contributing to the remanence. This would appear to be the case, as the highest T_B at which only the reset component is removed decreases systematically with distance from the dyke; this, according to McClelland-Brown (1982), is the characteristic behaviour of PTRM rather that CRM. There is, however, a degree of overlap of T_B spectra which may indicate a small additional CRM.

Using a contact temperature (T_c) range of 458 to 850°C and dyke width D=0.58m, it is possible to construct a temperature profile as in fig. 7.15, following Jaeger (1959).

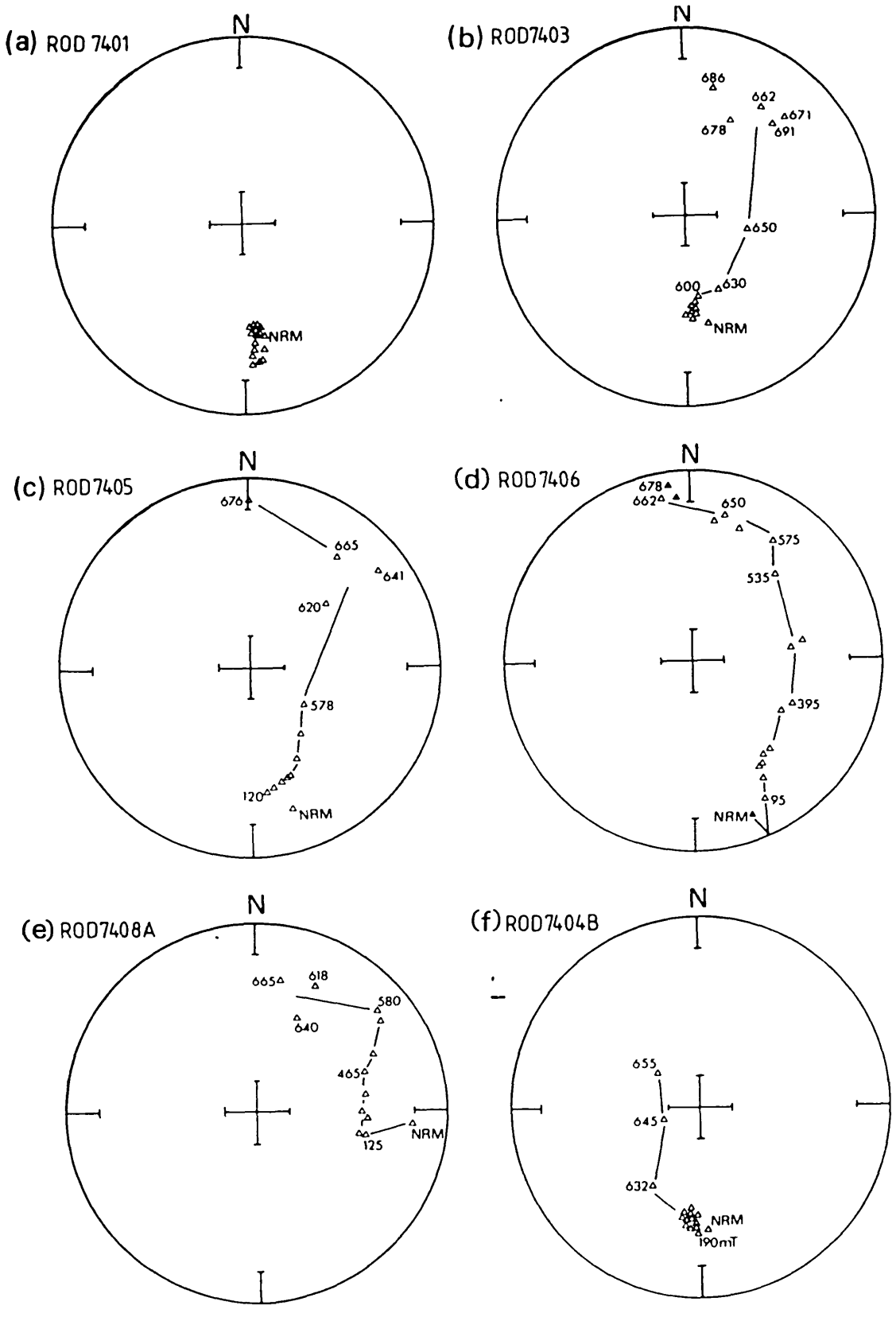


Fig. 7.14. ROD74: Progressive demagnetisation (stereographic projections). Compare relevant specimens with fig. 7.13. All subjected to thermal demagnetisation (temperatures in °C) apart from ROD7404B (firstly AF demagnetised to 190 mT).

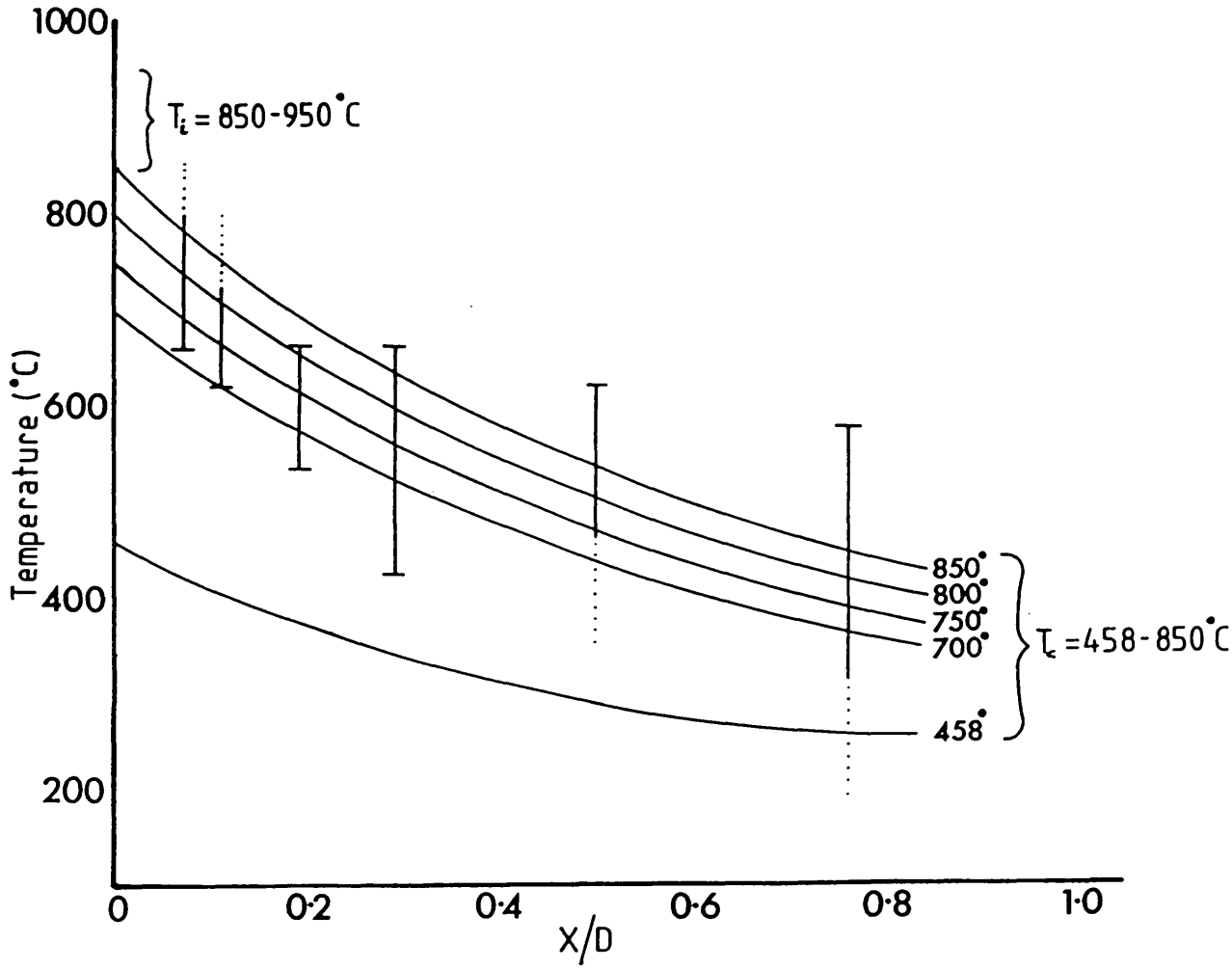


Fig. 7.15. ROD74: Variation of laboratory unblocking temperature with distance from the dyke margin (expressed as a fraction of dykewidth DW). Laboratory equivalent of temperature reached during contact metamorphism lies within vertical error bar range for each specimen. Theoretical single-pulse temperature profiles for various contact temperatures Tc shown as solid curves.

Jaeger (1964) suggests that it is valid to consider the dyke and its host rock to have similar thermal properties (conductivity K and diffusivity k). Ignoring latent heat of solidification L, the contact temperature T_c will then be approximated by

$$T_c = 0.5\ T_i$$

where T_i is the intrusion temperature.

If latent heat is taken into account, this has the same effect as considering the dyke to have an intrusion temperature T_i^*, where

$$T_i^* = T_i + L/c \quad (c = \text{specific heat}).$$

The contact temperature will now be

$$T_c = 0.5T_i^* = 0.5(T_i + L/c)$$

Using data from Jaeger (1959), L = 100 cal/g and c = 0.25 cal/g/°C, i.e. L/c = 400°C.

Fig. 7.15 suggests that the contact temperature in the dyke margin is within the range 700-800°C. This corresponds to an intrusion temperature range of

$$T_i = (2T_c - L/c) = 1000 \text{ to } 1200^\circ C.$$

These temperatures are consistent with the nature of the dyke; Rock (1983) suggests that intrusion temperatures

were around 950°C. The assumptions of the calculation (purely conductive heat transfer, lack of volatiles in the host rock and intrusion in a single, instantaneous pulse) would thus appear to be applicable.

Earlier work on dyke aureoles (Jaeger, 1959) suggested that basic dykes and sandstones should be considered to have contrasting thermal properties. Taking thermal conductivities of the dyke and country rock to be K_1=0.0043 and K_o=0.0128 and diffusivities k_1=0.008 and k_o=0.031 respectively, this would give an initial contact temperature of

$$T_c = \frac{\sigma T_1}{1 + \sigma} \qquad \text{where } \sigma = \frac{K_1 k_o^{1/2}}{K_1 k_o^{1/2}} = 0.66$$

i.e. $T = 358°C$.

Even when taking latent heat into account, T_c is unlikely to exceed 458°C. A thermal profile for such a contact temperature (fig. 7.15) shows that it is unrealistic.

To achieve a sufficiently elevated contact temperature under such constraints would require a greater net heat input, as would be the case if the dykes had acted as feeders to the surface allowing the passage of large volumes of magma, contrary to the observation of Watson (1985).

It is interesting to compare these data with that reported by Kynaston & Hill (1908). They record the alteration of the immediate contact zone of a camptonite dyke near Oban intruded into Dalradian phyllites to a black, vitreous buchite, speckled with cordierite, augite, magnetite and spinel. This corresponds to a contact temperature of 850-900°C (Rock, 1983). The thickness of the dyke is not recorded in the original publication but is about three feet according to N.Rock (pers. comm.). Fusion has occured up to 2 feet (0.7 DW) from the dyke, corresponding to temperatures of 600-650°C (Rock, 1983). Alteration, of a more minor degree, extends to between 5 and 6 feet (i.e. about 2 DW).

Bulk geochemical analyses from the fused phyllite and fresh country rock (Kynaston & Hill, op.cit.) show little or no evidence of transfusion of material from the dyke into the surrounding phyllites which might otherwise have explained the ease and completeness with which fusion took place. It would thus appear that here, possibly, an elevated contact temperature is required.

The mean of component I, representing dyke-induced remanence, is given in table 7.4. Discussion of this result in the regional context will be given in section 7.5. The significance of the high-T_B component H which, it is suggested, represents a magnetisation preceding dyke emplacement, is considered in chapters 4 and 9 along with other sites from the same formation.

7.4.4.2. Geochemical studies

As with site ROD2 in the lacustrine laminites (section 7.4.2.2.) ICP analyses were made for a full range of elements (appendix C1a). There appears to be little

systematic behaviour apart from a possible increase in calcium and decrease in magnesium towards the dyke, suggesting some redistribution of carbonate cements during emplacement (fig. 7.16a,b). Base metals are present in very much lower concentrations than in site ROD2, and that there is no systematic variation with distance (appendix C). This is consistent with syngenetic mineralisation in the laminites but with a generally low detrital contribution in clastic sediments.

The concentration of iron present does not appear to vary systematically with distance from the dyke (fig. 7.16c); beyond 6.5cm there is no significant variation from the background of about 4.5% Fe. It is possible to determine the oxidation state of the iron using wet chemistry (as there is no organic carbon present, unlike in the lacustrine sediments). There is no significant variation with distance (table 7.5).

Table 7.5
ROD74 Iron analyses (Whole rock)

Sample	Total Fe (ICP)	FeO
01	3.6%	0.68%
02	4.6%	-
03	4.4%	-
04	3.9%	0.71%
05	4.5%	-
07	4.6%	-
08	4.6%	-

Geochemical and palaeomagnetic evidence is thus consistent with dyke margin NRM being a pure TRM/PTRM with negligible CRM even immediately adjacent to the dyke. The most probable explanation of the observed intensity variation with distance (fig. 7.17) is that this represents the magnetic realignment of previously randomly-orientated

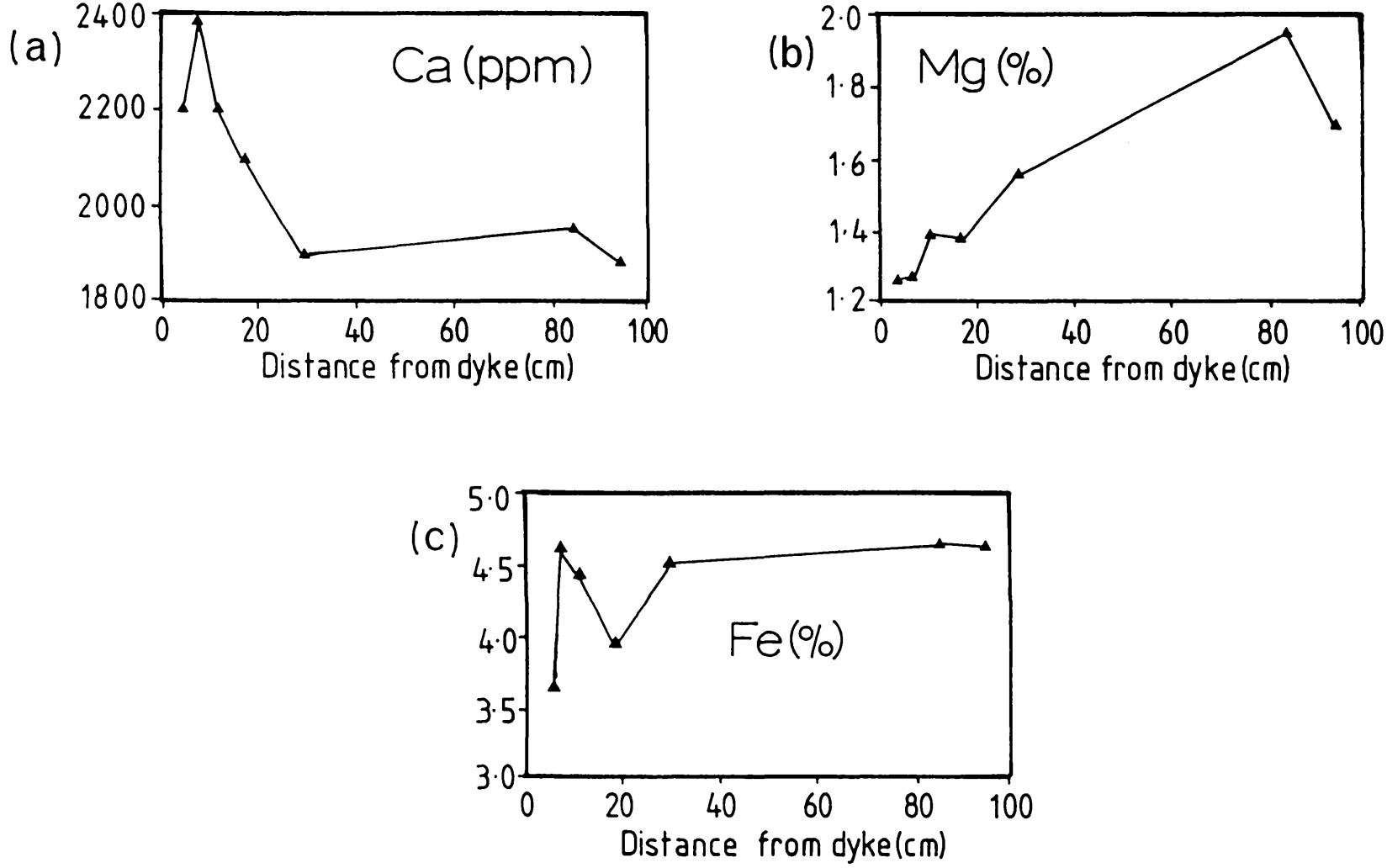


Fig. 7.16. ROD74: Selected ICP analyses showing variation with distance from dyke margin. Full analyses given in appendix C.

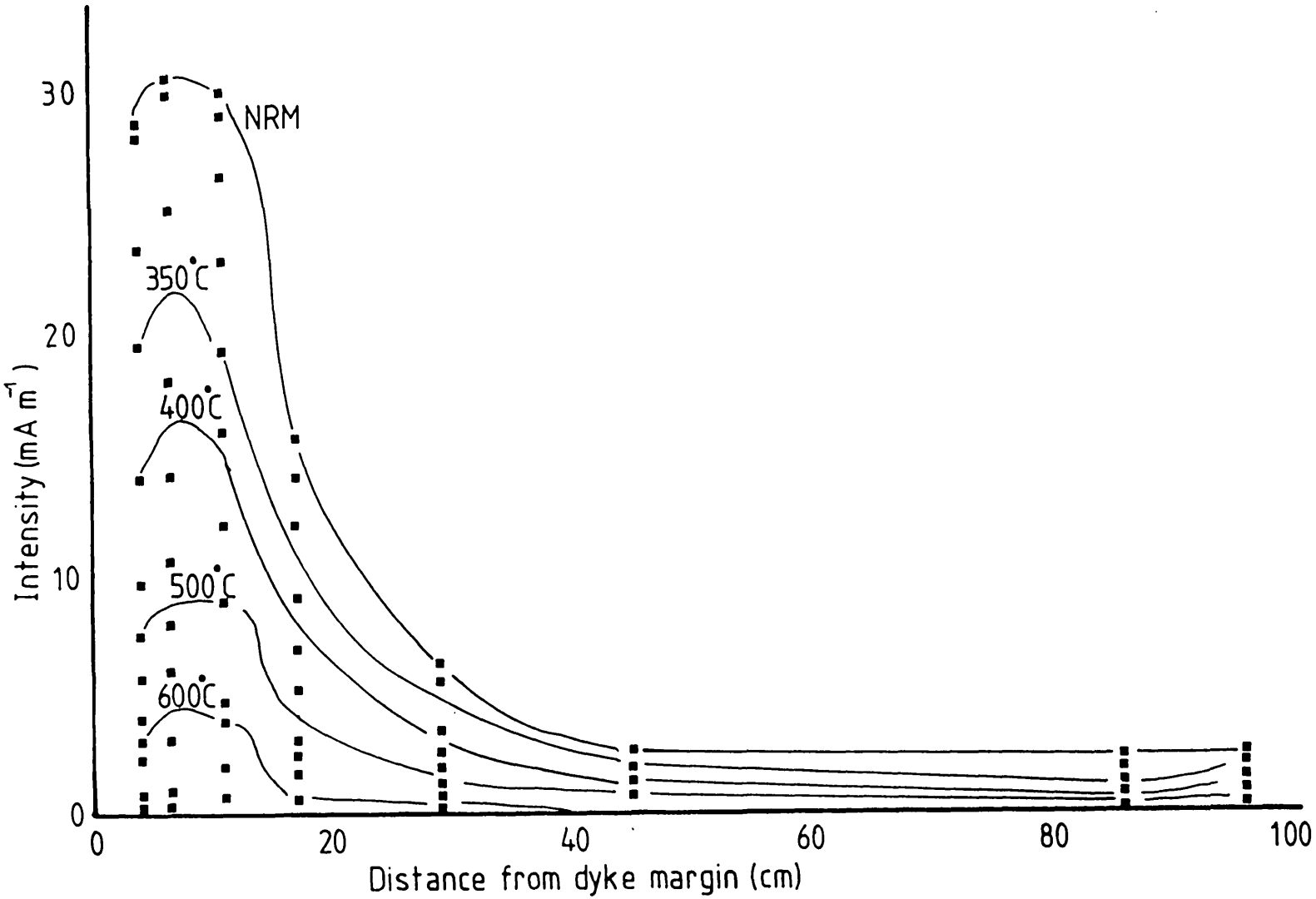


Fig. 7.17. ROD74: Intensity variation at various temperatures as a function of distance from the dyke. Details as for fig. 7.10.

iron oxide grains which would not originally have carried a net remanence. One candidate for this would be biotite flakes, oxidised prior to deposition. Such flakes would not acquire a significant DRM as crystal shape irregularity would be a far more efficient grain orientation controlling mechanism than alignment of inter-layer iron oxides with the ambient field. The extent of acquisition of a remanence during heating would thus be directly temperature-dependent, as discussed below.

7.5 Synthesis

It will be apparent (section 7.3) that material from dykes themselves is generally unsuitable for palaeomagnetic analysis, due to the effects of recent oxidation and high magnetic viscosity. Dyke margins, on the other hand, usually give an extremely well-defined direction. These directions are considered to represent a remanence dating from the time of dyke emplacement. Site mean directions are presented stereographically in fig.7.18 and in table 7.4, showing them to be distributed approximately along a north-south plane. If the observed apparent variation of corresponding pole position represents a true age variation then this would be between the extremes of ROD4 (lat. -30.5°, long. 003.6°) and ROD2 (lat. -58.1°, long. 346.5°), i.e. a range of 14-15 degrees of arc. Comparison of measured palaeomagnetic mean directions with expected directions in the Upper Palaeozoic - Mesozoic for the Orcadian Basin (fig. 7.19, after Briden & Mullan, 1984) shows that this represents an age span of perhaps mid Carboniferous (Visean-Namurian) to Upper Permian or later. However, each mean direction probably only represents a spot reading acquired almost instantaneously during secular variation. The mean direction for the dykes

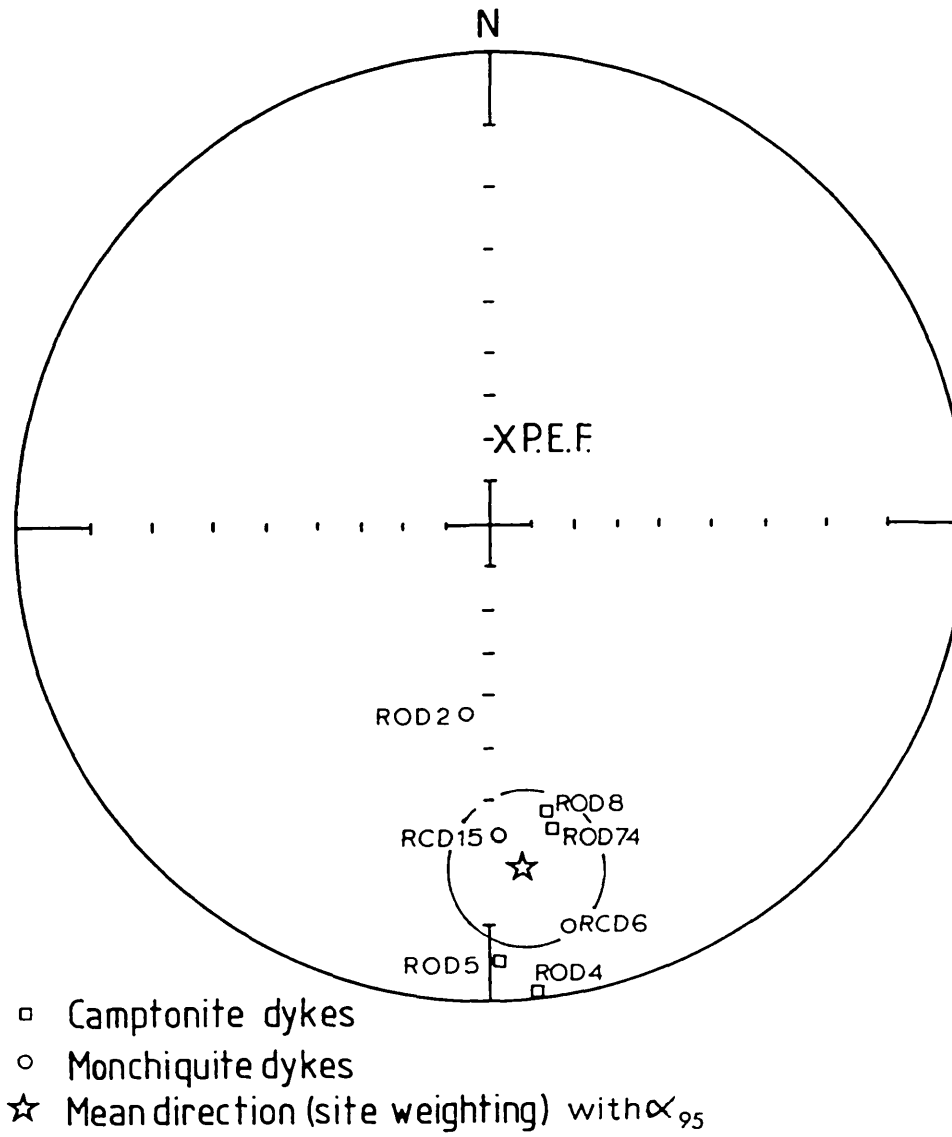


Fig. 7.18. Dyke margins: Site mean directions. Margins of camptonitic dykes distinguished from monchiquitic.

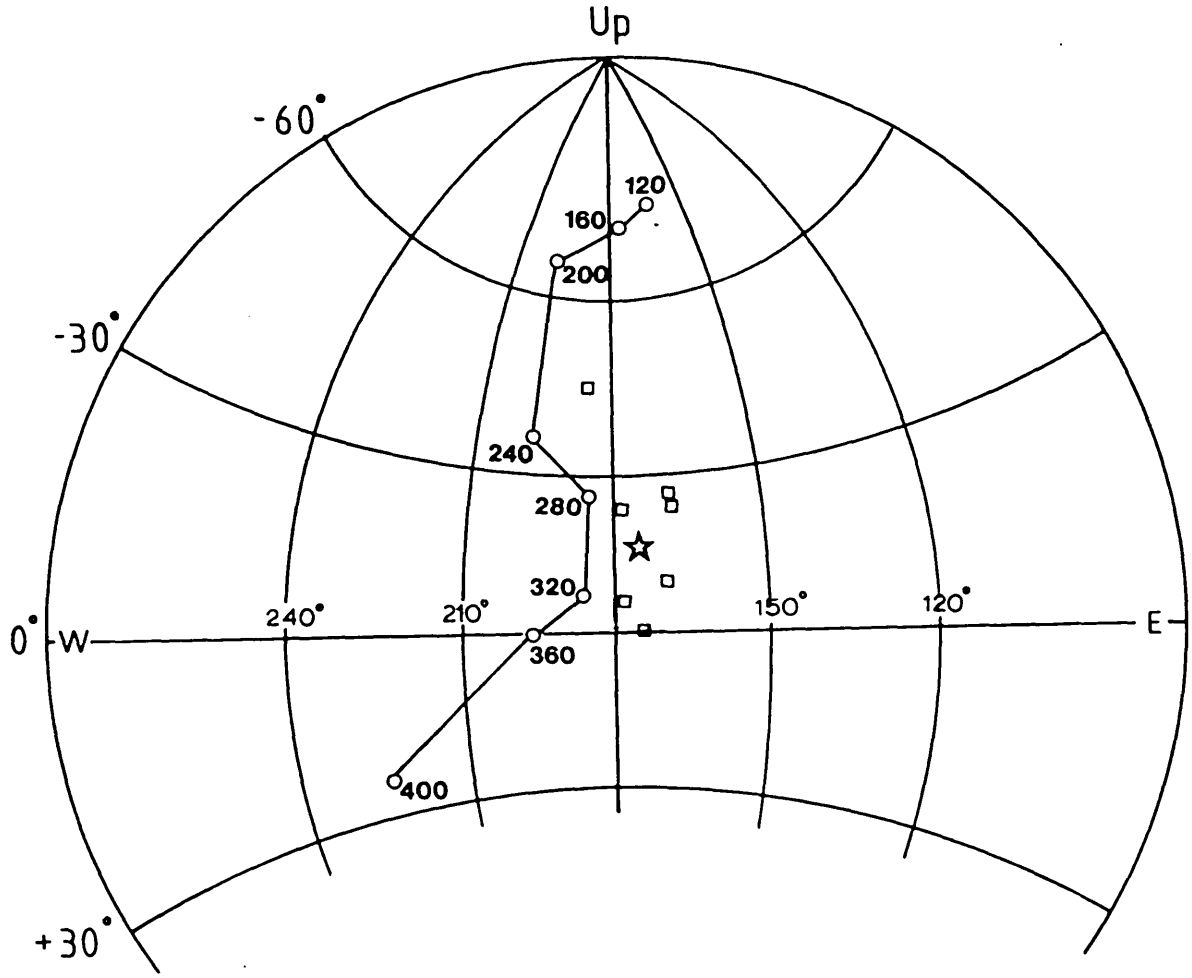


Fig. 7.19. Palaeomagnetic directions for Northern Scotland: Middle Devonian to mid Cretaceous. Time marked every 40m.y. Shows mean directions for individual dykes and the overall mean. (After Briden & Mullan, 1984; corrected for geographical location).

given in table 7.4 corresponds to an age of 290-310 Ma (Briden & Mullan, op. cit.), i.e. mid Carboniferous (de Souza, 1982). This is somewhat earlier than recently-reported isotopic dates of 252±10 Ma (Baxter & Mitchell, 1984) and 240±12 Ma (Brown, 1975) but the result may be somewhat imprecise if secular variation has not been sufficiently well averaged. Despite this, there is no *a priori* reason why dyke emplacement should necessarily be time-restricted; Permo-Carboniferous igneous activity is known to have occurred over a fairly long time span over Scotland as a whole. However, fig.7.18 shows that there is no apparent correlation between palaeomagnetic orientation and dyke composition or location, as may perhaps be expected if activity was over a long period of time; well-defined isotopic dates also tend to discount this hypothesis.

The nature of the dyke-related remanence in contact zones is highly variable and much dependent on the characteristics of the host rock in question, in particular the presence or absence of organic carbon. Immature lacustrine laminites have acquired a narrow inner zone within which iron, perhaps in the form of magnetite, appears to have been introduced; beyond this, severe temperature-dependent thermochemical alteration of the country rock has caused a TCRM overprint, the intensity of which decreases with distance. Relatively mature sandstones of the Upper ORS also have an inner zone of magnetite introduction and a thermal aureole beyond this carrying a hematitic TRM/PTRM.

In contrast, the Eday Marls appear to have suffered no significant geochemical alteration, acquiring a pure PTRM by remagnetisation of pre-existing randomly magnetised hematite. The peak temperature reached decreases

systematically with distance from the dyke. Peak temperatures reached are generally consistent with those predicted by theoretical thermal modelling, suggesting that the net heat input in the vicinity of dykes was compatible with a single-phase instantaneous intrusion.

The dykes have probably not, therefore, acted as feeders to the surface. This conclusion is consistent with that of Watson (1985) who suggests that short en echelon dyke segments separated by unbroken 'bridges' of country rock are incompatible with the free passage of magma.

The main conclusion, however, in the context of the present study is that Permo-Carboniferous dykes of the Orcadian Basin have not directly caused any regional remagnetisation of surrounding sediments, despite their apparent contemporaneity with the postulated remagnetisation described elsewhere in this volume.

CHAPTER 8

OTHER INTRUSIVE BODIES AND THEIR AUREOLES

8.1 Introduction.

In addition to the extensive suite of Permo-Carboniferous dykes discussed in the previous chapter, there are a number of vents in the Orcadian Basin, most or all of which are considered to be coeval with the dyke swarm. They are distributed along two major lineaments (fig. 8.1) suggesting a relationship with deep dislocations in the lower crust or mantle (Watson, 1985). The largest and most well-known is the vent at Duncansby Ness (fig.8.2) which bears numerous mantle xenoliths. In addition, there are several smaller vents, some of which are magmatic while others are formed almost exclusively of brecciated flagstones with little or no trace of magma.

The vent at Duncansby Ness has been extensively sampled in the present study, including basic matrix material, sedimentary xenoliths and also the contact zone in the John o'Groats Sandstone. In addition, other sites in the John o'Groats Sandstone from throughout its outcrop range are discussed (fig. 8.3), as remanence acquisition appears to be closely related to emplacement of the vent. The results from less intensive sampling of three other vents of varying character, including a possible cryptovent in the Upper ORS of Dunnet Head and two other vents on Orkney, are also discussed.

8.2 Duncansby Ness vent.

8.2.1. Geology, sampling and age.

The ultrabasic vent of Duncansby Ness is the only one

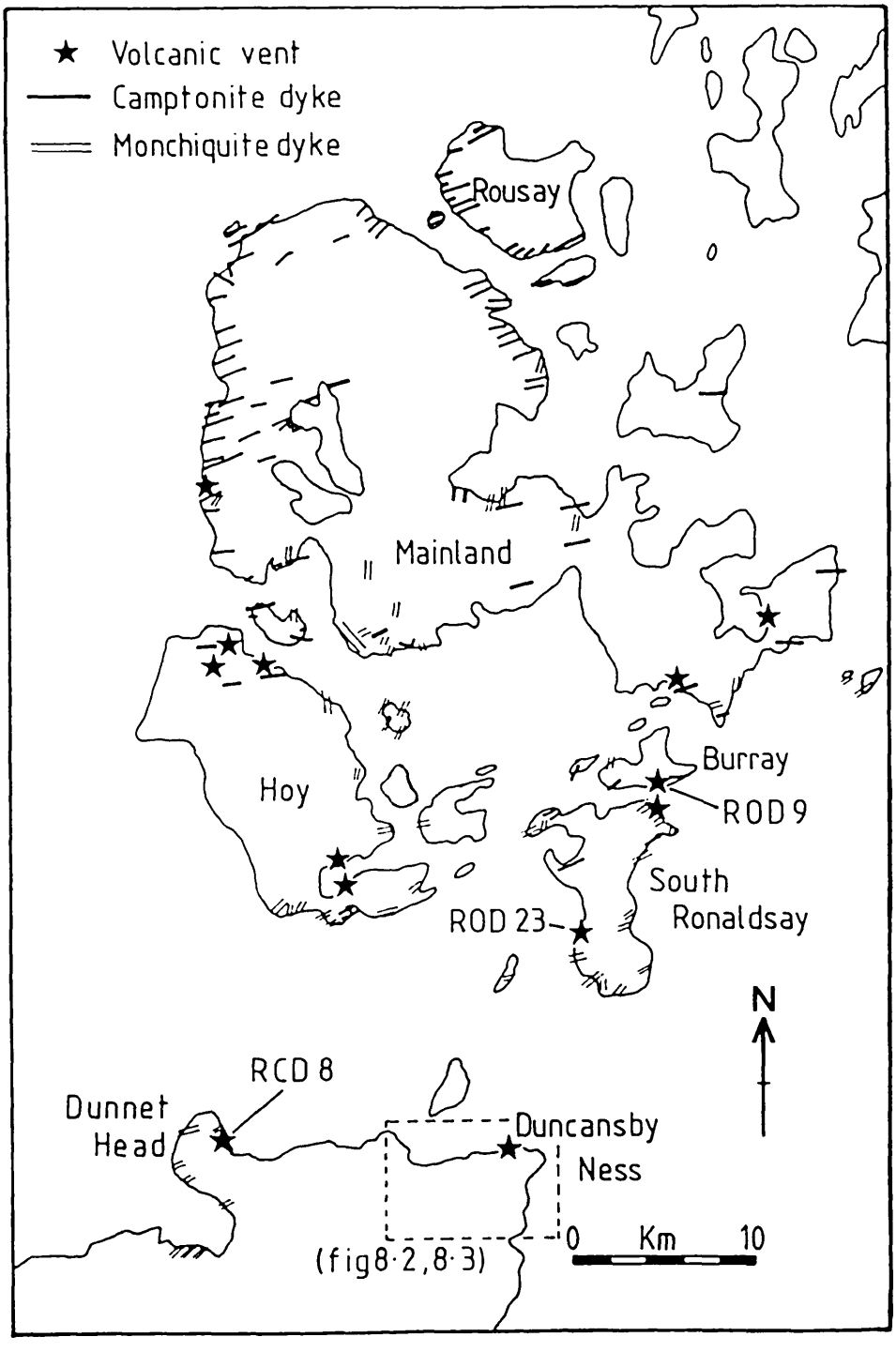


Fig. 8.1. Intrusive igneous bodies of the Orcadian Basin, with site locations. Vents lie on two northerly lineaments through Dunnet Head-Hoy and Duncansby Ness-Burray (see Watson, 1985, fig.9)

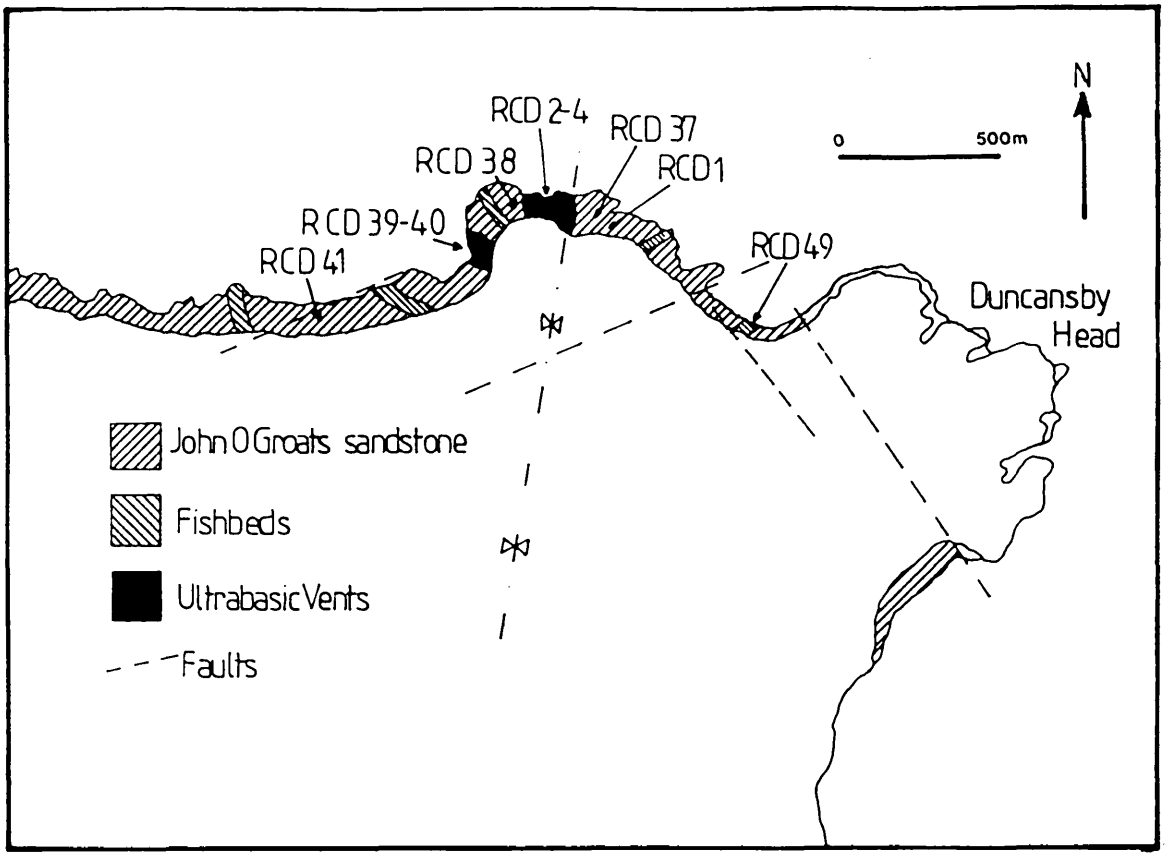


Fig. 8.2. Duncansby Ness: site locations in the vents and in nearby John o'Groats Sandstone. (after Foster, 1972)

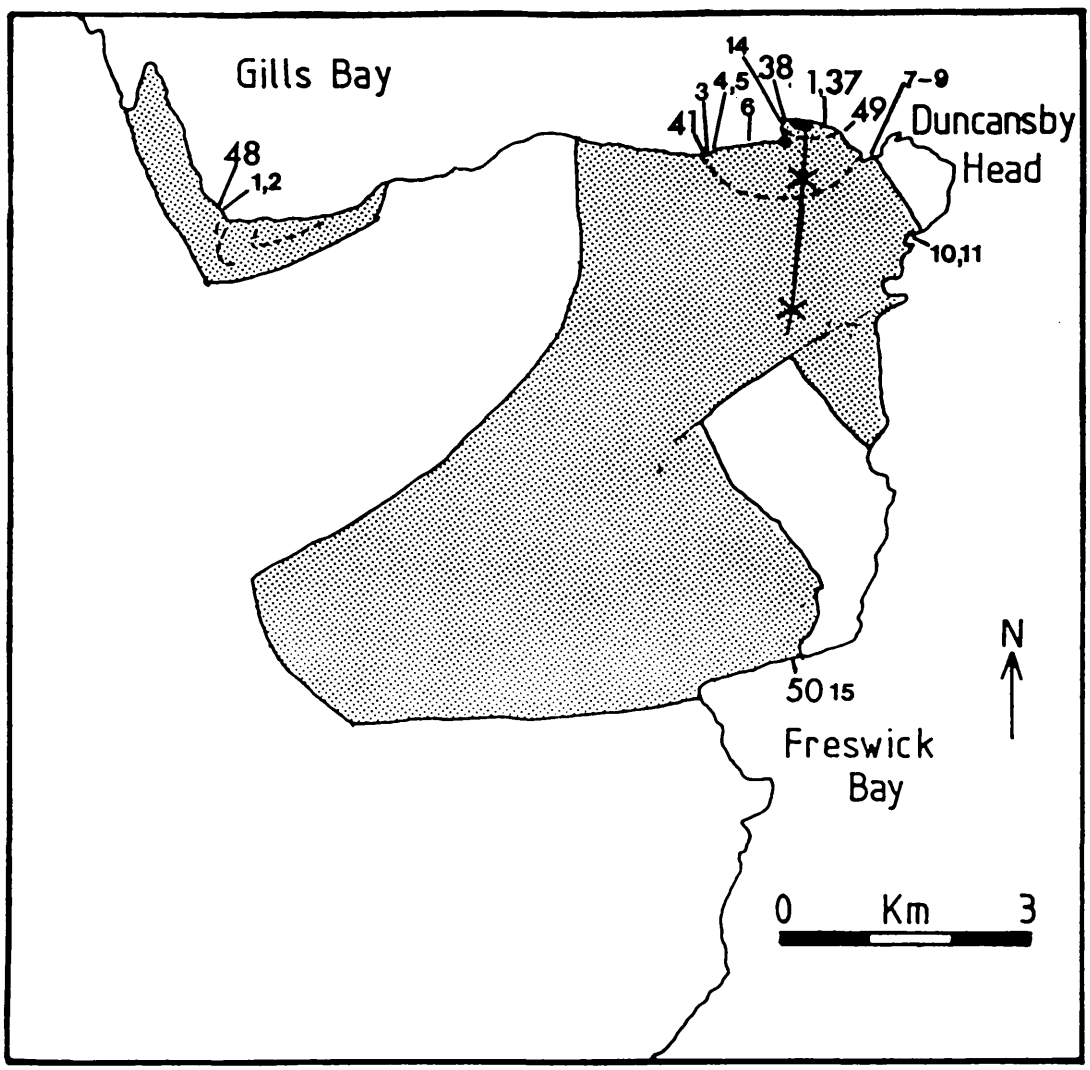


Fig. 8.3. The John o'Groats Sandstone: geographical range and site locations (see also fig. 8.2).

in the area to have been studied geochemically or isotopically in any detail, largely as a result of its numerous mantle xenoliths which include chrome-spinel lherzolite, wehrlite and spinel clinopyroxenite (Chapman, 1975). Matrix material is described as a nepheline-basalt (Crampton & Carruthers, 1914) or basanite (MacIntyre et al, 1981); it is generally somewhat decomposed, with olivine being serpentinised or replaced by carbonates. Other phenocrysts (augite, nepheline and biotite) are fairly fresh. Iron oxides occur within olivines or in the groundmass with decomposed glass and carbonates.

Included within the vent are numerous sedimentary xenoliths, up to 1.5m in diameter, predominantly of red or yellow sandstone with occasional flagstones or limestones, presumably representing material stoped into the vent during its ascent. Bedding orientations are clearly evident and are apparently random. Smaller fragments of sediment can be seen in thin section to be partially absorbed into the matrix.

There is no field evidence regarding the age of the vent, apart from the fact that it postdates sedimentation of the upper Middle ORS. However, a well-defined K-Ar date of 267±1 Ma (i.e. Permo-Carboniferous) is reported by MacIntyre et al (1981). Alternatively, Geikie (1878) and Storetvedt et al (1978) have suggested an Upper ORS age, the latter explaining their K-Ar date of 239-258 Ma as an underestimate due to radiogenic Ar loss during deep burial. Isotopic dating thus tends to confirm the Permo-Carboniferous age, based on similarity with the Fife volcanics, as suggested by Geikie (1897) and Crampton & Carruthers (1914). The apparent similarity in geochemical and field characteristics to the well-dated dykes of the basin (discussed in chapter 7) would

Table 8.1
Permian Vents: site details.

Site	Location	Site Details		Host Rock	N_{SA}	N_{SP}	None	Th	AF	Th+AF
RCD2		Sed. Xen.	(W)		10	16	6	2	-	8
RCD3	Duncansby	Matrix	(W)	John o'Groats	9	10	-	8	-	2
RCD4	Ness	Sed. xen.	(W)	Sandstone	5	11	6	5	-	-
RCD39		Matrix	(E)		8	13	-	3	10	-
RCD40		Sed. xen.	(E)		4	4	-	4	-	-
RCD8	Dunnet Head	Matrix		Upper ORS	6	6	-	1	5	-
ROD9	Burray	Matrix		Rousay Flags	7	8	-	4	-	4
ROD23	S. Ronaldsay	Matrix		S. Ronaldsay	7	10	3	1	6	-

(W) = Western outcrop N_{SA} = No. of samples
(E) = Eastern outcrop N_{SP} = No. of specimens
Sed. xen = Sedimentary xenolith within vent

also suggest a Permo-Carboniferous age.

The vent appears as two distinct outcrops (fig. 8.2) separated by recent beach and peat deposits; it is not clear whether these represent exactly the same body, although there is no doubt that they are coeval. Samples were collected from both outcrops (termed Western and Eastern) and also from a number of sedimentary xenoliths with varying bedding orientation (table 8.1). The host rock, the John o'Groats Sandstone, is discussed in section 8.3.

8.2.2. Palaeomagnetism.

(a) Matrix material.

The only published palaeomagnetic investigation of the volcanic vents of the Orcadian Basin is that of Storetvedt et al (1978), working on the Duncansby vent. They established a characteristic palaeomagnetic direction of Dec = 207.9°, Inc = -54.6° (henceforth referred to as the 'A' direction) which survived up to the Curie Point of magnetite. They suggest that this is a secondary magnetisation, acquired during prolonged deep burial prior to uplift in the Lower-Middle Jurassic. They recognise that burial to sufficient depth to effect such a remagnetisation is geologically improbable, so an additional contribution from chemical remagnetisation is envisaged.

They also report a high-T_B component (the 'B' component), contributing 1 to 5% of the total NRM intensity. This southerly, low-inclination direction is proposed as an estimate of the primary remanence direction of the vent, although a later re-interpretation of their data by Van der Voo & Scotese (1981) suggests that it has no validity. One of the principal aims, therefore, of further sampling of the

vent and its aureole is to establish conclusively whether the 'A' magnetisation is a true representation of the primary NRM or if there is in fact a meaningful high-T_B component.

Matrix material, as sampled by Storetvedt et al, (op. cit.) from the two outcrops (sites RCD3 and 39) gives a well-defined southerly, upwards characteristic direction after removal of a low-T_B viscous remanence. Maximum T_B, where determinable, is between 413 and 581 °C, although directional instability may occur before demagnetisation is complete. A number of specimens were AF demagnetised, with maximum demagnetising fields of around 75 mT. Typical examples are illustrated in fig. 8.4 and site mean directions included in table 8.2.

Table 8.2

Duncansby Ness: site mean directions.

Site no.	Location	In Situ Dec	In Situ Inc	N	k	a_{95}
RCD2	Sed. xen. (W)	210.8	-55.1	10	56	6.5
RCD3	Matrix (W)	201.6	-50.7	10	46	7.2
RCD4	Sed. xen. (W)	209.8	-52.7	5	72	9.1
RCD39	Matrix (E)	215.1	-56.2	12	38	7.1
RCD40	Sed. xen. (E)	223.8	-33.2	4	41	14.6
Mean, sample weighting		211.1	-52.2*	41	35	3.8
Mean, site weighting		213.0	-49.9	5	55	10.4

(W): Western outcrop; (E): Eastern outcrop.

* Palaeopole position: 124°N, 57°E (dp=3.6 dm=5.2)

Directional behaviour above the stability limit of the southerly, downwards component is erratic, as illustrated in fig. 8.5. This is in contrast to the findings of Storetvedt et al (op. cit.) but is not conclusive proof that a consistent high-T_B component is not present as this may be masked by viscous components.

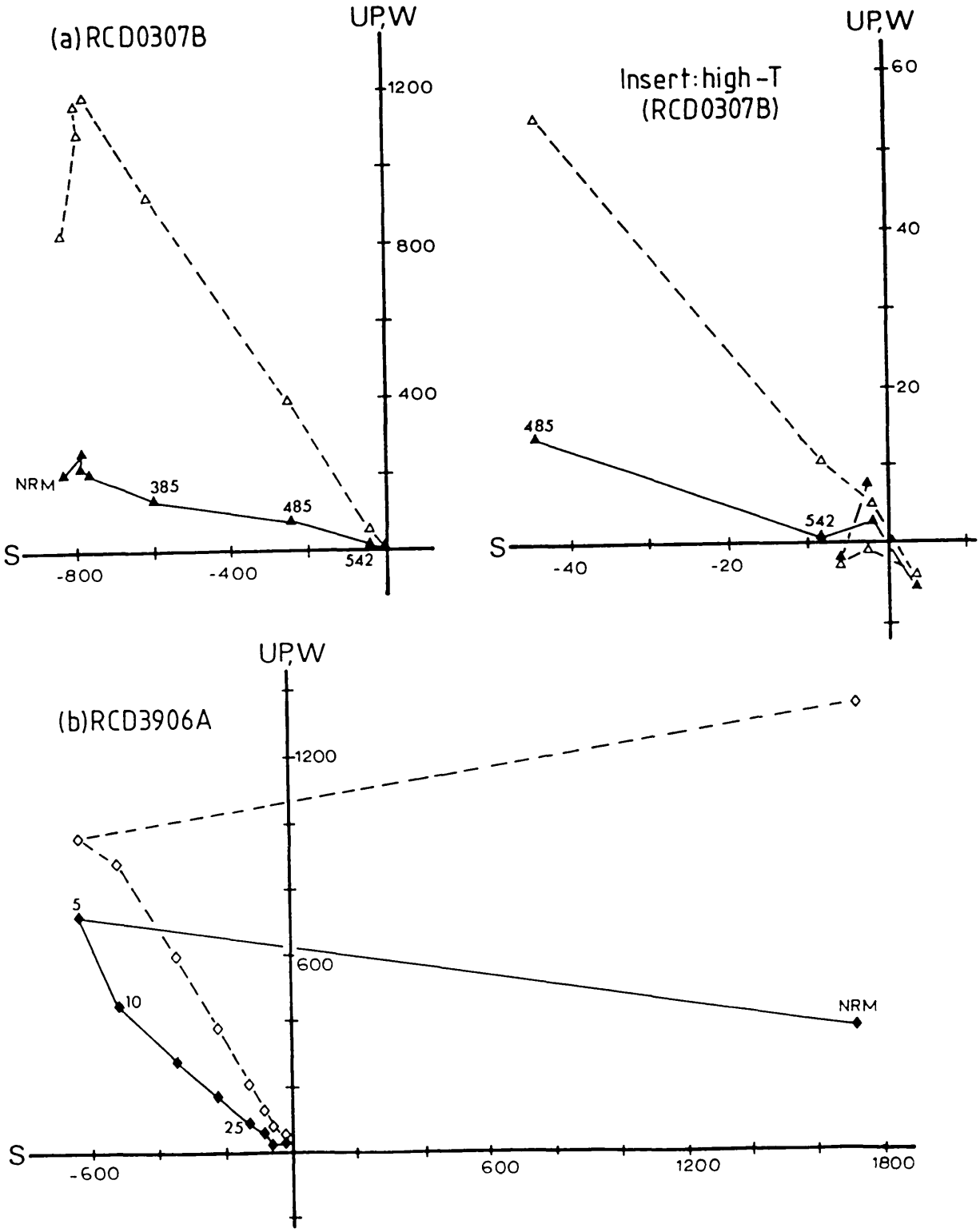


Fig. 8.4. Duncansby Ness Vents (matrix material): typical thermal demagnetisation of both the major and minor outcrops (fig. 8.2). Orthogonal projections; demagnetisation temperatures in °C (RCD0307B) or applied field in mT (RCD3906A). Axes in mA/m.

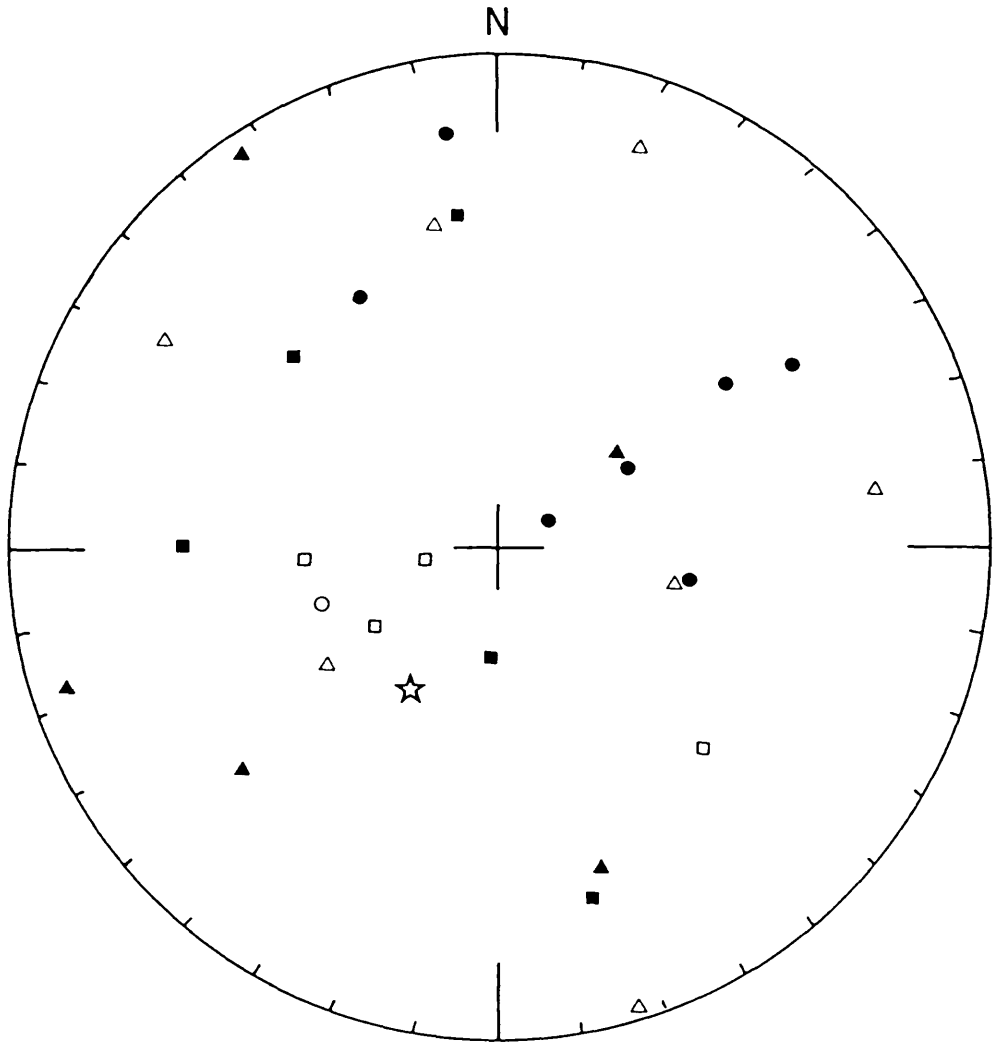


Fig. 8.5. Duncansby Ness Vents: thermal demagnetisation. Shows all specimen directions revealed during thermal demagnetisation after a departure of 10° or more from the dominant ('A') component direction. Demagnetisation was continued for one, two or more steps after directional instability had occurred. This demonstrates the absence of a southerly, low-inclination high-T_B remanence (see text).

(b) Sedimentary xenoliths.

Site RCD2 consists of samples collected from the eastern outcrop, from 4 discrete sedimentary xenoliths of varying bedding orientation. Two cores (two to four specimens) from the interiors of these xenoliths have been analysed. Xenoliths range in size from 7x15 cm to 45x45 cm, cores generally being taken from a fresh inner face exposed by recent fracturing. Site RCD4 consists of 5 cores from the interior of the largest xenolith in the eastern outcrop which is 1m in diameter. Samples are from minimum distances of 30 to 45 cm from its outer surface.

High-temperature or high-field directional stability is very much greater than that shown by matrix material (see above), presumably due to the absence of large, magnetically soft magnetite grains. Progressive demagnetisation of specimens from the smaller xenoliths of site RCD2 shows the remanence to be essentially single-component, directed upwards to the south, with Curie points of 625-680°C (fig. 8.6a). Demagnetisation is rapid around the Curie point of magnetite, but there is no directional change at this or higher temperatures. The presence of magnetite is confirmed by IRM experiments (see below). A number of specimens treated by a combination of AF and thermal methods still show no change from the 'A' direction.

Site RCD4, from the largest xenolith (1m in diameter) has very much lower NRM intensity (3.2 to 6.7 mA/m) than the smaller xenoliths of RCD2 (265 to 3335 mA/m) but still shows a southerly, upwards component during thermal demagnetisation (fig. 8.6b) with Curie points of 500-650°C. At higher temperatures, random directions are presumably associated with magneto-mineralogical alteration during

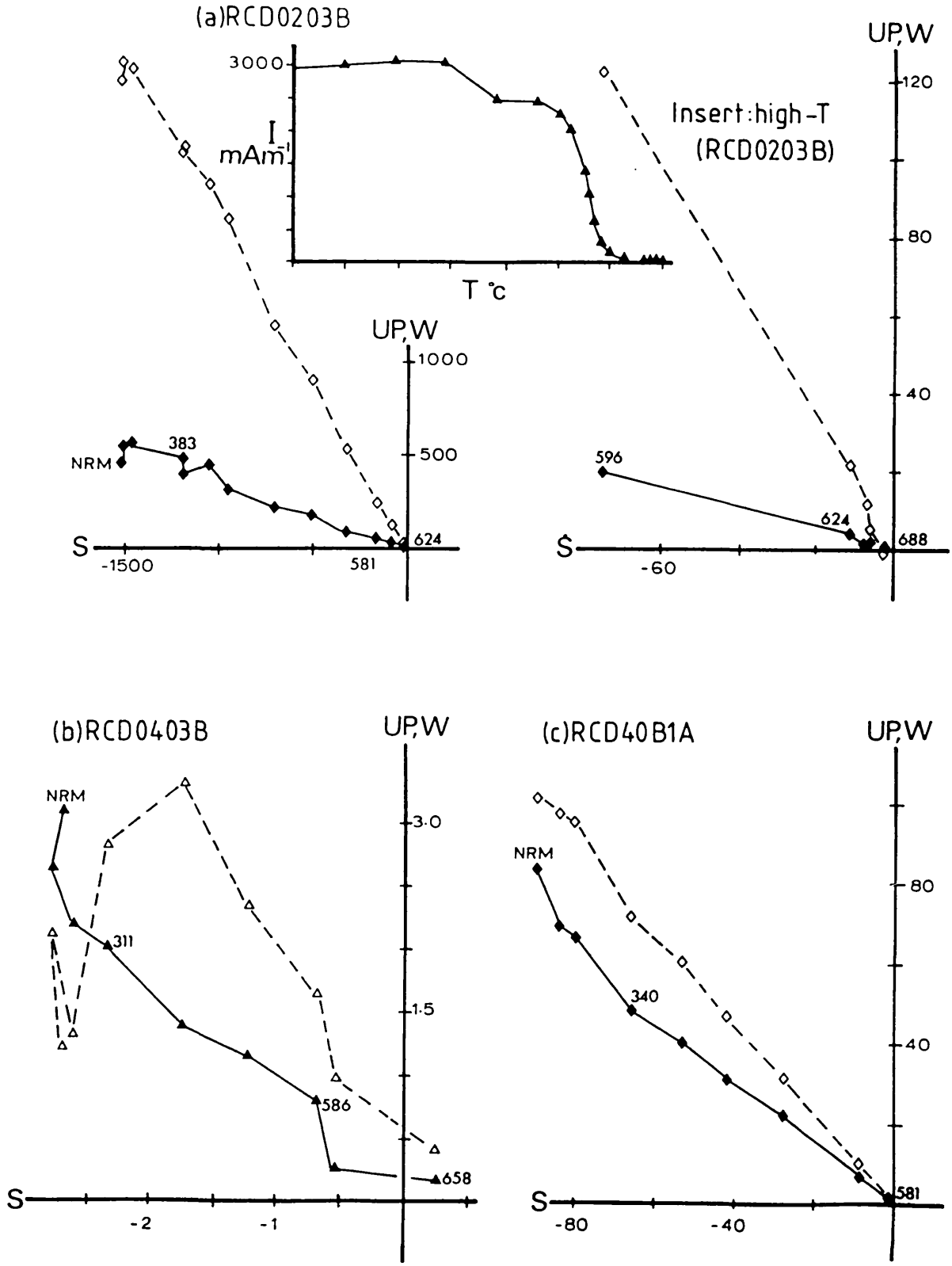


Fig. 8.6. Duncansby Ness Vents: thermal demagnetisation of sedimentary xenoliths. Orthogonal projections; demagnetisation temperatures in °C, axes in mA/m.

treatment, as suggested by large increases in susceptibility.

Site RCD40 is in a coarser-grained pale sandstone xenolith, 1x1.5 m in size, from the western outcrop. This again shows a stable southerly, upwards high-intensity (100-450 mA/m) single-component magnetisation which is fully demagnetised by 580°C, suggesting that the remanence carrier is magnetite. There is no high-T_B remanence equivalent to that found in RCD2 (fig. 8.6c)

Mean directions for the three sites are included in table 8.2. They can be seen to be very similar to mean directions found in the matrix material, as shown in fig. 8.7, suggesting that the remanence in the xenoliths may be a TCRM acquired during or very shortly after emplacement of the vent. The significantly lower NRM intensity of the largest xenolith suggests that the efficacy of the remagnetisation process is related to distance from vent matrix material, as it does not appear to have acquired a strong magnetitic remanence. The smaller xenoliths may have acquired a TCRM whereas remanence in the large clast of RCD4 may be a pure TRM. This conclusion is supported by IRM experiments (table 8.3) which show that M_{rs} for RCD4 is an order of magnitude lower than for RCD2. Neither of these saturate below 0.7T, indicating that hematite is present in both (probably an original characteristic of the rock). In contrast, matrix material saturates in 90-130 mT and M_{rs} is much greater than in either of the clasts analysed, suggesting that the dominant magnetic mineral present is magnetite.

The geochemical inter action of clasts and magma is

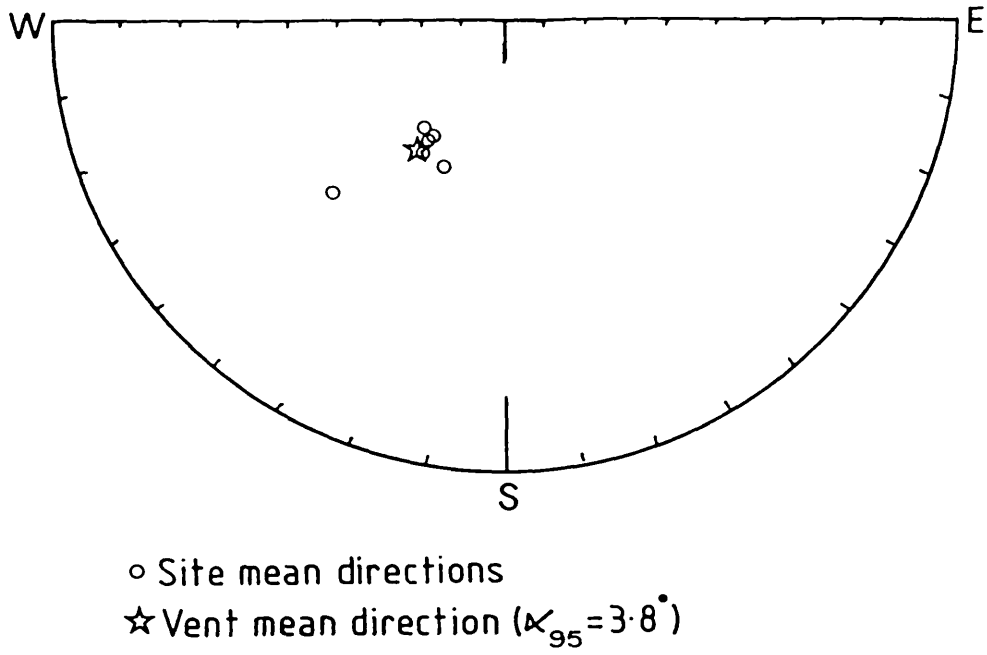
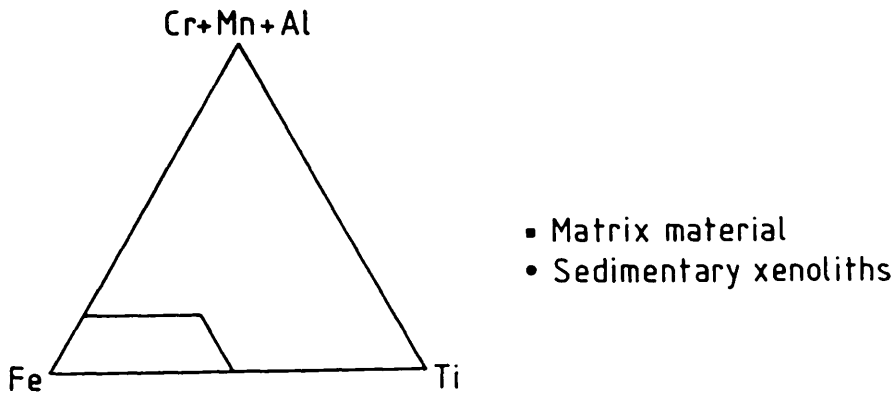


Fig. 8.7. Duncansby Ness Vents: site mean directions for both matrix and xenoliths. Error circle too small to show.



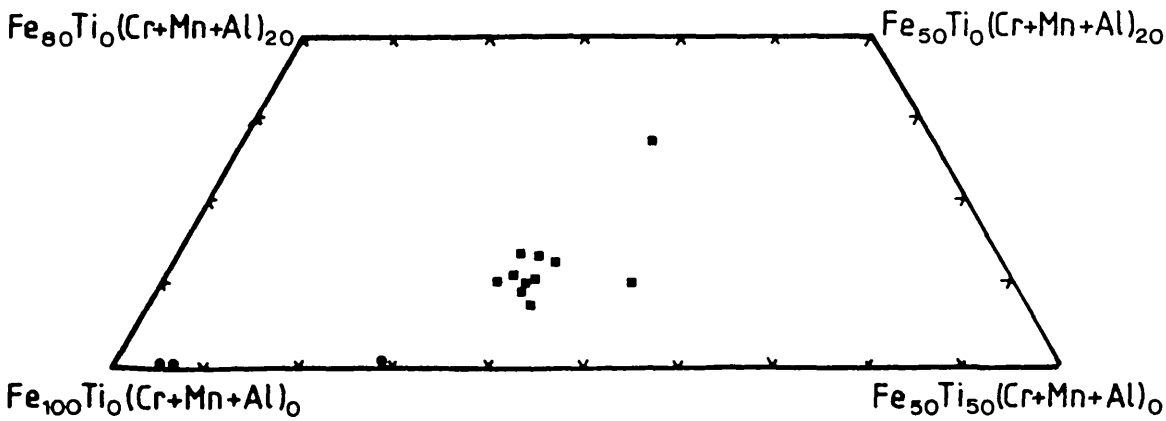


Fig. 8.8. EPMA analyses of titanomagnetite from the Duncansby Ness Vents. Matrix material is generally of high Ti while oxides from the xenoliths show very low Ti. (Full analyses in appendix D2iv).

Table 8.3
Duncansby Vent: IRM characteristics.

Specimen	Description	M_{rs} (mA/m)	B_c (mT)	B_s (mT)	Interpretation
RCD02B1A	Small clast	29700	<65	700	M + H
RCD0403A	Large clast	3130	155-290	1200	H ± M
RCD3908B	Matrix	526000	<50	130	M
RCD3802B	Contact (0.4m)	4000+	155-290	-	H
RCD3806C	Contact (7.0m)	4400+	155-290	-	H

M= Magnetite H= Hematite

also demonstrated by bulk geochemical data (appendix C). This shows that the average concentrations of Fe, Ca and Mg are about 50% higher in the small clasts of site RCD2 compared with those of RCD4. These elements may have been introduced from the magma into the smaller clasts but to a lesser extent, if atall, into the larger ones.

EPMA analyses of iron oxide grains using the electron microscope (fig. 8.8; appendix D) shows that those from matrix material have a mean metal composition of Fe 73.8%, Ti 20.0% and (Cr+Mn+Al) 6.2%. They show a much higher level of the latter elements than that found in similar grains from sedimentary clasts within the vent.

A pure titanomagnetite of this composition would have a Curie Temperature of around 350-450°C. This is lower than that revealed during thermal demagnetisation of matrix material. Very fine-scale exsolution may thus have occurred which is not apparent visually but which produces a mean composition as observed.

8.3 John o'Groats Sandstone.

8.3.1. Geology, age and sampling.

The outcrop range of the John o'Groats Group is limited to N.E. Caithness (fig. 8.3). It marks a rapid change in depositional environment from the underlying flagstones of the Mey Beds Subgroup (discussed in chapter 5), although the

exact nature of the change is not evident as all contacts are faulted; the relationship is presumably disconformable. The sediments bear a general similarity to the Upper ORS of Dunnet Head and Hoy (chapter 4) and also to clastic horizons of the lower Eday Group, with which they are equated (Donovan et al, 1974). Discussion of the Group in the context of the evolution of the basin as a whole is given in chapter 2.

The sediments of the Group (Crampton & Carruthers, 1914) are characteristically friable medium- to coarse-grained fluvial sandstones with much cross-bedding and frequent small-scale syn-depositional contortion. Cementation is predominantly calcareous, weathering to a honeycomb structure. The lower part of the Group is usually yellow-orange, reddening towards the top.

Within the Group, two thin bands of laminated fish-bearing lacustrine laminites occur (the Last House formation of Donovan et al, 1974), providing the only palaeontological control of stratigraphy. The fauna is highly distinctive (Crampton & Carruthers, 1914) and very different from underlying assemblages. Stratigraphy of the Group is discussed in great detail in Donovan et al (op. cit.), to which reference will be made without detailed discussion.

Sampling localities are shown in fig.8.3, both from this study and from that of Storetvedt & Carmichael (1979), as discussed in more detail below; individual characteristics of each site are given in table 8.4. The structure of the area is straightforward, the main feature being a gently plunging syncline with a N-S axis, along the hinge of which the volcanic vent is found.

Table 8.4
John o'Groats sandstone: site details.

Site	Formation	Location	N_{SA}	N_{SP}	Analysis None	Th	AF	AF+Th
RCD1	Knocking Stone		13	17	-	13	1	3
RCD37	Knocking Stone	Duncansby	8	17	15	2	-	-
RCD38	Roberts Haven	Ness	7	15	-	13	2	-
RCD41	Knocking Stone		6	10	-	10	-	-
RCD48	-	Gills Bay	6	13	5	8	-	-
RCD49	Last House	Dunc. Ness	6	10	-	5	5	-
RCD50	-	Freswick	6	12	7	5	-	-

N_{SA} = No. of samples N_{SP} = No. of specimens

8.3.2. Palaeomagnetism.

Palaeomagnetic characteristics of the John o'Groats Sandstone reported in Storetvedt & Carmichael (1979) are very similar to those described by Storetvedt et al (1978) for the nearby Duncansby Ness vent (section 8.2), with a characteristic southerly, upwards low-T_B component (the 'A' magnetisation) and an apparent flatlying, southerly direction at higher temperatures (the 'B' magnetisation). The latter component is open to the same objections (Van der Voo & Scotese, 1981) as the comparable one in the vent.

The 'A' magnetisation was shown to reside in the pigmented cement, as it decays rapidly during chemical demagnetisation which also produces a general bleaching of the rock. It appears to have been acquired prior to deformation; mean dip-corrected directions for sample components given in Storetvedt & Carmichael (op. cit.) have been recalculated, with components supposedly representing the reversed 'A' magnetisation being rejected (as they are indistinguishable from a recently acquired CRM). The corresponding *in situ* directions have also been calculated (table 8.5) showing that the precision parameter k, both at the site and sample level, is much greater after correction for tectonic dip. (The plunge of the fold, being very low, has not been taken into account). It should be noted,

however, that this result is dependent almost entirely upon the effects of tectonic correction on sites 7 and 8, rather than on the entire component population; the implications must therefore be considered with some care.

Site mean directions reported by Tarling et al (1976) also show an 'A' direction in each of four sites after thermal cleaning at 300°C. It is not apparent whether these results are corrected for tectonic dip.

Table 8.5
Recalculated mean directions for the John o'Groats sandstone using the data of Storetvedt & Carmichael (1979)

		In Situ		Dip corrected			
Site	N	Dec	Inc	Dec	Inc	k	a_{95}
1	1	191.0	-44.0	191.0	-44.0	-	-
4	9	175.5	-49.2	202.2	-38.5	195	3.7
5	3	187.6	-47.9	192.2	-32.8	132	10.7
7	4	253.3	-65.5	202.7	-34.8	66	11.4
8	6	244.6	-73.1	186.8	-38.7	255	4.2
10	10	182.6	-40.7	173.3	-45.5	71	5.8
11	2	177.9	-38.4	173.3	-40.4	-	-
Mean	35[1]	190.2	-54.4a			15	6.4
	35[1]			189.2b	-40.5	42	3.8
Mean	7[2]	192.4	-53.8			15	16.0
	7[2]			189.2	-39.8	62	7.7

(1) = Unit weighting to samples
(2) = unit weighting to sites

Palaeopoles: (a) In Situ 157°E, 65°N (dp= 6.3° dm= 9.0°)
(b) Dip corrected 162°E, 54°N (dp= 2.8° dm= 4.6°)

The John o'Groats sandstone has also been cursorily investigated by Turner (1977), who found only apparently random directions of magnetisation, despite good stability during thermal treatment.

Sampling in the present study is less extensive than that reported by Storetvedt & Carmichael (1979), the main aim here being to establish the exact relationship between the vent and remanence in the sandstone and also to determine which facies carry a stable remanence.

Remanence in the four clastic sites from the Duncansby

Ness area (all of which are within 500 m of the vent and correspond to sites 6 to 9 of Storetvedt & Carmichael, op. cit.; see fig. 8.3), is generally less well-defined in the present study than in Storetvedt & Carmichael (op. cit.). Sites RCD1 and 37, from the Knocking Stone formation east of the vent, do not show internally consistent behaviour; the two specimens analysed from site RCD37 have no stable remanence above 400°C while RCD1 is characterised by stable components of apparently random orientation; such findings are similar to those of Turner (1977) discussed above. They do not appear to be amenable to conventional interpretation.

Site RCD41, in the same formation but west of the vent, is of finer grain size than the remainder; it generally shows a poorly-defined component directed downwards to the south and with high (hematitic) T_B (fig. 8.9a; table 8.6) This site appears to be in approximately the same location as site 6 of Storetvedt & Carmichael (op. cit.); significantly, the single component reported by these authors for the site is also directed downwards to the south. It is suggested that the remanence at this site may predate the 'A' magnetisation and possibly represents a primary direction. This is discussed in the regional context in chapter 9.

Of all the sites analysed from the John o'Groats Sandstone, the only one to give a well-defined remanence similar to the 'A' magnetisation is site RCD38, in the Roberts Haven formation. It consists of 7 samples (15 specimens) at distances of 0.02 to 10.0 m from the vent on Duncansby Ness discussed above. All but one of the samples shows a clear, well-defined component directed upwards to the south, with a maximum T_B of 500 to 675°C (fig. 8.9b,c).

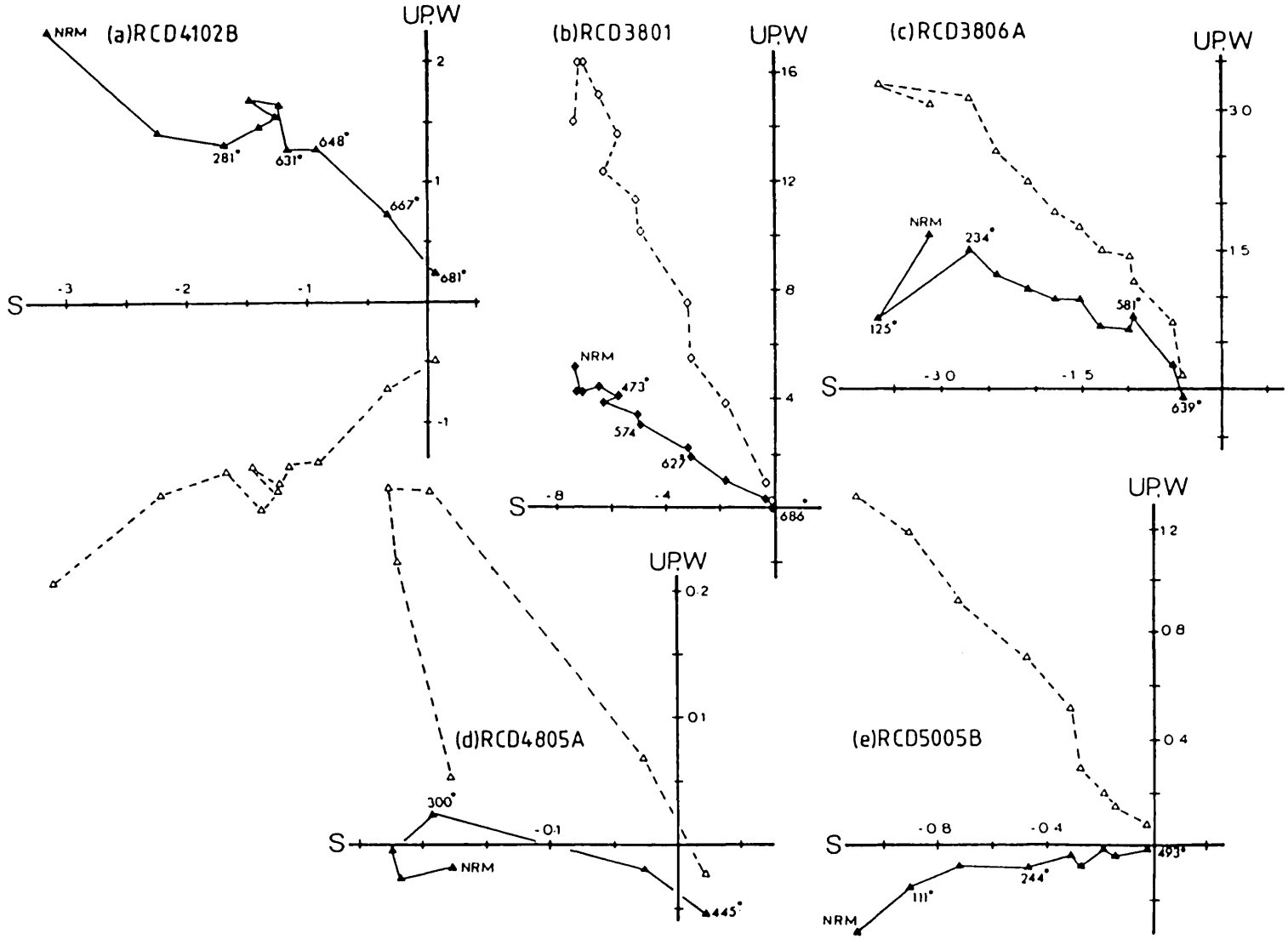


Fig. 8.9. John o'Groats Sandstone: thermal demagnetisation. Orthogonal projections; demagnetisation temperatures in °C, axes in mA/m.

Table 8.6
John o'Groats sandstone: site means.

Site no.	In Situ Dec	In Situ Inc	Dip Corrected Dec	Dip Corrected Inc	N	k	a_{95}
RCD38	202.8	-42.6	203.7	-32.7	9	27	10.0
RCD41*	213.1	29.0	213.9	46.0a	7	10	19.8
RCD48	172.3	-48.5	191.0	-41.0	4	8	33.7
RCD50	186.6	-50.9	174.3	-35.5	2	-	-
Mean,	193.6	-46.0b			15^{1}	16	10.0
'A' cpts			196.7	-35.6c	15^{1}	16	9.8
	187.8	-48.0			3^{2}	52	17.3
			189.8	-37.0	3^{2}	41	19.5

* = Not included in mean direction
(1) = Unit weighting to samples
(2) = Unit weighting to sites

Palaeopole positions: a 147°E, 0°N (dp=12.0° dm=21.8°)
b 154°E, 57°N (dp= 8.1° dm=12.7°)
c 152°E, 49°N (dp= 6.5° dm=12.3°)

There is usually also a small low-T_B viscous component and often an unresolved high-T_B component with minimum T_B of 475-640°C. This is never sufficiently well-defined to give an interpretable direction; it may possibly represent vestiges of a remanence acquired prior to the dominant 'A' magnetisation, as at site RCD41 above.

Spatial variation in remanence characteristics of the site gives only limited information regarding its exact relationship with the vent, although specimen RCD3801, 0.02 m from the contact, has significantly higher NRM intensity (16.9 mA/m) and susceptibility (26.0 $\times 10^{-5}$ mA/m) than the remainder (2.3 mA/m and 4.0 $\times 10^{-5}$ mA/m respectively). Beyond this, variation is erratic and within the range for the John o'Groats Sandstone as a whole.

The remaining two sites in the sandstone are characterised by NRM intensities generally lower than the remainder by an order of magnitude. Site RCD48, in a yellow horizon from Gills Bay, corresponds to sites 1 and 2 of Storetvedt & Carmichael (op. cit.) who report only one

specimen with an 'A' magnetisation, the others being too weakly magnetised to survive more than a few demagnetisation steps or showing erratic behaviour. The same pattern is found in the present study; of the 8 specimens analysed, only 4 give an 'A' direction (fig. 8.9d), the remainder being weakly magnetised and highly erratic (table 8.2).

Site RCD50 corresponds to site 15 of Storetvedt & Carmichael (op. cit.) who report no stable magnetisation. This was found to be the case in the present study with the exception of a single sample (RCD5003) which, in contrast to the yellow colour of the remainder of the site, has a red stained cement. This one sample (two specimens) has significantly higher NRM intensity (average 1.916 mA/m) than the remainder (average 0.202 mA/m) and shows a well-defined magnetisation directed upwards to the south (table 8.2; fig. 8.9e). Maximum T_B is 500 to 540°C.

Site RCD49, from the Last House formation (the John o'Groats Fishbed) will be discussed in chapter 5 with other sites in similar lithologies from elsewhere in the basin. It does not show an 'A' magnetisation.

Site mean directions for all sites in the John o'Groats Sandstone are given in table 8.6. Individual sample components are shown in fig. 8.10, both in situ and corrected for tectonic dip; there is no significant difference in precision between the two.

8.3.3. Origin of the NRM.

Fig. 8.11 shows the mean directions from the Duncansby Ness neck and the John o'Groats Sandstone, including data both from this study and from those of Storetvedt et al (1978) and Storetvedt & Carmichael (1979). It can be seen

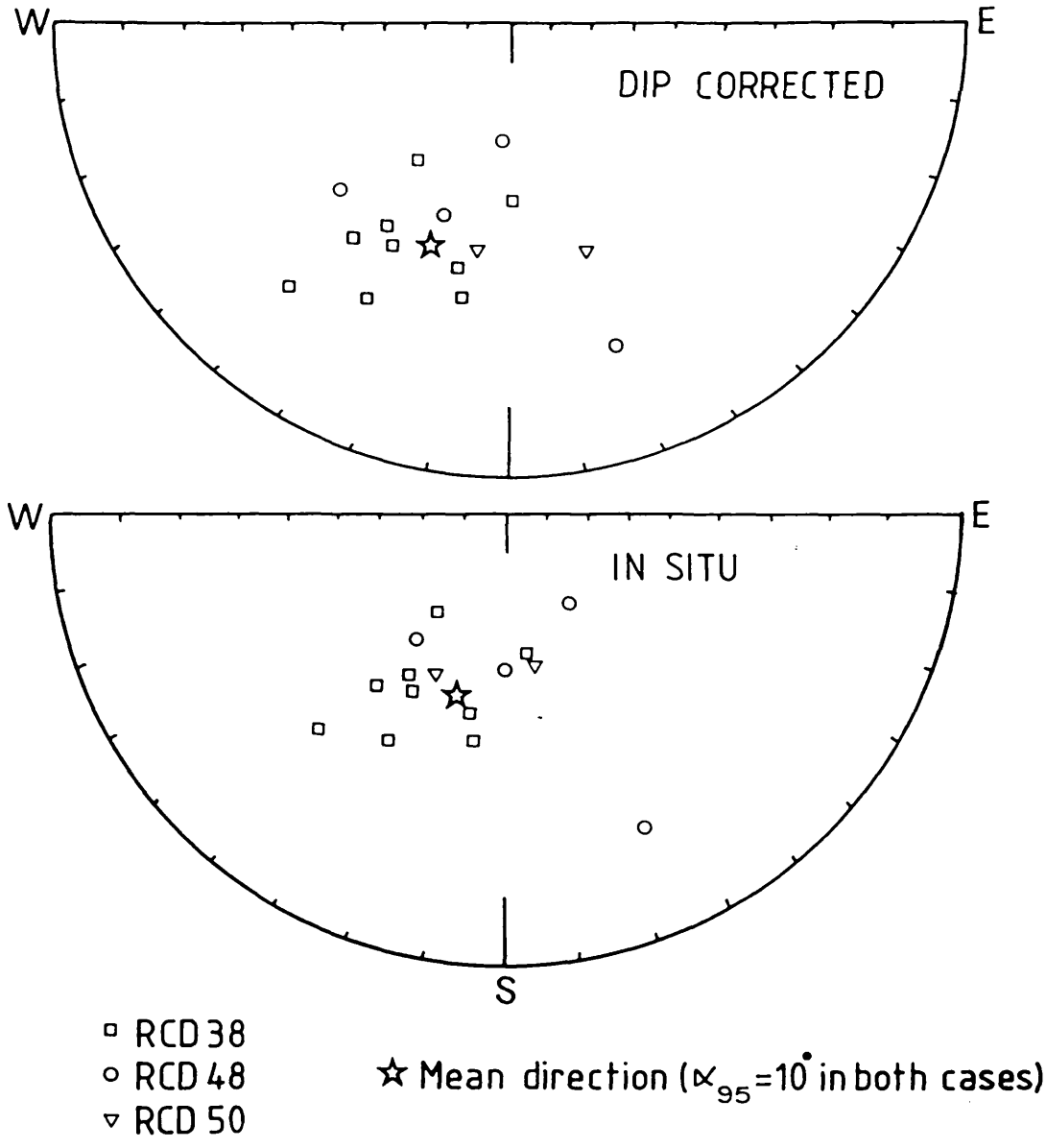
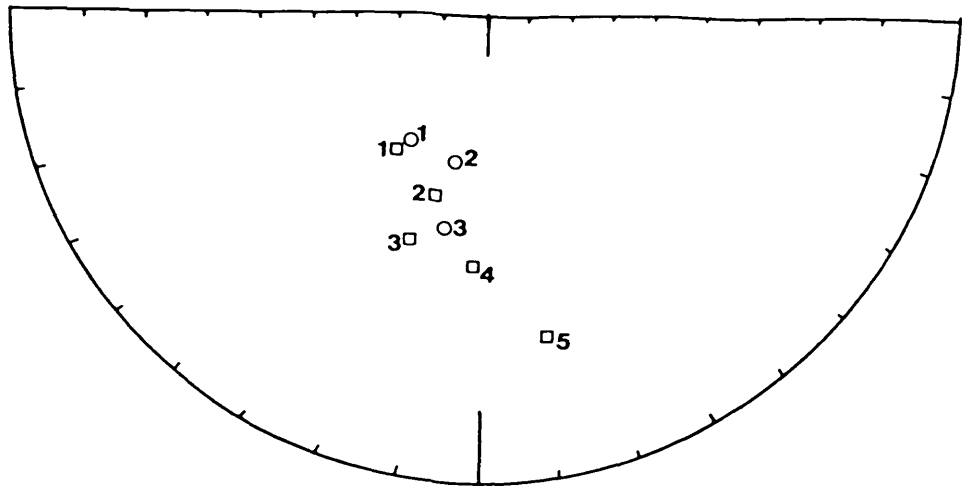


Fig. 8.10. John o'Groats Sandstone: specimen component directions by site, with overall mean direction (error circle not shown).



□ This study
○ Previous studies

Fig. 8.11. Mean directions, Duncansby Ness area.
(1): Duncansby Vent
(2): John o'Groats Sandstone (In Situ)
(3): John o'Groats Sandstone (Dip Corrected)
(4): Burray Vent
(5): Barswick Vent, South Ronaldsay.

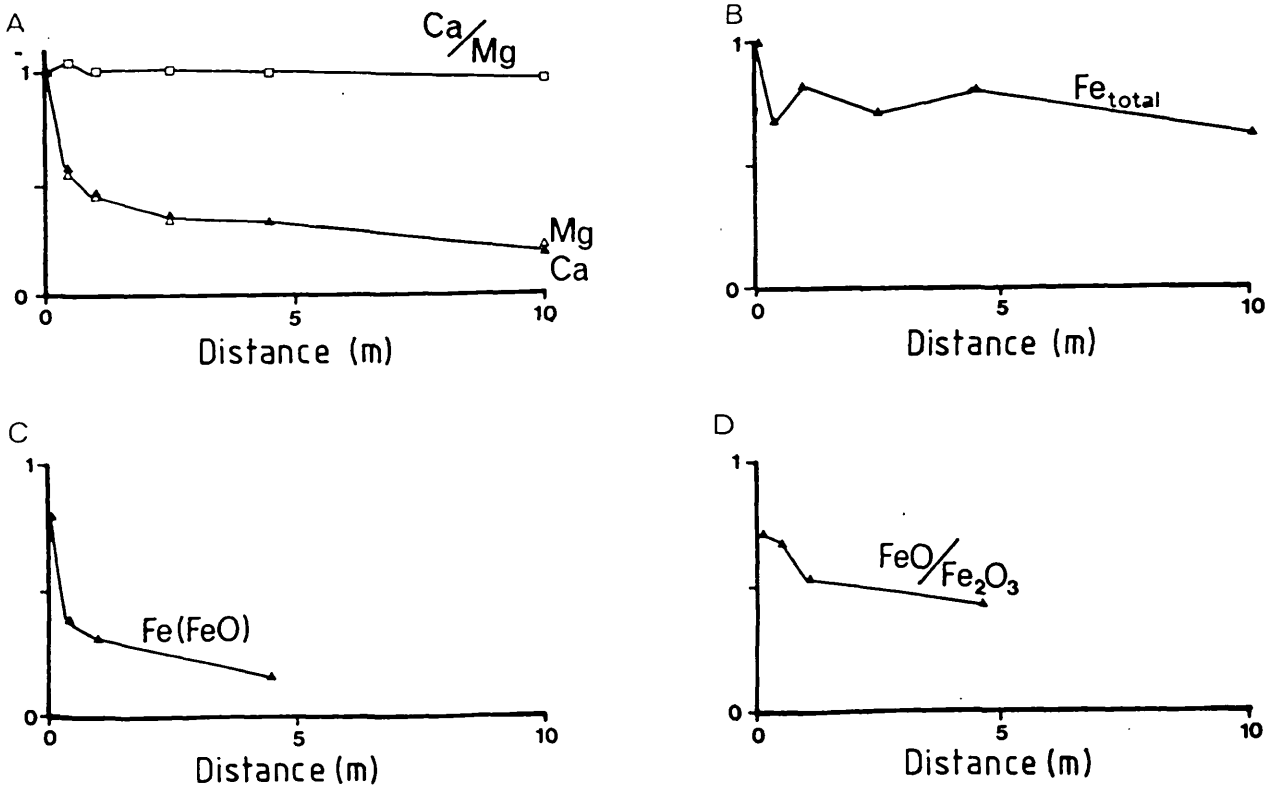


Fig. 8.12. Bulk analysis variation in the contact zone of the Duncansby Ness Vent (site RCD38). Ca, Mg and total Fe analyses from ICP (appendix CIg); FeO analyses from 'wet chemistry' (appendix E). All analyses normalised to specimen RCD3801.

that directional agreement between these studies is very good. It can also be seen that mean directions from the sandstone and the volcanic neck are similar and hence presumably approximately coeval. It remains to be shown whether this is coincidental (as in the case of the Permo-Carboniferous dykes and the regional Kiaman remagnetisation of the basin; see chapter 6) or if the two are related.

The remanence of sites showing the 'A' magnetisation has been shown by chemical demagnetisation (Storetvedt & Carmichael, op. cit.) to reside in the pigmented cement. This is confirmed by thin section observation; such sites can be seen to have been dedolomitised, with fine particulate hematite accompanying the carbonate cement. Such a process has recently been established as an effective method of secondary remanence acquisition (Elmore et al, 1985), as discussed in chapter 2. No other indications of secondary hematite generation can be seen.

Dedolomitisation fabrics have also been illustrated by Storetvedt & Carmichael (1979, plate 1f); this is recognised by the original authors as showing hematite formed as an alteration product of crystals within the matrix, but they do not note the significance of the shape of the relict structure outlined by secondary hematite grains: it strongly resembles a (dedolomitised) dolomite rhomb, as illustrated elsewhere in this volume.

Bulk analyses demonstrate why sites RCD48 and 50 show only a weak remanence, if any; total Fe analyses are 0.90% and 0.25% respectively (appendix C). Their highly mature mineralogy is demonstrated by very low total non-silicate analyses (8 and 6% respectively).

The only palaeomagnetic evidence directly linking the

remanence of the vent and of the sandstone, apart from the similarity of palaeomagnetic orientation, is the increase in NRM intensity immediately adjacent to the contact (section 8.3.2.) suggesting a limited thermo-chemical overprint.

The main feature of bulk geochemical variation with distance from the vent is a consistent increase in Ca and Mg (fig. 8.12a). These increase by a factor of three or more between 10.0 and 0.02 m, although the relative proportions remain approximately constant. This suggests either that extensive redistribution of the carbonate cement during emplacement has occured or that later removal of the cement has been inhibited in the aureole of the intrusion, perhaps by temperature-induced induration of the sediment.

The only other possibly significant variation is in iron concentration; total Fe is highest in RCD3801 (1.72% compared to a mean of 1.25% elsewhere in the site; fig. 8.12b). The bulk of the Fe is in the oxidised state (fig. 8.12c,d) although there is possibly a systematic decrease in FeO away from the vent. This would be in accordance with the net introduction of very small quantities of vent-derived magnetite during emplacement within only a few centimetres of the contact, with an associated increase in NRM intensity and susceptibility. Unfortunately, fresh material from sample RCD3801 is not available to confirm this by IRM analysis.

The emplacement of a vent such as that at Duncansby Ness would, under suitable circumstances, be accompanied by the hydrothermal circulation of large volumes of water (Robinson & McClelland Brown, in prep) The John o'Groats Sandstone, being generally of very high porosity and permeability, would be ideally suited to act as an aquifer

supplying such a system. The passage of large volumes of water through a rock is essential for the dedolomitisation process (chapter 2) which seems to have occured predominantly in the immediate vicinity of the vent but also, to a lesser degree, at the geographical extremes of the formation, 5 km away (sites RCD48 and 50). Remanence acquisition at such sites could thus be indirectly related to vent emplacement. Such a model would also explain why the less porous sandstone of RCD41 and the relatively impermeable fishbed (site RCD49) do not show an 'A' magnetisation. Neither of them show any evidence of dedolomitisation.

If, as it might appear, remanence in the sandstone is more or less directly related to emplacement of the vent, then mean directions for the sandstone (both dip-corrected and *in situ*) and the vent should be compared (fig. 8.10). Agreement between the two sets of directions is better if the *in situ* direction from the sandstone is used. This is contrary to evidence that remanence acquisition predates folding of the sandstones, although this test is not conclusive despite being statistically significant, as discused above (see also section 8.5).

8.4 Other vents

In addition to the vent at Duncansby Ness, three other vents, two on Orkney and one on Dunnet Head, Caithness, have been analysed (table 8.1). The plug on Burray, ROD9, is very similar to the Duncansby neck, with clasts of sediment in a basic matrix, although it is described in Wilson et al, 1935, as being composed of brecciated sandstone with no detected volcanic rocks. The other two, on Dunnet Head in the Upper ORS (Wilson et al, 1935, fig. 22) and Barswick,

South Ronaldsay, in the Lower Eday Sandstone, have very little or no volcanic material; they consist of an indurated flagstone/sandstone breccia. The Dunnet Head neck is highly decomposed and may be a cryptovent, as suggested by Crampton & Carruthers (1914) who equate it with nearby volcanism on Hoy.

Barswick vent appears to be closely related to faulting; small patches of vent material can be seen at several locations in cliffs along the outcrop of a vertical fault. Mykura (1976) suggests that it was formed by hot gases rising above an ascending magma coming into contact with pockets of water. (The vent appears to have been confused by Wilson et al, 1935, with the one on Burray; they describe it as monchiquitic with fragments of sandstone).

Both vents appear to have largely been replaced by carbonates. Mg and Ca together constitute over 60% of the total non-silica analysis (appendix C). Analyses are not available for site ROD9.

The monchiquitic vent on Burray, ROD9, has a straightforward two-component remanence; a viscous component is removed by 200-350°C or 5-10 mT, followed by a stable component directed upwards to the south with maximum T_B of 525-575°C. It is magnetised in a similar direction to the 'A' direction on Duncansby Ness (table 8.7); intensities and susceptibilities are also very similar. The vent, which has not been isotopically dated, would thus appear to be part of the same period of volcanism as the better-known vent on the mainland. The only site in nearby sediments (site ROD10 in the Rousay Flags; see chapter 5) shows no stable magnetisation.

Barswick vent on South Ronaldsay, probably formed by

gaseous fluxion above a rising magma, has very low NRM intensity (0.21 to 1.2 mA/m) and low magnetic stability; no consistent directions are found. Site RCD8, in the Upper ORS of Dunnet Head, is also very weakly magnetised (0.3 to 1.4 mA/m) but nevertheless all specimens give a poorly-defined component defining a mean direction directed upwards to the south (table 8.7; fig. 8.10). This suggests that it, too, may belong to the same Late Palaeozoic phase of volcanic activity.

Table 8.7
Site statistics, minor vents.

Vent	Site	Dec	Inc	N	k	a_{95}
Burray	ROD9	181.7	-32.8	8	29	10.4
Little Clett	RCD8	168.5	-19.8	6	8	25.9

Palaeopole positions:
Burray 175°E, 49°N (dp= 6.6 dm=11.7)
Little Clett 192°E, 41°N (dp=14.2 dm=27.1)

8.5 Summary.

The characteristic 'A' magnetisation in the Duncansby Ness vent has been shown to be the only ancient remanence present; it represents a primary TRM acquired during cooling, by both matrix material and also by sedimentary clasts stoped into the vent during its ascent. The high-T component reported by Storetvedt et al (1978) has been shown experimentally to be unreal, confirming the opinion of Van der Voo & Scotese (1981) who based this conclusion on the original data alone.

The majority of coarser-grained sites in the John o'Groats Sandstone carry a secondary hematitic remanence, acquired during a dedolomitisation event which has affected the whole outcrop area of the group but which was most effective in the immediate vicinity of the Duncansby vent.

This remanence bears a strong directional similarity to that in the vent. Only one site, in a fine-grained impermeable sandstone, carries an earlier magnetisation which is probably syn-depositional.

The timing of secondary remanence acquisition in the John o'Groats sandstone is somewhat uncertain, due to slight doubt about the reliability of the fold test reported by Storetvedt & Carmichael (1979). There are four possible scenarios regarding the times of acquisition of the secondary remanence, emplacement of the vent and formation of the syncline; conclusions which may be drawn from each of these are summarised in table 8.8

Table 8.8
John o'Groats Sandstone: possible remanence acquisition - deformation scenarios.

	Scenario A	B	C	D
Remanence in sst. related to vent emplacement?	Yes	Yes	No	No
Fold test significant?	Yes	No	Yes	No
conclusion: Folding postdates vent emplacement and 'A' component in sandstone.	+	n/i	n/i	n/i
Folding postdates 'A' component in sandstone.	+	n/i	+	n/i
Vent direction represents spot reading only	+	(+)	n/i	n/i

(n/i = no information)

In the author's opinion, remanence in the sandstone appears to be related to emplacement of the vent, and the grounds for rejecting the fold test are not sufficient. Scenario A is therefore considered as the most probable. This conclusion carries with it two important implications. Local folding must be uppermost Palaeozoic or later, which is contrary to the generally accepted timing of deformation in the basin (i.e. pre-Upper ORS). It also suggests that

the mean direction from the vent is only a spot reading acquired over a short period during secular variation, the average field at the time being of somewhat lower inclination; this might perhaps be expected taking into account the small size of the vent.

Mean directions for the three vents and the John o'Groats sandstone are considered in relation to data from the remainder of the Orcadian Basin and elsewhere in chapter 9.

CHAPTER 9

CONCLUSIONS

9.1. The syngenetic remanence in context

9.1.1. Intra-basin

Mean directions for all sites showing a suspected syngenetic (i.e. detrital or early diagenetic) remanence are shown in fig. 9.1; these are categorised into Lower, Middle and Upper ORS. It will be seen that reversed (i.e. southerly declination) components are confined to the upper Middle ORS, although normal components may be found within the Eday Group. There are sufficient data points for the upper Middle ORS to show that the distribution is approximately Fisherian; the one outlier is site ROD22 from the Eday Marls which is suspected of carrying a DRM and hence possibly recording secular variation.

The same data are shown at the formation or group level in fig. 9.2, based on the formation mean directions given in table 9.1. The Eday Group, as a result of intensive sampling, is subdivided into five formations. Fig. 9.2 also shows other directions from north of the Great Glen Fault which have been proposed as an estimate of the late Silurian or Devonian geomagnetic field with respect to northern Scotland. Respective merits of these and other studies have been discussed at depth in relevant chapters. Only those which are considered by this author to be valid and sufficiently precise are included; reasons for rejection of other data include improper statistical analysis and/or arbitrary component selection procedures.

It is interesting to compare directions found for the Lower ORS (Storhaug & Storetvedt 1985 and this study) and

F.R.S. LIBRARY

TABLE 9.1

PRIMARY MEAN DIRECTIONS (Dip Corrected)

Formation	Age	Specimen Weighting Dec.	Inc.	N	k	a_{95}	Site weighting Dec.	Inc.	N	k	a_{95}	Palaeopole position[1] Lat.	Long.	dp	dm	Source tables
Upper ORS	Du	353.3	-15.7	7	31	11	-	-	1	-	-	183.1E	23.9N	5.8	11.3	4.12
Upper Eday Sst.	Dm	193.6	41.6	23	8	11	191.9	38.6	4	14	26	164.7E	6.1N	8.6	14.1	4.7
Eday Marls	Dm *	198.3	31.4	31	7	10	197.3	32.7	6	11	21	149.1E	12.9N	6.4	11.4	4.7,4.8
Middle Eday Sst.	Dm *	186.8	24.4	22	17	8	187.4	28.8	7	29	11	170.2E	17.8N	4.4	8.3	4.7,4.8
Eday Volcanics	Dm	191.8	36.7	48	12	6	194.3	36.9	7	46	9	165.7E	10.3N	4.3	7.3	4.7
Lower Eday Sst.	Dm	192.0	35.8	14	14	11	182.8	34.0	3	18	30	165.9E	10.2N	7.5	12.9	4.7
John o'Groats	Dm	213.1	29.0	7	10	20	-	-	1	-	-	144.4E	11.1N	12.0	21.8	8.6
Lower ORS	Dl-m	013.0	-12.2	58	14	5	014.2	-10.6	8	14	14	162.5E	24.6N	2.7	5.3	4.1,4.3

*: Components of normal polarity converted to reversed equivalent
(1): Unit weighting to specimens

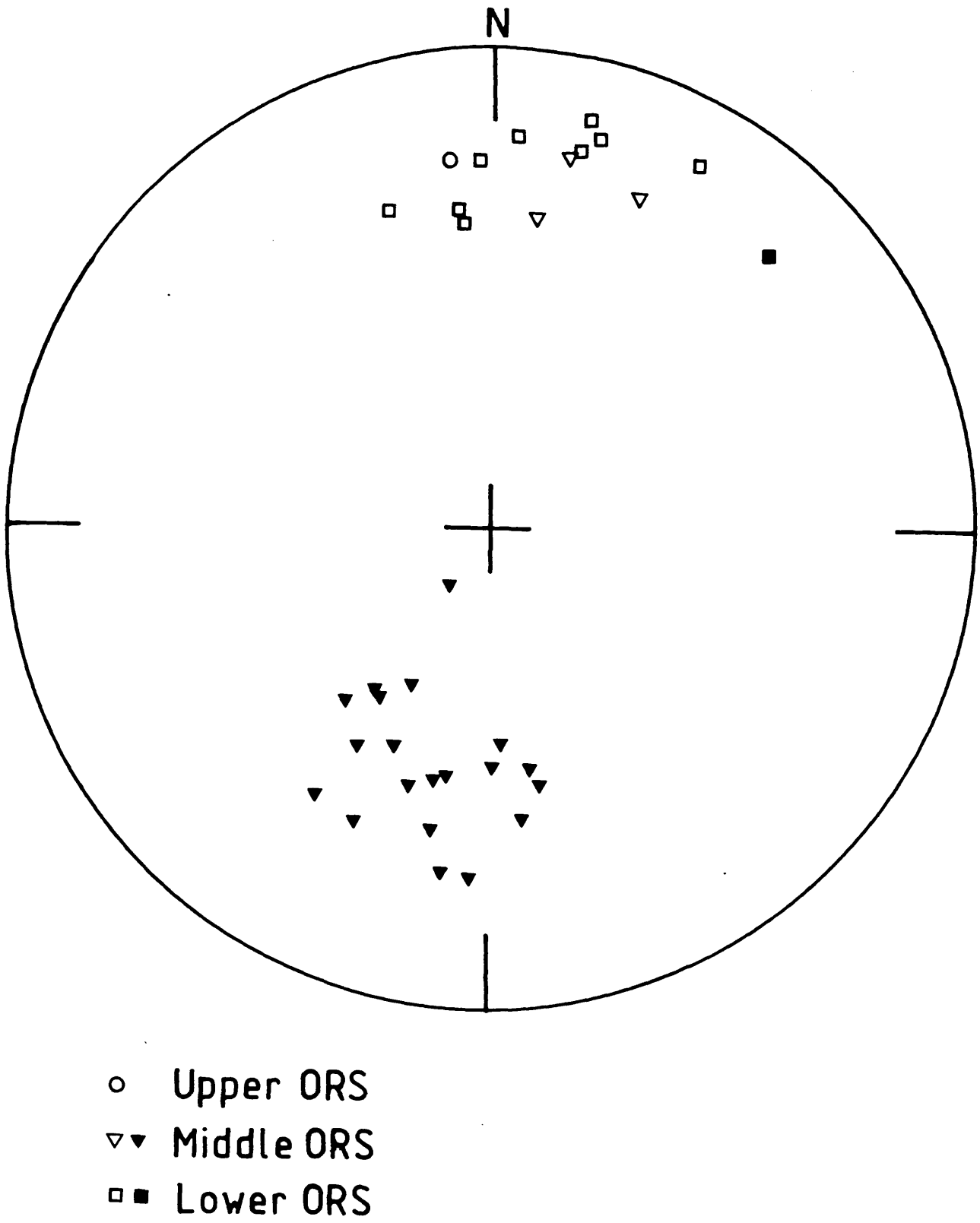


Fig. 9.1. Orcadian Basin: site mean directions for all suspected syngenetic remanence components. Categorised into Lower ORS sediments (largely Emsian), Middle ORS (both lavas and sediments, all of upper Middle ORS age), and Upper ORS (sediments). All corrected for tectonic dip as appropriate.

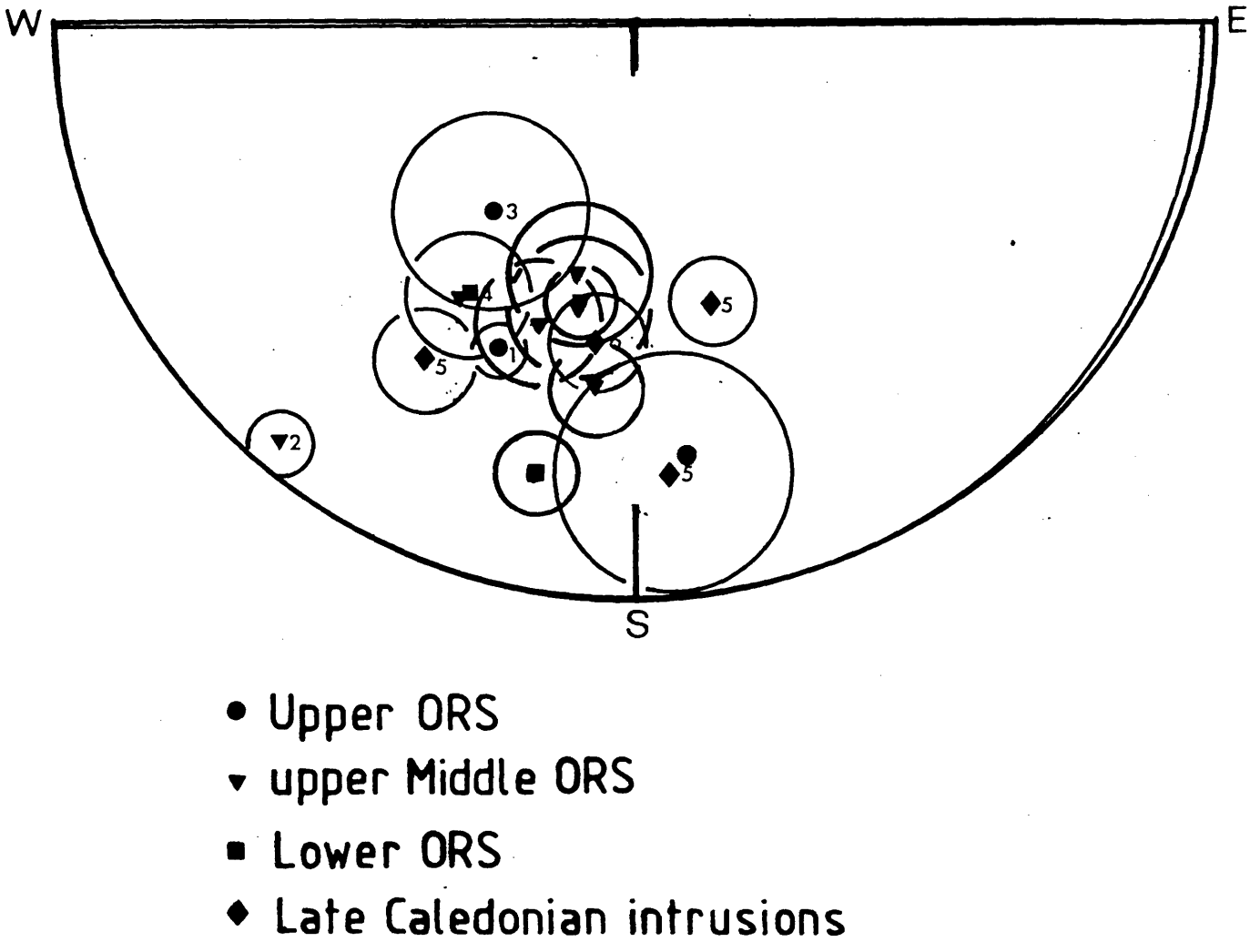


Fig. 9.2. Formation mean directions for the ORS of the Orcadian Basin (this study). Lower ORS includes Sarclet, Berriedale and Braemore. Upper Middle ORS directions are for five discrete formations from the Eday Group (see table 9.1), all with 95% error circles, and also from one site in the John o'Groats Sandstone (with no error circle). Upper ORS is represented by the one site from Dornoch showing a primary remanence (no error circle).

Overlay shows published estimates of primary late Silurian-Upper ORS directions from north of the GGF, with associated error circles. References (1) Storetvedt & Meland 1985; Hoy Lavas, northerly direction (see text); (2) Storetvedt & Torsvik 1985; Esha Ness Ignimbrite, Shetland; (3) Morris et al 1973; Orkney-Shetland Lavas; (4) Storhaug & Storetvedt 1985; Sarclet Sandstone, group I; (5) Turnell & Briden 1983; Borrolan Ledmoreite, Borrolan Pseudoleucite and Loch Ailsh; (6) Turnell 1985; Ratagan. Other published data considered unsatisfactory.

also for the upper Middle and Upper ORS (Morris et al, 1973; Storetvedt & Meland, 1985 and this study). It has been suggested (chapters 3 and 4) that there is sufficient evidence in this study to show that the directions believed to represent a syngenetic remanence do, in fact, do so. Concurrence with the above-mentioned studies is supportive evidence that this is indeed the case.

Mean primary directions derived for the upper Middle ORS are thus proposed as a faithful recorder of the contemporaneous geomagnetic field with respect to northern Scotland.

The status of mean directions from the Lower ORS is not quite as clearcut, largely as they are in significant disagreement with results from south of the GGF. This will be discussed in the following section. There is no reason to suspect that the single site mean direction from the Upper ORS of Dornoch is not a primary direction.

Intrusive igneous bodies of the Northern Highlands constitute the only additional source of late Silurian to Lower Carboniferous palaeomagnetic data from north of the GGF (Turnell & Briden, 1983; Turnell, 1985). Correlation with the sedimentary sequence is impossible but it is interesting to note a general similarity between the intrusions and sediments (see also the next section). Doubts are expressed by the original author (Torsvik, 1984, p176) about the reliability of mean directions derived from the Helmsdale and Foyers Granites so these are not considered further.

9.1.2. Great Britain

Palaeopole positions corresponding to formation mean directions for the ORS of the Orcadian Basin (as listed in

table 9.1) are shown in relation to similar poles from the remainder of the British Isles in fig. 9.3.

One of the most well-defined sections of the British Palaeozoic PWP is that based largely on early ORS lavas from the Midland Valley area. These can be seen to group closely around a palaeopole position of longitude 140-150°E and of very low inclination. Very little reliable data is available for the period between this and the early Carboniferous.

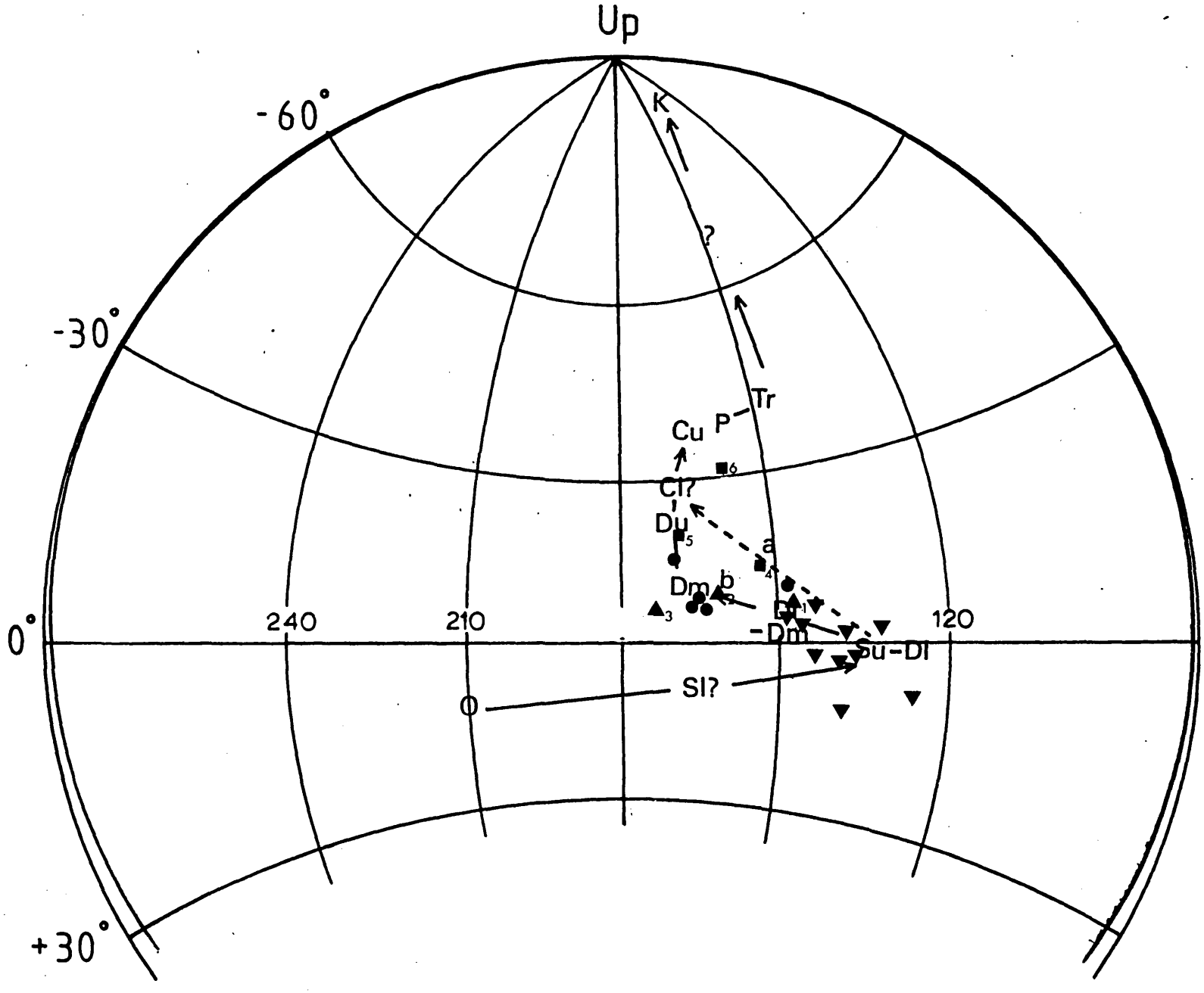
Lower ORS poles from the Orcadian Basin can be seen to have a more westerly longitude (on the given projection) than poles from the Midland Valley. It is suggested that the difference is largely a result of the significant age difference between them. The Midland Valley Lavas are probably of Geddinian or even Ludlovian age, whereas the Sarclet Group is considered to be uppermost Emsian or Eifelian and the Berriedale-Braemore sediments (also included in the Lower ORS mean) are even younger than this (fig. 4.3).

Upper Middle ORS poles plot in a broadly comparable, or more westerly, position compared with the Lower-basal Middle ORS. They suggest that the palaeopole position was of longitude 165-175°E and of latitude 5-10°N at the time with respect to the Orcadian Basin. Such a pole is consistent with the very few Upper ORS poles for the British Isles (poles 4,5 and 6, of which 4 should be considered to be somewhat unreliable due to non-rigorous laboratory treatment).

The main importance of the results reported here is that they demonstrate that the PWP followed a path more resembling 'b' (solid) than 'a' (dashed) during the Middle to Upper ORS. Prior to this study there was no certainty

Fig. 9.3. Portion of Upper Palaeozoic PWP for Great Britain. Formation mean directions: ▼ ?late Silurian-basal ORS volcanics of southern Scotland: source references Embleton, 1968; Briden, 1970; McMurry, 1970; Sallomy & Piper, 1973; Thorning, 1974; Latham & Briden, 1975; Piper, 1975; Torsvik, 1985. ▲ ?upper Lower ORS to basal Middle ORS sediments. Source references (1) Storhaug & Storetvedt 1985; Sarclet Group; (2) This study, Sarclet Group; (3) Turner & Archer 1975, Gamrie Outlier. ● upper Middle ORS; This study (see fig. 9.2 and table 9.1). ■ Upper ORS; source references (4) Storetvedt & Meland 1985, Hoy Volcanics; (5) Nairn, 1960; Jedburgh Sandstone; (6) Morris et al 1973; Bristol area.

Overlay shows an approximate PWP based on these observations. Earlier (pre-Upper Silurian) from Briden et al 1984; Later (post-Upper Devonian) from McElhinny 1973 and Turner & Tarling 1975. Uncertainty exists regarding the Lower Silurian. the Lower Carboniferous and the Jurassic. Symbols all shown solid irrespective of polarity.


Up
-60°
-30°
0°
+30°
240
210
120
K
?
Tr
P
Cu
Cl?
Du
Dm
a
b
-Dm
Su-Dl
Sl?
0

regarding the British PWP between basal ORS and basal Carboniferous.

It will be apparent that palaeomagnetic detection of any post-Silurian transcurrent movement on faults (such as the Great Glen Fault) will, in the author's opinion, have to be based on the data shown in fig. 9.3 alone. This is a substantially smaller data base than has often been used for such purposes in the past. There are little or no data of comparable age to the Midland Valley Lavas to the north of the GGF and little data of comparable age to that of the Orcadian Basin to the south of the fault. As fairly rapid APW would appear to have occurred during the Lower-Middle Devonian it is invalid to make comparisons across the fault using this data.

It is thus suggested that there is no palaeomagnetic basis at present for attempting to quantify transcurrent fault displacements in northern Scotland; if geological estimates of fault displacement (e.g. Smith & Watson, 1983) are valid then this will always be the case due to intrinsic uncertainties of the method.

Comparison of these data with supposed ORS poles from outside the British Isles is not attempted. This is for two reasons. The first is that inter-continental correlation of the ORS is very difficult due to the paucity of marine fossils within the predominantly continental facies of sediments typical of the time. Additionally, it is becoming apparent that much of the data for the ORS, particularly of N. America but also for much of Western Europe and the USSR, has been affected by Kiaman remagnetisation. As it is difficult or impossible to judge upon the validity or otherwise of published 'ORS' directions (particularly those

derived before the need for stringent laboratory treatment became apparent) then any attempted global reconstructions would be fraught with uncertainty.

9.2. Post-ORS directions in context

9.2.1. Remagnetised sediments

Site mean directions for all sediments which are considered to carry a post-ORS ancient remanence are shown in fig. 9.4 (based on data summarised in table 9.2).

With the exception of the Upper ORS (based on two sites only), it can be seen that the formation means lie on an approximately north-south trajectory. As this is not a Fisherian distribution, the overall mean direction is of questionable validity.

It would appear that formation means may define true APW, reflecting long-term acquisition of a secondary remanence (on the basin-wide, if not the local, scale). This could also invalidate mean directions at the formation level, as contemporaneous sediments may have been remagnetised in geographically discrete areas at different times.

It has been suggested (chapter 6) that there is strong evidence that the Lower ORS and the lower Middle ORS (i.e. lacustrine sediments) were remagnetised via the diagenesis of ferroan carbonates. On a first examination it would appear that the mean direction for these two groups of sediment are of significantly lower inclination than other (younger) sediments. However, previously-published secondary directions from similar rocks (fig. 9.4 overlay) do not show such a trend so it may not be valid.

Most formation means are of significantly shallower inclination (and hence older) than previously reported; this

TABLE 9.2

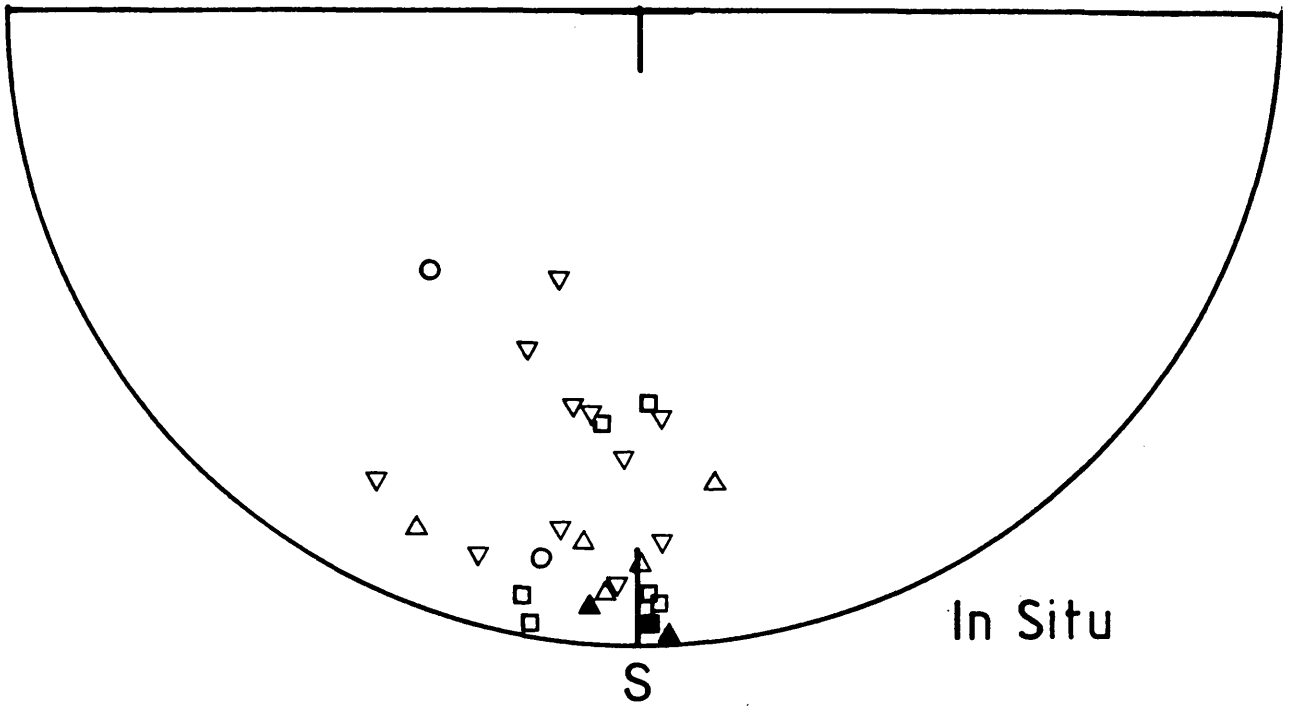
SECONDARY MEAN DIRECTIONS (SEDIMENTS: In Situ)

Formation	Age	Specimen weighting Dec.	Inc.	N	k	a_{95}	Site weighting Dec.	Inc.	N	k	a_{95}	Palaeopole position Lat.	Long.	dp	dm	Source tables
Upper ORS	Du	205.4	-24.4	10	10	16	202.7	-21.8	2	-	-	143.6E	40.5N	9.4	17.6	4.12
Upper Eday Sst.	Dm	194.4	-37.1	13	12	13	187.5	-33.4	4	12	27	155.9E	50.2N	8.7	14.8	4.9
Eday Marls	Dm	185.0	-15.5	26	19	7	183.4	-12.9	4	69	11	170.8E	38.6N	3.6	6.9	4.9
Middle Eday Sst.	Dm	193.3	-19.2	30	18	6	193.4	-18.8	6	36	11	159.8E	39.6N	3.5	6.7	4.9
lower Middle ORS	Dm	180.9	-7.1	54	12	6	183.3	-6.1	7	45	9	175.6E	34.6N	2.9	5.7	5.5
Lower ORS	Dl	182.3	-8.7	42	16	6	182.5	-8.5	7	40	10	173.6E	36.1N	2.9	5.7	4.1,4.3, 4.12
Mean ORS		186.1	-14.1	175	12	3	186.8	-14.7	30	22	6	168.6E	38.7N	1.7	3.3	

Fig. 9.4. Secondary directions in sediments of the Orcadian Basin. (a) Site mean directions. See table 9.2 for source tables. (b) Formation mean directions with overall mean direction for the ORS. Datails given in table 9.2.

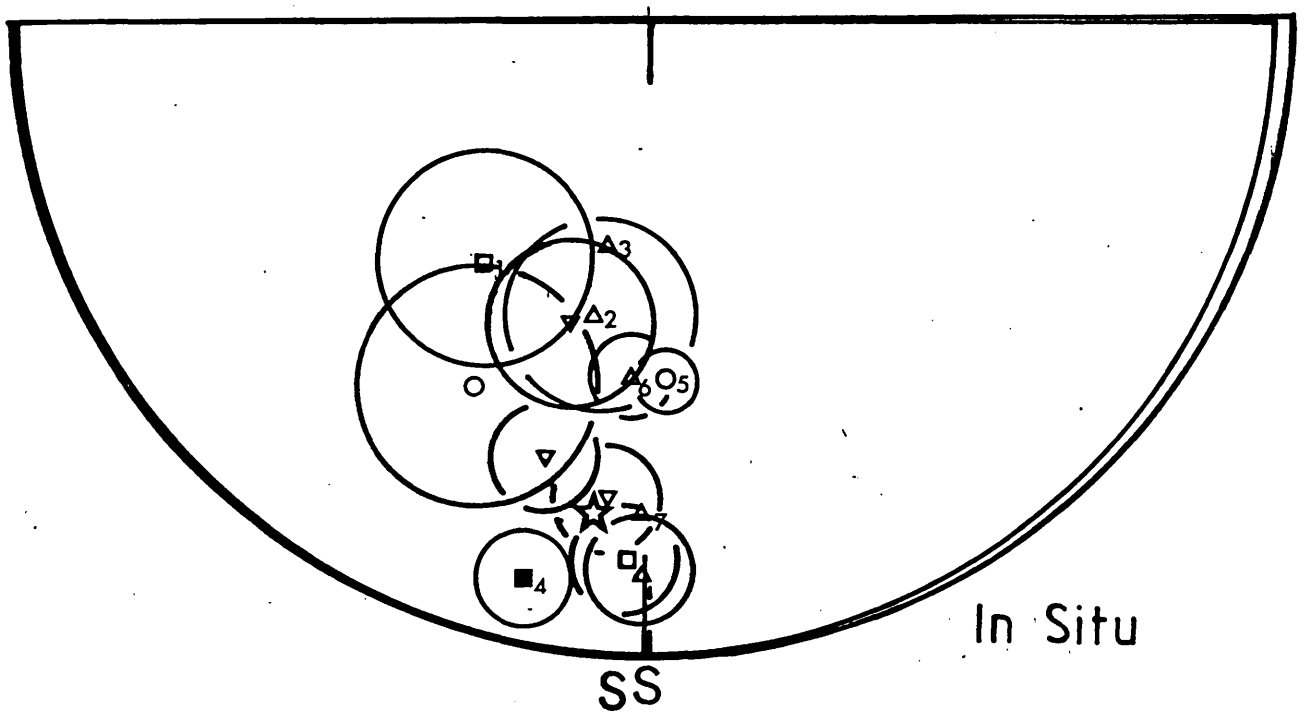
Overlay shows previously-determined secondary directions from the ORS of northern Scotland. (1) Turner & Archer 1975, Gamrie Outlier; (2) Tarling et al 1976, L-M ORS clastics; (3) Turner 1977, Achanarras Limestone; (4) Storhaug & Storetvedt 1985, Sarclet Group; (5) Storetvedt & Meland 1985, Upper ORS of Hoy; (6) Torsvik et al 1983, Helmsdale Granite; (7) Eustance 1981; Achanarras Limestone, estimated direction only. Error circles shown only for those data for which they are given in the original publication.

(a) Site mean directions



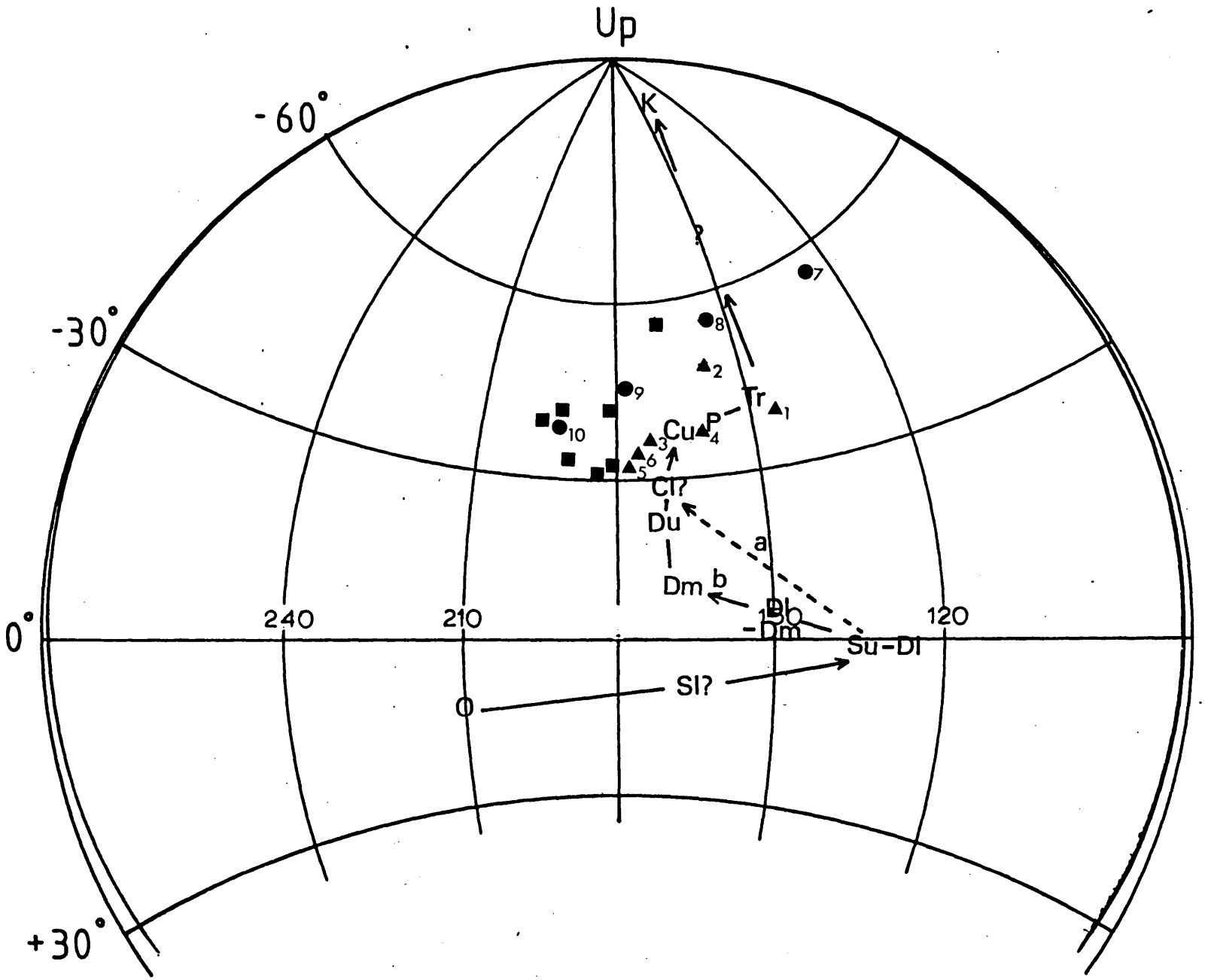
○ Upper ORS
▽ upper Middle ORS
▲ △ lower Middle ORS
■ □ Lower ORS

(b) Formation mean directions



☆ Mean ORS direction ($\alpha = 3^{\circ}$)

Fig. 9.5. Pole positions for secondary sediment remanence directions and for igneous bodies and their aureoles. ■ Dyke margins. ▲ Sediment remagnetisations: (1) Upper ORS (2) Upper Eday Sandstone (3) Eday Marls (4) Middle Eday Sandstone (5) lower Middle ORS (lacustrine sediments) (6) Lower ORS. ● Intrusive igneous vents: (7) Duncansby Ness (8) John o'Groats Sandstone (9) Burray Vent (10) Little Clett Vent.


Up
-60°
-30°
0°
+30°
240
210
120
K
?
Tr
P
Cu
Cl?
Du
Dm
a
b
Pl
Bb
Dm
Su-Dl
Sl?
0
1
2
3
4
5
6
7
8
9
10

applies particularly to the lacustrine sediments. It is suggested that this may largely be a function of the larger sample size and more intensive demagnetisation procedures (and hence better multicomponent resolution) in the present study.

Comparison of palaeopole positions corresponding to the formation means given in table 9.2 with the PWP derived in fig. 9.3 shows a close coincidence with most of the Upper Carboniferous/Lower Permian to Triassic portion of the path (fig. 9.5). Also of particular note is that every secondary remanence direction is of reversed (southerly) polarity. If the apparent time span suggested above is valid then these facts together would tend to suggest that remagnetisation occurred largely or entirely during the Kiaman magnetic interval. This lasted for 50-60Ma, from the Stephanian (late Carboniferous) to late Permian or even early Triassic (McElhinny 1973, section 4.2.3). Within this time period, large-scale plate movements (and hence net APW) could have occurred, as could very long-term diagenetic processes as described in this thesis.

9.2.2. Intrusive igneous activity

Mean directions and corresponding palaeopoles for intrusive igneous rocks (and their aureoles) are given in table 9.3. Comparison of poles from these rocks with those from remagnetised sediments (fig. 9.5) shows that dyke emplacement was contemporaneous with, or possible slightly earlier than, most of the oxidative remagnetisation of sediments. Dyke poles cluster around the Lower-Mid Carboniferous mean pole position, although it is not considered valid to attempt to use the dykes to refine the APW curve. This is for two reasons; firstly that each dyke

TABLE 9.3

INTRUSIVE IGNEOUS BODIES (In Situ)

Description	Mean Dec.	Inc.	N	k	a_{95}	Lat.	Long.	dp	dm	Source tables
Duncansby Vent	211.2	-52.2	41	35	3.8	124E	57N	3.6	5.2	8.2
John o'Groats Gp.	193.6	-46.0	15	16	10.0	154E	57N	12.0	21.8	8.6
Burray Vent	181.7	-32.8	8	29	10.4	175E	49N	6.6	11.7	8.7
Clett Vent	168.5	-19.8	6	8	25.9	192E	41N	14.2	27.1	8.7
Dykes	176.0	-24.1	74	17	4.1	182E	44N	2.3	4.3	7.4

may represent only a 'spot reading' which has not negated the effects of secular variation and secondly that it is not proven that the intrusion of dyke swarm was only of limited duration. Each dyke would have to be individually dated until this became apparent.

The pole for the Duncansby Vent falls closest to the mid-Upper Triassic mean pole. This would suggest a somewhat later date than that indicated by radiometric dating (MacIntyre et al 1981; see chapter 8).

9.3. Relevance to the continental remagnetisation hypothesis

9.3.1. A model for Kiaman remagnetisation

A substantial part of this thesis has been devoted to studies of the background to palaeomagnetic remanence, using methods and techniques which are not part of a typical palaeomagnetic investigation. This has been aimed largely at investigating the cause, extent and timing of remagnetisation, particularly of sediments. Of the numerous mechanisms by which a secondary remanence could have been generated in the sediments studied, some have been shown not to be applicable, some to have possibly played a major role and some to be of uncertain status. These will be summarised below.

(a) Detrital oxides. All of the sediments studied carry detrital 'opaques' to a greater or lesser degree, with the exceptions of lacustrine sediments of Middle ORS age and occasional sites in very mature sandstones which rarely show a stable ancient remanence. In all of the cases analysed, there is no evidence to suggest that any detrital grains have escaped oxidation at some stage of their history. Many show conclusive evidence of this oxidation (see plate 6.1). Analytical data would thus suggest that

magnetite is rare or absent.

A very small number of sites are suspected of carrying a primary magnetite remanence, this conclusion being based on palaeomagnetic and rock magnetic evidence alone. These sediments are, without exception, very fine grained. Unfortunately suitable material was not available from these two or three sites to confirm the presence of magnetite microscopically.

The majority of sites which carry a (hematitic) primary remanence are believed to have acquired this during early diagenetic oxidation of iron oxides, originally deposited as magnetite. This conclusion is based largely on the occurrence of closely associated green and red sediments of which the former carry a magnetitic component of normal polarity and the latter, which from field evidence would appear to have suffered post-depositional reddening, carry a hematitic remanence of similar age but opposite polarity.

The extent of early (syn-depositional) oxidation will largely be a function of original sedimentary environment, organic matter content, and physical characteristics of the sediment.

Sediments which carry only a later (remagnetised) hematite component may have been able to escape early oxidation (due to rapid burial, high organic content etc.). During the Kiaman, they were subjected to essentially similar physico-chemical conditions to those found on the earth's surface (i.e. vadose water system, high Eh etc.). Any magnetite which may have escaped syngenetic oxidation would now have a 'second chance' to become oxidised to hematite and thus acquire a Kiaman hematitic remanence.

(b) Secondary oxides. Secondary iron-titanium oxides,

readily distinguishable from primary grains on the basis of morphology, are widespread, particularly in remagnetised sediments. The source of the iron cannot be conclusively proven, although a late generation of at least some is suggested by the fact that it may grow into secondary porosity space, formed during late carbonate cement dissolution.

It is suggested that much of the iron in secondary oxide growths was sourced from ferroan carbonates during their diagenesis or dissolution by free-flowing groundwaters. Other sources, such as decomposing detrital grains or the detrital clay fraction, cannot be ruled out.

(c) Carbonates. As mentioned above, ferroan carbonates (which may originally have incorporated much of the free iron from decomposing detrital grains) may have acted as a delayed source of iron oxides in many clastic sediments. More concrete evidence of the role of ferroan carbonate diagenesis is found elsewhere, particularly in finer-grained clastic sediments of the Lower ORS and also in lacustrine sediments, both of which have been partially or fully remagnetised. Here, fine-scale calcitisation of ferroan dolomite can be seen; this has presumably been preserved due to limited fluid flow through the rock. It is suggested that the process acted as the chief agent of remagnetisation in such sediments.

Of particular importance are specimens which show both syngenetic and remagnetised hematite components with discrete stability ranges. Such sediments may have been fully oxidised during or shortly after deposition, acquiring a hematitic CRM from oxidation of detrital magnetite. Free iron in the sediment could have been incorporated into

ferroan dolomite which has later been calcitised and/or removed in solution, leaving a residue of iron oxide. This will tend to have differing physical characteristics to oxidised magnetite and hence they may well have discrete stability ranges.

This provides an important mechanism for the remagnetisation of sediments which may have been fully oxidised during deposition, as it does not involve postponement of oxidation (c.f. Tarling et al, 1976). A close link with free-flowing groundwater is likely; this could explain why the John o'Groats Sandstone (which is generally mature and probably oxidised during deposition) did not acquire a secondary remanence until the intrusion of the Duncansby Vent. Circulating hydrothermal fluids around this body may have effected the calcitisation/dissolution process resulting in a sediment remanence contemporaneous with the vent.

(d) Sheet silicates. Detrital sheet silicates, especially biotite, have often been oxidised and show iron oxides within cleavage planes. Oxidised portions of such grains have also lost potassium, suggesting that it was a vermiculisation process rather than high-temperature oxidation in the parent igneous body. It is suggested that much of the oxidation took place prior to deposition, as the occurrence of oxidised biotite shows no correlation with remanence characteristics. It is thus not an important mechanism of post-depositional remagnetisation.

(e) Fine-particle hematite. The role of fine-particle hematite, both as grain coatings and within interstitial clay material, is unclear largely due to the difficulty of performing chemical demagnetisation. Much is considered to

have originated through the dehydration of precursor goethite; this will generally be sufficiently fine-grained to behave superparamagnetically and hence not contribute to the stable remanence. Since dehydration probably took place synchronously with magnetite oxidation, the palaeomagnetic contribution of fine-particle hematite would be difficult to assess even if it was capable of carrying a stable remanence.

(f) Igneous bodies. Although intrusive igneous bodies were originally thought to have played a significant role in the remagnetisation of the Orcadian Basin, detailed study has shown that they imposed only limited effects on the surrounding sediment (with the exception of the Duncansby Vent which may have had a more profound influence on the John o'Groats Sandstone, as discussed above).

9.3.2. Extension to Laurentia-Baltica

The model outlined above for Kiaman remagnetisation of the Orcadian Basin may have relevance, with modifications as appropriate, to Kiaman remagnetisations elsewhere in the Laurentia-Baltica continent. The close association of such remagnetisations with carbonates or carbonate-bearing rocks has been noted before (section 2.4, 2.6). Although the calcitisation of ferroan dolomite has not previously been proposed as an important mechanism of remagnetisation on a continental scale, it would appear that it may play a very important role. The reason that it has only rarely (Elmore et al, 1985) been associated with Kiaman remagnetisation may

largely be one of the usual expectation that detrital grains, or occasionally ferromagnesian minerals, will play the dominant role in diagenetic remagnetisation.

9.4. Summary

Detailed palaeomagnetic investigation of varied sediments, contemporaneous lavas and intrusive igneous rocks has demonstrated the close association of primary, secondary and recent components, even on a very small scale. The study has demonstrated the absolute necessity of a detailed demagnetisation procedure in resolving a complex, multi-component remanence such as that usually found in Upper Palaeozoic sediments.

Suspected primary components have been derived from an extrusive lava and its baked contact, which have escaped later oxidation due to their very low permeability. Contemporaneous sediments show an intimate association of primary and secondary components. The former is considered to result chiefly from the early diagenetic oxidation of detrital magnetite, which may survive in unreddened sediments. Oxidation is intimately associated with reddening, which is believed to be largely due to the dehydration of iron oxyhydroxides.

Secondary components may have been acquired through the delayed oxidation of magnetite, which escaped early diagenesis as a result of its original sedimentary environment and conditions. An important additional mechanism for the delayed production of hematite is the diagenesis of ferroan carbonates, particularly the calcitisation of ferroan dolomite. This could operate even in sediments of very mature detrital mineralogy, which may carry an additional primary component of contrasting

stability range. Ferroan carbonate diagenesis is more apparent in fine-grained sediments of the Lower ORS and in lacustrine sediments, both of which are partially or wholly remagnetised. They are believed to have acquired much of their Kiaman remanence by this mechanism.

The environment of remagnetisation was one of extreme aridity associated with the low latitude of the continent during the Kiaman. A very depressed water table created conditions resembling those of the surface, under which oxidative diagenesis could occur to great depths, enabling a pervasive oxidative remagnetisation to occur.

REFERENCES

Addison,F.T., Turner,P. & Tarling,D.H., 1985. Magnetic studies of the Pendleside Limestone: evidence for remagnetisation and late-diagenetic dolomitisation during a post-Albian normal event. J. Geol. Soc. Lond. 142 p983-994

Ahmad,M.V., 1967. Some geophysical observations on the Great Glen Fault. Nature 213 p275-277.

Akimoto,T., Kinoshita,H. & Furuta,T., 1984. Electron probe microanalysis study on processes of low-temperature oxidation of titanomagnetite. Earth Planet. Sci. Lett. 71 p263-278.

Alderman,A.R. & Skinner,C.W., 1957. Dolomite sedimentation in the south-east of South Australia. Amer. J. Sci. 255 p561-567.

Al-Hashimi,W.S. & Hemingway,J.E., 1973. Recent dedolomitisation and the origin of rusty crusts of Northumberland. J. Sed. Petrol. 43 p82-91

Allen,P.A., 1981. Devonian lake margin environments and processes, S.E. Shetland, Scotland. J. Geol. Soc. Lond. 138 p1-14.

Anderson,W. & Dunham,K.C., 1953. Reddened beds in the coal measures beneath the Permian of Durham and south Northumberland. Proc. Yorks. Geol. Soc. 29 p21-32.

Anderton,R., Bridges,P.H., Leeder,M.R. & Selwood,B.W., 1979. A dynamic stratigraphy of the British Isles- a study in crustal evolution. George, Allen and Unwin, 301pp.

Anon, 1974. Putting the Highlands, a game for all comers. New Scientist 61 p4

Armstrong,M., 1977. The Old Red Sandstone of Easter Ross and the Black Isle. (in) The Moray Firth area geological studies, ed. Gill,G. Inverness Field Club.

As,J.A., 1960. Instruments and measuring methods in palaeomagnetic research. Med. Verh. Kon. Meteorol. Instit. 78

Astin,T.R., 1982. The Devonian geology of the Walls Peninsula, Shetland. PhD thesis, Univ. of Cambridge (unpubl.)

----------, 1985. The palaeogeography of the Middle Devonian Lower Eday Sandstone, Orkney. Scott. J. Geol. 21 p353-376.

Back,W., Hanshaw,B.B., Plummer,L.N., Rahn,P.H., Rightmire,C.T. & C.T., 1985. Process and rate of dedolomitisation: mass transfer and ^{14}C dating in a regional carbonate aquifer. Geol. Soc. Am. Bull. 94 p1415-1429.

WATTS LIBRARY

Bacon,M. & Chesher,J., 1975. Evidence against post-Hercynian transcurrent movement on the Great Glen Fault. Scott. J. Geol. 11 p79-82.

Bailey,E.B., 1926. Subterranean penetration by a desert climate. Geol. Mag. 63 p276-280.

Baker,P.A. & Burns,S.J., 1985. Occurrence and formation of dolomite in organic-rich continental margin sediments. Bull. Am. Assoc. Petrol. Geol. 69 p1917-1930.

Barber,A., 1985. A new concept of mountain building. Geology Today 1 p116-121.

Barker,A.J. & Gayer,R.A., 1985. Caledonide-Appalachian tectonic analysis and evolution of related rocks. (in) The tectonic evolution of the Caledonide-Appalachian orogen, ed. Gayer,R.A. (Vieweg & Sohn).

Baxter,A.N. & Mitchell,J.G., 1984. Camptonite-monchiquite dyke swarms of Northern Scotland; age relationships and tectonic implications. Scott. J. Geol. 20 p297-308

Beckinsale,R.D. & Obradovitch,J.D., 1973. Potassium-Argon ages for minerals from the Ross of Mull, Argyllshire, Scotland. Scott. J. Geol. 9 p147-156

Berner,R.A., 1969. Goethite stability and the origin of redbeds. Geochim. Cosmochim. Acta 33 p267-273.

----------, 1984. Sedimentary pyrite formation: an update. Geochim. Cosmochim. Acta 48 p605-615.

---------- & Raiswell,R., 1983. Burial of organic carbon and pyrite sulphur in sediments over Phanerozoic time: a new theory. Geochim. Cosmochim. Acta 47 p855-862.

Bott,M.H.P., 1981. Crustal doming and the mechanism of continental rifting. Tectonophysics 73 p1-8.

----------. & Watts,A.B., 1970. Deep sedimentary basins proved in the Shetland-Hebridean continental shelf and margin. Nature 225 p265-268.

Bramlette, M.N., 1941. The stability of minerals in sandstone. J. Sed. Petrol. 11 p32-36.

Brewer,J.A. & Smythe,D.K., 1984. MOIST and the continuity of crustal reflectors along the Caledonian-Appalachian orogen. J. Geol. Soc. Lond. 141 p105-120.

Briden,J.C., 1970. Palaeomagnetic results from the Arrochar and Garabal Hill - Glen Fyne igneous complexes, Scotland. Geophys. J. Roy. Astron. Soc. 21 p457-470.

---------- & Arthur,G.R., 1981. Precision of measurement of remanent magnetisation. Can. J. Earth Sci. 18 p527-538.

---------- & Mullan,A.J., 1984. Superimposed Recent, Permo-Carboniferous and Ordovician palaeomagnetic remanence in the Builth volcanic series, Wales. Earth Planet. Sci. Lett. 69 p413-421.

----------, Turnell,H.B. & Watts,D.R., 1984. British palaeomagnetism, Iapetus Ocean and the Great Glen Fault. Geology 12 p428-431.

Brown,G., 1961. The x-ray identification and crystal structure of clay minerals. Min. Soc. Lond. pp370-387: Iron oxides and hydroxides.

Browne,J.F., 1975. Potassium-Argon evidence of a Permian age for the camptonite dykes, Orkney. Scott. J. Geol. 11 p259-262.

Carroll,D., 1958. The role of clay minerals in the transportation of iron. Geochim. Cosmochim. Acta 14 p1-28.

Chamalaun,F.H., 1964. Origin of the secondary magnetisation of the Old Red Sandstone of the Anglo-Welsh Cuvette. J. Geophys. Res. 69 p4327-4337.

---------- & Creer,K.M., 1964. Thermal demagnetisation studies on the Old Red Sandstone of the Anglo-Welsh Cuvette. J. Geophys. Res. 69 p1607-1616.

Chapman,N.A., 1975. An experimental study of spinel-clinopyroxenite xenoliths from the Duncansby Ness vent, Caithness, Scotland. Contrib. Mineral. Petrol. 51 p223-230.

Chesher,J.A., 1977. A review of the offshore geology of the Moray Firth. (in) The Moray Firth area geological studies, ed. Gill, G. (Inverness Field Club).

Chevalier,R., 1951. Proprietes magnetiques de l'oxyde ferrique rhombohedrique (α-Fe_2O_3). J. Phys. Rad. 12 p178-188.

Chilingar,G.V. & Bissell,H.J., 1963. Is dolomite formation favoured by high or low pH? Sedimentology 2 p171-172.

Collins,A.G. & Donovan,R.N., 1977. The age of two Old Red Sandstone sequences in southern Caithness. Scott. J. Geol. 13 p53-57.

Collinson,D.W., 1965a. Depositional remanent magnetisation in sediments. J. Geophys. Res. 70 p4663-4668.

----------, 1965b. Origin of remanent magnetisation and initial susceptibility of certain red sandstones. Geophys. J. Roy. Astron. Soc. 9 p203-217.

----------, 1974. The role of pigment and specularite in the remanent magnetism of red sediments. Geophys. J. Roy. Astron. Soc. 38 p253-264.

----------, 1980. An investigation of the scattered remanent magnetisation of the Dunnet Head Sandstone. Geophys. J. Roy. Astron. Soc. 62 p393-402.

----------, 1982. Methods in rock magnetism and palaeomagnetism: Techniques and instrumentation. Chapmann & Hall, London. 500pp.

Courtillot,V., Chambon,P., Matte,P. & Feist,R., 1985. Remagnetisation of Devonian limestones from the Montagne Noir (S. France). Terra Cognita 5 p140 (abstr).

Craig,G.Y., 1956. The Lower Carboniferous outlier of Kirkbean, Kirkudbrightshire. Trans. Geol. Soc. Glasg. 22 p113-132.

Crampton,C.B. & Carruthers, R.G., 1914. The geology of Caithness. (Mem. Geol. Surv. U.K.)

Creer,K.M., 1957. The NRM of certain stable rocks from Great Britain: (3) The NRM of the Old Red Sandstone of the Anglo-Welsh Cuvette. Philos. Trans. 250A p113-123.

----------, Thomson,R., Molyneux,L. & Mackereth,F.J.H., 1972. Geomagnetic secular variation recorded in the stable magnetic remanence of Recent sediments. Earth Planet. Sci. Letts. 14 p115-127.

----------, 1968. Palaeozoic Palaeomagnetism. Nature 219 p246-250

---------- & Embleton,B.J.J., 1967. Devonian palaeomagnetic pole for Europe and North America. Nature 214 p42-43.

Day,R., 1977. TRM and its variation with grain size: a review. J. Geomagn. Geoelectr. 29 p233-266.

Deer,W.A., Howie,R.A. & Zussman,J., 1962. Rock-forming minerals, vol. V: non-silicates. Longmans, Green & Co., London. 371pp.

---------, ---------- & ----------, 1966. An introduction to the rock-forming minerals. Longmans, Green & co., London. 528pp.

De Groot,K., 1967. Experimental dedolomitisation. J. Sed. Petrol. 37 p1216-1220.

De Souza,H.A.F., 1979. The geochronology of Scottish Carboniferous volcanism. PhD thesis,Univ. of Edinburgh (unpubl.).

---------------, 1982. Age data from Scotland and the Carboniferous time scale. (in) Numerical dating in stratigraphy, ed. Odin,G.S. (John Wiley & Sons ltd) p455-465.

Deutsch,E.R. & Prasad,J.N., 1985. Palaeomagnetism of Early to Mid Ordovician limestones from the Western Platform of Newfoundland. Eos 66 p257 (abstr).

Dewey,J.F., 1983. Plate tectonics and the evolution of the British Isles. J. Geol. Soc. Lond. 139 p371-412.

Dodson,M.H. & McClelland Brown,E.A., 1980. Magnetic blocking temperatures of single-domain grains during slow cooling. J. Geophys. Res. 85B p2625-2637.

Donovan,R.N., 1975. Devonian lacustrine limestones at the margin of the Orcadian Basin, Scotland. J. Geol. Soc. Lond. 131 p489-510

----------, 1980. Lacustrine cycles, fish ecology and stratigraphic zonation in the Middle Devonian of Caithness. Scott. J. Geol. 16 p35-50.

----------, Archer,R., Turner,P. & Tarling,D.H., 1976. Devonian palaeogeography of the Orcadian Basin and the Great Glen Fault. Nature 259 p550-551.

----------, Foster,R.J. & Westoll,T.S., 1974. A stratigraphical revision of the Old Red Sandstone of N.E. Caithness. Trans. Roy. Soc. Edin. 69 p167-201.

---------- & Meyerhoff,A.A., 1982. Comment on 'Palaeomagnetic evidence for a large (2000 km) sinistral offset along the Great Glen Fault in Carboniferous time.' Geology 10 p604-605.

Dubey,A.C. & Dunlop,D.J., 1971. Superparamagnetism in hematites of goethite origin. Eos 52 p191 (abstr).

Dubois,R.L., Peck,C.J. & Elmore,R.D., 1985. Early and Late Palaeozoic remagnetisation of the Upper Cambrian Peerless Formation, central Colorado. Eos 66 p258 (abstr).

Duff,B., 1978. Palaeomagnetic and rock magnetic studies of Lower Palaeozoic rocks on Jersey and the adjacent regions of the Armorican Massif. PhD thesis, Univ. of Leeds (unpubl).

Dunlop,D.J., 1971. Magnetic properties of fine-particle hematite. Annales de Geophysique 27 p269-293.

----------, 1972a. Magnetite: behaviour near the single-domain threshold. Science 176 p41-43.

----------, 1972b. Magnetic mineralogy of unheated and heated red sediments by coercivity spectrum analysis. Geophys. J. Roy. Astron. Soc. 27 p37-55.

----------, 1979. On the use of Zijderfeld vector diagrams in multi-component palaeomagnetic studies. Phys. Earth Plan. Int. 20 p12-24.

----------, 1983. Determination of domain structure in igneous rocks by alternating field and other methods. Earth Planet. Sci. Lett. 63 p353-367.

Edel,J-B. & Coulon,M., 1984. Late Hercynian remagnetisation of Tournasian series from the Laval Syncline, Armorican Massif, France. Earth Planet. Sci. Lett. 68 p343-350

Elmore,R.D., Dunn,W. & Peck,C., 1985. Absolute dating of dedolomitisation by means of palaeomagnetic techniques. Geology 13 p558-561.

---------- & Loucks,V.L., 1985. Remagnetisation of the Cambrian Morgan Creek limestone, central Texas. Eos 66 p258 (abstr).

Embleton,B.J.J., 1968. Laboratory stability tests applied to Devonian lavas from Scotland. Geophys. J. Roy. Astron. Soc. 16 p239-251.

Esang,C.B. & Piper,J.D.A., 1984a. Palaeomagnetism of the Carboniferous E-W dyke swarm in Argyllshire. Scott. J. Geol. 20 p309-314.

---------- & ----------, 1984b. Palaeomagnetism of Caledonian intrusive suites in the Northern Highlands of Scotland: constraints to tectonic movement within the Caledonian orogenic belt. Tectonophysics 104 p 1-34

Eugster,H.P. & Wones,D.R., 1962. Stability relations of the ferruginous biotite, annite. J. Petrol. 3 p82-125.

Eustance,N.B., 1981. Palaeomagnetism and diagenesis of sedimentary rocks. PhD thesis, Univ. of Newcastle-Upon-Tyne. (unpubl.)

Evamy,B.D., 1963. The application of a chemical staining technique to a study of dedolomitisation. Sedimentology 2 p164-170.

----------, 1967. Dedolomitisation and the development of rhombohedral pores in limestone. J. Sed. Petrol. 37 p1204-1215.

Eyles,V.A. & MacGregor,A.G., 1952. The Great Glen crush belt. Geol. Mag. 89 p426-436.

Fannin,N.G.T., 1970. The sedimentary environment of the Old Red Sandstone of Western Orkney. PhD thesis, Univ. of Reading (unpubl.)

Farmer,V.C., Russell,J.D., McHardy,W.T., Norman,A.C.D., Alrichs,J.L. & Rimsaite,J.Y.H., 1971. Evidence for loss of protons and octohedral iron from oxidised biotites and vermiculites. Min. Mag. 38 p121-137.

Fassell,V.A. & Kniseley,R.N., 1974. Inductively Coupled Plasma-Optical emission spectroscopy. Anal. Chem. 46 p1110A-1155A.

Fisher,R.A., 1953. Dispersion on a sphere. Proc. Roy. Soc. Lond. 217A p295-305.

Flett,J.S., 1898. The Old Red Sandstone of the Orkneys. Trans. Roy. Soc. Edin. 39 p383-424.

----------, 1900. The trap dykes of the Orkneys. Trans. Roy. Soc. Edin. 39 p865-905.

Flinn,D., 1975. Comment on 'Evidence for post-Hercynian transcurrent movement on the Great Glen Fault.' Scott. J. Geol. 11 p266-267.

Folkman,Y., 1968. Diagenetic dedolomitisation in the Albian-Cenomanian Yagur Dolomite on Mount Carnel (Northern Israel). J. Sed. Petrol. 38 p380-385

Foster,R.J., 1972. Solid geology of N.E. Caithness. PhD thesis, Univ. of Newcastle-upon-Tyne. (unpubl.)

Francis,E.H., 1968. Review of Carboniferous-Permian volcanicity in Scotland. Geol. Rundsch. 57 p219-246.

Frank,J.R., 1981. Dedolomitisation in the Taum Sauk Limestone (Upper Cambrian), southwest Missouri. J. Sed. Petrol. 51 p7-17.

Friedman,I. & Muruta,K.J., 1979. Origin of dolomite in Miocene Monterey Shale and related formations of the Tremblor Range, California. Geochim. Cosmochim. Acta 43 p1357-1365.

Friend,P.F., 1966. Clay fractions and colour of some Devonian red beds in the Catskill Mountains, USA. J. Geol. Soc. Lond. 122 p273-292.

----------, Harland,W.B. & Gilbert-Smith,A., 1970. Reddening and fissuring associated with the Caledonian Unconformity in north-west Arran. Proc. Geol. Assoc. 81 p75-85.

Furuta,T. & Otsuki,M., 1985. Quantitative electron probe microanalysis of oxygen in titanomagnetites with implications for oxidation processes. J. Geophys. Res. 90B p3145-3150.

Gallagher,K.J., Feitrecht,W. & Mannweiller,U., 1968. Mechanism of oxidation of magnetite to γ-Fe_2O_3. Nature 217 p1118-1121.

Garrels,R.M. & Christ,C.L., 1965. Solutions, minerals and equilibria. Harper & Row, New York (450pp).

Garson,M.S. & Plant,J., 1972. Possible dextral movements on the Great Glen and Minch Faults, Scotland. Nature 240 p31-32.

Gawthorpe,R.L., 1985. Sedimentation, tectonics and diagenesis: the Dinantian sequence of the Bowland Basin, Northern England. PhD thesis, Univ. of Leeds (unpubl).

----------, in press. Burial dolomitisation and porosity development in a mixed carbonate-clastic sequence: an example from the Bowland Basin, Northern England. (submitted to Sedimentology).

Geikie,A., 1878. On the Old Red Sandstone of Western Europe. Trans. Roy. Soc. Edin. 28 p345-452.

---------, 1897. Ancient volcanoes of Great Britain, vol.II. (London)

Goddard,E.N., 1951. Rock Colour Chart. Geol. Soc. America, New York.

Goldstein,J.I., Newbury,D.E., Echlin,P., Joy,D.C., Fiori,C. & Lifshin,E., 1981. Scanning electron microscopy and x-ray microanalysis. Plenum Press; 673pp.

Goree,W.S. & Fuller,M.D., 1976. Magnetometers using RF-driven squids, and their application in rock magnetism and palaeomagnetism. Rev. Geophys. Space Phys. 14 p591-608.

Graham,J.W., 1949. The stability and significance of magnetism in sedimentary rocks. J. Geophys. Res. 54 p131-167.

----------, 1954. Rock magnetism and the earth's magnetic field in Palaeozoic time. J. Geophys. Res. 59 p215-222.

Graham,K.W.T., 1961. The remagnetisation of a surface outcrop by lightning currents. Geophys. J. Roy. Astron. Soc. 6 p85-102.

Haggerty,S.E., 1976. Opaque mineral oxides in terrestrial igneous rocks. (in) Oxide Minerals, ed. Rumble,D,III. Min. Soc. Am. short course notes, vol.3. (Southern Printing Co., Virginia).

Halliday,A.N., McAlpine,A, & Mitchell,J.G., 1977. The age of the Hoy Lavas, Orkney. Scott. J. Geol. 13 p43-52.

Halls,H.C., 1976. A least-squares method to find a remanence direction from converging remagnetisation circles. Geophys. J. Roy. Astron. Soc 45 p297-304.

----------, 1978. The use of converging remagnetisation circles in palaeomagnetism. Phys. Earth Planet. Int. 16 p1-11.

Harwood,G.M., 1981. Controls on mineralisation in the Cadeby Formation (Lower Magnesian Limestone). PhD thesis, Open Univ. (unpubl).

Heaton,R.C., 1979. The geology of the area around Prestonmill, Solway, S.W. Scotland. Undergraduate thesis, Univ. of Leeds (unpubl).

Hedley,I.G., 1968. Chemical remanent magnetisation of the FeO.OH, Fe_2O_3 system. Phys. Earth Planet. Int. 1 p103-121.

Henry,S.G., 1979. Chemical demagnetisation: methods, proceedures and applications through vector analysis. Can. J. Earth Sci. 16 p1832-1841.

Higham,J.C., 1976. Sedimentology and diagenesis of the red Lower and Middle Devonian sediments in Northern Scotland. PhD thesis, Univ. of Hull (unpubl).

Hillerbrand,W.F., Lundall,G.E.F., Bright,H.A. & Hoffman,J.I., 1953. Applied inorganic analysis, second edition.

Hillier,S. & Marshall,J.E.A., 1985. Hydrocarbon source rocks, thermal maturity and burial history of the Orcadian Basin, Scotland. (abstr.) Lacustrine Petroleum Source Rocks: IGCP project 219 (Geol. Soc. Lond.).

Holgate,N., 1969. Palaeozoic and Tertiary transcurrent movements on the Great Glen Fault. Scott. J. Geol. 5 p97-139.

Hornafius,J.S., 1984. Origin of remanent magnetisation in dolomite from the Monterey Formation. (in) Dolomites of the Monterey Formation and other organic-rich units, ed. Garrison,R.E., Kastner,M. & Zenger,D.H. (SEPM vol.41).

House,M.R., Richardson,J.B., Chaloner,W.G., Allen,J.R.L., Holland,C.H. & Westoll,T.S., 1977. A correlation of the Devonian rocks in the British Isles. Geol. Soc. Lond. Spec. Rep. 8 (110pp).

Institute of Geological Sciences (1979). Regional Geochemical AtlasSouth Orkney and Caithness. I.G.S., London.

Irving,E,1964. Palaeomagnetism and its application to geological and geophysical problems. John Wiley, New York. 399pp

--------- & Strong,D.F., 1984a. Evidence against large-scale Carboniferous strike-slip faulting in the Appalachian-Caledonian orogen. Nature 310 p762-764.

--------- & Strong,D.F., 1984b. Palaeomagnetism of the Early Carboniferous Deer Lake Group, western Newfoundland: no evidence for mid-Carboniferous displacement of 'Acadia'. Earth Planet. Sci. Lett. 69 p379-390.

--------- & Strong,D.F., 1985. Palaeomagnetism of rocks from Burin Peninsula, Newfoundland: hypothesis of late Palaeozoic displacement of Acadia criticised. J. Geophys. Res. 90B p1949-1962.

Irwin,H., 1980. Early diagenetic carbonate precipitation and pore fluid migration in the Kimmeridge Clay of Dorset, England. Sedimentology 27 p577-591.

--------, Curtis,C.D. & Coleman,M., 1977. Isotopic evidence for source of diagenetic carbonates formed during burial of organic-rich sediments. Nature 269 p209-213.

Ismail,F.T., 1970. Biotite weathering and clay formation in arid and humid regions, California. Soil Science 109 p257-262.

Ixer,R.A., Turner,P. & Waugh,B., 1979. Authigenic iron and titanium oxides in Triassic red beds (St. Bees Sandstone), Cumbria, Northern England. Geol. Journal 14 p179-192.

Jaeger,J.C., 1959. Temperatures outside a cooling intrusive sheet. American J. Science 257 p44-54.

Jaeger, J.C., 1964. Thermal effects of intrusions. Rev. Geophys. 2, p443-466.

Jelenska,M.B., 1985. Palaeomagnetism of Mesozoic and Palaeozoic rocks from Spitsbergen; tectonic implications. Terra Cognita 5 p141 (abstr).

Katz,A., 1971. Zoned dolomite crystals. J. Geol. 79 p38-51.

Kellock,E, 1969. Alkaline basic igneous rocks in the Orkneys. Scott. J. Geol. 5 p140-153.

Kennedy,W.Q., 1946. The Great Glen Fault. Q. Jl. Geol. Soc. Lond. 102 p41-72.

Kent,D.V., 1979. Palaeomagnetism of the Devonian Onondaga Limestone revisited. J. Geophys. Res. 84 p3576-3588.

---------, 1982. Palaeomagnetic evidence for post-Devonian displacement of the Avalon Platform (Newfoundland). J. Geophys. Res. 87 p8709-8716.

---------, in press. Thermoviscous remagnetisation in some Appalachian limestones.

--------- & Opdyke,N.D., 1978. Palaeomagnetism of the Devonian Catskill red beds: evidence of motion of the coastal New England-Canadian Maritime Region relative to cratonic North America. J. Geophys. Res. 83 p4441-4450.

--------- & ----------, 1979. The early Carboniferous palaeomagnetic field of North America and its bearing on the tectonics of the Northern Appalachians. Earth Planet. Sci. Lett. 44 p365-372.

--------- & ----------, 1985. Multicomponent magnetisations from the Mississippian Mauch Chunk Formation of the central Appalachians and their tectonic implications. J. Geophys. Res. 90B p5371-5384.

Kent,J.T., Briden,J.C. & Mardia,K.V., 1983. Linear and planar structure in ordered multivariate data, as applied to progressive demagnetisation of palaeomagnetic remanence. Geophys. J. Roy. Astron. Soc. 75 p593-622.

Kent,P.E., 1975. The tectonic devolepment of Great Britain and the surrounding areas. (in) Woodland,A.D.(ed), Petroleum and the continental shelf of N.W.Europe, p3-28. Applied Science Publ.

King,R.F., 1955. The remanent magnetisation of artificially deposited sediments. Mon. Not. R. Astron. Soc. 7 p115-134.

Kneen,S.J., 1973. The palaeomagnetism of the Foyers plutonic complex, Inverness-shire. Geophys. J. Roy. Astron. Soc. 32 p53-63.

Kono,M., 1979. Palaeomagnetism and palaeointensity studies of Scottish Devonian volcanic rocks. Geophys. J. Roy. Astron. Soc. 56 p385-396.

Krinsley,D.H., Pye,K. & Kearsley,A.T., 1983. Application of backscattered electron microscopy in shale petrology. Geol. Mag. 120 p109-114.

Kynaston,H & Hill,J.B., 1908. 1-inch sheet memoirs, Oban & Dalmally sheet 45. Geol. Surv. Gt. Br. (Scotland).

Land,L.S., 1980. The isotopic and trace element geochemistry of dolomite: the state of the art. (in) Concepts and models of dolomitisation, ed. Zenger,D.H., Dunham,J.B. & Ethington,R.L. Spec. Pub. Soc. Econ. Palaeontol. Minerol. 28 p87-110.

Langmuir,D., 1971. Particle size effect on the reaction goethite = hematite + water. Am. J. Sci. 271 p147-156.

Larsen,G. & Chilingar,G.V., 1979. Diagenesis in sediments and sedimentary rocks. Elsevier, Holland (579pp).

Larson,E.E. & Walker,T.R., 1975. Development of chemical remanent magnetisation during early stages of red bed formation in late Cenozoic sediments, Baja California. Geol. Soc. Am. Bull. 86 p639-650.

Larson,E.E., Walker,T.R., Patterson,P.E., Hoblitt,R.P & Rosenbaum,J.G., 1982. Palaeomagnetism of the Moenkopi Formation, Colorado Plateau: basis for long-term model of acquisition of CRM in red beds. J. Geophys. Res. 87 p1081-1106.

Latham,A.G. & Briden,J.C., 1975. Palaeomagnetic field directions in Siluro-Devonian lavas of the Lorne Plateau, Scotland, and their regional significance. Geophys. J. Roy. Astron. Soc. 43 p243-252.

Leeder,M.R., 1982. Upper Palaeozoic basins of the British Isles: Caledonide inheritance versus Hercynian plate margin processes. J. Geol. Soc. Lond. 139 p479-491.

LePichon,X., Sibuet,J.C. & Francheteau,J., 1977. The fit of the continents around the North Atlantic Ocean. Tectonophysics 38 p169-209.

Lie,L.G., Storetvedt,K.M. & Gjellestad,G., 1969. The palaeomagnetism of the Kvamshesten Old Red sequence, south-west Norway. Nor. Geol. Tiddskr. 49 p241-249

Lindsley,D.H., 1976. The crystal chemistry and structure of oxide minerals as exemplified by the Fe-Ti oxides. (in) Oxide Minerals, ed. Rumble,D.,III. (Min. Soc. Am. short course notes, pL1-L60).

Lippmann,F., 1973. Sedimentary carbonate minerals. Springer-Verlag, New York (228pp).

Livermore,R.A., Smith,A.G. & Briden,J.C., 1985. Palaeomagnetic constraints on the distribution of continents in the late Silurian and early Devonian. Philos. Trans. R. Soc. Lond. B309 p29-56.

Lovlie,R., Torsvik,T., Jelenska,M. & Levandowski,M., 1984. Evidence for detrital remanent magnetisation carried by hematite in Devonian red beds from Spitsbergen: palaeomagnetic implications. Geophys. J. Roy. Astron. Soc. 79 p573-588.

MacDonald,W.D., 1980. Net tectonic rotation, Apparent tectonic rotation and the structural tilt correction in palaeomagnetic studies. J. Geophys. Res. 85 p3659-3669.

MacGregor,M & MacGregor,A.G., 1948. The Midland Valley of Scotland (second edition). British Regional Geology, H.M.S.O.

MacIntyre,R.M., Cliff,R.A. & Chapman,N.A., 1981. Geochronological evidence for phased volcanic activity in Fife and Caithness necks, Scotland. Trans. Roy. Soc. Edin. 72 p1-7.

Marshall,J.E.A., Brown,J.F. & Hindmarsh,S., 1985. Hydrocarbon source rock potential of the Orcadian Basin. Scott. J. Geol. 21 p301-320.

McAlpine,A., 1978. The Upper Old Red Sandstone of Orkney, Caithness and neighbouring areas. PhD thesis, Univ. of Newcastle-upon-Tyne. (unpubl.)

McCabe,C., van der Voo,R & Ballard,M.M., 1984. Late Palaeozoic remagnetisation of the Trenton Limestone. Geophys. Res. Lett. 11 p979-982.

---------, ----------, Peacor,D.R., Scotese,C.R. & Freeman,R., 1983. Diagenetic magnetite carries ancient yet secondary remanence in some Palaeozoic sedimentary carbonates. Geology 11 p221-223.

McClelland Brown,E.A., 1980. Palaeomagnetic studies in thermal aureoles. PhD thesis, Univ. of Leeds. (unpubl.)

----------, 1981. Palaeomagnetic estimates of temperatures reached in contact metamorphism. Geology,9, p112-116

----------, 1982. Discrimination of TRM and CRM by blocking temperature spectrum analysis. Phys. Earth Planet. Int. 30 p405-414.

----------, 1983. Palaeomagnetic studies of fold development and propagation in the Pembrokeshire Old Red Sandstone. Tectonophysics 98 p131-150.

McElhinny,M.W., 1964. Statistical significance of the fold test in palaeomagnetism. Geophys. J. Roy. Astron. Soc. 8 p338-340.

----------, 1973. Palaeomagnetism and plate tectonics. Cambridge University Press, 358pp.

---------- & Cowley,J.A., 1977. Palaeomagnetic results from the USSR. ANU (Research School of Earth Sciences) publication no. 1268.

---------- & ----------, 1979. Palaeomagnetic results from the USSR: supplement no.1. ANU (Research School of Earth Sciences) publication no. 1377.

----------, Luck,G.R. & Edwards,D., 1971. A large-volume magnetic field free space for thermal demagnetisation and other experiments in palaeomagnetism. Pure Applied Geophys. 90 p126-130.

McFadden,P.L. & Jones,D.L., 1981. The fold test in palaeomagnetism. Geophys. J. Roy. Astron. Soc. 67 p53-58.

---------- & Lowes,F.J., 1981. The discrimination of mean directions drawn from Fisher distributions. Geophys. J. Roy. Astron. Soc. 67 p19-33.

McKenzie,D.P., 1978. Some remarks on the development of sedimentary basins. Earth Plan. Sci. Lett. 40 p25-32.

McMurry,E.W., 1970. Palaeomagnetic results from Scottish lavas of Lower Devonian age. (in) Palaeogeophysics, ed. Runcorn,S.K., p253-262. (Academic Press)

McQuillin,R., 1968. Geophysical surveys in the Orkney Islands. Geophys. paper no. 4, Inst. Geol. Sci., p1-18.

Merrill,R.T., 1981. Toward a better theory of Thermal Remanent Magnetism. J. Geophys. Res. 86 p937-949.

Michie,U. McL. & Cooper, D.C., 1979. Uranium in the Old Red Sandstone of Orkney. Rep. Inst. Geol. Sci. 78/16; 35pp.

Miller,J.D. & Kent,D.V., 1985. Another look at the Catskill. Eos 66 p257 (abstr).

Morad,S. & Ala Adin Aldahan, 1982. Authigenesis of titanium minerals in two Proterozoic sedimentary rocks from Southern and Central Sweden. J. Sed. Petrol. 52 p1295-1305.

Morris, W.A., 1976. Transcurrent motion determined palaeomagnetically in the northern Appalachians and Caledonides and the Acadian orogeny. Can. J. Earth Sci. 13 p1236-1243.

----------, Briden,J.C., Piper,J.D.A. & Sallomy,J.T., 1973. Palaeomagnetic studies in the British Caledonides: V Miscellaneous new data. Geophys. J. Roy. Astron. Soc. 34 p69-106.

Mould,D.D.C.P., 1946. The geology of the Foyers granite and the surrounding country. Geol. Mag. 83 p249-265.

Muir,A., Hardie,H.G.M., Mitchell,R.L. & Phemister,J., 1956. The limestones of Scotland: chemical analyses and petrography. Mem. Geol. Surv. Gt. Br. Min. Resources 37

Muir,R.O. & Ridgway,J.M., 1975. Sulphide mineralisation of the continental sediments of Orkney (Scotland). Mineralium deposita 10 p205-215.

Muller,G., Irion,G. & Forstner,U., 1972. Formation and diagenesis of inorganic carbonates in the lacustrine environment. Naturwissenschaften 59 p158-164.

Munro,M., 1973. Structures in the south-eastern portion of the Strontian granitic complex, Argyllshire. Scott. J. Geol. 9 p99-108.

Mykura,W., 1960. The replacement of coal by limestone and the reddening of coal measures in the Ayrshire Coalfield. Bull. Geol. Surv. Gt. Br. 16 p69-109.

----------, 1975. Possible large-scale strike-slip sinistral displacement along the Great Glen Fault in Scotland. Geol. Mag. 112 p91-94.

----------, 1976. British Regional Geology: Orkney and Shetland. H.M.S.O.

----------, 1982. The Old Red Sandstone east of Loch Ness, Inverness-shire. Rep. Inst. Geol. Sci. 82/13.

Nairn,A.E.M., 1960. Palaeomagnetic results from Europe. J. Geol. 68 p285-306.

Neel,L., 1949. Theorie du trainage magnetique des ferromagnetiques en grains fins avec applications aux terres cuites. Ann. Geophys. 5 p99-136.

-------, 1950. Theorie du trainage magnetique des substances massives dans le domaine de Rayleigh. J. Phys. Radium 12 p339-351.

Newman,A.C.D. & Brown,G., 1966. Chemical alteration during the alteration of micas. Clay Miner. 6 p297-310.

O'Reilly,W., 1984. Rock and mineral magnetism. Chapman & Hall; 270pp.

Palmer,J.A., Perry,S.P.G. & Tarling,D.H., 1985. Carboniferous magnetostratigraphy. J. Geol. Soc. Lond. 142 p945-955.

Parnell, J.T., 1981. Post-depositional processes in the Old Red Sandstone of the Orcadian Basin, Scotland. PhD thesis, Imperial College, London (unpubl.)

----------, 1982. Comment on 'Palaeomagnetic evidence for a large (2000 km) displacement along the Great Glen Fault during Carboniferous time.' Geology 10 p605.

----------, 1983a. Ancient duricrusts and related rocks in perspective: a contribution from the Old Red Sandstone. (in) Residual Deposits: surface-related weathering processes and materials, ed. Wilson, R.C.L. Geol. Soc. Spec. Pub. 11 p197-209.

----------, 1983b. The distribution of hydrocarbon minerals in the Orcadian Basin. Scot. J. Geol. 19 p205-210.

----------, 1985a. Sedimentology of lacustrine source rocks in the Orcadian Basin. (abstr.) Lacustrine petroleum source rocks: I.G.C.P. project 219 (Geol. Soc. Lond.)

----------, 1985b. Hydrocarbon source rocks, reservoir rocks and migration in the Orcadian Basin. Scott. J. Geol. 21 p321-336.

----------, 1985c. Evidence for evaporites in the ORS of Northern Scotland: replaced gypsum horizons in Easter Ross. Scott. J. Geol. 21 p377-380.

Parry, J.H., 1957. The problem of reversed magnetisations and its study by magnetic methods. Adv. Phys. 6 p299-305.

Payne, M.A., 1981. SI and CGS units, conversions and equations for use in geomagnetism. Phys. Earth Planet. Int. 26 p10-16.

---------- & Verosub, K.L., 1982. The acquisition of post-depositional DRM in a variety of natural sediments. Geophys. J. Roy. Astron. Soc. 68 p625-642.

Perroud, H., Robardet, M., van der Voo, R., Bonhommet, N. & Paris, F., in press. Revision of the age of magnetisation of the Montmartin red beds, Normandy, France.

---------- & van der Voo, R., 1984. Secondary magnetisations from the Clinton-type iron ores of the Silurian Red Mountain Formation, Alabama. Earth Planet. Sci. Lett. 67 p391-399.

Perry, S.P.G., 1979. Palaeomagnetic studies of British carbonate sediments. PhD thesis, Univ. of Newcastle-upon-Tyne (unpubl).

Pettijohn, F.J., 1963. Chemical composition of sandstones - excluding carbonate and volcanic sands. USGS prof. paper 440S (21pp).

Phillips,W.E.A., Stillman,C.J. & Murphy,T., 1976. A Caledonian plate tectonic model. J. Geol. Soc. Lond. 132 p579-609.

Pickering,K.T., 1984. The Upper Jurassic 'boulder beds' and related deposits: a fault-controlled submarine slope, N.E. Scotland. J. Geol. Soc. Lond. 141 p357-374.

Piper,J.D.A., 1975. Palaeomagnetism of Silurian lavas of Somerset and Gloucestershire, England. Earth Planet. Sci. Lett. 25 p355-360.

Price,G.D., 1980. Exsolution microstructures in titanomagnetites and their magnetic significance. Phys. Earth Planet. Int. 23 p2-12.

Purucker,M.E., Elston,D.P. & Shoemaker,E.M., 1980. Rapid acquisition of remanent magnetisation in red beds of the Moenkopi Formation (Triassic), Gray Mountain, Arizona. J. Geophys. Res. 85 p997-1012.

Pye,K., 1985. Electron microscope analysis of zoned dolomite rhombs in the Jet Rock Formation (Lower Toarcian) of the Whitby area, U.K. Geol. Mag. 122 p279-286.

Pye,K. & Krinsley,D.H., 1983. Mudrocks examined by backscattered electron microscopy. Nature 301 p412-413.

Radke,B.M. & Mathis,R.L., 1980. On the formation and occurrence of saddle dolomite. J. Sed. Petrol. 50 p1149-1168.

Rayner,D.H., 1963. The Achanarras limestone of the Middle Old Red Sandstone, Caithness, Scotland. Proc. Yorks. Geol. Soc. 18 p5-20.

Readman,P.W. & O'Reilly, 1972. Magnetic properties of oxidised (cation deficient) titanomagnetites. J. Geomagn. Geoelectr. 24 p69-70.

Reeder,R.J., 1983. Crystal chemistry of the rhombohedral carbonates. (in) Carbonates: Mineralogy and chemistry, ed. Reeder,R.J. (Min. Soc. Am. Reviews in Mineralogy 11)

Reynolds,R.L., 1982. Post depositional alteration of titanomagnetite in a Miocene sandstone, south Texas. Earth Planet. Sci. Lett. 61 p381-391

Richey,J.E., 1939. The dykes of Scotland. Trans. Edin. Geol. Soc. 13 p393-435.

Rice,C.M. & Williams,J.M., 1969. A Mossbauer study of biotite weathering. Min. Mag. 37 p210-215.

Ridgway,J.M., 1974. Sedimentology of the Eday Group, Middle Old Red Sandstone, Orkney. PhD thesis, Univ. of London. (unpubl.)

Rigby,S., 1984. Aspects of fracturing, fissuring and fluid movement at red bed unconformities. PhD thesis, Univ. of Leeds (unpubl).

Robinson,M.A., 1985. Palaeomagnetism of volcanics and sediments of the Eday Group, southern Orkney. Scott. J. Geol. 21 p285-300.

Robinson,M.A. & McClelland Brown (in prep.). Cooling of the Rhum Intrusion: a palaeomagnetic investigation (provisional title).

Rock,N.M.S., 1983. The Permo-Carboniferous camptonite-monchiquite dyke suite of the Scottish Highlands and Islands: distribution, field and petrological aspects. Rep. Inst. Geol. Sci. Lond. 82/14.

Roy,J.L. & Morris,W.A., 1983. A review of palaeomagnetic results from the Carboniferous of North America: the concept of Carboniferous geomagnetic field horizon markers. Earth Planet. Sci. Lett. 65 p167-181.

-------- & Park, J.K., 1972. Red beds: DRM or CRM? Earth Planet. Sci. Lett. 17 p211-216.

Rumble,D.,III, 1976. Oxide Minerals. Min. Soc. of America short course notes, vol. III. Southern Printing Co., Virginia.

Sallomy,J.T. & Piper,J.D.A., 1973. Palaeomagnetic studies in the British Caledonides IV: Lower ORS lavas of the Strathmore region. Geophys. J. Roy. Astron. Soc. 34 p47-68.

Salmon,E., Edel,J.B., Pique,A. & Westphal,M., 1985. Evidence for late Carboniferous-Permian overprintings on Middle to late Devonian limestones from the Tafilalet (southern Morocco). Terra Cognita 5 p140 (abstr).

Schmalz,R.F., 1968. Formation of redbeds in modern and ancient deserts: Discussion. Geol. Soc. Am. Bull. 79 p277-280.

Schmidt,V., 1965. Facies, diagenesis and related reservoir properties in the Gigas Beds (Upper Jurassic), northwestern Germany. (in) Dolomitisation and limestone diagenesis: a symposium; ed. Pray,L.C. & Murray,R.C. Soc. Econ. Palaeontol. Miner. Spec. Pub. 13 p124-168.

Schwarz,E.J., 1977. Depth of burial from remanent magnetisation: the Sudbury irruptive at the time of diabase intrusion (1250 Ma). Can J. Earth Sci. 14 p82-88.

Scotese,C.R., van der Voo,R. & McCabe,C., 1982. Palaeomagnetism of the Upper Silurian and Lower Devonian carbonates of New York State: evidence for secondary magnetisations residing in magnetite. Phys. Earth Planet. Int. 30 p385-395.

Shand,S.J., 1951. Mylonites, slickensides and the Great Glen Fault. Geol. Mag. 88 p423-428.

Shearman,D.J., Khouri,J. & Taha,S., 1961. On the replacement of dolomite by calcite in some Mesozoic limestones from the French Jura. Proc. Geol. Assoc. 72 p1-13.

Shive,P.N., 1986. Suggestions for the use of SI units in magnetism. Eos 67 p25.

Smit,D.E. & Swett,K., 1968. Devaluation of 'dedolomitisation'. J. Sed. Petrol. 39 p379-380.

Smith,D.I., 1977. The Great Glen Fault. (in) The Moray Firth area geological studies, ed. Gill,G. Inverness Field Club.

---------- & Watson,J.V., 1983. Scale and timing of movements on the Great Glen Fault, Scotland. Geology 11 p523-526.

Soper,N.J. & Hutton,D.H.W., 1984. Late Caledonian sinistral displacements in Britain: Implications for a three-plate collision model. Tectonics 3 p781-794.

Speight,J.M. & Mitchell,J.G., 1979. The Permo-Carboniferous dyke swarm of northern Argyll and its bearing on dextral displacement of the Great Glen Fault. J. Geol. Soc. Lond. 136 p3-11.

Stacey,F.D., 1967. The Koenigsberger ratio and the nature of thermoremanence in igneous rocks. Earth Planet. Sci. Lett. 2, p67-68.

---------- & Bannerjee,S.K., 1974. The physical principles of rock magnetism. Elsevier, Amsterdam (195pp).

Steiger,R.H. & Jaeger,E., 1977. Submission on geochronology: convention on the use of decay constants in geo- and cosmochronology. Earth Planet. Sci. Lett. 36 p359-362.

Steiner,M.B., 1983. DRM in hematite. J Geophys. Res. 88 p6253-6539.

Stephenson,D., 1972. Middle Old Red Sandstone fan and talus deposits at Foyers, Inverness-shire. Scott. J. Geol. 8 p121-127.

----------, 1977. Intermontane basin deposits associated with an early Great Glen feature in the Old Red Sandstone of Inverness-shire. (in) The Moray Firth area geological studies, ed. Gill,G. (Inverness Field Club)

Storetvedt,K.M., 1968a. A synthesis of the Palaeozoic palaeomagnetic data for Europe. Earth Plan. Sci. Lett. 3 p444-448.

----------, 1970a. The Devonian palaeomagnetic field for Europe. (in) Palaeogeophysics, ed. Runcorn,S.K. (Academic Press).

----------, 1970b. On remagnetisation problems in palaeomagnetism: further considerations. Earth Planet. Sci Lett. 9 p407-415.

----------, 1972. Old Red Sandstone palaeomagnetism of central Spitsbergen and the Upper Devonian (Svalbardian) phase of deformation. Norsk. Polarinst. Arb. p59-69.

----------, 1974a. A possible large-scale sinistral displacement along the Great Glen Fault in Scotland. Geol. Mag. 111 p23-30.

----------, 1974b. Great Glen Fault. Nature 249 p777

----------, 1975. A possible large-scale sinistral displacement along the Great Glen Fault in Scotland. (Reply). Geol. Mag. 112 p94-96.

----------, 1977. Devonian palaeogeography of N. Britain. Nature 265 p764.

----------, Carmichael,C.M., Hayatsu,A. & Palmer,H.C., 1978. Palaeomagnetism and Potassium-Argon results from the Duncansby volcanic neck, N.E. Scotland: superimposed magnetisations, age of igneous activity, and tectonic implications. Phys. Earth Planet. Int. 16 p379-392.

---------- & ----------, 1979. Resolution of superimposed magnetisations in the Devonian John o'Groats sandstone, N.Scotland. Geophys. J. Roy. Astron. Soc. 58 p759-784.

---------- & Gjellestad,G., 1966. Palaeomagnetic evolution of an Old Red Sandstone formation of southern Norway. Nature 212 p59-61

---------- & Halvorsen,E., 1968. On the palaeomagnetic reliability of the Scottish Devonian lavas. Tectonophysics 5 p447-457.

----------, ---------- & Gjellestad,G., 1968. Thermal analysis of the NRM of some Upper Silurian red sandstones in the Oslo region. Tectonophysics 5 p413-426.

---------- & Meland,A.H., 1985. Geological interpretation of palaeomagnetic results from Devonian rocks of Hoy, Orkney. Scott. J. Geol. 21 p337-352.

---------- & Petersen,N., 1972. Palaeomagnetic properties of the Middle-Upper Devonian volcanics of the Orkney Islands. Earth Planet. Sci. Lett. 14 p269-278.

---------- & Torsvik,T.H., 1983. Palaeomagnetic re-examination of the basal Caithness Old Red Sandstone: aspects of local and regional tectonics. Tectonophysics 98 p151-164.

---------- & ----------, 1985. Palaeomagnetism of the Middle-Upper Devonian Esha Ness ignimbrite, W.Shetland. Phys. Earth Planet. Int. 37 p169-173.

Storhaug,K. & Storetvedt,K.M., 1985. Palaeomagnetism of the Sarclet Sandstone (Orcadian Basin): age perspectives. Scott. J. Geol. 21 p275-284.

Stubbs,P.H.S., 1958. Continental Drift and Polar Wandering, a palaeomagnetic study of British and European Trias and of the British Old Red Sandstone. PhD thesis, Univ. of London. (unpubl.).

Sunderland,J., 1972. Deep sedimentary basin in the Moray Firth. Nature 236 p24-25.

Sutton,J., 1963. Some events in the evolution of the Caledonides. (in) The British Caledonides, ed. Johnson, M.R.W. & Stewart, F.H. (Oliver & Boyd; 289pp)

Tarling,D.H., Donovan,R.N., Abou-Deeb,J.M. & El-Batrouk,S.I., 1976. Palaeomagnetic dating of hematite genesis in Orcadian Basin sediments. Scott. J. Geol. 12 p125-134.

Tauxe,L. & Kent,D.V., 1984. Properties of a detrital remanence carried by hematite, from study of modern river deposits and laboratory redeposition studies. Geophys. J. Roy. Astron. Soc. 76 p543-562.

--------, --------- & Opdyke,N.D., 1978. Magnetic components contributing to the NRM of Middle Siwalik red beds. Earth Planet. Sci. Lett. 47 p279-284.

Thirlwall, M.F., 1981. Implications for plate tectonic models of chemical data from volcanic rocks of the British Old Red Sandstone. J. Geol. Soc. Lond. 138 p123-138.

Thorning,L., 1974. Palaeomagnetic results from Lower Devonian rocks of the Cheviot Hills, northern England. Geophys. J. Roy. Astron. Soc. 36 p487-496.

Tighem, N.J., 1976. Experimental techniques. (in) Electron Microscopy in mineralogy, ed. Wenk,H.R. p144-173. (Springer Verlag).

Torsvik, T.H., 1984. Palaeomagnetism of the Foyers and Strontian granites, Scotland. Phys. Earth Planet. Int. 36 p163-177.

----------, 1985a. Palaeomagnetic results from the Peterhead granite, Scotland; implication for regional late Caledonian magnetic overprinting. Phys. Earth Planet. Int. 39 p108-117.

----------, 1985b. Magnetic properties of the Lower Old Red Sandstone lavas in the Midland Valley, Scotland; palaeomagnetic and tectonic considerations. Phys. Earth Plan. Int. 39 p194-207.

----------, Lovlie,R. & Storetvedt,K.M., 1983. Multicomponent magnetisation in the Helmsdale Granite, north Scotland: geotectonic implication. Tectonophysics 98 p111-130.

----------, --------- & Sturt,B.A., 1985. Palaeomagnetic argument for a stationary Spitsbergen relative to the British Isles (Western Europe) since late Devonian and its bearing on North Atlantic reconstruction. Earth Planet. Sci. Lett. 75 p278-288.

Trewin,N.H., 1976. Correlation of the Achanarras and Sandwick fishbeds, Middle Old Red Sandstone, Scotland. Scott. J. Geol. 12 p205-208.

Trotter,F.M., 1939. Reddened Carboniferous beds in the Carlisle Basin and Edenside. Geol. Mag. 76 p408-416.

----------, 1953. Reddened beds of Carboniferous age in North-West England and their origin. Proc. Yorks. Geol. Soc. 29 p1-20.

----------, 1954. Reddened beds in the Coal Measures of South Lancashire. Bull. Geol. Surv. Gt. Br. 5 p61-80.

Turnell,H.B., 1982. Palaeomagnetism of Lower Palaeozoic intrusions in the Scottish Highlands. PhD thesis, Univ. of Leeds (unpubl).

----------, 1985. Palaeomagnetism and Rb-Sr ages of the Ratagan and Comrie intrusions. Geophys. J. Roy. Astron. Soc. 83 p363-378.

---------- & Briden,J.C., 1983. Palaeomagnetism of NW Scotland syenites in relation to local and regional tectonics. Geophys. J. Roy. Astron. Soc. 75 p217-234.

Turner,P., 1974. Origin of red beds in the Ringerike Group (Silurian) of Norway. Sed. Geol. 12 p215-235.

---------, 1977. Remanent magnetism of Middle Old Red Sandstone lacustrine and fluvial sediments from the Orcadian Basin, Scotland. J. Geol. Soc. Lond. 133 p37-50.

---------, 1979. The palaeomagnetic evolution of continental redbeds. Geol. Mag. 116 p289-301.

---------, 1980. Continental Redbeds. Developments in Sedimentology 29. Elsevier, 562pp.

--------- & Archer,R., 1975. Magnetisation history of Lower Old Red Sandstones from the Gamrie Outlier, Scotland. Earth Planet. Sci. Lett. 27 p240-250.

--------- & ---------, 1977. The role of biotite in the diagenesis of redbeds from the Devonian of N. Scotland. Sed. Geol. 19 p241-251.

--------- & Ixer,R.A., 1977. Diagenetic development of unstable and stable magnetisations in the St. Bees Sandstone (Triassic) of N. England. Earth Planet. Sci. Lett. 34 p113-124.

---------, Metcalfe,I. & Tarling,D.H., 1979. Palaeomagnetic studies of some Devonian limestones from the Craven Basin and a contribution to Asbian magnetostratigraphy. Proc. Yorks. Geol. Soc. 42 p371-396.

--------- & Tarling,D.H., 1975. Implications of new palaeomagnetic results from the Carboniferous period of Britain. J. Geol. Soc. Lond. 131 p469-488.

---------, ----------, Archer,R. & Donovan,R.N., 1976. A palaeomagnetic argument concerning post-Devonian displacement along the Great Glen Fault. Geol. Mag. 113 p365-370.

---------, Vaughan,D.J. & Tarling,D.H., 1978. Palaeomagnetic and mineralogical studies of Devonian lacustrine sediments from Caithness, Scotland. Phys. Earth. Planet. Int. 16 p73-83.

van der Voo,R., French,A.N. & French,R.B., 1979. A palaeomagnetic pole position from the folded Upper Devonian Catskill redbeds, and its tectonic implications. Geology 7 p345-348.

---------- & McCabe,C., 1985. Remagnetisations in the eastern U.S. and Canada. Eos 66 p257.

---------- & Scotese,C., 1981. Palaeomagnetic evidence for a large (2000 km) sinistral offset along the Great Glen Fault during Carboniferous time. Geology 9 p583-589.

---------- & ----------, 1982. Palaeomagnetic evidence for a large (2000 km) sinistral offset along the Great Glen Fault during Carboniferous time (Reply). Geology 10 p606-607.

van Hilten,D., 1965. Discussion of some recent papers on ancient continental configurations reconstructed from palaeomagnetic evidence. Tectonophysics 1 p521-530.

van Houten,F.B., 1968. Iron oxides in redbeds. Geol. Soc. Am. Bull. 79 p399-416.

----------, 1973. Origin of redbeds: A review 1961-1972. Ann. Rev. Earth Planet. Soc. 1 p39-61.

Veizer,J., 1983. Trace elements and isotopes in sedimentary carbonates. (in) Carbonates: mineralogy and chemistry, ed. Reeder,R.J. Reviews of Mineralogy 11. (Min. Soc. America).

Verosub,K.L., 1977. Depositional and post-depositional processes in the magnetisation of sediments. Rev. Geophys. & Space Phys. 15 p129-143

Waage,H.L. & Storetvedt,K.M., 1973. The Devonian geomagnetic axis relative to the Orcadian Basin, N. Scotland. Z. Geophys. 39 p937-951.

Walker,T.R., 1967. Formation of redbeds in modern and ancient deserts. Geol. Soc. Am. Bull. 78 p353-368.

---------- & Honea,R.M., 1969. Iron content of modern deposits in the Sonoran Desert: A Contribution to the origin of redbeds. Geol. Soc. Am. Bull. 80 p535-544.

Walker,T.R. & Larson,E.E., 1976. Hematite authigenesis in the Moenkopi Formation (Triassic age), Colorado Plateau: a contribution to the origin of magnetism in red beds. Geol. Soc. Am. abstracts, p1158.

Walker,T.R., Larson,E.E. & Hoblitt,R.P., 1981. Nature and origin of hematite in the Moenkopi Formation (Triassic), Colorado Plateau: A contribution to the origin of magnetism in red beds. J. Geophys. Res. 86 p317-333.

----------, Ribbe,P.H. & Honea,R.M., 1967. Geochemistry of hornblende alteration in Pliocene redbeds, Baja California, Mexico. Geol. Soc. Am. Bull. 78 p1055-1060.

----------, Waugh,B. & Crone,A.J., 1978. Diagenesis in first-cycle desert alluvium of Cenozoic age, southwestern United States, and northwestern Mexico. Geol. Soc. Am. Bull. 89 p19-32.

Watson,J.V., 1984. The ending of the Caledonian Orogeny in Scotland. J. Geol. Soc. Lond. 141 p193-214.

----------, 1985. Northern Scotland as an Atlantic-North Sea divide. J. Geol. Soc. Lond. 142 p221-243.

---------- & Plant,J.A., 1979. Regional geochemistry of uranium as a guide to deposit formation. Philos. Trans. R. Soc. London A291 p321-338.

Weaver,L.E. & Pollard,L.D., 1973. The chemistry of clay minerals. Developments in sedimentology 15. Elsevier, Amsterdam (213pp).

Welton,J.E., 1984. SEM petrology atlas. Am. Ass. Petrol. Geol; 237pp

White,S.H., Shaw,H.F & Huggett,J.M., 1984. The use of back-scattered electron imaging for the petrographic study of sandstones and shales. J. Sed. Petrol. 54 p487-494.

Wilkinson,J.F.G., 1957. Titanomagnetites from a differentiated teschenite sill. Min. Mag. 31 p443-453.

Wilson,G.V., Edwards,W, Knox,J, Jones,R.C.B. & Stevens,J.V., 1935. The geology of the Orkneys. Mem. Geol. Surv. Gt. Br.

Wilson,J.T., 1966. Did the Atlantic close and then re-open? Nature 211 p676-681.

Wilson,M.J., 1971. Clay mineralogy of the Old Red Sandstone (Devonian) of Scotland. J. Sed/ Petrol. 41 p995-1007.

----------. & Duthie,D.M.L., 1981. Some aspects of intrastratal alteration of biotite in the Old Red Sandstone. Scott. J. Geol. 17 p65-72.

Winchester,J.A., 1973. Pattern of regional metamorphism suggests a sinistral displacement of 160.km along the Great Glen Fault. Nature 246 p81-84.

---------------, 1974. Pattern of regional metamorphism suggests a sinistral displacement of 160.km along the Great Glen Fault (Reply). Nature 249 p777.

Wones,D.R. & Eugster,H.P., 1965. Stability of biotite: experiment, theory and application. Am. Miner. 50 p1228-1272.

Wood,G.V. & Armstrong,A.K., 1975. Diagenesis and stratigraphy of the Lisburne Group Limestones of the Saddlerochit Mountains and adjacent areas of nertheastern Alaska. US Geol. Surv. Prof. Paper 857 (47pp).

Woodcock,N.H., 1977. Specification of fabric shapes using an eigenvalue method. Geol. Soc. Am. Bull. 88 p1231-1236.

Zenger,D.H., 1973. Syntaxial calcite borders on dolomite crystals, Little Falls Formation (Upper Cambrian), New York. J. Sed. Petrol. 43 p118-124.

Zijderfeld,J.D.A., 1967. A.C. demagnetisation of rocks: analysis of results. (in) Methods in palaeomagnetism, ed. Collinson,D.W., Creer,K.M. & Runcorn,S.K., p254-286.

Appendix A.

Experimental Techniques.

A.1. Palaeomagnetic methods and techniques.

A.1.1. Spinner Magnetometer.

The principle of the Spinner Magnetometer (Collinson 1982, section 9.3) is that a sample rotating within a coil produces an alternating voltage in that coil, the amplitude of which is proportional to the component of magnetic moment perpendicular to the rotation axis. The phase of the voltage is related to the direction of the component with respect to the sample.

The instrument used was a Digico Spinner Magnetometer, connected to an on-line Digico Micro 16E minicomputer which performs correction for sample orientation, and also tectonic corrections if appropriate.

Sensitivity is generally lower than the Cryogenic magnetometer (see below) although reproducibility down to a magnetic intensity of around 0.1 to 0.2 mA/m may be achieved.

A.1.2. Cryogenic Magnetometer.

The Cryogenic (or SQUID: Superconducting Quantum Interference Device) Magnetometer is described by Goree & Fuller (1977) and Collinson (1982), section 9.4. A specimen is introduced into a gap in a superconducting ring maintained at liquid helium temperature. This induces a current in the ring, proportional to the magnetic moment along the axis of the ring and measured using a SQUID device.

Sensitivity is somewhat greater than with the spinner

magnetometer, with reproducibility below 0.1 mA/m. It is also faster to use, and hence is more amenable to repeat measurements which will tend to improve accuracy.

A.1.3. Thermal demagnetisation.

The majority of thermal demagnetisations were performed in the large demagnetiser built at Leeds University to the design of McElhinny et al (1971) and modified by McClelland Brown (1980). This has a large 'field-free space' (a cube of side 20 cm) within which the field is less than 5nT. The field may be monitored and adjusted as often as is necessary. Up to 15-20 specimens may be treated at any one time. The peak temperature, which may be precisely pre-determined, is measured at four points within the array of specimens.

Some specimens were treated on the 'bench' thermal demagnetiser described by Turnell (1982). This has a smaller capacity (maximum 9) and a large thermal gradient (monitored by three dummy specimens). Peak temperatures are less predictable and for this reason the larger model was generally preferred.

A.1.4. AF demagnetisation.

During AF demagnetisationa a specimen is cycled through magnetic hysteresis loops of decreasing amplitude, starting from the peak field. This peak field is progressively increased during progressive demagnetisation. At each step, a component of progressively higher coercivity will be demagnetised. The AF demagnetiser used consists of a two-axis tumbler within a set of Helmholtz coils; these are able to annul the earth's field to about ± 200 nT. The maximum AF field strength available is 190 mT. There is a slight

tendency for specimens of low coercivity to pick up a random magnetisation above 30-60 mT. Results were generally not as good as found with thermal demagnetisation, especially in separating a multi-component hematitic remanence.

A.1.5. Susceptibility.

The susceptibility of the majority of specimens analysed was measured, prior to treatment, on a low-field susceptibility bridge. It was also repeatedly monitored during thermal demagnetisation to determine whether any gross magneto-chemical changes were occuring during heating. The reasons for such changes (e.g. maghemite inversion, oxy-hydroxide dehydration, oxidation of magnetite etc.) are discussed in Eustance (1981).

The ratio of NRM intensity to susceptibility (the Koenigsberger Ratio, Q: Stacey, 1967; Collinson, 1982, section 2.7) can be a useful guide to magnetic stability of igneous rocks. High Q may generally be indicative of high magnetic stability, although it is highly susceptible to error (e.g. natural IRM or viscous decay of NRM) and should not be relied on.

Changes in susceptibility frequently occured. Where this was accompanied by irrational demagnetisation behaviour (e.g. rapid intensity changes) treatment was usually terminated. It was found that heating in nitrogen did not reduce such effects.

A.1.6. Hysteresis of NRM.

The magnetic mineralogy of some specimens is not apparent from demagnetisation characteristics; determination of the hysteresis of NRM of representative samples from this

category is a useful additional investigative tool (Collinson, 1982, chapter 3).

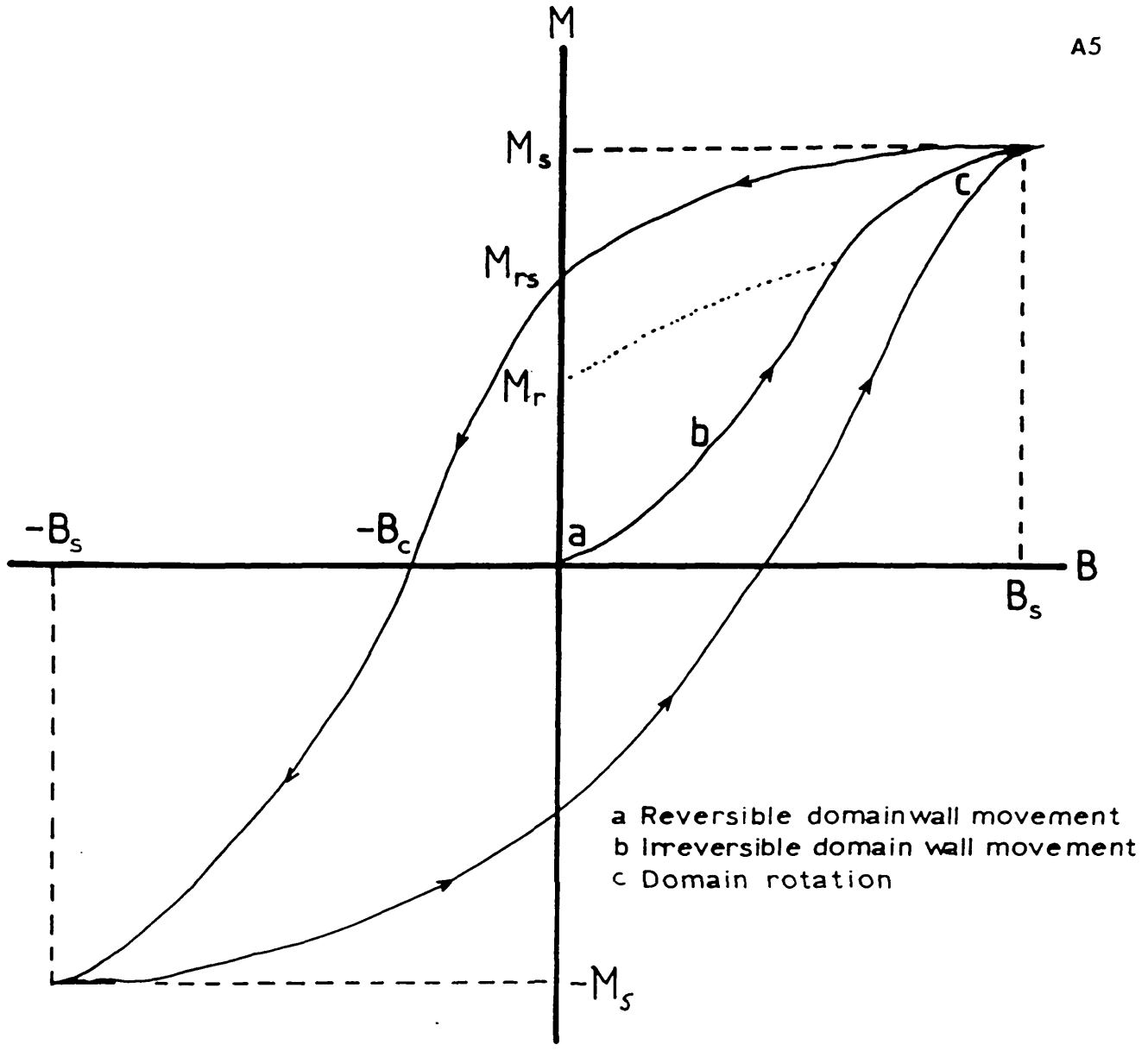
The demagnetised rock is given a series of IRMs of increasing field strength in a direction parallel to the z-axis of the specimen. Measurement is made after each increment until saturation, or until the peak available field (1.2 T) is reached. The specimen is then inverted and the process repeated until saturation in the reverse direction occurs. Three main parameters may be determined (fig. A.1):

(i) Saturation Remanent Magnetisation, M_S This is a measure of the total magnetic content of the specimen; extremes of 60 mA/m (lacustrine laminites) and 800 000 mA/m (basic lavas) were encountered.

(ii) Saturation Field Strength, B_S Hematite will only rarely saturate in the maximum available field whereas (titano)magnetite should saturate in 0.2 to 0.4 T, dependant on domain state and composition.

(iii) Coercivity of Maximum Remanence, B_c This is the field needed to exactly oppose an induced saturation magnetisation. For magnetite it is generally between 20 and 50 mT whereas for hematite it often exceeds 100 mT.

In the case of a specimen with a mixed mineralogy, care must be taken in interpreting the above parameters as, for example, the magnetite in a rock containing both magnetite and hematite could effectively swamp M_S and B_c due to hematite alone and may give a false impression of the true mineralogy.



B: Applied field
M: Magnetisation

M_s: Saturation magnetisation
B_s: Saturating field
M_{rs}: Saturation IRM
B_c: Coercive force
M_r: Unsaturated IRM

Fig. A.1. Hysteresis loop for an ideal ferromagnetic material

A.2. Other methods and techniques.

A.2.1. Electron Microscopy.

Two machines were used, a Jeol 733 at Imperial College, London, and also a Jeol JXA-50A electron microprobe at Leeds University. Both have on-line ZAF corrections using LINK software. A beam current of 1 nA and accelerating voltage of 20 kV were standard operating conditions.

Both machines were used largely in the Backscattered Electron Image (BEI) mode, although a Secondary Electron Image (SEI) was used on occasion on the Jeol 733 both on polished thin sections and rough samples. These were coated with carbon and gold respectively.

The BEI mode is highly sensitive to compositional contrast, i.e. the mean atomic number of the target. Resolution of Z is about ± 0.1 for low Z, although this increases for higher Z. Relative brightness on BEI microphotographs is thus directly proportional to mean Z.

Spot analyses were made using Electron Probe Microanalysis (EPMA). Details are given in Goldstein et al (1981). During analysis, the volume of the specimen affected by electron collisions is directly proportional to the accelerating voltage and inversely proportional to Z. For example, this volume for Al may be an order of magnitude or more greater than for Au under similar working conditions. Analytical resolution on a finer scale than this volume (typically 1 μ) is not possible without using a Transmission Electron Microscope.

The analysis of iron oxide grains using EPMA is described by Akimoto et al (1984) and Furuta & Otsuki (1985)

with particular reference to the oxidation state of titanomagnetite. The analysis of sediments is described by Krinsley et al (1983), Pye & Krinsley (1983) and White et al (1984) and carbonates in particular by Pye (1985).

A.2.2. Optical Microscopy.

Conventional optical microscopy was widely used, although it often acted as a 'backup' to electron microscopy, largely as a result of the generally small grain size of many of the sediments investigated. It was of particular use, however, in the study of carbonates. Most thin sections were stained with Alizarin Red and Potassium Ferricyanide, using the method described by Evamy (1963). Carbonate minerals stain as follows:

Calcite:	Red
Ferroan calcite:	Mauve to blue
Dolomite:	No stain
Ferroan dolomite:	Turquoise

A.2.3. Ferrous Iron Determination.

The method used for ferrous iron determination is the modified Pratt method, largely as described by Hillerbrand et al (1953). The procedure is as follows:

Weigh accurately 0.25 to 0.5g of sample into a Pt crucible. Add 5ml of distilled water and loosen. Add 5ml of 50% H_2SO_4, 10ml of HF and cover. Heat to boiling and maintain for 5 minutes to keep an atmosphere of steam over the contents to avoid aerial oxidation. Plunge crucible and contents into 200ml of a solution of 1% H_3BO_3, 2%H_3PO_4 and 3% H_2SO_4. Using Ba diphenylamine as an indicator, titrate

with standard $K_2Cr_2O_7$ solution. Repeat determination using a different sample weight.

The main sources of error are the presence of insoluble residues (Pyrite, barite) Organic carbon will tend to be oxidised by the titrant and hence will give false results.

Full results are given in appendix E and discussed as appropriate in the main text.

A.2.4. X-Ray Diffraction (XRD). This method which, it was hoped, would assist in the identification of iron oxide minerals, was found to be of limited use only. Analysis of whole-rock powder gave little information that was not evident from thin-section observation and it proved impossible to extract sufficient quantities of heavy mineral concentrate from sediments to obtain reliable results. Although extensive trials were made using XRD, the results are usually not referred to in the text.

A.2.5. ICP analysis.

Crushed and temaed samples from many of the sites investigated in this study were analysed using Inductively Coupled Plasma (ICP) spectroscopy. This gives a whole-rock analysis of all major and most minor elements except for silicon. Results are presented as an actual mass proportion of the total rock composition. The balance of the analysis will, in the case of sediments, largely consist of silicon and anions.

Material analysed was chosen from offcuts of several drilled specimens per site wherever possible. It was hoped that this would give a somewhat better mean analysis than a single specimen. Care was taken to avoid weathered surfaces

found on the tops of drilled cores. A few analyses were made of thermally demagnetised cores due to lack of fresh material. These may show a falsely high Cu analysis; they are specifically identified in appendix C1. Such material was not used for valency state determinations.

Full results are tabulated in appendix C1 and extracts from this discussed elsewhere in the main text as appropriate. Results are given only to the limit of accuracy of the method, as shown below. This explains the apparent lack of consistency in precision within a set of data.

Proportion present	Reported Accuracy
0-1.99 ppm	±0.01 ppm
2.0-19.9 ppm	±0.1 ppm
20-199 ppm	±1 ppm
200-1990 ppm	±10 ppm
0.2-1.99 %	±0.01 %
2.0-19.9 %	±0.1 %
>20 %	±1 %

A.2.6. Colour Determination. Colours were determined for most clastic sediments, using finely-ground and temaed dry rock flour (appendix B). The standard Munsell Colour Chart (Goddard, 1951) was used.

Any particular colour description consists of three parts: (i) Hue, e.g. 10YR (ii) Value or lightness; gradational from 1 (dark) to 8 (light) and (iii) Chroma or degree of saturation; gradational from 0 (low saturation) to 6 (most vivid colouration).

Appendix B: Site Details.

Site	Location	Grid Ref.	Group/Fmn.		Rock type	Bedding	Colour	Chapter	Core/Block
RCD01	Duncansby	ND394737	John o'Groats		Sandstone	12/270	10R6/6	8	C
RCD02	Duncansby	ND391738	Dunc. Vent	*	Xenoliths	n/a	-	8	C+B
RCD03	Duncansby	ND390738	Dunc. Vent	*	Matrix	n/a	-	8	C
RCD04	Duncansby	ND390738	Dunc. Vent	*	Xenoliths	n/a	-	8	C
RCD05	Thurso	ND185683	UCF		Laminite	05/275	-	5	B
RCD06	Thurso	ND187693	UCF	*	Dyke Margin	08/290	-	7	C
RCD07	Thurso	ND187693	UCF		Laminite	08/290	-	5	C
RCD08	Dunnet Head	ND217746	Vent	*	Matrix	n/a	10R8/4	8	C
RCD09	Dunnet Head	ND218745	Upper ORS		Sandstone	08/240	10YR8/2	4	C
RCD10	Dunnet Head	ND218744	Upper ORS	*	Sandstone	08/240	5YR7/2	4	C
RCD11	Dunnet Head	ND218744	Upper ORS		Sandstone	08/240	N8	4	C
RCD12	Dunnet Head	ND215700	Upper ORS		Sandstone	06/230	5YR7/4	4	C
RCD13	Dunnet Head	ND215700	Upper ORS		Sandstone	06/230	-	4	C
RCD14	Dunnet Head	ND215700	Upper ORS		Sandstone	06/230	-	4	C
RCD15	Dunnet Head	ND213700	Upper ORS	*	Dyke Margin	06/230	10YR8/4	4	C
RCD16	Dunnet Head	ND213700	Upper ORS	+	Dyke Margin	06/230	10YR6/2	4	C
RCD17	Dunnet Head	ND213700	Upper ORS		Dyke Margin	06/230	10YR6/2	4	C
RCD18	Wick	ND385521	LCF		Laminite	17/250	-	5	C
RCD19	Sarclet	ND353434	Sarclet Sst.	*	Sandstone	0/0	10YR7/2	4	C
RCD20	Sarclet	ND353434	Sarclet Sst.	*	Sandstone	0/0	10YR7/2	4	B
RCD21	Wick	ND348546	UCF		Laminite	28/285	-	5	C
RCD22	Wick	ND348546	UCF		Laminite	42/140	-	5	C
RCD23	Achanarras	ND174542	UCF	+	Laminite	0/0	-	5	C
RCD24	Achanarras	ND174542	UCF	+	Laminite	0/0	-	5	C
RCD25	Blackpark	NH677832	Niandt FB	*	Fishbed	0/0	-	5	C
RCD26	Achanarras	ND150545	Niandt FB	*	Fishbed	0/0	-	5	C
RCD27	Inverness	NH754428	Niandt FB	*	Fishbed	0/0	-	5	C
RCD28	Inverness	NH760448	Niandt FB		Fishbed	08/060	-	5	C
RCD29	Foyers	NH501215	Lower ORS	*	Sandstone	36/325	5YR8/1	4	B
RCD30	Foyers	NH504207	Lower ORS	*	Sandstone	35/280	5RP7/2	4	B
RCD31	Elgin	NJ203585	M.ORS		Sandstone	06/230	10R6/4	4	C
RCD32	Nairn	NH875571	Upper ORS		Sandstone	10/310	10R7/2	4	C
RCD33	Nairn	NH875571	Upper ORS		Sandstone	09/290	-	4	C
RCD34	Nigg	NH873755	Niandt FB	*	Fishbed	16/275	10R7/4	5	C
RCD35	P/mahomack	NH907842	Upper ORS		Sandstone	20/220	-	4	C
RCD36	Baligill	NC856662	Niandt FB		Fishbed	0/0	5YR7/4	5	C+B
RCD37	Duncansby	ND391737	John o'Groats		Sandstone	18/270	5YR7/4	8	C
RCD38	Duncansby	ND390738	John o'Groats	*	Vent Margin	08/295	-	8	C
RCD39	Duncansby	ND388738	Dunc. Vent	*	Matrix	n/a	-	8	C
RCD40	Duncansby	ND388738	Dunc. Vent	*	Xenolith	n/a	-	8	B
RCD41	Duncansby	ND385735	John o'Groats	*	Sandstone	17/300	5YR7/2	8	C
RCD42	Sarclet	ND329413	E.G. Cong.	*	Conglomerate	20/190	5R6/2	4	C+B
RCD43	Sarclet	ND352426	Sarclet Cong.	*	Conglomerate	17/240	5R6/2	4	C+B
RCD44	Sarclet	ND353434	Sarclet Sst.	*	Sandstone	0/0	5R6/2	4	C
RCD45	Sarclet	ND353434	Sarclet Sst.	*	Sandstone	0/0	10YR6/2	4	B
RCD46	Sarclet	ND353434	Sarclet Sst.	*	Sandstone	0/0	10YR7/2	4	B
RCD47	Dunnet Head	ND219745	Upper ORS	*	Sandstone	08/240	5YR7/4	4	C
RCD48	Duncansby	ND325730	John o'Groats	*	Sandstone	20/340	5YR7/2	8	C
RCD49	Duncansby	ND394737	John o'G FB		Laminite	15/270	-	5	C
RCD50	Duncansby	ND386678	John o'Groats	+	Sandstone	20/200	N8	8	B
RCD51	Sarclet	ND365476	Hillhead RB	*	Sandstone	08/195	-	4	C
RCD52	Braemore	ND071305	Lower ORS	*	Sandstone	40/032	5YR7/4	4	C
RCD53	Helmsdale	ND065191	Lower ORS	*	Sandstone	35/320	5YR6/2	4	B
RCD54	Dornoch	NH806895	Upper ORS	*	Sandstone	14/020	5YR7/4	4	C
RCD55	Sarclet	ND327407	E.G. Cong.	*	Conglomerate	22/190	5YR7/1	4	C

Appendix B: Site Details (contd.)

Site	Location	Grid Ref.	Group/Fmn.		Rock type	Bedding	Colour	Chapter	Core/Block	Grain size
ROD01	Kirkwall	HY443126	Dyke		Camptonite	n/a	-	7	C	
ROD02	Kirkwall	HY397130	Rousay Flags	*	Dyke Margin	12/330	-	7	C	
ROD03	Brough	HY255287	Dyke		Camptonite	n/a	-	7	C	
ROD04	Brough	HY255287	USF	*	Dyke Margin	07/230	-	7	C	
ROD05	Brough	HY255287	USF	*	Dyke Margin	07/230	-	7	C	
ROD06	Brough	HY255287	USF		Laminite	07/230	-	5	C	
ROD07	Yesnaby	HY220161	Dyke		Camptonite	n/a	-	7	C	
ROD08	Yesnaby	HY220161	LSF	*	Dyke Margin	12/220	-	7	C	
ROD09	Burray	ND482954	Vent	*	Matrix	n/a	-	8	C	
ROD10	Burray	ND482954	Rousay Flags		Laminite	28/315	-	5	C	
ROD11	Deerness	HY590064	L. Eday Sst.		Liesegang	20/220	10YR8/5	4	C	M
ROD12	Deerness	HY590064	L. Eday Sst.		Sandstone	20/220	10YR6/4	4	C	M
ROD13	Deerness	HY555034	L. Eday Sst.		Liesegang	24/350	10YR8/4	4	C	M
ROD14	Yesnaby	HY219159	Lower ORS	*	Sandstone	(18/270)	5YR8/2	4	C	
ROD15	Yesnaby	HY219159	Lower ORS		Sandstone	(32/350)	5Y7/1	4	C	
ROD16	Deerness	HY567037	M. Eday Sst.	*	Sandstone	18/355	5YR8/1	4	C	C
ROD17	Deerness	HY567037	M. Eday Sst.	*	Sandstone	18/355	10R6/2	4	C	F
ROD18	Deerness	HY574041	M. Eday Sst.	+	Sandstone	10/160	5R6/2	4	C	F
ROD19	Deerness	HY592036	Eday Flags	*	Below lavas	10/190	-	3	C	
ROD20	Deerness	HY592036	Eday Lavas	*	-	10/190	-	3	C	C
ROD21	S.Ronaldsay	ND464973	U. Eday Sst.	*	Sandstone	14/270	10R5/6	4	C	F
ROD22	S.Ronaldsay	ND451938	Eday Marls	*	Marl	10/240	5YR7/4	4	C	
ROD23	S.Ronaldsay	ND434867	Vent		Matrix	n/a	10YR7/4	8	C	
ROD24	S.Ronaldsay	ND428892	M. Eday Sst.	*	Sandstone	15/230	10R5/6	4	C	C
ROD24A	"	ND428892	M. Eday Sst.	*	Sandstone	15/230	10R5/6	4	B	C
ROD25	Kirkwall	HY458113	Niandt FB	*	Fishbed	20/270	-	5	C	
ROD26	Cruaday	HY245215	Niandt FB	*	Fishbed	07/180	-	5	C	
ROD27	Brough	HY258288	USF		Laminite	-	-	5	B	
ROD28	Hoy	(Hoy)	Upper ORS		Sandstone	-	-	8	B	
ROD29	Skaill	HY234196	Niandt FB	*	Fishbed	07/170	-	5	C	
ROD30	Kirkwall	HY486119	Eday Marls	*	Sandstone	13/170	5R6/4	4	C	M
ROD31	Kirkwall	HY487120	Eday Marls	*	Sandstone	28/060	5R6/2	4	C	F
ROD32	Kirkwall	HY479088	Eday Flags		Laminite	20/230	-	3	B	
ROD33	Kirkwall	HY443081	Eday Marls	+	Sandstone	62/220	10R5/6	4	C	M
ROD34	Deerness	HY563033	Eday Lavas		-	26/334	-	3	C	
ROD35	Deerness	HY563033	Eday Lavas		-	26/334	-	3	C	
ROD36	Deerness	HY563033	Eday Flags		Laminite	26/330	-	3	B	
ROD37	Deerness	HY562032	Eday Flags		Laminite	17/290	-	3	B	
ROD38	Deerness	HY591039	Eday Lavas	*	-	10/090	-	3	B	
ROD39	Eday	HY570303	U. Eday Sst.	*	Sandstone	64/310	5YR6/4	4	B	M
ROD40	Eday	HY578297	U. Eday Sst.	*	Sandstone	40/255	5YR7/4	4	B	M
ROD41	Eday	HY574287	U. Eday Sst.		Sandstone	30/220	5YR7/2	4	B	M
ROD42	Eday	HY543314	M. Eday Sst.		Sandstone	33/345	5R7/2	4	C	M
ROD43	Eday	HY537314	M. Eday Sst.		Sandstone	16/345	5YR6/2	4	C+B	F
ROD44	Eday	HY534337	L. Eday Sst.	*	Sandstone	28/005	5YR7/4	4	C	M
ROD45	Eday	HY537334	M. Eday Sst.		Sandstone	23/360	5YR7/2	4	C+B	M
ROD46	Eday	HY565340	L. Eday Sst.	+	Sandstone	18/210	5YR7/4	4	C	
ROD47	Eday	HY566339	L. Eday Sst.		Sandstone	18/210	5YR6/4	4	C	M
ROD48	Eday	HY554381	U. Eday Sst.	*	Sandstone	20/220	5YR7/1	4	C	M
ROD49	Eday	HY554381	U. Eday Sst.	*	Sandstone	20/220	10R6/2	4	C	M

Appendix B: Site Details (contd.)

Site	Grid Ref.	Group/Fmn.		Rock Type	Bedding	Colour	Chapter	Core/Block	Grain size
ROD50 Eday	HY551371	M. Eday Sst.	*	Sandstone	22/210	5YR6/3	4	C	M
ROD51 Eday	HY549363	Eday Marls	*	Sandstone	12/210	5YR7/2	4	C	F
ROD52 Eday	HY549365	Eday Marls		Sandstone	12/210	5YR6/3	4	C	M
ROD53 Eday	HY555361	M. Eday Sst.	*	Marl	14/220	10R6/3	4	C	VF
ROD54 Eday	HY555361	M. Eday Sst.	*	Marl	14/220		4	B	VF
ROD55 Eday	HY566335	L. Eday Sst.		Sandstone	15/200	5YR6/4	4	B	M
ROD56 Eday	HY566334	L. Eday Sst.		Sandstone	14/180	5Y7/2	4	B	M
ROD57 Sanday	HY607373	L. Eday Sst.		Sandstone	50/130	5YR7/4	4	C	M
ROD58 Sanday	HY607373	L. Eday Sst.		Sandstone	50/130	5Y7/2	4	C	C
ROD59 Sanday	HY607373	L. Eday Sst.	*	Sandstone	50/130	10R5/6	4	C	C
ROD60 Sanday	HY607373	L. Eday Sst.		Sandstone	50/130	10YR8/4	4	C	C
ROD61 Sanday	HY608373	U. Eday Sst.		Sandstone	26/150	10R6/4	4	C	C
ROD62 Sanday	HY613381	U. Eday Sst.		Sandstone	12/210	5YR6/4	4	C	M
ROD63 Sanday	HY615377	M. Eday Sst.		Sandstone	12/165	5Y7/1	4	B	C
ROD64 Sanday	HY600356	L. Eday Sst.		Sandstone	63/195	5YR6/2	4	B	M
ROD65 Sanday	HY600356	L. Eday Sst.		Sandstone	22/360	5YR6/2	4	B	M
ROD66 Sanday	HY600356	L. Eday Sst.		Sandstone	-	5YR6/2	4	B	M
ROD67 Sanday	HY611373	Eday Marls	*	Marl	28/160	5YR6/4	4	C	VF
ROD68 Sanday	HY526150	Eday Lavas	*	-	14/200	-	3	C	
ROD69 Sanday	HY526150	Eday Flags		Below lavas	14/200	-	3	C	
ROD70 Sanday	HY526150	Eday Flags	*	Below lavas	14/200	-	3	C	
ROD71 Sanday	HY526150	Eday Flags	*	Below lavas	14/200	-	3	C	
ROD72 Sanday	HY524148	Eday Lavas		-	14/200	-	3	C	
ROD73 Sanday	HY524148	Eday Lavas	*	-	14/200	-	3	C	
ROD74 Burray	ND455956	Eday Marls	*	Dyke Margin	08/280	5YR6/4	7	C	VF
ROD75 Burray	ND455956	Dyke	+	Camptonite	n/a	-	7	C	
ROD76 Burray	ND455956	Eday Marls		Sandstone	08/280	10YR6/2	4	C+B	M
ROD77 Copinsay	HY594020	Eday Lavas		-	-	-	4	C	
ROD78 Copinsay	HY595020	Eday Lavas		-	-	-	4	B	
ROD79 Yesnaby	HY225153	Lower ORS		Sandstone	07/250	5Y7/2	4	B	
ROD80 Yesnaby	HY258094	Lower ORS		Conglomerate	08/320	5Y6/1	4	C	
ROD81 Yesnaby	HY258094	Lower ORS		Laminite	08/320	-	4	B	

LSF/USF: Lower/Upper Stromness Flags.
FB: Fishbed.

n/a: Not applicable.

Grain size: (see app. A)
C Coarse
M Medium
F Fine
VF Very fine

Appendix C1.

ICP whole-rock analyses (ppm).

(a) Dyke Margins

	RCD			ROD													
	Upper ORS			Rousay			Flags				Eday			Marls			
	15	16	17	0201	0202	0206	0207	0209	0210	0211	7401	7402	7403	7404	7405	7407	7408
x(m)	0.05	1.30	10.0	0.05	0.05	0.09	0.14	0.33	0.47	0.58	0.04	0.065	0.11	0.17	0.29	0.86	0.96
Na	6300	5400	4600	2900	4600	4900	5000	5700	4800	4700	12600	13400	12500	12700	12600	12900	12300
K	17800	18600	16100	44000	45000	47000	44000	50000	48000	52000	35000	34000	36000	32000	33000	33000	34000
Mg	1680	1720	1340	23000	10800	11700	14800	16400	27000	24000	12500	12600	13800	13700	15500	19600	16900
Ca	62000	29000	37000	112000	149000	153000	132000	78000	94000	83000	2200	2400	2200	2100	1890	1950	1880
Al	29000	33000	29000	42000	48000	49000	47000	58000	59000	62000	69000	71000	77000	69000	73000	78000	75000
Ti	1070	1080	1130	2200	2600	2500	2600	3300	3100	3300	4300	4100	4400	4800	4600	4700	4900
Fe	10200	12700	9100	84000	15800	11600	19200	32000	29000	25000	36000	39000	44000	44000	45000	46000	46000
Li	90	28	25	143	43	48	22	18	17	18	40	36	40	41	48	58	59
Rb	43	70	50	142	121	159	147	179	168	194	136	125	147	114	124	133	130
Sr	155	98	161	900	690	780	740	500	770	590	88	93	87	82	81	96	96
Ba	380	510	750	189	290	280	290	320	420	390	470	480	500	510	470	620	480
La	18	14	13	20	23	23	23	25	25	25	19	18	23	28	28	34	32
V	22	23	18	70	75	79	71	83	91	97	91	82	94	91	95	100	99
Cr	12	13	12	35	42	37	43	58	60	59	71	60	63	81	78	76	79
Mo	4	6	3	7	11	8	8	9	9	9							
Mn	220	610	157	620	800	750	730	540	740	640	250	250	330	360	340	1050	440
Co	97	99	86	37	41	19	22	24	22	29	28	21	29	25	21	27	25
Ni	16	14	9	112	63	32	49	52	35	47	46	42	48	52	54	62	59
Cu	25	12	8	31	44	41	31	27	35	31	14	*	18	21	*	*	*
Ag				3	3	1	1	1		1							
Zn	4	16	10	2800	2300	1710	860	470	340	720	45	63	55	60	71	86	83
Cd				14	17	14	5	5	2	3							
Pb	9	14	8	780	700	470	620	152	144	250	24	23	25	24	34	26	25
P	260	240	200	380	480	400	430	520	500	460	670	710	820	820	760	750	750
Total (%)	12.9	10.3	10.0	31.5	28.1	28.4	26.9	24.6	26.8	25.7	17.3	17.8	19.2	18.0	18.8	19.9	19.3

(* for Cu analyses: Contamination by sample holder after thermal demagnetisation)
(x = distance from dyke in metres)
(= below detectable limit)

Appendix C1.

ICP whole-rock analyses (ppm).

(b) Eday Flags beneath lavas.

	ROD														
	Deerness							Shapinsay							
	1911	1908	1912	1907	1906	1901	1904	69A	69B	70A	70B	7101	7102	7103	7105
x(m)	0.03	0.08	0.12	0.20	0.40	0.80	1.20	0.11	0.14	0.22	0.25	0.31	0.35	0.39	0.45
Na	9400	9200	9200	7600	7300	8300	7800	12100	10600	9100	10500	10000	10700	10600	10600
K	29000	30000	30000	31000	36000	39000	35000	23000	23000	21000	22000	28000	22000	29000	32000
Mg	22000	22000	20000	13700	15600	13300	16400	13600	13600	10900	11400	17600	11400	19900	20000
Ca	30000	25000	32000	74000	46000	49000	54000	32000	68000	114000	91000	55000	80000	33000	32000
Al	62000	51000	53000	49000	50000	52000	54000	50000	50000	44000	47000	60000	46000	65000	67000
Ti	3700	3700	3700	3400	4000	3600	3800	3000	2500	2400	2600	3400	2700	3600	3800
Fe	34000	35000	34000	26000	29000	25000	32000	23000	23000	18800	19000	29000	20000	32000	34000
Li	58	55	49	30	34	28	37	45	39	42	42	47	29	49	50
Rb	120	114	108	133	149	140	152	52	61	49	43	79	41	75	84
Sr	110	91	103	260	107	115	173	128	240	370	250	161	220	112	126
Ba	460	450	460	430	430	520	420	670	1070	1060	690	470	470	460	780
La	30	29	26	24	20	21	22	26	28	24	22	30	23	30	28
V	75	77	79	50	76	81	52	47	46	41	40	83	44	73	73
Cr	51	52	59	49	66	59	69	40	37	31	33	45	35	64	64
Mo	9	8	8	7	9	7	8								
Mn	400	350	390	910	440	520	650	380	610	1030	810	500	670	360	380
Co	44	33	40	48	41	47	45	16	15	13	12	19	13	23	20
Ni	62	61	58	38	54	42	53	34	32	26	25	44	26	49	50
Cu	14	16	42	27	17	19	13	14	6	17	7	*	*	21	*
Ag															
Zn	60	57	57	30	31	30	33	25	19	25	21	31	25	42	41
Cd	1	1	1	1	2	1	1								
Pb	17	14	15	16	17	18	17	9	7	6	7	11	9	10	8
P	600	570	560	540	530	490	590	770	640	520	520	610	550	540	560
Total (%)	19.2	17.7	18.4	20.7	19.0	19.2	20.5	15.9	19.3	22.3	20.6	20.5	19.5	19.5	20.1

(* for Cu analyses: Contamination by sample holder after thermal demagnetisation)
(x = distance from lava in metres)
(= below detectable limit)

Appendix C1.

ICP whole-rock analyses (ppm).

(c) Permian Vents.

	Duncansby RCD							Ness RCD						Other Vents		
	Sedimentary clasts in main vent							Baked margin in John o'Groats Sst.								
	02B1	02B2	02B3	02B4	0401	0402	0403	3801	3802	3803	3804	3805	3807	RCD 40	RCD 08	ROD 23
x(m)	0.20	0.10	0.04	0.07	0.40	0.45	0.30	0.1	0.4	1.0	2.5	4.5	10.0			
Na	9840	9500	8500	10500	10400	10200	10400	10300	11900	10600	11500	11400	12000	2300	470	2200
K	22000	24000	25000	22000	14800	15300	15000	14300	17500	16500	17300	17700	18400	33000	12500	27000
Mg	17400	15800	13200	18500	9600	13100	10300	28000	16400	14700	11900	11100	8000	11300	26000	29000
Ca	36000	32000	32000	42000	22000	28000	22000	53000	33000	28000	23000	21000	14900	18200	64000	86000
Al	39000	43000	40000	39000	33000	34000	33000	30000	36000	34000	34000	36000	36000	32000	22000	38000
Ti	2100	2200	2500	1510	2100	1660	1780	1190	1760	1600	1290	1470	2200	1900	1780	2000
Fe	13400	17000	15500	12100	13600	9800	9400	17200	11800	14100	12000	13800	10600	12100	19300	23000
Li	11	17	20	14	24	25	24	7	6	6	6	6	6	25	17	41
Rb	66	87	84	58	29	37	36	29	29	43	59	42	59	108	46	78
Sr	260	250	117	220	136	167	146	122	88	68	71	67	64	82	370	520
Ba	310	740	350	410	270	280	450	260	350	290	320	320	310	200	320	500
La	21	22	20	16	16	18	16	17	18	17	16	16	19	14	19	20
V	27	32	46	24	21	21	20	38	20	21	19	19	21	22	44	50
Cr	21	26	26	13	14	13	15	11	13	14	11	14	22	17	41	28
Mo	7	7	6	6	5	4	7	6	6	7	8	7	7	7	6	6
Mn	410	450	560	470	430	380	400	650	370	460	470	410	210	260	740	670
Co	63	72	37	56	7	5	114	65	52	65	81	104	83	87	44	27
Ni	29	31	31	22	12	14	12	73	21	16	14	13	13	12	83	31
Cu	21	12	15	10	40	30	6	18	11	9	8	7	7	5	35	8
Ag	1															
Zn	15	15	11	10	19	19	14	17	15	15	15	14	13	6	39	37
Cd	1	1	1				1		1	1	1	1	1	1	1	1
Pb	20	16	15	9	13	12	11	8	10	14	15	13	16	11	20	129
P	430	380	470	310	340	280	330	250	270	260	250	300	400	280	530	380
Total (%)	14.1	14.5	13.8	14.7	10.7	11.3	7.0	15.6	12.9	12.1	11.2	11.4	10.3	11.2	14.8	20.0

(x = distance from vent material or vent margin as appropriate)
(= below detectable limit)

Appendix C1.

ICP whole-rock analyses (ppm)

(d) Laminated lacustrine sediments, Middle ORS.

	RCD							ROD				
	25	26	27	28	34	36	49	25	26	29	32	36
Na	290	23000	48000	10300	9400	13400	4900	16200	17200	18200	6100	11900
K	10700	20000	14200	21000	15500	31000	28000	32000	13000	15300	29000	21000
Mg	10100	19900	14200	19200	16900	6300	31000	27000	25000	22000	37000	4800
Ca	260000	56000	43000	45000	151000	71000	69000	53000	126000	116000	92000	76000
Al	25000	56000	70000	38000	41000	52000	58000	65000	42000	48000	44000	41000
Ti	1510	3500	4200	1480	2000	3400	3100	3900	2800	3200	2500	2000
Fe	11100	27000	33000	11800	19100	18500	26000	37000	21000	23000	25000	10900
Li	14	14	69	13	35	18	77	54	42	53	26	18
Rb	20	86	220	69	53	71	80	75	36		84	71
Sr	450	370	400	300	510	182	240	340	1130	1120	350	159
Ba	190	430	590	430	360	470	570	590	440	480	350	400
La	17	27	29	16	21	30	26	26	26	24	28	21
V	55	67	109	22	95	67	86	95	95	109	116	33
Cr	40	60	75	135	36	48	53	88	66	90	48	23
Mo		6	6	7	9			10	11	11		
Mn	900	1070	470	420	760	980	730	380	560	520	780	610
Co	19	65	21	37	18	45	43	40	35	27	14	11
Ni	24	51	47	262	24	28	55	70	43	45	33	15
Cu	15	4	34	14	32	12	76	29	36	42	45	4
Ag			1				1					
Zn	45	18	260	13	51	80	47	140	37	43	38	10
Cd		1		1	1							
Pb	20	22	53	10	24	26	15	310	22	18	20	10
P	300	590	650	340	400	510	510	580	1510	520	670	400
Total (%)	32.1	20.8	22.9	14.9	25.7	19.8	22.2	23.6	25.1	24.9	23.8	16.9

(= below detectable limit)

Appendix C1.

ICP whole-rock analyses (ppm)

(e) Lower ORS

	Mainland Scotland (RCD)										Orkney (ROD)				
	19	20	42	43	44	46	29	52	53	55	14	14H	15	79	80
Na	13300	13100	24000	12600	18600	18100	17400	16700	18400	19600	680	500	770	630	3500
K	34000	33000	25000	36000	44000	33000	24000	25000	25000	28000	12200	1140	10200	24000	36000
Mg	5500	2200	8000	1970	10000	2100	12100	24000	9800	2700	21000	42000	27000	460	1790
Ca	60000	27000	60000	22000	4700	7600	21000	22000	3900	30000	111500	150000	69000	360	3200
Al	51000	42000	53000	48000	67000	52000	59000	63000	56000	47000	16500	2900	16100	25000	39000
Ti	3900	2300	3100	3100	38000	3100	3800	3900	5500	2400	510	45	540	920	2300
Fe	24000	18200	22000	18700	31000	16500	28000	33000	32000	13400	12100	69000	19500	10400	19400
Li	6	2	6	2	12	2	18	35	24	5	4	1	6	8	21
Rb	108	106	56	105	140	98	108	79	82	80	26	20		34	69
Sr	147	96	151	151	93	103	147	116	100	111	730	2000	3200	430	300
Ba	1350	620	420	1490	550	700	650	490	520	750	750	2700	330	450	300
La	30	25	29	25	22	28	33	30	44	25	14	7	15	6	18
V	50	33	46	40	76	52	49	88	71	29	22	19	36	14	34
Cr	61	40	40	46	63	54	45	90	178	17	8	4	15	13	41
Mo	6	7					7				4	5	8		42
Mn	1070	1230	1050	750	250	850	600	980	880	420	960	3100	1110	60	250
Co	65	104	53	41	73	83	77	43	76	83	40	7	147	9	38
Ni	51	22	15	18	105	20	35	108	58	9	7	17	10	4	25
Cu	4	5	3	3	4	*	4	27	13	5	8	2	10	8	16
Ag									2	1					2
Zn	18	6	14	6	32	12	53	72	56	15	230	60	260	26	144
Cd	1	1					1				1	1	1		
Pb	22	16	14	13	27	15	22	23	29	19	47		85	17	1220
P	590	430	630	520	580	560	620	660	1260	370	3300	157	2400	290	320
Total (%)	19.5	14.0	19.7	14.5	21.5	13.5	16.8	19.0	15.4	14.5	17.8	13.9	15.0	6.2	10.8

(* for Cu analysis: Contamination by sample holder after thermal demagnetisation).
(= below detectable limit)

Appendix C1.

ICP whole-rock analyses (ppm)

(f) Eday Group, Orkney

(i) Lower Eday Sandstone (ROD)

	11L	11N	44	46	47	55	56	57	58	59	60	64	
Na	7700	7700	7700	11000	10800	11500	16000	5400	7900	7600	7900	11500	
K	25000	26000	23000	27000	27000	29000	37000	13200	19800	15100	15400	22000	
Mg	2300	1420	3100	1010	950	1290	2600	1410	3100	1170	1190	1390	
Ca	2400	540	57000	880	890	630	1010	32000	19100	950	1070	780	
Al	35000	35000	32000	37000	38000	42000	54000	32000	40000	31000	32000	35000	
Ti	1170	1460	1750	810	790	1050	1280	2200	2200	2000	2600	1110	
Fe	15900	8800	11700	3900	370	22000	8200	14200	14600	10700	5000	14500	
Li	4	4	2	3	3	5	5	86	85	72	91	4	
Rb	81	69	28	28	46	85	126	38	75	45	28	51	
Sr	70	66	66	102	107	77	90	88	109	75	75	67	
Ba	810	710	450	620	620	540	680	590	460	250	260	470	
La	15	14	16	8	10	10	14	23	21	19	18	30	
V	15	16	21	9	9	25	45	28	34	23	22	84	
Cr	13	12	23	3	3	20	12	23	29	24	23	59	
Mo	6	3											
Mn	590	56	530	14	9	162	230	510	550	101	53	750	
Co	104	88	19	17	10	29	20	19	18	37	27	25	
Ni	16	11	10	3	3	12	21	9	18	9	10	49	
Cu	6	5	7	31	37	10	3	7	7	17	12	22	
Ag	1			1	2					2	1		
Zn	8	6	10	10	10	14	11	9	16	7	11	69	
Cd	1												
Pb	20	15	8	11	14	21	21	10	12	12	12	24	
P	290	280	340	149	144	400	280	480	380	510	510	590	
Total (%)	9.1	8.2	13.8	8.3	8.0	10.9	12.1	10.2	10.8	6.9	6.6	8.8	
													Mean
Na/K	0.31	0.30	0.33	0.41	0.40	0.40	0.43	0.41	0.40	0.50	0.51	0.53	0.38
Mg+Ca	0.47	0.20	6.01	0.19	0.18	0.19	0.36	3.34	2.22	0.21	0.23	0.21	1.15%

(= below detectable limit)

11L: With liesegang ring structures.
11N: Without liesegang ring structures.

Appendix C1.

ICP whole-rock analyses (ppm)

(f) Eday Group, Orkney (contd.)

(ii) Middle Eday Sandstone (ROD)

	16	17	18	24	42	43	45	50	53	54G	54P	63	
Na	15800	10300	11500	1110	7900	10700	9500	12500	11400	11400	11300	10200	
K	23000	32000	31000	15000	29000	33000	27000	18900	29000	25000	26000	22000	
Mg	2700	17300	12900	930	1970	7100	2700	4900	23000	17400	20000	550	
Ca	49000	34000	31000	370	610	8300	710	1370	67000	74000	75000	800	
Al	41000	58000	49000	27000	36000	50000	40000	39000	66000	59000	60000	38000	
Ti	860	3800	2600	1000	1790	2800	1430	2400	3600	3300	3300	550	
Fe	4500	34000	24000	10900	8700	21000	9500	16600	32000	24000	29000	2500	
Li	9	34	27	26	2	17	4	17	58	46	48	30	
Rb	69	113	111	54	85	84	31		136	66	102	51	
Sr	290	198	130	88	67	84	81	79	197	161	174	179	
Ba	5000	1260	560	330	470	480	540	510	510	1260	420	1070	
La	14	26	24	10	14	19	15	26	31	26	29	16	
V	10	69	47	14	22	40	16	29	65	94	121	14	
Cr	5	58	33	9	18	40	12	30	62	45	49	8	
Mo	5	8	7	5									
Mn	430	540	470	15	59	186	88	590	640	650	680	64	
Co	56	38	77	99	37	23	20	21	22	18	19	25	
Ni	6	47	32	8	7	27	7	22	43	35	37	3	
Cu	4	7	8	9	16	12	11	15	15	410	165	2	
Ag					1								
Zn	7	42	27	9	8	27	27	29	54	49	47	2	
Cd	1	1	1										
Pb	19	23	22	20	17	15	15	16	20	15	18	13	
P	175	570	410	178	159	550	62	390	600	570	590	230	
Total (%)	14.3	19.2	16.4	5.7	8.7	13.4	9.2	9.7	23.4	21.7	22.7	7.6	
													Mean
Na/K	0.69	0.32	0.37	0.07	0.27	0.32	0.35	0.66	0.39	0.46	0.43	0.46	0.40
Mg+Ca	5.17	5.13	4.39	0.13	0.26	1.54	0.34	0.53	10.00	9.14	9.50	0.13	3.85%

(= below detectable limit)

54G: Green horizon.
54P: Purple horizon.

Appendix C1.

ICP whole-rock analyses (ppm)

(f) Eday Group, Orkney (contd.)

(iii) Eday Marls and Upper Eday Sandstone (ROD).

	Eday Marls									Upper Eday Sandstone						
	22	30	31	33	51	52	67	74M	76	21	39	40	41	49	61	62
Na	13300	4900	13000	2300	13500	13000	11900	12700	15800	760	12600	12500	11200	9500	10900	11200
K	22000	16900	23000	21000	16300	16300	32000	34000	18300	15700	19400	17900	18100	18900	15100	18800
Mg	16000	1610	2600	1840	2800	2900	20000	14900	2500	1060	1690	1040	1790	4900	1320	1190
Ca	29000	350	1640	19400	1310	930	48000	2100	1410	250	1030	880	840	1370	880	1120
Al	52000	34000	50000	27000	34000	34000	70000	73000	40000	28000	34000	33000	33000	39000	32000	33000
Ti	3300	1760	3500	1280	1590	930	3800	4500	1430	1160	1470	1750	1610	2400	1030	1930
Fe	22000	9000	21000	8800	8600	7700	35000	43000	9300	13600	8400	7900	7400	16600	15100	14400
Li	26	18	19	8	9	10	68	46	20	20	4	6	8	19	91	7
Rb	90	47	65	32	46		107	130	71	61	26	48	62	24	36	20
Sr	112	84	115	300	70	78	164	89	100	103	70	68	69	77	74	74
Ba	610	380	490	410	430	450	860	500	420	560	460	430	440	470	340	460
La	24	13	21	13	16	13	30	26	12	24	11	13	13	14	9	21
V	39	21	52	18	19	15	84	93	24	47	20	22	22	22	16	27
Cr	44	13	41	13	17	9	59	73	15	33	13	20	13	16	15	23
Mo	9									7						
Mn	600	77	310	145	65	65	750	430	80	470	39	54	44	210	82	280
Co	44	18	17	22	28	17	25	25	16	77	26	31	43	17	22	28
Ni	24	8	16	2	7	6	49	52	9	32	3	3	5	8	8	8
Cu	14	17	11	8	17	22	22	8	28	8	10	11	19	23	9	14
Ag					1								1			
Zn	37	27	17	6	14	27	69	66	12	12	10	8	15	38	5	14
Cd	1	1								1						
Pb	24	13	20		17	11	24	26	18	16	11	14	18	14	12	13
P	610	98	590	280	320	200	590	75	300	189	300	250	220	270	190	410
Total (%)	16.0	6.9	11.6	8.4	7.9	7.7	22.3	18.6	9.0	6.2	7.9	7.6	7.5	9.4	7.7	16.0
															Mean	
															EM	UES
Na/K	0.60	0.29	0.57	0.11	0.83	0.80	0.37	0.37	0.86	0.05	0.65	0.70	0.62	0.50	0.72	0.60	0.53	0.55
Mg+Ca	3.50	0.20	0.42	2.12	0.41	0.38	6.80	1.70	0.39	0.13	0.17	0.19	0.26	0.63	0.22	0.23	1.76%	0.26%

(= below detectable limit)

74M: Mean of analyses given in appendix C1(a).

Appendix C1.

ICP whole-rock analyses (ppm)

(g) Middle and Upper ORS clastics, mainland Scotland (RCD).

	John o'Groats Sandstone					Middle & Upper ORS							
	01	37	41	48	50	10	11	13L	13N	31D	31L	51	54
Na	10200	11300	13000	7300	1820	3600	1470	6200	6000	580	700	16900	850
K	17400	13100	17400	16000	21000	23000	12500	18100	19000	19600	19300	30000	15900
Mg	10600	10100	10800	4400	1550	5500	2700	1670	1510	2300	1250	18900	1830
Ca	19200	40000	67000	15300	230	14900	57000	750	10400	102000	120000	29000	88000
Al	35000	32000	39000	26000	28000	45000	20000	32000	31000	40000	29000	58000	34000
Ti	1880	2100	1910	590	1580	3300	730	1230	1000	3300	1920	4000	1680
Fe	13900	16200	14800	9000	2500	21000	5200	9900	9400	23000	10300	32000	12100
Li	23	16	15	26	7	19	9	34	31	12	7	44	7
Rb	55	38	65	61	59	74	33	64	87	91	65	106	35
Sr	74	79	196	107	59	290	240	157	162	66	98	117	76
Ba	430	420	880	360	410	280	490	880	1770	470	490	560	370
La	18	18	16	11	15	19	13	14	14	30	19	25	18
V	23	18	29	10	14	49	13	19	19	55	32	75	20
Cr	22	23	22	5	10	86	9	13	10	41	12	66	15
Mo	7	7	4	5	3	6	3	4	5	4	2	9	
Mn	220	1130	630	142	3	194	230	5300	1180	830	910	470	490
Co	122	70	50	80	80	74	58	10	69	52	48	32	43
Ni	14	10	16	9	6	16	7	15	13	12	5	52	8
Cu	9	4	6	7	8	6	7	8	6	5	5	6	7
Ag	1					4							
Zn	13	8	18	8	6	21	7	14	14	20	21	54	12
Cd	1	1	1	1		1			1	1	1	1	
Pb	12	12	12	14	12	15	5	22	14	22	16	24	14
P	410	510	340	151	96	340	138	220	197	590	290	550	340
Total (%)	10.9	12.7	16.6	7.9	5.7	11.7	10.1	7.6	8.2	19.3	18.4	19.1	15.5

(* for Cu analysis: Contamination by sample holder after thermal demagnetisation).
(= below detectable limit)

13L: With liesegang rings 13N: Without liesegang rings.
31D: Darker colouration 31L: Lighter colouration.

Appendix C2.

ICP Analyses: Mean values.

	Caithness L. ORS	John o'Groats Sandstone	Caithness M-U. ORS	Orkney Eday gp.	Fishbed	Global Mean[1]	Eday Group Formations LES	MES	EM	UES
Na	1.72	0.87	0.45	1.01	1.49	4.46	0.95	1.03	1.11	0.98
K	3.10	1.74	1.96	2.22	2.09	0.92	2.54	2.59	1.67	1.77
Mg	0.78	0.75	0.44	0.95	2.03	0.72	1.74	0.93	0.54	0.18
Ca %	2.58	2.83	5.28	1.36	9.65	2.21	0.98	2.85	0.87	0.09
Al	5.38	3.20	3.61	3.87	4.83	4.46	3.69	4.69	3.45	3.31
Ti	0.35	0.16	0.21	0.18	0.28	0.30	0.15	0.23	0.18	0.16
Fe	2.37	1.13	1.54	1.38	1.54	2.36	1.08	1.81	1.37	1.19
Li	11	17	20	26	36	15	30	26	25	22
Rb	85	56	70	63	73	60	58	81	65	40
Sr	121	103	150	110	460	35	83	144	127	76
Ba	754	500	665	665	440	300	540	1030	505	450
La	28	16	19	18	23	<1	16	21	19	15
V	53	19	35	36	79	15	28	45	41	25
Cr	63	16	31	24	63	15	20	31	32	19
Mo*	2.0	5.2	4.1	1.1	5.0	0.2	0.8	2.1	0.8	0.6
Mn ppm	810	425	1200	295	680	500	300	370	280	170
Co	70	80	48	33	31	<1	35	38	23	35
Ni	44	11	16	17	58	2	14	23	19	10
Cu	7	6.8	6.2	16	28	15	19	10	20	13
Ag*	0.3	0.2	0.5	0.1	0.2	<0.1	0.6	0.1	0.1	0.2
Zn	28	11	20	22	65	16	15	27	31	16
Cd*	0.3	0.8	0.6	0.2	0.2	<0.1	0.1	0.2	0.2	0.2
Pb	20	12	15	16	46	9	15	18	17	14
P	620	300	330	340	580	400	360	375	340	260

* Inaccurate mean due to proximity to detection limit of ICP.

(1) Mean global composition from Pettijohn, 1963, table 13.

Appendix D1. EPMA analyses (Carbonates).

(i) Dolomite-Ferroan Dolomite-Ankerite.

Analysis	013	014	015	016	017	018	020	021	022	027	028	029	030	040	041	072
Site	RCD19	RCD19	RCD19	RCD19	RCD19	RCD19	RCD19	RCD19	RCD19	RCD19	RCD19	RCD19	RCD19	ROD17	RCD26	RCD19
Na_2O	0.056	0.042	0.237	0.200	0.266	0.000	0.220	0.120	0.285	0.339	0.274	0.193	0.052	0.107	0.000	0.047
MgO	10.783	12.887	18.834	12.680	13.027	12.428	13.008	12.704	12.835	12.183	12.566	13.571	21.389	20.312	20.561	15.220
Al_2O_3	0.126	0.145	0.348	0.558	0.217	0.227	0.203	0.000	0.000	0.094	0.767	0.214	0.229	0.113	0.103	0.528
SiO_2	4.229	0.538	0.776	1.237	0.482	1.535	0.369	0.253	0.276	0.455	2.523	0.459	0.371	0.503	0.436	1.439
K_2O	0.000	0.000	0.000	0.139	0.000	0.000	0.000	0.000	0.000	0.000	0.013	0.000	0.077	0.036	0.075	0.231
CaO	28.427	29.612	30.040	29.274	29.641	28.386	28.857	29.850	29.348	29.198	27.765	28.617	31.625	32.586	33.602	27.958
TiO_2	0.060	0.124	0.108	0.112	0.000	0.000	0.000	0.075	0.000	0.079	0.000	0.001	0.000	0.046	0.172	0.071
Cr_2O_3	0.113	0.000	0.000	0.000	0.108	0.122	0.000	0.000	0.014	0.000	0.080	0.000	0.020	0.055	0.139	0.007
MnO	0.324	0.745	1.054	0.826	0.768	1.087	1.324	0.915	1.230	0.652	1.086	1.323	0.000	0.082	0.048	0.382
FeO	12.441	10.892	1.489	10.554	10.571	11.520	11.396	11.168	11.236	12.283	9.855	11.404	0.186	0.158	0.179	6.939
Total	57.881	54.985	52.386	55.580	55.079	55.305	55.378	55.085	55.224	55.282	54.931	55.782	53.950	54.000	55.314	52.813
$MgCO_3$	24.136	27.376	40.606	27.338	27.711	26.831	27.449	26.779	27.056	25.911	28.146	28.418	44.131	42.096	41.660	34.070
$CaCO_3$	53.850	53.574	55.160	53.753	53.701	52.192	51.860	53.590	52.688	52.889	52.965	51.418	55.573	57.519	57.985	53.303
$MnCO_3$	0.562	1.207	1.761	1.380	1.266	1.819	2.166	1.495	2.010	1.075	1.885	2.147	0.000	0.132	0.076	0.633
$FeCO_3$	21.452	17.536	2.473	17.529	17.322	19.158	18.525	18.135	18.246	20.125	17.004	18.936	0.295	0.252	0.279	11.966

Analysis	073	074	075	078	079	080	081	082	083	084	085	086	087	088	089	097	098
Site	RCD19	RCD19	RCD19	RCD19	RCD19	RCD19	RCD19	RCD19	RCD19	RCD19	RCD19	RCD19	RCD19	RCD19	RCD19	ROD14	ROD14
Na_2O	0.340	0.381	0.000	0.019	0.070	0.000	0.024	0.000	0.018	0.117	0.440	0.000	0.138	0.049	0.000	0.047	0.000
MgO	13.357	12.380	12.052	12.190	12.394	12.129	13.056	13.004	13.847	13.251	11.844	12.623	12.797	13.279	13.157	18.817	9.909
Al_2O_3	0.231	0.057	0.343	0.268	0.059	0.028	0.155	0.000	0.392	0.569	0.163	0.290	0.434	0.248	0.123	0.000	0.277
SiO_2	0.483	0.349	0.650	0.716	0.633	0.568	0.358	0.261	0.552	1.156	0.613	0.281	0.880	0.484	0.286	0.108	0.251
K_2O	0.030	0.000	0.061	0.000	0.006	0.000	0.000	0.002	0.000	0.021	0.000	0.025	0.038	0.046	0.031	0.000	0.021
CaO	29.218	28.034	27.419	29.559	31.544	30.715	31.137	31.634	31.867	30.442	31.599	30.513	30.263	30.299	29.795	31.074	30.467
TiO_2	0.068	0.000	0.000	0.058	0.155	0.084	0.063	0.026	0.115	0.000	0.053	0.107	0.000	0.078	0.000	0.000	0.000
Cr_2O_3	0.010	0.033	0.000	0.000	0.048	0.000	0.068	0.011	0.000	0.000	0.078	0.035	0.193	0.131	0.000	0.040	0.000
MnO	0.780	0.792	0.656	0.986	0.811	0.745	0.739	0.696	0.739	1.187	0.756	0.772	0.759	1.173	1.287	0.083	0.421
FeO	9.453	11.722	11.150	12.115	11.607	11.433	11.214	11.590	11.548	11.854	12.346	11.843	11.746	10.753	11.392	2.758	12.947
CoO	0.000	0.000	0.000	0.197	0.079	0.000	0.016	0.017	0.000	0.000	0.311	0.018	0.060	0.124	0.000	0.000	0.100
Total	53.969	53.749	52.331	56.109	57.406	55.711	56.830	57.241	59.178	58.597	58.204	56.506	57.310	56.665	56.073	53.559	54.392
$MgCO_3$	28.956	27.283	27.082	25.684	25.381	25.443	26.762	26.316	27.444	26.917	24.244	26.117	26.546	27.506	27.237	39.197	21.468
$CaCO_3$	53.946	51.464	52.470	53.042	55.018	54.873	54.357	54.524	53.790	52.665	55.088	53.768	53.464	53.452	52.531	56.245	56.217
$MnCO_3$	1.312	1.353	1.143	1.610	1.288	1.211	1.174	1.092	1.135	1.869	1.200	1.238	1.221	1.883	2.065	0.134	0.707
$FeCO_3$	15.786	19.900	19.301	19.663	18.311	18.474	17.707	18.068	17.631	18.549	19.468	18.876	18.769	17.158	18.167	4.425	21.068

n.b. Carbonate analyses normalised to 100%.

Appendix D1. EPMA analyses (Carbonates).

(i) Dolomite, Ferroan dolomite and Ankerite (contd).

Analysis	099	100	101	102	103	105	106	107	108	110	111	112	114	133	135	139	140
Site	ROD14	ROD14	ROD14	ROD14	ROD14	ROD14	ROD14	ROD14	ROD14	ROD14	ROD14	ROD14	ROD14	RCD02	RCD02	RCD26	RCD26
Na_2O	0.179	0.058	0.079	0.108	0.218	0.253	0.000	0.016	0.041	0.000	0.000	0.413	0.268	0.000	0.000	0.170	0.091
MgO	12.219	10.931	12.343	11.208	6.510	19.638	18.261	13.237	19.387	13.306	10.167	17.250	17.816	17.688	18.718	20.868	13.743
Al_2O_3	0.282	0.221	0.203	0.269	0.029	0.189	0.237	0.150	0.000	0.407	1.503	0.000	0.153	0.073	0.468	0.261	0.631
SiO_2	0.152	0.214	0.154	0.167	0.116	0.299	0.179	0.185	0.156	0.987	2.395	0.234	0.231	0.592	1.535	0.548	1.690
K_2O	0.000	0.000	0.000	0.000	0.000	0.000	0.000	0.000	0.000	0.076	0.211	0.000	0.000	0.044	0.361	0.000	0.229
CaO	31.905	31.845	31.657	31.166	31.778	31.860	31.113	31.134	30.738	30.952	30.793	29.966	31.767	31.225	28.682	30.789	29.014
TiO_2	0.004	0.140	0.000	0.013	0.000	0.000	0.025	0.000	0.000	0.000	0.000	0.000	0.000	0.000	0.000	0.080	0.133
Cr_2O_3	0.077	0.037	0.015	0.000	0.000	0.000	0.011	0.085	0.000	0.027	0.067	0.022	0.000	0.000	0.000	0.000	0.000
MnO	0.463	0.604	0.355	0.607	1.319	0.982	0.676	0.514	0.491	0.758	0.926	0.579	0.406	0.030	0.303	0.000	0.105
FeO	12.174	13.438	12.072	14.116	18.988	3.504	3.234	10.240	3.601	12.926	11.071	5.683	5.371	4.912	4.410	0.484	10.497
CoO	0.184	0.000	0.069	0.093	0.104	0.183	0.040	0.201	0.099	0.000	0.174	0.000	0.000	0.000	0.036	0.072	0.135
Total	57.640	57.488	56.949	57.748	59.061	56.908	53.776	55.761	54.512	59.439	57.307	54.148	56.012	54.568	54.512	53.312	56.269
$MgCO_3$	24.823	22.366	25.364	22.829	13.225	39.094	38.223	27.554	39.793	26.759	22.277	36.240	36.120	36.782	40.015	43.967	29.478
$CaCO_3$	55.377	55.494	55.402	54.064	54.983	54.018	55.465	55.197	53.733	53.012	57.464	53.618	54.852	55.301	52.221	55.247	53.003
$MnCO_3$	0.729	0.957	0.561	0.958	2.077	1.515	1.097	0.430	0.781	1.182	1.573	0.943	0.638	0.049	0.502	0.000	0.174
$FeCO_3$	19.052	21.181	19.109	22.149	29.716	5.373	5.215	16.420	5.694	19.127	18.686	9.198	8.388	7.868	7.262	0.785	17.344

Analysis	142	143	144	199	238	239	240	241	242	243	244	245	246	247	250	252	253
Site	RCD26	ROD17	RCD26	ROD26	ROD26	ROD26	ROD26	ROD26	ROD26	ROD26	ROD26	ROD26	ROD26	ROD26	ROD26	ROD26	ROD26
Na_2O	0.101	0.343	0.392		0.000	0.415	0.166	0.000	0.218	0.219	0.320	0.240	0.205	0.446	0.126	0.113	0.291
MgO	13.127	21.455	11.837	20.549	21.354	14.681	15.178	22.008	21.875	16.255	16.682	22.649	22.732	22.224	18.745	16.141	16.222
Al_2O_3	0.232	0.896	0.366	0.041	0.000	0.524	0.202	0.000	0.025	0.578	1.277	0.000	0.000	0.033	0.031	0.000	0.315
SiO_2	0.439	2.250	0.704	0.722	0.642	1.714	0.221	0.282	0.280	1.457	2.526	0.185	0.172	0.163	0.215	0.214	0.485
K_2O	0.000	0.456	0.061		0.000	0.000	0.000	0.058	0.000	0.088	0.228	0.000	0.000	0.006	0.038	0.026	0.070
CaO	28.960	30.228	28.389	31.733	31.935	31.595	32.175	31.718	32.255	31.099	30.975	33.156	32.735	32.568	33.654	29.851	32.043
TiO_2	0.000	0.000	0.000	0.017	0.000	0.000	0.093	0.000	0.000	0.081	0.000	0.041	0.037	0.110	0.005	0.000	0.008
Cr_2O_3	0.026	0.000	0.222	0.123	0.027	0.099	0.148	0.000	0.000	0.113	0.000	0.000	0.065	0.101	0.041	0.000	0.003
MnO	0.200	0.000	0.085	0.000	0.089	0.362	0.360	0.000	0.000	0.244	0.159	0.077	0.000	0.000	0.771	0.027	0.292
FeO	12.341	0.484	15.098	0.387	0.167	6.556	6.505	0.150	0.203	5.650	4.268	0.293	0.179	0.172	2.741	8.283	6.555
CoO	0.000	0.047	0.108														
Total	55.427	56.160	57.261	53.572	54.214	55.944	55.048	54.217	54.855	55.782	56.254	56.642	56.125	55.823	56.367	54.656	56.285
$MgCO_3$	27.663	45.100	24.809	42.923	43.803	31.425	31.706	44.789	44.190	34.452	35.895	44.456	44.793	44.365	37.405	33.651	33.250
$CaCO_3$	51.977	54.117	50.675	56.454	55.791	57.600	57.242	54.976	55.494	56.137	56.765	55.427	54.936	55.371	57.195	53.003	55.937
$MnCO_3$	0.327	0.000	0.138	0.000	0.141	0.164	0.583	0.000	0.000	0.186	0.266	0.000	0.000	0.000	1.186	0.436	0.464
$FeCO_3$	20.034	0.783	24.377	0.623	0.264	10.810	10.468	0.235	0.316	9.224	7.074	0.116	0.272	0.265	4.213	13.303	10.350

n.b. Carbonate analyses normalised to 100%.

Appendix D1 EPMA analyses (Carbonates).

(i) Dolomite, Ferroan Dolomite and Ankerite (contd).

Analysis	254	255	256	259	260	261	262	265	266	267	268	270	273	274	275	276	277
Site	ROD26	ROD26	ROD26	ROD26	ROD26	ROD26	ROD26	ROD26	ROD26	ROD25	ROD25	ROD25	RCD26	RCD26	RCD26	RCD26	RCD26
Na_2O	0.020	0.156	0.161	0.281	0.155	0.292	0.153	0.329	0.060	0.527	0.277	0.205	0.247	0.175	0.139	0.315	0.027
MgO	17.026	16.497	16.621	17.701	16.629	18.632	17.931	17.370	16.478	19.925	19.367	16.964	18.178	17.258	11.649	14.612	12.912
Al_2O_3	0.189	0.000	0.034	0.186	0.000	0.098	0.122	0.085	0.080	0.028	0.067	0.840	0.177	0.055	0.000	0.438	0.142
SiO_2	0.374	0.360	0.369	0.278	0.178	0.184	0.157	0.228	0.682	0.195	0.577	1.790	0.445	0.458	0.372	0.980	0.684
K_2O	0.002	0.000	0.042	0.000	0.000	0.000	0.022	0.000	0.000	0.032	0.000	0.119	0.022	0.031	0.073	0.060	0.080
CaO	32.999	32.327	32.417	35.686	35.231	35.105	34.156	34.447	32.541	32.003	31.347	30.020	31.357	33.045	29.716	29.694	29.439
TiO_2	0.081	0.051	0.075	0.000	0.159	0.000	0.110	0.000	0.164	0.069	0.124	0.101	0.055	0.029	0.000	0.038	0.042
Cr_2O_3	0.118	0.093	0.000	0.047	0.000	0.000	0.004	0.000	0.136	0.000	0.000	0.000	0.000	0.026	0.000	0.061	0.009
MnO	0.003	0.166	0.261	0.238	0.302	0.428	0.539	0.211	0.000	0.166	0.351	0.575	0.017	0.201	0.324	0.393	0.457
FeO	3.638	3.633	4.038	0.642	1.078	0.678	0.829	4.037	3.740	1.793	1.621	4.074	2.621	2.353	12.187	9.648	11.301
CoO																	
Total	54.550	53.282	54.018	55.060	53.733	55.417	54.023	56.707	53.881	54.736	53.731	54.688	53.119	53.630	54.461	56.239	55.093
$MgCO_3$	35.760	35.133	34.961	36.293	34.683	37.729	37.297	34.753	35.005	40.921	40.700	36.786	38.746	36.432	24.999	30.673	27.447
$CaCO_3$	58.410	58.633	58.073	62.315	62.905	60.542	60.507	58.698	58.875	55.978	56.105	55.442	56.922	59.412	54.313	53.086	53.295
$MnCO_3$	0.005	0.274	0.424	0.379	0.491	0.671	0.869	0.327	0.000	0.264	0.572	0.966	0.029	0.329	0.539	0.640	0.753
$FeCO_3$	5.824	5.960	6.525	1.014	1.741	1.058	1.329	6.222	6.120	2.837	2.624	6.805	4.304	3.826	20.147	15.400	18.506

n.b. Carbonate analyses normalised to 100%.

Appendix D1: EPMA analyses (carbonates).

(ii) Calcite

Analysis	025	052	062	091	104	109	113	120	124	131	248	249
Site	RCD19	ROD17	RCD42	ROD17	ROD14	ROD14	ROD14	RCD43	RCD43	RCD43	ROD26	ROD26
Na_2O	0.651	0.102	0.000	0.082	0.363	0.085	0.444	0.043	0.174	0.125	0.000	0.152
MgO	0.172	0.152	0.061	1.149	0.293	1.446	1.950	0.229	0.368	0.278	1.216	0.812
Al_2O_3	0.000	0.021	0.020	0.135	0.000	0.084	0.293	0.027	0.091	0.025	0.000	0.049
SiO_2	0.000	0.319	0.373	0.311	0.319	0.311	0.327	0.356	0.290	0.301	0.143	0.296
K_2O	0.000	0.000	0.000	0.038	0.000	0.000	0.000	0.139	0.000	0.000	0.000	0.000
CaO	51.722	60.385	58.904	59.287	56.763	57.707	52.396	59.633	58.372	56.645	55.394	56.720
TiO_2	0.083	0.000	0.014	0.054	0.062	0.106	0.000	0.084	0.190	0.148	0.000	0.002
Cr_2O_3	0.000	0.003	0.000	0.149	0.000	0.322	0.000	0.004	0.032	0.000	0.090	0.113
MnO	0.000	0.134	0.809	0.510	0.042	0.172	0.252	0.842	0.292	0.172	0.360	0.240
FeO	0.705	1.476	0.579	0.088	0.041	0.346	1.128	1.136	0.501	0.101	0.297	0.457
CoO			0.137	0.000	0.000	0.082	0.000	0.000	0.126	0.000		
SO_2				0.076	0.000			0.038	0.018	0.418		
Total	53.333	62.594	60.896	61.877	57.884	60.661	56.791	62.530	60.452	58.214	57.499	58.841
$MgCO_3$	0.384	0.288	0.118	2.205	0.601	2.836	4.145	0.436	0.722	0.570	2.486	1.635
$CaCO_3$	98.403	97.363	97.790	96.906	96.380	96.380	94.872	96.657	98.075	98.997	96.475	97.282
$MnCO_3$	0.000	0.197	1.223	0.758	0.262	0.262	0.415	1.242	0.444	0.274	0.570	0.375
$FeCO_3$	1.213	0.869	0.869	0.130	0.523	0.523	0.567	1.665	0.758	0.160	0.468	0.709

Analysis	251	257	258	263	264	269	271	272	281	282	283
Site	ROD26	ROD26	ROD26	ROD26	ROD26	ROD25	ROD25	ROD25	ROD67	ROD67	ROD67
Na_2O	0.053	0.000	0.024	0.197	0.212	0.177	0.000	0.040	0.177	0.083	0.032
MgO	0.955	1.829	1.003	1.122	0.851	0.288	0.325	0.551	0.759	0.866	0.942
Al_2O_3	0.105	0.000	0.089	0.058	0.079	0.173	0.084	0.082	0.027	0.074	0.003
SiO_2	0.328	0.306	0.201	0.221	0.215	0.555	0.319	0.323	0.188	0.464	0.305
K_2O	0.000	0.000	0.006	0.080	0.000	0.010	0.045	0.000	0.005	0.000	0.095
CaO	56.439	54.092	54.781	54.574	56.163	55.597	56.283	56.438	53.979	53.515	53.500
TiO_2	0.000	0.000	0.015	0.041	0.209	0.000	0.000	0.001	0.022	0.079	0.034
Cr_2O_3	0.002	0.003	0.016	0.059	0.031	0.086	0.000	0.080	0.000	0.000	0.030
MnO	0.443	0.324	0.281	0.282	0.213	0.279	0.253	0.053	1.119	0.773	0.153
FeO	0.460	0.380	0.460	0.426	0.359	0.659	0.545	0.000	0.082	0.040	0.000
NiO									0.042	0.277	0.076
Total	58.874	56.934	56.876	57.060	58.333	57.826	57.854	57.569	56.402	56.172	55.170
$MgCO_3$	1.921	3.776	2.079	2.330	1.733	0.596	0.665	1.133	1.592	1.840	2.021
$CaCO_3$	96.675	95.102	96.535	96.535	97.368	97.908	98.075	98.784	96.455	96.823	97.325
$MnCO_3$	0.691	0.519	0.454	0.454	0.336	0.447	0.401	0.085	1.820	1.273	0.254
$FeCO_3$	0.713	0.604	0.682	0.563	0.563	1.050	0.859	0.000	0.133	0.065	0.000

n.b. Carbonate analyses normalised to 100%.

Appendix D2: EPMA Analyses (Iron-Titanium Oxides).

(i) Sarclet Group

Analysis	058	070	071	116	118	126	127	129	130	145	147	148	149
Site	RCD42	RCD42	RCD42	RCD51	RCD51	RCD43	RCD43	RCD43	RCD43	RCD46	RCD46	RCD46	RCD46
	S	S	S	S	S	S	D	S	S	D	S	S	S
Na_2O	0.343	0.526	0.808	0.279	0.343	0.490	0.240	0.517	0.188	1.662	0.000	0.793	0.000
MgO	0.286	0.187	0.379	0.468	0.000	0.473	0.082	0.302	0.249	0.474	0.078	0.000	0.589
Al_2O_3	0.370	0.231	0.029	0.415	0.148	1.618	0.119	0.436	0.846	0.266	0.000	0.232	0.409
SiO	1.017	0.679	0.780	1.175	0.951	2.545	0.425	1.015	1.810	0.733	0.147	0.392	1.207
K_2O	0.196	0.000	0.000	0.035	0.197	0.531	0.032	0.000	0.000	0.076	0.039	0.029	0.240
CaO	0.250	0.097	0.181	0.164	0.068	0.000	0.000	0.033	0.000	0.105	0.150	0.000	1.088
TiO_2	2.186	0.719	3.230	3.657	2.847	3.960	3.937	3.303	3.965	8.098	4.439	0.398	4.133
Cr_2O_3	0.200	0.368	0.110	0.165	0.151	0.131	0.513	0.086	0.217	0.312	0.043	0.000	0.011
MnO	0.000	0.016	0.116	0.000	0.029	0.177	0.000	0.000	0.196	0.000	0.000	0.000	0.133
FeO	84.372	88.010	85.122	83.243	84.674	82.264	86.242	84.387	82.592	80.111	84.574	89.996	80.491
CoO	0.216	0.286	0.524	0.251	0.038	0.008	0.000	0.266	0.000	0.103	0.155	0.077	0.340
Total	89.435	91.121	91.280	89.852	89.446	92.197	91.590	90.345	90.063	91.942	89.624	91.917	88.641
FeO -	4.931	20.103	21.553	8.684	5.030	29.875	24.323	10.582	10.983	27.490	6.632	27.265	(0)
Fe_2O_3	95.069	79.897	78.467	91.316	94.970	70.215	75.677	89.418	89.017	72.510	93.368	72.735	(100)

Analysis	150	151	154	155	156	161	162	163	164	165	185	186
Site	RCD46	RCD46	RCD20	RCD20	RCD20	RCD20	RCD20	RCD20	RCD20	RCD20	RCD42	RCD42
	D	S	S	S	S	D	S	S	S	S	S	S
Na_2O	0.426	0.070	0.005	0.165	0.000	0.248	0.275	0.023	0.401	0.260	0.745	0.111
MgO	0.567	0.001	0.038	0.000	0.000	0.000	0.000	0.114	0.113	0.000	0.332	0.000
Al_2O_3	0.165	0.317	0.120	0.040	0.472	0.127	0.013	0.000	0.239	0.261	0.340	0.000
SiO_2	0.559	0.392	0.347	0.533	0.752	0.400	0.381	0.482	0.544	1.013	0.873	0.474
K_2O	0.157	0.068	0.104	0.060	0.029	0.101	0.120	0.000	0.000	0.215	0.090	0.000
CaO	0.000	0.000	0.079	0.000	0.000	0.386	0.076	0.042	0.000	0.000	0.070	0.106
TiO_2	11.755	9.088	3.140	7.438	0.207	6.854	1.613	7.172	6.326	2.403	6.193	7.498
Cr_2O_3	0.381	0.337	0.000	0.188	0.004	0.000	0.046	0.088	0.242	0.184	0.234	0.083
MnO	0.000	0.000	0.140	0.137	0.000	0.163	0.314	0.156	0.011	0.000	0.298	0.077
FeO	76.869	78.514	86.127	83.689	87.413	83.406	88.275	82.618	82.505	83.698	81.449	82.889
CoO	0.020	0.005	0.310	0.015	0.686	0.047	0.000	0.000	0.000	0.061	0.000	0.000
Total	90.900	88.792	90.410	92.266	89.565	91.732	91.112	90.893	90.381	88.095	90.624	91.237
FeO	18.114	(0)	13.705	30.406	6.101	25.601	20.022	18.051	13.444	(0)	15.630	21.146
Fe_2O_3	81.886	(100)	86.295	69.594	93.899	74.978	79.978	81.949	86.556	(100)	84.370	78.854

D: Detrital S: Secondary

Appendix D2: EPMA Analyses (Iron-Titanium oxides)

(ii) Eday Group.

Analysis	093	094	095	187	188	189	191	192	192a	192b	193
Site	ROD17	ROD17	ROD17	ROD16	ROD16	ROD16	ROD16	ROD18	ROD17	ROD17	ROD18
Formation	MES	MES	MES	MES	MES	MES	MES	MES	MES	MES	MES
	D	D	D	D	D	D	D	D	D	D	D
Na_2O	0.454	0.322	0.115								
MgO	0.209	0.118	0.000	0.309	0.471	0.067	0.000	0.175	0.178	0.176	0.064
Al_2O_3	0.956	0.772	0.137	0.477	0.168	0.000	1.330	0.431	0.436	0.431	0.343
SiO_2	2.953	1.207	0.378	0.701	0.704	0.836	0.911	0.690	0.696	0.688	0.991
K_2O	0.093	0.236	0.089								
CaO	0.284	0.025	0.031	0.025	0.016	0.063	0.087	0.063	0.062	0.062	0.050
TiO_2	0.529	1.363	7.036	6.668	15.007	15.239	15.829	10.680	10.581	10.454	0.084
Cr_2O_3	0.068	0.043	0.029	0.294	0.027	0.030	0.135	0.162	0.155	0.154	0.283
MnO	0.211	0.120	0.115	0.057	0.360	0.303	0.208	0.819	0.665	0.657	0.434
FeO	80.957	85.473	84.648	83.214	76.341	76.014	71.801	80.256	80.325	79.445	89.195
CoO	0.000	0.352	0.413								
NiO				0.000	0.000	0.030	0.000	0.019	0.160	0.158	0.000
Total	86.711	90.030	92.991	91.745	93.095	92.582	90.301	93.294	93.258	92.224	91.444
FeO	(0)	10.420	36.930	25.718	37.866	33.249	10.294	39.656	39.332	30.028	23.009
Fe_2O_3	(100)	89.580	63.070	74.282	66.751	66.751	89.706	60.344	60.668	69.972	76.991

Analysis	193a	197	198	200	201	202	203	206	207	209	210
Site	ROD17	ROD17	ROD17	ROD17	ROD19	ROD17	ROD17	ROD17	ROD17	ROD22	ROD22
Formation	MES	MES	MES	MES	EV	MES	MES	MES	MES	EM	EM
	D	D	D	S		S	D	D	D	S	S
Na_2O					0.241	0.572	0.284	0.755	0.190	0.392	0.560
MgO	0.065	0.000	0.139	0.280	0.169	0.454	0.203	0.165	0.119	0.270	0.350
Al_2O_3	0.345	0.165	0.060	1.201	0.405	0.870	0.435	0.596	0.513	0.205	0.288
SiO_2	0.991	0.535	0.520	1.084	0.852	3.197	1.216	0.428	0.771	0.532	0.830
K_2O					0.000	0.124	0.179	0.059	0.108	0.145	0.063
CaO	0.049	0.104	0.100	0.091	0.128	0.862	0.090	0.159	0.225	0.121	0.106
TiO_2	0.082	9.513	10.520	2.160	5.748	1.994	5.040	6.456	18.790	4.142	2.838
Cr_2O_3	0.270	0.022	0.075	0.000	0.348	0.035	0.095	1.252	1.304	0.089	0.091
MnO	0.270	0.048	0.058	0.168	0.000	0.723	0.000	0.000	0.000	0.000	0.049
FeO	88.436	81.440	80.720	85.463	77.521	74.820	76.160	74.404	63.951	78.705	77.924
CoO					0.000	0.657	0.300	0.086	0.423	0.000	0.000
NiO	0.024	0.000	0.071	0.000							
Total	90.532	91.826	92.264	90.446	85.413	84.306	84.003	84.359	86.393	84.602	83.099
FeO	14.802	26.447	30.388	14.019	(0)	(0)	(0)	(0)	(0)	(0)	(0)
Fe_2O_3	85.198	73.553	69.612	85.971	(100)	(100)	(100)	(100)	(100)	(100)	(100)

D: Detrital S: Secondary

Appendix D2: EPMA Analyses (Iron-Titanium oxides)

(ii) Eday Group (contd).

Analysis	211	224	225	226	227	228a	228b	229a	229b	230
Site	ROD22	ROD67	ROD67	ROD67	ROD67	ROD67	ROD67	ROD67	ROD67	ROD22
Formation	EM	EM	EM	EM	EM	EM	EM	EM	EM	EM
	S	D	D	D	D	D	D	D	D	D
Na_2O	0.105									
MgO	0.144	0.334	0.065	0.000	0.105	0.304	0.303	0.213	0.219	0.719
Al_2O_3	0.660	0.518	0.000	0.487	0.526	0.330	0.342	0.379	0.387	0.957
SiO_2	1.339	0.626	0.372	0.521	1.366	2.790	2.819	0.792	0.803	0.945
K_2O	0.184									
CaO	0.067									
TiO_2	1.952	0.137	9.220	0.441	0.823	4.832	4.889	9.737	9.914	21.409
V_2O_5		0.360	0.000	0.409	0.460	0.009	0.021	0.000	0.000	0.578
Cr_2O_3	0.129	0.000	0.097	0.303	0.266	0.080	0.075	0.110	0.106	0.049
MnO	0.050	0.160	0.277	0.000	0.192	0.344	0.327	1.658	1.662	0.015
FeO	80.955	87.782	81.288	87.277	86.788	81.435	82.442	76.558	77.996	65.819
NiO		0.000	0.000	0.047	0.028	0.000	0.000	0.000	0.000	0.015
ZnO		0.000	0.047	0.101	0.000	0.023	0.022	0.244	0.244	0.013
CoO	0.170									
Total	87.755	89.917	91.365	89.587	90.544	90.147	91.240	89.693	91.332	90.518
FeO	(0)	9.268	22.298	6.299	14.910	13.768	21.173	7.253	22.001	14.677
Fe_2O_3	(100)	90.732	77.702	93.701	85.090	86.232	78.827	92.747	77.999	85.323

Analysis	231	232	233	234	235	236	237	284	285	286
Site	ROD30	ROD30	ROD30	ROD30	ROD30	ROD30	ROD30	ROD39	ROD39	ROD39
Formation	EM	EM	EM	EM	EM	EM	EM	UES	UES	UES
	D	S	S	S	S	S	S	S	D	D
Na_2O		0.413	0.693	0.448	0.499	0.576	0.278	0.393	0.088	0.428
MgO	0.000	0.169	0.590	0.477	0.000	0.000	0.000	0.220	0.000	0.098
Al_2O_3	0.131	0.258	0.391	0.000	0.085	0.000	0.000	0.016	0.049	0.002
SiO_2	1.064	0.917	0.869	0.631	0.475	0.396	0.257	0.524	0.298	0.290
K_2O		0.070	0.027	0.007	0.076	0.029	0.000	0.000	0.000	0.000
CaO		0.000	0.000	0.000	0.000	0.000	0.018	0.090	0.073	0.008
TiO_2	9.819	5.796	1.653	0.047	1.579	1.120	0.963	0.179	6.108	5.843
V_2O_5	0.094									
Cr_2O_3	0.054	0.163	0.104	0.184	0.067	0.136	0.174	0.000	0.228	0.037
MnO	0.003	0.131	0.246	0.393	0.187	0.000	0.042	0.033	0.000	0.000
FeO	77.864	79.589	84.995	86.127	85.462	86.480	87.027	87.117	84.024	84.259
NiO	0.000							0.000	0.000	0.065
ZnO	0.048									
Total	89.077	87.506	89.569	88.313	88.429	88.737	88.759	88.570	90.868	91.031
FeO	1.710	(0)	6.137	(0)	(0)	(0)	(0)	(0)	17.826	19.293
Fe_2O_3	98.290	(100)	93.863	(100)	(100)	(100)	(100)	(100)	82.174	80.707

D: Detrital S: Secondary

Appendix D2: EPMA Analyses (Iron-Titanium oxides).

(iii) Other sediments.

	Lower ORS (Foyers)			John o'Groats Sst.		U.ORS (Dunnet)		Upper ORS (Dornoch)					
Analysis	166	167	168	152	153	004	007	172	173	177	181	182	183
Site	RCD29	RCD29	RCD29	RCD01	RCD01	RCD16	RCD16	RCD54	RCD54	RCD54	RCD54	RCD54	RCD54
	D	D	S	D	D	D	D	D	D	D	D	D	D
Na_2O	0.499	0.024	0.166	0.249	0.369	0.028	0.091	0.000	0.322	0.651	0.000	0.440	0.476
MgO	0.049	0.002	0.237	0.126	0.328	0.022	1.278	0.000	0.309	0.164	0.157	0.270	0.120
Al_2O_3	0.134	0.034	0.071	1.314	0.300	0.255	0.336	0.801	2.849	0.000	0.115	0.477	0.273
SiO_2	0.662	0.512	0.761	2.060	0.727	0.657	0.375	0.811	0.984	0.367	0.143	0.559	0.416
K_2O	0.000	0.135	0.095	0.169	0.048	0.000	0.020	0.187	0.106	0.000	0.026	0.000	0.098
CaO	0.421	0.232	0.534	0.094	0.036	0.022	0.000	0.118	0.389	0.268	0.127	0.146	0.142
TiO_2	6.573	20.362	4.492	0.820	0.359	4.944	18.270	3.211	6.454	8.949	11.567	14.182	12.213
Cr_2O_3				0.196	0.385								
MnO	0.178	0.376	0.052	0.000	0.000	0.093	0.387	0.255	0.000	0.000	0.263	0.000	0.170
FeO	83.238	69.163	85.770	83.924	85.366	82.633	70.214	84.519	78.148	83.826	81.415	76.291	80.758
CoO	0.058	0.000	0.000	0.224	0.837			0.528	0.199	0.000	0.000	0.350	0.055
Total	91.811	90.480	92.178	89.176	88.755	88.654	90.971	90.429	89.758	94.225	93.813	92.715	94.821
FeO	26.312	14.335	29.614	2.601	(0)	(0)	18.753	13.876	7.838	48.034	38.657	34.440	53.397
Fe_2O_3	73.688	85.666	70.386	97.399	(100)	(100)	81.247	86.124	92.612	51.966	61.343	65.554	46.603

(iv) Duncansby Vent.

	Xenoliths								Matrix					
Analysis	003	157	158	212	213	214	215	216	217	218	219	221	222	223
Site	RCD02	RCD02	RCD02	RCD03	RCD03	RCD03	RCD03	RCD03	RCD03	RCD03	RCD03	RCD03	RCD03	RCD03
Na O	0.449	0.456	0.000	0.387	0.390	0.429	0.723	0.247	0.227	0.290	0.722	0.240	0.402	0.661
MgO	0.167	0.375	0.000	0.328	0.038	0.231	0.424	0.019	0.000	0.626	0.102	2.654	0.312	0.279
Al_2O_3	0.092	0.248	0.000	1.978	2.618	2.670	2.187	1.278	2.045	3.123	0.591	5.792	2.430	2.082
SiO_2	0.581	0.711	0.437	0.397	0.415	0.535	0.392	0.565	0.475	0.556	0.653	0.601	0.440	0.395
K_2O	0.066	0.097	0.169	0.081	0.016	0.057	0.000	0.104	0.051	0.000	0.107	0.138	0.000	0.000
CaO	0.016	0.452	0.542	0.431	0.350	0.355	0.254	0.553	0.405	0.525	0.654	0.320	0.248	0.568
TiO_2	13.224	2.976	2.271	16.248	17.449	17.874	17.253	22.255	16.768	17.018	17.979	18.570	16.152	15.363
Cr_2O_3				2.101	0.231	0.718	0.000	0.091	0.128	0.995	0.000	5.073	0.431	0.323
MnO	0.167	0,000	0.000	1.773	2.071	2.151	2.381	3.158	2.209	1.775	2.504	0.866	2.090	2.022
FeO	77.791	84.517	83.760	65.373	66.792	65.030	65.848	62.301	66.215	64.925	66.187	55.928	68.706	66.953
CoO		1.073	0.681	0.000	0.000	0.458	0.011	0.217	0.136	0.086	0.520	0.000	0.180	0.308
Total	92.387	90.095	87.859	89.097	90.370	90.507	89.472	90.789	88.660	89.920	90.019	90.183	91.391	88.955
FeO	31.495	10.870	(0)	1.890	13.345	14.578	5.264	17.115	(0)	9.295	10.186	11.662	22.532	0.612
Fe_2O_3	68.505	89.130	(100)	98.110	86.655	85.422	94.736	82.885	(100)	90.705	89.814	88.338	77.468	99.388

D: Detrital S: Secondary

Appendix D2: EPMA Analyses (Iron-Titanium Oxides).

(v) Stoichimetric Recalculation.

	Analysis 224				Analysis 225				Analysis 227				Analysis 228a			
	3 oxygens		4 oxygens		3 oxygens		4 oxygens		3 oxygens		4 oxygens		3 oxygens		4 oxygens	
	Ox. %	Form.	Ox. %	Form.	Ox. %	Form.	Ox. %	Form.	Ox. %	Form.	Ox. %	Form.	Ox. %	Form.	Ox. %	Form.
Mg	0.33	0.013	0.33	0.020	0.07	0.003	0.07	0.004	0.11	0.006	0.11	0.006	0.30	0.012	0.30	0.018
Al	0.52	0.016	0.52	0.024	0.00	0.000	0.00	0.000	0.53	0.016	0.53	0.024	0.33	0.010	0.33	0.015
Si	0.63	0.017	0.63	0.025	0.37	0.010	0.37	0.015	1.37	0.036	1.37	0.054	2.79	0.074	2.79	0.110
Ti	0.14	0.003	0.14	0.004	9.22	0.183	9.22	0.274	0.82	0.016	0.82	0.024	4.83	0.096	4.83	0.144
V	0.36	0.002	0.36	0.003	0.00	0.000	0.00	0.000	0.46	0.003	0.46	0.004	0.01	0.000	0.01	0.000
Cr	0.00	0.000	0.00	0.000	0.10	0.002	0.10	0.003	0.27	0.006	0.27	0.008	0.08	0.002	0.08	0.002
Mn	0.16	0.004	0.16	0.005	0.28	0.006	0.28	0.009	0.19	0.004	0.19	0.006	0.34	0.008	0.34	0.012
Fe2+	97.56	1.944	63.41	1.900	81.31	1.616	47.88	1.427	93.56	1.860	60.77	1.807	82.36	1.641	49.78	1.482
Fe3+	0.000	0.000	30.72	1.023	8.13	0.179	38.21	1.264	2.60	0.057	32.11	1.061	7.33	0.162	36.65	1.212
Ni	0.00	0.000	0.00	0.000	0.00	0.000	0.00	0.000	0.03	0.001	0.03	0.001	0.00	0.000	0.00	0.000
Zn	0.00	0.000	0.00	0.000	0.05	0.001	0.05	0.001	0.00	0.000	0.00	0.000	0.02	0.000	0.02	0.001
Total	99.69	1.999	96.27	3.005	99.51	2.000	96.16	2.997	99.93	2.004	96.64	2.997	98.40	2.005	95.14	2.997

	Analysis 229a				Analysis 229b				Analysis 230				Analysis 231			
	3 oxygens		4 oxygens		3 oxygens		4 oxygens		3 oxygens		4 oxygens		3 oxygens		4 oxygens	
	Ox. %	Form.	Ox. %	Form.	Ox. %	Form.	Ox. %	Form.	Ox. %	Form.	Ox. %	Form.	Ox. %	Form.	Ox. %	Form.
Mg	0.21	0.009	0.21	0.013	0.22	0.009	0.22	0.013	0.72	0.029	0.72	0.043	0.00	0.000	0.00	0.000
Al	0.38	0.012	0.38	0.018	0.39	0.012	0.39	0.018	0.96	0.030	0.96	0.045	0.13	0.004	0.13	0.006
Si	0.79	0.021	0.79	0.032	0.80	0.021	0.80	0.032	0.95	0.025	0.95	0.038	1.06	0.029	1.06	0.043
Ti	9.74	0.196	9.74	0.294	9.91	0.196	9.91	0.294	21.41	0.433	21.41	0.649	9.82	0.200	9.82	0.300
V	0.00	0.000	0.00	0.000	0.00	0.000	0.00	0.000	0.58	0.004	0.58	0.006	0.09	0.001	0.09	0.001
Cr	0.11	0.002	0.11	0.004	0.11	0.002	0.11	0.003	0.05	0.001	0.05	0.002	0.05	0.001	0.05	0.002
Mn	1.66	0.038	1.66	0.056	1.66	0.037	1.66	0.056	0.01	0.000	0.01	0.001	0.00	0.000	0.00	0.000
Fe2+	76.58	1.547	44.24	1.338	78.01	1.548	45.07	1.338	51.20	1.036	18.29	0.555	75.29	1.536	42.40	1.298
Fe3+	7.66	0.172	36.75	1.234	7.80	0.172	37.44	1.235	19.75	0.444	49.36	1.664	10.12	0.229	39.71	1.351
Ni	0.00	0.000	0.00	0.000	0.00	0.000	0.00	0.000	0.01	0.000	0.01	0.000	0.00	0.000	0.00	0.000
Zn	0.24	0.005	0.24	0.007	0.24	0.005	0.24	0.007	0.01	0.000	0.01	0.000	0.05	0.001	0.05	0.001
Total	97.37	2.002	94.13	2.996	99.15	2.002	95.85	2.996	95.65	2.003	92.35	3.004	96.62	2.001	93.33	3.003

Appendix D3: EPMA Analyses (Miscellaneous).

(i) High-Titanium oxides.

Analysis	051	146	159	170	171	175	176	178	180	195	204	205
Site	ROD17	RCD46	RCD02	RCD29	RCD29	RCD54	RCD54	RCD54	RCD54	ROD17	ROD17	ROD17
Na_2O	0.508	0.234	0.666	0.057	0.251	0.338	0.000	0.281	0.549		0.000	0.126
MgO	0.679	0.424	0.225	0.139	0.218	0.709	0.719	0.365	0.097	0.046	0.072	0.110
Al_2O_3	0.190	0.295	0.012	0.112	0.196	0.000	0.118	0.112	0.777	0.045	0.127	0.596
SiO	0.368	0.738	0.263	0.731	0.781	0.616	0.486	0.452	1.721	0.694	0.480	1.278
K_2O	0.104	0.185	0.000	0.058	0.150	0.000	0.000	0.073	0.101		0.050	0.125
CaO	0.158	0.000	0.107	0.050	0.196	0.193	0.000	0.180	0.317	0.117	0.123	0.205
TiO_2	60.695	62.671	28.848	53.817	59.668	50.125	49.767	65.795	28.060	57.534	57.600	27.966
Cr_2O_3	0.108	0.282	68.308	0.205	0.362						0.144	0.109
MnO	1.276	0.176	0.207	0.000	0.050	2.696	2.309	0.105	1.400	1.377	0.000	0.104
FeO	36.052	32.697	0.247	45.861	39.842	48.899	48.372	30.570	60.273	36.340	33.136	57.111
CoO	0.000	0.000	0.000	0.000	0.000	0.000	0.429	0.000	0.827		0.000	0.252
Total	100.407	97.702	98.884	101.029	101.714	103.578	102.210	97.934	94.120	96.152	91.732	87.983

(ii) Sheet silicates.

Analysis	009	024	042	043	059	065	090	117	Intra-cleavage oxides 066	208
Site	RCD19 (BIO)	RCD19 (CHL)	ROD17 (BIO)	ROD17 (BIO)	RCD42 (BIO)	RCD42 (CHL)	ROD17 (BIO?)	RCD51 (BIO)	RCD42	ROD22
Na_2O	0.313	0.297	0.213	0.590	0.066	0.171	0.183	0.050	0.897	0.414
MgO	0.262	15.532	6.079	0.272	17.410	11.504	21.860	18.928	4.367	0.170
Al_2O_3	30.607	20.683	16.952	33.644	18.927	22.684	21.444	14.477	5.093	0.659
SiO_2	44.571	26.245	35.288	46.428	30.742	25.699	27.757	29.106	5.969	1.184
K_2O	10.134	0.042	8.233	7.010	1.241	0.062	0.496	2.066	0.156	0.228
CaO	0.084	0.066	0.185	0.079	0.191	0.116	0.201	0.089	0.169	0.110
TiO_2	1.554	0.264	4.470	1.289	0.034	0.023	0.426	1.388	2.658	0.205
V_2O_5	0.000									
Cr_2O_3	0.000	0.124	0.000	0.000	0.082	0.031	0.060	0.000	0.063	0.204
MnO	0.000	0.158	0.255	0.082	0.062	0.317	0.157	0.232	0.000	0.000
FeO	4.583	25.086	23.067	1.463	21.921	30.177	15.701	19.354	78.769	80.745
CoO	0.000		0.042	0.071	0.166	0.287	0.000	0.000	0.000	0.000
NiO	0.000									
Total	92.109	88.522	94.785	90.928	90.844	91.072	88.285	85.690	98.142	83.918

BIO = Biotite CHL = Chlorite MUS = Muscovite

Appendix E.

Ferrous Iron Determinations.

Sample no.	FeO (%) Analysis 1	Analysis 2	Mean	%Fe
RCD10	0.569	-	0.57	2.1
RCD11	0.277	-	0.28	0.5
RCD3801	0.165	0.148	0.16	1.7
RCD3802	0.102	0.099	0.10	
RCD3803	0.097	0.090	0.09	1.4
RCD3805	0.075	0.072	0.07	1.4
ROD0201	1.542	-	1.54	8.4
ROD0211	2.484	-	2.48	2.5
ROD1911	2.412	-	2.41	3.4
ROD1908	2.499	-	2.50	3.5
ROD1907	1.369	-	1.37	2.6
ROD1906	1.680	-	1.68	2.9
ROD1901	1.054	-	1.06	2.5
ROD1904	1.530	-	1.53	3.2
ROD54G	1.285	1.254	1.27	2.4
ROD54P	1.289	1.311	1.30	2.9
ROD7401	0.696	0.673	0.68	3.6
ROD7404	0.719	0.689	0.70	4.4

(1): As calculated.
(2): To 2 decimal places.
(3): From ICP analysis (Appendix C).
(4): Highly inaccurate due to organic carbon.

APPENDIX F

CARBONIFEROUS SEDIMENTS OF THE KIRKBEAN OUTLIER

Study of ORS sediments described in this volume has indicated that they have undergone severe oxidative remagnetisation during the Kiaman reversed polarity interval, this often involving the diagenesis of ferroan carbonate cements.

If such processes have affected most ORS sediments then they should also be expected to have affected younger (but pre-Kiaman) sediments. In order to test this hypothesis, a reconnaissance study was made of folded Carboniferous sediments on Southerness Point, northern Solway Firth. These are generally believed to have been deformed during the late Carboniferous; the timing of acquisition of any stable ancient remanence should thus be referrable to the age of deformation.

Structure and sedimentology of the area is described by Craig (1956) and Heaton (1979). Specimens were drilled in nine sites around two folds in the Gillfoot Beds (fig. F.1). The sediments sampled were a medium-grained red sandstone; sites 6 to 9 are from are finer-grained sandy mudstone within a generally somewhat coarser sequence.

Progressive demagnetisation of one pilot specimen from each of the nine sites showed the remanence to be essentially two-component. A low stability component was demagnetised by 200-350°C, above which the demagnetisation trajectory was usually directed towards the origin (fig F.2). A maximum T_B of 620-680°C showed the remanence to be carried in hematite. Based on this information, most specimens were thermally cleaned at 400-550°C. Site mean directions are

given in table F.1, and illustrated in figs. F3, F4.

Precision can be seen to be greater in situ than dip corrected, although site mean directions show a surprising degree of dispersion considering the precision with which individual components are defined.

Comparison of the precision parameter k for in situ and dip corrected mean directions gives a ratio of 1.51; this is insufficient to pass the fold test at the 95% confidence level (as described by McElhinny, 1964) but would tend to suggest that remanence was largely acquired after deformation.

Time has not permitted a detailed petrological study, although calcitisation of ferroan dolomite has been reported from the area. It is thus proposed as an indication that such processes may have affected pre-Kiaman sediments younger than the ORS.

Table F.1
Site mean directions

	In Situ		Dip Corrected		N	k	a_{95}
Site	Dec	Inc	Dec	Inc			
1	161.2	3.0	161.7	-11.2	8[1]	25.4	11.2
2	168.1	-8.5	169.1	-23.1	9[1]	10.2	17.0
3	195.9	5.8	196.1	-7.9	8[1]	15.8	14.4
4	171.6	-17.8	172.5	-33.6	10[1]	24.2	10.0
5	174.1	-11.2	168.8	-25.9	10[1]	12.2	4.4
6	137.0	-19.3	132.3	5.1	10[1]	26.9	9.5
7	132.8	-27.9	120.1	-19.9	5[1]	31.7	13.8
8	170.6	-25.5	179.1	-41.0	6[1]	14.6	18.1
9	163.2	3.1	183.7	-44.4	10[1]	45.6	7.2
Mean	164.4	-10.3			9[2]	13.3	14.7
			164.2	-24.2	9[2]	8.8	18.3

(1) Unit weighting to specimens
(2) Unit weighting to sites

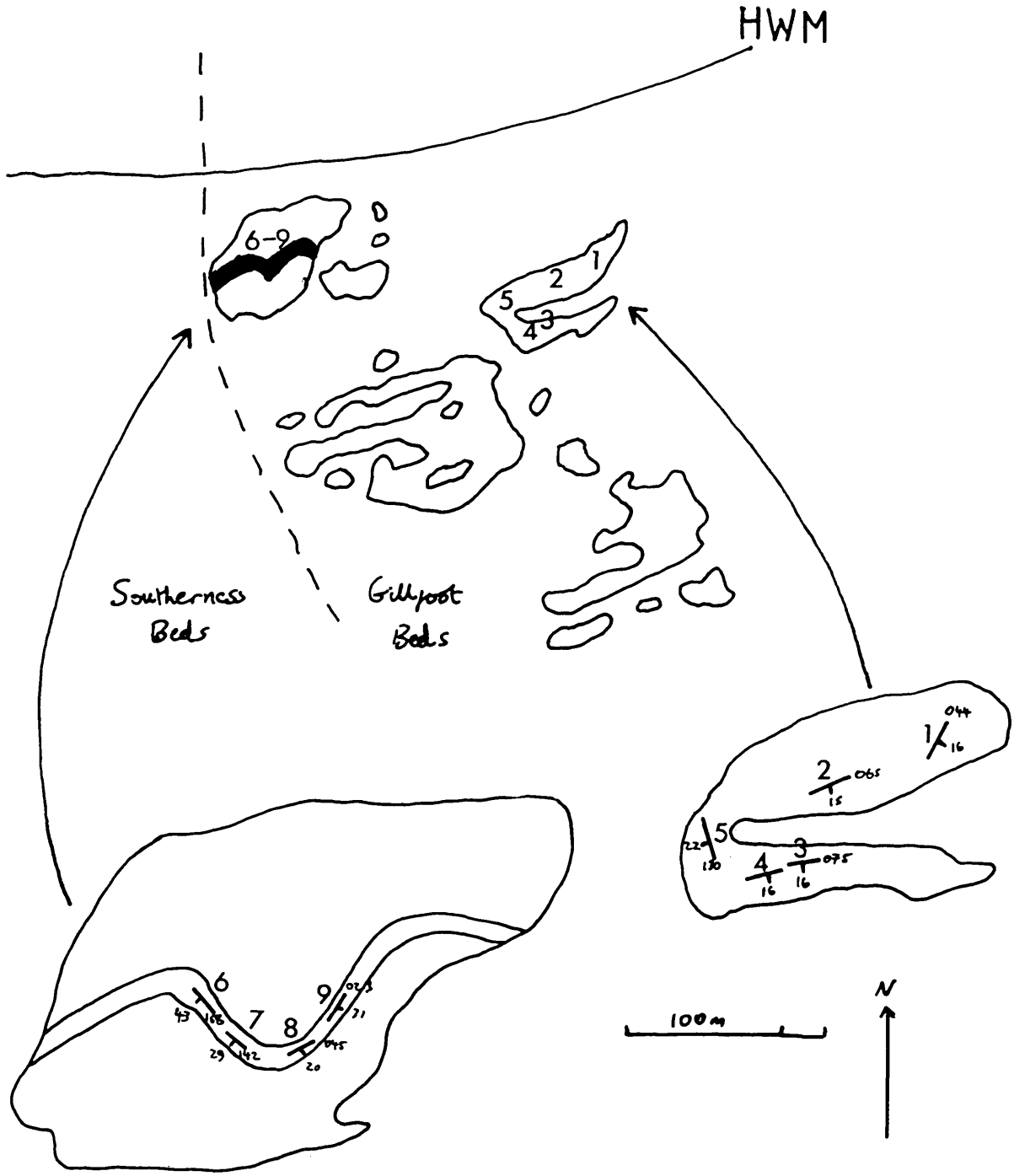
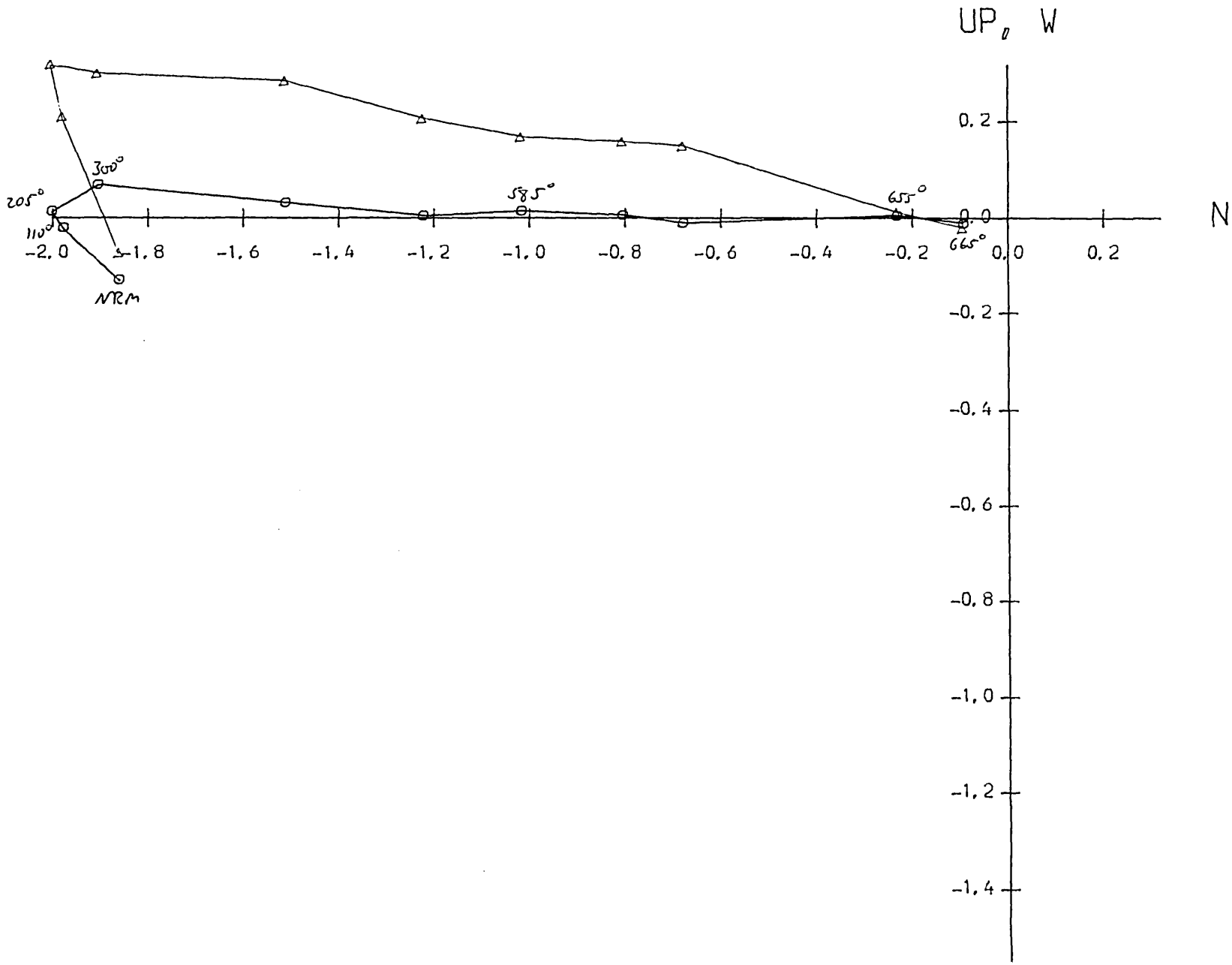


Fig. F.1. Location map, Kirkbean Outlier, immediately south of Southerness Hotel. GR 975543; see Heaton, 1979. Shows site numbers and corresponding dedding orientation.

RSC0501B


UP, W
N
0.2
0.0
-0.2
-0.4
-0.6
-0.8
-1.0
-1.2
-1.4
-2.0
-1.8
-1.6
-1.4
-1.2
-1.0
-0.8
-0.6
-0.4
-0.2
0.0
0.2
205°
300°
110°
585°
655°
665°
NRM

KIRKBEAN SITE MEANS I.S.

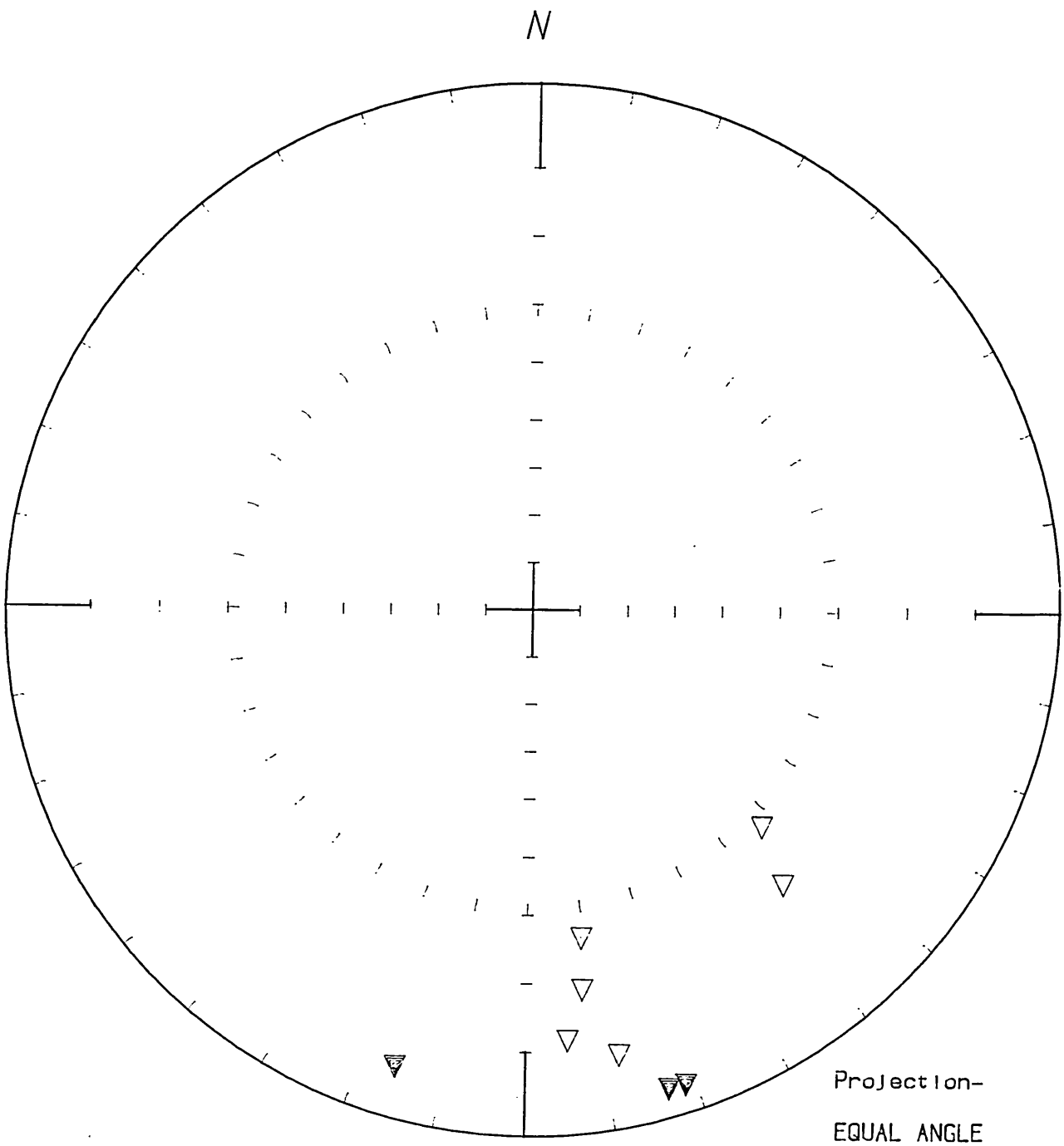


Fig F3

KIRKBEAN SITE MEANS D. C.

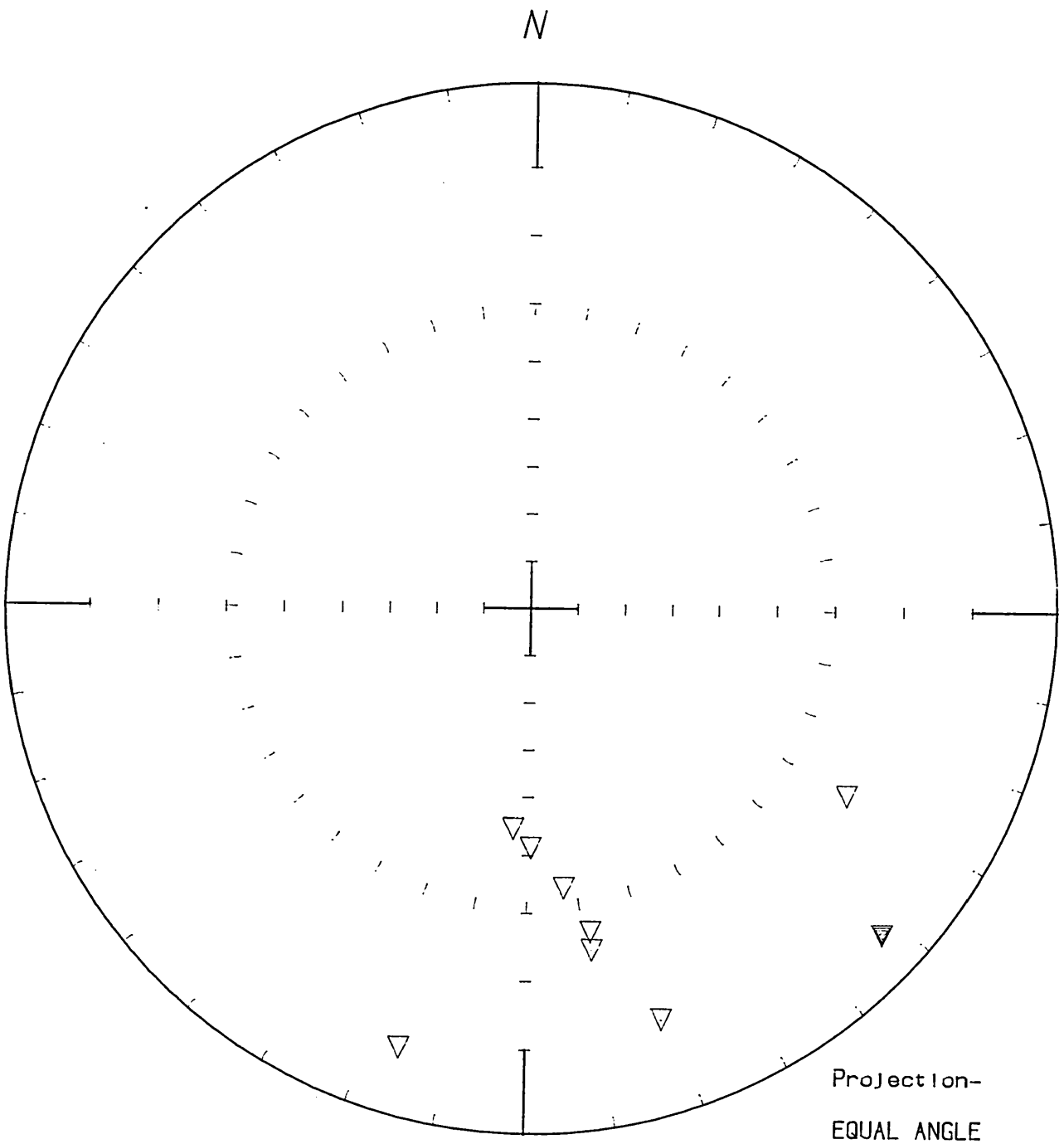


Fig F4